U.P.V. E.H.U.

Actas de las II Jornadas de Inteligencia Computacional

JIC'08

Ramón Moreno Jiménez
Alexandre Manhães Savio

Affi, Italia

Prefacio

El presente libro de actas recoge las presentaciones realizadas en las II Jornadas de Inteligencia Computacional que el grupo de Inteligencia Computacional de la UPV/EHU realizó en la localidad de Affi en la provincia de Verona en Italia, en los días 12 al 18 de Mayo de 2008. La primera pregunta que debe contestar este prefacio es: ¿por qué Affi? ¿por qué un grupo de investigación con sede en San Sebastián, Gipuzkoa, España, se va hasta una pequeña localidad italiana a realizar un periodo de concentración? La primera razón, la operativa, es que el grupo cuenta con un miembro originario de esta población (Flavio Banterla) que ha puesto toda su capacidad organizativa a nuestro servicio, para localizar alojamiento barato y tranquilo en el que pudiéramos realizar las sesiones de trabajo, para organizar actividades de relajación tras las horas de sesiones (efectivamente: desde las 9 de la mañana hasta las 13h y desde las 15h hasta las 19h). La segunda razón es de costo: el viaje y la estancia se han realizado a precios muy por debajo de los costos habituales en congresos y reuniones científicas, beneficiándonos de la hospitalidad de Villa Elena. Aquí mantenemos un recuerdo entrañable del personal de Villa Elena por su amabilidad y extraordinario calor humano. La tercera razón es que el acto viajar y encontrar una manifestación vital semejante y, al mismo tiempo, distinta, añade una dimensión de universalidad a la experiencia que estimula la imaginación y nos recuerda que somos ciudadanos del mundo. La última razón es también pragmática, alejarse del entorno habitual facilita considerablemente la concentración en la tarea y evita vías de escape que destrozarían la dinámica de trabajo deseada.

La experiencia de estas jornadas ha sido extraordinariamente positiva, en todos los aspectos. La convivencia ha sido agradable y fluida, el lugar magnífico y la hospitalidad de sus gentes memorable. El intenso trabajo de preparación, asistencia y presentación ha sido estimulante (y agotadora) para todos los miembros del grupo. Las presentaciones tenían una duración estimada de una hora, que en general resultó ser un tiempo corto para el material preparado por los ponentes. Un objetivo de esta jornada era el establecimiento de una base común de trabajo y conocimiento, algo bastante difícil habida cuenta de la variedad de intereses y formaciones de los miembros del grupo. Las jornadas han supuesto un paso adelante en este camino, que esperamos se vaya consolidando en el futuro, en las III Jornadas que realizaremos en la primavera de 2009. Por de pronto han servido para muchos de los miembros hayan realizado un trabajo de revisión del estado del arte de sus áreas de trabajo que sienta bases de sus propios trabajos personales.

El presente libro electrónico, que se publicará en la web del grupo (www.ehu.es/ccwintco) es atípico en varios aspectos, el primero y primordial es que se trata de una recolección de presentaciones, desprovistas de literatura. La ventaja de las presentaciones como documentación es precisamente su capacidad de proporcionar de forma inmediata la información y los elementos más importantes del tema. Este libro presenta de forma sumaria el espectro de trabajos e intereses de los miembros del grupo que atendieron a las jornadas y presentaron su trabajo. No están todos los que son, pero son todos los que están. Es una muestra importante de los intereses y capacidad de

trabajo del Grupo de Inteligencia Computacional de la UPV/EHU. En lo referente al lenguaje, algunas de las presentaciones están redactadas en inglés mientras que otras están en castellano, dado que no impusimos restricciones ni de lengua ni de formato en las presentaciones. Las presentaciones han sufrido un proceso de revisión, que ha supuesto cambios profundos en algunas de ellas y en otras la corrección de erratas y pequeños errores. Dicho proceso de revisión se ha llevado a cabo en una instalación de un sistema de gestión de congresos (Myreview).

La temática de las presentaciones abarca campos diversos, desde el proceso de la imagen digital, hasta la sociología y neurosicología, pasando por la revisión de algunos fundamentos teóricos (filtros Kalman, Markov Random Fields, Redes Neuronales Competitivas) y algunas aplicaciones computacionales de la inteligencia computacional como la gestión de información multimedia o los Sistemas de Información Geográfica (GIS). Resulta obligado en todo prefacio hacer una breve introducción de cada una de las aportaciones.

Ramón Moreno presentó sus trabajos y el estado del arte en el análisis de reflectancia en imágenes digitales basado en el Modelo Dicromático de Reflexión, que es el modelo más extendido en este tipo de análisis. El objetivo de estos trabajos es la eliminación de los efectos de iluminación, incluyendo la identificación de los píxeles de la imagen correspondientes a regiones puramente especulares. La identificación de la cromaticidad de la fuente de iluminación es una de las técnicas claves para obtener dicha identificación y separación de las regiones especulares de la imagen.

Flavio Banterla presentó un estado del arte de las aplicaciones de Realidad Virtual en Neuropsicología. La Realidad Virtual proporciona un instrumento de gran valor para la observación de la conducta y la medición precisa de las respuestas de los sujetos experimentales o pacientes en casos clínicos. También aporta herramientas para la rehabilitación en algunas patologías. El grado de inmersión que induce la Realidad Virtual lleva consigo una mayor Validez Ecológica que otras técnicas de evaluación neuropsicologica.

Abdelmalik Moujahid presentó la aplicación de técnicas de sincronización de sistemas dinámicos para la detección de estructuras jerárquicas en redes complejas de agentes. Partiendo de un estado completamente sincronizado de los agentes, el cambio dinámico de los parámetros de interacción produce de forma espontanea un clustering jerarquico progresivo que detecta de manera completa la estructura modular de la red de agentes. La evidente implicación sociológica de estos trabajos encontró eco inmediato en otro de los ponentes (Patxi) y ha dado lugar a una estrecha colaboración.

Elsa Fernández presento la aplicación de técnicas de clustering al estudio y análisis de información de imagen funcional de Resonancia Magnética (fMRI). La señal de fMRI viene dada por la evolución temporal de la señal debida a la oxigenación en distintas zonas del cerebro (señal BOLD) que mide de forma indirecta la actividad neuronal. Esta información temporal puede someterse a procesos de clustering para encontrar los patrones representativos de las diversas fases de activación neuronal.

Ivan Villaverde hizo una revisión de la formulación matemática de los filtros de Kalman

y sus derivaciones finales en filtros de partículas. Los filtros de Kalman son el mecanismo básico de estimación del estado para el control de sistemas con incertidumbre en su estado y observaciones ruidosas. Son algoritmos predictores/correctores: corrigen la predicción del estado en función de la observación, estimando la incertidumbre de la estimación a través de su matriz de covarianza.

Alexandre Manhaes nos presentó una revisión del estado del arte en el registro de imágenes de Resonancia Magnética de cerebro, un campo muy activo debido al intenso estudio actual sobre las enfermedades neurodegenerativas. En su presentación introdujo los atlas cerebrales y sus métodos de construcción, puesto que son elementos centrales en la definición de los procesos de registro. La presentación incluyó la descripción somera de los métodos rígidos y elásticos de registro, los problemas del registro Inter.-sujeto y de los registros multimodales, especialmente de información funcional y anatómica.

Jose Orlando Maldonado presentó el estado del arte en sistemas de acceso a bases de datos de imágenes basados en contenidos (CBIR) con mecanismos de realimentación basados en la relevancia de las respuestas obtenidas mediante interacción con el usuario que realiza la pregunta. La presentación revisa las aproximaciones basadas en redes neuronales artificiales y en las formulaciones bayesianas del mecanismo de relevancia y su realización.

Miguel Angel Veganzones presenta una revisión de los diversos métodos de extracción de endmembers en imágenes hiperespectrales. El proceso de análisis que consiste en la descomposición del espectro cada píxel en la mezcla de un conjunto de espectros, conocido como linear unmixing precisa de la identificación de los espectros que constituyen la base de la mezcla, los endmembers. La presentación incluye una técnica para la detección del número de endmembers en la imagen, y revisa los métodos geométricos, morfológicos (basados en Lattice Computing) y heurísticos.

Carmen Hernández realizó una presentación de los resultados básicos de la teoría de campos aleatorios Markovianos. Los campos aleatorios Markovianos tienen aplicación en el modelado de imágenes y procesos espaciales para su procesado bayesiano en aplicaciones de restauración de imagen, segmentación e interpretación. Además de las definiciones básicas la presentación recorre una extensa variedad de tipos de campos, caracterizados por expresiones particulares de la función de energía.

Josune Gallego en colaboración con Jose Luis Jiménez preparó una presentación de conceptos básicos sobre contraste de hipótesis o test estadísticos. Desde el punto de vista metodológico, los tests estadísticos tienen una gran importancia en todos los campos de la ciencia, y también en la Inteligencia Computacional. Nos permiten realizar afirmaciones sobre propiedades de nuestros datos de forma rigurosa.

Maite García Sebastián presentó una revisión del estado del arte de métodos de segmentación con corrección de inhomogeneidades de intensidad en imágenes de Resonancia Magnética. Estos métodos se basan en un modelo común simple que asume respuesta constante para tejidos homogéneos, pero abarcan una diversidad de aproximaciones desde las redes neuronales articiales, los sistemas borrosos (fuzzy) hasta

técnicas bayesianas usando modelos construidos mediante campos aleatorios markovianos.

Alicia d'Anjou presentó una introducción a los sistemas de información geográfica los cuales constituyen una de las fuentes más ricas de información digital en la actualidad. La proliferación de los sistemas de localización GPS así como los sistemas de distribución de mapas vía Internet, liderado por Google, han popularizado este tipo de sistemas,

Como conclusión a este prefacio debo expresar mi mas profundo agradecimiento personal a las personas que hicieron posible este evento con su presencia. Desde los comienzos de mi carrera universitaria he deseado poder realizar un encuentro cómo el que realizamos en la Villa Elena en Affi. Cada uno de los presentes contribuyo con su color especial al maravilloso cuadro que dibujamos en esos días. Mi deseo es que contemplar este libro como uno de los frutos de aquel trabajo anime a los asistentes y aotros miembros del Grupo de Inteligencia Computacional a continuar trabajando en este mundo incierto pero fascinante que es la investigación al nivel universitario. Un mundo con fuertes limitaciones pero con un aire de libertad que no existe en ningún otro ambiente, a pesar de las piedras en el camino que nos ponen desde dentro y fuera de la Universidad. Este humilde librito, con su aparentemente inocuo contenido, reclama con orgullo la herencia de siglos de amor al conocimiento y a la libertad de pensamiento.

Manuel Graña Romay
San Sebastián, 12 Noviembre de 2008

Agradecimientos

A Manuel Graña y al resto de los integrantes del Grupo de Inteligencia Computacional de la Universidad del País Vasco (UPV/EHU) por su confianza y por la oportunidad de llevar a cabo la edición de este libro y la organización de las II Jornadas de Inteligencia Computacional.

A todos los autores por sus contribuciones, sin las cuales esta publicación no hubiera sido posible.

A Flavio, a su familia, a la población de Affi en general y al personal de Villa Elena en particular por su cálida acogida.

Lista de Presentaciones

- Reflectance Analysis Based on the Dichromatic Reflection Model

  Ramón Moreno

- State of the art of virtual reality applications in neuropsychology

  Flavio Banterla

- Clustering Dinámico y estructuras modulares en redes complejas

  Abdel Moujahid

- Comparación de técnicas de clustering para fMRI

  Elsa Fernández

- Introducción a los filtros Kalmans

  Ivan Villaverde

Lista de Presentaciones

- Brain Image Registration

Alexandre Manhães

- Relevance Fedback for CBIR Systems

Orlando Maldonado

- Linear Mixing Model for Hyperspectral Imagery. Virtual Dimensionality, Endmembers Induction Methods and Unmixing techniques

Miguel A. Veganzones

Lista de Presentaciones

- Markov Random Fields

Carmen Hernández

- Contraste de Hipotesis

Josune Gallego

- Métodos de segmentación y corrección de la inhomogeneidad de intensidad en imágenes de RM

Maite García-Sebastián

- Introduction to GIS

Alicia D'Anjou

Lista de Presentaciones

- Redes Sociales. Una aproximación desde la Teoría General de Sistemas

Blanca Cases y Patxi Olasagasti

- Algunas ideas sobre redes neuronales competitivas y mixtas

Manuel Graña

- Robust Multimedia Information. Retrieval in Basque Context

Eloy Irigoyen

Reflectance Analysis

Based on the Dichromatic Reflection Model

R. Moreno
Computational Intelligence Group
Universidad del País Vasco

JIC 2008

Outline

1. Reflectance
2. DRM
   - Chromaticity
3. Illumination Chromaticity
   - Dichromatic-based color constancy using dichromatic slope and dichromatic line space
   - Color constancy thought Inverse-Intensity chromaticity space
   - On determining the color Illuminant using the dichromatic reflection model
4. Components Separation
   - Robby-Ikeuchi Method
   - Kuk-jin Method

Reflectance

Figure: Specular and diffuse reflection in natural scene

- The dichromatic reflection model proposed by Safer [4], describes the surface reflection for dielectric materials as the sum of two components, the **diffuse** and **specular** terms.
- The **diffuse reflection** component exhibits the color by material as different wavelenght are more or less absorbed within the material as light is scattered.
- The **specular reflection** component is essentially determined by the color of incident light.

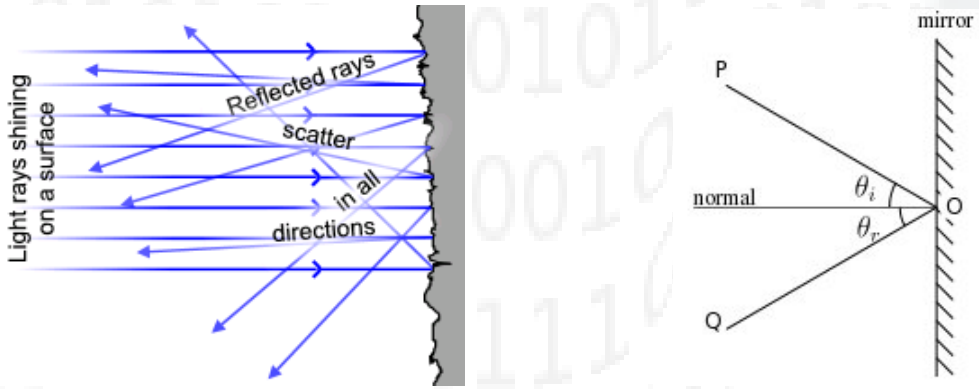

Figure: Diffuse and Specular reflections

Dichromatic Reflection Model

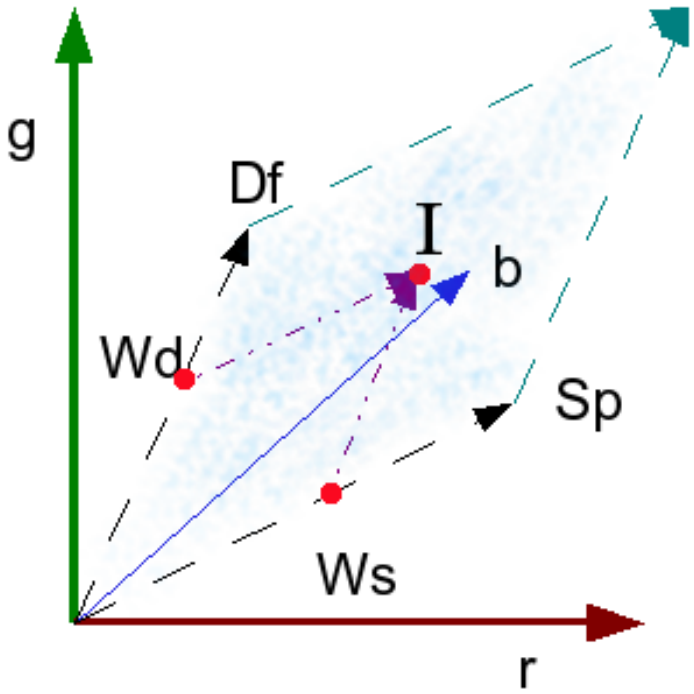

Figure: Dichromatic Reflection Model Scheme

$$I = w_d Df + w_s Sp$$

- The color of a uniform color surface is represented by the blue region, where *Df* is the body color (depending of diffuse albedo), *Sp* is the light color.
- Because the geometry is different at each point, the scale factors w_d and w_s vary from point to point.

Model of a image taken with a CCD digital camera

$$I(x) = w_d(x) \int_{\Omega} S(\lambda, x) E(\lambda) q(\lambda) d\lambda + w_s(x) \int_{\Omega} E(\lambda) q(\lambda) d\lambda \quad (1)$$

- $I = \{I_r, I_g, I_b\}$ is the color of image intensity or camera sensor.
- $x = \{x, y\}$ are the two dimensional space coordinates.
- $q = \{q_r, q_g, q_b\}$ is the three-element-vector of sensor sensitivity.
- $w_d(x)$ and $w_s(x)$ are the weighting factors for diffuse and specular components, they depend of the geometric structure at location x.
- $S(\lambda, x)$ is the diffuse spectral reflectance.
- $E(\lambda)$ is the spectral power distribution function of illumination source, it is independent of the spatial location x because we assume a uniform illuminant light color.
- The integration is done over the visible spectrum Ω.

Model of a image taken with a CCD digital camera

Model of a image taken with a CCD digital camera

$$I(x) = w_d B(x) + w_s G \tag{2}$$

- $B(x) = \int_\Omega S(\lambda, x) E(\lambda) q(\lambda) d\lambda$
- $G = \int_\Omega E(\lambda) q(\lambda) d\lambda$

Outline

1. Reflectance
2. DRM
   - Chromaticity
3. Illumination Chromaticity
   - Dichromatic-based color constancy using dichromatic slope and dichromatic line space
   - Color constancy thought Inverse-Intensity chromaticity space
   - On determining the color Illuminant using the dichromatic reflection model
4. Components Separation
   - Robby-Ikeuchi Method
   - Kuk-jin Method

Chromaticity

Normalized RGB

$$\sigma(x) = \frac{I(x)}{I_r + I_g + I_b} \tag{3}$$

Diffuse Chromaticity

$$\Lambda(x) = \frac{B(x)}{B_r + B_g + B_b} \tag{4}$$

Specular or Illumination Chromaticity

$$\Gamma = \frac{G}{G_r + G_g + G_b} \tag{5}$$

Image expressed in terms of chromaticity

Image model expressed in terms of chromaticity

$$I(x) = m_d(x)\Lambda(x) + m_s(x)\Gamma \tag{6}$$

where

- $m_d(x) = w_d(x)\left[B_r(x) + B_g(x) + B_b(x)\right]$
- $m(x) = w_s(x)\left(G_r + G_g + G_b\right)$

In addition, from their definitions we can obtain:

$$(\sigma_r + \sigma_g + \sigma_b) = (\Lambda_r + \Lambda_g + \Lambda_b) = (\Gamma_r + \Gamma_g + \Gamma_b) = 1$$

Methods

In this section, we will to describe some methods for the Illumination chromaticity estimation:

1. Dichromatic-based color constancy using dichromatic slope and dichromatic line space[8]
2. Color constancy thought Inverse-Intensity chromaticity space[5]
3. On determining the color illuminant using the dichromatic reflection model[2]
4. Color line search for illuminant estimation in real-world scenes [1]

Outline

1. Reflectance
2. DRM
   - Chromaticity
3. Illumination Chromaticity
   - Dichromatic-based color constancy using dichromatic slope and dichromatic line space
   - Color constancy thought Inverse-Intensity chromaticity space
   - On determining the color Illuminant using the dichromatic reflection model
4. Components Separation
   - Robby-Ikeuchi Method
   - Kuk-jin Method

Image chromaticity and dichromaticity line space

This method is based on the specularity invariant dichromatic slope and the three-dimensional dichromatic line space.
From equations (3) and (6) we can derive the following equation:

$$I_c(x) = \Lambda_c(x) + \frac{m_s(x)}{m_d(x) + m_s(x)} (\Gamma_c - \Lambda_c(x)) \quad (7)$$

Defining *s(x)* as

$$s(x) = \frac{m_s(x)}{m_d(x) + m_s(x)} \quad (8)$$

and $0 < s(x) \leq 1$.

Dichromatic slope

Image chromaticity can be expressed as:

$$I(x) = \Lambda(x) + s(x)\left(\Gamma - \Lambda(x)\right) \tag{9}$$

We can derive the following equation from (9) by differentiating image chromaticity $i_r(x)$ w.r.t x.

$$\frac{\partial i_r(x)}{\partial x} = \frac{\partial \Lambda_r(x)}{\partial x} + \frac{\partial}{\partial x}\left[s(x)\left(\Gamma_r - \Lambda_r(x)\right)\right] \tag{10}$$

Dichromatic slope

$\frac{\partial \Gamma_r(x)}{\partial x}$ is assumed to be zero under a single uniform illumination. In addition $\frac{\partial i_g(x)}{\partial x}$ is close enough to zero to be neglected. Then equation (10) can be simplified to:

$$\frac{\partial i_r(x)}{\partial x} = \frac{\partial s(x)}{\partial x}\left(\Gamma_r - \Lambda_r(x)\right) \tag{11}$$

We can derive respect $i_g(x)$:

$$\frac{\partial i_g(x)}{\partial x} = \frac{\partial s(x)}{\partial x}\left(\Gamma_g - \Lambda_g(x)\right) \tag{12}$$

Dichromatic slope

Finally, using (11) and (12)

Dichromatic slope $\alpha(x)$

$$\frac{\frac{\partial i_r(x)}{\partial x}}{\frac{\partial i_g(x)}{\partial x}} = \frac{\Gamma_r - \Lambda_r(x)}{\Gamma_g - \Lambda_g(x)} \triangleq \alpha(x) \tag{13}$$

Dichromatic Line Space

In the two dimensional space, a line can be described by identifying one point on it and its slope.

Dichromatic line

$$g(r) = \alpha(x)(r - i_r(x)) + i_g(x) \tag{14}$$

- $(i_r(x), i_g(x))$ and $\alpha(x)$are the image chromaticity and the chromaticity slope at x.
- In a three-dimensional space (i_r, i_g, α) represents a line that passes(i_r, i_g) with slope α.

Illuminant Chromaticity Estimation

- Illuminant chromaticity can be estimated by finding the intersections of dichromatic lines when are two or more colors.

1. The first step is to detect specular pixels and project them in to the dichromatic line space according to their chromaticities and dichromatic slopes.
2. Local maxima in the dichromatic line space are detected. A maximun in the dichromatic line space represents a line in the dichromatic space.

Illuminant Chromaticity Estimation

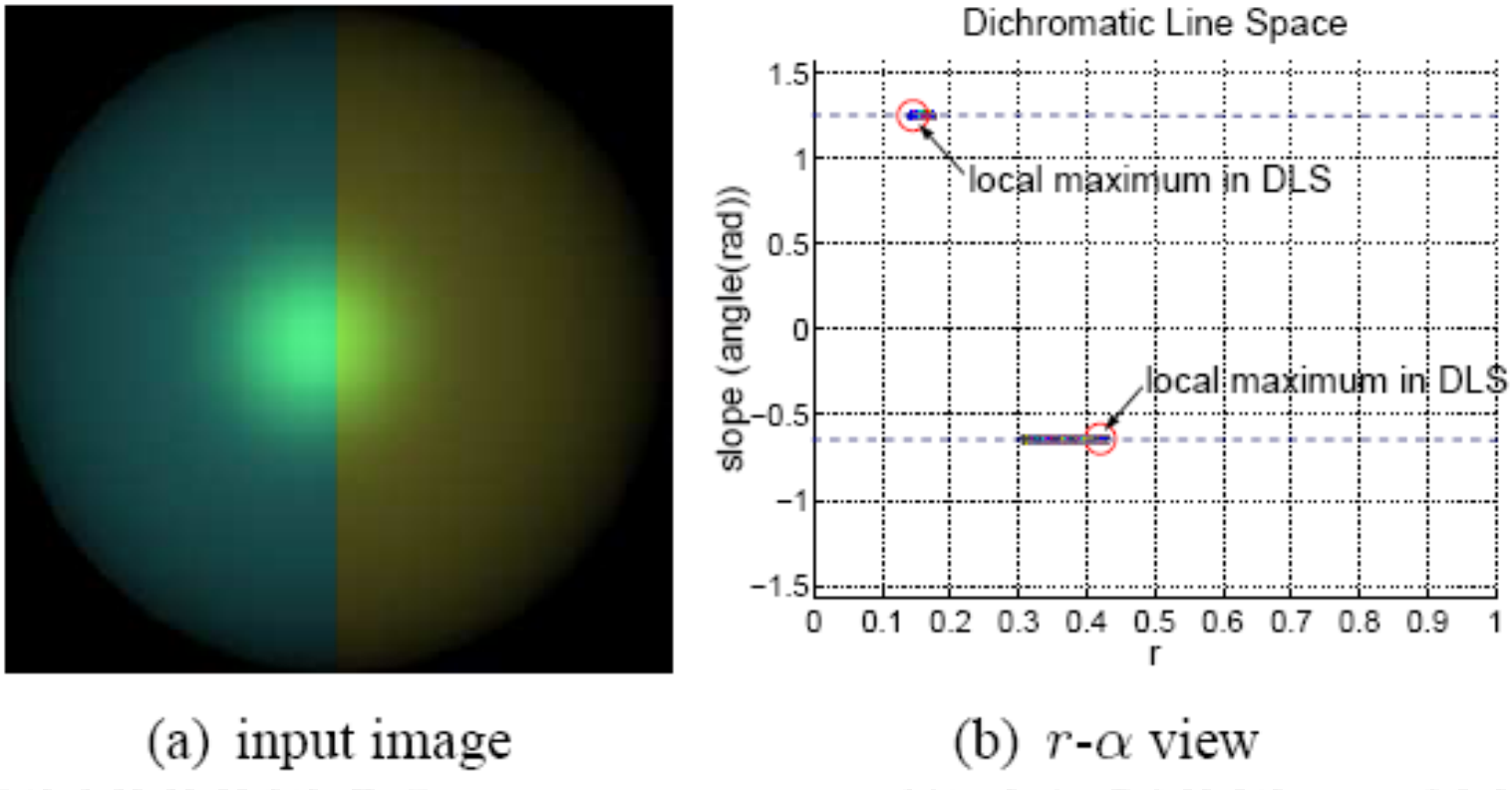

(a) input image (b) r-α view

Figure: Dichromatic Line Space for a synthetic surface

Illuminant Chromaticity Estimation

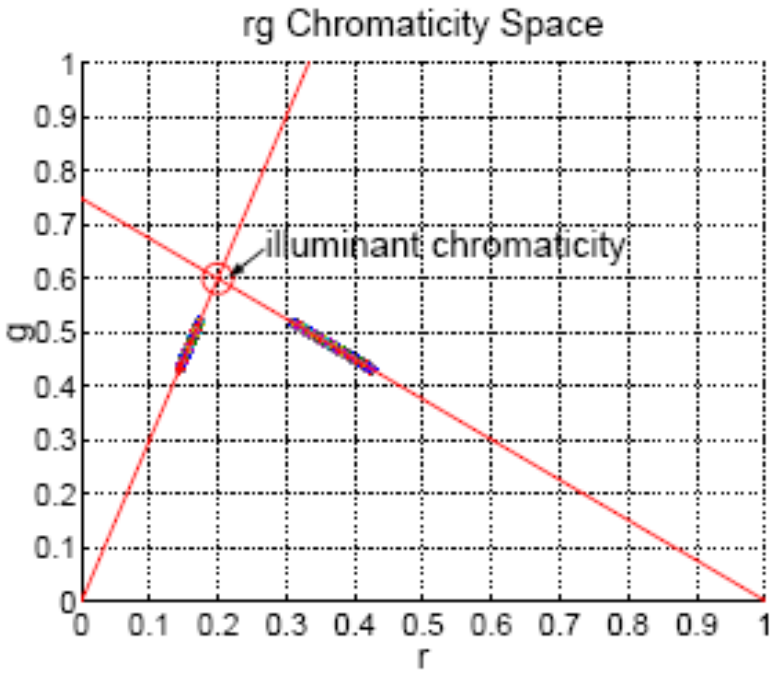

(c) dichromatic lines

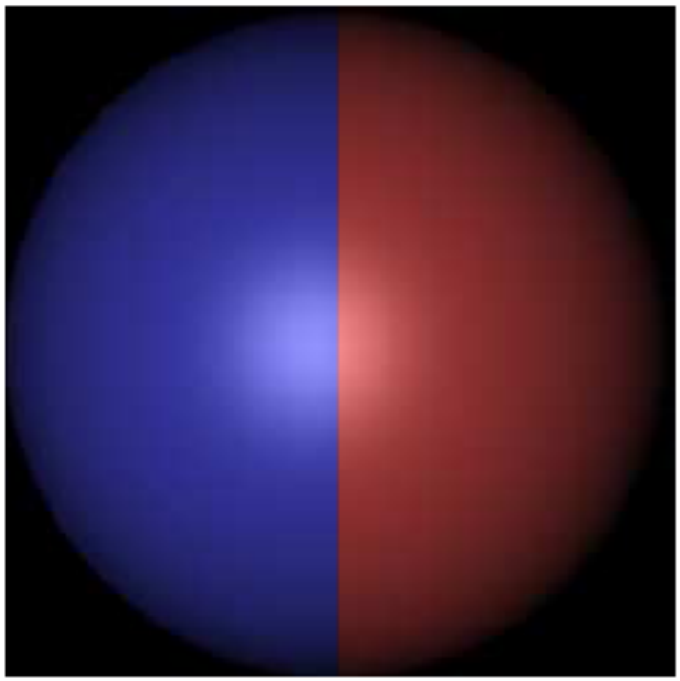

(d) normalized image

Figure: Dichromatic Line Space for a synthetic surface

Illuminant Chromaticity Estimation

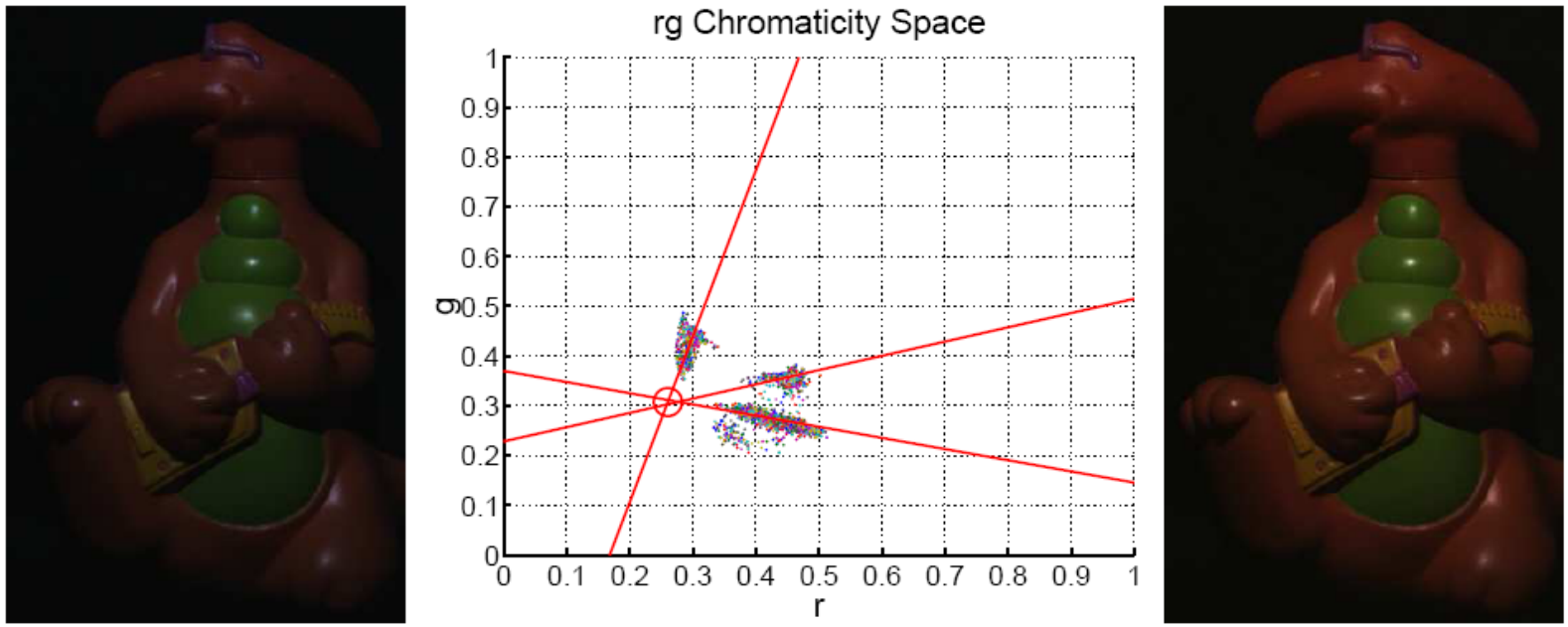

(a) input image (b) dichromatic lines (c) normalized

Figure: Dichromatic Line Space for a natural surface

Outline

1. Reflectance
2. DRM
   - Chromaticity
3. Illumination Chromaticity
   - Dichromatic-based color constancy using dichromatic slope and dichromatic line space
   - Color constancy thought Inverse-Intensity chromaticity space
   - On determining the color Illuminant using the dichromatic reflection model
4. Components Separation
   - Robby-Ikeuchi Method
   - Kuk-jin Method

Image Chromaticity and Intensity

By substituting each color channel's intensity in equation (3) with its definition (6) the chromaticity can written in terms of dichromatic reflection model:

Chromaticity expressed in DRM

$$\sigma(x) = \frac{m_d(x)\Lambda_c(x) + m_s(x)\Gamma_c}{m_d(x)\Sigma\Lambda_i(x) + m_s(x)\Gamma_i} \tag{15}$$

By deriving the last equation, we can obtain the relation between specular and diffuse coefficients

$$m_s = \frac{m_d(\Lambda_c - \sigma)}{\sigma - \Gamma_c} \tag{16}$$

Image Chromaticity and Intensity

Then substituting (16) in (6) we can obtain:

Illumination expressed in DRM

$$I_c = m_d \left(\Lambda_c - \Gamma_c\right) \left(\frac{\sigma}{\sigma - \Gamma_c}\right) \tag{17}$$

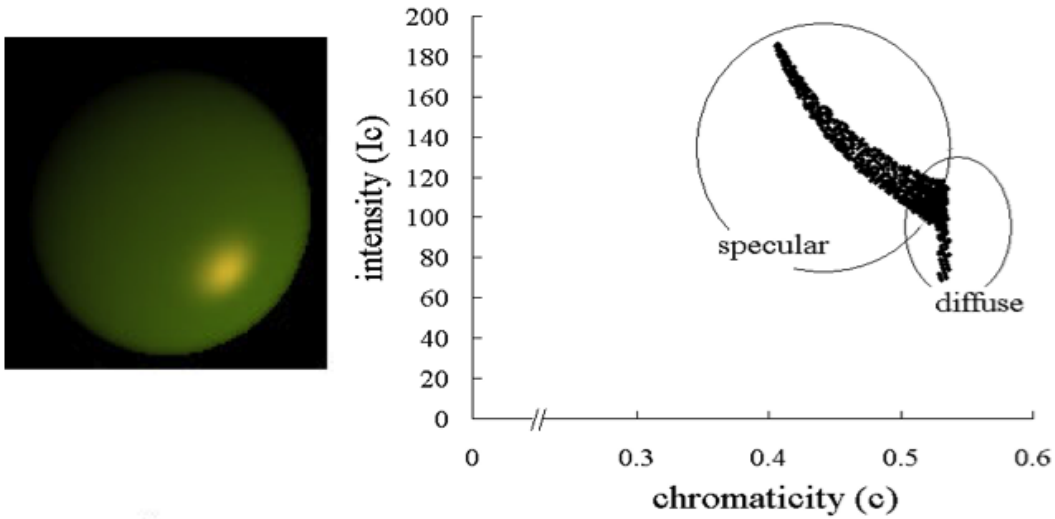

Figure: Chromaticity-Intensity Space

Image Chromaticity and Illumination Chromaticity

By introducing $p = m_d(\Lambda_c - \Gamma_c)$ we can derive the next equation:

The core of method

$$\sigma = p\frac{1}{\Sigma I_i} + \Gamma_c \tag{18}$$

The specular pixels can be grouped in into a number of clusters with the same value m_d. In this group, we can consider p as a constant. Equation (18) become a linear function, with p as a its constant gradient.

Image Chromaticity and Illumination Chromaticity

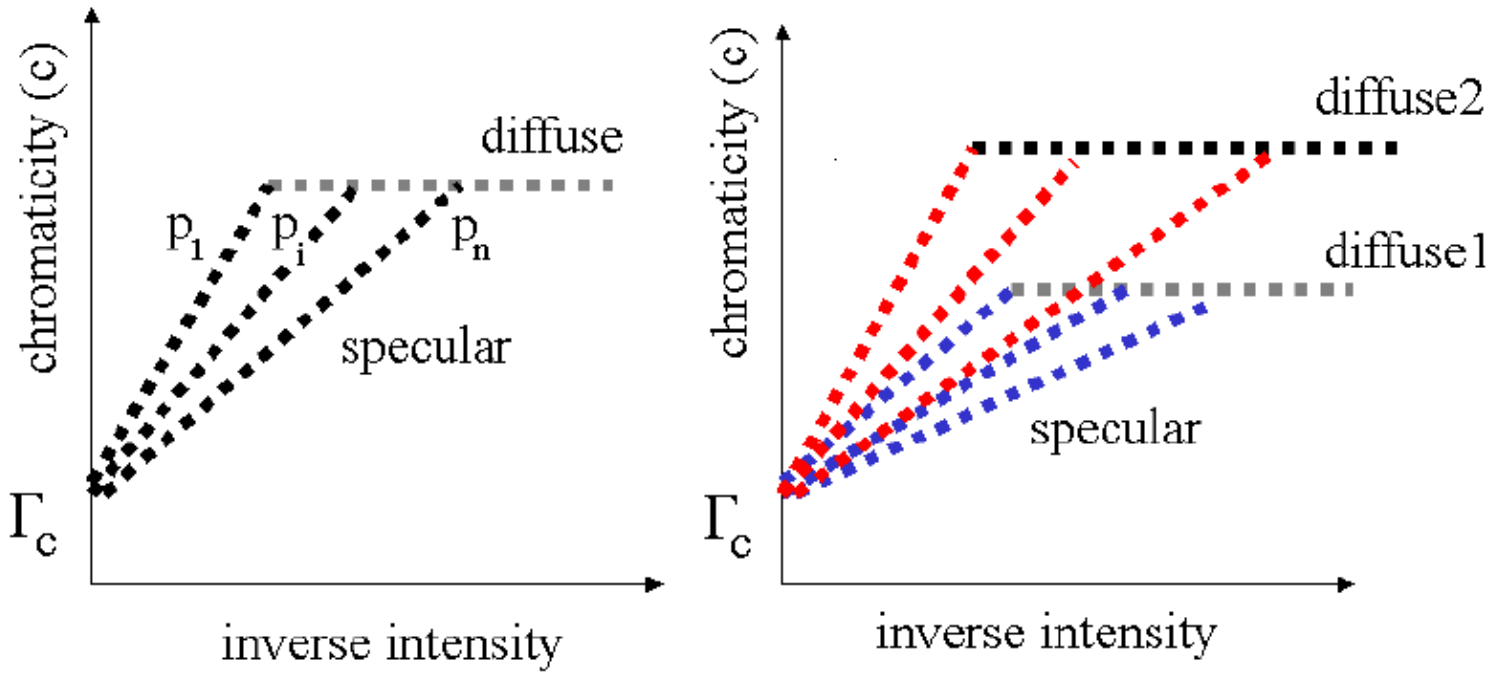

Figure: Sketch of specular points of a single surface in inverse-intensity chromaticity space

Image Chromaticity and Illumination Chromaticity

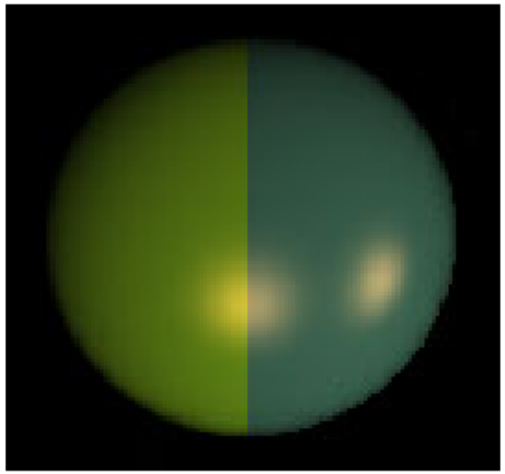

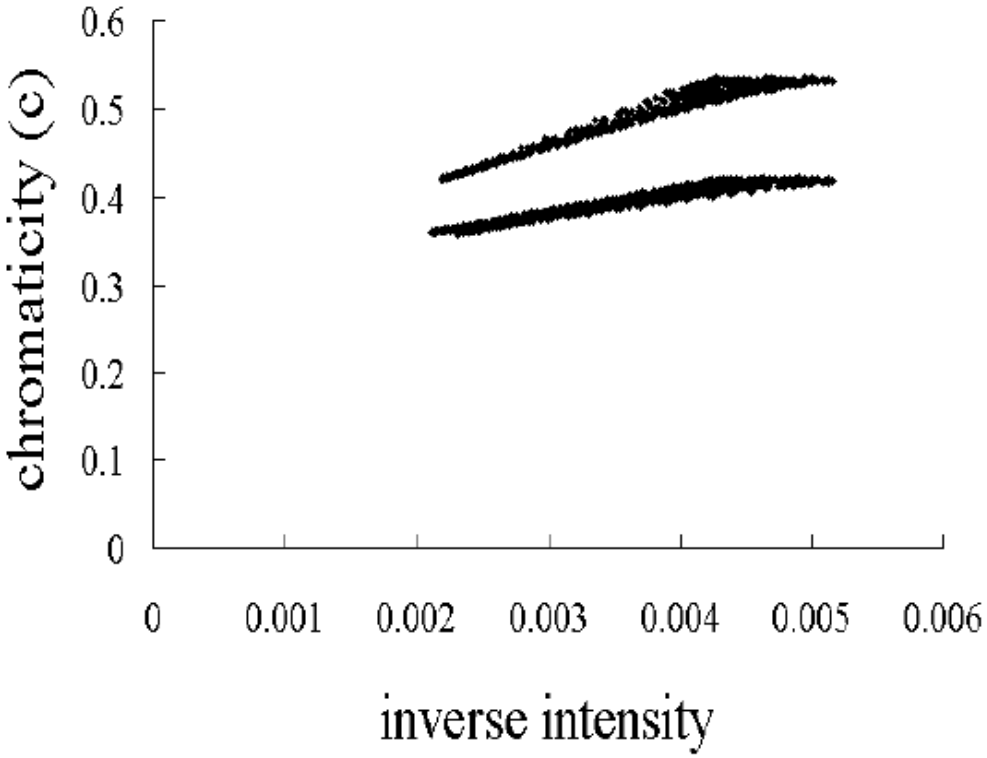

a. b.

Figure: Synthetic image with multiple surface colors

Estimating Illumination Chromaticity

- Hough transform.
- x-axis represent Γ_c and y-axis represent p
- All intersections will be concentrated in in a single value Γ_c, with a small range of p's values.

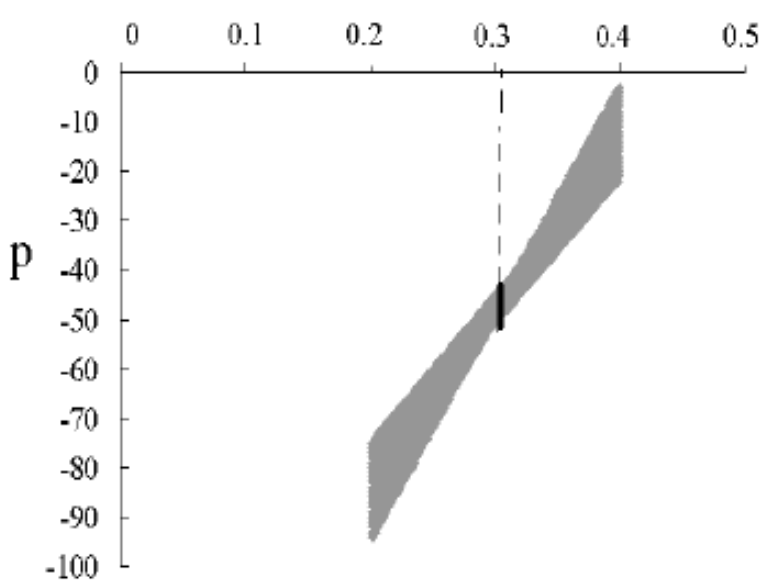

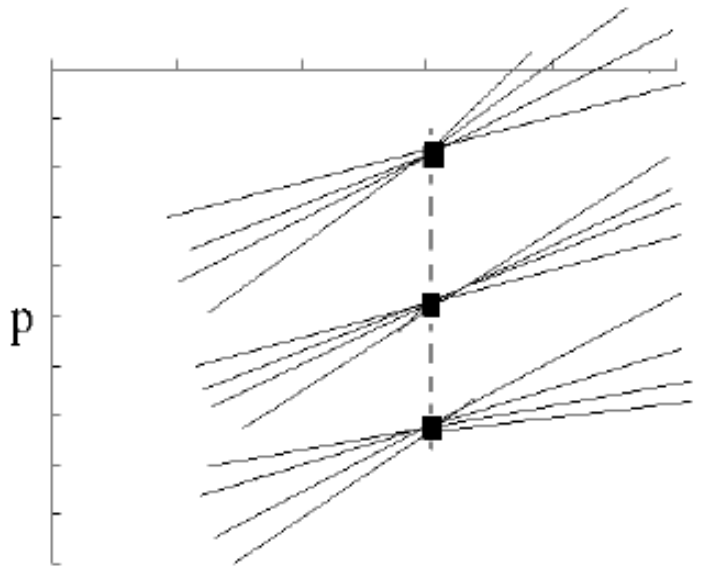

Estimating Illumination Chromaticity

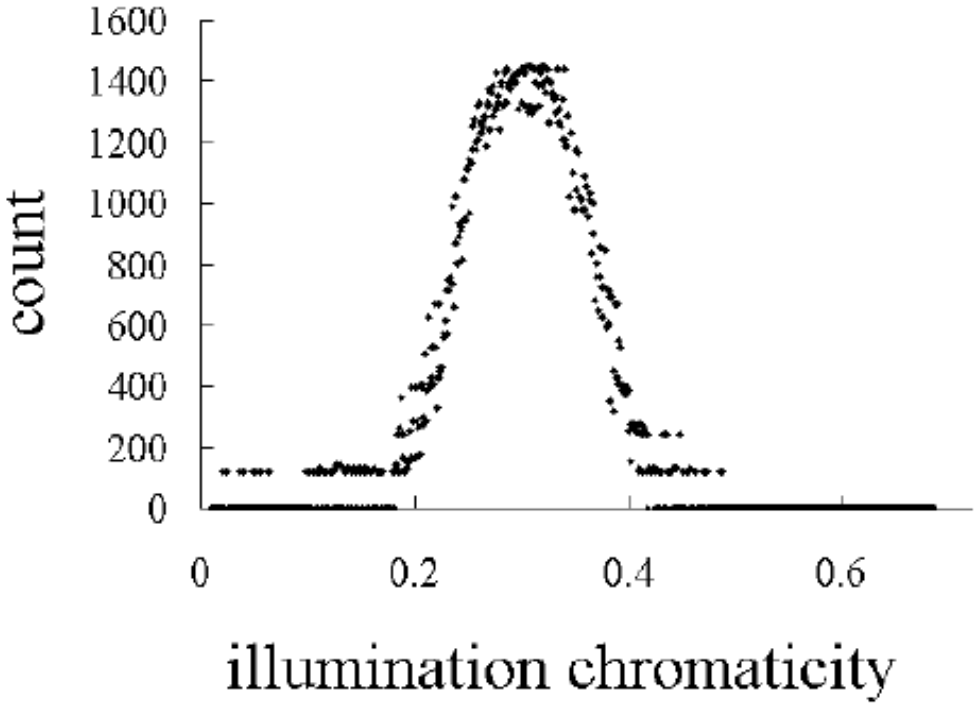

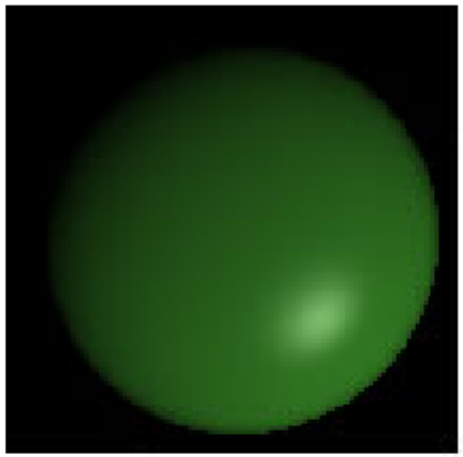

b.

Figure: Intersection counting distribution in the green chromaticity channel of chromaticity

Outline

1. Reflectance
2. DRM
   - Chromaticity
3. Illumination Chromaticity
   - Dichromatic-based color constancy using dichromatic slope and dichromatic line space
   - Color constancy thought Inverse-Intensity chromaticity space
   - On determining the color Illuminant using the dichromatic reflection model
4. Components Separation
   - Robby-Ikeuchi Method
   - Kuk-jin Method

DRM

Image in DRM

$$I = \int_{-\infty}^{+\infty} [s_M R_M(\lambda) E(\lambda) + s_S R_S(\lambda) E(\lambda)] S(\lambda) d\lambda \qquad (19)$$

- $R_M(\lambda)$ is the object reflectance with regard to the matte reflection
- $R_S(\lambda)$ is the object reflectance with regard to the specular reflection
- s_M and s_s are scaling factors depending of the geometry
- $E_i(\lambda)$ is the irradiance falling onto the object
- $S(\lambda)$ is the vector with the response functions of the sensor

DRM

Image in DRM

$$I_i = s_M R_{M,i} E_i + s_S R_{S,i} E_i \tag{20}$$

Assuming that the specular reflection behaves like a perfect mirror $R_{S,i} = 1$

$$I_i = s_M R_{M,i} E_i + s_S E_i \tag{21}$$

- $C_M = [R_{M,r}E_r, R_{M,g}E_g, R_{M,b}E_b]$ be set the measured matte color and
- $C_s = [E_r, E_g, E_b]$ be the color of illuminant
- The two vector, C_M and C_s , define a plane inside RGB space

DRM

- The points are projected in the *r+g+b=1* plane
- The two points which define the line are the chromaticities of the measured object color $[r_O, g_O]^T$ and the chromaticities of the color illuminant $[r_E, g_E]^T$.

Dichromatic line

$$\begin{pmatrix} r \\ g \end{pmatrix} = s \begin{pmatrix} r_O \\ g_O \end{pmatrix} + (1-s) \begin{pmatrix} r_E \\ g_E \end{pmatrix} \quad (22)$$

For some scaling factor *s*. The data points which belong to a uniformly colored surface will all be distributed along this line.

Estimating the Illuminant's color

- The noise is removed by pre-filtering the image using a Gaussian or median filter.
- Achromatic regions are removed.
- The dichromatic line $\mathscr{L}_j$ of region j is given by $\mathscr{L}_j = \{a_j + se_j | with s \in \mathbb{R}\}$
  - a_j is the average chromaticity
  - e_i is the normalized eigenvector which corresponds to the largest eigenvalue for the region j.

Estimating color in the CIELab Space

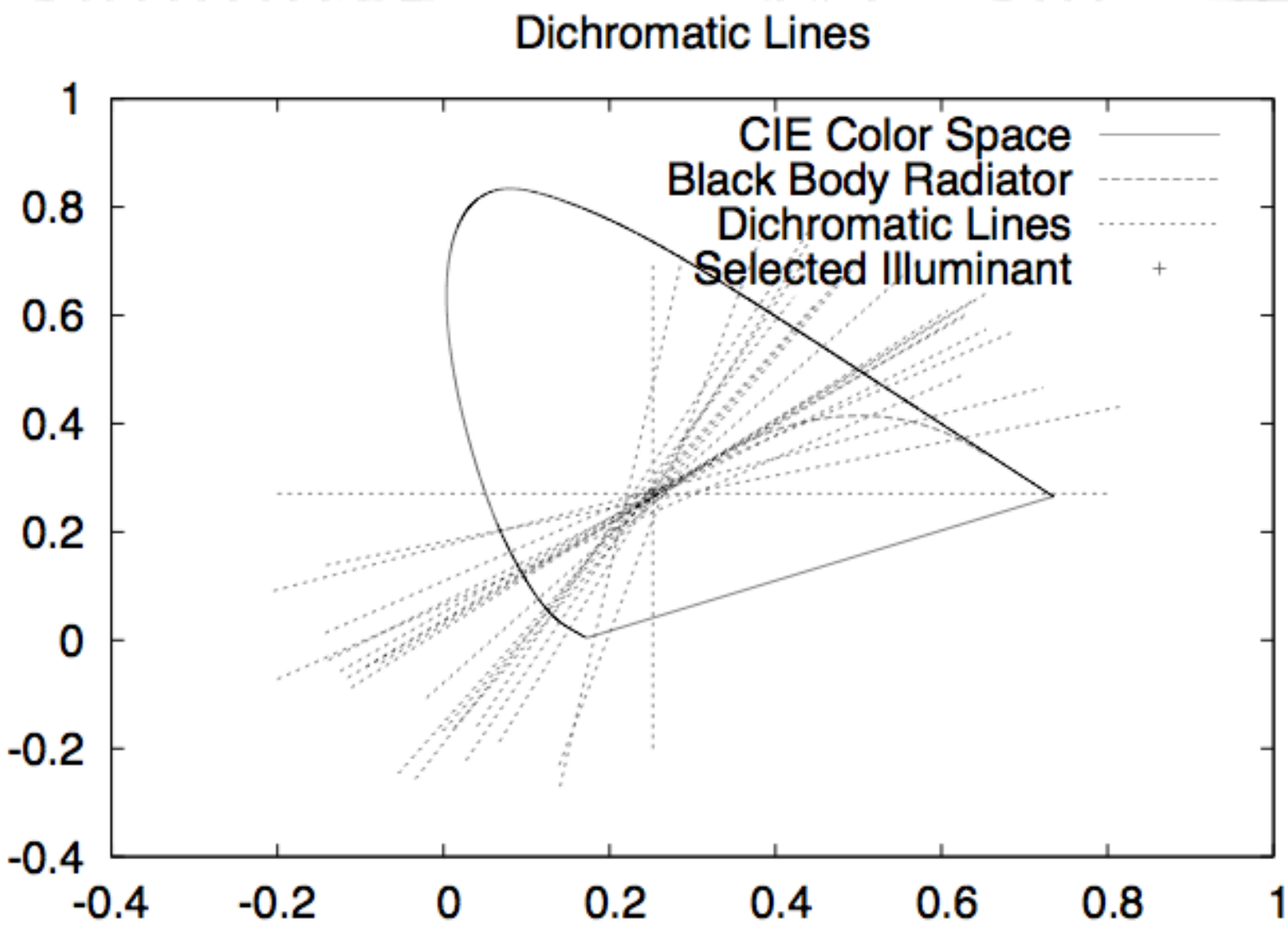

There are a number of methods for separate specular and diffuse components

1. Separating reflection components of textured surfaces using a single image [7, 6]
2. Fast separation of reflection components using a specularity-invariant image representation [9]
3. Dichromatic Reflection separation from a single image [10]
4. Separation of Highlight Reflections on textured surfaces [3]

Outline

1. Reflectance
2. DRM
   - Chromaticity
3. Illumination Chromaticity
   - Dichromatic-based color constancy using dichromatic slope and dichromatic line space
   - Color constancy thought Inverse-Intensity chromaticity space
   - On determining the color Illuminant using the dichromatic reflection model
4. Components Separation
   - Robby-Ikeuchi Method
   - Kuk-jin Method

Normalization

- The specular component must be pure white ($\Gamma_r = \Gamma_g = \Gamma_b$)
- This process requires the value of Γ^{est}, which can be obtained by some previously shown methods

Normalized Image

$$I'(x) = m'_d(x)\Lambda'(x) + \frac{m'_s(x)}{3} \tag{23}$$

Renormalization

$$m_d(x)\Lambda(x) = [m'_d(x)\Lambda'(x)]\Gamma^{est} \tag{24}$$

$$m_s(x)\Gamma = \left[\frac{m'_s(x)}{3}\right]\Gamma^{est} \tag{25}$$

Specular-to-diffuse Mechanism

Maximum chromaticity

$$\tilde{\sigma}' = \frac{max\left(I'_r(x), I'_g(x), I'_b(x)\right)}{I'_r(x) + I'_g(x) + I'_b(x)} \tag{26}$$

$$\tilde{\sigma}'_{diff} > \tilde{\sigma}'_{spec} \tag{27}$$

$$\tilde{\Lambda}' > \frac{1}{3} \tag{28}$$

Specular-to-diffuse Mechanism

Curved line

$$\tilde{I}'(x) = m_d'(x)\frac{\left(\tilde{\Lambda}'(x) - \frac{1}{3}\right)\tilde{\sigma}'(x)}{\tilde{\sigma}'(x) - \frac{1}{3}} \quad (29)$$

Diffuse weighting factor

$$m_d'(x_1) = \frac{\tilde{I}'(x_1)\left[3\tilde{\sigma}'(x_1) - 1\right]}{\tilde{\sigma}'(x_1)\left[3\tilde{\Lambda}'(x_1) - 1\right]} \quad (30)$$

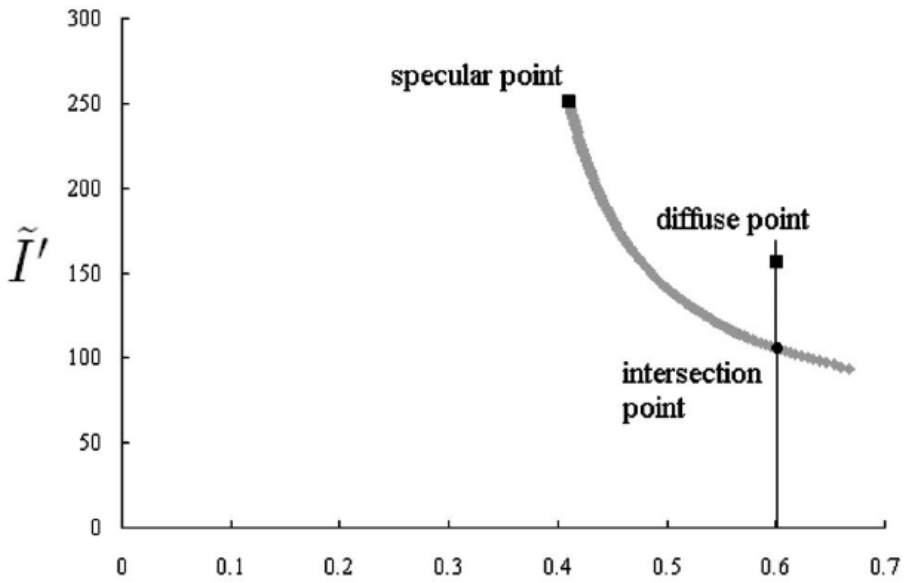

Specular Free Image

- We need a geometrically identical image without specular component.
- To generate a Specular Free Image, we simply set the diffuse maximum chromaticity equal to an arbitrary scalar value $\frac{1}{3} < \tilde{\Lambda}' \leq 1$.

We formally describe a Specular Free Image as:

$$\overset{\circ}{I}(x) = \overset{\circ}{m}_d(x)\overset{\circ}{\Lambda}(x) \tag{31}$$

Specular Free Image

$$\overset{\circ}{m}_d(x) = m'_d(x)\frac{3\tilde{\Lambda}'(x)-1}{3\tilde{\Lambda}^{new}(x)-1} \tag{32}$$

$$\overset{\circ}{I}(x) = m'_d(x)k(x)\overset{\circ}{\Lambda}(x) \tag{33}$$

where $k(x) = \frac{3\tilde{\Lambda}'(x)-1}{3\tilde{\Lambda}^{new}(x)-1}$

Separation Method

$$log(I'(x)) = log(m'_d(x_1) + log(\Lambda')$$

$$log(\mathring{I}(x_1)) = log(m'_d(x_1) + ... \\ ... + log(k) + log(\mathring{\Lambda})$$

$$\frac{\partial}{\partial x} log(I'(x)) = \frac{\partial}{\partial x} log(m'_d(x_1))$$

$$\frac{\partial}{\partial x} log(\mathring{I}(x)) = \frac{\partial}{\partial x} log(m'_d(x_1))$$

Separation Method

The method is based in the difference of the differential logarithmic

$$\triangle(x) = dlog(I'(x)) - dlog(\overset{\circ}{I}(x)) \tag{34}$$

if $\triangle(x)$= 0, then is a diffuse pixel, otherwise is a specular or discontinuity pixel .

Color discontinuity

$$(\triangle r > thR \ \ and \ \ \triangle g > thG) \begin{cases} true: & Color\, discontinuity \\ false: & Otherwise \end{cases} \tag{35}$$

Specularity reduction

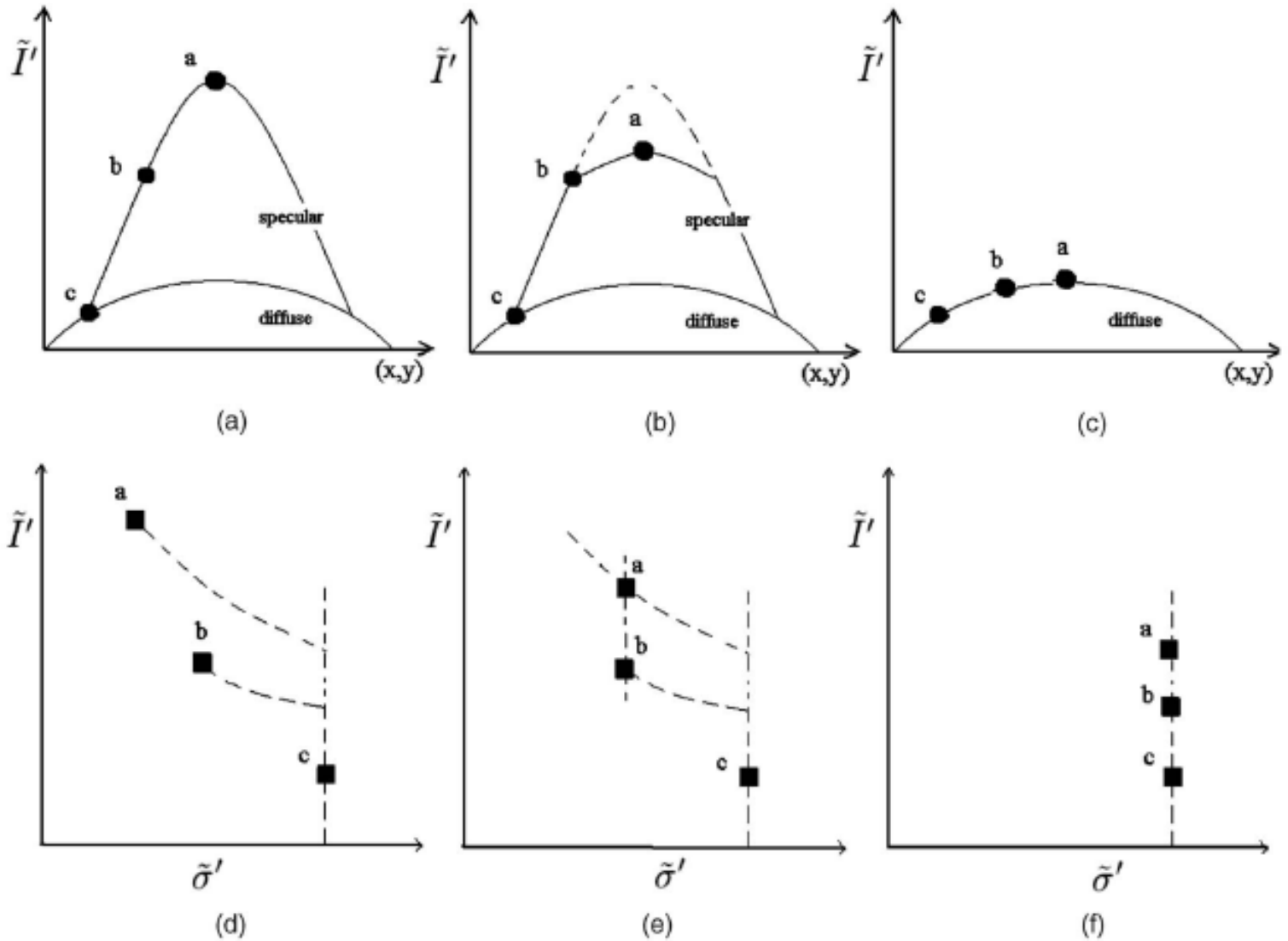

Outline

1. Reflectance
2. DRM
   - Chromaticity
3. Illumination Chromaticity
   - Dichromatic-based color constancy using dichromatic slope and dichromatic line space
   - Color constancy thought Inverse-Intensity chromaticity space
   - On determining the color Illuminant using the dichromatic reflection model
4. Components Separation
   - Robby-Ikeuchi Method
   - Kuk-jin Method

Specularity-Invariant color image representation

When $I_g(x_1) \geq I_r(x_1)$ and $I_g(x_2) \geq I_r(x_2)$

- $\hat{I}(x_1) = I_g(x_1) - I_r(x_1)$
- $\hat{I}(x_2) = I_g(x_2) - I_r(x_2)$

$\hat{I}$ *is independent* of the specular reflection component and depends only of the diffuse reflection component.

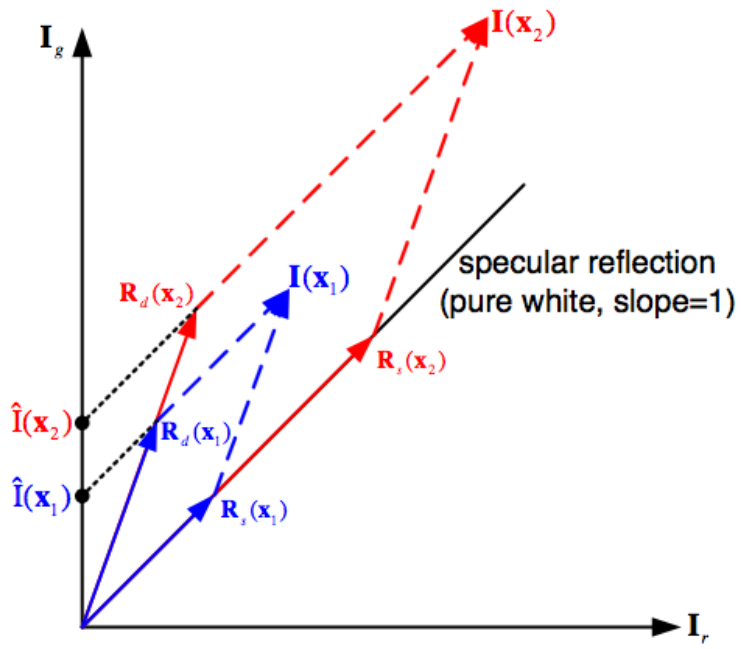

Figure: Specularity-invariant value and radio

Specular-Free Two-Band Image Generation

$$\tilde{I}(x) = min\{I_r(x), I_g(x), I_b(x)\}$$

$$\tilde{\Lambda}(x) = min\{\Lambda_r(x), \Lambda_g(x), \Lambda_b(x)\}$$

$$\tilde{I}(x) = m_d(x)\tilde{\Lambda}(x) + \frac{m_s}{3} \quad (36)$$

Specular-free two-band

$$\hat{I}(x) = I(x) - \tilde{I}(x) = m_d(x)\left[\Lambda(x) - \tilde{\Lambda}(x)\right] \quad (37)$$

Local Ratios

Diffuse Ratio

$$r_d = \frac{\sum_{c\in\{r,g,b\}} \hat{I}_c(x_1)}{\sum_{c\in\{r,g,b\}} \hat{I}_c(x_2)} = \frac{m_d(x_1)}{m_d(x_2)} \tag{38}$$

Diffuse and Specular Ratio

$$r_{d+s} = \frac{\sum_{c\in\{r,g,b\}} I_c(x_1)}{\sum_{c\in\{r,g,b\}} I_c(x_2)} = \frac{m_d(x_1)+m_s(x_1)}{m_d(x_2)+m_s(x_1)} \tag{39}$$

- If x_1 and x_2 are specular pixels, then r_d and r_{d+s} are the same because $m_s(x_1)$ and $m_s(x_2)$ are equal to zero.
- We can generate a diffuse image making $r_{d+s} = r_d$.

Iterative Framework

Iteration when $r_{d+s} > r_d$

$$I^{t+1}(x_1) = I^t(x_1) - \frac{m}{3} \tag{40}$$

$$m = \sum_{c\in\{r,g,b\}} I_c^t(x_1) - r_d \sum_{c\in\{r,g,b\}} I_c^t(x_2)$$

Iteration when $r_{d+s} < r_d$

$$I^{t+1}(x_2) = I^t(x_2) - \frac{m}{3} \tag{41}$$

$$m = \sum_{c\in\{r,g,b\}} I_c^t(x_2) - \frac{\sum_{c\in\{r,g,b\}} I_c^t(x_1)}{r_d}$$

References I

- Thomas M. Lehmann and Christoph Palm.
  color line search for illuminant estimation in real-word scenes.
  Journal of the Optical Society of America A, 18:2679–2691, 2001.
- christian Herrmmannn Marc Ebner.
  On determining the color of the illuminant using the dichromatic reflection model.
  In Springer Berlin / Heidelberg, editor, *Pattern Recognition*, volume 3663/2005, pages 1–8, 2005.
- S. Ping Tan; Long Quan; Lin.
  Separation of highlight reflections on textured surfaces.
  Computer Vision and Pattern Recognition, 2:1855 – 1860, 2006.

References II

Steven A. Shafer.
Using color to separate reflection components.
color research and aplications, 10:43–51, april 1984.

Robby T Tan, Ko Nishino, and Katsushi Ikeuchi.
Color constancy through inverse-intensity chromaticity space.
J Opt Soc Am A Opt Image Sci Vis, 21(3):321–334, Mar 2004.

Robby T Tan, Ko Nishino, and Katsushi Ikeuchi.
Separating reflection components based on chromaticity and noise analysis.
IEEE Trans Pattern Anal Mach Intell, 26(10):1373–1379, Oct 2004.

References III

R.T. Tan and K. Ikeuchi.
Separating reflection components of textured surfaces using a single image.
In *Computer Vision, 2003. Proceedings. Ninth IEEE International Conference on*, pages 870–877vol.2, 13-16 Oct. 2003.

Kuk-Jin Yoon, Yoo Jin Chofi, and In-So Kweon.
Dichromatic-based color constancy using dichromatic slope and dichromatic line space.
In *Image Processing, 2005. ICIP 2005. IEEE International Conference on*, volume 3, pages III–960–3, 11-14 Sept. 2005.

References IV

- Kuk-Jin Yoon, Yoojin Choi, and In So Kweon.
  Fast separation of reflection components using a specularity-invariant image representation.
  In *Image Processing, 2006 IEEE International Conference on*, pages 973–976, 8-11 Oct. 2006.
- Shen Cherng3 Yun-Chung Chung1, Shyang-Lih Chang2 and Sei-Wang Chen1.
  Dichromatic Reflection Separation from a Single Image, pages 225–241.
  Springer, 2007.

State of the art of virtual reality applications in neuropsychology

Definitions

- Neuropsychology: interdisciplinary branch of psychology and neuroscience that aims to understand how the structure and function of the brain relate to specific psychological processes and explicit behaviors. (Wikipedia)
- Psychology: applied discipline involving the scientific study of mental processes and behavior. (Wikipedia)
- Neuroscience is a field that is devoted to the scientific study of the nervous system. (Wikipedia)
- Virtual reality: is a technology, which allows a user to interact with and immerse in a computer-simulated environment, be it a real or imagined one. (Wikipedia)

Applications of Neuropsychology

- Assessment of Brain Functions by observing behaviors
- Rehabilitation of Brain Functions by modifying behavior

Brain functions

- arousal (awakening)
- **attention**
- consciousness
- decision making
- **executive functions**
- language
- **learning**
- **memory**
- motor coordination
- sensory perception
- **planning**
- **problem solving**
- thought

Definitions of brain functions

- **Attention** is the cognitive process of selectively concentrating on one aspect of the environment while ignoring other things. (Wikipedia)
- **Executive functions** is a collection of brain processes whose role is to guide thought and behavior in accordance with internally generated goals or plans. (Wikipedia)
- **Learning** is the acquisition and development of memories and behaviors, including skills, knowledge, understanding, values, and wisdom. (Wikipedia)

Definitions of brain functions

- **Memory** is an organism's ability to store, retain, and subsequently retrieve information. (Wikipedia)
- **Planning** is both the organizational process of creating and maintaining a plan; and the psychological process of thinking about the activities required to create a desired future on some scale. (Wikipedia)
- **Problem Solving** is a higher-order cognitive process that requires the modulation and control of more routine or fundamental skills (Goldstein & Levin, 1987). It occurs if an organism or an artificial intelligence system does not know how to proceed from a given state to a desired goal state. It is part of the larger problem process that includes problem finding and problem shaping. (Wikipedia)

in short

Neuropsychology	**Brain Functions**
Assessment	Observing behaviors
Rehabilitation	Modifying behaviors

Why Virtual Reality in Neuropsychology?

Well-known Virtual Reality Applications

- Entertainment: Videogames, IMAX
- Training: Manufacturing, Surgical training, NASA Hubble repair
- Education: Virtual Science, Process simulation, …

Virtual Reality Key Elements

Visualization Technologies

Interaction Technologies

Immersion

Virtual Reality Visualization Technologies

Z800 3DVisor by eMagin

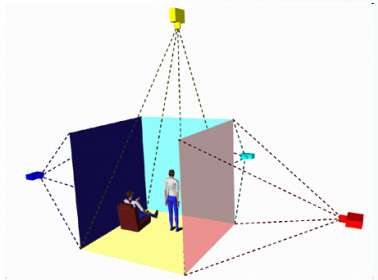

CAVE University of Illinois at Chicago

VisionStation by Elumens

SGI France

Examples of Interaction Technologies

VirtuSphere by VirtuSphere

Wiimote and WiiFit by Nintendo

GestureTek gesture-control using Computer Vision

Brain Computer Interaction - Emotiv EPOC™

Virtual reality and behavioral studies

1. VR provides a life-like, three-dimensional highly interactive environment in which a person becomes involved in rather than an observer of the scenario
2. VR offers safety from potential dangers that could arise in an actual situation
3. VR can increase motivation because of its gaming, interactive, and immersive qualities
4. VR features are easily modified and allow for multiple application

Virtual reality and behavioral studies

Within the controllable, dynamic and interactive 3D stimulus environments generated by the Virtual Reality, behavioral action can be recorded and measured

Virtual Reality Key Elements

Visualization Technologies

Interaction Technologies

↓

Immersion

↓

record and measure behavioral data

VR in Neuroscience

- “Virtual reality has finally come of age for serious applications in the behavioral neurosciences…
- …VR is attractive for both research and real-world applications in neuroscience, cognitive science and psychology…”

Tarr, MJ & Warren, WH (2002). Virtual Reality in behavioral neuroscience and beyond. Nature Neuroscience, S-5, 326-332

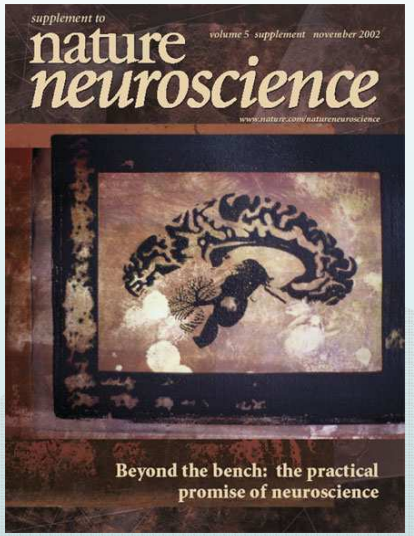

“*Analysis of Assets for Virtual Reality Applications in Neuropsychology*”

Albert A. Rizzo, Maria Schultheis, Kimberly A. Kerns, and Catherine Mateer

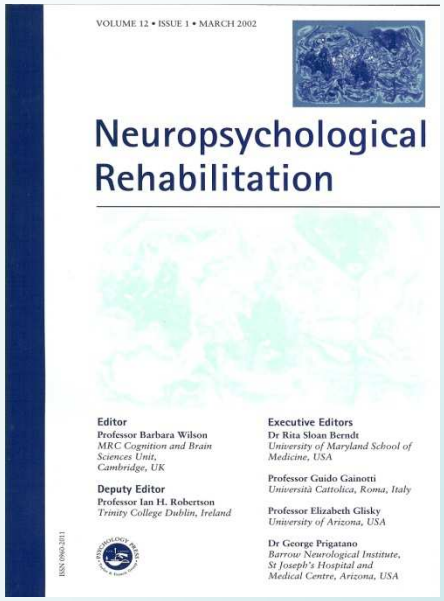

Neuropsychological Rehabilitation Vol. 14(1), 207-239 (2004)

Ecological validity of a test

- Ecological validity is the degree of relevance or similarity that a test or training system has relative to the “real” world (Neisser, 1978)
- Is the functional and predictive relation between the patient execution in the neuropsychological exploration and his/her behavior in a real life situation. Sbordone (1928)
- The ecological validity of a test is determined by the degree of generalization of its results (Burgess *et al*., 2006)

Methodological considerations

- Correlation “r”: indicates the strength and direction of a linear relationship between two random variables
- Statistical significance “p”: a result is called statistically significant if it is unlikely to have occurred by chance
- The “f” Test prove the hypothesis that the means of multiple normally distributed populations are equal

Index of papers

1. A Simulated Reality Scenario Compared with the Computerized Wisconsin Card Sorting Test: An Analysis of Preliminary Results (Elkins et al., 2001)
2. Probing memory and executive functions with virtual reality: past and present studies (Pugnetti et al. 1926)
3. A Virtual Environment for Investigating Schizophrenic Patients' Characteristics: Assessment of Cognitive and Navigation Ability (Peled et al., 2005)
4. The Virtual Classroom: A Virtual Reality Environment for the Assessment and Rehabilitation of Attention Deficits (Rizzo et al., 2000)
5. A controlled clinical comparison of attention performance in children with ADHD in a virtual reality classroom compared to standard neuropsychological methods (Thomas D. Parsons et al., 2006)
6. Initial Validation of a Virtual Environment for Assessment of Memory Functioning: Virtual Reality Cognitive Performance Assessment Test (Thomas D. Parsons et al., 2008)

A Simulated Reality Scenario Compared with the Computerized Wisconsin Card Sorting Test: An Analysis of Preliminary Results

JAMES S. ELKIND, ERICA RUBIN, SAUL ROSENTHAL, BARRY SKOFF, PENNY PRATHER

CYBERPSYCHOLOGY & BEHAVIOR
Volume 4, Number 4, 2001

Neuropsychology	**Brain Functions Involved:** problem solving, executive functions
Assessment	X
Rehabilitation	

A Simulated Reality Scenario Compared with the Computerized Wisconsin Card Sorting Test: An Analysis of Preliminary Results

JAMES S. ELKIND, ERICA RUBIN, SAUL ROSENTHAL, BARRY SKOFF, PENNY PRATHER

CYBERPSYCHOLOGY & BEHAVIOR
Volume 4, Number 4, 2001

Wisconsin Card Sorting Test:

- Is a neuropsychological test of "set-shifting", i.e. the ability to display flexibility in the face of changing schedules of reinforcement
- The test is widely used by psychiatrists, neurologists and neuropsychologists in patients with acquired brain injury, neurodegenerative disease, or mental illness such as schizophrenia

A Simulated Reality Scenario Compared with the Computerized Wisconsin Card Sorting Test: An Analysis of Preliminary Results

JAMES S. ELKIND, ERICA RUBIN, SAUL ROSENTHAL, BARRY SKOFF, PENNY PRATHER

CYBERPSYCHOLOGY & BEHAVIOR

Computerized WCST

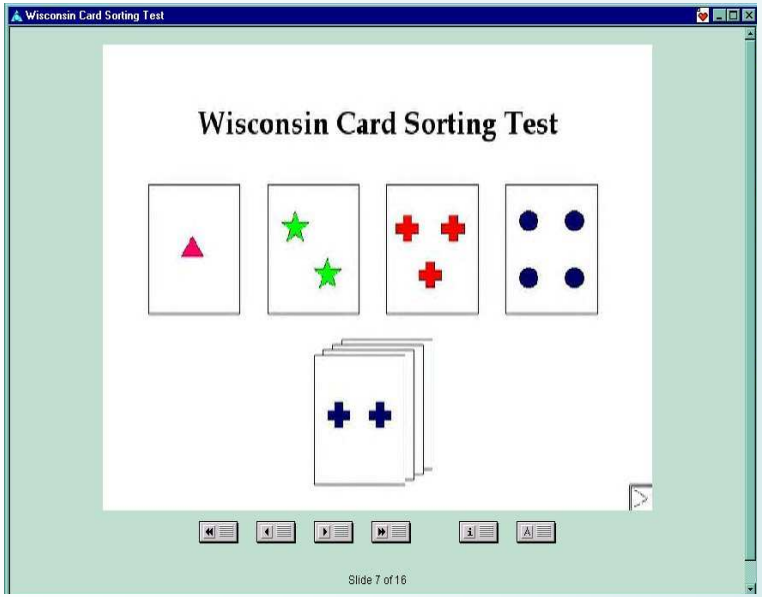

PAR Psychological Assessment Resources, Inc.

A Simulated Reality Scenario Compared with the Computerized Wisconsin Card Sorting Test: An Analysis of Preliminary Results

JAMES S. ELKIND, ERICA RUBIN, SAUL ROSENTHAL, BARRY SKOFF, PENNY PRATHER

CYBERPSYCHOLOGY & BEHAVIOR

Look For A Match (LFAM)

A Simulated Reality Scenario Compared with the Computerized Wisconsin Card Sorting Test: An Analysis of Preliminary Results

JAMES S. ELKIND, ERICA RUBIN, SAUL ROSENTHAL, BARRY SKOFF, PENNY PRATHER

CYBERPSYCHOLOGY & BEHAVIOR

- Data were available from 63 participants (data from one participant was unavailable due to technical problems).
- Ages ranged from 18 to 74, with a median age of 29 years. Most of the participants were women (71%) and Caucasian (72%).
- Fifty-six percent had completed a degree beyond high school

A Simulated Reality Scenario Compared with the Computerized Wisconsin Card Sorting Test: An Analysis of Preliminary Results

JAMES S. ELKIND, ERICA RUBIN, SAUL ROSENTHAL, BARRY SKOFF, PENNY PRATHER

CYBERPSYCHOLOGY & BEHAVIOR
Volume 4, Number 4, 2001

- This initial study compares several functions assessed by the Wisconsin Card Sorting Test (WCST) with our three-dimensional, stereographic scenario, Look for a Match (LFAM)
- Participants completed questionnaires, alternately began with either the WCST or LFAM, and then took the second test

Experimental Variables

- Perseverative errors: failures to change sorting strategy after negative feedback
- Conceptual responses: strategy to change contextual contingencies
- Trials to first category: number of trials to learn the first rule (Categories: color, shape, number)

Data results

TABLE 1. CORRELATIONS COMPARING LFAM AND WCST PERFORMANCE.

Total errors	*Perseverative errors*	*Nonperseverative errors*	*Conceptual responses*	*Trials to first category*	*Failure to maintain set*
0.50***	0.02	0.44***	0.48***	0.58***	0.33**

**$p < 0.01$.
***$p < 0.001$.
LFAM, Look for a Match; WCST, Wisconsin Card Sorting Test.

Data results

Subjective Data:

More enjoyable

More interesting

More difficult

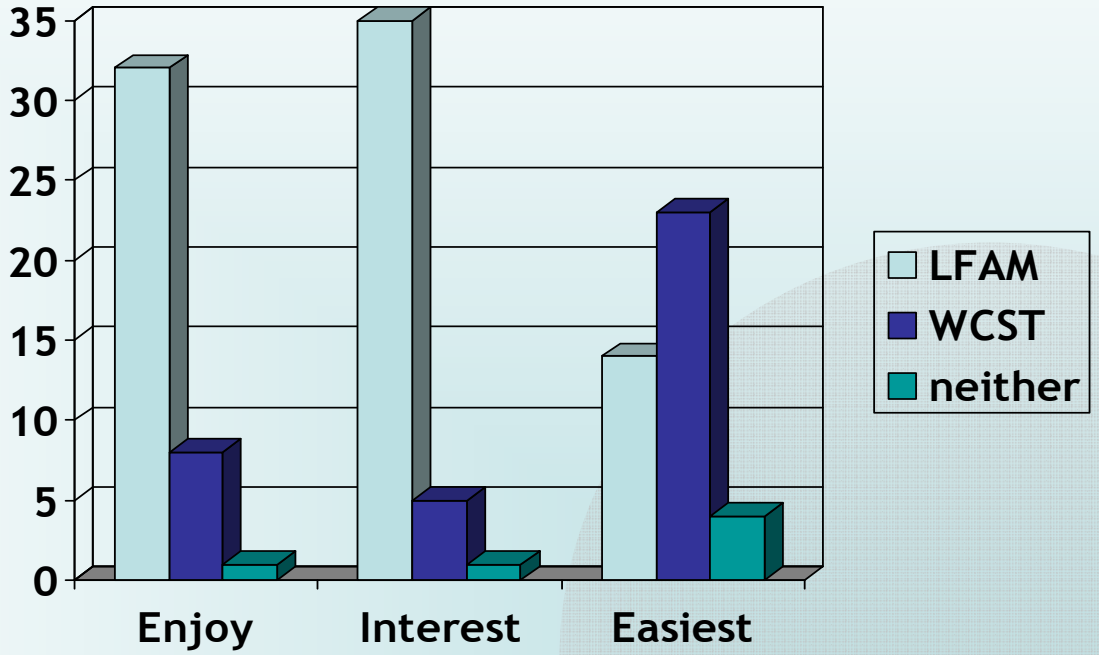

Discussion

- Overall performance without regard to order, suggested that the LFAM was a more difficult, yet enjoyable and engaging task than the WCST: is it a benefit to the assessment?
- The comparison with the computerized WCST doesn't prove the ecological validity with the real test

Index of papers

1. A Simulated Reality Scenario Compared with the Computerized Wisconsin Card Sorting Test: An Analysis of Preliminary Results (Elkins et al., 2001)
2. Probing memory and executive functions with virtual reality: past and present studies (Pugnetti et al. 1926)
3. A Virtual Environment for Investigating Schizophrenic Patients' Characteristics: Assessment of Cognitive and Navigation Ability (Peled et al., 2005)
4. The Virtual Classroom: A Virtual Reality Environment for the Assessment and Rehabilitation of Attention Deficits (Rizzo et al., 2000)
5. A controlled clinical comparison of attention performance in children with ADHD in a virtual reality classroom compared to standard neuropsychological methods (Thomas D. Parsons et al., 2006)
6. Initial Validation of a Virtual Environment for Assessment of Memory Functioning: Virtual Reality Cognitive Performance Assessment Test (Thomas D. Parsons et al., 2008)

Probing memory and executive functions with virtual reality: past and present studies

CyberPsychology & Behavior 1:151–162 Pugnetti, L., Mendozzi, L., Attree, E., et al. (1928) **Volume 4, Number 4, 2001**

Neuropsychology	**Brain Functions Involved:** problem solving, memory, executive functions
Assessment	X
Rehabilitation	

Probing memory and executive functions with virtual reality: past and present studies

CyberPsychology & Behavior 1:151–162 Pugnetti, L., Mendozzi, L., Attree, E., et al. (1928)

- The task was to reach the exit of a virtual building. The virtual environment comprised 32 rooms of variable shapes, each with a number of rooms that lead to dead-end corridors, the next room, or, in the case of the final room only, the exit
- The strategy was to match either the shape or the color of the door which lead to the next room, and the criterion was changed every seven consecutive correct selections
- They compared the performance of patients with neurological impairments and non-impaired control participants on the WCST and their VR-based version

Probing memory and executive functions with virtual reality: past and present studies

CyberPsychology & Behavior 1:151–162 Pugnetti, L., Mendozzi, L., Attree, E., et al. (1928)

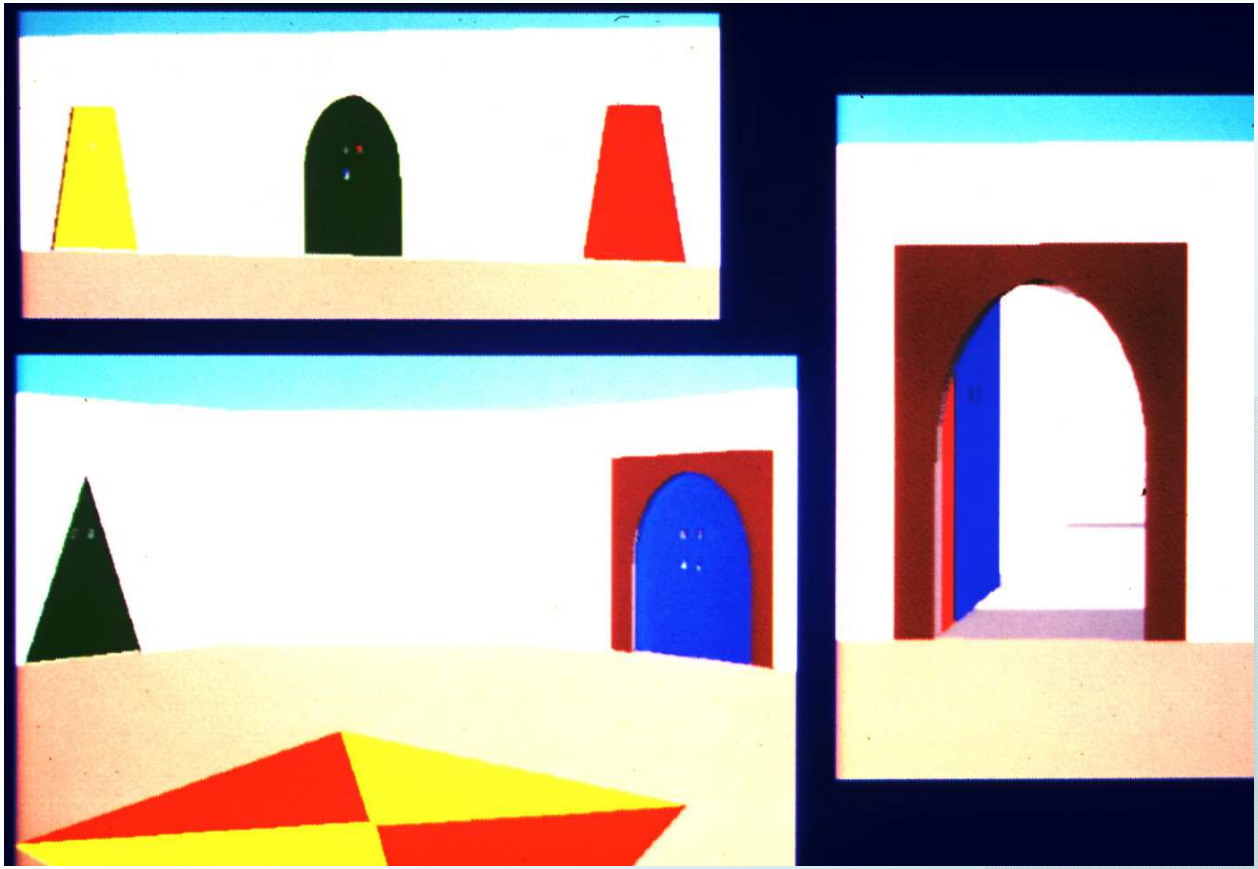

Results

- Controls performed better than patients in both tests
- There was a modest correlation between the two tests
- In the WCST, there was an almost linear increase in the number of errors up to the fourth or fifth set, whereas in the VR test, errors decreased sharply from the first to the second and third categories
- A clearly significant difference between patients and controls only emerged after the fourth category in the WCST, whereas this difference was apparent in the first category in the VR test

Discussion

- The differences between patients and controls was apparent in the first category in the VR test: the more complex (and complete) cognitive demands of the VE setting at the beginning of the test when perceptuomotor, visuospatial (orientation), memory, and conceptual aspects of the task need to be fully integrated into an efficient routine
- The detection of these early “integrative” difficulties may be particularly relevant for the task of predicting real world capabilities from test results

Index of papers

1. A Simulated Reality Scenario Compared with the Computerized Wisconsin Card Sorting Test: An Analysis of Preliminary Results (Elkins et al., 2001)
2. Probing memory and executive functions with virtual reality: past and present studies (Pugnetti et al. 1926)
3. A Virtual Environment for Investigating Schizophrenic Patients' Characteristics: Assessment of Cognitive and Navigation Ability (Peled et al., 2005)
4. The Virtual Classroom: A Virtual Reality Environment for the Assessment and Rehabilitation of Attention Deficits (Rizzo et al., 2000)
5. A controlled clinical comparison of attention performance in children with ADHD in a virtual reality classroom compared to standard neuropsychological methods (Thomas D. Parsons et al., 2006)
6. Initial Validation of a Virtual Environment for Assessment of Memory Functioning: Virtual Reality Cognitive Performance Assessment Test (Thomas D. Parsons et al., 2008)

A Virtual Environment for Investigating Schizophrenic Patients' Characteristics: Assessment of Cognitive and Navigation Ability (Peled et al., 2005)

Neuropsychology	**Brain Functions Involved:** problem solving, memory, executive functions, attention
Assessment	X
Rehabilitation	

A Virtual Environment for Investigating Schizophrenic Patients' Characteristics: Assessment of Cognitive and Navigation Ability (Peled et al., 2005)

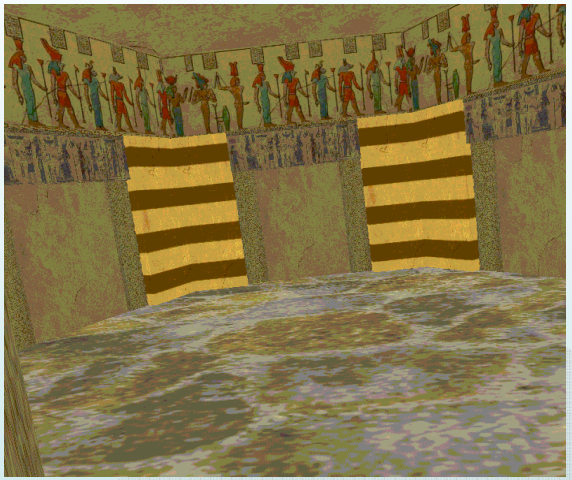

- Working memory
- Executive Function
- Cognitive flexibility

Method

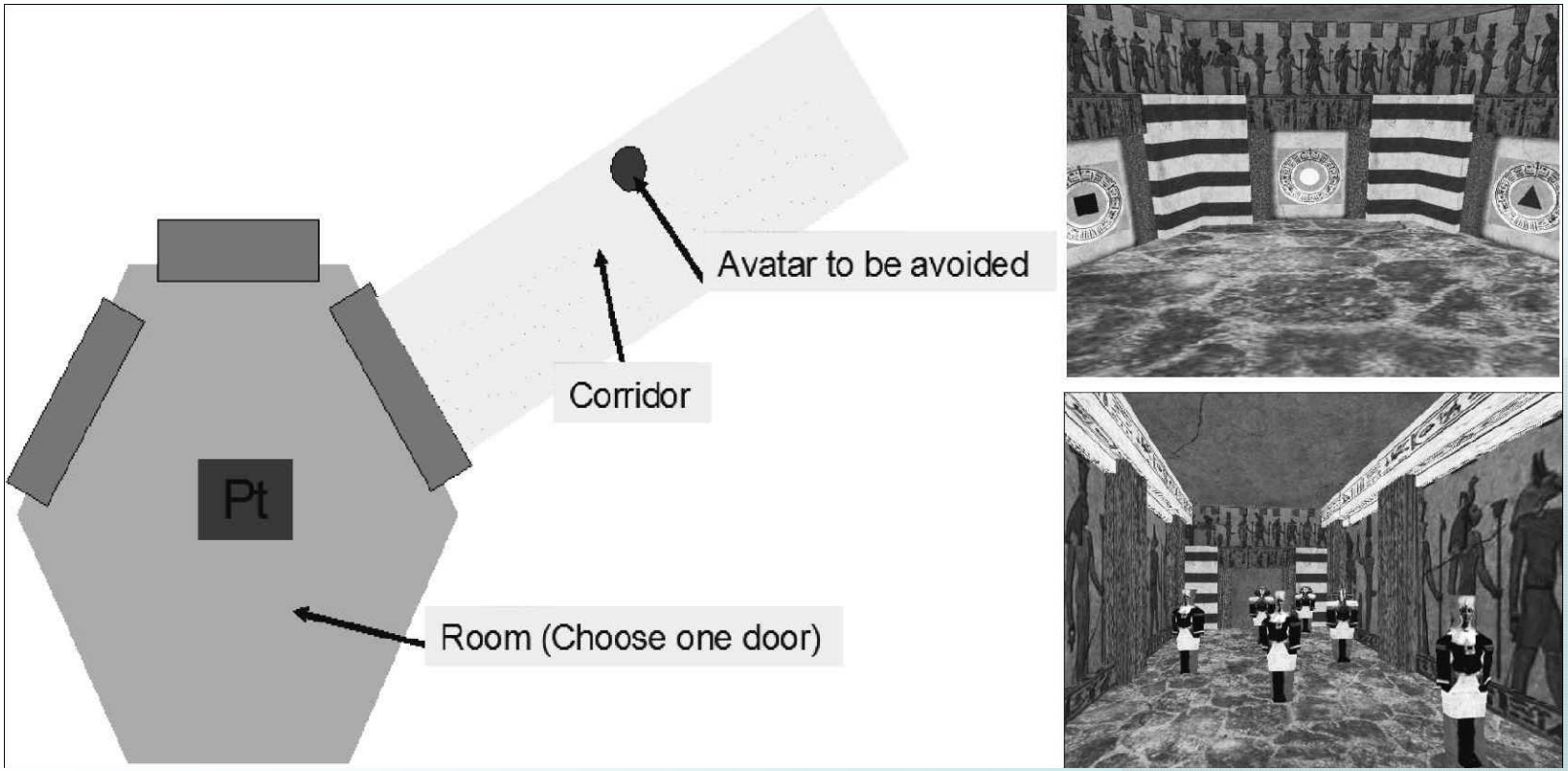

Method

- The virtual environment consists of rooms, which look like Egyptian pyramids, with three doors in each. The rooms are linked by corridors
- Every door has a colored shape on its surface and a sound is played when subject looks at the door. In every room, the subject must choose one door, if the wrong door is chosen, a vibration signal is given to indicate a mistake, but the door opens anyway
- The corridors contain avatars-mummies, obstacles that have to be avoided
- The difficulty level is associated by the number of times the rules are changed during the course of the game, e.g., by the length and the crowdedness of the corridors
- The subject has to get out of the pyramid with doors, which behave in a Wisconsin card fashion

Experimental Variables

- Perseveration: failures to change sorting strategy after negative feedback
- Rule finding: strategy to change contextual contingencies

Results and Discussion

TABLE 5. THE CORRELATIONS BETWEEN VR INDEXES AND WCST INDEXES

		WCST Indexes		
		Perseveration	*Rule finding*	*Total*
VR Index (WOD)	Perseveration	−0.585[b]	−0.108	0.157
	Rule finding	−0.505[a]	−0.327	−0.453[a]
	Total Index	−0.636[b]	−0.151	−0.373
VR Index (WD)	Perseveration	0.585[b]	0.034	0.264
	Rule finding	−0.438[a]	−0.653[b]	−0.672[b]
	Total Index	−0.607[b]	−0.396	−0.547[a]

[a]Correlation is significant at the 0.05 level (2-tailed).
[b]Correlation is significant at the 0.01 level (2-tailed).

There are more correlations in a condition with distractors

Results and Discussion

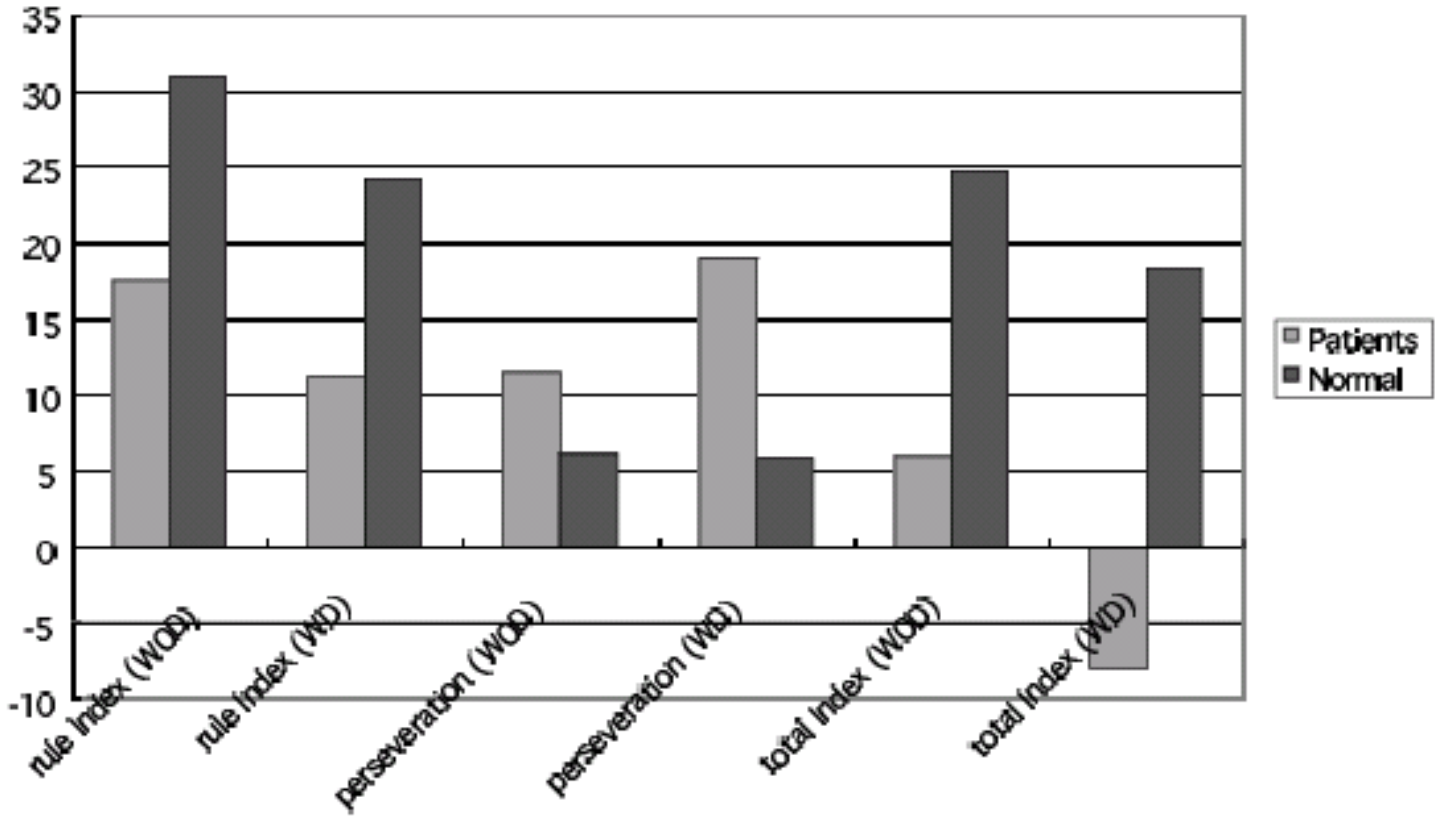

FIG. 3. Comparison between WOD and WD in each index.

Results and Discussion

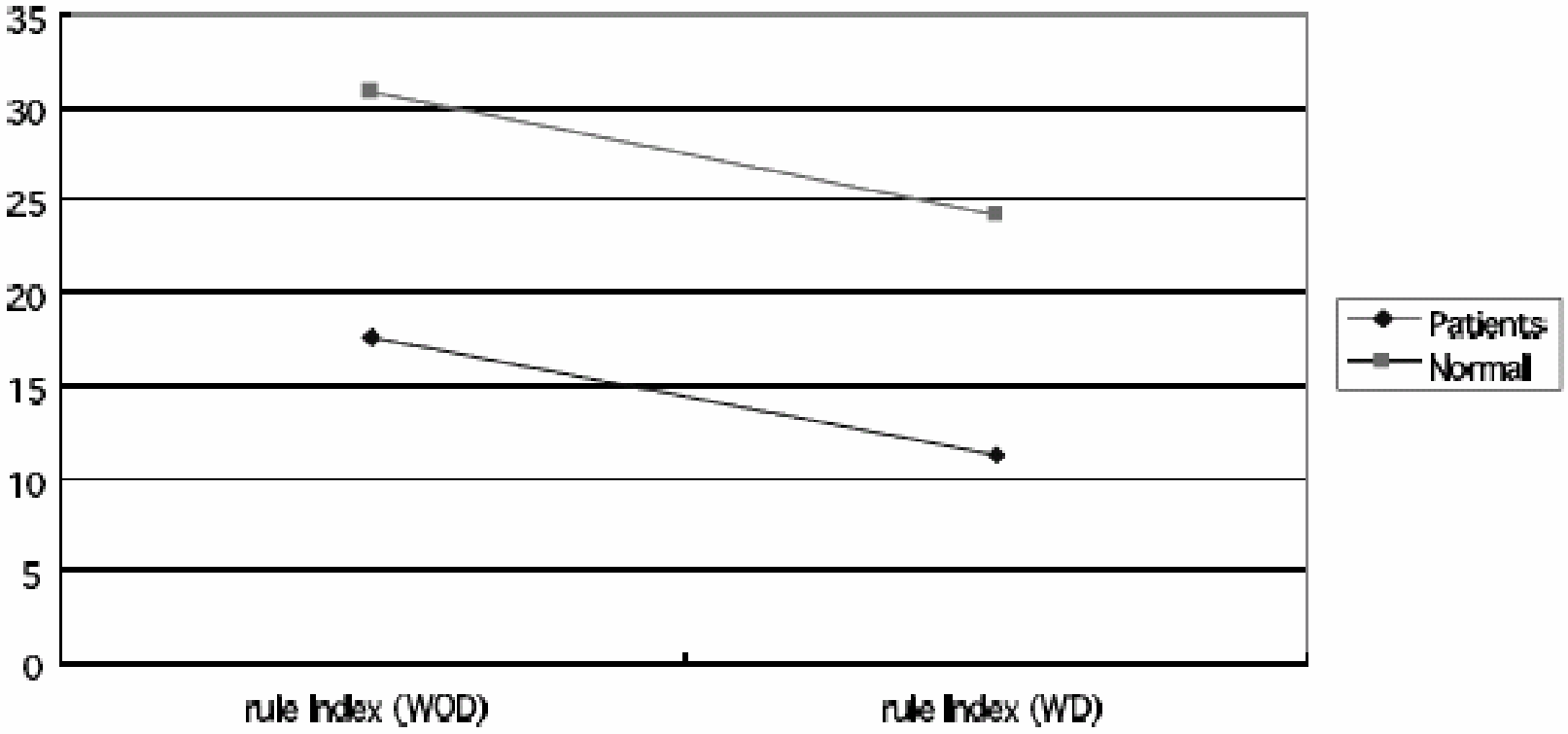

FIG. 4. Comparison of rule finding index between WOD and WD in both groups.

Results and Discussion

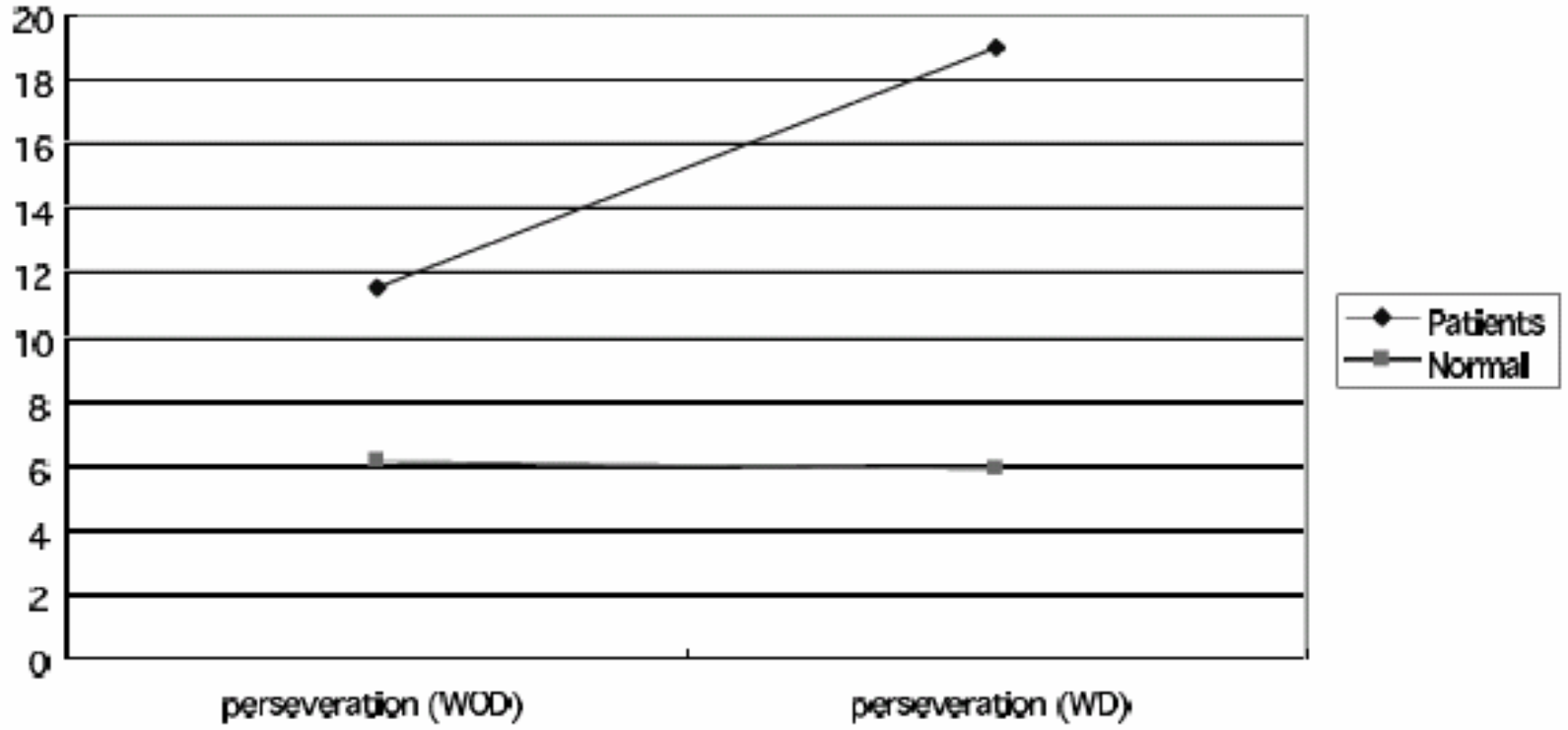

FIG. 5. Comparison of perseveration index between WOD and WD in both groups.

Results and Discussion

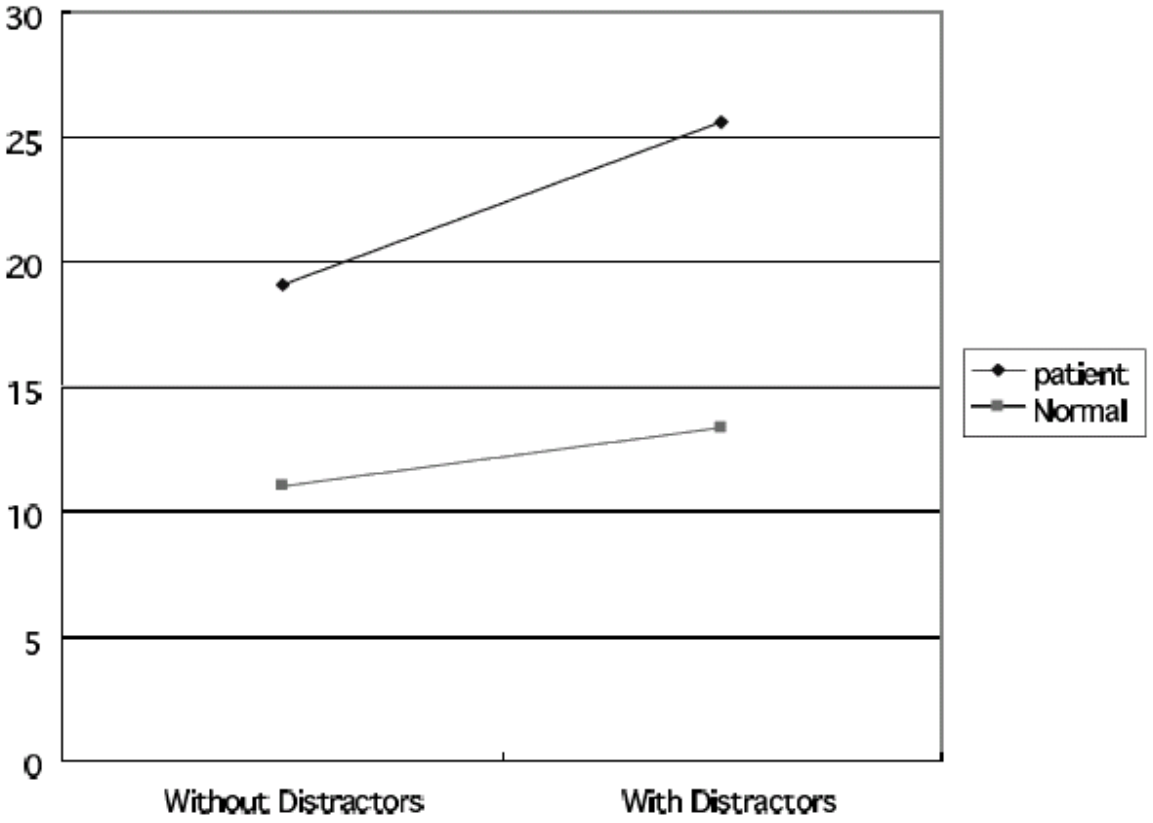

FIG. 6. Comparison of navigation index between WOD and WD in both groups.

Index of papers

1. A Simulated Reality Scenario Compared with the Computerized Wisconsin Card Sorting Test: An Analysis of Preliminary Results (Elkins et al., 2001)
2. Probing memory and executive functions with virtual reality: past and present studies (Pugnetti et al. 1926)
3. A Virtual Environment for Investigating Schizophrenic Patients' Characteristics: Assessment of Cognitive and Navigation Ability (Peled et al., 2005)
4. The Virtual Classroom: A Virtual Reality Environment for the Assessment and Rehabilitation of Attention Deficits (Rizzo et al., 2000)
5. A controlled clinical comparison of attention performance in children with ADHD in a virtual reality classroom compared to standard neuropsychological methods (Thomas D. Parsons et al., 2006)
6. Initial Validation of a Virtual Environment for Assessment of Memory Functioning: Virtual Reality Cognitive Performance Assessment Test (Thomas D. Parsons et al., 2008)

The Virtual Classroom: A Virtual Reality Environment for the Assessment and Rehabilitation of Attention Deficits

A.A. RIZZO et al. CYBERPSYCHOLOGY & BEHAVIOR Volume 3, Number 3, 2000

Neuropsychology	**Brain Functions Involved:** attention
Assessment	X
Rehabilitation	

The Virtual Classroom: A Virtual Reality Environment for the Assessment and Rehabilitation of Attention Deficits

A.A. RIZZO et al. CYBERPSYCHOLOGY & BEHAVIOR Volume 3, Number 3, 2000

- Attention Deficit-Hyperactivity Disorder (ADHD) is a behavioral condition identified by the DSM-IV (Diagnostic and Statistical Manual of Mental Disorders, 4th Edition)
- ADHD is a neurobehavioural developmental disorder affecting about 3-5% of the world's population under the age of 19
- It typically presents itself during childhood, and is characterized by a persistent pattern of inattention and/or hyperactivity, as well as forgetfulness, poor impulse control or impulsivity, and distractibility
- ADHD is currently considered to be a persistent and chronic condition for which no medical cure is available
- ADHD is most commonly diagnosed in children and, over the past decade, has been increasingly diagnosed in adults

The Virtual Classroom: A Virtual Reality Environment for the Assessment and Rehabilitation of Attention Deficits

A.A. RIZZO et al. CYBERPSYCHOLOGY & BEHAVIOR Volume 3, Number 3, 2000

- ADHD Assessment:
  - History taking
  - Psychometric testing
  - Behavioral observation/rating scales
  - Flatscreen computer-delivered tests CPT (continuous performance tests)

- Some difficulties with traditional ADHD assessment tools:
  - Limited control of multiple stimuli
  - Limited assessment of alternating and divided multi-sensory attention components
  - Limited use of distraction
  - Little integrated assessment of motor behavior
  - Poor ecological validity

The Virtual Classroom: A Virtual Reality Environment for the Assessment and Rehabilitation of Attention Deficits

A.A. RIZZO et al. CYBERPSYCHOLOGY & BEHAVIOR Volume 3, Number 3, 2000

Within the Virtual Classroom

- Systematic presentation of both auditory and visual stimulus challenges:
  - Visual Stimuli appear on blackboard
  - Audio Stimuli appear via the “teacher’s” voice
  - Mixed Audio/Visual integration tasks
- Systematic response capture of integrated cognitive and motor response components:
  - Measurement of reaction time, response variability and omission/commission error performance on attention challenges
  - Motor “hyper” activity can be quantified via head, hand, and leg trackers

Initial Clinical Trial

- Boys aged 8-12
- Sample size: ADHD=8 Control=10
- ADHD group was physician referred
- All testing done in morning prior to standard medication intake
- No Significant Differences on:
  - Age
  - Grade level
  - Ethnicity
  - Handedness

Material

- Pentium 3 processor with the nVIDIA G2 graphics card
- The HMD used in this study was the V8 model from Virtual Research
- Tracking of the head, arm and leg used three 6DF magnetic “Flock of Birds” trackers from Ascension Technology Corp

Virtual environment

- Standard rectangular classroom containing
  - desks
  - a female teacher
  - a blackboard across the front wall
  - a side wall with a large window
  - a pair of doorways through which activity occurred
- Children's attention performance was assessed while a series of common classroom distracters:
  - ambient classroom noise
  - activity occurring outside the window

Attention Test (CPT)

- It was a vigilance performance task delivered on the blackboard that required the participants to hit a wireless mouse button whenever they saw the letter “X” preceded by the letter “A”
- Two 10-minute conditions were presented to participants:
  - one without distraction
  - one with distractions (pure audio, pure visual and mixed A/V)

Experimental variables

- Hit reaction time
- Omission errors
- Commission errors
- Response variability

Summary of results

- ADHD children had slower correct hit reaction time compared with normal controls on the distraction condition (760ms vs. 610ms; t (1,16) = -2.76, p <.03).
- ADHD children had higher reaction time variability on correct hits compared with normal controls on both the no-distraction (SD= 220ms vs. 160ms; t (1,16) = -2.22, p < .05) and distraction conditions (SD= 250ms vs. 170ms; t (1,16) = -2.52, p < .03).
- ADHD children made more Omission errors (missed targets) compared with normal controls on both the no-distraction (14 vs. 4.4; t (1,16) = -4.37, p < .01) and distraction conditions (21 vs. 7.2; t (1,16) = - 4.15, p < .01).
- ADHD children made more Commission errors (impulsive responding in the absence of a target) compared with normal controls on both the no-distraction (16 vs. 3.7; t (1,16) = -3.15, p < .01) and distraction conditions (12.1 vs. 4.2; t (1,16) = -3.22, p < .01)

Summary of results

- ADHD children made more Omission errors in the distraction condition compared to the non-distraction condition (21 vs. 14; $t(1,14) = -3.50$, $p < .01$). No such differences on Omission and Commission errors were found with the non-diagnosed children across no-distraction and distraction conditions.
- Exploratory analysis of motor movement in ADHD children (tracked from head, arm and leg) indicated higher activity levels on all metrics compared to non-diagnosed children across both conditions.
- Exploratory analysis of motor movement in ADHD children also indicated higher activity levels on all metrics in the distraction condition compared to the non-distraction condition. This difference was not found with the normal control children.
- An exploratory analysis using a neural net algorithm trained to recognize a stereotypic leg movement on the first five participants in each group was able to accurately discriminate the remaining subjects to groups at 100%.

Without Distraction

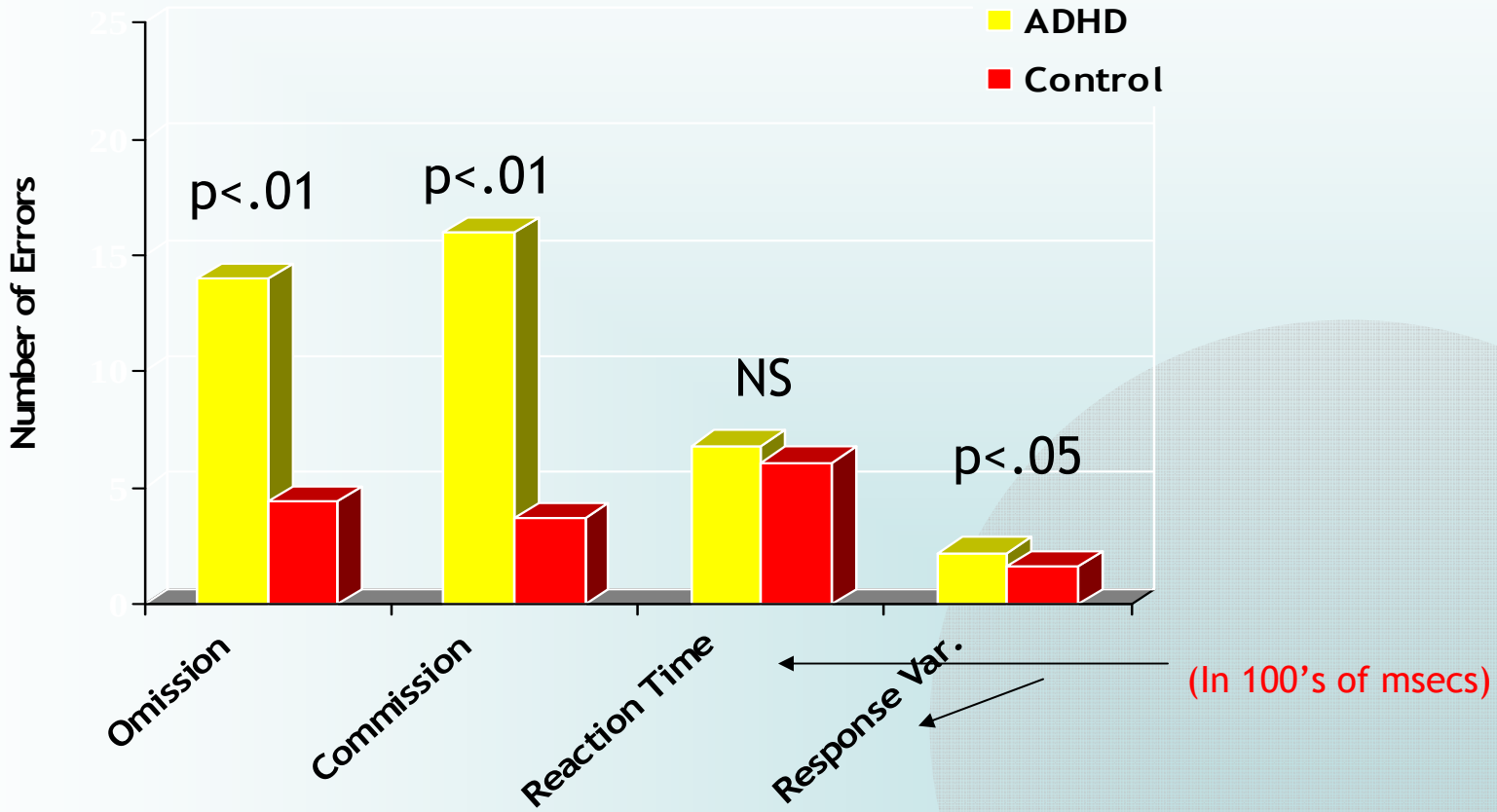

With Distraction

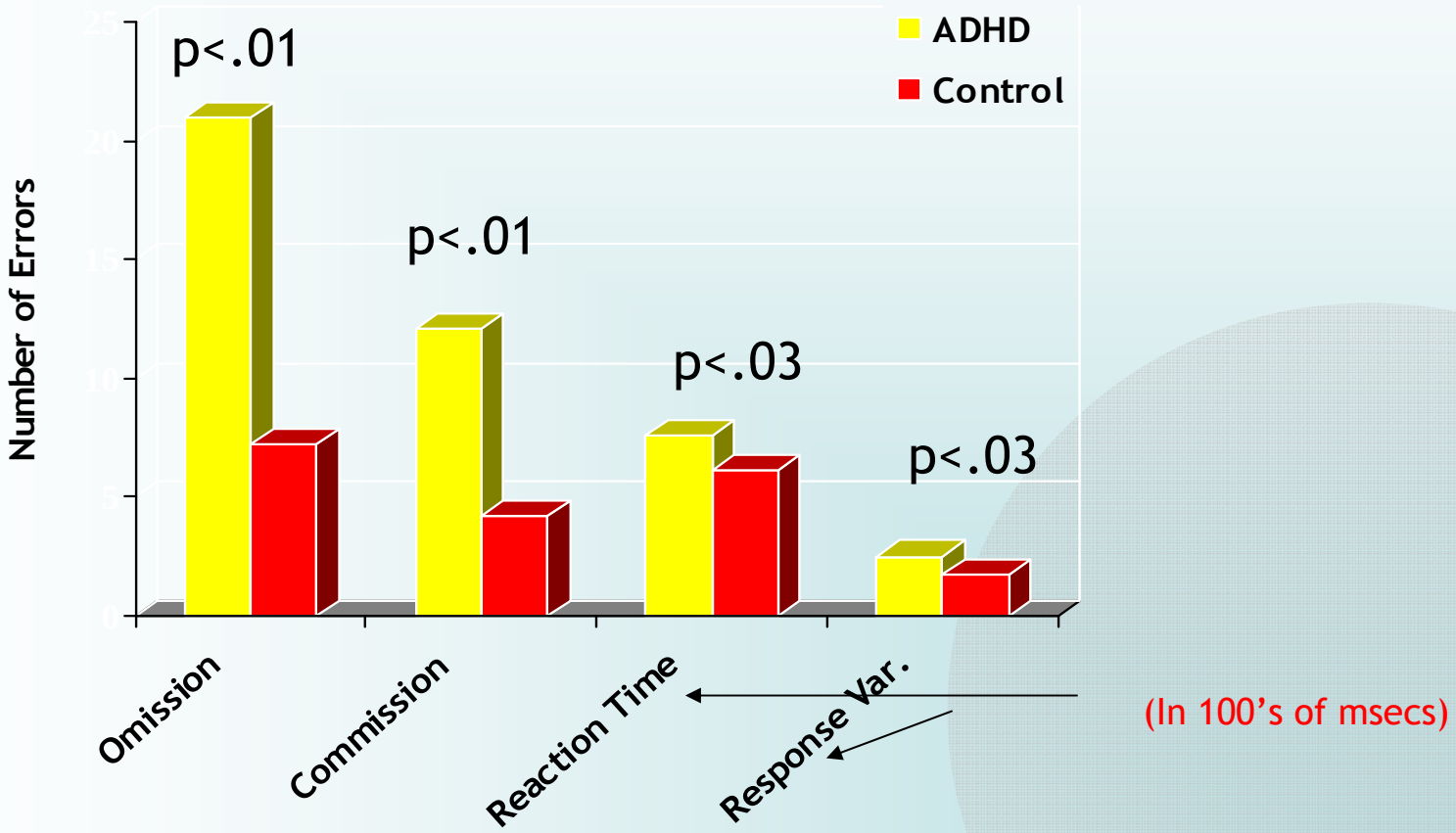

Sample Movement Measures

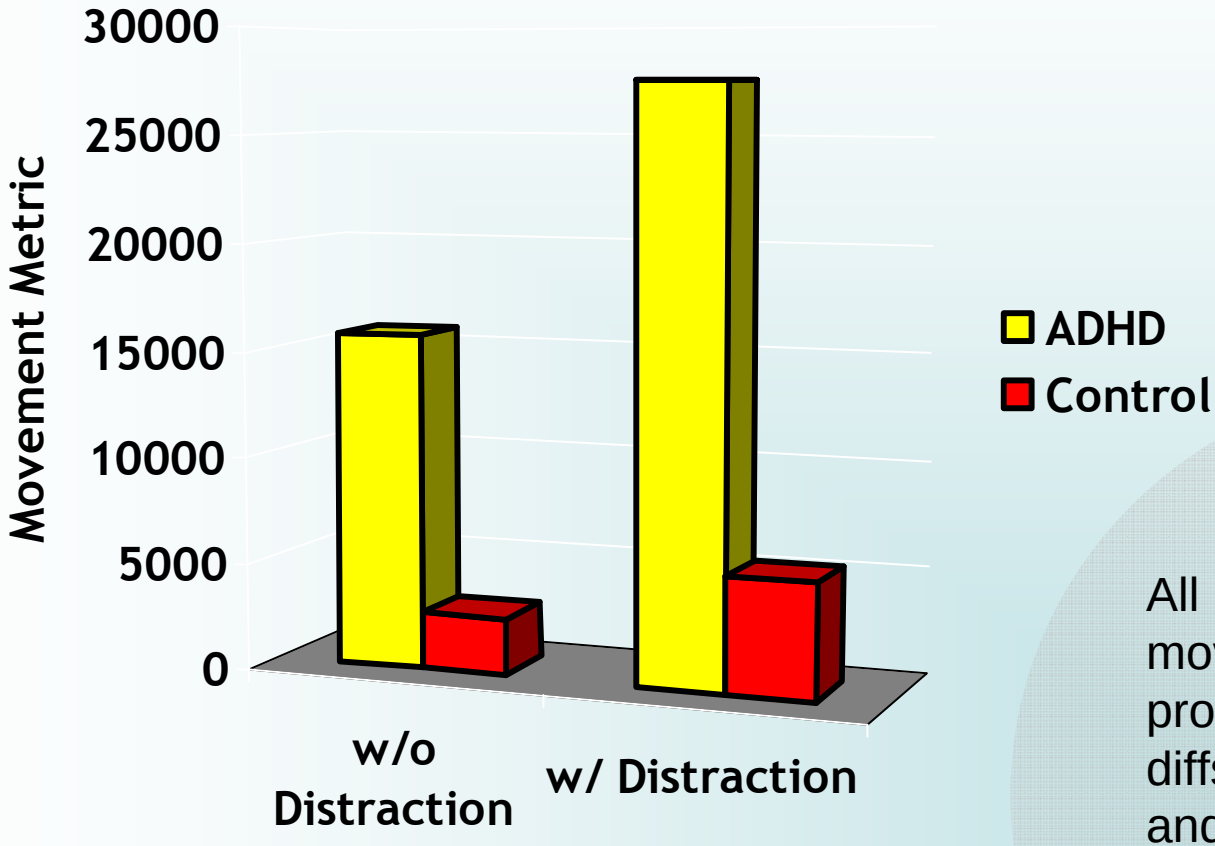

All 18 component movement metrics produced significant diffs. between groups and across distraction conditions!

All tracked movement metrics from Head, Arm & Leg

- A Support Vector Machine analysis was used to classify the tracked movements metric
- After training system on first five subjects per group, 100% discrimination on groups for stereotypic rotation movement of the leg was uncovered.

Support Vector Machine analysis of tracked movement metrics from Head, Arm & Leg

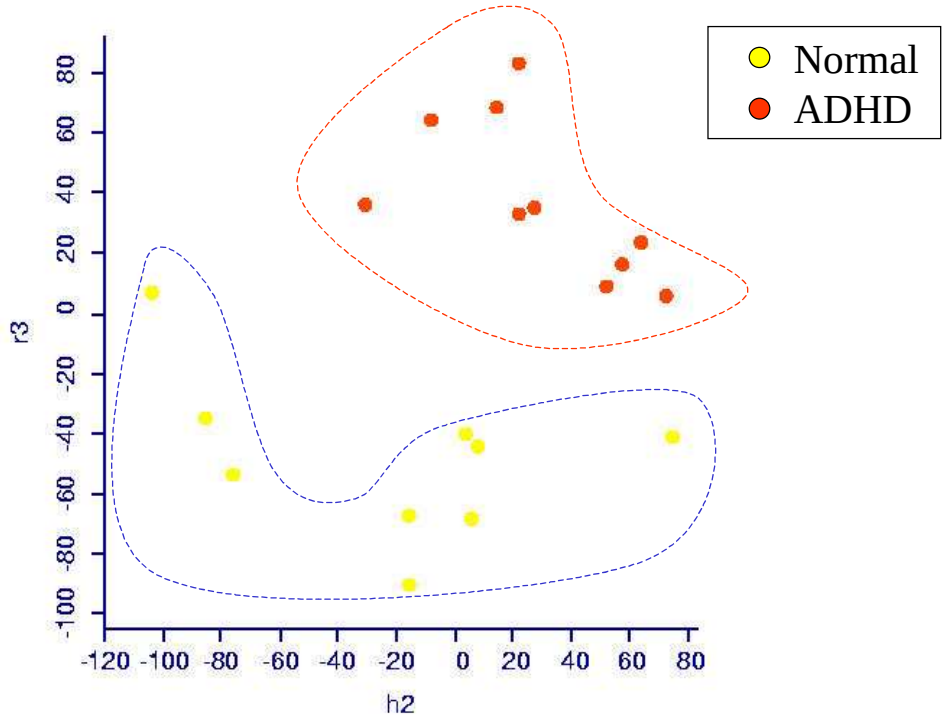

Discussion

- The Virtual Classroom had good potential as an efficient, cost-effective and scalable tool for conducting attention performance measurement beyond what exists using traditional methodologies
- The system allowed for controlled performance assessment within an ecologically valid environment and appeared to parse out significant effects due to the presence of distraction stimuli
- The capacity to integrate measures of movement via the tracking technology further added value to this form of assessment when compared to traditional analog tests and rating scales

Index of papers

1. A Simulated Reality Scenario Compared with the Computerized Wisconsin Card Sorting Test: An Analysis of Preliminary Results (Elkins et al., 2001)
2. Probing memory and executive functions with virtual reality: past and present studies (Pugnetti et al. 1926)
3. A Virtual Environment for Investigating Schizophrenic Patients' Characteristics: Assessment of Cognitive and Navigation Ability (Peled et al., 2005)
4. The Virtual Classroom: A Virtual Reality Environment for the Assessment and Rehabilitation of Attention Deficits (Rizzo et al., 2000)
5. A controlled clinical comparison of attention performance in children with ADHD in a virtual reality classroom compared to standard neuropsychological methods (Thomas D. Parsons et al., 2006)
6. Initial Validation of a Virtual Environment for Assessment of Memory Functioning: Virtual Reality Cognitive Performance Assessment Test (Thomas D. Parsons et al., 2008)

The Virtual Classroom: A Virtual Reality Environment for the Assessment and Rehabilitation of Attention Deficits

A.A. RIZZO et al. CYBERPSYCHOLOGY & BEHAVIOR Volume 3, Number 3, 2000

Neuropsychology	**Brain Functions Involved:** attention
Assessment	X
Rehabilitation	

A controlled clinical comparison of attention performance in children with ADHD in a virtual reality classroom compared to standard neuropsychological methods

Thomas D. Parsons et all. - *Child Neuropsychology Volume 13, Issue 4 July 2007 , pages 363 - 381*

Standard neuropsychological methods

- Clinical Interviews and Rating Scales
  - they have limited predictive validity (Lahey et al., 2006) and treatment utility (Scotti et al., 1926)
  - lack sensitivity to low base rates, which raters may underestimate (Fabiano et al., 2004)
  - bias is an inherent possibility in teacher (Abikoff et al., 1923) and parental ratings of ADHD (Sayal & Taylor, 2005)
- Neuropsychological Tests
  - They reliably discriminate between the ADHD and normal childs: Stroop, Controlled Oral Word Association Test, and Picture Arrangement from the Wechsler Intelligence Scale for Children-III
  - Limited ecological validity
- Laboratory-Based Measures
  - more cost effective and require less time and effort than complete comprehensive diagnostic evaluations
  - less influenced by extraneous factors
  - more time efficient descriptions of the impact of treatments on ADHD symptoms
  - easier use for administers (i.e. teachers and parents) in multifarious settings
  - the most popular of the laboratory-based measures is the **Continuous Performance Test (CPT)**

A controlled clinical comparison of attention performance in children with ADHD in a virtual reality classroom compared to standard neuropsychological methods

Thomas D. Parsons et all. - *Child Neuropsychology Volume 13, Issue 4 July 2007 , pages 363 - 381*

- Future advances in the ecological validity of laboratory-based measures may result from
  - assessments of the target behaviors in natural settings
  - the combination of the more promising laboratory-based measures into a standardized battery
- Within VR it is possible to systematically present cognitive tasks targeting attention performance beyond what are currently available using traditional methods

Hypothesis

H1: There would be differences in Virtual Classroom Performance between children with ADHD and nonclinical controls

H2: The children with ADHD would display more distractibility than controls as measured by their responses to systematically delivered pure auditory, pure visual, and mixed distractors

H3: Virtual Classroom measures would be correlated with traditional psychometric measures of attention and parent reports of inattention, impulsivity, and hyperactivity

Methods: Participants

- Ten boys diagnosed with ADHD and ten normal control boys
- The groups did not significantly differ in mean age, grade level, ethnicity, or handedness
- Mean ages:
  - ADHD: 10.6 years (range 8-12)
  - Normal: 10.2 years (range 8-12)

Methods: Measures

- Assessment measures selected:
  - SWAN Behavior Checklist
  - Conners' CPT II
- Neuropsychological measures selected:
  - Stroop
  - Trail Making tests
  - NEPSY
  - WISC-III
  - Judgment of Line Orientation

Methods: Experimental Condition

- Three 10-min conditions followed the 1-min hit command phase. The participant was instructed to view a series of letters presented on the blackboard and to hit the response button only after he viewed the letter “X” preceded by an “A”
- *Condition 1 (AX task without distraction)*
- *Condition 2 (AX task with distraction):*
  - *pure auditory—ambient classroom* sounds (i.e., whispering, pencils dropping, chairs moving, etc.) “behind” the student;
  - *pure visual—3D paper airplane flying directly across the participant’s field of view;*
  - *mixed audio/visual*
- *Condition 3 (Boston Naming Test Match):*
  - *the player has to* hit the response pad every time the Virtual Teacher incorrectly named the object
  - after 4.5 min the criterion for response shifted to requiring the participant to hit the response pad after correct matches

Results

Table 2 Comparison of Means for Psychometric Measures between ADHD Group and Normal Control

	ADHD (n=9)*		Normal (n=10)		Entire Sample (n=19)		
Measures	*M*	*SD*	*M*	*SD*	*M*	*SD*	*f*
SWAN[a]	0.83	0.88	−1.54	1.11	−0.35	1.56	−5.29**
Conners CPT II[b]							
Omission	60.14	21.67	45.05	4.73	52.59	17.12	−2.15*
Commission	52.12	6.42	43.64	8.56	47.88	8.55	−2.51*
Hit RT	55.45	14.37	47.00	4.77	51.22	11.29	−1.76†
Stroop Test[c]							
Word	50.00	4.71	49.60	5.40	49.80	4.94	−.18
Color	48.60	9.71	48.80	4.24	48.70	7.29	0.06
Color-Word	46.00	7.89	55.20	6.48	50.60	8.46	2.85*
NEPSY[d]							
Visual Attention	10.10	2.92	13.20	3.01	11.65	3.30	2.34*
Design Fluency	11.50	1.84	12.30	1.77	11.90	1.80	0.99
Verbal Fluency	12.20	3.29	14.90	2.18	13.55	3.05	2.16*
WISC-III[e]							
Digit Span	9.90	2.81	13.40	1.58	11.65	2.85	3.44**
Coding B	9.30	3.68	10.90	2.89	10.10	3.32	1.08
Arithmetic	8.90	2.08	12.80	2.04	10.85	2.83	4.23**
Vocabulary	12.60	3.72	15.20	2.35	13.90	3.31	1.87†
Trail Making Test[f]							
Part A	0.78	0.68	0.70	0.48	0.74	0.57	−0.32
Part B	0.37	1.18	1.02	0.40	0.70	0.92	1.65
JLO[g]	19.60	5.32	25.40	2.68	22.50	5.06	3.08**

**p < .01
*p < .05
†p < .10

Results

H1: Group differences in Virtual Classroom performance

Table 3 Comparison of Means for Virtual Classroom Measures Between ADHD Group and Normal C

Measures		ADHD[a] *M*	ADHD[a] *SD*	Normal *M*	Normal *SD*	Entire Sample *M*	Entire Sample *SD*	*F*
Condition 1 (AX Task without Distraction)								
Omission[b]		16	10.34	4	2.98	9.68	9.48	−3.52**
Commission		16.33	10.54	3.4	4.5	9.53	10.17	−3.55**
Hit RT[c]		0.52	0.24	0.6	0.07	0.57	0.17	1.05
Body Movement[d]	X	37.78	27.03	9.7	9.86	23	24.1	−3.07**
	Y	27.44	17.19	9.1	5.82	17.79	15.39	−3.19**
	Z	102.44	88.98	25.8	22.31	62.11	72.9	−2.64*
	R	14349	10253	3805	5833	8800	9643	−2.79*
	P	7150	4889	1628	1685	4244	4479	−3.37**
	H	15742	13534	2632	2752	8842	11420	−3.00**
Condition 2 (AX Task with Distraction)								
Omission		22.89	10.06	7	5.52	14.53	11.25	−4.33**
Commission		12.11	8.81	2	1.89	6.79	7.95	−3.55**
Hit RT		0.56	0.29	0.59	0.09	0.58	0.2	0.33
Body Movement	X	59.67	30.39	12.2	10.58	34.68	32.55	−4.65**
	Y	40.44	19.74	10	6.6	24.42	20.95	−4.61**
	Z	135	92.1	30.9	23.07	80.21	83	−3.47**
	R	27434	24727	6770	6005	16558	20053	−2.57*
	P	10794	5257	2437	2310	6395	5773	−4.57**
	H	27579	18367	5418	5588	15915	17169	−3.64**
Condition 3 (BNT Match)								
Omission		0.33	0.71	0	0	0.16	0.5	−1.5
Commission		6.67	6.42	2.6	3.41	4.53	5.34	−1.75†
Hit RT		0.57	0.06	0.58	0.06	0.58	0.06	0.46
Body Movement	X	26.22	14.18	11.2	9.2	18.32	13.82	−2.77*
	Y	19.11	11.04	8.6	4.62	13.58	9.69	−2.76*
	Z	65	34.23	30.5	20.98	46.84	32.46	−2.68*
	R	12802	12905	3518	2754	7916	10025	−2.23*
	P	5635	3223	2212	1895	3136	2249	−2.86*
	H	13982	15731	4796	4318	7217	6320	−1.78†

**p < .01
*p < .05
†p < .10

Results

H2: Children with ADHD would display more distractibility than controls

Table 4 Comparison of Virtual Classroom Performance Degradation from Condition 1 to Condition 2 between ADHD Group and Normal Control Group.

	ADHD[a] (n=9)		Normal (n=10)			
Measures[b]	*M*	*SD*	*M*	*SD*	*f*	*r*[c]
Omission	6.89	6.57	3.00	5.60	−1.39	1.94†
Commission	−4.22	6.57	−1.4	3.81	1.16	1.00
Hit RT	0.04	0.15	−0.01	0.10	−0.89	0.81
Body Movement						
X	21.89	14.99	2.50	6.40	−3.74**	3.07**
Y	13.00	9.72	0.90	4.33	−3.57**	2.81*
Z	32.56	28.92	5.10	13.45	−2.70*	2.37*
R	13085	16564	2965	6448	−1.79†	0.51
P	3644	2598	809	1434	−2.99*	2.46*
H	11838	8189	2786	4359	−3.05**	1.67

**p < .01
*p < .05
†p < .10

Results

H3: Virtual Classroom correlated with traditional psychometric measures

We considered those correlations that met the criterion of *p < .05*

- On the AX task (CPT) total, omission and commission errors in the Virtual Classroom were moderately correlated with parent behavioral ratings on the SWAN Behavior checklist (*r=.51; and r=.59, respectively)*
- Correlations of Virtual Classroom body movement with behavior ratings were slightly higher in the distracting condition (*r=.61)* than the non-distracting condition (*r=.47)*
- On the “incorrect match” BNT task condition, commission errors in the Virtual Classroom were moderately correlated (*r=.51) with parent behavioral ratings on the SWAN Behavior checklist*
- Virtual Classroom body movement measures were moderately correlated with parent behavioral ratings in both BNT task conditions (*r=.41; and r=.49, respectively)*
- In the non-distracting condition (Condition 1), commission errors but not omission errors in the Virtual Classroom were correlated with errors, and average reaction time for hits on the Conners’ CPT II (*r=.51; and r=.75, respectively)*
- When distractions were introduced, commission errors in the Virtual Classroom were still correlated with errors, and average reaction time for hits on the Conners’ CPT II (*r=.44; r=.79, respectively)*
- In the non-distracting condition, Virtual Classroom body movement was correlated with omission errors (*r=.73),* commission errors (*r=.46), and average reaction time for hits (r=.49) on the Conners’ CPT II*

Results

H3: Virtual Classroom correlated with traditional psychometric measures

- Correlations between Virtual Classroom measures and the Conners' CPT II were more variable between the two BNT task conditions. In both conditions, commission errors in the Virtual Classroom were correlated with errors, and average reaction time for hits on the Conners' CPT II (*r=.39; and r=.70, respectively).*
- Omission errors in the Virtual Classroom were not correlated with any Conners' CPT II variables in the incorrect match BNT condition, but they were moderately correlated with Conners' CPT II omission errors and average reaction time on hits in the correct match BNT condition (*r=.52)*
- Virtual Classroom body movement measures were not related to any of the Conners' CPT II variables in either of the two BNT task conditions.
- When correlations were calculated separately for each group, however, it was noticed that in the correct match BNT condition very strong individual group correlations were working in opposite directions and actually reducing the total sample correlation for one measure.
- Specifically, it was found that strong positive correlations exist between Virtual Classroom body movement and commission errors on the Conners' CPT II for the normal control group (*r=.77). In* contrast, strong negative correlations exist between Virtual Classroom body movement and commission errors on the Conners' CPT II for the participants with ADHD (*r=−.82).*

Discussion

1. H1: Participants with ADHD exhibited more omission errors, commission errors, and overall body movement than normal control children in the Virtual Classroom
2. H2: Participants with ADHD were more impacted by distraction than normal control children in the Virtual Classroom
3. H3: Virtual Classroom measures were correlated with traditional ADHD assessment tools, the behavior checklist and flatscreen CPT
4. No negative side effects were associated with use of the Virtual Classroom
5. Greater overall hyperactivity could result in greater inattention to the task and in turn less commission errors

Index of papers

1. A Simulated Reality Scenario Compared with the Computerized Wisconsin Card Sorting Test: An Analysis of Preliminary Results (Elkins et al., 2001)
2. Probing memory and executive functions with virtual reality: past and present studies (Pugnetti et al. 1926)
3. A Virtual Environment for Investigating Schizophrenic Patients' Characteristics: Assessment of Cognitive and Navigation Ability (Peled et al., 2005)
4. The Virtual Classroom: A Virtual Reality Environment for the Assessment and Rehabilitation of Attention Deficits (Rizzo et al., 2000)
5. A controlled clinical comparison of attention performance in children with ADHD in a virtual reality classroom compared to standard neuropsychological methods (Thomas D. Parsons et al., 2006)
6. Initial Validation of a Virtual Environment for Assessment of Memory Functioning: Virtual Reality Cognitive Performance Assessment Test (Thomas D. Parsons et al., 2008)

The Virtual Classroom: A Virtual Reality Environment for the Assessment and Rehabilitation of Attention Deficits

A.A. RIZZO et al. CYBERPSYCHOLOGY & BEHAVIOR Volume 3, Number 3, 2000

Neuropsychology	**Brain Functions Involved:** Learning, Memory, Executive functions, Attention, Processing speed, Verbal fluency
Assessment	X
Rehabilitation	

Initial Validation of a Virtual Environment for Assessment of Memory Functioning: Virtual Reality Cognitive Performance Assessment Test

THOMAS D. PARSONS, Ph.D. and ALBERT A. RIZZO, Ph.D.

CYBERPSYCHOLOGY & BEHAVIOR Volume 11, Number 1, 2008

- VRCPAT is a virtual environment–based measure of learning and memory
- Hypothesis:
  - H1: the performance on the VRCPAT would correlate significantly with performance on traditional neuropsychological measures of memory
  - H2: the performance on the VRCPAT would not correlate with performance on traditional other neuropsychological measures than memory

Methods

- 30 healthy participants (15 males and 15 females)
- The VRCPAT software is a 3D VE programmed to simulate a city environment
- Three-dimensional visual imagery is presented using the eMagin z800 Head Mounted Display
- During immersion in the VRCPAT, participants are seated at a desk and have a complete 360-degree view of the city environment

Methods

- Participants completed a neuropsychological battery administered under standard conditions (1.5 hours):
  - Hopkins Verbal Learning Test—Revised (HVLT-R)
  - Brief Visuospatial Memory Test—Revised (BVMT-R)
  - Controlled Oral Word Association Test (FAS)
  - Semantic Fluency (Animals)
  - Digit Symbol Coding and Digit Span (Forward and Backward) from the Wechsler Adult Intelligence Scale, Third Edition (WAIS-III)
  - Trail Making Test Parts A and B (TMT)
  - Stroop Color and Word Test
  - Wechsler Test of Adult Reading (WTAR)
- Using this battery the following variables are studied:
  - Learning
  - Memory
  - Executive functions
  - Attention
  - Processing speed
  - Verbal fluency

Methods

VRCPAT is a 15-minute measure made of:

- *Acquisition phase:*
  - Users were presented with 10 pieces of language-based information to be learned without any context for what they would need to do with this information (blue car, intact barrel, red shipping container , etc.)
  - Three 1-minute trials. At the end of each trial, users were asked to name the objects they studied as an assessment of initial declarative recall memory. A psychometrist scored the **VRCPAT's learning score** by recording the total recall

- *VR interface and task training phase*

Methods

VRCPAT is a 15-minute measure made of:

- *Retrieval phase:*
  - The users “travel” to five zones in the city.
  - At each zone, the users were exposed to both targets (items from the 10-item list in the acquisition phase) and foils (items that were similar to or different the targets)
- *Debriefing phase:*
  - Users were asked to recall the original list of stimuli and at which target zones they were found
  - A psychometrist scored the **VRCPAT’s memory score** by recording the total delayed recall both from within the five zones and again at the end of the VR scenario

Results

TABLE 1. MEANS AND STANDARD DEVIATIONS (RAW SCORES)

	Mean	*Variance*	*Standard deviation*	*Standard error*
VRCPAT				
Total learning	35.67	189.06	13.75	2.51
Total memory	6.04	5.05	2.25	0.41
Neuropsychological measures				
HVLT Trials 1–3	27.90	21.40	4.63	0.84
BVMT Trials 1–3	28.90	20.51	4.53	0.83
HVLT Retention	10.27	3.65	1.91	0.35
BVMT-R Retention	11.00	2.21	1.49	0.27
Trail Making Test, Part B	46.30	184.70	13.59	2.48
Stroop Interference	97.07	373.44	19.32	3.53
Digit Span Forward	7.37	1.34	1.16	0.21
Digit Span Backward	6.00	2.21	1.49	0.27
Trail Making Test, Part A	24.10	82.02	9.06	1.65
Digit-Symbol Coding	86.10	310.16	17.61	3.22
Semantic Fluency	27.20	29.20	5.40	0.99
Phonemic Fluency	47.97	139.14	11.80	2.15

Note: For all analyses, $N = 30$.
HVLT, Hopkins Verbal Learning Test; BVMT-R, Brief Visuospatial Memory Test—Revised.

Results

TABLE 2. CORRELATIONS BETWEEN TRADITIONAL TEST COGNITIVE DOMAIN SCORES AND VRCPAT LEARNING AND MEMORY SCORES

	VRCPAT learning		*VRCPAT memory*	
	r	*p*	*r*	*p*
Learning	0.69	<0.01	0.73	<0.01
Memory	0.67	<0.01	0.65	<0.01
Executive functions	0.21	0.25	0.13	0.48
Attention	0.25	0.18	0.12	0.50
Processing speed	0.12	0.50	0.15	0.43
Verbal fluency	0.27	0.15	0.25	0.18

Results

TABLE 3. CONVERGENT VALIDITY: CORRELATIONS BETWEEN TRADITIONAL NEUROCOGNITIVE TEST SCORES AND VRCPAT TOTAL MEMORY SCORE

	$r\ (x,y)$	r^2	t	p
Learning				
HVLT Trials 1–3	0.58	0.34	3.78	<0.01
BVMT-R Trials 1–3	0.75	0.56	6.01	<0.01
Memory				
HVLT Retention	0.50	0.25	3.05	<0.01
BVMT-R Retention	0.40	0.16	2.29	<0.01

TABLE 4. DISCRIMINANT VALIDITY: CORRELATIONS BETWEEN TRADITIONAL NEUROCOGNITIVE TEST SCORES AND VRCPAT TOTAL MEMORY SCORE

	$r\ (x,y)$	r^2	t	p
Executive functions				
Trail Making Test: Part B	0.34	0.12	1.94	0.07
Stroop Interference	0.30	0.09	1.66	0.11
Attention				
Digit Span Forward	0.13	0.02	0.68	0.48
Digit Span Backward	0.05	0.00	0.29	0.80
Processing speed				
Trail Making Test: Part A	0.30	0.09	1.67	0.11
Digit-Symbol Coding	0.07	0.01	0.39	0.70
Verbal fluency				
Animals	0.32	0.10	1.79	0.08
Letter fluency	0.16	0.03	0.86	0.38

Discussion

1. The VRCPAT was significantly related to all of the other measures (both individual and composites) used to assess learning and memory
2. VRCPAT memory scores did not correlate with nonmemory measures drawn from the traditional neuropsychological test battery
3. This removed the possibility that results reflected correlates of the nontarget construct (i.e., executive function, attention, processing speed, and verbal fluency)
4. **The ability of the VRCPAT to accurately classify participants into memory impaired and nonimpaired groups based on carefully established critical values must be evaluated. It must be evaluated by the performance indices of:**
   - Sensitivity
   - Specificity
   - Predictive value of a positive test
   - Predictive value of a negative test
5. Small sample size

State of the art of virtual reality applications in neuropsychology

GRAZIE

Clustering Dinámico y estructuras modulares en redes complejas

A. Moujahid

Grupo de Inteligencia Computacional

Universidad del País Vasco

Mayo, 2008

Contenido

Introducción

Estructuras modulares jerárquicas en redes complejas

Técnicas de detección de estructuras modulares

clustering dinámico y fenómeno de sincronización

Conclusión

Referencias

Introducción

- El fenómeno de la sincronización es un concepto clave para estudiar grandes poblaciones de individuos (o sistemas) que interactúan. Gran parte de la investigación realizada en ésta área ha sido inspirada a partir de sistemas biológicos, físicos, sociales o fisiológicos asimilándolos a un conjunto de osciladores [Strogatz, S.H. (2003)].
- En la década del 80, Y. Kuramoto propuso un enfoque para el problema de la sincronización que consiste en modelar cada miembro de la población como un oscilador de fase, dando lugar a uno de los modelos más representativos conocido como modelo de Kuramoto [Juan A. Acebrón et al. (2005)].

Introducción

La dinámica del modelo Kuramoto viene dada por:

$$\dot{\theta}_i(t) = \omega_i + \frac{K}{N} \sum_{j=1}^{N} sin(\theta_j - \theta_i)$$

donde $\theta_i(t)$ es la fase del oscilador i en el instante t,y ω_i su frecuencia natural. Las frecuencias naturales son independientes del tiempo. El parámetro $K \geq 0$ mide la fuerza de acoplamiento como término global de acoplamiento.

Introducción

- Para valores pequeños de K, cada oscilador tiende a oscilar independientemente con su propia frecuencia, mientras para valores grandes de K, el acoplamiento tiende a forzar los osciladores a entrar en un régimen sincronizado global.
- Kuramoto ha mostrado que este modelo, a pesar de la diferencia en las frecuencias naturales de los osciladores, exhibe una transición espontanea desde un régimen incoherente hacia un régimen de sincronización colectiva, a medida que el parámetro K supera un cierto umbral K_c [Strogatz, S.H. (2003)].

Introducción

- En [Oh E. et al. (2005);Moreno, Y. et al (2004)] se ha mostrado que conjuntos de osciladores altamente interconectados sincronizan más facilmente que aquellos con escasas conexiones.
- Este escenario sugiere que para una red compleja con un patrón de conectividad no trivial, partiendo de unas condiciones iniciales arbitrarias, aquellas unidades altamente interconectadas y que forman clusters locales, sincronizarían antes que las demás.
- Después, de acuerdo a un proceso secuencial, otras estructuras espaciales harán lo mismo hasta alcanzar un estado final en el cual la población total oscila a la misma frecuencia.
- Este proceso ocurre a diferentes escalas temporales si existe una clara estructura modular de la red.

Introducción

Una versión modificada del modelo de Kuramoto adaptada para redes sociales complejas, conocida como OCR (Opinion Changing Rate) model, viene dada por [Pluchino A. et al.(2005)]:

$$\dot{x}_i(t) = \omega_i + \frac{K}{N} \sum_{j=1}^{N} \alpha sin(x_j - x_i) e^{-\alpha |x_j - x_i|}$$

aquí $x_i(t)$ es un número real que representa la opinion del individuo i en el instante t,y ω_i su *natural opinion changing rate*, es decir, la tendencia natural que tiene cada individuo para cambiar su opinion. $K \geq 0$ es el factor de acoplamiento.

Introducción

- Generalmente, se utiliza una distribución uniforme $g(\omega)$ centrada en su primer momento ω_0 para generar aleatoriamente los ω_i.
- para valores menores a ω_0 los individuos tienden a mantener su opinión.
- para valores cercanos a ω_0 los individuos son más flexibles.
- para valores mayores a ω_0 los individuos son más abiertos a nuevas sugerencias y ideas anticipando los demás.
- El factor exponencial en el término de acoplamiento asegura que, para distancias recíprocas mayores a un cierto umbral, controlado por el parámetro α, no habrá influencias mutuas entre las opiniones.

Estructuras modulares jerárquicas en redes complejas

- El estudio de las redes complejas fue motivado por la necesidad de entender el comportamiento de varios sistemas reales, que van desde redes de comunicación hasta redes ecológicas, pasando por Internet, World wide web, las colaboraciones y citaciones científicas, los metabolismos y ecosistemas.
- Muchas de estas redes complejas comparten muchas propiedades topológicas tales como la existencia de caminos relativamente cortos entre cada par de nodos, coeficientes de clustering relativamente altos, correlaciones en los grados y la presencia de estructuras modulares.

Estructuras modulares jerárquicas en redes complejas

- Esta última propiedad se describe como la habilidad que tienen las redes para organizarse en comunidades o estructuras modulares, es decir, la división de los nodos (elementos) de la red en grupos dentro de los cuales las conexiones son densas, mientras que entre los distintos grupos las conexiones son escasas.
- Históricamente, la noción de comunidad, y la primera formalización de este concepto para redes, fue propuesta en las ciencias sociales [Wasserman S. and Faust K. (1994)] .

Estructuras modulares jerárquicas en redes complejas

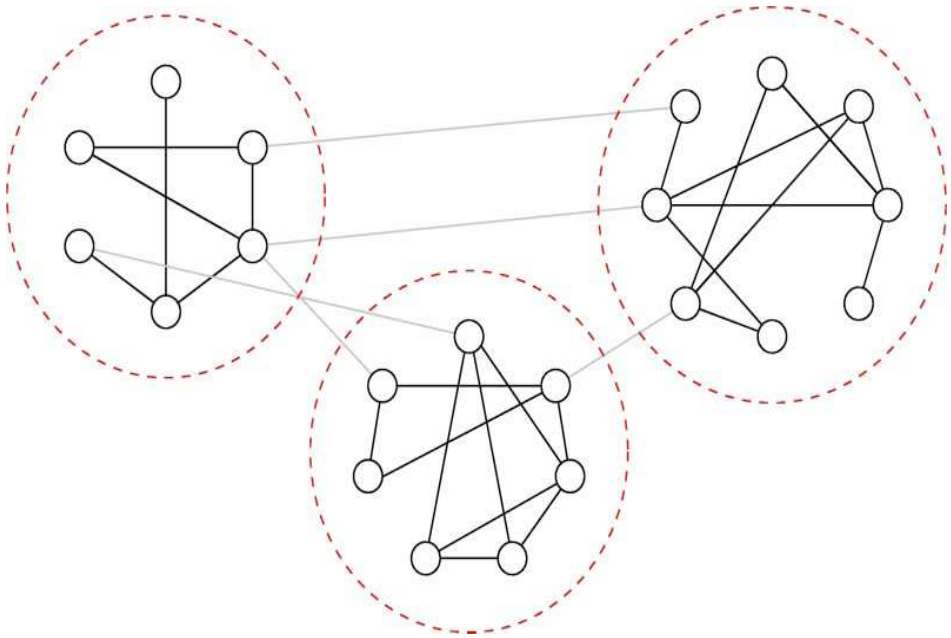

Ejemplo de una red divida en estructuras modulares. Figura tomada de la ref. [Newman M.E.J. and Girvan M. (2004)].©2004 by the American Physical Society.

Técnicas de detección de estructuras modulares

- La habilidad de detectar una estructura modular en una red podría tener aplicaciones prácticas claras. Las comunidades en una red social pueden representar agrupamientos sociales reales; en una red de citación pueden representar trabajos relacionados con un único tema; en una red metabólica pueden representar ciclos o otros agrupamientos funcionales; en la web pueden representar páginas sobre algún tema.
- El problema de detección de estructuras modulares en redes complejas es formalmente equivalente al problema clásico de particionamiento de un grafo, que consiste en encontrar la mejor partición de la red en subgrafos que representan módulos (o estructuras modulares) de acuerdo a una definición dada.

Técnicas de detección de estructuras modulares

El método tradicional para detectar la estructura de comunidad en redes (sociales) es el clustering jerárquico [Scott, J. (2000); Wasserman S. and Faust K.(1994)]. La idea básica acerca de esta técnica consiste en:

- definir una cierta medida de similitud x_{ij} entre pares (i, j) de vértives basada en la estructura de la red.
- una vez definida esta medida, entonces, partiendo de una red vacía de n vertices y ninguna arista, se añaden aristas entre pares de vertices según el orden decreciente de la similitud, empezando con el par de vertices con mayor valor de similitud.

Técnicas de detección de estructuras modulares

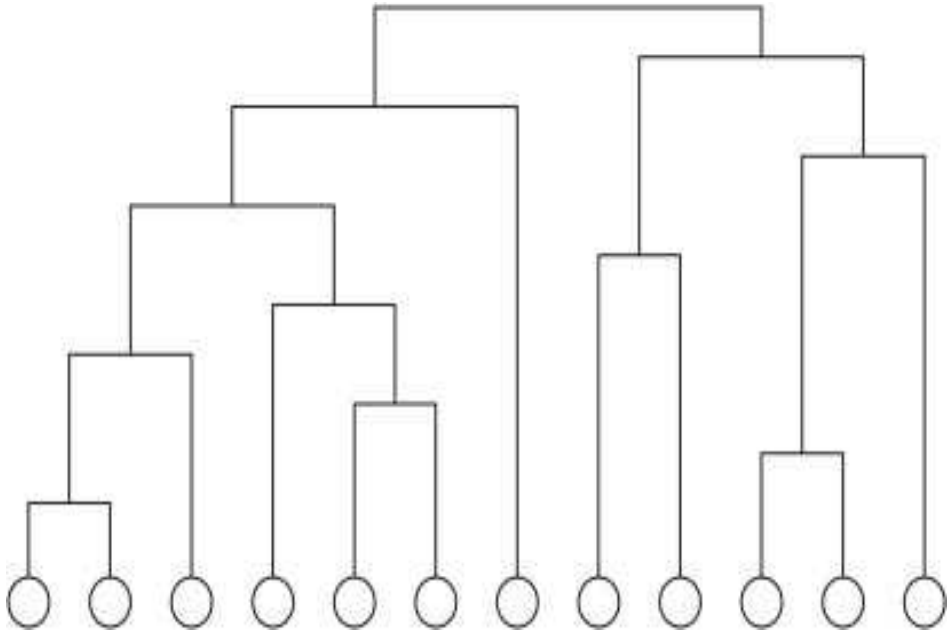

Ejemplo de un pequeño árbol (o dendrograma) de clustering jerárquico. Los círculos abajo representan los vértices en la red, y el árbol muestra el orden en el cual los vértices están agrupados para formar comunidades.

Técnicas de detección de estructuras modulares

- En muchas redes complejas la organización de los nodos no puede ser representada completamente con una única partición, sino con un conjunto de estructuras modulares que aparecen a diferentes escalas topológicas.
- El estudio de los sistemas biológicos complejos, en particular, el análisis de grandes poblaciones de osciladores acoplados, muestra que la aparición de régimenes de sincronización en estos sistemas esta estrechamente relacionado con la topología subyacente a las interacciones entre los diferentes osciladores.

Clustering dinámico y fenómeno de sincronización

Basandose el modelo OCR [Boccaletti S. et al. (2007)], se asocia a cada nodo i de un grafo no dirigido, no ponderado con N nodos y K aristas, descrito por la matriz de adyacencias $A = a_{ij}$, una variable dinámica $x_i(t) \in]-\infty, +\infty[$ descrita por el siguiente modelo:

$$\dot{x}_i(t) = \omega_i + \frac{\sigma}{\sum_{j \in N_i} b_{ij}^{\alpha(t)}} \sum_{j \in N_i} b_{ij}^{\alpha(t)} sin(x_j - x_i) \beta e^{-\beta |x_j - x_i|}$$

Clustering dinámico y fenómeno de sincronización

- donde ω_i es la frecuencia natural del nodo i. σ es el factor de acoplamiento, N_i es el conjunto de nodos adyacentes al nodo i, β es un factor que controla la interacción entre dos nodos del grafo; cuando la distancia de fase entre dos nodos supera un cierto umbral, se considera que los nodos no interactuan.
- La interacción entre dos nodos adyacentes i y j es ponderada por el término $b_{ij}^{\alpha(t)} / \sum_{j \in N_i} b_{ij}^{\alpha(t)}$, donde b_{ij} es la *betweenness* de la arista que une los nodos i, j. $\alpha(t)$ es un exponente dependiente del tiempo tal que $\alpha(0) = 0$.

Clustering dinámico y fenómeno de sincronización

La noción de betweenness, originalmente introducida para cuantificar la importancia de un individuo en una red social, es la medida estándard de relevancia de un nodo, y se conoce como node betweenness:

$$b_i = \sum_{j,k \in N, j \neq k} \frac{n_{jk}(i)}{n_{jk}}$$

donde n_{jk} el número de caminos cortos que conectan j y k, mientras $n_{jk}(i)$ es el número de caminos cortos conectando j y k y que pasan por i.

Clustering dinámico y fenómeno de sincronización

El concepto de node betweenness puede ser extendido a las aristas dando lugar a la noción de edge betweenness [Newman M.E.J. and Girvan M. (2004)]: se buscan todos los caminos cortos entre todos los pares de vértices y se cuenta cuantas veces se pasa por cada arista. Newman [Newman M.E.J. (2001)] y Brandes [Brandes U. (2001)] han propuesto un algoritmo que permite encontrar todas las betweenness en un tiempo $O(mn)$ para un grafo de m aristas y n nodos.

Clustering dinámico y fenómeno de sincronización

- Para identificar las estructuras modulares de una red compleja descrita por el modelo anterior, el algoritmo de clustering dinámico propuesto por Boccaletti consiste en fijar el valor σ de la fuerza de acoplamiento a un valor arbitrario tal que la red no ponderada ($\alpha = 0$) es completamente sincronizada, y se resuelva el modelo dinámico anterior decrementando de manera gradual el valor de α.
- Ya que las aristas conectando nodos que pertenecen al mismo módulo (o a distintos módulos) tienen, en general, una betweenness pequeña (grande), cuando α decrece, la fuerza de interacción correspondiente a estas aristas se mejora (o se degrada).

Clustering dinámico y fenómeno de sincronización

- Por otra parte, a medida que el valor de α decrece, el estado de sincronización original se divide de manera jerárquica en clusters de elementos sincronizados, de acuerdo a la jerárquia de los módulos presentes en la red.
- El procedimiento consiste entonces en monitorizar el conjunto de clusters sincronizados para cada valor de α.
- Para identificar la mejor partición del grafo, es decir, el mejor valor de α, se utiliza una medida conocida como "Modularity"Q, definida de la siguiente manera [Newman M.E.J. and Girvan M.(2004)]:

Clustering dinámico y fenómeno de sincronización

- Dada una división particular de la red en k módulos, se define una matriz simétrica e cuyos elementos e_{ij} representan la proporción de todas las aristas en la red que unen nodos en el módulo i con nodos en el módulo j (cada arista es contada sólo una vez en la matriz e_{ij}).
- La traza de esta matriz $Trace(e) = \sum_i e_{ii}$ permite calcular la proporción de aristas en la red que unen nodos que pertenecen al mismo módulo. Por tanto, la mejor división de la red en módulos le corresponde una valor alto de $Trace(e)$.

Clustering dinámico y fenómeno de sincronización

- Sin embargo, utilizar sólo la $Trace(e)$ para cuantificar la calidad de la división, no es un buen indicador.
- Entonces, se definen las sumas por fila (o columna) $a_i = \sum_j e_{ij}$, que representan la proporción de aristas que tienen conexión con nodos del módulo i.
- Finalmente, se define la Modularity Q como

$$Q = \sum_i (e_{ii} - a_i^2)$$

Clustering dinámico y fenómeno de sincronización

- Para evaluar la precisión de este método se ha considerado un conjunto de grafos generados por ordenador con una cierta estructura modular. Todos los grafos son generados con $N = 128$ nodos y $K = 1024$ aristas. Los nodos se dividen en 4 comunidades de 32 nodos cada una.
- Sea P_{in} (P_{out}) la probabilidad de que dos nodos que pertenecen al mismo módulo (o distintos módulos) están conectados.
- La probabilidad P_{out} es definida de manera que el número promedio, Z_{out}, de aristas que un nodo forma con miembros de otra comunidad, sea controlado.
- La probabilidad P_{in} es definida de manera que mantenga un valor promedio para los grados constante, es decir, $< k >= 16$.

Clustering dinámico y fenómeno de sincronización

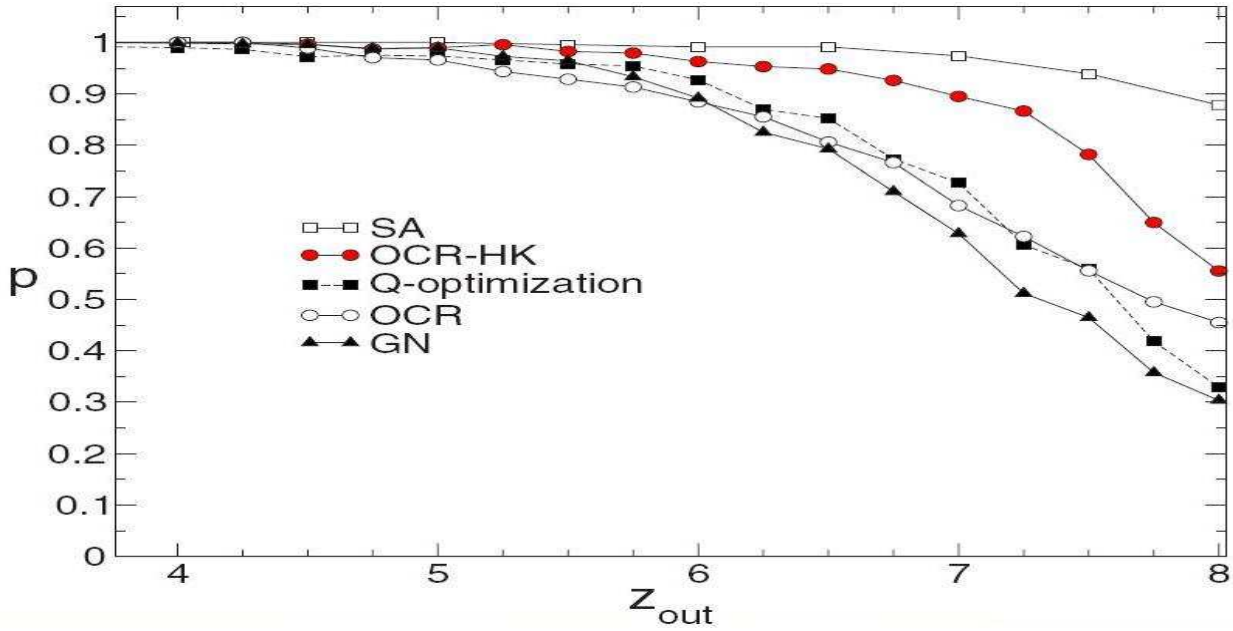

Fracción p de nodos identificados correctamente en función de z_{out}, el número promedio de aristas inter-modulares por nodo. Los resultados son obtenidos para un grafo con $N = 128$ nodos, 4 comunidades y un valor promedio de grados $< k >= 16$. [Boccaletti S. et al. 2007].©2007 by the American Physical Society.

Clustering dinámico y fenómeno de sincronización

Para testear este modelo en redes del mundo real, se ha considerado la red Zachary Karate Club formada por $N = 34$ y $K = 78$ [Zachary W.W. (1977)]. Tenemos un conocimiento a priori de los módulos existentes. Para esta red se conocen dos comunidades pequeñas.

Clustering dinámico y fenómeno de sincronización

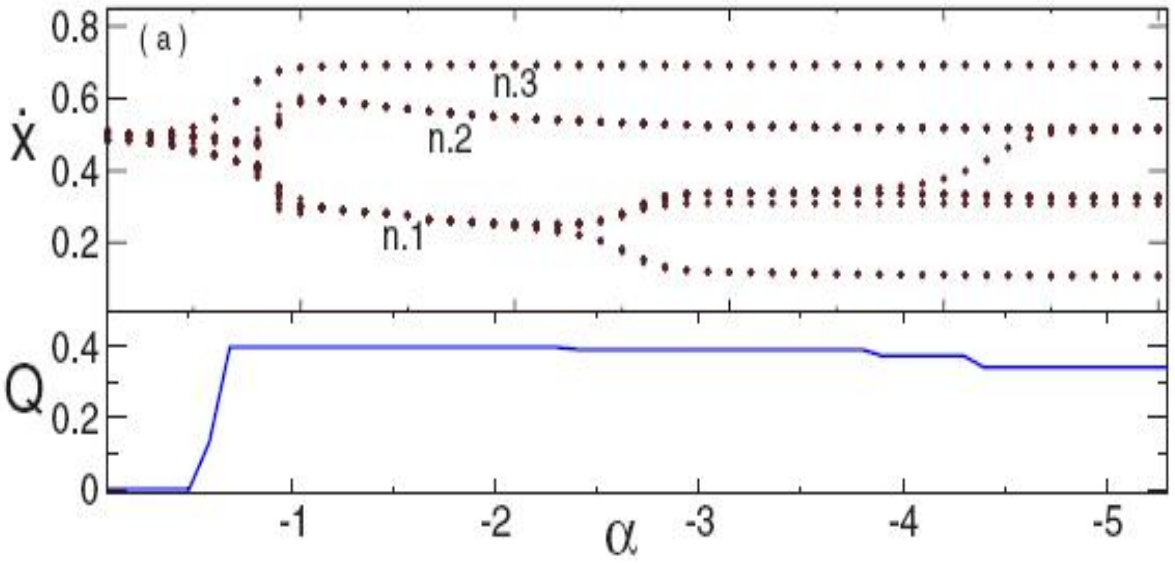

Distribución de las frecuencias instantáneas y sus correspondientes modularidades en función del factor α. El proceso de simulación se ha realizado con $\sigma = 5{,}0$ y $\delta\alpha = 0{,}1$. $n1$, $n2$ y $n3$ representan los 3 módulos detectados por el algoritmo. [Boccaletti S. et al. 2007].©2007 by the American Physical Society.

Conclusión

En este trabajo se ha presentado un algoritmo eficiente para detectar e identificar estructuras modulares en redes complejas combinando tanto información topológica como dinámica. Partiendo de un estado totalmente sincronizado de todos los nodos (o unidades dinámicas) de la red, un cambio dinámico en los pesos de las interacciones, las cuales recogen información sobre la distribución original de la Betweenness, da lugar a un clustering jerárquico progresivo que detecta de manera completa las estructuras modulares.

Referencias

1 Boccaletti S. et al. Physical Review E 75, 045102(R) (2007)

2 Arenas A. et al. Physical Review Letters 96, 114102 (2006)

3 Pluchino A. et al. Int. J. Mod. Phys. C 16, 515 (2005)

4 Juan A. Acebrón et al. Reviews of Modern Physics, 77 (2005)

5 Chavez M. et al. Physical Review Letters 94, 218701 (2005)

6 Oh E. et al. Physical Review E 72, 047101 (2005)

7 Newman M.E.J. and Girvan M., Physical Review E 69, 026113 (2004)

8 Moreno, Y. et al. Physica A (Amsterdam) 343, 279 (2004)

9 Strogatz, S.H. (2003), SYNC:the emerging Science of Spontenous Order (Hyperion, New York)

10 Boccaletti S. et al. Phys. Rep. 366, 1 (2002)

11 Réka Albert and Albert-László Barabási, Reviews of Modern Physics, 74 (2002)

Referencias

12 Wasserman S. and Faust K., Social Networks Analysis (Cambridge University Press), Cambridge, 1994

13 Pothen A. et al. SIAM J: Matrix Anal. Appl. 11, 430 (1990)

14 Newman M.E.J. Physical Review E 64, 016132 (2001)

15 Brandes U., J. Math. Sociol. 25, 163 (2001)

16 Scott, J. Social Network Analysis: A Handbook. Sage, London. 2nd edition (2000)

Comparación de técnicas de clustering para fMRI

Elsa Fernández Gómez de Segura[1]

[1]Computational Intelligence Group
Basque Country University

2nd Conference on Computational Intelligence, 2008

Contenido I

1. Introducción histórica.
2. Principios Físicos
3. MRI vs. fMRI.
4. Señal BOLD
5. Experimentos reales
6. Procesado de los datos fMRIs
7. Métodos de clustering.
8. Datos y métodos
9. Resultados
10. Bibliografía

Contenido

1 Introducción histórica.
2 Principios Físicos
3 MRI vs. fMRI.
4 Señal BOLD
5 Experimentos reales
6 Procesado de los datos fMRIs
7 Métodos de clustering.
8 Datos y métodos
9 Resultados
10 Bibliografía

Primeros experimentos

- **Joseph Francis Gall** desarrolló la teoría de la Frenología alrededor de 1800. Estableció la doctrina de la localización en partes del cerebro de varios procesos mentales.

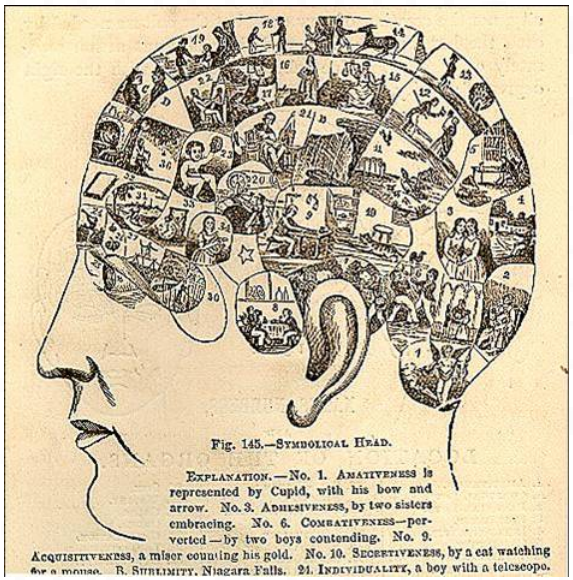

Fig. 145.—Symbolical Head.

Explanation.—No. 1. Amativeness is represented by Cupid, with his bow and arrow. No. 3. Adhesiveness, by two sisters embracing. No. 6. Combativeness—perverted—by two boys contending. No. 9. Acquisitiveness, a miser counting his gold. No. 10. Secretiveness, by a cat watching for a mouse. B. Sublimity. Niagara Falls. 21. Individuality, a boy with a telescope.

Primeros experimentos

- **Bertino's Brain:** "Un campesino italiano del siglo XIX llamado Bertino sobrevivió a un terrible accidente que le dejó sin un pedazo de cráneo y el cerebro expuesto cubierto sólo por una fina capa de tejido. Su médico, Angelo Mosso, notó otra cosa muy extraña. Cada vez que sonaban las campanas de la iglesia local, la presión sanguínea de las venas del cerebro de Bertino aumentaba. Mosso supuso que la sangre fluía más porque las campanas le recordaban a la oración. Cuando Mosso preguntó a Bertino directamente, "¿las campanas te hacen pensar en la oración?" Bertino respondió: "Sí." En ese momento las pulsaciones aumentaron en las venas expuestas. Mosso Luego preguntó: "¿Cuanto es de 8 por 12?" Bertino respondió "96." Aún más pulsaciones."

$\Downarrow$

Primera conexión entre el flujo sanguíneo y la actividad cerebral

$\Downarrow$

fMRI

Esfigmógrafo

- Esfigmógrafo: instrumento utilizado para registrar las pulsaciones arteriales.

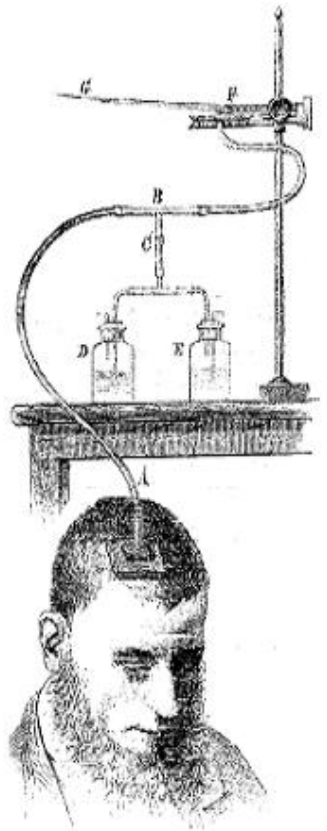

Figure: Esfigmógrafo de Mosso

Historia de las fMRIs

- **Historia de las fMRI:**
  - **1990:** Seiji Ogawa detecta variaciones en la oxigenación del tejido local al utilizar contraste dependiente del nivel de oxígeno de la sangre. Se pasó a llamar el efecto BOLD (blood oxygenation level dependent contrast).
  - **1991:** Belliveau experimenta con las primeras imágenes de resonancia magnética funcional usando un agente de contraste.
  - **1992:** John W. Belliveau, Peter Bandettini y Seiji Ogawa publican de forma independiente sus estudios sobre la respuesta cerebral a la estimulación sensorial para los que utilizan imágenes obtenidas por resonancia magnética funcional.

Incremento de las publicaciones

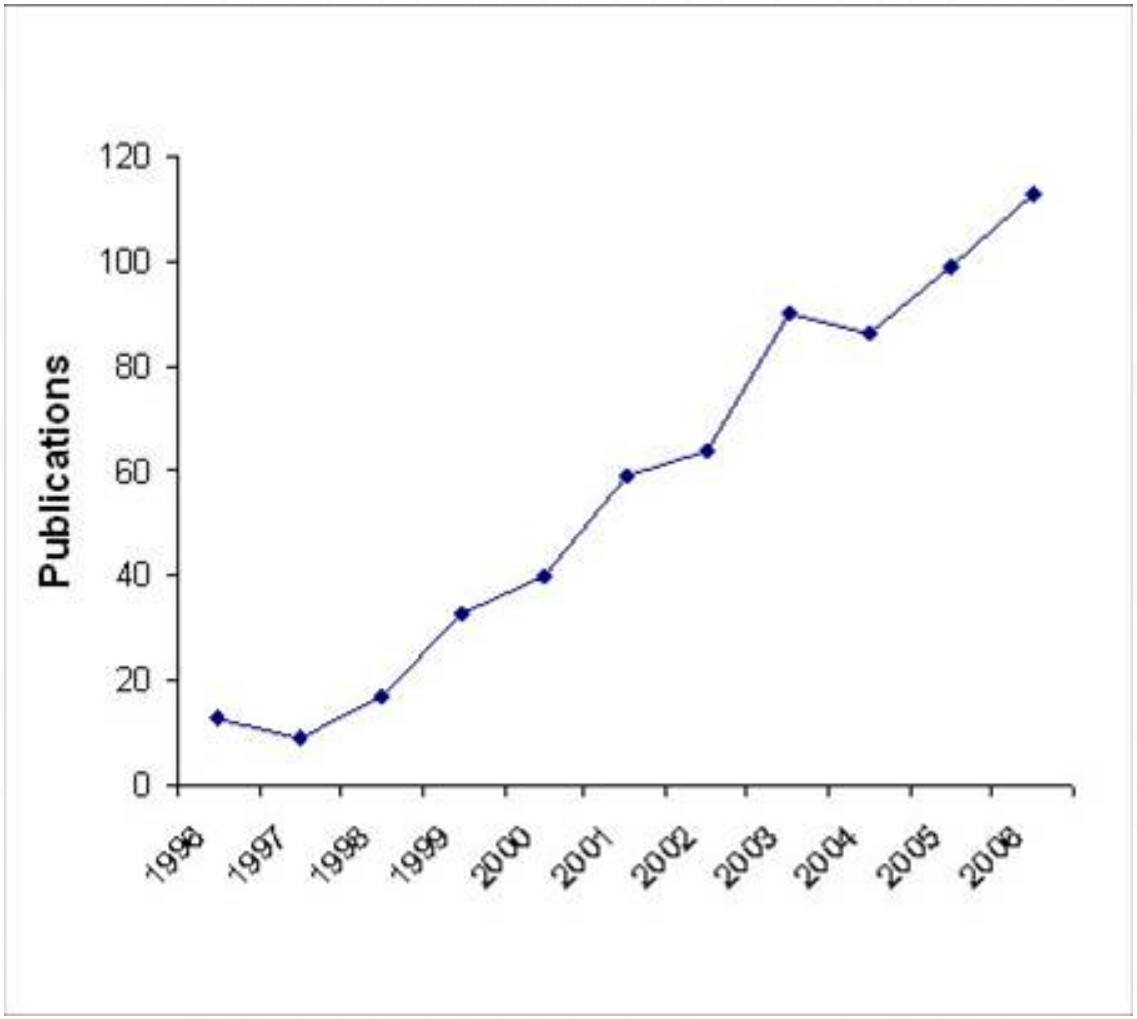

Figure: Número de artículos publicados desde 1996 con el término "fMRI" en su título.

Contenido

1. Introducción histórica.
2. Principios Físicos
3. MRI vs. fMRI.
4. Señal BOLD
5. Experimentos reales
6. Procesado de los datos fMRIs
7. Métodos de clustering.
8. Datos y métodos
9. Resultados
10. Bibliografía

Algunos términos importantes

- B_0 - se llama así al campo magnético principal también conocido como magnetización longitudinal.
  Los objetos colocados en un campo B_0 se alinearán gradualmente a este campo (relajación longitudinal)
- M_0 - se denota así al momento neto de un objeto con un B_0.
  El M_0 se produce debido a un alineamiento de los spines con un campo B_0 que es la base para crear imágenes RM.
- Pulso RF - pulso de radiofrecuencia. Para leer el M_0 producido por la presencia del campo magnetico B0 se necesita mandar un pulso RF con una cierta frecuencia y gradiente.

Algunos términos importantes

- B_0 - se llama así al campo magnético principal también conocido como magnetización longitudinal.
  Los objetos colocados en un campo B_0 se alinearán gradualmente a este campo (relajación longitudinal)
- M_0 - se denota así al momento neto de un objeto con un B_0.
  El M_0 se produce debido a un alineamiento de los spines con un campo B_0 que es la base para crear imágenes RM.
- Pulso RF - pulso de radiofrecuencia. Para leer el M_0 producido por la presencia del campo magnetico B0 se necesita mandar un pulso RF con una cierta frecuencia y gradiente.

Algunos términos importantes

- B_0 - se llama así al campo magnético principal también conocido como magnetización longitudinal.
  Los objetos colocados en un campo B_0 se alinearán gradualmente a este campo (relajación longitudinal)
- M_0 - se denota así al momento neto de un objeto con un B_0.
  El M_0 se produce debido a un alineamiento de los spines con un campo B_0 que es la base para crear imágenes RM.
- Pulso RF - pulso de radiofrecuencia. Para leer el M_0 producido por la presencia del campo magnetico B0 se necesita mandar un pulso RF con una cierta frecuencia y gradiente.

Algunos términos importantes

- B_0 - se llama así al campo magnético principal también conocido como magnetización longitudinal.
  Los objetos colocados en un campo B_0 se alinearán gradualmente a este campo (relajación longitudinal)
- M_0 - se denota así al momento neto de un objeto con un B_0.
  El M_0 se produce debido a un alineamiento de los spines con un campo B_0 que es la base para crear imágenes RM.
- Pulso RF - pulso de radiofrecuencia. Para leer el M_0 producido por la presencia del campo magnetico B0 se necesita mandar un pulso RF con una cierta frecuencia y gradiente.

Algunos términos importantes

- Imán el imán que produce el campo magnético B_0.
- Bobinas de gradiente pequeños imanes que se usan para inclinar el momento neto (M_0) del sujeto alineándolo con B_0
  Existen tres bobinas de gradiente, ortogonales entre sí para que puedan aplicarse en los planos x, y y z.
- Bobina de RF bobina de radiofrecuencia se usan para medir el M_0 cierto tiempo después de haber aplicado los pulsos RF.

Algunos términos importantes

- Imán el imán que produce el campo magnético B_0.
- Bobinas de gradiente pequeños imanes que se usan para inclinar el momento neto (M_0) del sujeto alineándolo con B_0
  Existen tres bobinas de gradiente, ortogonales entre sí para que puedan aplicarse en los planos x, y y z.
- Bobina de RF bobina de radiofrecuencia, se usan para medir el M_0 cierto tiempo después de haber aplicado los pulsos RF.

Algunos términos importantes

- Imán el imán que produce el campo magnético B_0.
- Bobinas de gradiente pequeños imanes que se usan para inclinar el momento neto (M_0) del sujeto alineándolo con B_0
  Existen tres bobinas de gradiente, ortogonales entre sí para que puedan aplicarse en los planos x, y y z.
- Bobina de RF bobina de radiofrecuencia se usan para medir el M_0 cierto tiempo después de haber aplicado los pulsos RF.

Polarización: Concepto general de RM

- La Resonancia Magnética Nuclear (RMN) es un fenómeno que ocurre cuando los núcleos de ciertos átomos son sometidos a un campo magnético.

Núcleos con espín

^{1}H, ^{15}N, ^{19}F, ^{23}Na, ^{31}P y ^{13}C

La absorción de radiación EM a una frecuencia específica por un núcleo con un momento magnético no nulo sometido a un campo magnético externo.

Polarización: Concepto general

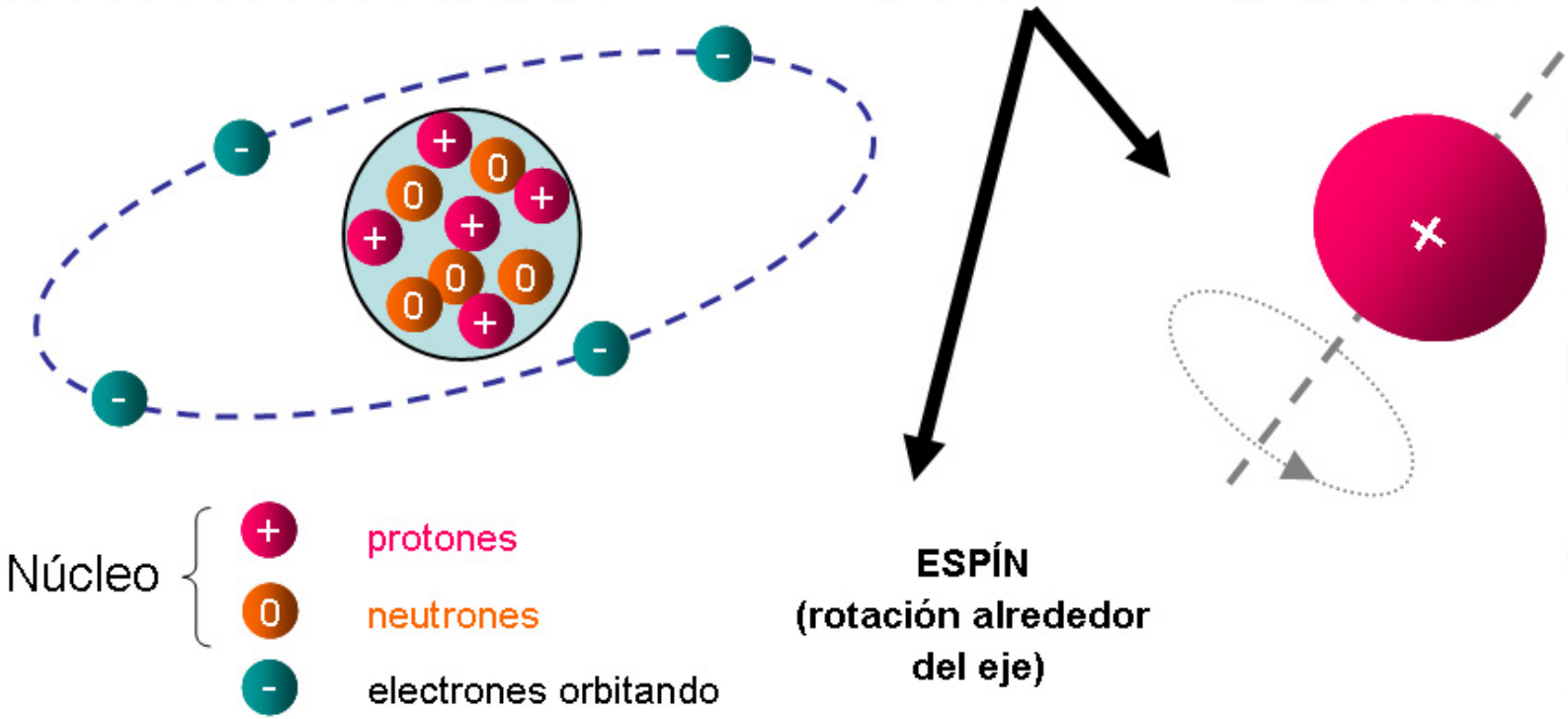

Propiedad de los espines

Sin campo magnético externo

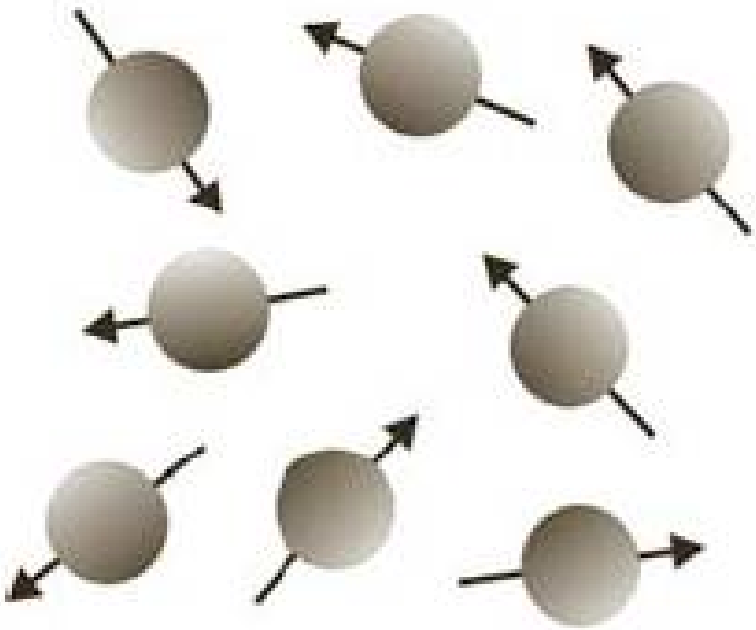

Con campo magnético externo aplicado

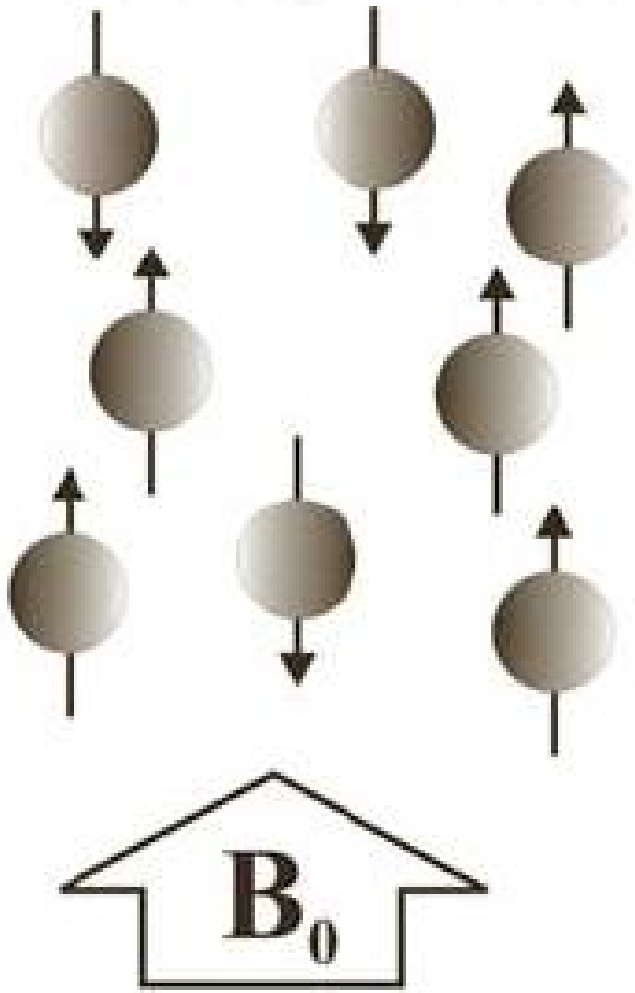

Precesión

Ley de Larmor: describe la dependencia entre el campo magnético B_0 y la frecuencia angular a la que están precesando dichos espines.

$$w_i = \gamma(B_0 + G \times r_i)$$

- w_i es la frecuencia del protón en la posición r_i
- G es un vector que representa la amplitud del gradiente y su dirección
- γ es la constante giromagnética. Para H es igual a 42.58MHz/T

Excitación

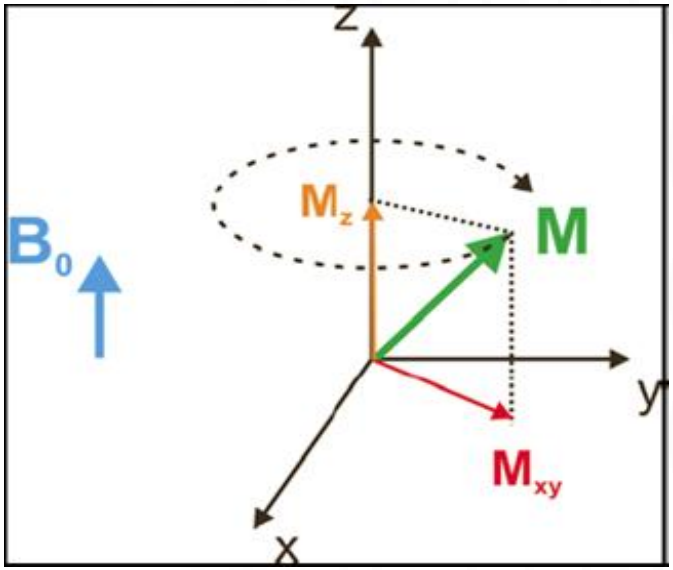

- M_z : Componente longitudinal de la magnetización M
- M_{xy} : Componente transversal de la magnetización M

Relajación: T1 y T2

- T1 mide la relajación longitudinal (a lo largo de Z) o la velocidad a la cual el objeto (y las partes que constituyen ese objeto) alcanzan el equilibrio magnético.
- T2 mide la relajación transversal (a lo largo del plano XY) o la velocidad de decaimiento (relajación) de la señal después de ser sometido al pulso RF.
- T1 recuperación al estado de equilibrio magnético
- T2 velocidad de relajación después de la excitación

Tejido	Tiempo de relajación T2 (en un imán de 1.5 T)
Sustancia blanca	70 msec
Sustancia gris	90 msec
CSF	400 msec

Relajación

- Las imágenes en T1 y T2 son inversas las unas de las otras, las T1 se usan para formar imágenes que estudien la anatomía y T2* se usa típicamente en fMRI.
- T2: descenso intrínseco de la magnetización transversal sobre una región microscópica (5-10 microns)
  - 50-100 msec (menor con un B_0 mayor)
- T2*: descenso generalizado de la magnetización transversal sobre una región macroscópica (mm)
  - desciende más rápidamente que T2.

Relajación

- Las imágenes en T1 y T2 son inversas las unas de las otras, las T1 se usan para formar imágenes que estudien la anatomía y T2* se usa típicamente en fMRI.
- T2: descenso intrínseco de la magnetización transversal sobre una región microscópica (5-10 microns)
  - 50-100 msec (menor con un B_0 mayor)
- T2*: descenso generalizado de la magnetización transversal sobre una región macroscópica (mm)
  - desciende más rápidamente que T2.

Relajación

- Las imágenes en T1 y T2 son inversas las unas de las otras, las T1 se usan para formar imágenes que estudien la anatomía y T2* se usa típicamente en fMRI.
- T2: descenso intrínseco de la magnetización transversal sobre una región microscópica (5-10 microns)
  - 50-100 msec (menor con un B_0 mayor)
- T2*: descenso generalizado de la magnetización transversal sobre una región macroscópica (mm)
  - desciende más rápidamente que T2.

Relajación

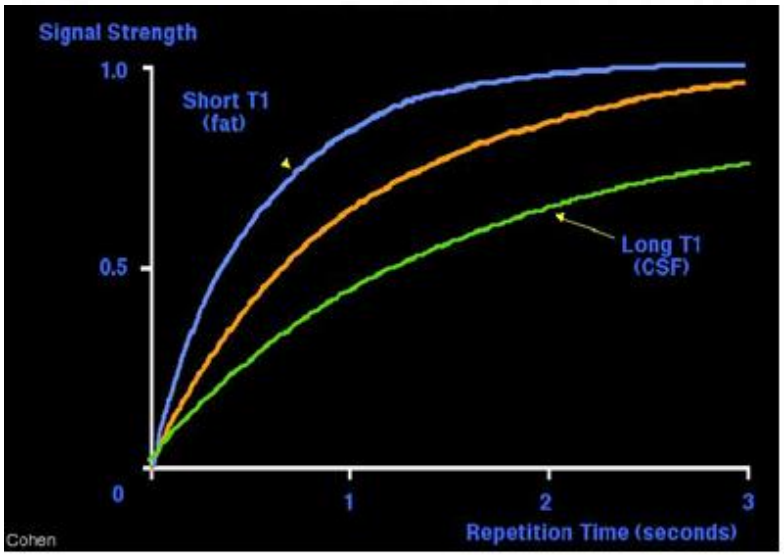

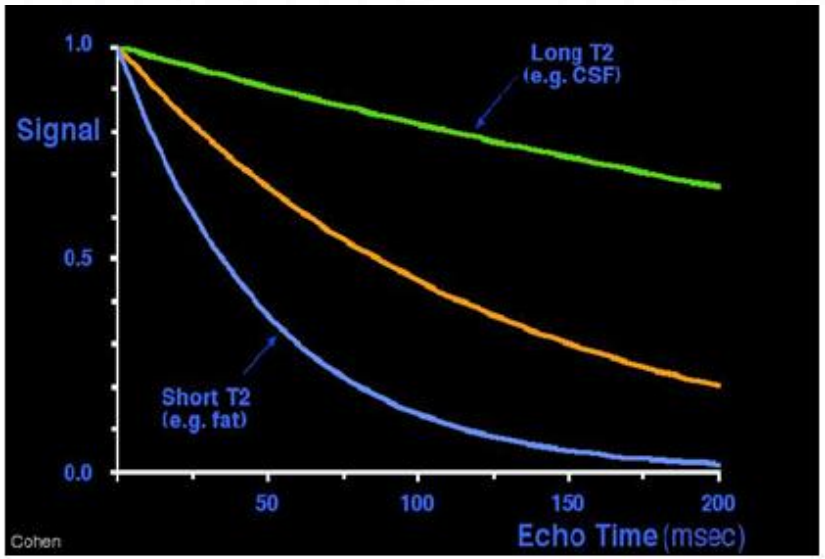

T1 mide la velocidad con la que los protones se realinean con el campo magnético principal

T2 mide la velocidad con la que los protones emiten energía al volver al equilibrio.

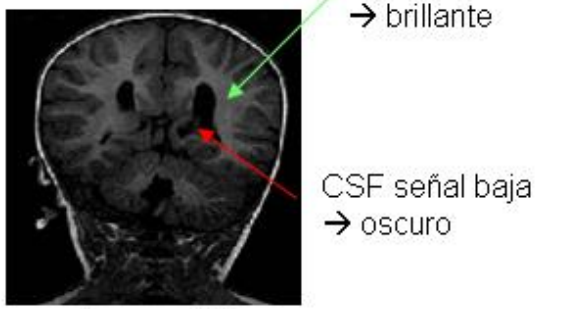

Imagen T1

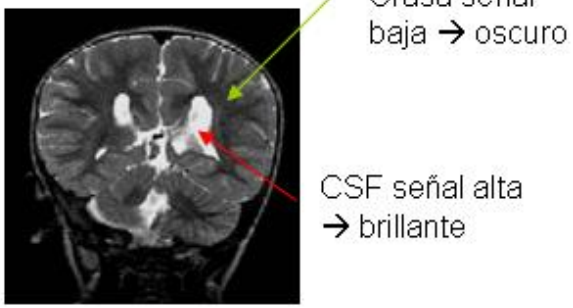

Imagen T2

Generación de la imagen

- La imagen se genera digitalizando y almacenando las distintas señales de eco de radiofrecuencia.
- Se almacenan por filas en un espacio denominado K, cuyas dimensiones son:
  - Filas (Ky) : Representan la fase de la señal
  - Columnas (Kx) : Representan la frecuencia de la señal
- Mediante transformaciones de Fourier se pasa a imagen.

Generación de la imagen

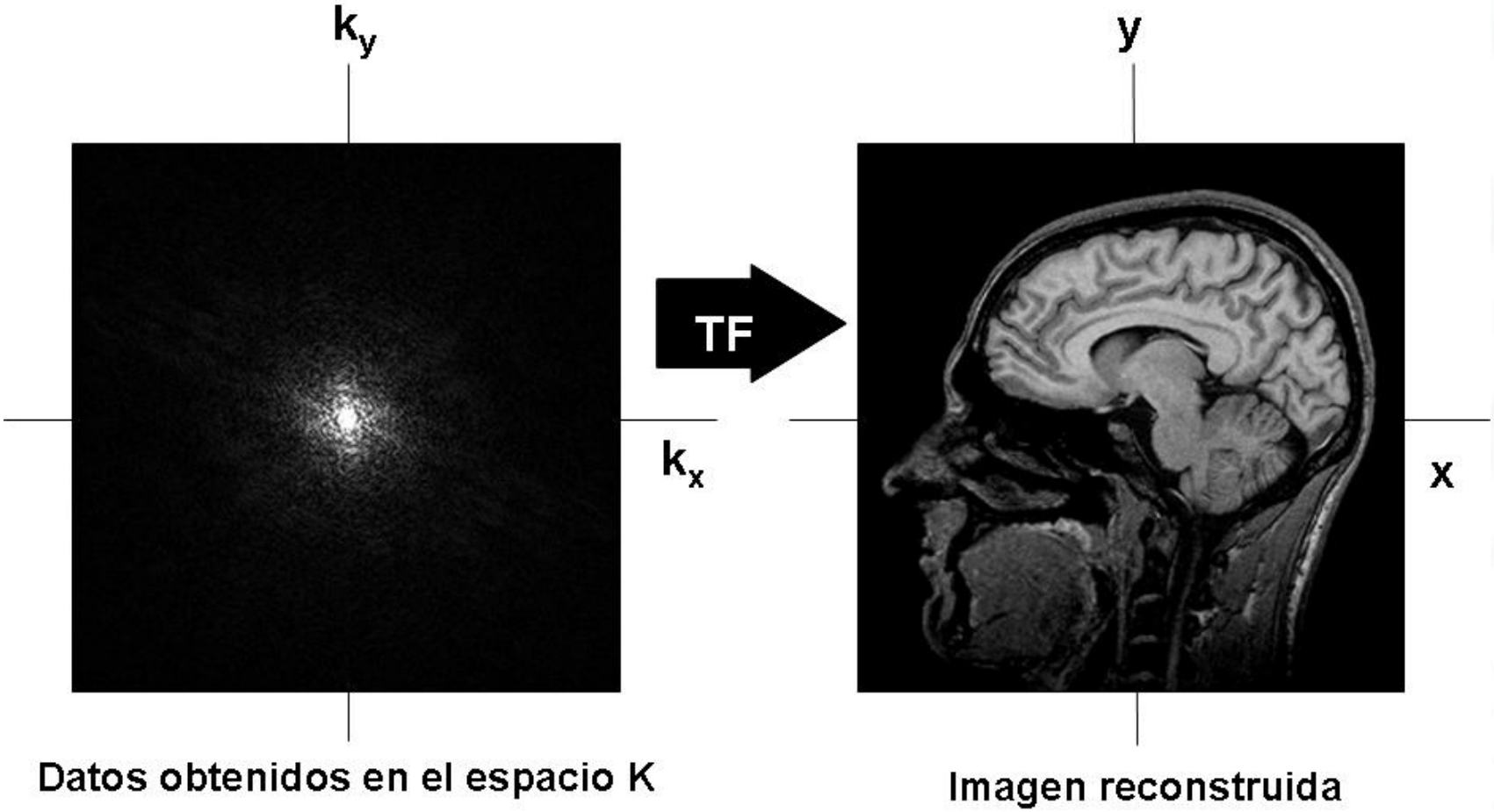

Contenido

1. Introducción histórica.
2. Principios Físicos
3. MRI vs. fMRI.
4. Señal BOLD
5. Experimentos reales
6. Procesado de los datos fMRIs
7. Métodos de clustering.
8. Datos y métodos
9. Resultados
10. Bibliografía

MRI vs. fMRI.

MRI

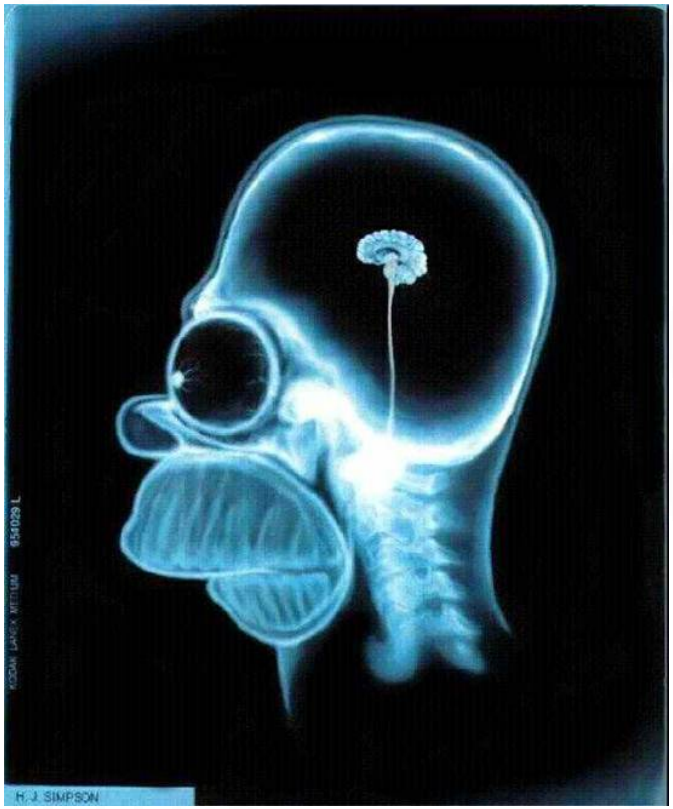

Estructuras anatómicas

MRI funcional

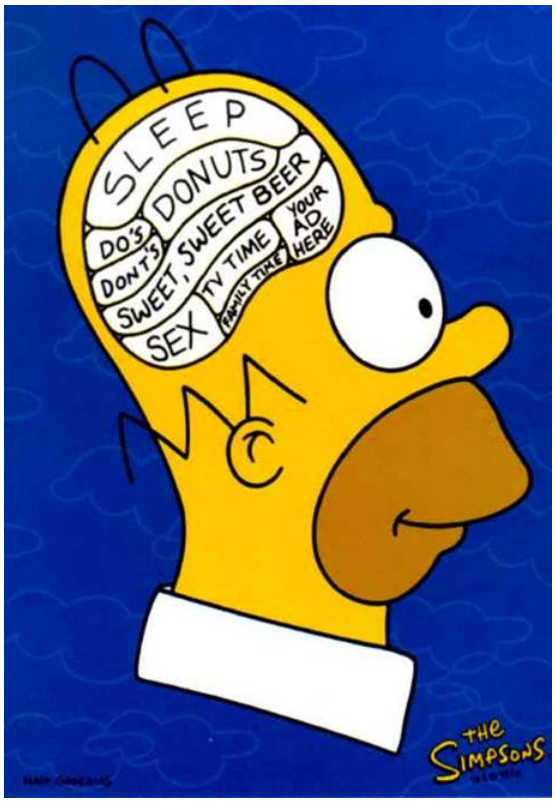

Funciones metabólicas

MRI vs. fMRI.

MRI	fMRI
Alta resolución espacial	Baja resolución espacial
Estudio de Estructuras Anatómicas	Estudio de funciones metabólicas
Sensible al B_0	Muy sensible a la elección del B_0(1,5 o 3T)
Imágenes en T1, T2 y PD	Imágenes en T2*

MRI vs. fMRI.

Alta resolución
(1 mm)

MRI

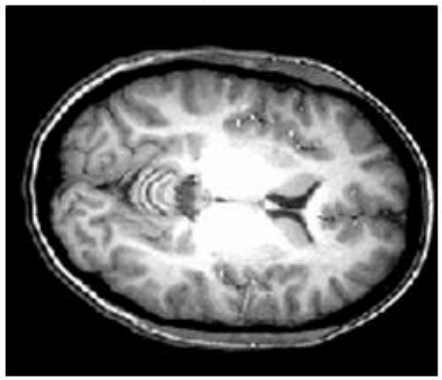

Una imagen

fMRI

Baja resolución
(~3 mm)

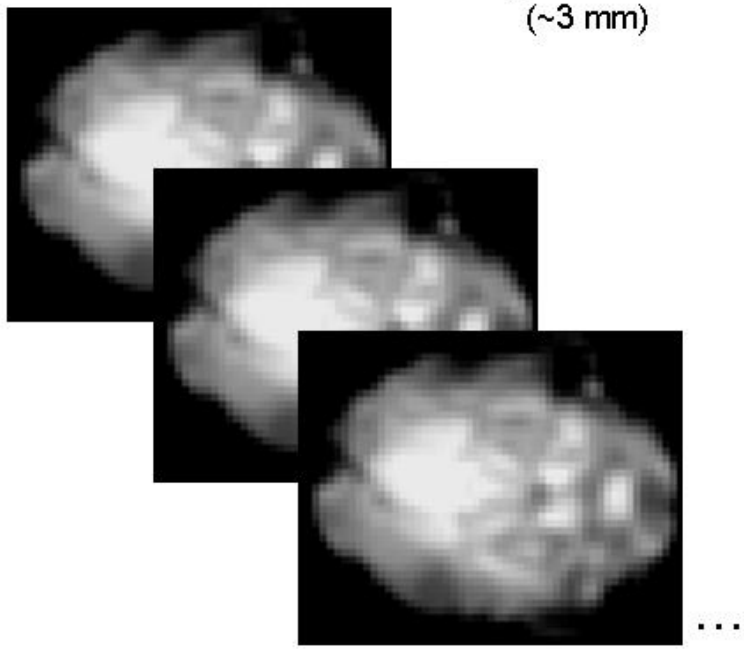

...

Muchas imágenes
(p. ej., cada 2" durante 5')

Contenido

1. Introducción histórica.
2. Principios Físicos
3. MRI vs. fMRI.
4. Señal BOLD
5. Experimentos reales
6. Procesado de los datos fMRIs
7. Métodos de clustering.
8. Datos y métodos
9. Resultados
10. Bibliografía

Señal BOLD

Blood Oxygen Level Dependent signal

Señal dependiente del nivel de oxigenación de la sangre

↑ actividad neuronal →↑ flujo sangre →↑ oxihemoglobina →↑ T2* →↑ Señal MR

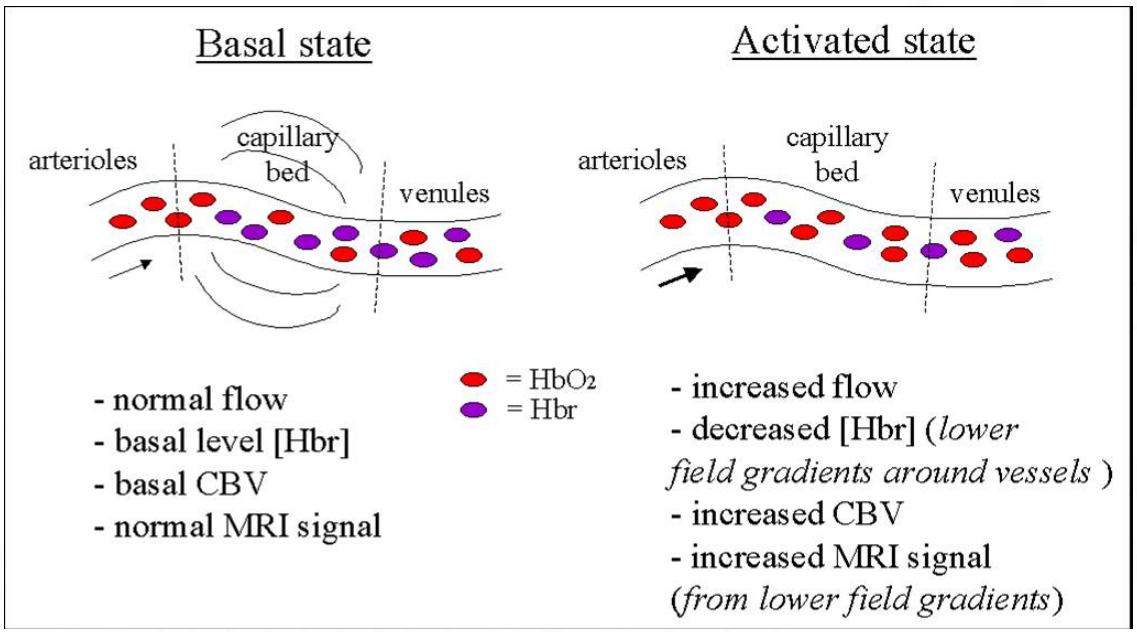

Proceso metabólico: BOLD

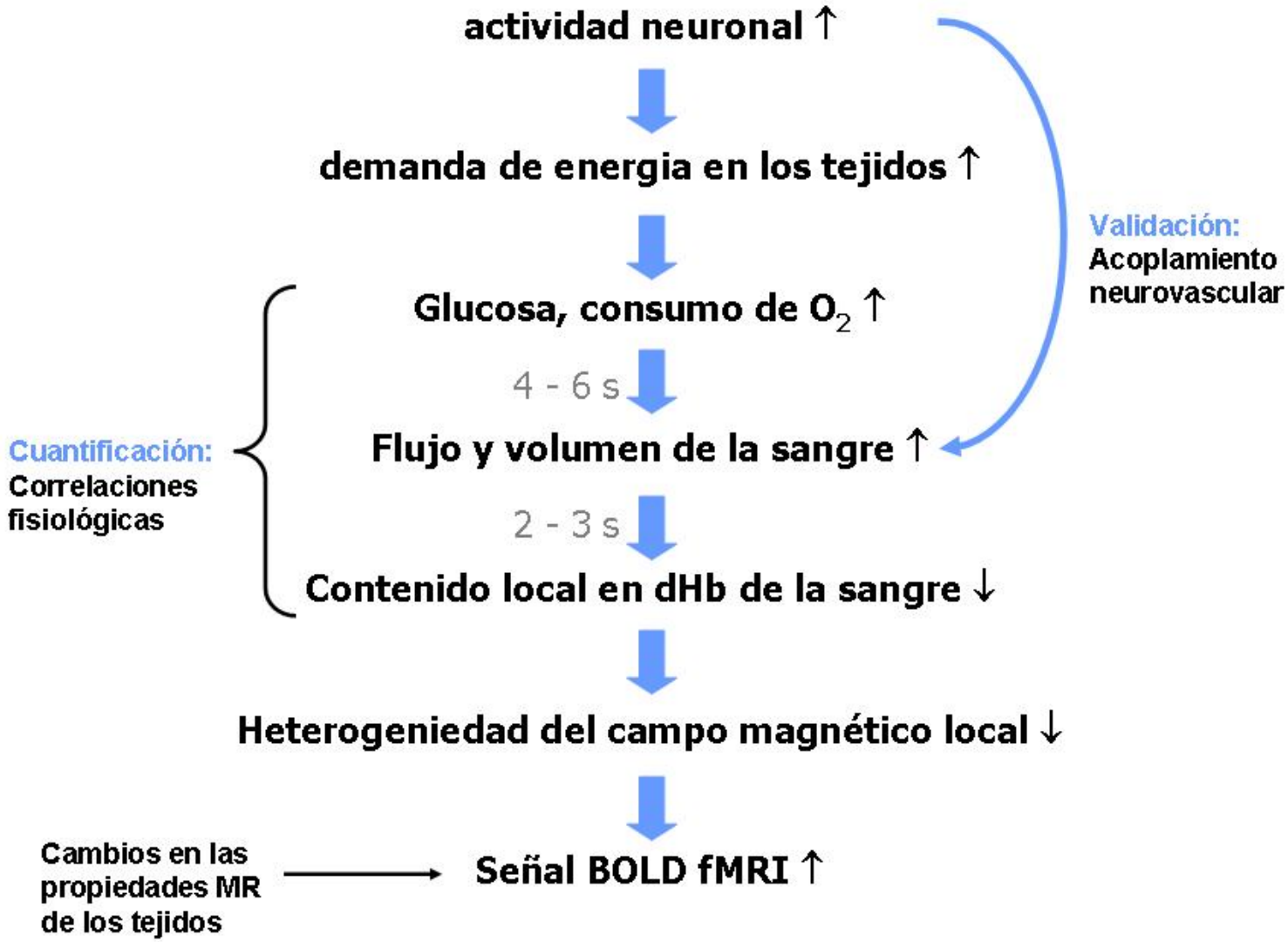

Señal BOLD

- La susceptibilidad magnética (χ) se refiere a la respuesta magnética de un material colocado en un campo B_0.
  Las células sanguíneas muestran un cambio en χ durante la activación.
- Básicamente, la oxihemoglobina en los glóbulos rojos (HbO_2) se transforma en deoxihemoglobina (Hb):
  - Se vuelve paramagnética.
  - La susceptibilidad es diferente en el complejo vascular y en sus alrededores. (la susceptibilidad induce cambios en el campo).

Señal BOLD

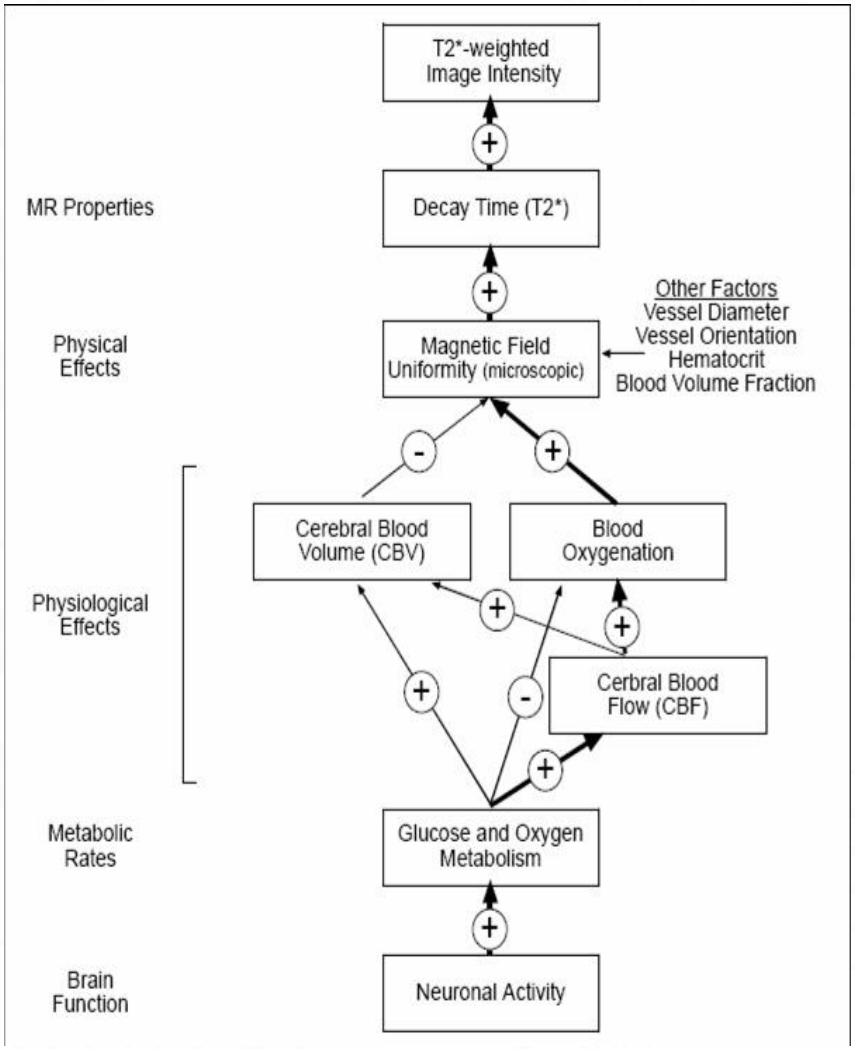
T2*-weighted
Image Intensity
MR Properties
Decay Time (T2*)
Other Factors
Vessel Diameter
Vessel Orientation
Hematocrit
Blood Volume Fraction
Physical
Effects
Magnetic Field
Uniformity (microscopic)
Cerebral Blood
Volume (CBV)
Blood
Oxygenation
Physiological
Effects
Cerbral Blood
Flow (CBF)
Metabolic
Rates
Glucose and Oxygen
Metabolism
Brain
Function
Neuronal Activity

Señal BOLD
Función de respuesta hemodinámica

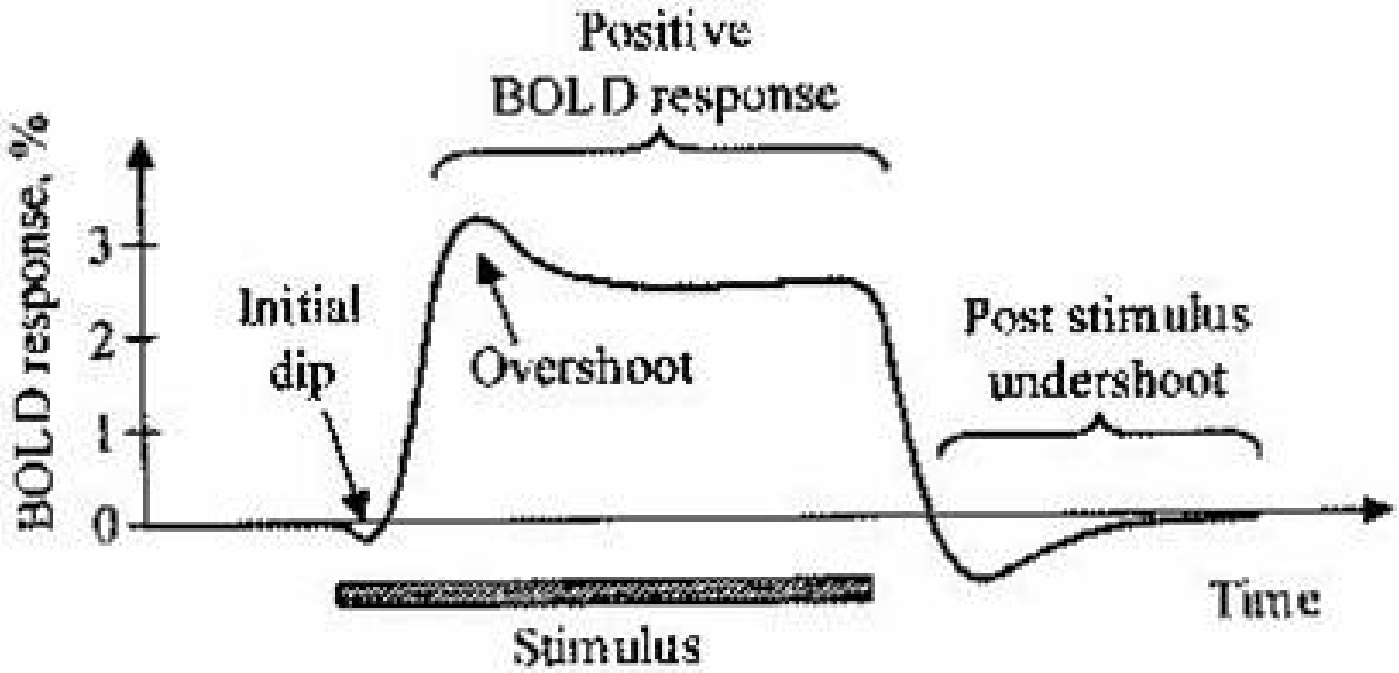

Señal BOLD: T2*

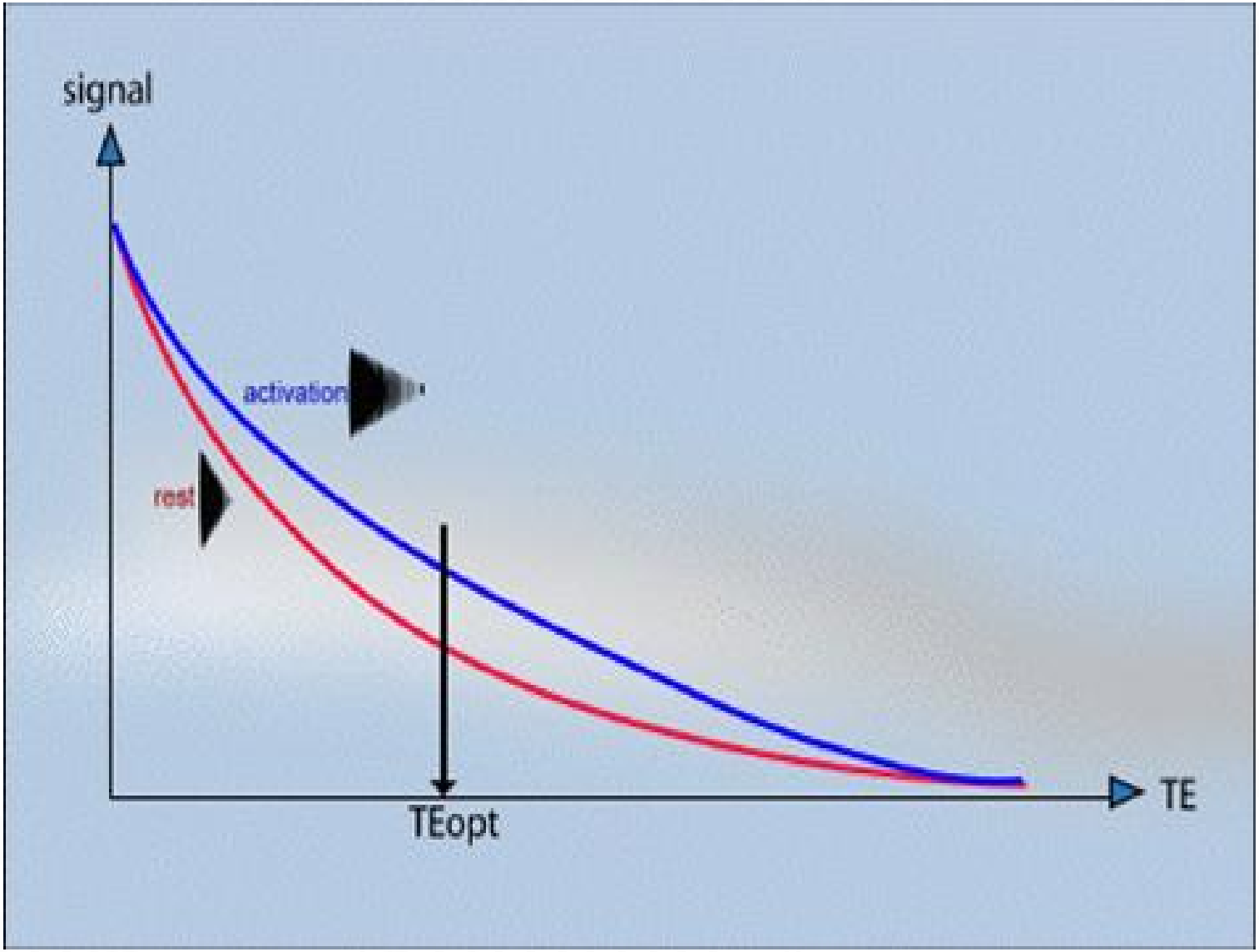

Contenido

1. Introducción histórica.
2. Principios Físicos
3. MRI vs. fMRI.
4. Señal BOLD
5. Experimentos reales
6. Procesado de los datos fMRIs
7. Métodos de clustering.
8. Datos y métodos
9. Resultados
10. Bibliografía

Experimentos reales

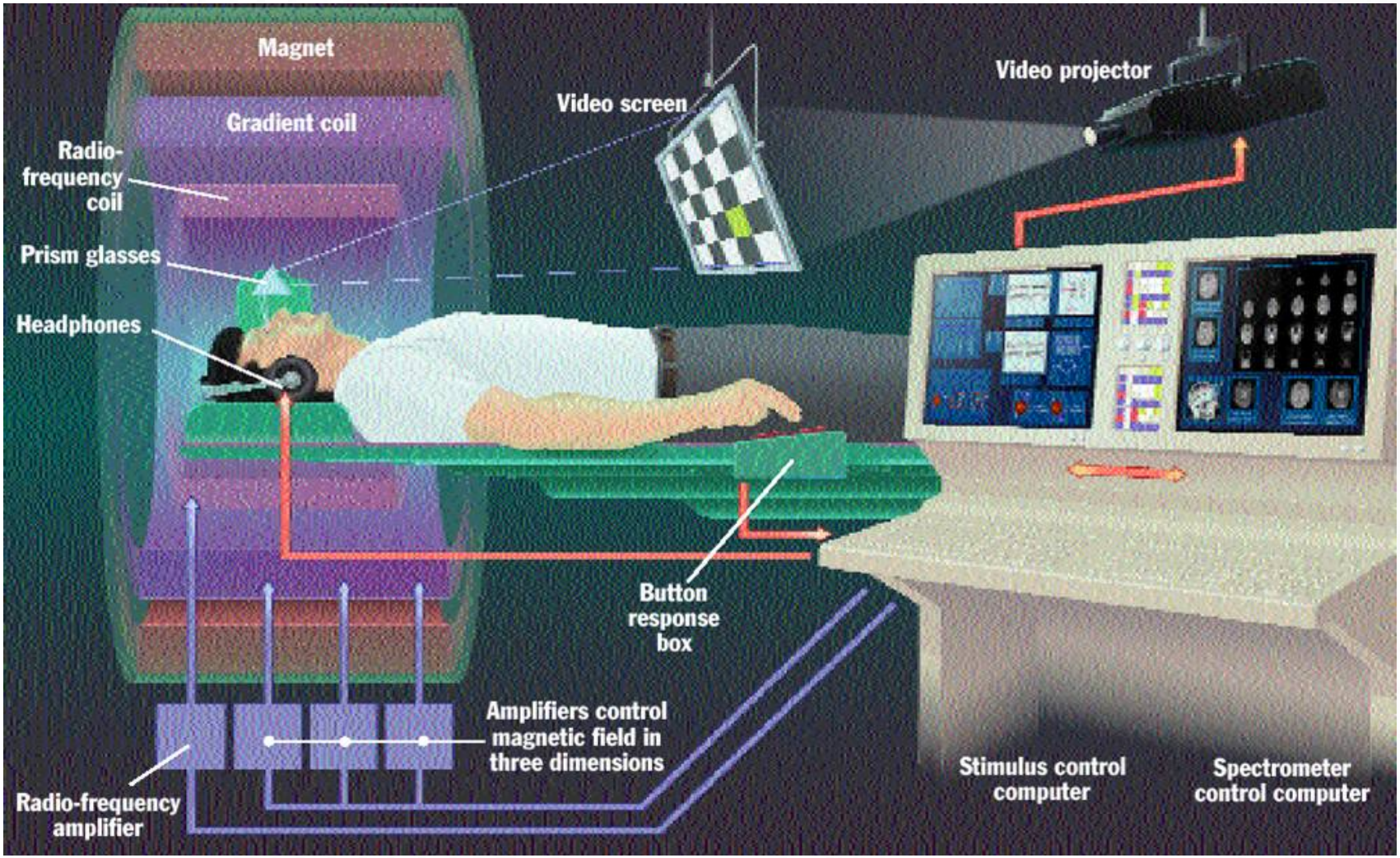

Experimentos reales I

Proceso:

1. Preparar al sujeto
   - Formulario de consentimiento informado.
   - Evaluación de seguridad.
   - Instrucciones.
2. Shimming (ajuste del campo magnético)
   - Colocar el cuerpo en un campo magnético
   - Ajuste a las 3 bobinas ortogonales para hacer el campo magnético lo más homogéneo y uniforme posible.
3. Sagitales Tomar imágenes en una linea media para planear los cortes.

Experimentos reales I

5. Toma de imágenes anatómicas en T1

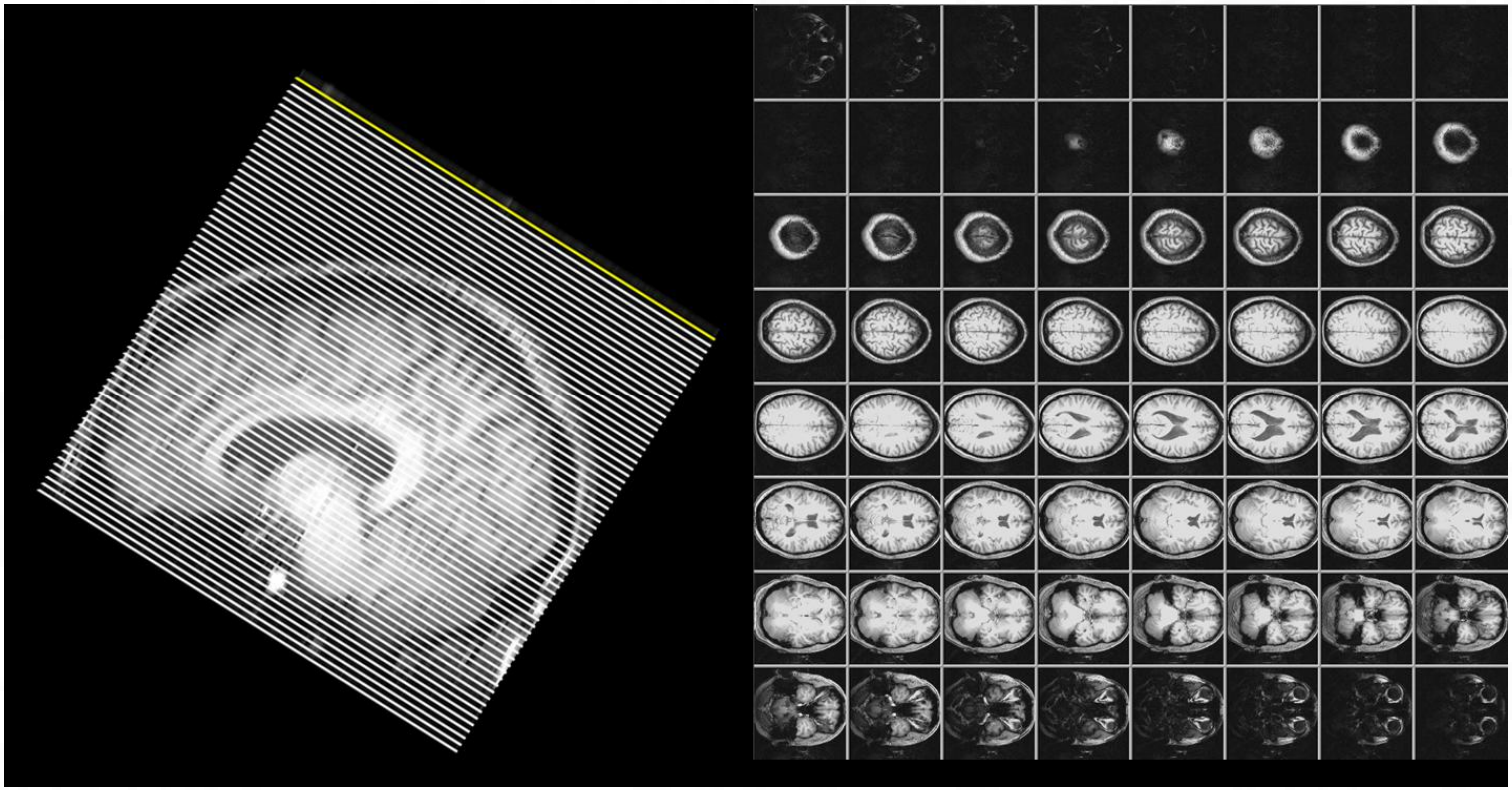

Experimentos reales

6. Toma de imágenes funcionales en T2*
   - Las imágenes están relacionadas indirectamente con la actividad neuronal
   - Son de baja resolución (3x3x5 mm.)
   - Todos los cortes a la vez= volumen
   - Muestrear muchos volúmenes (puntos en el tiempo)(P.Ej., un volumen cada 2 seg.)
   - Datos 4D: 3 espaciales, 1 temporal.

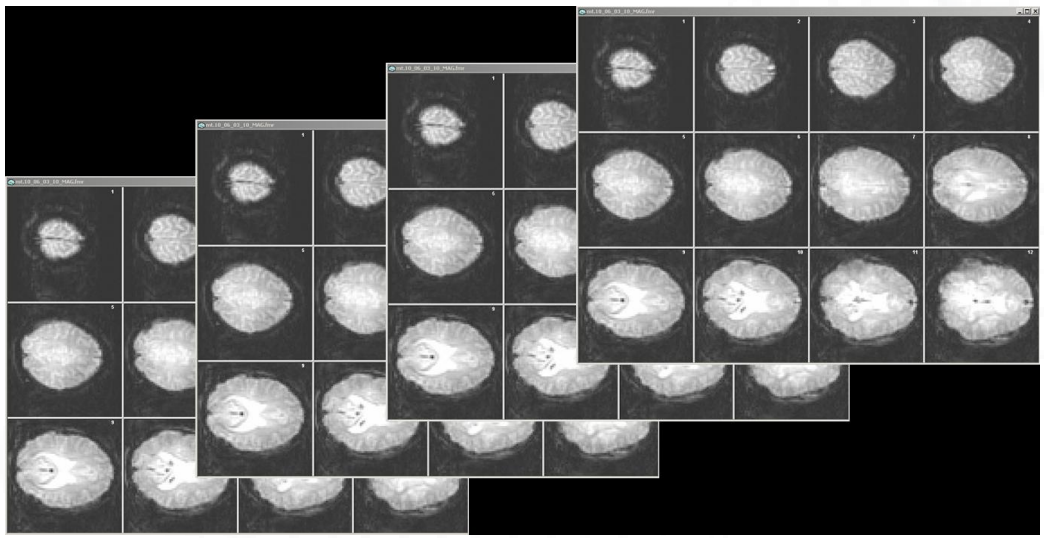

Experimentos reales

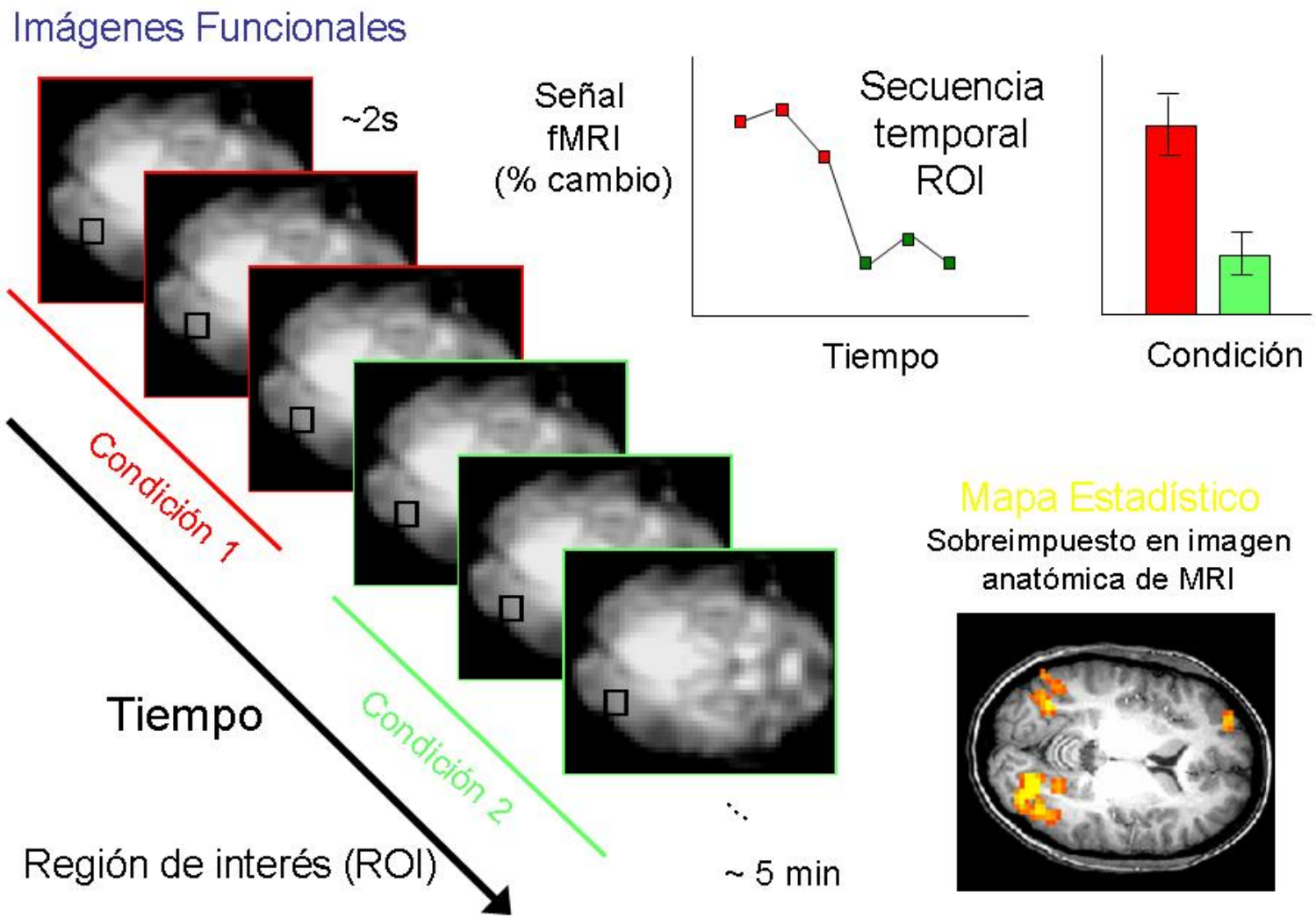

Diseño de paradigmas:Ejecuciones

Sesión: todos las imágenes escaneadas obtenidas de un sujeto en un día.

Ejecución (o escaneo): un periodo continuo de escaneo (5-7 min).

Experimento: conjunto de condiciones que se tienen que comparar unas con otras.

Condición: un conjunto de estímulos o una tarea.

Contenido

1 Introducción histórica.
2 Principios Físicos
3 MRI vs. fMRI.
4 Señal BOLD
5 Experimentos reales
6 Procesado de los datos fMRIs
7 Métodos de clustering.
8 Datos y métodos
9 Resultados
10 Bibliografía

Preprocesado

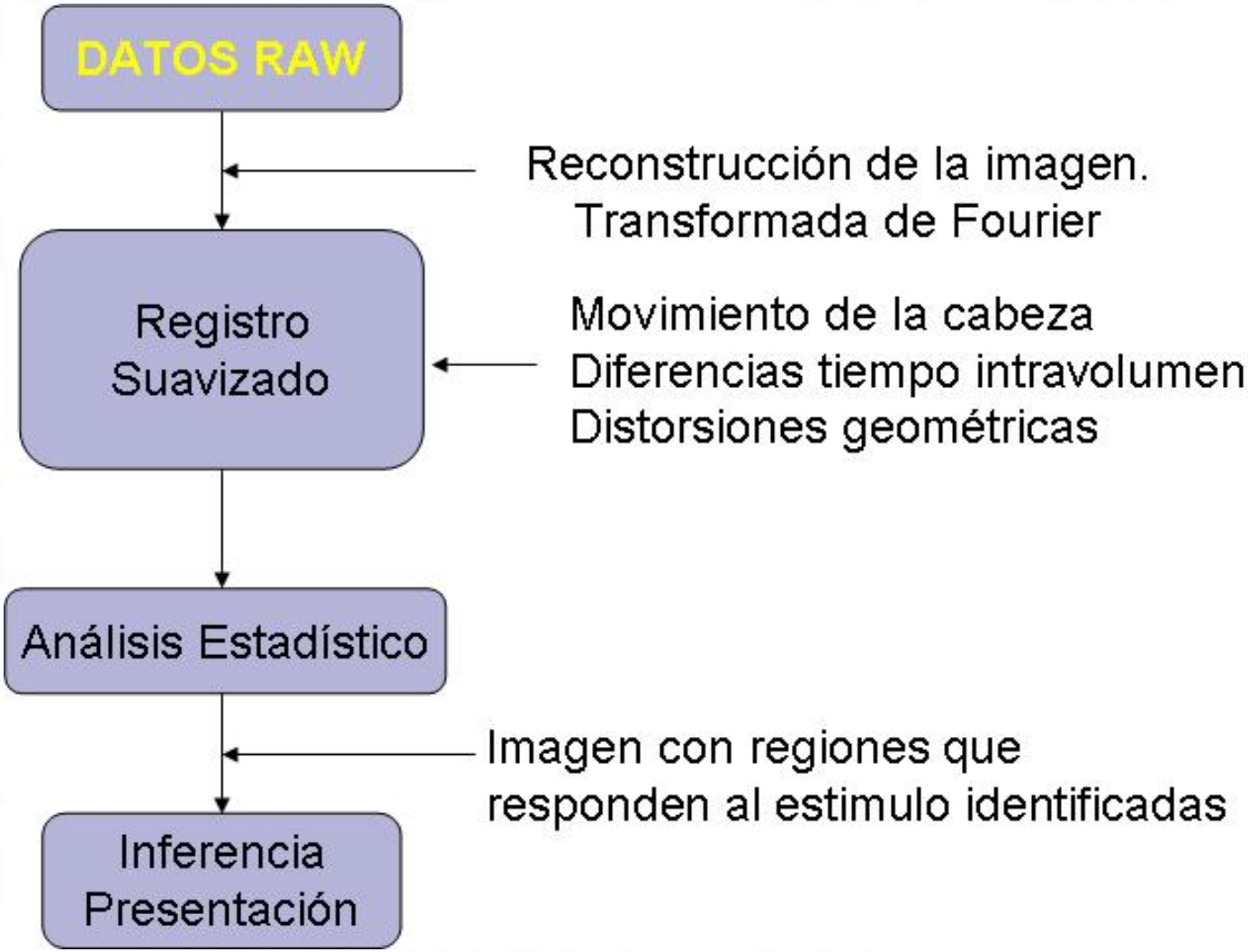

Preprocesado:Análisis Estadístico

- Técnicas de substracción.
- Técnicas de correlación.
- Modelo lineal general.
- Test de Hipótesis (T-test).
- Análisis de Varianza (Anova).
- Otras técnicas de Análisis:
  - PCA, ICA.
  - Fuzzy clustering
  - Redes Neuronales

Contenido

1. Introducción histórica.
2. Principios Físicos
3. MRI vs. fMRI.
4. Señal BOLD
5. Experimentos reales
6. Procesado de los datos fMRIs
7. Métodos de clustering.
8. Datos y métodos
9. Resultados
10. Bibliografía

Introducción

fMRI:

- Evaluación de la actividad cerebral (variaciones hemodinámicas locales)
- Método óptimo que combina resolución espacial y temporal para el mapeo de la actividad cerebral.
- Métodos estadísticos basados en el modelo que estiman la función de respuesta hemodinámica (HRF)

Introducción

Metódos de análisis:

- Exploratory data analysis (EDA):
  No necesitan información a priori y pueden identificar artefactos pero producen degradación de la calidad de los datos. Se usan para estimar respuestas cerebrales inesperadas o donde los modelos biofísicos son muy complejos.
- Cluster Analysis: identifica regiones con un patrón de activación similar.

Motivación Clustering fMRI

Cada vez que hay una activación, sucede en un grupo de píxeles, no en uno sólo.

Contenido

1. Introducción histórica.
2. Principios Físicos
3. MRI vs. fMRI.
4. Señal BOLD
5. Experimentos reales
6. Procesado de los datos fMRIs
7. Métodos de clustering.
8. Datos y métodos
9. Resultados
10. Bibliografía

Datos fMRI típicos

Dos tipos de datos:

- Simulados:
  Serie temporal (35 instancias) de cortes transversales cerebrales (128x128) con texturas invariantes en el tiempo y 3 regiones de activación (49 píxeles).
- Híbridos:
  Una serie de 140 imágenes reales MRI a las que se han añadido la activación artificialmente(5x5 píxeles) con una relación contraste-ruido (CNR) de 2, 1.66, 1.33.

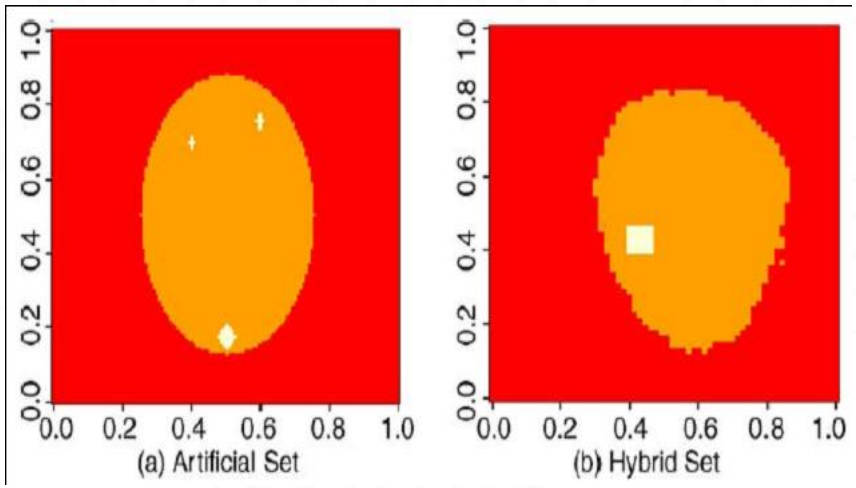

Hierarchical Clustering

Procedimiento:

1. El primer paso es calcular las distancias entre todos los pares de objetos. Esto es lo mismo que asumir que cada objeto constituye un cluster: C1, ...,CN(N clusters iniciales).
2. Encontrar el par de clusters más cercano y fusionarlos en un sólo cluster.
3. Calcular de nuevo las distancias entre el nuevo cluster y los demás.
4. Repetir los pasos (2) y (3) hasta que todos los puntos estén clasificados en un cluster de tamaño N.

Hierarchical Clustering

- Se utiliza la fórmula de semejanza de Lance-Williams

$$\Omega(K_{ij}, K_t) = \alpha(i) \cdot \Omega(K_i, K_t) + \alpha(j) \cdot \Omega(K_j, K_t) + \beta \cdot \Omega(K_i, K_j) + \gamma \cdot |\Omega(K_i, K_t) - \Omega(K_j, K_t)|$$

- En el paso 3 se utiliza el **single link** que considera la distancia entre clusters como la mínima distancia entre los miembros de los dos clusters.

Hierarchical Clustering

Dendrogramas:Ejemplo en Matlab.

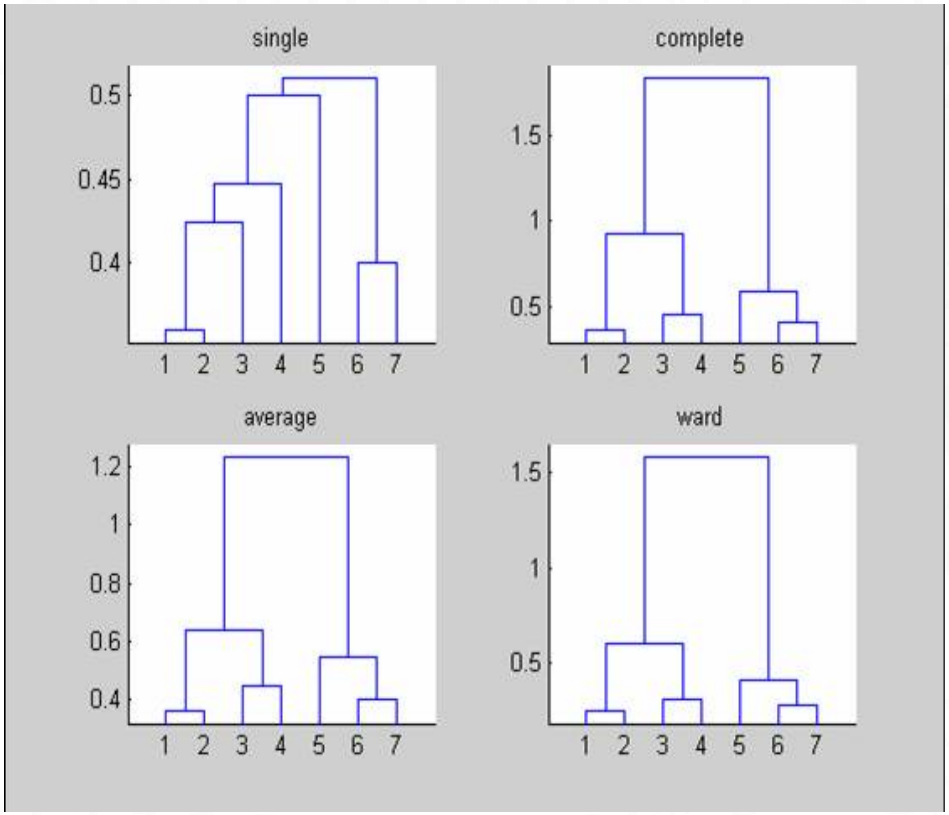

Figure: Tipos de linkaje

Crisp clustering

Algoritmos comparados:

- Maximin-distance
- K-means
- CLARA
- Hard competitive learning
- Neural Gas
- SOM

Maximin-distance

Algoritmo:

1. Inicializar el conjunto $C = \{c_1, c_2, ..., c_k\}$ $(K << N)$ con sólo un vector central w_{cj} elegido aleatoriamente del conjunto de datos y calcular la distancia de ese punto a todos los demás del conjunto.
2. Encontrar el punto más alejado que pasa a ser el próximo centro del cluster.
3. Calcular las distancias entre cada punto restante a los centros encontrados. Nos quedamos con la distancia mínima y buscamos el máximo entre esas distancias mínimas. Si la distancia es mayor que un umbral predefinido ese punto pasa a ser el nuevo centro.
4. Repetir hasta que la distacia máxima en un paso no cumpla la condicion de creación de un nuevo cluster o hasta que se alcance un número de clusters deseado.

K-means

Algoritmo:

1. Inicializar el conjunto $C = \{c_1, c_2, ..., c_k\}$ $(K << N)$ con sólo un vector central w_{cj} elegido aleatoriamente del conjunto de datos y calcular la distancia de ese punto a todos los demás del conjunto.
2. Calcular el centro de todos los clusters.
3. Generar una nueva partición del conjunto de datos correspondiedo cada punto con el cluster donde la distancia al centro sea la más cercana.
4. Si las particiones cambian ir al paso (2), sino parar.

Clustering Large Applications:CLARA

Tiene dos fases: la primera se basa en el algoritmo k-medioides (PAM). Se extrae una muestra de los datos que posteriormente es clasificada en k clusters mediante el PAM. Cada punto que no pertenezca a la muestra se asigna al representante más cercano.

1. Coger un punto x_i (no seleccionado aún).
2. Considerar un punto x_j no seleccionado y calcular la diferencia entre su disimilaridad D_j con el más similar elegido previamente y su disimilitud d(i,j) con el punto x_j.
3. Si la diferencia es positiva, x_j contribuye a la decisión de seleccionar x_i. $C_{ij} = max(D_j - d(i,j), 0)$.
4. El coste total por seleccionar x_i es :$\sum_j C_{ji}$.
5. Elegir el x_i que maximice $max_i \sum_j C_{ji}$. Parar cuando se hayan elegido los k medoides.

Clustering Large Applications:CLARA

Segunda fase: una vez seleccionados los medoides, se obtiene una mejora considerando todos los pares de puntos (x_i, x_l) donde x_i es un punto representativo y x_l no lo es. Como medida de disimilaridad se usa la distacia euclídea.
El tiempo de computación y el espacio en disco requerido para conjuntos de datos grandes hacen que este algoritmo sea impracticable.

Hard competitive learning (hardcl)

Es un algoritmo online estocástico de descenso por el gradiente que minimiza la distacia media de un conjunto de datos a su centro más cercano.
Algoritmo:

1. Inicializar el conjunto $C = \{c_1, c_2, ..., c_k\}$ $(K << N)$ con sólo un vector central $w_{cj} \in \Re^d$ elegido aleatoriamente del conjunto de datos. Inicializar el contador t=0.
2. Extraer un patrón de entrada x_i del conjunto de datos.
3. Seleccionar el ganador $s(x_i)$:

$$s(x_i) = argmin_c \|x_i - w_c\|$$

4. Mover el vector centro del ganador a lo largo del gradiente de $\|x_i - w_c\|$ hacia x_i. En el caso de la norma euclídea, esto es $_{s(x_i)} = \varepsilon(x_i - w_{s(x_i)})$ donde ε es la velocidad de aprendizaje.
5. $t = t + 1;'$ si $t < t_max$ entonces ir al paso (2).

Neural Gas I

Algoritmo de aprendizaje competitivo. No sólo se adapta la unidad ganadora al introducir un patrón de entrada, sino también otras unidades.

Algoritmo:

1. Inicializar el conjunto $C = \{c_1, c_2, ..., c_k\}$ con los vectores centrales $w_{cj} \in \Re^d$ elegidos aleatoriamente del conjunto de datos. Inicializar el contador t=0.
2. Extraer un patrón de entrada x_i del conjunto de datos.
3. Ordenar todos los elementos de C según su distancia a x_i, encontrar la secuencia de índices $(l_0, l_1, ..., l_{k-1})$ tales que w_{l0} es el vector más cercano al patrón, w_{l1} el segundo, etc. Denotamos el número asociado con w_l como $m_l(x_i, c)$.

Neural Gas II

4. Adaptar los centros según:

$$\Delta w_l = \varepsilon_t h_\lambda (m_l(x_i, C)) \nabla \|(x_i - w_l)\|$$

donde

$$\lambda_t = \lambda_{ini} \left(\frac{\lambda_{fin}}{\lambda ini} \right)^{(t/t_{max})}$$

$$\varepsilon_t = \varepsilon_{ini} \left(\frac{\varepsilon_{fin}}{\varepsilon ini} \right)^{(t/t_{max})}$$

$$h_\alpha(m) = exp\left(\frac{-m}{\lambda_t} \right)$$

y $\nabla \|(x_i - w_l)\|$ es la función de distancia.

5. $t = t + 1;'$ si $t < t_max$ entonces ir al paso (2).

Self-Organizing Maps (SOM)

Algoritmo de aprendizaje competitivo.

Algoritmo:

1. Inicializar el conjunto $C = \{c_1, c_2, ..., c_k\}$ $(K << N)$.
2. Definir una relación de vecindario. Usualmente esta función de vecindario es una malla. Inicializar el contador t a cero.
3. Extraer un punto x_i del conjunto de datos.
4. Calcular el nodo ganador $s(x_i)$:

$$s(x_i) = argmin_c \|x_i - w_c\|$$

Self-Organizing Maps (SOM)

6. Adaptar los centros de acuerdo a la regla aprendizaje:

$$\Delta w_l = \varepsilon_t \phi(l, s(x_i))(x_i - w_l)$$

donde ε_t es la velocidad de aprendizaje y $\phi(l, s(x_i))$ es la función vecindario. Debido a esta función, no sólo el centro ganador aprende sino también los vectores de su vecindario topológico.

7. Incrementar $t = t + 1$; si $t < t_{max}$ continuar en el paso (3).

Fuzzy clustering

Algoritmos revisados:

- C-means
- Unsupervised fuzzy competitive learning

Fuzzy C-Means

Es unos de los algoritmos clásicos en agrupamiento difuso. Contrariamente a sus variantes en aprendizaje competitivo, es un método off-line, es decir las actualizaciones se basan en todo el conjunto de entrenamiento.

- Fijar el número de clusters $k, 2 \leq k < N$ donde N es el número de puntos. Fijar q, $1 < q < \infty$.
- Inicializar el contador t a cero y los centros de los clusters v_i.
- Calcular la matriz de partición difusa:

$$U_{t+1} = u_{ij,t+1} = \left[\sum_{t=1}^{k} \left(\frac{\|x_i - v_{j,t}\|}{\|x_i - v_{l,t}\|} \right)^{2/(q-1)} \right]^{-1}$$

Fuzzy C-Means

y actualizar los clusters según

$$V_{t+1} = v_{t+1} = \frac{\sum_{i=1}^{N} (u_{ij,t+1})^q x_i}{\sum_{i=1}^{N} (u_{ij,t+1})^q}$$

donde $1 \leq i \leq N$ y $1 \leq j \leq k$

- Si $\|U_t - U_{t-1}\| \leq \varepsilon$ entonces parar, sino $t = t + 1$

Unsupervised fuzzy competitive learning I

Unsupervised fuzzy competitive learning(UFCL): Es la versión on-line del algoritmo fuzzy c-means. Cada vez se que se presenta un patrón nuevo extraído del conjunto de datos se calcula su valor de membresía y se actualizan los centros de los clusters.

$$v_{j,t} = v_{j,t-1} + \alpha_t u_{ij,t}^{q} [x_i - v_{j,t-1}]$$

donde $\alpha_t = \alpha_0(1 - t/T)$

Correlation coefficient

La correlación entre el centro del cluster de activación identificado y el centro de la clase de activación de referencia se mide mediante:

$$CC = \frac{\sum(c_i - \overline{c})(c_i^* - \overline{c}^*)}{\sqrt{\sum(c_i - \overline{c})^2 \sum(c_i^* - \overline{c}^*)^2}}$$

Weighted Jaccard coefficient (wJC)

Partiendo de la función JC ($JC = a/(a+b+c)$) y añadiendo pesos que son las funciones inversas de las probabilidades de los true-positives, false-negatives y false-positives bajo la hipótesis que cada pixel tiene la misma probabilidad perteneciendo a una clase de activación o de no-activación.

$$wJC = \frac{a + (1/P(a))}{(a + 1/P(a) + b + 1/P(b) + c + 1/P(c))}$$

donde a es el número de TP, b es el número de FN y c es el número de FP y sus probabilidades:

$$P(a) = (a+c)x(a+b)/n^2$$
$$P(b) = (b+d)x(a+b)/n^2$$
$$P(c) = (a+c)x(c+d)/n^2$$

Como este coeficiente incide en el número de TPs, es una buena medida de la calidad de los clusters activados.

Contenido

1. Introducción histórica.
2. Principios Físicos
3. MRI vs. fMRI.
4. Señal BOLD
5. Experimentos reales
6. Procesado de los datos fMRIs
7. Métodos de clustering.
8. Datos y métodos
9. Resultados
10. Bibliografía

Resultados

Table 1 *CC* ranks for artificial data sets

	t6			*t5*			*t4*			Mean
	5cl	10cl	20cl	5cl	10cl	20cl	5cl	10cl	20cl	
ngas	0.83 (1)	1.00 (1)	1.00 (1)	0.82 (1)	0.91 (1)	1.00 (1)	0.79 (2)	0.89 (1)	0.95 (1)	0.91
kmeans	0.83 (2)	0.94 (3)	1.00 (2)	0.81 (3)	0.91 (2)	0.98 (3)	0.79 (1)	0.86 (2)	0.93 (2)	0.89
hardcl	0.80 (3)	1.00 (2)	1.00 (3)	0.81 (2)	0.87 (3)	0.99 (2)	0.67 (3)	0.81 (3)	0.90 (3)	0.87
som	0.63 (5)	0.82 (4)	0.90 (5)	0.63 (5)	0.81 (4)	0.88 (4)	0.61 (4)	0.81 (4)	0.87 (4)	0.77
maximin	0.80 (4)	0.80 (5)	0.74 (6)	0.75 (4)	0.75 (5)	0.75 (5)	0.35 (7)	0.64 (5)	0.61 (5)	0.69
clara	0.32 (8)	0.76 (6)	0.49 (8)	0.34 (8)	0.63 (6)	0.52 (6)	0.35 (8)	0.44 (7)	0.54 (6)	0.49
cmeans	0.39 (6)	0.44 (7)	0.51 (7)	0.44 (6)	0.46 (7)	0.48 (7)	0.47 (5)	0.49 (6)	0.51 (7)	0.47
ufcl	0.39 (7)	0.35 (8)	0.94 (4)	0.36 (7)	0.35 (8)	0.39 (8)	0.38 (6)	0.41 (8)	0.43 (8)	0.44

Resultados

Table 3 *wJC* ranks for artificial data sets

	t6			*t5*			*t4*			Mean
	5cl	10cl	20cl	5cl	10cl	20cl	5cl	10cl	20cl	
maximin	0.98 (1)	0.98 (1)	0.98 (1)	0.97 (1)	0.98 (1)	0.98 (1)	0.09 (8)	0.87 (1)	0.91 (1)	0.86
ngas	0.44 (2)	0.98 (3)	0.98 (2)	0.40 (2)	0.75 (3)	0.98 (2)	0.37 (1)	0.69 (2)	0.90 (2)	0.72
kmeans	0.43 (3)	0.84 (5)	0.98 (3)	0.39 (3)	0.73 (4)	0.95 (4)	0.37 (2)	0.67 (3)	0.88 (3)	0.69
hardcl	0.37 (4)	0.98 (4)	0.98 (4)	0.33 (5)	0.60 (5)	0.96(3)	0.29 (5)	0.55 (6)	0.80 (4)	0.65
clara	0.37 (5)	0.98 (2)	0.61 (7)	0.37 (4)	0.78 (2)	0.65 (7)	0.36 (3)	0.61 (4)	0.62 (7)	0.59
cmeans	0.32 (6)	0.55 (6)	0.61 (6)	0.31 (6)	0.53 (6)	0.72 (6)	0.31 (4)	0.57 (5)	0.72 (6)	0.52
som	0.14 (7)	0.50 (7)	0.81 (5)	0.14 (7)	0.49 (7)	0.80 (5)	0.13 (6)	0.48 (7)	0.78 (5)	0.47
ufcl	0.10 (8)	0.04 (8)	0.98 (4)	0.10 (8)	0.04 (8)	0.01(8)	0.09 (7)	0.04 (8)	0.01 (8)	0.15

Contenido

1. Introducción histórica.
2. Principios Físicos
3. MRI vs. fMRI.
4. Señal BOLD
5. Experimentos reales
6. Procesado de los datos fMRIs
7. Métodos de clustering.
8. Datos y métodos
9. Resultados
10. Bibliografía

Bibliografía I

R Baumgartner, L Ryner, W Richter, R Summers, M Jarmasz, and R Somorjai.
Comparison of two exploratory data analysis methods for fmri: fuzzy clustering vs. principal component analysis.
Magnetic resonance imaging, 18:89–94, 2000.
PMID: 10642106.

R Baumgartner, G Scarth, C Teichtmeister, R Somorjai, and E Moser.
Fuzzy clustering of gradient-echo functional mri in the human visual cortex. part i: reproducibility.
Journal of magnetic resonance imaging : JMRI, 7:1094–101, 1997.
PMID: 9400854.

Bibliografía II

R Baumgartner, R Somorjai, R Summers, W Richter, L Ryner, and M Jarmasz.
Resampling as a cluster validation technique in fmri.
Journal of magnetic resonance imaging : JMRI, 11:228–31, February 2000.
PMID: 10713959.

K H Chuang, M J Chiu, C C Lin, and J H Chen.
Model-free functional mri analysis using kohonen clustering neural network and fuzzy c-means.
IEEE transactions on medical imaging, 18:1117–28, December 1999.
PMID: 10695525.

Evgenia Dimitriadou, Markus Barth, Christian Windischberger, Kurt Hornik, and Ewald Moser.
A quantitative comparison of functional mri cluster analysis.
Artificial Intelligence in Medicine, 31:57–71, May 2004.

Bibliografía III

M J Fadili, S Ruan, D Bloyet, and B Mazoyer.
A multistep unsupervised fuzzy clustering analysis of fmri time series.
Human brain mapping, 10:160–78, August 2000.
PMID: 10949054.

Jay Hegdé.
Time course of visual perception: Coarse-to-fine processing and beyond.
Progress in Neurobiology, 84:405–439, April 2008.

O. Lange, A. Meyer-Baese, M. Hurdal, and S. Foo.
A comparison between neural and fuzzy cluster analysis techniques for functional mri.
Biomedical Signal Processing and Control, 1:243–252, July 2006.

Bibliografía IV

A. Meyer-Baese, A. Saalbach, O. Lange, and A. WismÃ¼ller.
Unsupervised clustering of fmri and mri time series.
Biomedical Signal Processing and Control, 2:295–310, October 2007.

A Meyer-Baese, Axel Wismueller, and Oliver Lange.
Comparison of two exploratory data analysis methods for fmri: unsupervised clustering versus independent component analysis.
IEEE transactions on information technology in biomedicine : a publication of the IEEE Engineering in Medicine and Biology Society, 8:387–98, September 2004.
PMID: 15484444.

Bibliografía V

E Moser, M Diemling, and R Baumgartner.
Fuzzy clustering of gradient-echo functional mri in the human visual cortex. part ii: quantification.
Journal of magnetic resonance imaging : JMRI, 7:1102–8, 1997.
PMID: 9400855.

Mohamed L Seghier, Karl J Friston, and Cathy J Price.
Detecting subject-specific activations using fuzzy clustering.
NeuroImage, 36:594–605, July 2007.
PMID: 17478103.

Christian Windischberger, Markus Barth, Claus Lamm, Lee Schroeder, Herbert Bauer, Ruben C. Gur, and Ewald Moser.
Fuzzy cluster analysis of high-field functional mri data.
Artificial Intelligence in Medicine, 29:203–223, November 2003.

Gracias por su atención

eman ta zabal zazu
Universidad del Pais Vasco
Euskal Herriko Unibertsitatea

Introducción a los filtros Kalman

Ivan Villaverde
Grupo de Inteligencia Computacional
JIC 2008

Contenidos

eman ta zabal zazu
Universidad del Pais Vasco
Euskal Herriko Unibertsitatea

- Un poco de historia
- Qué es un filtro Kalman
- *Discrete Kalman Filter*
- *Extended Kalman Filter*
- *Unscented Kalman Filter*
- Otras variaciones

Un poco de historia

- Desarrollado por R. E. Kalman y R. S. Bucy a principios de los 60.
  - Basado en trabajos de Stratonovich, Thiele y Swerling.
- Primera aplicación práctica: estimación de trayectorias para proyecto Apolo por Stanley Schmidt.
- Múltiples aplicaciones, desde seguimiento de objetivos a economía.

Qué es un filtro Kalman

- Método recursivo para estimar el estado de un sistema dinámico
- Modelo lineal de predicción.
- Entrada con ruido --> estimación del estado robusta.
- Proceso predicción-corrección retroalimentado:
  1. Predicción del estado usando el modelo lineal.
  2. Corrección de la predicción usando las observaciones de la realidad.

Qué es un filtro Kalman

- Para predecir el estado siguiente:
  - Modelo del proceso: modelo que describe cómo el estado cambia en el tiempo.
- Para corregir la predicción:
  - Modelo de la observación: modelo que describe cómo se observan (miden) el entorno desde un estado dado.

Qué es un filtro Kalman
(un ejemplo gráfico)

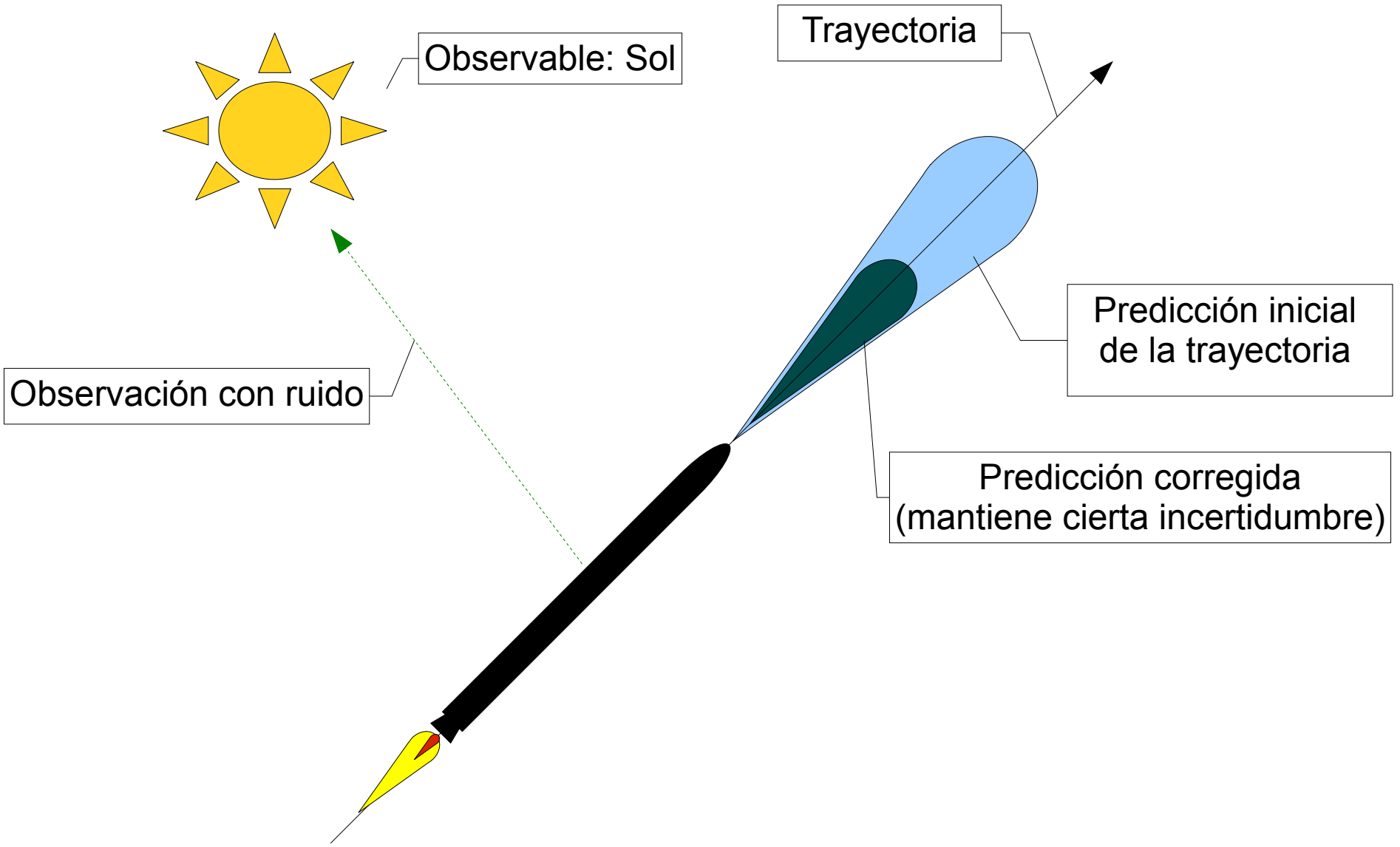

Discrete Kalman Filter

Discrete Kalman Filter

Formalizando conceptos básicos

eman ta zabal zazu
Universidad del Pais Vasco
Euskal Herriko Unibertsitatea

- Estimar el estado $x \in \Re^n$ de un proceso temporal asumiendo un modelo lineal de tiempo discreto:

$$x_k = Ax_{k-1} + Bu_{k-1} + w_{k-1}, \tag{1.1}$$

- Con un modelo lineal de las observaciones $z \in \Re^m$

$$z_k = Hx_k + v_k. \tag{1.2}$$

- Y las fuentes de ruido se asumen variables aleatorias con distribución de probabilidad gausiana con matriz de covarianza conocida:

$$p(w) \sim N(0, Q), \tag{1.3}$$

$$p(v) \sim N(0, R). \tag{1.4}$$

Discrete Kalman Filter
Formalizando conceptos básicos

eman ta zabal zazu
Universidad del Pais Vasco
Euskal Herriko Unibertsitatea

- Estimación *a priori* del estado, $\hat{x}_k^- \in \Re^n$
  - Dada por el modelo del proceso.
- Estimación *a posteriori* del estado, $\hat{x}_k \in \Re^n$
  - Obtenida tras la medición.
- Error a *priori* y *a posteriori*: $e_k^- \equiv x_k - \hat{x}_k^-, \quad e_k \equiv x_k - \hat{x}_k.$
- Covarianza del error *a priori*: $P_k^- = E[e_k^- e_k^{-T}],$
- Covarianza del error *a posteriori*: $P_k = E[e_k e_k^T].$

Discrete Kalman Filter
¿Cómo lo hacemos?

eman ta zabal zazu
Universidad del Pais Vasco
Euskal Herriko Unibertsitatea

- Objetivo: calcular la estimación del estado *a posteriori* como una combinación lineal de la estimación *a priori* y la observación:

$$\hat{x}_k = \hat{x}_k^- + K(z_k - H\hat{x}_k^-)$$

- La diferencia $(z_k - H\hat{x}_k^-)$ entre la predicción de la observación y la observación realizada es el *residual*.

Discrete Kalman Filter
¿Cómo lo hacemos?

eman ta zabal zazu
Universidad del Pais Vasco
Euskal Herriko Unibertsitatea

- *K*: factor de ganancia (*Kalman Gain*)
  - Estimado minimizando la covarianza del error *a posteriori*:

$$K_k = P_k^- H^T (H P_k^- H^T + R)^{-1} = \frac{P_k^- H^T}{H P_k^- H^T + R}$$

  - Resultados básicos sobre la precisión del filtro:
    - Confianza en las observaciones: $\lim_{R_k \to 0} K_k = H^{-1}.$
    - Confianza en el modelo de proceso: $\lim_{P_k^- \to 0} K_k = 0.$

Discrete Kalman Filter
Algoritmo

eman ta zabal zazu
Universidad del Pais Vasco
Euskal Herriko Unibertsitatea

- Estimación del estado de un proceso dinámico mediante un algoritmo predictor-corrector.
- Fase de predicción (*time update*)

$$\hat{x}_k^- = A\hat{x}_{k-1} + Bu_{k-1} \qquad (1.9)$$

$$P_k^- = AP_{k-1}A^T + Q \qquad (1.10)$$

Discrete Kalman Filter
Algoritmo

eman ta zabal zazu
Universidad del Pais Vasco
Euskal Herriko Unibertsitatea

- Fase de corrección basada en la actualización de las observaciones (*measurement update*)

$$K_k = P_k^- H^T (H P_k^- H^T + R)^{-1} \qquad (1.11)$$

$$\hat{x}_k = \hat{x}_k^- + K_k (z_k - H\hat{x}_k^-) \qquad (1.12)$$

$$P_k = (I - K_k H) P_k^- \qquad (1.13)$$

Discrete Kalman Filter
Algoritmo

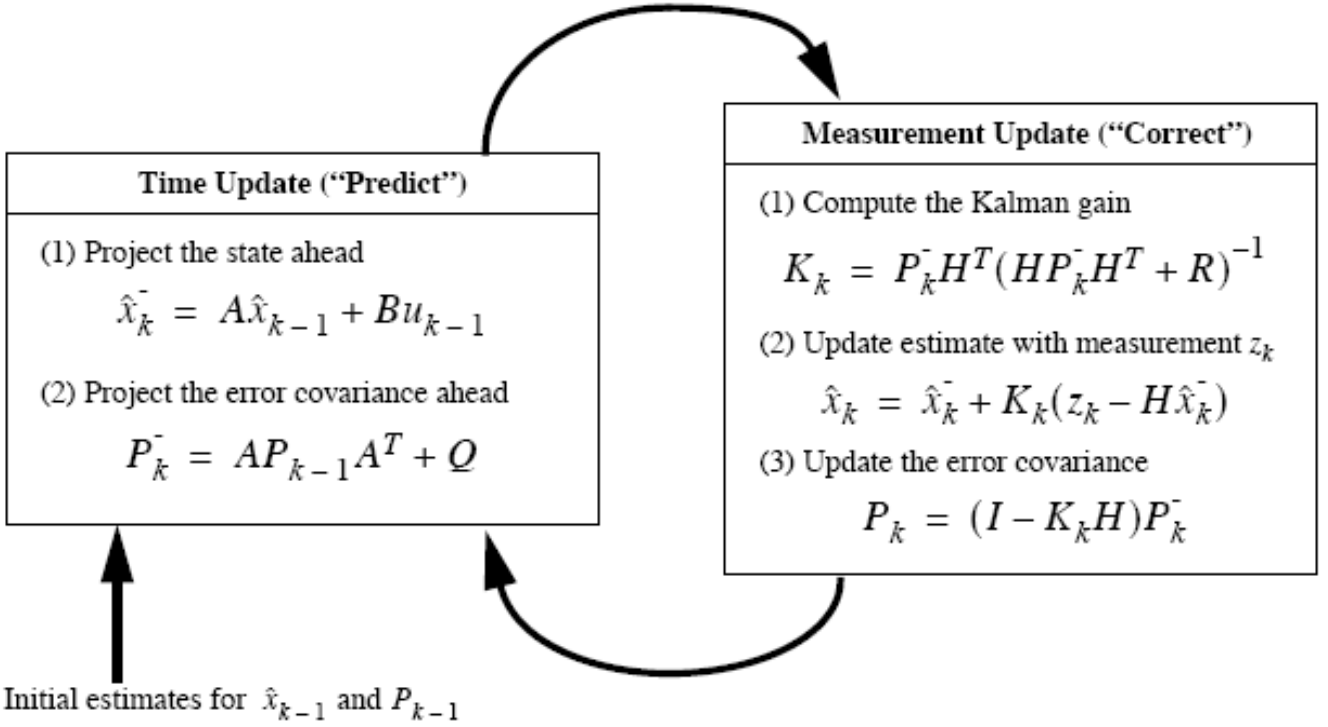

Discrete Kalman Filter
Ajuste de parámetros

eman ta zabal zazu
Universidad del Pais Vasco
Euskal Herriko Unibertsitatea

- Identificación del sistema: proceso de ajuste fino de Q y R.
- R generalmente se calcula antes de la aplicación del filtro.
  - Es posible tomar observaciones.
- No siempre es posible estimar Q.
  - No siempre se puede observar el proceso.
  - Puede compensar malos modelos de proceso inyectando incertidumbre.
- Si Q y R son constantes, P_k y K_k se estabilizan rápidamente.

Discrete Kalman Filter

Un ejemplo sencillo:
Estimar la posición de una locomotora

Discrete Kalman Filter

Un ejemplo sencillo

- Una locomotora se mueve por una vía ideal.

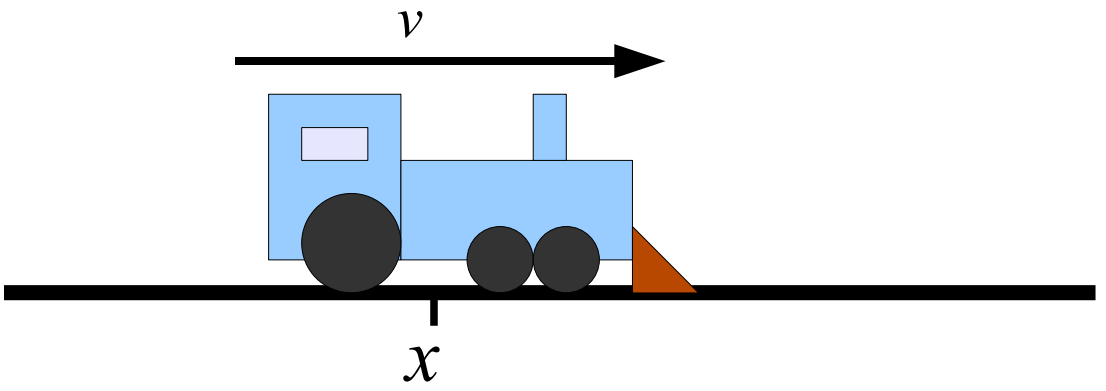

$$x = \begin{bmatrix} x \\ v \end{bmatrix}$$

- Entre los instantes *k-1* y *k* sufre aceleración aleatoria a_k con distribución normal de media 0 y desviación σ_a

$$x = Ax_{k-1} + Ga_k \qquad A = \begin{bmatrix} 1 & \Delta t \\ 0 & 1 \end{bmatrix} \qquad G = \begin{bmatrix} \Delta t^2/2 \\ \Delta t \end{bmatrix}$$

$$Q = cov(Ga) = E[(Ga)(Ga)^T] = G\,E[a^2]G^T = G[\sigma_a^2]G^T = \sigma_a^2 G\,G^T$$

Discrete Kalman Filter

Un ejemplo sencillo

eman ta zabal zazu
Universidad del Pais Vasco
Euskal Herriko Unibertsitatea

- Ruido de observación: variable aleatoria de media 0 y desviación σ_z:

$$z_k = Hx_k + v_k \qquad H = \begin{bmatrix} 1 & 0 \end{bmatrix}$$

$$R = E\left[v_k v_k^T\right] = \left[\sigma_z^2\right]$$

- Estado inicial:

$$\hat{x}_0 = \begin{bmatrix} 0 \\ 0 \end{bmatrix} \qquad P_0 = \begin{bmatrix} 0 & 0 \\ 0 & 0 \end{bmatrix}$$

- Estado inicial desconocido: $P_0 = \begin{bmatrix} B & 0 \\ 0 & B \end{bmatrix}$

Discrete Kalman Filter

Un ejemplo con resultados: Estimar un escalar constante

[Welch & Bishop 2001]

Discrete Kalman Filter

Un ejemplo con resultados

- Estimar un escalar aleatorio constante: un voltaje.
- Observaciones corrompidas ±0.1V.
- Ecuación: $x_k = Ax_{k-1} + Bu_{k-1} + w_k = x_{k-1} + w_k$
  - El estado no cambia: $A = 1$
  - No hay control: $u = 0$
- Observación: $z_k = Hx_k + v_k = x_k + v_k$
  - El estado es constante: $H = 1$

Discrete Kalman Filter

Un ejemplo con resultados

eman ta zabal zazu
Universidad del Pais Vasco
Euskal Herriko Unibertsitatea

- Ecuaciones del filtro:
  - Predicción:

$$\hat{x}_k^- = \hat{x}_{k-1},$$

$$P_k^- = P_{k-1} + Q,$$

  - Corrección:

$$K_k = P_k^-(P_k^- + R)^{-1} = \frac{P_k^-}{P_k^- + R}$$

$$\hat{x}_k = \hat{x}_k^- + K_k(z_k - \hat{x}_k^-)$$

$$P_k = (1 - K_k)P_k^-.$$

- Se asume una varianza del proceso muy pequeña:

$$Q = 1\,e^{-5}$$

- Se va a estimar una distribución: $\hat{x}_{k-1} = 0$
- Valor inicial ha de ser P ≠ 0: $P_0 = 1$

Discrete Kalman Filter

Un ejemplo con resultados

eman ta zabal zazu
Universidad del Pais Vasco
Euskal Herriko Unibertsitatea

- Primera simulación (*R* óptimo):

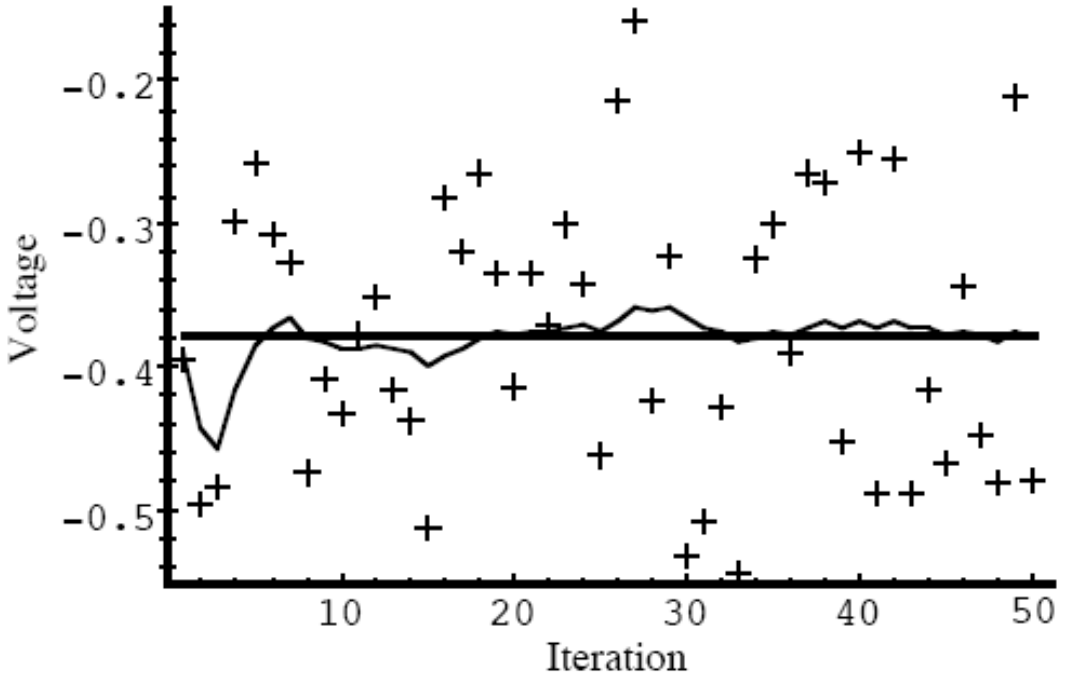

Figure 3-1. The first simulation: $R = (0.1)^2 = 0.01$. The true value of the random constant $x = -0.37727$ is given by the solid line, the noisy measurements by the cross marks, and the filter estimate by the remaining curve.

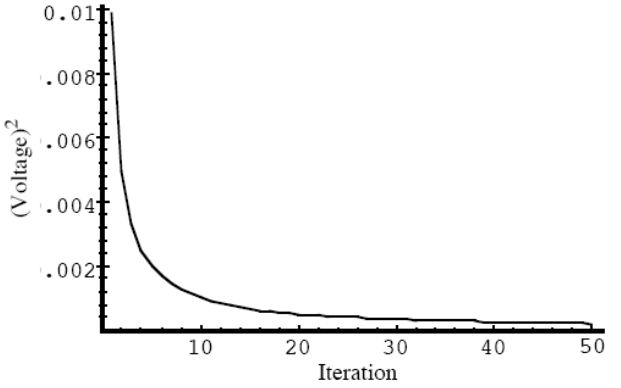

Figure 3-2. After 50 iterations, our initial (rough) error covariance P_k^- choice of 1 has settled to about 0.0002 (Volts^2).

Discrete Kalman Filter

Un ejemplo con resultados

eman ta zabal zazu
Universidad del Pais Vasco
Euskal Herriko Unibertsitatea

- Segunda simulación (*R* alto):

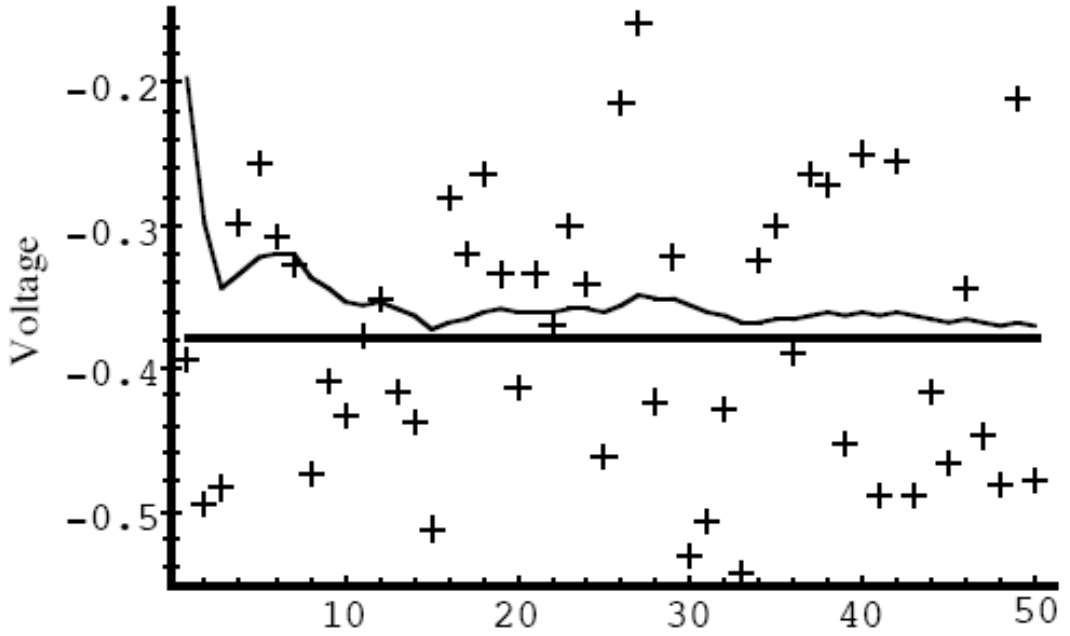

Figure 3-3. Second simulation: $R = 1$. The filter is slower to respond to the measurements, resulting in reduced estimate variance.

Discrete Kalman Filter

Un ejemplo con resultados

- Tercera simulación (*R* bajo):

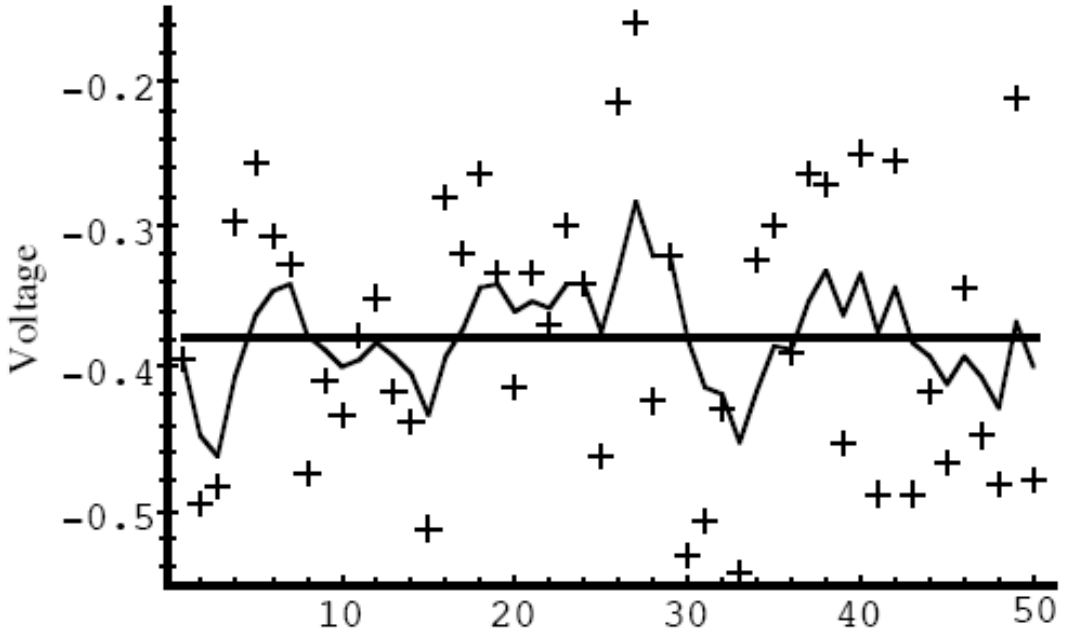

Figure 3-4. Third simulation: $R = 0.0001$. The filter responds to measurements quickly, increasing the estimate variance.

Discrete Kalman Filter

eman ta zabal zazu
Universidad del Pais Vasco
Euskal Herriko Unibertsitatea

- Ventajas:
  - Los posteriores son estimados *on-line*.
  - Mantiene un cierto nivel de incertidumbre.
  - Fuerte convergencia.
- Limitaciones:
  - Asume ruido gaussiano (independiente y limitado).
  - Mapeo: problema de correspondencia.
  - Limitado a sistemas lineales.

Sistemas no lineales
Extended Kalman Filter

Sistemas no lineales

eman ta zabal zazu
Universidad del Pais Vasco
Euskal Herriko Unibertsitatea

- KF asume un sistema lineal:
  - Sólo operaciones con matrices.
  - Las observaciones son funciones lineales del estado.
  - El siguiente estado es una función lineal del estado anterior.
- ¿Cómo lo adaptamos a un sistema no-lineal?
  - Funciones en lugar de matrices.
  - Jacobianos para proyectar hacia adelante y relacionar mediciones y estados.

Extended Kalman Filter
Formalizando conceptos básicos

eman ta zabal zazu
Universidad del Pais Vasco
Euskal Herriko Unibertsitatea

- Estimar el estado $x \in \Re^n$ en procesos dinámicos gobernados por una función no-lineal:

$$x_k = f(x_{k-1}, u_{k-1}, w_{k-1}), \tag{2.1}$$

- Con observaciones no lineales $z \in \Re^m$:

$$z_k = h(x_k, v_k), \tag{2.2}$$

- Ruido desconocido: se usan aproximaciones utilizando la anterior estimación *a posteriori*:

$$\tilde{x}_k = f(\hat{x}_{k-1}, u_{k-1}, 0) \tag{2.3}$$

$$\tilde{z}_k = h(\tilde{x}_k, 0), \tag{2.4}$$

Extended Kalman Filter
¿Cómo lo hacemos?

eman ta zabal zazu
Universidad del Pais Vasco
Euskal Herriko Unibertsitatea

- Linealizar estimaciones

$$x_k \approx \tilde{x}_k + A(x_{k-1} - \hat{x}_{k-1}) + W w_{k-1}, \quad (2.5)$$

$$z_k \approx \tilde{z}_k + H(x_k - \tilde{x}_k) + V v_k. \quad (2.6)$$

  - x_k y z_k son el estado y la observación reales.
  - $\tilde{x}_k$ y $\tilde{z}_k$ son las aproximaciones del estado y la observación de (2.3) y (2.4).
  - Las variables aleatorias w_k y v_k representan el ruido de proceso y observación.

Extended Kalman Filter
¿Cómo lo hacemos?

eman ta zabal zazu
Universidad del Pais Vasco
Euskal Herriko Unibertsitatea

- *A* es la matriz Jacobiana de las derivadas parciales de *f* respecto a *x*:

$$A_{[i,j]} = \frac{\partial f_{[i]}}{\partial x_{[j]}}(\hat{x}_{k-1}, u_{k-1}, 0),$$

- *W* es la matriz Jacobiana de las derivadas parciales de *f* respecto a *w*:

$$W_{[i,j]} = \frac{\partial f_{[i]}}{\partial w_{[j]}}(\hat{x}_{k-1}, u_{k-1}, 0),$$

- *H* es la matriz Jacobiana de las derivadas parciales de *h* respecto a *x*:

$$H_{[i,j]} = \frac{\partial h_{[i]}}{\partial x_{[j]}}(\tilde{x}_k, 0),$$

- *V* es la matriz Jacobiana de las derivadas parciales de *h* respecto a *v*:

$$V_{[i,j]} = \frac{\partial h_{[i]}}{\partial v_{[j]}}(\tilde{x}_k, 0).$$

Extended Kalman Filter
¿Cómo lo hacemos?

eman ta zabal zazu
Universidad del Pais Vasco
Euskal Herriko Unibertsitatea

- Error de predicción: $$\tilde{e}_{x_k} \equiv x_k - \tilde{x}_k, \qquad (2.7)$$
- Residual: $$\tilde{e}_{z_k} \equiv z_k - \tilde{z}_k. \qquad (2.8)$$
- Nuevas ecuaciones de error:

$$\tilde{e}_{x_k} \approx A(x_{k-1} - \hat{x}_{k-1}) + \varepsilon_k, \qquad (2.9)$$

$$\tilde{e}_{z_k} \approx H\tilde{e}_{x_k} + \eta_k, \qquad (2.10)$$

where ε_k and η_k represent new independent random variables having zero mean and covariance matrices WQW^T and VRV^T, with Q and R as in (1.3) and (1.4) respectively.

$$p(\tilde{e}_{x_k}) \sim N(0, E[\tilde{e}_{x_k}\tilde{e}_{x_k}^T])$$

$$p(\varepsilon_k) \sim N(0, WQ_kW^T)$$

$$p(\eta_k) \sim N(0, VR_kV^T)$$

- Estimación del estado *a posteriori*:

$$\hat{x}_k = \tilde{x}_k + \hat{e}_k. \qquad (2.11)$$

$$\hat{e}_k = K_k\tilde{e}_{z_k}. \qquad (2.12)$$

- Sustituyendo: $$\hat{x}_k = \tilde{x}_k + K_k\tilde{e}_{z_k} = \tilde{x}_k + K_k(z_k - \tilde{z}_k) \qquad (2.13)$$

Extended Kalman Filter
Algoritmo

- Fase de predicción:

$$\hat{x}_k^- = f(\hat{x}_{k-1}, u_{k-1}, 0) \qquad (2.14)$$

$$P_k^- = A_k P_{k-1} A_k^T + W_k Q_{k-1} W_k^T \qquad (2.15)$$

- Fase de corrección:

$$K_k = P_k^- H_k^T (H_k P_k^- H_k^T + V_k R_k V_k^T)^{-1} \qquad (2.16)$$

$$\hat{x}_k = \hat{x}_k^- + K_k(z_k - h(\hat{x}_k^-, 0)) \qquad (2.17)$$

$$P_k = (I - K_k H_k) P_k^- \qquad (2.18)$$

Extended Kalman Filter
Algoritmo

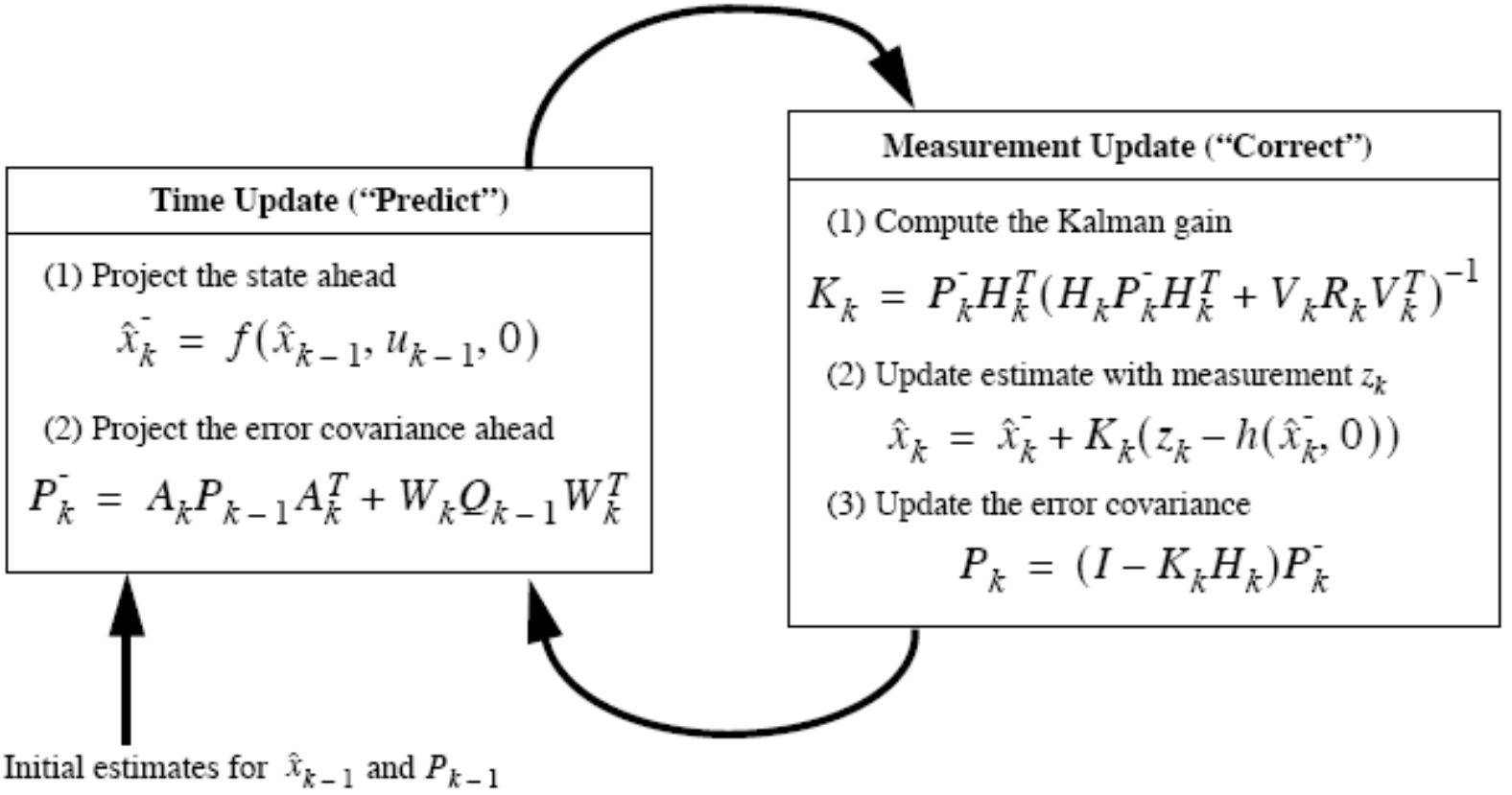

Extended Kalman Filter
Problemas

eman ta zabal zazu
Universidad del Pais Vasco
Euskal Herriko Unibertsitatea

- No es un estimador óptimo.
- Muy sensible a estimaciones iniciales incorrectas.
- Muy sensible a malos modelos de proceso.
- Aun así, es el estándar *de facto* en problemas de navegación.

Sistemas no lineales
Unscented Kalman Filter

Unscented KF

- Estimador basado en la *unscented transformation*:
  - Medias y covarianzas de distribuciones de probabilidad se parametrizan por medio de puntos escogidos.
- Generaliza sistemas no-lineales sin los pasos de linealización del EKF.
- Rendimiento similar al del KF en sistemas lineales.

Unscented KF

- Problema del EFK:
  - Transformación con series de Taylor.
  - Se descartan los términos de orden mayor que dos.
  - Si esos términos no son despreciables:
    - Introduce error.
    - Transformación sesgada.
  - Se puede compensar introduciendo ruido controlado.
    - Difícil de ajustar correctamente.
    - No evita el sesgo.

Unscented KF
Unscented Transformation

- Idea básica:
  - Calcular las estadísticas (media, varianza) de una variable aleatoria que ha de pasar por una transformación no lineal.
  - ¿Por qué?: Es más fácil aproximar una gaussiana que una función no lineal arbitraria.
  - ¿Cómo?: Se escoge un conjunto de puntos cuya media y covarianza sean $\bar{x}$ y P_{xx}. Se aplica la función no-lineal a esos puntos y se obtienen las estadísticas $\bar{y}$ y P_{yy} de esos puntos transformados.

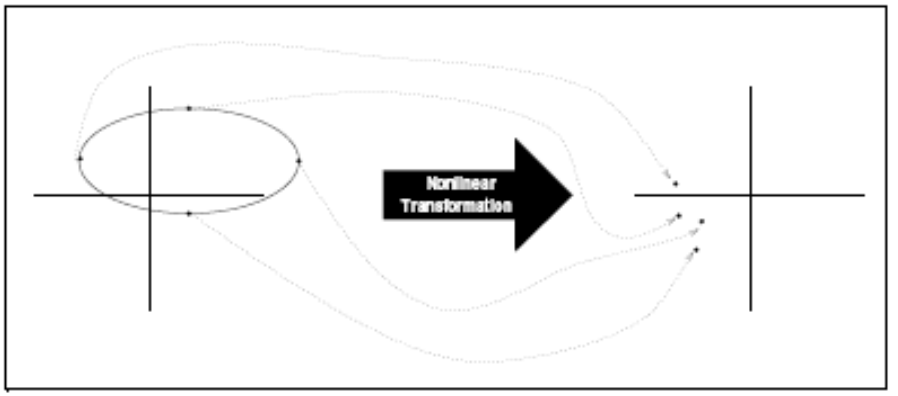

Unscented KF
Unscented Transformation

eman ta zabal zazu
Universidad del Pais Vasco
Euskal Herriko Unibertsitatea

- Una variable *x* de dimensión *n* se aproxima por 2*n*+1 puntos.

$$\begin{aligned}
\boldsymbol{\mathcal{X}}_0 &= \bar{\mathrm{x}} & W_0 &= \kappa/(n+\kappa) \\
\boldsymbol{\mathcal{X}}_i &= \bar{\mathrm{x}} + \left(\sqrt{(n+\kappa)\mathbf{P}_{xx}}\right)_i & W_i &= 1/2(n+\kappa) \\
\boldsymbol{\mathcal{X}}_{i+n} &= \bar{\mathrm{x}} - \left(\sqrt{(n+\kappa)\mathbf{P}_{xx}}\right)_i & W_{i+n} &= 1/2(n+\kappa)
\end{aligned}$$

- Se calculan las estadísticas de los puntos transformados.

$$\boldsymbol{\mathcal{Y}}_i = \mathrm{f}\left[\boldsymbol{\mathcal{X}}_i\right].$$

$$\bar{\mathrm{y}} = \sum_{i=0}^{2n} W_i \boldsymbol{\mathcal{Y}}_i.$$

$$\mathbf{P}_{yy} = \sum_{i=0}^{2n} W_i \left\{\boldsymbol{\mathcal{Y}}_i - \bar{\mathrm{y}}\right\}\left\{\boldsymbol{\mathcal{Y}}_i - \bar{\mathrm{y}}\right\}^T.$$

Unscented KF
Algoritmo

- Paso previo:
  - El vector de estado se amplía con el ruido:

$$\mathbf{x}^a(k) = \begin{bmatrix} \mathbf{x}(k) \\ \mathbf{v}(k) \end{bmatrix}.$$

  - Los puntos se extraen a partir de:

$$\hat{\mathbf{x}}^a(k \mid k) = \begin{pmatrix} \hat{\mathbf{x}}(k \mid k) \\ \mathbf{0}_{q\times 1} \end{pmatrix} \text{ and } \mathbf{P}^a(k \mid k) = \begin{bmatrix} \mathbf{P}(k \mid k) & \mathbf{P}_{xv}(k \mid k) \\ \mathbf{P}_{xv}(k \mid k) & \mathbf{Q}(k) \end{bmatrix}.$$

Unscented KF
Algoritmo

eman ta zabal zazu
Universidad del Pais Vasco
Euskal Herriko Unibertsitatea

- Predicción:
  - Se instancia cada punto siguiendo el modelo del proceso.

$$\boldsymbol{\mathcal{X}}_i\left(k+1 \mid k\right) = \mathbf{f}\left[\boldsymbol{\mathcal{X}}_i^a\left(k \mid k\right), \mathbf{u}\left(k\right), k\right].$$

  - Se predice la media (estado):

$$\hat{\mathbf{x}}\left(k+1 \mid k\right) = \sum_{i=0}^{2n^a} W_i \boldsymbol{\mathcal{X}}_i^a\left(k+1 \mid k\right).$$

  - Covarianza del proceso.

$$\mathbf{P}\left(k+1 \mid k\right) \sum_{i=0}^{2n^a} W_i \left\{\boldsymbol{\mathcal{X}}_i\left(k+1 \mid k\right) - \hat{\mathbf{x}}\left(k+1 \mid k\right)\right\} \left\{\boldsymbol{\mathcal{X}}_i\left(k+1 \mid k\right) - \hat{\mathbf{x}}\left(k+1 \mid k\right)\right\}^T$$

Unscented KF
Algoritmo

- Corrección:
  - Se instancia cada punto siguiendo el modelo de observación. $\boldsymbol{\mathcal{Z}}_i(k+1 \mid k) = \mathbf{h}[\boldsymbol{\mathcal{X}}_i(k+1 \mid k), \mathbf{u}(k), k]$
  - Se estima la observación. $\hat{\mathbf{z}}(k+1 \mid k) = \sum_{i=1}^{2n^a} W_i \boldsymbol{\mathcal{Z}}_i(k+1 \mid k).$
  - Covarianza de innovación.

$$\mathbf{P}_{\nu\nu}(k+1 \mid k) = \mathbf{R}(k+1) + \sum_{i=0}^{2n^a} W_i \{\boldsymbol{\mathcal{Z}}_i(k \mid k-1) - \hat{\mathbf{z}}(k+1 \mid k)\} \{\boldsymbol{\mathcal{Z}}_i(k \mid k-1) - \hat{\mathbf{z}}(k+1 \mid k)\}^T$$

  - Matriz de correlación cruzada.

$$\mathbf{P}_{xz}(k+1 \mid k) = \sum_{i=0}^{2n^a} W_i \{\boldsymbol{\mathcal{X}}_i(k \mid k-1) - \hat{\mathbf{x}}(k+1 \mid k)\} \{\boldsymbol{\mathcal{Z}}_i(k \mid k-1) - \hat{\mathbf{z}}(k+1 \mid k)\}^T$$

  - Ganancia: $K_t = P_{xz} P_{vv}^{-1}$
  - *A posteriori* del estado y su covarianza igual que EKF.

Otras variaciones

Variaciones del KF

eman ta zabal zazu
Universidad del Pais Vasco
Euskal Herriko Unibertsitatea

- *Kalman-Bucy*.
- *Ensemble Kalman Filter* (EnKF).
- *Fast Kalman*.
- *Perturbation KF*.
- *Iterated Extended KF*.
- *FastSLAM*.
- Filtro de partículas *Rao-Blackwell*.
- Algoritmo *Lu/Milios*

Referencias

- Kalman, R. E. 1960. “A New Approach to Linear Filtering and Prediction Problems”, *Transaction of the ASME—Journal of Basic Engineering*, pp. 35-45 (March 1960).
- S. J. Julier and J. K. Uhlmann. “A new extension of the Kalman filter to nonlinear systems”. In *Proceedings of AeroSense: The 11th International Symposium on Aerospace/Defence Sensing, Simulation and Controls*, 1997.
- Maybeck, Peter S. 1979. *Stochastic Models, Estimation, and Control, Volume 1*, Academic Press, Inc.
- Sorenson, H. W. 1970. “Least-Squares estimation: from Gauss to Kalman,” *IEEE Spectrum*, vol. 7, pp. 63-68, July 1970
- Thrun, S. “Robotic Mapping: A Survey”, *Exploring Artificial Intelligence in the New Millenium.* Lakemeyer, G and Nebel, B. (eds), 2002.
- Welch, G. and Bishop, G. “An Introduction to the Kalman Filter”, SIGGRAPH 2001 course 8. In *Computer Graphics, Annual Conference on Computer Graphics & Interactive Techniques*. ACM Press, Addison-Wesley, Los Angeles, CA, USA (August 12--17)

Brain Image Registration

Alexandre Manhães Savio[1]

[1]Grupo de Inteligencia Computacional
Basque Country University

2nd Jornadas de Inteligencia Computacional, 2008

Presentation Outline

- This presentation consists on two separate presentations:
  1. An introduction to brain image registration
  2. A survey on brain image registration techniques

Brain Image Registration

Alexandre Manhães Savio[1]

[1]Grupo de Inteligencia Computacional
Basque Country University

2nd Jornadas de Inteligencia Computacional, 2008

Outline

1. Introduction
   - Definition
   - Brain Image Processing
2. Brain Atlases and Templates
   - Application
   - Definitions
   - Examples of Brain Atlases
3. Registration Methods
   - Introduction

Outline

1. Introduction
   - Definition
   - Brain Image Processing
2. Brain Atlases and Templates
   - Application
   - Definitions
   - Examples of Brain Atlases
3. Registration Methods
   - Introduction

Definitions of Image Registration I

- Image registration is the problem of determining the spatial transform that map points from one image to homologous points on an object in the second image. [1]

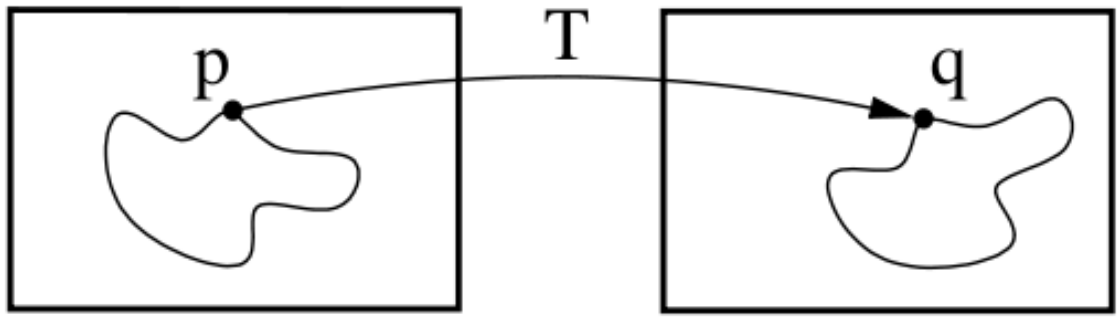

Figure 8.1: Image registration is the task of finding a spatial transform mapping on image into another.

Definitions of Image Registration II

- Image registration aligns the images and so establishes correspondences between different features seen on different imaging modalities, allows monitoring of subtle changes in size or intensity over time or across a population, and establishes correspondence between images and physical space. [2]

Outline

1. Introduction
   - Definition
   - Brain Image Processing
2. Brain Atlases and Templates
   - Application
   - Definitions
   - Examples of Brain Atlases
3. Registration Methods
   - Introduction

Applications

- Combining information from multiple imaging modalities.
- Monitoring changes in size, shape or image intensity over time intervals.
- Relating preoperative images and surgical plans to the physical reality of the patient in the operating room.
- Relating an individual's anatomy to a standardized atlas. [2]

Applications

- Combining information from multiple imaging modalities.
- Monitoring changes in size, shape or image intensity over time intervals.
- Relating preoperative images and surgical plans to the physical reality of the patient in the operating room.
- Relating an individual's anatomy to a standardized atlas. [2]

Applications

- Combining information from multiple imaging modalities.
- Monitoring changes in size, shape or image intensity over time intervals.
- Relating preoperative images and surgical plans to the physical reality of the patient in the operating room.
- Relating an individual's anatomy to a standardized atlas. [2]

Applications

- Combining information from multiple imaging modalities.
- Monitoring changes in size, shape or image intensity over time intervals.
- Relating preoperative images and surgical plans to the physical reality of the patient in the operating room.
- Relating an individual's anatomy to a standardized atlas. [2]

Application Fields

- Brain Image Processing has applications in many medical fields, for example:
  - Neuroscience
  - Neuropathological studies
  - Neurosurgery

Terminology of Brain Image Studies

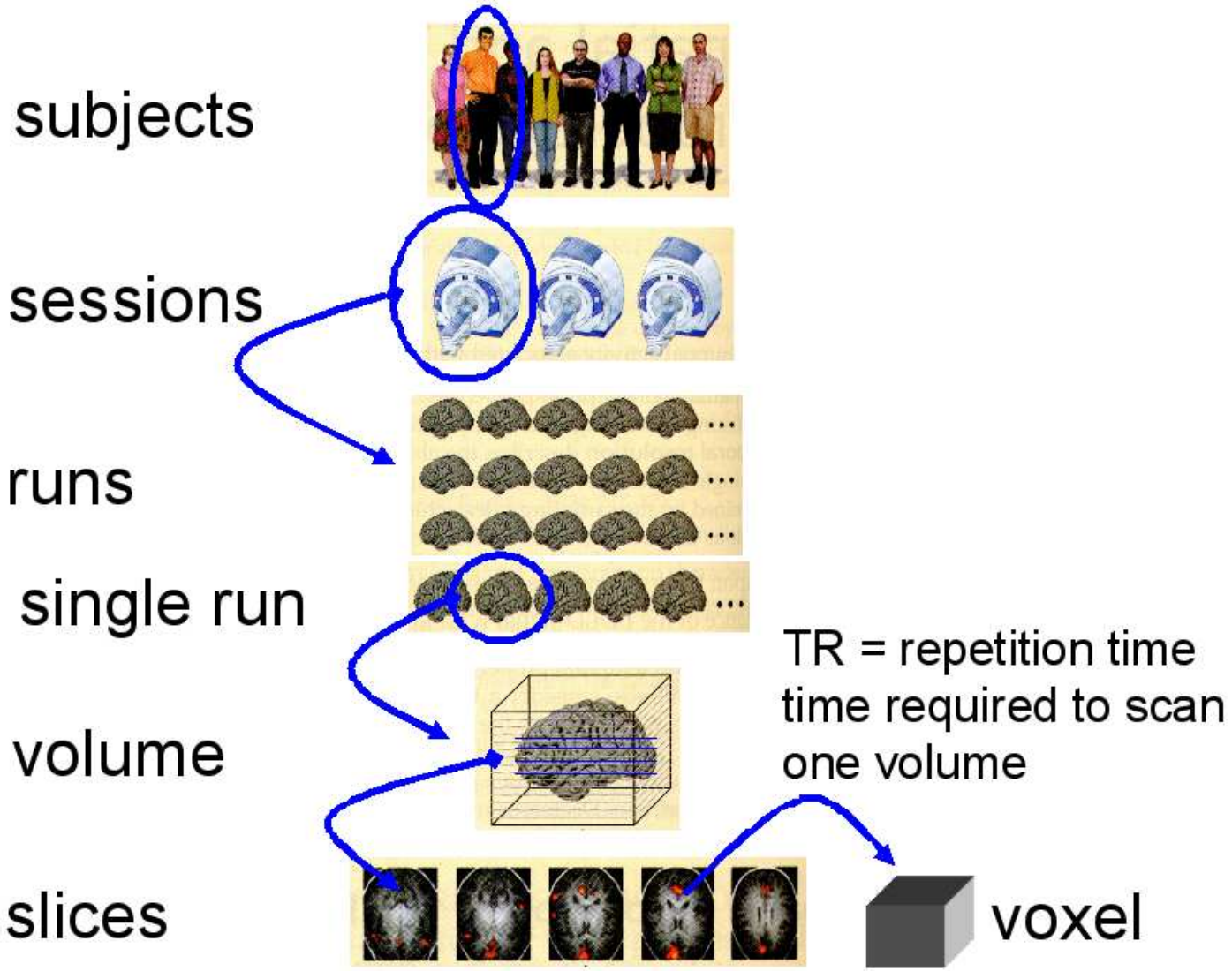

Outline

1. Introduction
   - Definition
   - Brain Image Processing
2. Brain Atlases and Templates
   - Application
   - Definitions
   - Examples of Brain Atlases
3. Registration Methods
   - Introduction

Application

- In group analysis studies the images of different subjects can only be compared and analyzed if the anatomical variations are compensated via appropriate mapping to a brain template or brain atlas. [3]

- In functional localization they provide a standard basis for activation labeling.

Outline

1. Introduction
   - Definition
   - Brain Image Processing
2. Brain Atlases and Templates
   - Application
   - Definitions
   - Examples of Brain Atlases
3. Registration Methods
   - Introduction

Brain Atlases

Brain Atlases

- A brain atlas provides a standard high-resolution structural brain which normally contains coordinate, anatomic, cytoarchitectonic and functional labels and is basically used for activation labeling. [3]

Brain Templates

Brain Templates

- Brain templates can be considered to be a subclass of brain atlases, which do not need to have labels or extra information about the anatomic or functional significance of locations, and are normally used as reference images for group analysis studies.
- For reporting the results in a standard coordinate system with a standard activation labeling, the brain template should be mapped to a standard brain atlas. [3]

Brain Templates

Brain Templates

- Brain templates can be considered to be a subclass of brain atlases, which do not need to have labels or extra information about the anatomic or functional significance of locations, and are normally used as reference images for group analysis studies.

- For reporting the results in a standard coordinate system with a standard activation labeling, the brain template should be mapped to a standard brain atlas. [3]

Construction of Brain Templates and Atlases

- Due to large variations in the brain structure of human populations, the construction and use of standard brain atlases and brain templates pose a fundamental challenge in human brain mapping and in particular in brain functional localization.[3]

Outline

1. Introduction
   - Definition
   - Brain Image Processing
2. Brain Atlases and Templates
   - Application
   - Definitions
   - Examples of Brain Atlases
3. Registration Methods
   - Introduction

Atlas of Talairach and Tournoux

- Introduced in 1988 by Talairach and Tournoux.
- Stereotaxic atlas of the human brain based on post mortem sections of a subject's brain.
- Based on two relatively invariant subcortical point landmarks (AC and PC).
  - Origin: AC (anterior commissure).
  - y-axis: AC-PC (posterior commissure).
  - z-axis: vertical line through inter-hemispheric fissure.
  - x-axis: line passing through AC and at right angles to the y and z axis.
- Divided into 12 cubic rectangular regions.

Atlas of Talairach and Tournoux

- Introduced in 1988 by Talairach and Tournoux.
- Stereotaxic atlas of the human brain based on post mortem sections of a subject's brain.
- Based on two relatively invariant subcortical point landmarks (AC and PC).
  - Origin: AC (anterior commissure).
  - y-axis: AC-PC (posterior commissure).
  - z-axis: vertical line through inter-hemispheric fissure.
  - x-axis: line passing through AC and at right angles to the y and z axis.
- Divided into 12 cubic rectangular regions.

Atlas of Talairach and Tournoux [4]

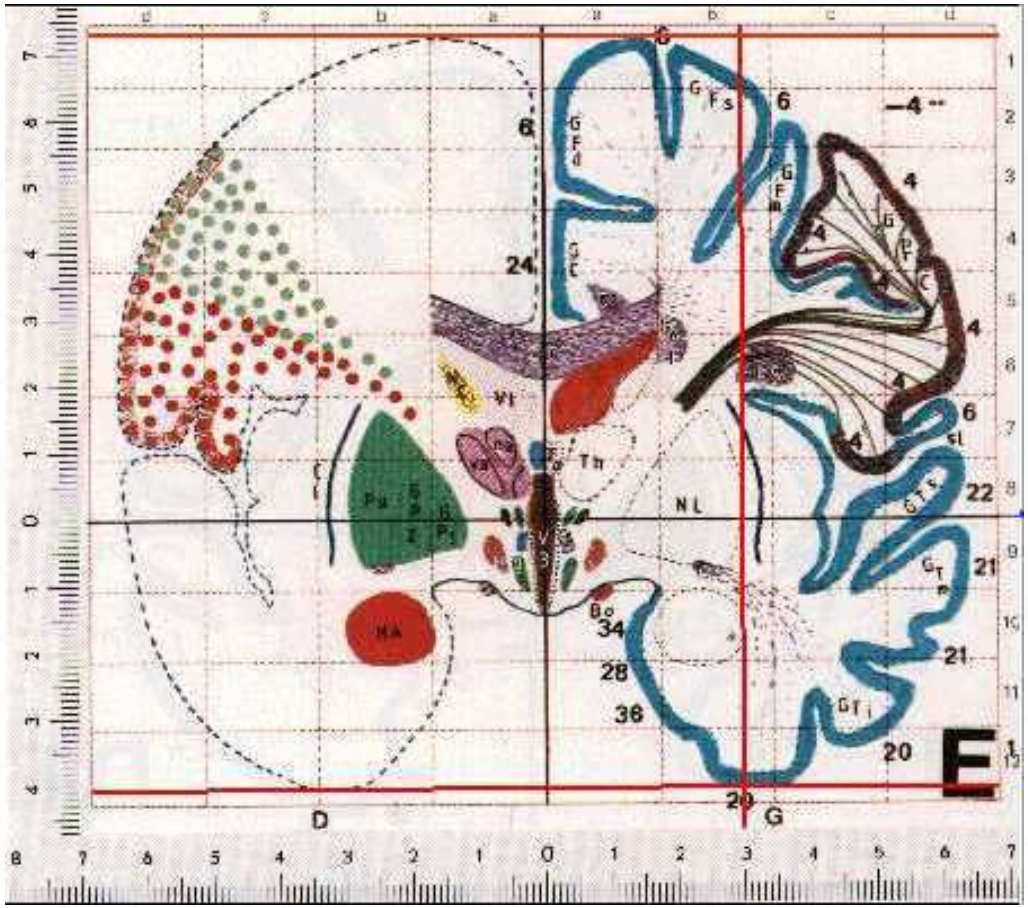

Talairach and Tournoux' atlas slice

Problems of the Talairach Atlas

- Talairach atlas problems:
  - Not sufficiently representative.
  - Cannot compensate for the anatomic variability of the differente brains.

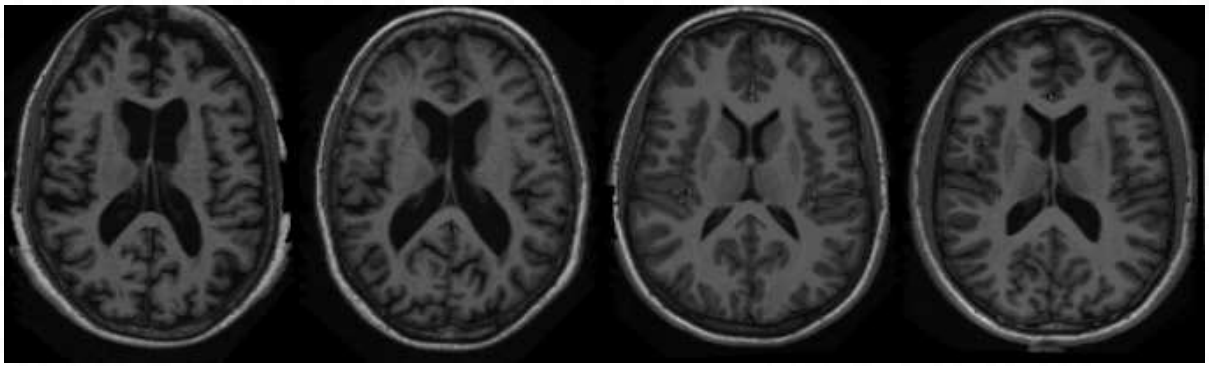

Different subjects from OASIS, linearly registered.

Digital Brain Atlases

- Based on high-resolution anatomical brain images, it involves the following stages:

1. Registration to the Talairach stereotaxic space.
2. Computing a geometric average brain.
3. Intensity averaging over the images registered to the computed geometric average brain.

Probabilistic Atlases

- Probability-encoded map of anatomic variability in the brain.
- Problem of blurring of the brain structures in the averaging process.
- Reliant upon the generality and reliability of the statistical samples and methods.
- New efforts in this field:
  - Maximum probability anatomical brain atlas.
  - Diffeomorphic probabilistic brain atlas.

Deformable Atlases

- Can be elastically transformed into the anatomy of individual brains using nonrigid registration techniques.
- Also used in joint registration and segmentations, providing automatic basis for functional localization and labeling.
- Characterizing the structural and anatomical differences is an ongoing research focus in clinical applications.
- Its effects on functional medical imaging have not been fully explored. [3]

MNI/ICBM Brain Templates

- Montreal Neurological Institute/International Consortium of Brain Mapping.
- MNI305 based on averaging a relatively large number of normal MRI brain images.
- ICBM adopted a MNI standard template named ICBM152 by registering 152 normal brain scans using a 9 parameter affine transformation.

Brain Phantoms

- Brain simulation images provide a way of generating data where ground truth is known and where realistic complexity may be taken into account when a realistic numerical phantom used as input to the simulator and the simulator reproduces the physics of data generation. [5]

- Simulations allow the control of various acquisition parameters, whereas real acquisitions are limited to the types of scan acquired.

Brain Phantoms

- Since some subtle real effects may not be included in simulations, these simulations are not sufficient to evaluate image processing methods.

- The ground truth and the realistic complexity of the simulated data allow the simulations to be an extremely helpful tool during the process of method of validation.

Brain Phantoms

- Physical Brain Phantoms:
  - Multimodality contrast and realistic motion, distortions and imaging issues.
  - Suffer from the lack of quantitative registration validity measures.
  - Not be easily deformed in a controlled manner.
- Digital Brain Phantoms:
  - More flexible.
  - Construction of accurate and realistic digital brain phantoms is a complicated task. [6]

Brain Phantoms

- Physical Brain Phantoms:
  - Multimodality contrast and realistic motion, distortions and imaging issues.
  - Suffer from the lack of quantitative registration validity measures.
  - Not be easily deformed in a controlled manner.
- Digital Brain Phantoms:
  - More flexible.
  - Construction of accurate and realistic digital brain phantoms is a complicated task. [6]

Outline

1. Introduction
   - Definition
   - Brain Image Processing
2. Brain Atlases and Templates
   - Application
   - Definitions
   - Examples of Brain Atlases
3. Registration Methods
   - Introduction

Classification of Registration Methods

- By transformation models:
  - Rigid registration.
  - Non-rigid registration.
- By subject relationship:
  - Intra-subject.
  - Inter-subject.

Classification of Registration Methods

- By transformation models:
  - Rigid registration.
  - Non-rigid registration.
- By subject relationship:
  - Intra-subject.
  - Inter-subject.

Image Registration Components [1]

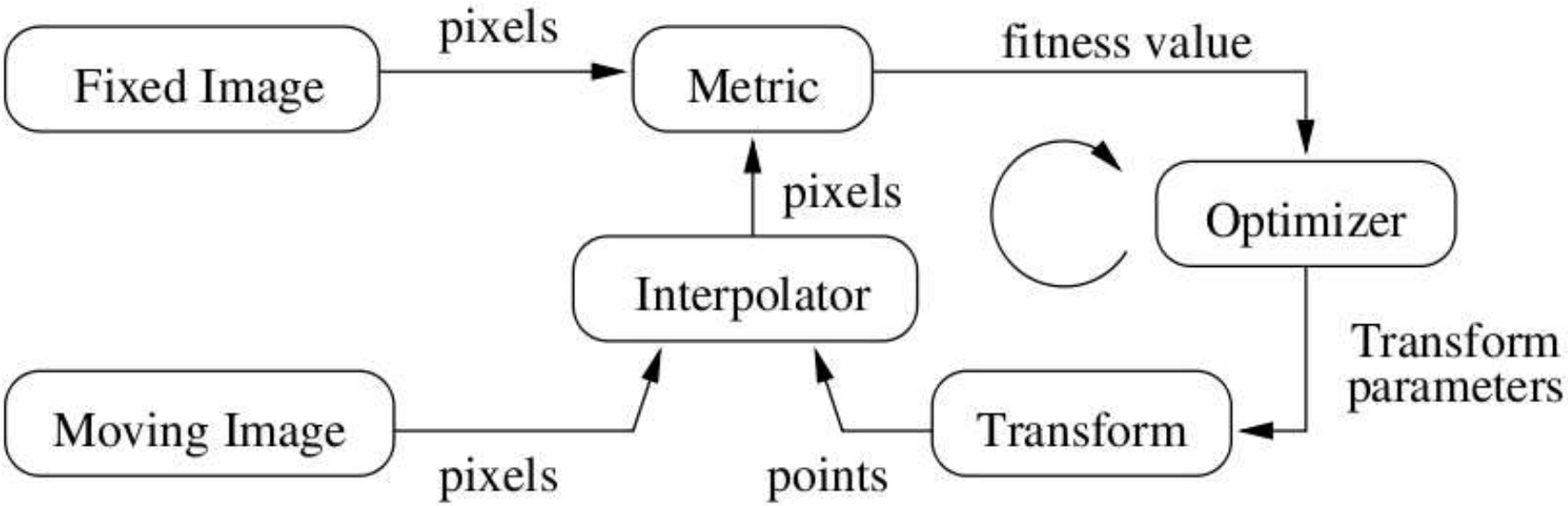

The basic components of the registration framework are two input images, a transform, a metric, an interpolator and an optimizer.

- Schroeder, L. I. W., [*The ITK Software Guide 2.4*], Kitware, Inc. (Nov. 2005).
- Hajnal, J. V., Hill, D. L., and Hawkes, D. J., [*Medical Image Registration*], CRC, 1 ed. (June 2001).
- Gholipour, A., Kehtarnavaz, N., Briggs, R., Devous, M., and Gopinath, K., "Brain functional localization: A survey of image registration techniques," *Medical Imaging, IEEE Transactions on* **26**, 427–451 (2007).
- for Neuroimaging at UCL, W. T. C., "http://www.fil.ion.ucl.ac.uk/spm/," (2006).
- Aubert-Broche, B., Evans, A. C., and Collins, L., "A new improved version of the realistic digital brain phantom," *NeuroImage* **32**, 138–145 (Aug. 2006).

Collins, D., Zijdenbos, A., Kollokian, V., Sled, J., Kabani, N., Holmes, C., and Evans, A., "Design and construction of a realistic digital brain phantom," *Medical Imaging, IEEE Transactions on* **17**, 463–468 (1998).

Brain Image Registration

Alexandre Manhães Savio[1]

[1]Grupo de Inteligencia Computacional
Basque Country University

2nd Jornadas de Inteligencia Computacional, 2008

Outline

1. Inter-Subject Registration
   - Introduction
   - Spatial Normalization
   - Volume Registration
   - Validation
   - Cortical Surface Registration
2. Functional-to-Anatomical Registration Methods
   - Correspondence Basis
   - Transformation Model
   - Optimization
   - Interpolation
   - Validation
3. Discussion

Outline

1. Inter-Subject Registration
   - Introduction
   - Spatial Normalization
   - Volume Registration
   - Validation
   - Cortical Surface Registration
2. Functional-to-Anatomical Registration Methods
   - Correspondence Basis
   - Transformation Model
   - Optimization
   - Interpolation
   - Validation
3. Discussion

- Normal and pathological aspects of brain functional localization
- Variability of brain anatomy between subjects is a major problem in analyzing groups of functional images
  - Loss of accuracy and reliability for statistical analysis
  - Problems in activation labeling and comparing results of different studies

Inter-Subject Registration

- Anatomical variability is highly nonlinear

Spatial Normalization

- To perform intersubject registration, all of the brain images are registered to a standard brain atlas or brain template

Inter-Subject Registration

- Anatomical variability is highly nonlinear

Spatial Normalization

- To perform intersubject registration, all of the brain images are registered to a standard brain atlas or brain template

Brain-Warping Techniques

- Volume registration techniques
  - Match the size and shape of different brains with each other or
  - Warp them into a standard brain template.
  - Based upon:
    - Voxel intensity values or
    - Anatomical features, utilizing internal landmarks as well as surface boundaries.
- Surface registration techniques
  - Utilizes the layered structure of the sulcal and gyral structures on the cortical surface

Brain-Warping Techniques

- Volume registration techniques
  - Match the size and shape of different brains with each other or
  - Warp them into a standard brain template.
  - Based upon:
    - Voxel intensity values or
    - Anatomical features, utilizing internal landmarks as well as surface boundaries.
- Surface registration techniques
  - Utilizes the layered structure of the sulcal and gyral structures on the cortical surface

Outline

1. Inter-Subject Registration
   - Introduction
   - Spatial Normalization
   - Volume Registration
   - Validation
   - Cortical Surface Registration
2. Functional-to-Anatomical Registration Methods
   - Correspondence Basis
   - Transformation Model
   - Optimization
   - Interpolation
   - Validation
3. Discussion

Spatial Normalization

- Simplest practical form of spatial normalization is the piecewise linear Talairach transformation
  - Cannot adequately deal with the anatomical variability
- Most of the newer developments are towards the use of spatial normalization in the high-resolution anatomical space of brain images.

Outline

1. Inter-Subject Registration
   - Introduction
   - Spatial Normalization
   - Volume Registration
   - Validation
   - Cortical Surface Registration
2. Functional-to-Anatomical Registration Methods
   - Correspondence Basis
   - Transformation Model
   - Optimization
   - Interpolation
   - Validation
3. Discussion

Volume Registration

- The choice of appropriate transformation models and correspondence bases has been controversial in volume registration techniques for spatial normalization.[1]
- Studies:
  - The use of various nonrigid transformation models and hybrid intensity and feature-based correspondence bases
  - Constraining the deformation fields to be smooth and physically correct with regularization techniques

Transformation Models

- Parametric Transformation Models
- Non-Parametric Transformation Models

Parametric Transformation Models

- FFD (Free-Form Deformation) models
  - Regular grid of control points, typically based on B-spline basis functions or radial basis functions. [2]
- Elastic-body spline warping models such as thin plate spline (TPS) warping models
- Local affine transformations
- Wavelet-mediated deformations

Non-Parametric Transformation Models

- Partial differential equations describing the deformation of elastic material
- The external forces are computed through the similarity measures, and the internal forces are normally formulated as cost functions penalizing excessive deformations.

Non-Parametric Transformation Models

- The deformation field models are normally described by:
  - Navier-Stokes equations in continuum mechanics
  - Euler-Lagrange in a variational framework
- Solved through FEM or the calculus of variations
- Optical Flow models and the dense deformation fields of grid points in the Demons algorithm.
  - Considered as an approximation of viscous fluid registration.

Regularization of the Brain-Warping

- Aims at constraining the solution of nonrigid registration to achieve physically acceptable and topologically correct smooth deformation fields

Regularization of the Brain-Warping

- Inherent in parametric nonrigid transformation models based on basis function interpolators such as
  - TPS (thin plate spline)
  - B-splines in FFD models.

Regularization of the Brain-Warping

- Control of the elasticity degree of the deformation field.
- Determine the elasticity and resolution of the transformation.
- Smoothness constraints formulated as the bending energy have been used for a regular grid of control points in the FFD model.
- Jacobian of transformation has also been incorporated as constraints for topology preservation via interval analysis optimization in a nonrigid registration algorithm.

Regularization of the Brain-Warping

- The PDE-based (partial differential equations) elastic models are generally more flexible than the parametric basis function models.
- The degree of elasticity is determined by the elastic Lamé constants
- Smoothness constraints have been formulated based on derivative, Laplacian, or Jacobian transforms of the deformation field in different studies.

Outline

1. Inter-Subject Registration
   - Introduction
   - Spatial Normalization
   - Volume Registration
   - Validation
   - Cortical Surface Registration
2. Functional-to-Anatomical Registration Methods
   - Correspondence Basis
   - Transformation Model
   - Optimization
   - Interpolation
   - Validation
3. Discussion

Validation of Inter-Subject Registration Techniques

- Several quantitative methods for validation [3]
- Not considered as an appropriate indicator of performance

Validation of Inter-Subject Registration Techniques

- Some methods:
  - Cross-validation through the use of similarity measures other than those utilized in each registration technique:
    - Average brain
    - Tissue overlap
    - Sulcus distance
  - Validation through manual expert segmentation

Validation of Inter-Subject Registration Techniques

- Qualitative validation of the registration results has also been carried out through:
  - Visual inspection
  - Matching of detected landmarks and segmentation
  - Postanalysis and interpretation of the loci of activation maps

Validation of Inter-Subject Registration Techniques: Example

- In a more comprehensive comparison of six intersubjects registration techniques, Hellier et al. utilized four different classes of performance measures:
  - Quantitative similarity measures (MSE (mean square error), CC (global correlation coefficient of intensity values) y MI (mutual information)) between the registered brains and the average brain volume as well as visual inspection of the sharpness of the average brain volume
  - Tissue overlap measures
  - Correlation of differential characteristics
  - Sulcal shape and distance measures

Validation of Inter-Subject Registration Techniques: Example

- Compared to an affine transformation, the higher dimensional registration techniques performed much better according to the first three performance criteria, but they did not perform better at matching cortical sulci structures.

Conclusion

Intersubject cortical variability remains a severe challenge for volume registration techniques.
It, thus, appears to be necessary to incorporate new track of studies on cortical surface registration into the spatial normalization procedure.

Validation of Inter-Subject Registration Techniques: Example

- Compared to an affine transformation, the higher dimensional registration techniques performed much better according to the first three performance criteria, but they did not perform better at matching cortical sulci structures.

Conclusion

Intersubject cortical variability remains a severe challenge for volume registration techniques.
It, thus, appears to be necessary to incorporate new track of studies on cortical surface registration into the spatial normalization procedure.

Outline

1. Inter-Subject Registration
   - Introduction
   - Spatial Normalization
   - Volume Registration
   - Validation
   - Cortical Surface Registration
2. Functional-to-Anatomical Registration Methods
   - Correspondence Basis
   - Transformation Model
   - Optimization
   - Interpolation
   - Validation
3. Discussion

Why is it needed for functional localization?

- Most of the normal anatomical variability in the brain is in the cortical layered structure
- The cortical surface structures, sulci and gyri, subdivide the brain into anatomically separate areas needed for activation labeling.
- Due to the highly folded nature of the cortical surface, a small inaccuracy in volume registration may result in large inaccuracies in structural localization

Cortical Surface Registration

- The evolution of cortical surface techniques involves a sequence of geometrical image processing algorithms including surface reconstruction, segmentation and structural modeling, inflation, flattening, and mapping to a surface-based coordinate system. [4, 5]

- Surface reconstruction is an unfolding procedure to represent or visualize the folded geometry of the cortical surface.

Cortical Surface Registration

- Most of the implemented tools are based on initial segmentations for white matter, gray matter, and cerebrospinal fluid tissue classification, triangular tessellation for reconstruction, and a topology correction method to provide geometrical smoothness and topology preservation.
- The required steps to go from the cortical surface reconstruction to the surface registration and visualization for functional localization include cortical surface inflation, flattening and probably more advanced structural segmentation.

Cortical Surface Registration

- Inflation is useful for visualization, and flattening to planar, spherical or ellipsoidal maps is a simplification to permit registration of the cortical surface-based standard coordinates.

- Detection of structural surface features, i.e., sulci and gyri, has a direct impact on surface registration techniques.

Cortical Surface Registration

- The newer cortical surface registration techniques are based on geometrical features or sulcus models and maps.
- The final stage of functional localization, activation labeling, is highly affected by the previous steps. Cortical surface reconstruction is useful primarily for visualizing the 3D location of activation maps as well as for high-level manual neuroanatomic labeling.

Automatic Neuroanatomic Labeling

- Thanks to accurate surface registration and sulcus matching techniques.
- Validation of the automatic labeling techniques includes:
  - Statistical analysis of consistency, accuracy and efficiency with respect to experts' manual labeling
- Nevertheless, due to the difficulties in sulcus matching, most of the algorithms have been used to produce assisted labeling rather than fully automated labeling.

Automatic Neuroanatomic Labeling

- Brain labeling algorithms:
  - Anatomical automatic labeling by Tzourio-Mazoyer [6] for SPM2.
  - Program for assisted labeling of sulcal regions (PALS) by Rettman [7].
  - Mindboggle by Klein and Hirsch [8]. Can be downloaded from NITRC `http://www.nitrc.org/projects/mindboggle`.
  - Automatic Nonlinear Image Matching and Anatomical Labeling (ANIMAL) by Collins and Evans [9]. Included within the ICBM software tools.

Outline

1. Inter-Subject Registration
   - Introduction
   - Spatial Normalization
   - Volume Registration
   - Validation
   - Cortical Surface Registration
2. Functional-to-Anatomical Registration Methods
   - Correspondence Basis
   - Transformation Model
   - Optimization
   - Interpolation
   - Validation
3. Discussion

Correspondence Basis [10]

- Find correspondences between functional to anatomical images.
- Spatial resolution, signal-to-noise ratio and contrast are less in functional images than those in anatomical images.
- Brain structures quite vague in fMRI and even more in PET and SPECT.

Extrinsic Correspondence Methods

- Artifical fiduciary markers visible in both functional and anatomical images.

Intrinsic Correspondence Methods

1. Feature-based methods.
2. Intensity-based methods

Feature-based Methods

- Automatic feature extraction or segmentation
- Manual or semi-automatic landmark detection
- For example: "head-and-hat" [11, 12], chamfer matching [13], iterative closest point (ICP) [14]
  - Very few recent papers

Intrinsic Correspondence Methods

- Intensity based methods
  - Absolute or sum-of-square intensity differences [15]
  - Cross-correlation of intensity values
  - Variance of intensity ratios [16]
  - Similarity measures based upon information theory [17, 18]
    - Normalized mutual information (NMI)
    - Entropy correlation coefficient
    - Drawback: ignorance of space information

Similarity Measures and Information Theory

- Research on quantifying the joint histogram of two brain images was redirected to use similarity measures based upon information theory, i.e., the concept of entropy and joint entropy of images, which resulted in the introduction of mutual information (MI) as a generally applicable similarity measure. [19, 20]

- The MI of two images describes the amount of information in the joint histogram of the images, hence its maximization results in the best match of intensity correspondences between the images for registration.

Research on Similarity Measure

1. Improve computational accuracy and efficiency of joint histogram and joint entropy estimation
2. Incorporate spatial information into MI
   - Jumarie entropy [21]
   - Combination of gradient information and MI [22]
   - Spatial feature vectors, multifeature MI and regional MI based on higher dimensional histograms
   - Quantitative-qualitative measure of MI (Q-MI), to improve noise rebustness
3. Utilize more generalized measures from information theory
   - f-information measures used in quantifying the divergence of probability density functions (PDFs) [23]

Outline

1. Inter-Subject Registration
   - Introduction
   - Spatial Normalization
   - Volume Registration
   - Validation
   - Cortical Surface Registration
2. Functional-to-Anatomical Registration Methods
   - Correspondence Basis
   - Transformation Model
   - Optimization
   - Interpolation
   - Validation
3. Discussion

Transformation Model

- Rigid transformation
- Affine transformation
  - 3 coordinates for: translation, rotation, scale, shearing
  - 12 degrees of freedom transformation
  - Fully modeled as 4x4 matrices
- Used because of presence of local nonrigid geometric distortions in fast functional imaging due to:
  - Eddy current effects
  - Field inhomogeinity
  - Susceptibility artifacts
  - Dephasing effects

Non-Rigid Transformation

- High dimensional non-rigid transformations for functional-to-anatomical brain image registration
  - Unidirectional B-spline basis functions [24]
  - Optical flow model [25]
  - Free form deformation with regular grid of control points [26]

- The most important challenge is the definition of appropriate constraints to avoid excessive deformations
  - Regularization methods
  - Smoothness and diffeomorphic constraints

Outline

1. Inter-Subject Registration
   - Introduction
   - Spatial Normalization
   - Volume Registration
   - Validation
   - Cortical Surface Registration
2. Functional-to-Anatomical Registration Methods
   - Correspondence Basis
   - Transformation Model
   - Optimization
   - Interpolation
   - Validation
3. Discussion

Optimization

- Search of those parameters of the transformation model that minimize a cost function [27]
- Cost functions:
  - Function of correspondences or similarity between source and target images
  - Can contain explicit regularization terms for smoothness and diffeomorphic constraints

Optimization

- Search of those parameters of the transformation model that minimize a cost function [27]
- Cost functions:
  - Function of correspondences or similarity between source and target images
  - Can contain explicit regularization terms for smoothness and diffeomorphic constraints

Optimization

- Optimization algorithms:
  - Global techniques such as evolutionary algorithms and simulated annealing rarely used in medical image registration
  - Multiresolution and multiscale optimization frameworks faster and more robust
    - Gradient descent, quasi-Newton and Levenberg-Marquardt require derivative calculation. Not easy for cost functions, although possible
    - State-of-the-art optimization algorithm: Parzen window estimation [28]

Outline

1. Inter-Subject Registration
   - Introduction
   - Spatial Normalization
   - Volume Registration
   - Validation
   - Cortical Surface Registration
2. Functional-to-Anatomical Registration Methods
   - Correspondence Basis
   - Transformation Model
   - Optimization
   - Interpolation
   - Validation
3. Discussion

Interpolation

- Used within each iteration of the registration algorithm to resample the transformed source image to the physical space of the target image. [29]
- Interpolation kernels:
  - Trilinear, quadratic and B-spline kernels seem to be the most popular in registration applications.
  - Partial Volume (PV) interpolation for marginal PDF estimation. Continuous and differentiable registration criterion.

Interpolation

- Used within each iteration of the registration algorithm to resample the transformed source image to the physical space of the target image. [29]
- Interpolation kernels:
  - Trilinear, quadratic and B-spline kernels seem to be the most popular in registration applications.
  - Partial Volume (PV) interpolation for marginal PDF estimation. Continuous and differentiable registration criterion.

Outline

1. Inter-Subject Registration
   - Introduction
   - Spatial Normalization
   - Volume Registration
   - Validation
   - Cortical Surface Registration
2. Functional-to-Anatomical Registration Methods
   - Correspondence Basis
   - Transformation Model
   - Optimization
   - Interpolation
   - Validation
3. Discussion

Validation

- Necessary to guarantee the fidelity and usefulness of registration techniques
  - Accuracy and robustness
  - Consistency and reliability
  - Resource requirements and computational complexity
  - Impact
- Problem: Find appropriate correspondences between images of different modalities.

Validation

- Most promising current similarity measures in multimodality image registration operate in the intensity domain, thus, they do not provide useful information about the correctness of registration, and errors.
- Independent quantitative and qualitative assessments of registration fidelity are essential to prove the usefulness of any multimodality image registration algorithm.
  - Accuracy and robustness
  - Consistency and reliability

Validation

- Quantitative validation is only possible when a ground truth is available.
  - Extrinsic Markers
  - Brain phantoms [25]

Brain Atlases and Brain Templates

- The success of a brain atlas depends upon how well the brains of different anatomies can be matched to the representation of anatomy in the atlas.
- Deformable and probabilistic brain atlases have been proposed to obtain more accurate representations of the anatomy in the atlas.
- Cortical surface registration, sulcus matching techniques, and advanced nonrigid registration techniques can be utilized as tools in the construction of more realistic and accurate deformable brain atlases.

Brain Atlases and Brain Templates

- Structural variability in the cortical morphology is a real challenge for developing a standard cortical map of the brain.
- More brain variability when comparing the function and structure of different groups of subjects
- Considerable variations of brain anatomy in psychiatric and mental diseases have been the motivation for developing disease-specific brain atlases.
- The choice of an atlas or template, in standard coordinates or based on deformable subpopulation atlases, depends on the type of clinical and scientific studies and may greatly affect the interpretation and comparison of the results.

Functional-to-Anatomical Registration

- Functional-to-anatomical brain image registration still remains and important research area.
- In single-subject analysis and specification in neurosurgical applications, the accuracy and reliability is the limiting factor.
- In group-analysis, spatial normalization is the most prominent source of inaccuracy. In practice, the current functional-to-anatomical registration techniques involve the optimization of an affine transformation model in a multiresolution framework to maximize a similarity measure.
- Mutual information or normalized mutual information has shown to be the most robust and accurate similarity measure in many studies.

Functional-to-Anatomical Registration

- The research is now focused on finding appropriate correspondences through more general and reliable similarity measures upon information theory, i.e., extending MI to incorporate spatial information.
- Nonrigid registration has been proposed to deal with the effect of nonlinear local distortions in functional images, specifically in EPI images used for fMRI.
- In-vivo validation of nonrigid multimodality registration techniques is extremely difficult due to the lack of reliable and accurate local correspondences between images.

Inter-Subject Registration

- Current spatial normalization techniques, such as the low-frequency cosine basis functions in SPM, the Demons algorithm, ANIMAL, OSN, HAMMER, and PASHA, seem to perform satisfactorily in common neuroscience applications.

- More accurate functional localization is often desired, especially as images of higher resolution become available, for more demanding applications.

Inter-Subject Registration

- Development of methods such as:
  - Cortical reconstruction
  - Segmentation
  - Tissue classification
  - Flattening and mapping to planar, ellipsoidal or spherical surfaces
- Utilizes powerful tools from differential geometry, image processing and computer vision, including deformable active statistical shape models.

Final Conclusion

- Technical advances in functional brain image and automatic functional localization are leading to clinical and scientific applications with higher spatial and temporal resolutions.
- The construction of standard and subpopulation brain atlases and brain templates, functional-to-anatomical registration, and spatial normalization through volumetric registration and cortical surface registration are deemed important fields of study in this burgeoning area of research.

- Rueckert, D., Frangi, A., and Schnabel, J., "Automatic construction of 3-d statistical deformation models of the brain using nonrigid registration," *Medical Imaging, IEEE Transactions on* **22**, 1014–1025 (2003).
- Tustison, Avants, Sundaram, Duda, and Gee, "A generalization of free-form deformation image registration within the itk finite element framework," (2006).
- Liu, T., Shen, D., and Davatzikos, C., "Deformable registration of cortical structures via hybrid volumetric and surface warping," *NeuroImage* **22**, 1790–1801 (Aug. 2004).
- Xu, C., Pham, D., Rettmann, M., Yu, D., and Prince, J., "Reconstruction of the human cerebral cortex from magnetic resonance images," *Medical Imaging, IEEE Transactions on* **18**, 467–480 (1999).

- Drury, H. A., Essen, D. C. V., Corbetta, M., and Snyder, A. Z., [*Surface-Based Analyses of the Human Cerebral Cortex*], 337–361, Academic Press, San Diego (1999).
- Tzourio-Mazoyer, N., Landeau, B., Papathanassiou, D., Crivello, F., Etard, O., Delcroix, N., Mazoyer, B., and Joliot, M., "Automated anatomical labeling of activations in spm using a macroscopic anatomical parcellation of the mni mri single-subject brain," *NeuroImage* **15**(1), 273–289 (2002).
- Rettmann, M. E., Tosun, D., Tao, X., Resnick, S. M., and Prince, J. L., "Program for assisted labeling of sulcal regions (pals): description and reliability," *NeuroImage* **24**(2), 398–416 (2005).
- Klein, A., Mensh, B., Ghosh, S., Tourville, J., and Hirsch, J., "Mindboggle: Automated brain labeling with multiple atlases," *BMC Medical Imaging* **5**(1), 7 (2005).

- Collins, D. L. and Evans, A. C., "Animal: Validation and applications of nonlinear registration-based segmentation," *IJPRAI* **11**(8), 1271–1294 (1997).
- Gholipour, A., Kehtarnavaz, N., Briggs, R., Devous, M., and Gopinath, K., "Brain functional localization: A survey of image registration techniques," *Medical Imaging, IEEE Transactions on* **26**, 427–451 (2007).
- Levin, D. N., Pelizzari, C. A., Chen, G. T., Chen, C. T., and Cooper, M. D., "Retrospective geometric correlation of mr, ct, and pet images," *Radiology* **169**, 817–23 (Dec. 1988). PMID: 3263666.

- Pelizzari, C. A., Chen, G. T., Spelbring, D. R., Weichselbaum, R. R., and Chen, C. T., "Accurate three-dimensional registration of ct, pet, and/or mr images of the brain," *Journal of Computer Assisted Tomography* **13**(1), 20–6 (1989). PMID: 2492038.
- Borgefors, G., "Hierarchical chamfer matching: A parametric edge matching algorithm," *IEEE Trans. Pattern Anal. Mach. Intell.* **10**, 849–865 (Nov. 1988).
- Besl, P. and Mckay, H., "A method for registration of 3-d shapes," *Pattern Analysis and Machine Intelligence, IEEE Transactions on* **14**(2), 239–256 (1992).
- Friston, K., Ashburner, J., Frith, C., Poline, J., Heather, J. D., and Frackowiak, R., "Spatial registration and normalization of images," *Human Brain Mapping* **2**, 165–189 (1995).

- Woods, R. P., Mazziotta, J. C., and Cherry, S. R., "Mri-pet registration with automated algorithm," *Journal of Computer Assisted Tomography* **17**(4), 536–46 (1993). PMID: 8331222.
- Pluim, J., Maintz, J., and Viergever, M., "Mutual-information-based registration of medical images: a survey," *Medical Imaging, IEEE Transactions on* **22**(8), 986–1004 (2003).
- Maes, F., Vandermeulen, D., and Suetens, P., "Medical image registration using mutual information," *Proceedings of the IEEE* **91**(10), 1699–1722 (2003).
- Maes, F., Collignon, A., Vandermeulen, D., Marchal, G., and Suetens, P., "Multimodality image registration by maximization of mutual information," *Medical Imaging, IEEE Transactions on* **16**, 187–198 (1997).

- Klein, S., Staring, M., and Pluim, J., "Evaluation of optimization methods for nonrigid medical image registration using mutual information and b-splines," *Image Processing, IEEE Transactions on* **16**, 2879–2890 (2007).
- Rodriguez-Carranza, C. E. and Loew, M. H., "Weighted and deterministic entropy measure for image registration using mutual information," **3338**, 155–166 (June 1998).
- Pluim, J., Maintz, J., and Viergever, M., "Image registration by maximization of combined mutual information and gradient information," *Medical Imaging, IEEE Transactions on* **19**(8), 809–814 (2000).
- Chung, A. C. S., Iii, W. M. W., Norbash, E., Eric, W., and Grimson, L., "Multi-modal image registration by minimising kullback-leibler distance," *H.-M. Chan and A.C.S. Chung* **2002**, 525—532 (2002).

- Kybic, J., Nirkko, A., and Unser, M., "1 unwarping of unidirectionally distorted epi images," *IEEE Trans. Medical Image Analysis* (2000).
- Ardekani, S. and Sinha, U., "Constrained free form deformation based algorithm for geometric distortion correction of echo planar diffusion tensor images," in [*Biomedical Imaging: Nano to Macro, 2004. IEEE International Symposium on*], 340–343 Vol. 1 (2004).
- Studholme, C., Constable, R., and Duncan, J., "Accurate alignment of functional epi data to anatomical mri using a physics-based distortion model," *Medical Imaging, IEEE Transactions on* **19**(11), 1115–1127 (2000).

- Maes, F., Vandermeulen, D., and Suetens, P., "Comparative evaluation of multiresolution optimization strategies for multimodality image registration by maximization of mutual information," *Medical Image Analysis* **3**(4), 373–386 (1999).
- Unser, M., "Optimization of mutual information for multiresolution image registration," *IEEE Transactions on Image Processing* **9**, 2083—2099 (2000).
- Meijering, E., "A chronology of interpolation: from ancient astronomy to modern signal and image processing," *Proceedings of the IEEE* **90**, 319–342 (2002).

Relevance Fedback for CBIR Systems

José Orlando Maldonado Bautista

UPV/EHU

JIC-2008

1 CBIR Systems

2 Relevance Feedback

3 Early approaches

4 Neural Network Based

5 SVM's based

6 Bayesian approach

Introduction

- Content-based image retrieval (CBIR), is any technology that in principle helps to organize digital picture archives by their visual content.
- In the CBIR systems, the images are indexed by descriptors based on features of images such as color, texture, shape, spatial relations, and so.

Introduction

- Typical framework for content-based image retrieval

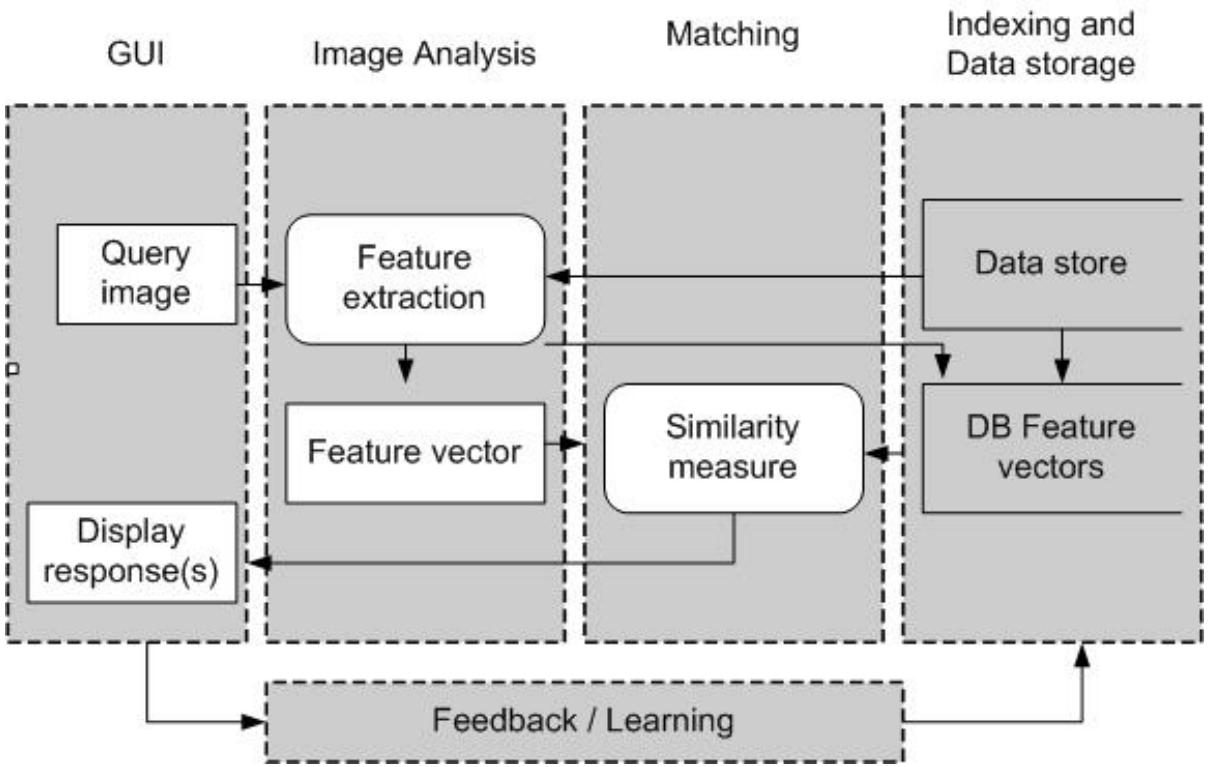

Introduction

- GUI examples of CBIR systems

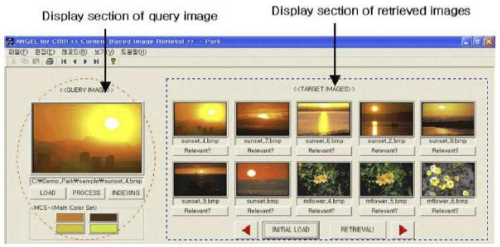

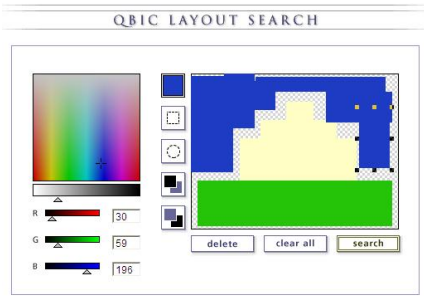

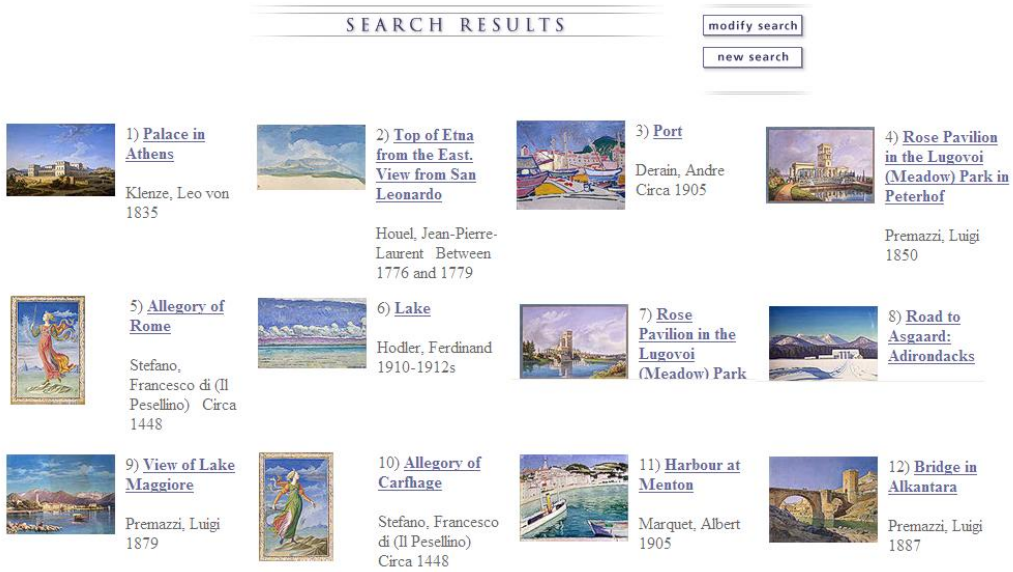

Image Domain & Semantic Gap

- A narrow domain has a limited and predictable variability in all relevant aspects of its appearance. (e.g. catalogues of parts).
- A broad domain has an unlimited and unpredictable variability in its appearance even for the same semantic meaning. (e.g. photographical stocks).

Image Domain & Semantic Gap

- Semantics is a categorization of objects according to some criterion of similarity.
- The user's semantic in time of search is the category of the objects that he/she has in mind.
- The lack of agreement between these two categorizations is known as the semantic gap.

Idea

- Relevance feedback (RF) is a query modification technique which attempts to capture the user's precise needs through iterative feedback and query refinement, and thus contribute in narrowing the semantic gap.

Flow diagram

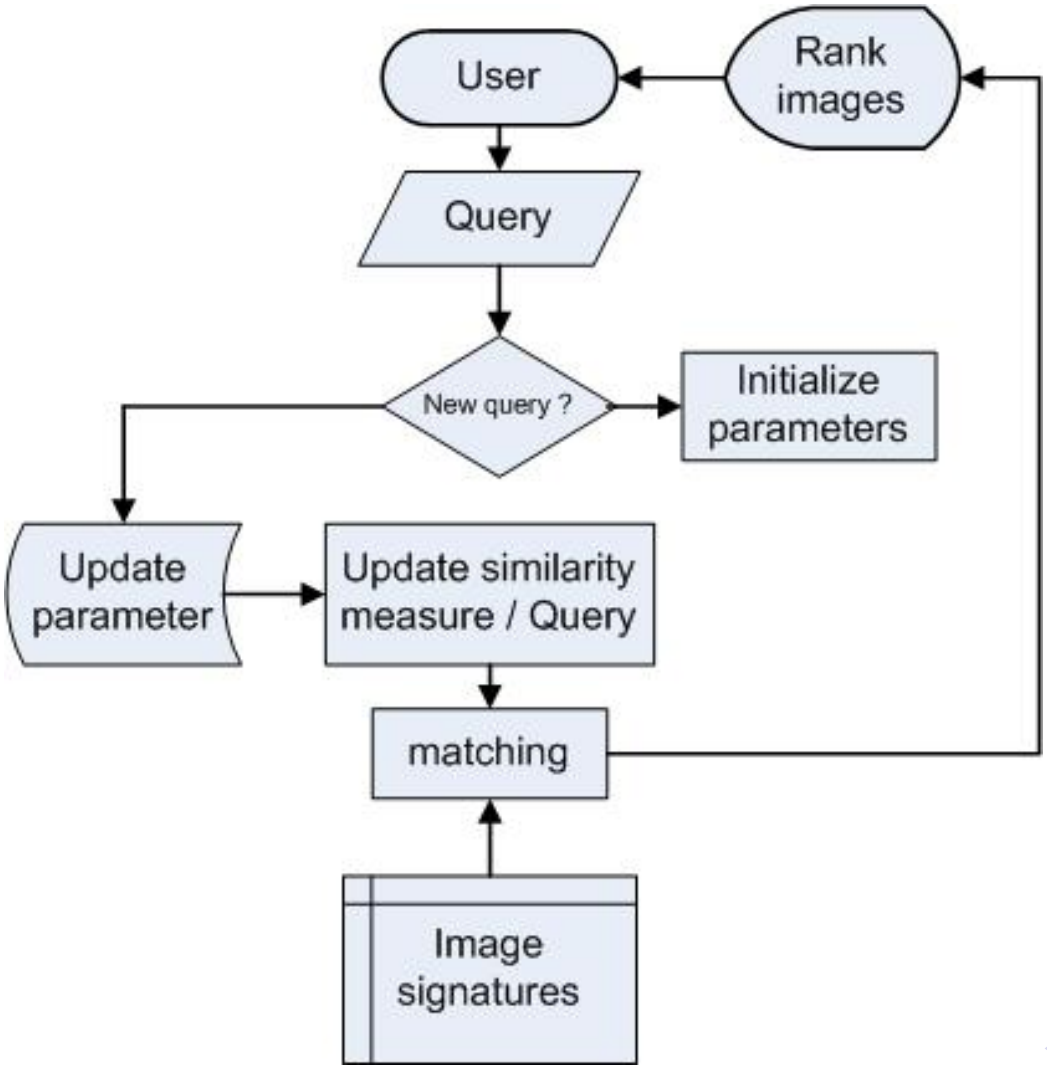

Heuristic methods

[Rui et al, 1998] An image object O is represented as: $O = O(D, F, R)$:

- D: is the raw image data, e.g., a JPEG image.
- $F = \{f_i\}$a set of low-level visual features such as color, texture, and shape.
- $R = \{r_{ij}\}$a set of representations for a given feature e.g., both color histogram and color moments are representations for the color feature.
- $rij = [r_{ij1}; ::::; r_{ijk}; ::::; r_{ijK}]$, where K is the length of the vector.

Together with a set of similarity measures $M = \{m_{ij}\}$, it has a CBIR model (D, F, R, M). Different similarity measures may be used for different feature representations.

Heuristic methods

- Weights exist at various levels W_i, W_{ij},W_{ijk}, and are associated with features representations and components respectively.

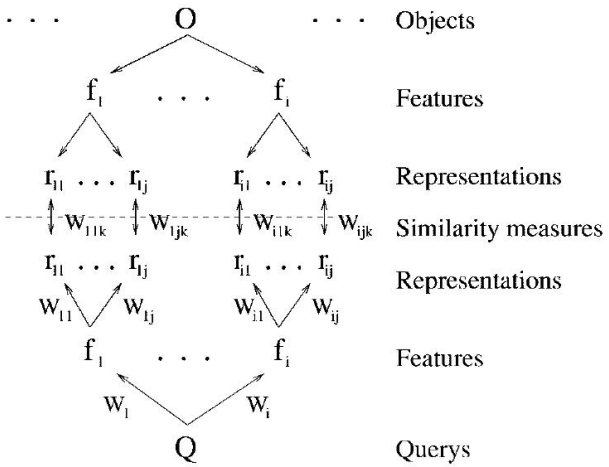

- The goal of relevance feedback is to find the appropriate weights to model the user's information need.

Heuristic methods

The retrieval process is as follow:
1. Initialize the weights W_i, W_{ij}, W_{ijk}.
2. The objects' similarity to the query, in terms of r_{ij} is calculated:

$$S(r_{ij}) = m_{ij}\left(r_{ij}, W_{ijk}\right).$$

3. Each representation's similarity values and the overall similarity are calculated:

$$\begin{aligned} S(f_i) &= \sum_j W_{ij} S(r_{ij}) \\ S &= \sum_j W_i S(f_i) \end{aligned}$$

Heuristic methods

4. The N most similar images are returned to the user.
5. For each of the retrieved objects, the user marks it as *highly relevant, relevant, no opinion, nonrelevant, or highly nonrelevant*, according to his information need and perception subjectivity.
7. The system updates the weights according to the user's feedback.
8. Go to step 2) with the adjusted and start a new iteration of retrieval.

Heuristic methods

NORMALIZATION

- Intranormalization: This normalization process puts equal emphasis on each r_{ijk} component within a representation vector r_{ij}.

$$V_{m,k} = \frac{V_{m,k} - \mu_k}{3\sigma_k}$$

- Where $V = r_{ij}$ and $V_m = [V_{m,1}, ..V_{m,K}]$ is the representation vector for image m where K is the length of vector V, and $m = 1, ..M$.

Heuristic methods

NORMALIZATION

- Internormalization: ensures equal emphasis of each individual similarity value $S(r_{ij})$ within the overall similarity value S.
- For any pair of images I_m, I_n and in the image collection compute $S_{m,n}(r_{ij}) = m_{ij}(r_{ij}, W_{ijk})$.
- Treat them as a data sequence, and find the mean and standard deviation of the sequence.
- When a query Q is presented, compute the raw similarity values between Q and the images in the database. $S_m, Q(r_{ij}) = mij(r_{ij}, W_{ijk})$.
- Normalize the raw similarity values as follows:

$$S'_{m,Q} = \frac{S_{m,Q}(r_{ij}) - \mu_{ij}}{3\sigma_{ij}}.$$

Heuristic methods

WEIGHT UPDATING

Update of W_{ij} (Interweight)

- Let be RT the set of the most similar N objects according to the overall similarity value S. Thus $RT = \{RT1, ..RTl, ..RTN\}$
- Let be Score the set containing the relevance scores fedback by the user for $RTl's$:
  - highly relevant (3),
  - relevant (1),
  - no opinion (0),
  - nonrelevant (-1),
  - highly nonrelevant (-3).
- For each r_{ij} let RT_{ij} be the set containing the most similar N objects to the query Q according to the similarity values $S(r_{ij}).RT_{ij} = \{RT_{1ij}, ..RT_{lij}, ..RT_{Nij}\}$.

Heuristic methods

WEIGHT UPDATING

Update of W_{ijk} (Intraweight)

- To stack vector $r'_{ij}s$, for those objects that are marked *highly relevant or relevant* by the user form a $M'xK$ matrix, then compute:

$$Wijk = \frac{1}{\sigma_{ijk}},$$

where σ_{ijk} *is the standard deviation of the length-* M' *sequence of* $W'_{ijk}s$.

- Finally, weights $W'_{ijk}s$ are normalized in the way:

$$W_{ij} = \frac{W_{ij}}{\sum W_{ij}}$$

Heuristic methods

EXPERIMENTAL RESULTS

- The first image collection contains 286 ancient African and Peruvian artifacts, and is part of the Museum Educational Site Licensing Project (MESL):

$$F = f_i = \{color, texture, shape\}$$

$$\begin{aligned} R \quad = \quad & r_{ij} = \{r_1, .., r_6\} = \{colorhistogram, colormoments, Tamura, \\ & cooccurrencematrix, Fourierdescriptor, \\ & Chamfershapedescriptor\} \end{aligned}$$

- The second image collection contains more than 70 000 images covering a wide range of more than 500 categories:

$$R = r_{ij} = \{r_1, r_2, r_3\} = \{colorhistogram, colormoments, cooccurrencematrix\}.$$

Heuristic methods

EXPERIMENTAL RESULTS

For the MESL, the six moderate and the six significant offset testing weights are:

$$W_1^* = [0.5\ 0.1\ 0.1\ 0.1\ 0.1\ 0.1]$$
$$W_2^* = [0.1\ 0.5\ 0.1\ 0.1\ 0.1\ 0.1]$$
$$W_3^* = [0.1\ 0.1\ 0.5\ 0.1\ 0.1\ 0.1]$$
$$W_4^* = [0.1\ 0.1\ 0.1\ 0.5\ 0.1\ 0.1]$$
$$W_5^* = [0.1\ 0.1\ 0.1\ 0.1\ 0.5\ 0.1]$$
$$W_6^* = [0.1\ 0.1\ 0.1\ 0.1\ 0.1\ 0.5].$$

$$W_7^* = [0.75\ 0.05\ 0.05\ 0.05\ 0.05\ 0.05]$$
$$W_8^* = [0.05\ 0.75\ 0.05\ 0.05\ 0.05\ 0.05]$$
$$W_9^* = [0.05\ 0.05\ 0.75\ 0.05\ 0.05\ 0.05]$$
$$W_{10}^* = [0.05\ 0.05\ 0.05\ 0.75\ 0.05\ 0.05]$$
$$W_{11}^* = [0.05\ 0.05\ 0.05\ 0.05\ 0.75\ 0.05]$$
$$W_{12}^* = [0.05\ 0.05\ 0.05\ 0.05\ 0.05\ 0.75].$$

For the Corel Stock test set, offset testing weights are:

$$W_1^* = [0.6\ 0.2\ 0.2]$$
$$W_2^* = [0.2\ 0.6\ 0.2]$$
$$W_3^* = [0.2\ 0.2\ 0.6].$$

$$W_4^* = [0.8\ 0.1\ 0.1]$$
$$W_5^* = [0.1\ 0.8\ 0.1]$$
$$W_6^* = [0.1\ 0.1\ 0.8].$$

Heuristic methods

EXPERIMENTAL RESULTS

- Convergence ratio curves. (a) MESL test set. (b) Corel test set.

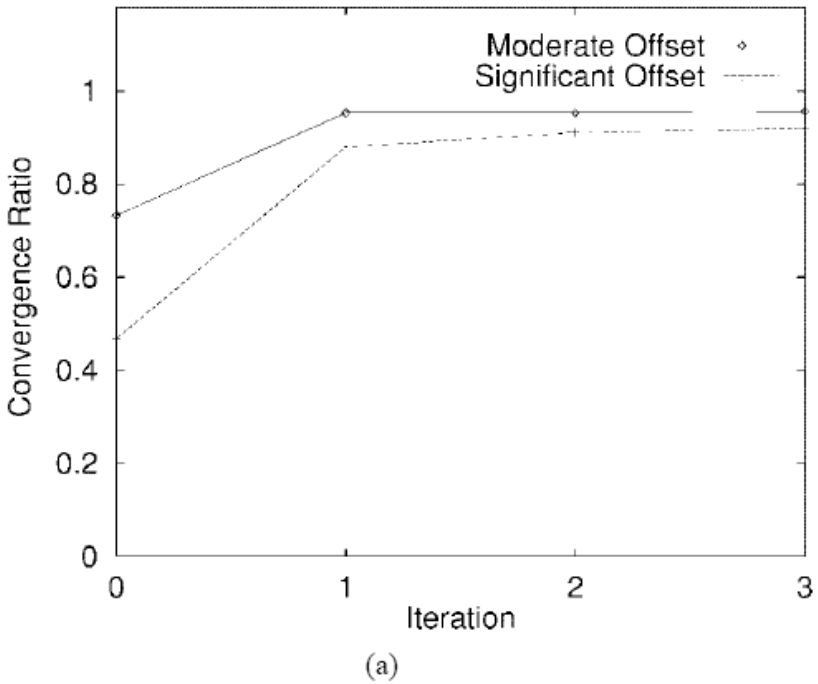

(a)

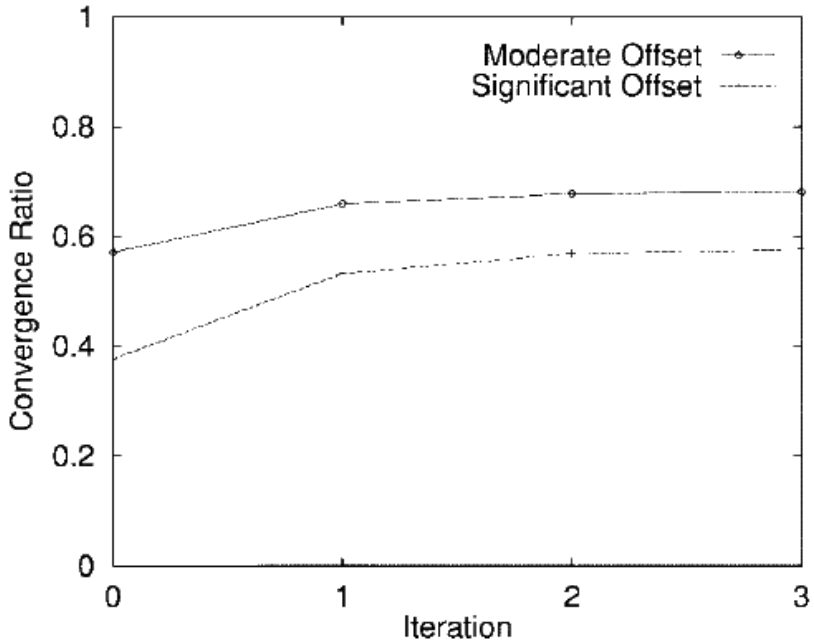

(b)

Heuristic methods

EXPERIMENTAL RESULTS

- Convergence ratio for MESL test set with w_7^*

TABLE V
CONVERGENCE RATIO FOR MESL TEST SET WITH W_7^*

N_{NT}	0 feedback	1 feedback	2 feedbacks	3 feedbacks
10	40.4	89.7	97.4	98.6
12	40.9	89.6	97.4	98.5
14	40.8	90.2	97.9	98.4
16	40.2	91.3	98.0	98.2
18	40.4	93.2	97.8	98.0
20	40.5	95.9	97.8	97.9

- Convergence ratio for Corel test set with w_4^*

TABLE VI
CONVERGENCE RATIO FOR COREL TEST SET WITH W_4^*

N_{NT}	0 feedback	1 feedback	2 feedbacks	3 feedbacks
850	40.6	63.4	68.5	69.6
900	40.9	63.8	69.0	70.1
950	41.2	64.2	69.6	70.6
1000	41.4	64.6	70.0	71.1
1050	41.6	65.1	70.6	71.7
1100	41.9	65.5	70.9	72.0

Using Radial Basis Function Network [Lee & Yoo, 2002]

- DB Searcher: compares each query feature to the corresponding feature vector of DB images and returns the compared metric value vector.
- MC: Combine the compared metric values, <v1,v2,..,vr>, using the RBF network and yields the ranked list of retrieved images.
- User mark according to his perception subjectivity

$$UF(q) = \begin{cases} 0,9 & \text{if alike} \\ 0,5 & \text{if similar} \\ 0 & \text{if diferent} \end{cases}$$

Using Radial Basis Function Network

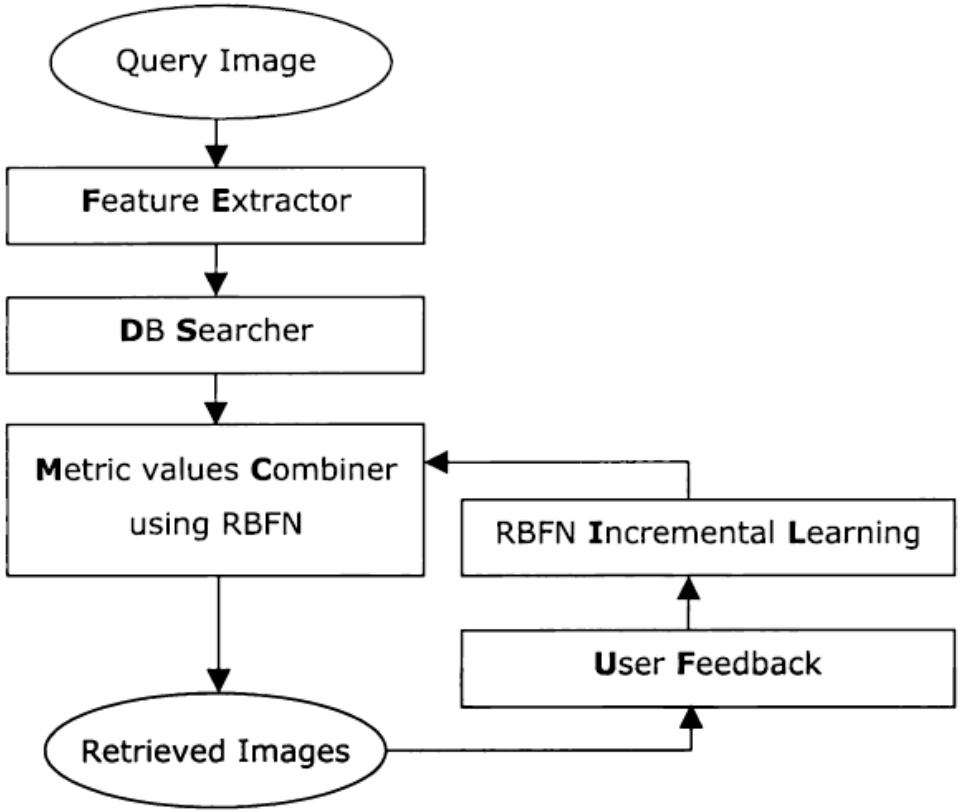

NNIR system.

Using Radial Basis Function Network

- The RBF network has been proved to be a universal function approximator.

$$
\begin{aligned}
y &= f(\bar{v}) + \varepsilon \\
f(\bar{v}) &= \sum_{j}^{p} w_j \left(g\left(\bar{v} - c_j \right) \right) \\
g\left(\|\bar{v}\| - c_j \right) &= exp\left(\frac{\|\bar{v} - c_j\|}{2\sigma} \right)
\end{aligned}
$$

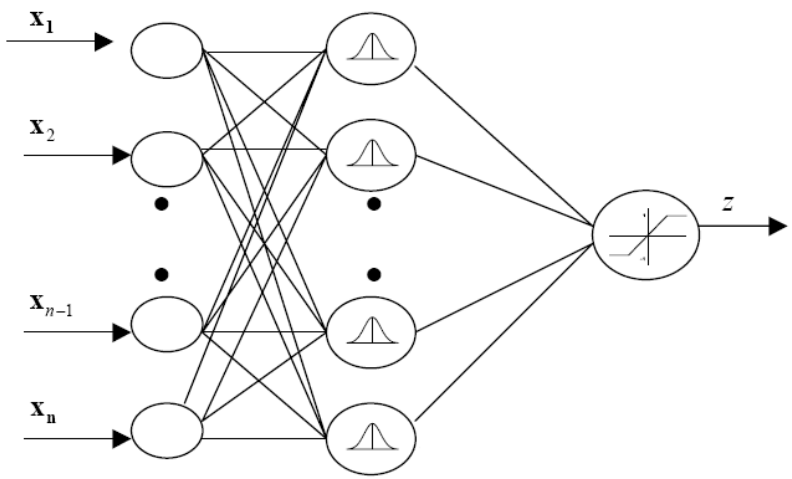

The RBF parameter w_j is determined by solving de following linear equation: $(G + \lambda I)\,\bar{w} = \bar{y}$

Using Radial Basis Function Network

- Each neuron of the hidden layer specializes in a particular region of the input space. The relationship between the input and output is a sum of local and non-linear functions.
- Learning faster: the weight change only affects the hidden neuron associated with this.

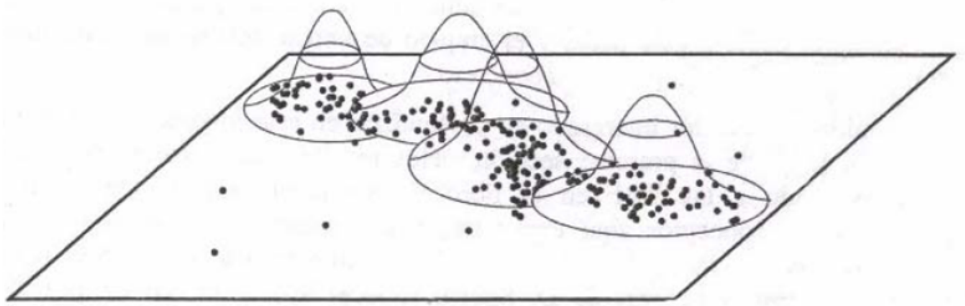

Using Radial Basis Function Network

Experimental Results

- Experiments are realized over four image databases generated from 145 selected images from the Web Clip Empire 250.000 by XOOM. For each images, author ran program that automatically transform it into six different images which belong to the same class.
- To train RBF network, 100 pairs of data with know output were fed to the network. The Maximum number of centers was limited to 130. The spread parameter was set to 1, and the error goal was set to 0.005. The centers are added to the network using OLS(*orthogonal least squares*) algorithm.

Using Radial Basis Function Network

Experimental Results

- Recall $R = \frac{NR}{RT}$, where NR is the number of relevant images retrieved, RT is the total number of relevant images in the database.
- Precision $P = \frac{NR}{RI}$, where NR is the number of relevant images retrieved, IR is the total number of images retrieved.

Average performance measures for 188 query images.

	Performance		
Method	Recall for a window size W = 8	Precision at 100% recall	Combining Time
NNIR	94.35%	81.45%	16.92 msec
BP-based method	82.54%	49.08%	10.00 msec
Linear combining method	77.84%	35.82%	7.33 msec

Using Self Organizing Map [Laaksonen et al, 2001]

- The SOM is an unsupervised, self-organizing neural algorithm widely used to visualize and interpret large high-dimensional data sets.
- The neuron with weight vector most similar to the input is called the best matching unit (BMU).
- During the training, the weights of the BMU and neurons close to it in the SOM lattice are adjusted towards the input vector.
- The magnitude of the change decreases with time and with distance from the BMU.

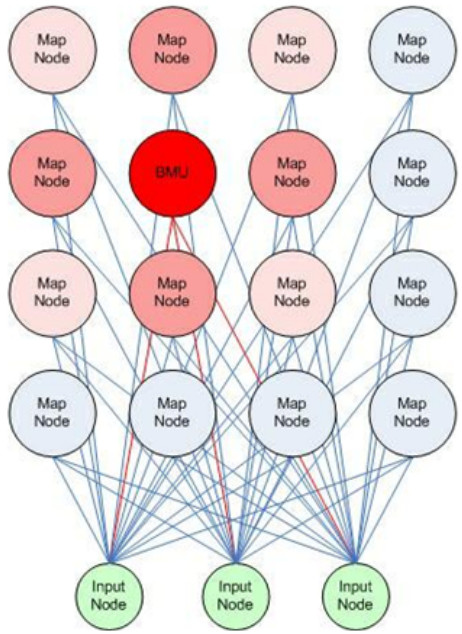

Using Self Organizing Map

For each sample $x(t)$, first the winner index c (best match) is identified by the condition:

$$\forall i, \|\mathbf{x}(t) - \mathbf{m}_c(t)\| \leq \|\mathbf{x}(t) - \mathbf{m_i}(t)\|.$$

After that, all model vectors or a subset of them that belong to nodes centered around node c = c(x) are updated as:

$$\mathbf{m_i}(t+1) = \mathbf{m}_i(t) + h_{c(x),i}(\boldsymbol{x}(t)\,\mathbf{m_i}(t)).$$

Here $h_{c(x),i}$ is the "neighborhood function", a decreasing function of the distance between the *ith* and *cth* nodes on the map grid.

Using Self Organizing Map

TS- SOM

- To speed up the search of the best-matching unit, In [Koikkalainen and Oja, 1990], authors introduced a variant of SOM called the Tree Structured Self-Organizing Map (TS-SOM).
- TS-SOM is a tree-structured vector quantization algorithm that uses normal SOMs at each of its hierarchical levels.
- The search space for the best-matching vector on the underlying SOM level is restricted to a predefined portion just below the best-matching unit on the above SOM.

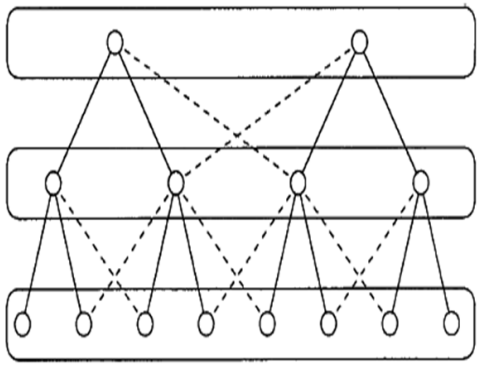

Using Self Organizing Map

TS- SOM on CBIR

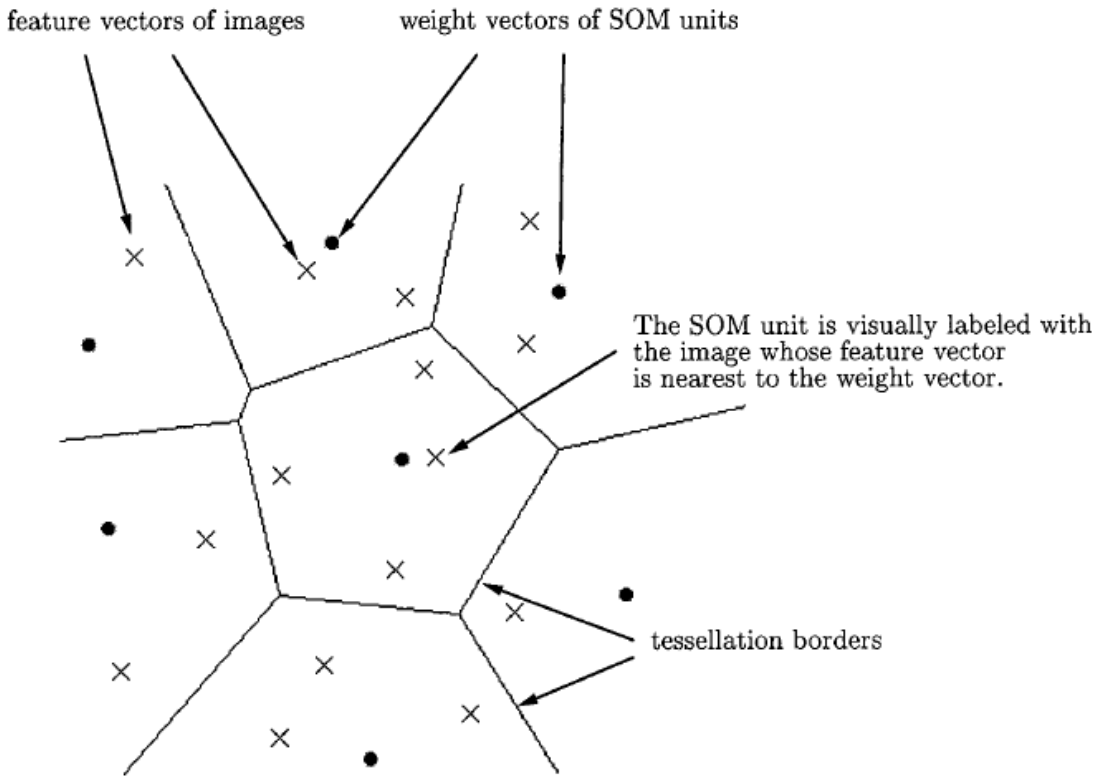

Using Self Organizing Map

TS- SOM on CBIR

- The surface of the 16 x 16-sized SOM formed with the average RGB colour feature.

Using Self Organizing Map

RF with TS- SOM on CBIR

- The system presents an initial set of tentative images.
- The user selects the subset of these images which best matches her/his expectations.
- The map units are scored with a fixed positive value for each positive image mapped in them. Likewise, negative images contribute negative values.
- The system remembers all image responses the user has given since the query was started.

Using Self Organizing Map

RF with TS- SOM on CBIR

An example showing how the levels of a TS-SOM, on which the images selected and rejected by the user are shown with white and black marks, respectively, are convolved with lowpass filters.

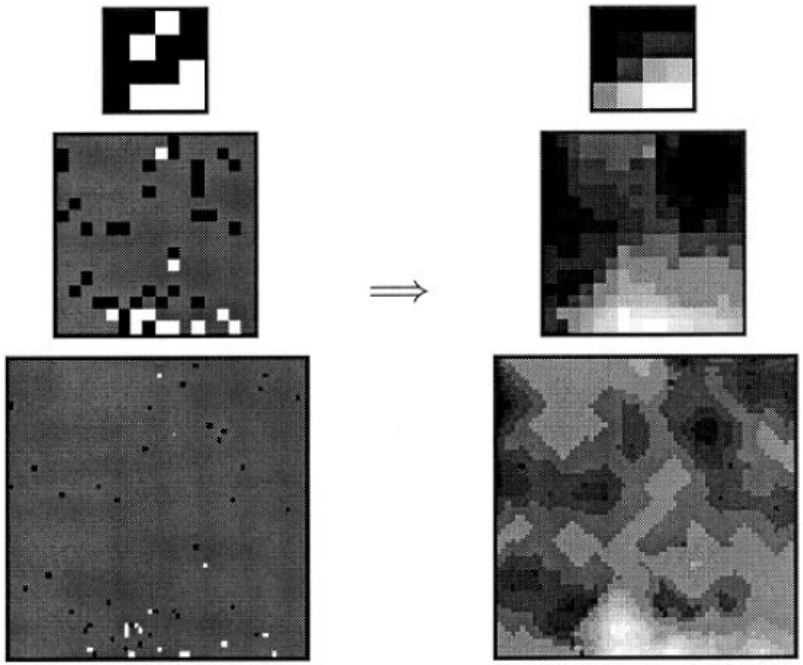

Using Self Organizing Map

RF with TS- SOM on CBIR

The stages of image selection in CBIR.

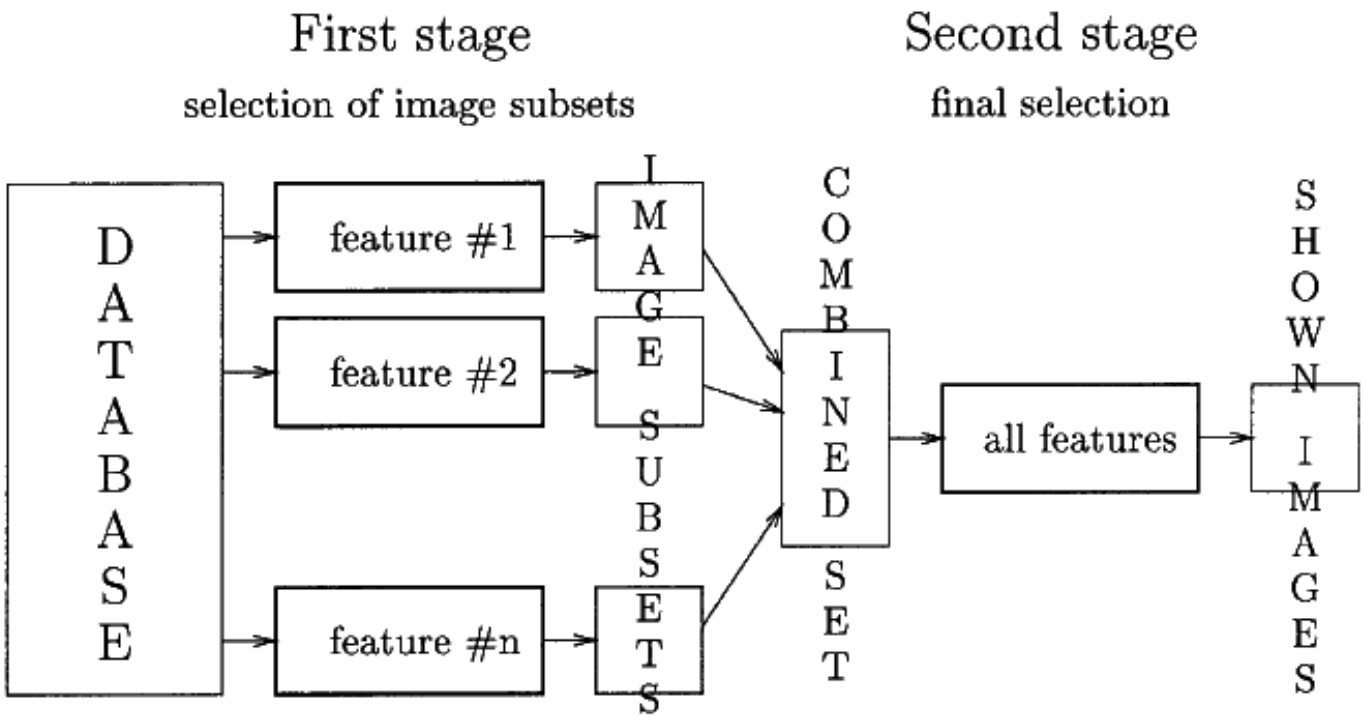

Using Self Organizing Map

Results of TS- SOM on CBIR

- As retrieval performance, was applied a quantitative figure denoted by author as the τ measure.
- The τ measure equals the average number of images the system retrieves before the correct one is found.
- The τ measure for class C is obtained by dividing the average number of shown images by the size of the database, N.

$$\tau \in \left[\frac{\rho_c}{2}, 1 - \frac{\rho_c}{2}\right] \text{ where } \rho_c = \frac{N_c}{N}$$

- N_c is the cardinality of the class.

Using Self Organizing Map

Results of TS- SOM on CBIR

τ-measure results of the PicSOM and reference systems and their two variations for retrieving the three hand-picked image classes of the Corel database:

τ	PicSOM	PicSOM+ distance	reference	reference+ distance
cars	0.177	0.193	0.212	0.187
faces	0.209	0.229	0.235	0.181
planes	0.137	0.147	0.203	0.185
average	0.174	0.190	0.217	0.184

Basic Theory of SVM

- Given a set of training vectors $(x1, y1)$,..(xm, ym), $xi \in Rn, yi \in \{-1, 1\}$ SVM maps the input data into a highdimensional feature space through a mapping function $z = \varphi(x)$ and finds the optimal separating hyperplane with the minimal classification errors. $\mathbf{w}\mathbf{z} + b = 0$.
- The optimal hyperplane can be obtained by solving the following optimization problem:

$$\text{Minimize } L(\mathbf{w}) = \frac{1}{2}\|\mathbf{w}\|^2 - C\sum_{i=1}^{m}\xi_i.$$

$$\text{Subject to } y_i(\mathbf{w}\cdot\mathbf{z}_i + b) \geq 1 - \xi_i, \xi_i \geq 0, i = 1, .., m.$$

- C is a regularization parameter, ξ is the slack variable, that is related to classification errors.

Basic Theory of SVM

Classification between two classes using hyperplanes: (a) arbitrary hyperplanes *l*, *m*, and *n* and (b) the optimal separating hyperplane with the largest margin identified by the dashed lines, passing the support vectors.

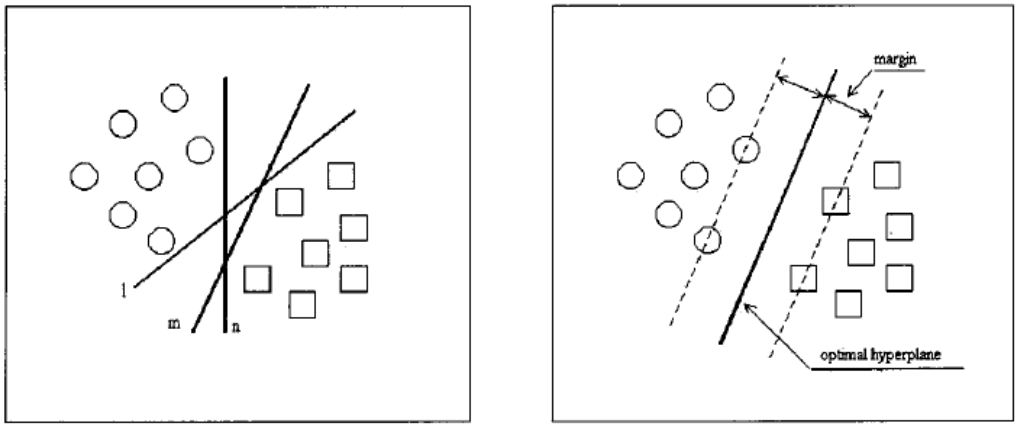

(a) (b)

Basic Theory of SVM

The optimization problem can be transformed into the following equivalent dual problem:

$$\text{Maximize } \sum_{i=1}^{m} \alpha_i - \frac{1}{2} \sum_{i=1}^{m} \sum_{j=1}^{m} \alpha_i \alpha_j y_i y_j \mathbf{z}_i \mathbf{z}_j$$

$$\text{Subject to } \sum_{i=1}^{m} y_i \alpha_i = 0, 0 \leq \alpha_i \leq C, i = 1, .., m.$$

Where α_i is the Lagrange multiplier.

Basic Theory of SVM

The decision function of the *SVM* can be represented as:

$$\begin{aligned} f(\mathbf{x}) &= \mathbf{w} \cdot \mathbf{z} + b = \sum_{i=1}^{m} \alpha_i y_i \varphi(\mathbf{x}_i) \cdot \varphi(\mathbf{x}) + b \\ &= \sum_{i=1}^{m} \alpha_i y_i K(\mathbf{x}_i \cdot \mathbf{x}) + b, \end{aligned}$$

where $K(\mathbf{x}_i, \mathbf{x})$ is the kernel function in the input space that computes the inner product of two data points in the feature space.

SVM approach for RF on CBIR [Guo et al, 2002]

Authors propose to use an "irregular" nonsphere boundary to enclose the similar images inside and the Euclidean distance measure is applied only to those images inside the boundary.

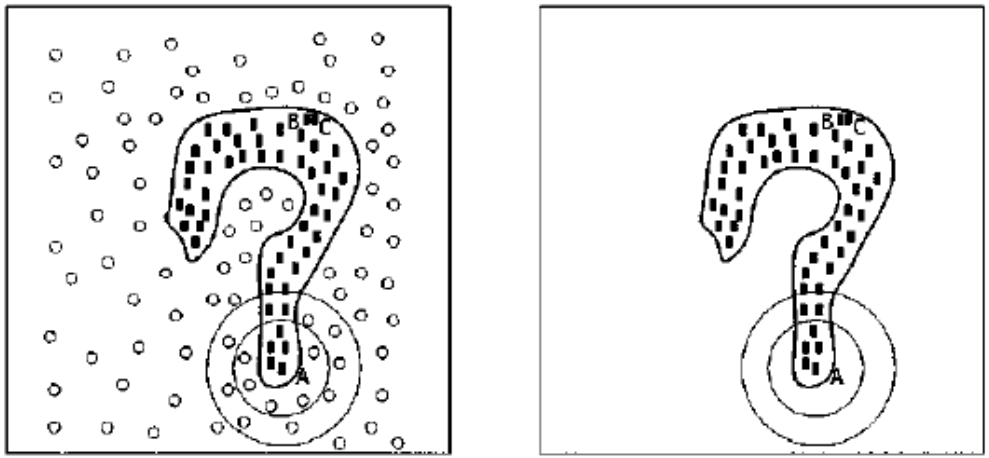

(a) (b)

SVM approach for RF on CBIR

- The authors concatenate color and texture features into one feature vector of dimension 435 to represent each image in the database. The features are normalized into a normal distribution in each dimension, separately.
- The gaussian radial basis function ($GRBF$) is choosen as the kernel function in experiments, which has the form $K(X, Y) = exp(-(x - y)^2/\sigma^2)$
- For a given kernel function, the SVM classifier is given by:

$$f(\mathbf{x}) = sign\left(\sum_{i=1}^{m} \alpha_i y_i K\left(\mathbf{x_i}, \mathbf{x}\right) + b\right).$$

SVM approach for RF on CBIR

- The restricted similarity measure can be formulated as follows:

$$S(\mathbf{x}, q) = \begin{cases} ED(\mathbf{x}, q), & \text{if } D(\mathbf{x}, \theta) \geq 0 \\ M - D(\mathbf{x}, q), & \text{oherwise,} \end{cases}$$

where $S(\mathbf{x}, q)$ denotes the similarity measure of the image $\mathbf{x}$ with respect to the query q, and $D(\mathbf{x}, \theta)$ represents the distance of $\mathbf{x}$ to the boundary characterized by a parameter set.

- The distance of the image to the boundary is given by:

$$D(\mathbf{x}, \theta) = \sum_{i=1}^{m} \alpha_i y_i K(\mathbf{x_i}, \mathbf{x}) + b,$$

M is the maximum Euclidean distance among the positive images to the query.

SVM approach for RF on CBIR

Experiment results

- Authors construct an image database 10009 images of 79 groups.
- 40 images are shown to the user each time, and the user clicks all the similar images to submit positive examples.
- Just the negative examples submitted by the user in the first round are selected, and keep them unchanged. In later stage, the users only submit positive examples to the system.
- The system learns a boundary, and the boundary is updated iteratively in response to user's interaction in later steps.

SVM approach for RF on CBIR

Experiment results

Precision and recall curves:

- Recall is the ratio of the number of relevant images returned to the total number of relevant images
- Precision is the ratio of the number of relevant images returned to the total number of images returned.
- Precision and recall curves for concepts of "Flower"

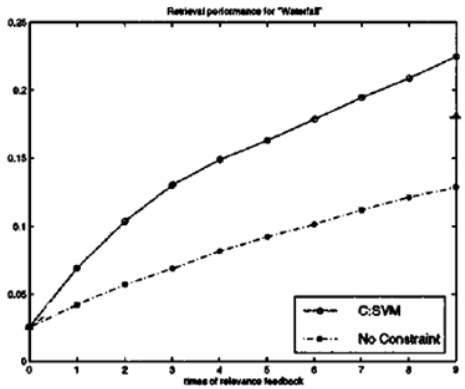

(a)

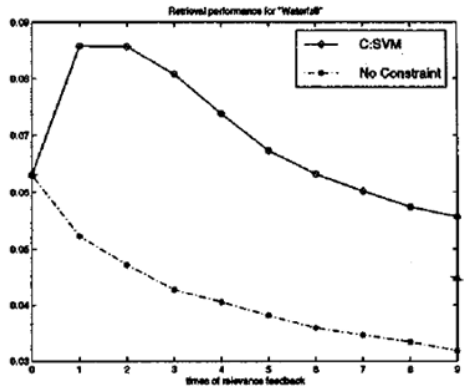

(b)

SVM approach for RF on CBIR

Experiment results

- Precision and recall curves for concepts of "Leopard", "Mountains" and "Sunsets"

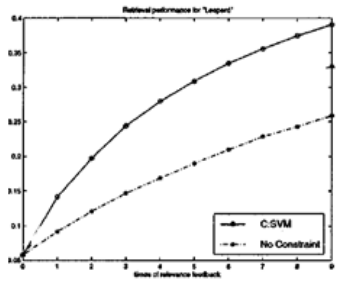

(a)

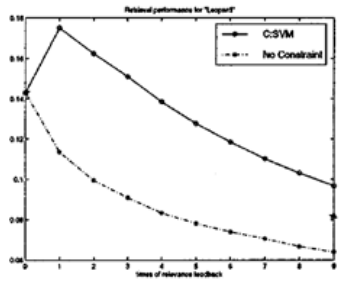

(b)

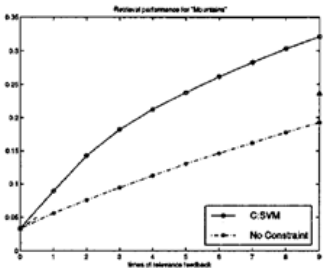

(a)

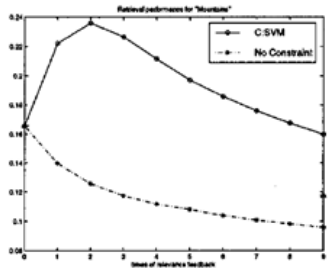

(b)

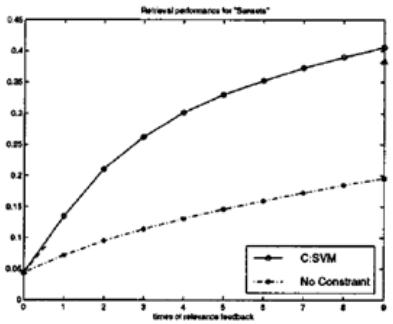

(a)

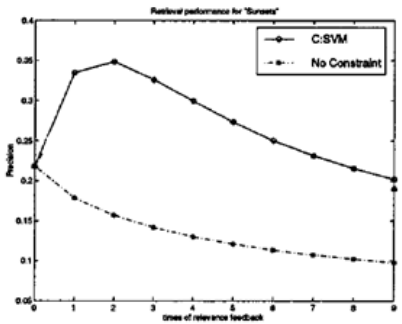

(b)

Fuzzy SVM approach for RF on CBIR [Wu and Yap, 2006]

The small sample problem arises in interactive CBIR systems even for a powerful learning machine such as *SVM*. They propose Active Learning with Pseudo-Labeled Images.

- Proposed Framework:
  1. Given a user-submitted query, the system performs the $K - NN$ search using the Euclidean distance for similarity matching. The top l_0 most similar images are shown to the user for feedback.
  2. The user provides the feedback on the l_0 images as either relevant or irrelevant. Based on the l_0 labeled images, an initial *SVM* classifier is trained.
  3. The *SVM* active learning is employed by selecting l unlabeled images that are closest to the current *SVM* decision boundary for the user to label.

Fuzzy SVM approach for RF on CBIR

- Proposed Framework:
  4. After the user labels the *l* images, add them to the previously labeled training set.
  5. A two-stage clustering is performed separately on the labeled relevant and irrelevant images. The formed clusters are then used for unlabeled images selection and pseudolabel assignment.
  6. A fuzzy metric is employed to evaluate the soft relevance membership of the pseudo-labeled images.
  7. An FSVM is trained using a hybrid of the labeled and pseudo-labeled images.
  8. Repeat steps (III)–(VII) until the retrieval performance is satisfactory.

Fuzzy SVM approach for RF on CBIR

Formulation of FSVM

- FSVM is an extension of SVM that takes into account the different significance of the training samples. For FSVM, each training sample is associated with a fuzzy membership value $\{\mu_i\}_{i=1}^{n} \in [0, 1]$. The μ_i value reflects the fidelity of the data.
- The optimization problem of the FSVM is formulated as follows:

$$\text{Minimize } L(\mathbf{w}) = \frac{1}{2}\|\mathbf{w}\|^2 - C\sum_{i=1}^{m}\mu\xi_i.$$

$$\text{Subject to } y_i(\mathbf{w}\cdot\mathbf{z}_i + b) \geq 1 - \xi_i, \xi_i \geq 0, i = 1, .., m.$$

Fuzzy SVM approach for RF on CBIR

Formulation of FSVM

- Similar to the conventional SVM, the optimization problem of FSVM can be transformed into its dual problem as follows:

$$\text{Maximize} \sum_{i=1}^{m} \alpha_i - \frac{1}{2} \sum_{i=1}^{m} \sum_{j=1}^{m} \alpha_i \alpha_j y_i y_j \mathbf{z}_i \mathbf{z}_j$$

$$\text{Subject to} \sum_{i=1}^{m} y_i \alpha_i = 0, 0 \leq \alpha_i \mu_i \leq C, i = 1, .., m.$$

- Solving above equation will lead to a decision function:

$$f(\mathbf{x}) = \sum_{i=1}^{m} \alpha_i y_i K(\mathbf{x_i}, \mathbf{x}) + b$$

Fuzzy SVM approach for RF on CBIR

Unlabeled Image Selection and Pseudo-Label Estimation

- The basic idea is to identify certain samples in the unlabeled image population, which are similar to the labeled images, to perform pseudo-labeling and fuzzy membership estimation.
- First, it performs K-means clustering (before, subtractive clustering is employed as a preprocessing step to estimate the number and structure of clusters).
- After that, select K nearest unlabeled neighbors for each labeled cluster based on their Euclidean distances to the center of the labeled cluster. The label (relevant or irrelevant) of each labeled cluster is then propagated to the unlabeled neighbors. This is referred to as pseudo-labeling process.

Fuzzy SVM approach for RF on CBIR

Estimation of Soft Relevance Membership Function for Pseudo-Labeled Images

- The objective is to find a mapping $g(\mathbf{x}^P) : \Re^n \rightarrow [0, 1]$, that assigns a proper relevance value between zero and one to each pseudo-labeled image $\mathbf{x}^P$.

$$w_1(\mathbf{x}_P) = \begin{cases} \exp\left(-a_1 \dfrac{\min\limits_i (\mathbf{x}_P - \mathbf{v}_{Si})^{\mathrm{T}}(\mathbf{x}_P - \mathbf{v}_{Si})}{\min\limits_j (\mathbf{x}_P - \mathbf{v}_{Oj})^{\mathrm{T}}(\mathbf{x}_P - \mathbf{v}_{Oj})}\right) & \text{if } \dfrac{\min\limits_i (\mathbf{x}_P - \mathbf{v}_{Si})^{\mathrm{T}}(\mathbf{x}_P - \mathbf{v}_{Si})}{\min\limits_j (\mathbf{x}_P - \mathbf{v}_{Oj})^{\mathrm{T}}(\mathbf{x}_P - \mathbf{v}_{Oj})} < 1 \\ 0 & \text{otherwise} \end{cases}$$

- $\mathbf{v}_{Si}$ denotes the center of the ith cluster with the same class label as the pseudo-labeled image $\mathbf{x}^P$, while $\mathbf{v}_{Oj}$ denotes the center of the *jth* cluster with the opposite class label to the pseudo-labeled image $\mathbf{x}^P$.

Fuzzy SVM approach for RF on CBIR

Estimation of Soft Relevance Membership Function for Pseudo-Labeled Images

- The second factor of the fuzzy function is chosen as a sigmoid function as follows:

$$w_2(\mathbf{x}_P) = \begin{cases} \dfrac{1}{1+\exp(-a_2\gamma)} & \text{pseudo-label is positive} \\ \dfrac{1}{1+\exp(a_2\gamma)} & \text{otherwise,} \end{cases}$$

where $a_2 > 0$ is a scaling factor. γ is the directed distance of the pseudo-labeled image $\mathbf{x}^P$ to the SVM boundary (the decision function output of SVM for the pseudo-labeled image $\mathbf{x}^P$).

- The fuzzy membership function is: $g\left(\mathbf{x}^P\right) = w_1\left(\mathbf{x}^P\right) w_2\left(\mathbf{x}^P\right)$.

Fuzzy SVM approach for RF on CBIR

Experimental results

- The image database adopted in our experiment contains 10,000 color images from 100 predefined categories.
- Color and texture descriptors of the images are extracted and used to index the images.
- The performance of the proposed PLFSVM method is evaluated and compared with active learning using SVM.
- One hundred queries with one from each category are selected for evaluation.

Fuzzy SVM approach for RF on CBIR

Experimental results

Retrieval accuracy of the PLFSVM and SVM methods. (a) Retrieval accuracy in top 10 results, (b) Retrieval accuracy in top 20 results.

$$\text{Retrieval accuracy} = \frac{\text{relevant images retrieved in top } T \text{ return}}{T}.$$

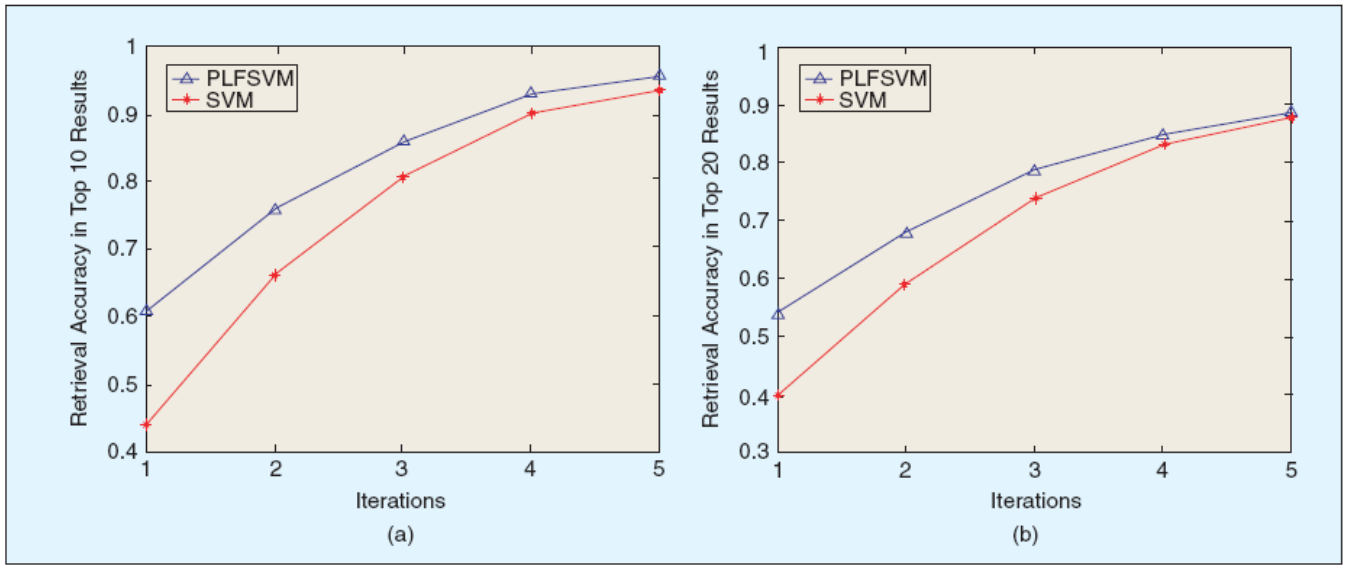

Problem definition [Zhang & Zhang, 2006]

The problem of determining whether an image Img_i is (ir)relevant to the query image and the corresponding (ir)relevancy confidence is reduced to estimating the conditional *pdfs* $p(Img_i|R)$ and $p(Img_i|I)$, respectively, the prior probabilities $P(R)$ and $P(I)$, respectively, and the *pdf* $p(Img_i)$ in the continuous feature space.

$$P(R \mid Img_i) = \frac{p(Img_i \mid R)\,P(R)}{p(Img_i)}$$

$$P(I \mid Img_i) = \frac{p(Img_i \mid I)\,P(I)}{p(Img_i)}$$

Problem definition

- Authors perform vector quantization before the *pdf* estimations to ease the computation intensity.
- The *pdf* $p(Img_i)$ is estimated by statistically counting the percentage of the quantized feature vectors in the feature space of the whole image data set.

Estimating the conditional *pdf* of the positive samples

- The *pdf* of each feature dimension of all the relevant images to a given query image satisfies the Gaussian distribution.

$$p(x_k \mid R) = \frac{1}{\sqrt{2\pi\sigma_k}} \exp\left(-\frac{(x_k - m_k)^2}{2\sigma_k}\right),$$

where x_k is the *kth* dimension of the feature vector of an image, m_k is the mean value of the x_k of all relevant images to the query image, and s_k is the standard deviation of the *kth* dimension of the relevant images.

Estimating the conditional pdf of the positive samples

Assume that $L = \{l_1, l_2, .l_N\}$ is the relevant sample set provided by a user. Applying the maximum-likelihood method, we obtain the following unbiased estimations of the mean *mk* and the standard deviation *sk* for the *kth* dimension of the features.

$$\hat{m}_k = \frac{1}{N} \sum_{i=1}^{N} l_{ki}$$

$$\hat{\sigma}_k = \frac{1}{N-1} \sum_{i=1}^{N} (l_{ki} - \hat{m}_k)^2$$

where l_{ki} denotes the *kth* dimension of the feature vector l_i.

Estimating the conditional pdf of the positive samples

- To describe the different conformity degrees to Gaussian distributions among different dimensions in the feature space we introduce a measure, called *trustworthy* degree,

$$w_k = \frac{\sigma_k^{-1}}{\max_{j=1}^{T} \sigma_k^{-1}},$$

for each dimension $k, k = 1, ., T$, where T is the number of dimensions of the feature space.

- The *pdf* of positive samples is determined as a trustworthy degree pruned joint *pdf*:

$$p(x \mid R) = \prod^{T} p(x_k \mid R), k = 1, w_k \geq \delta.$$

Estimating the conditional pdf of the *negative* samples

- Authors assume that each negative sample represents a unique potential semantic class, and they apply the kernel density estimator
- Consequently, the overall *pdf* for the negative samples is the agglomeration of all the kernel functions.
- They choose the kernel function in the estimator as an isotropic Gaussian function (assuming all the feature vectors have been normalized).

Estimating the conditional pdf of the *negative* samples

- The window of the estimation is a hyper-sphere centered at each negative sample $x_j, j = 1, 2, ., N$, assuming that there are N negative samples in total.
- The conditional *pdf* to be estimated for the sample x_i in the feature space is given by:

$$p\left(xi \mid I\right) = \sum_{j=1}^{N} \text{kernel}\left(x_i, x_j\right) = \sum_{j=1}^{N} \exp\left\{-\frac{\|x_i - x_j\|_2^2}{2r_j^2}\right\}$$

where $\|x_i - x_j\|_2$ is the Euclidean distance between the neighboring sample x_j and the center feature vector x_i.

Estimating the conditional pdf of the *negative* samples

- r is a constant bandwidth based on the maximum distance from all the negative samples to their closest neighbor D defined as follows:

$$r = \lambda D = \lambda \max_{x_k} \left[\min_{x_l} \left(\|x_k - x_l\|_2 \right) \right],$$

where λ is a scalar. Author find in their experiments that with well-normalized feature vectors, a λ between 1 and 10 often gives good results.

Estimating the conditional pdf of the *negative* samples

Authors generate additional negative samples based on the kernel distributions for each semantic class, the generation of the unlabeled samples follows a probability function defined by the following Gaussian pdf function:

$$p(y) = \frac{1}{\sqrt{2\pi}\sigma} \exp\left\{ -\frac{\|y - x_i\|_2^2}{2\sigma^2} \right\},$$

where $\|x_i - x_j\|_2$ is the Euclidean distance between the unlabeled sample y and the corresponding labeled sample x_i. σ is the standard deviation defined as follows:

$$\sigma = \frac{1}{N(N-1)} \sum_{i=1}^{N} \sum_{j=1, j\neq i}^{N} \|x_i - x_j\|_2$$

Estimating the conditional pdf of the negative samples

- The *pdf* function may be represented in another form as a function of the Euclidian distance z, between the unlabeled sample y and the labeled sample x_i:

$$p(z) = \frac{1}{\sqrt{2\pi}\sigma}\exp\left(-\frac{z^2}{2\sigma^2}\right).$$

In the following algorithm, *NUM* is the number of the unlabeled negative samples we intend to generate for each labeled sample. τ is a parameter to adjust the range centered at the positions with a distance d to the labeled sample, in which we select the unlabeled samples. In our experiments, τ is set to d/NUM.

Estimating the conditional pdf of the negative samples

input : S, Labeled negative example set
output : R, Extended negative sample set
begin
  $R = \{\}$;
  for *each labeled negative example* $s \in S$ **do**
    $i = 0$;
    Create an array A with $NUM + 1$ elements, each element $v_k = \frac{k}{NUM} * \frac{1}{\sqrt{2\pi}\sigma}$, where $k \in [0, NUM]$;
    while $i < NUM$ **do**
      $d = 0$;
      Generate a random number $t = rand()$ in $[0, \frac{1}{\sqrt{2\pi}\sigma}]$;
      Search array A to find the k with $v_{k-1} < t \leq v_k$;
      Determine the distance d based on the function $v_k = p(d)$ defined in Eq. 12;
      Randomly sample the feature space until a feature V is found with a distance s in $[d - \tau, d + \tau]$;
      $R = R \cup \{V\}$;
      $i = i + 1$;
    end
  end
  return R;
end

Determining the prior probabilities

- Given a query image, for each image Img_i in the image data set, it has:

$$p\left(Img_i\right) = p\left(Img_i \mid R\right) P\left(R\right) + p\left(Img_i \mid I\right) P\left(I\right),$$

and for the query image we also have:

$$P\left(R\right) + P\left(I\right) = 1$$

Combining before equations, it immediately has:

$$P_i\left(R\right) = \frac{p\left(Img_i\right) - p\left(Img_i \mid I\right)}{p\left(Img_i \mid R\right) - p\left(Img_i \mid I\right)}.$$

Determining the prior probabilities

- Thus, the final prior probability $P(R)$ is determined by an average of all the images in the data set, i.e.,

$$P(R) = \frac{1}{M} \sum_{i=1}^{M} P_i(R)$$

- It is noted that although this estimation of $P(R)$ is not really legitimate from the perspective of strict statistics, it is effective in empirical Bayes' approaches.

Ranking scheme

The Rocchio's formula for relevance feedback is frequently used to estimate 'optimal query' Q' with an initial query Q in relevance feedback for sets of relevant documents D_R and irrelevant documents D_I given by the user:

$$Q' = \alpha Q + \beta \left(\frac{1}{N_R} \sum_{d_j \in D_R} d_j \right) - \gamma \left(\frac{1}{N_I} \sum_{d_j \in D_I} d_j \right)$$

where α, β, and γ are suitable constants; N_R and N_I are the numbers of documents in D_R and D_I, respectively.

Ranking scheme

- Based on the Rocchio's formula, $SD(Img_i)$ is defined as follows:

$$\begin{aligned} SD(Img_i) &= log(1 + P(R \mid Img_i)) \\ &\quad + \beta \left\{ \frac{1}{N_R} \sum_{k \in D_R} [(1 + P(R \mid Img_k)) U_{ik}] \right\} \\ &\quad - \gamma \left\{ \frac{1}{N_I} \sum_{k \in D_I} [(1 + P(I \mid Img_k)) U_{ik}] \right\}, \end{aligned}$$

where N_R and N_I are the sizes of the positive and negative labeled sample sets D_R and D_I, respectively, in the relevance feedback, and U_{ik} is the feature-based distance between the images Img_i and Img_k (e.g., $Uik = \|Img_i - Img_k\|_2$).

Experimental results

- The following evaluations are performed on a general purpose color image database containing 10,000 images from the COREL collection with 96 categories. All images are indexed as described above, and 1500 images are randomly selected from all categories to be the query set.

Experimental results

The precision in top N returned images based on FD, $P(Rj$ Img), and SD metrics for the 10 categories

Category	FD				$P(Rj$Img)				SD			
	Top 20	Top 30	Top 50	Average	Top 20	Top 30	Top 50	Average	Top 20	Top 30	Top 50	Average
Africa	0.23	0.20	0.12	0.18	0.41	0.26	0.22	0.30	0.59	0.31	0.25	0.38
Beach	0.32	0.25	0.20	0.26	0.62	0.55	0.48	0.55	0.60	0.58	0.50	0.56
Buildings	0.38	0.30	0.24	0.31	0.51	0.31	0.29	0.37	0.49	0.38	0.30	0.39
Buses	0.62	0.58	0.52	0.57	0.51	0.49	0.50	0.50	0.62	0.60	0.55	0.59
Dino-saurs	0.80	0.72	0.69	0.74	0.73	0.65	0.58	0.65	0.81	0.75	0.70	0.75
Elephants	0.58	0.50	0.43	0.50	0.61	0.59	0.50	0.57	0.60	0.55	0.51	0.55
Flowers	0.81	0.72	0.70	0.74	0.90	0.81	0.82	0.65	0.91	0.86	0.80	0.83
Horses	0.91	0.85	0.60	0.79	0.69	0.65	0.61	0.65	0.91	0.86	0.80	0.86
Moun-tains	0.52	0.46	0.30	0.43	0.76	0.69	0.60	0.68	0.80	0.73	0.65	0.73
Food	0.41	0.32	0.20	0.31	0.81	0.73	0.69	0.74	0.79	0.75	0.68	0.74

The 'Average' column for each distance metric is the average of the corresponding three left columns (Top 20, Top 30, and Top 50, respectively).

Experimental results

Comparison between Bayesian approach and SVM approach on the average precision in the top 100 images returned. The number of positive sample images is set as 20.

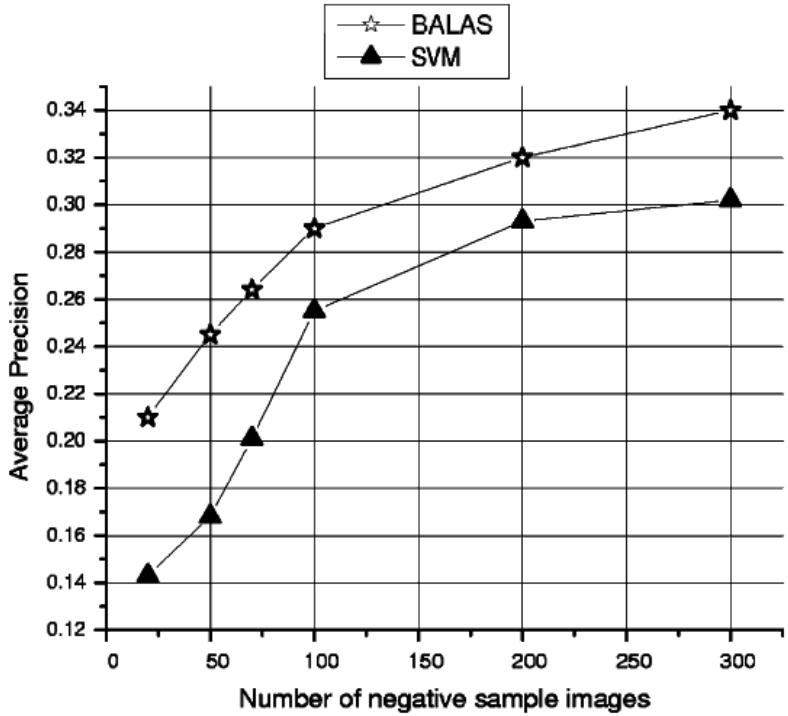

References

- Relevance Feedback: A Power Tool for Interactive Content-Based Image Retrieval. Yong Rui, Thomas S. Huang IEEE Transactions on Circuits and Systems for Video Technology, vol. 8, no. 5, september 1998.
- Self-Organising Maps as a Relevance Feedback Technique in Content-Based Image Retrieval. Jorma Laaksonen, Markus Koskela, Sami Laakso and Erkki Oja. Pattern Analysis & Applications (2001)4:140–152.
- Learning Similarity Measure for Natural Image Retrieval With Relevance Feedback. Guo-Dong Guo, Anil K. Jain, Wei-Ying Ma, Hong-Jiang Zhang. Ieee transactions on neural networks, vol. 13, no. 4, july 2002

References

- Nonlinear Combining of Heterogeneous Features in Content-Based Image Retrieval. Hyoung K. Lee, Suk I. Yoo. International Journal of Computer Research, Vol. 11, No. 3, 2002
- Fuzzy SVM for Content-Based Image Retrieval. Kui Wu and Kim-Hui Yap IEEE. Computational Intelligence Magazine, May 2006. 1556-603
- BALAS: Empirical Bayesian learning in the relevance feedback for image retrieval. Ruofei Zhang , Zhongfei (Mark) Zhang. Image and Vision Computing 24 (2006) 211–223
- Koikkalainen P, Oja E. Self-organizing hierarchical feature maps. Proceedings International Joint Conference on Neural Networks, San Diego, CA, 1990; II:279–284

Linear Mixing Model for Hyperspectral Imagery

Virtual Dimensionality, Endmembers Induction Methods and Unmixing techniques

Miguel A. Veganzones

Computational Intelligence Group
Basque Country University

2nd Conference on Computational Intelligence, Verona 2008

Outline

1. Motivation
2. Linear unmixing
3. Virtual Dimensionality
   - Introduction
   - Neyman-Pearson Detection Theory-Based Eigen-Thresholding Analysis (HFC Method)
   - Noise Whitening HFC Analysis (NWHFC Method)
   - Noise Subspace Projection Analysis (NSP Method)
4. Endmember induction methods
   - Geometric approaches
   - Lattice computing approaches
   - Heuristic approaches

Hyperspectral Imagery

- High dimensionality data.
- Data measured in several parts of the electromagnetic spectrum.
- Example: AVIRIS, 224 bands (visible, IR).

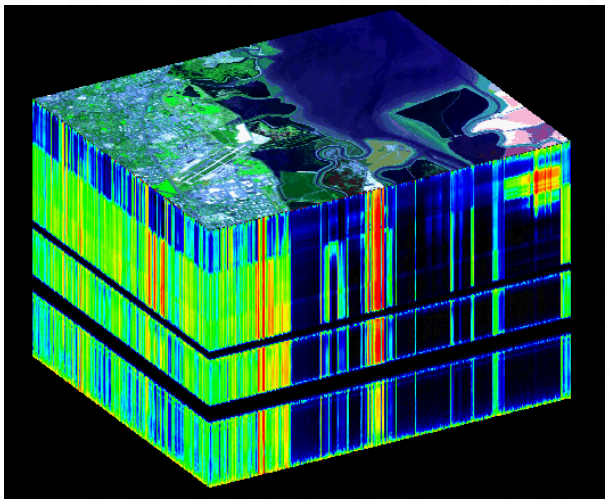

Hyperspectral analysis

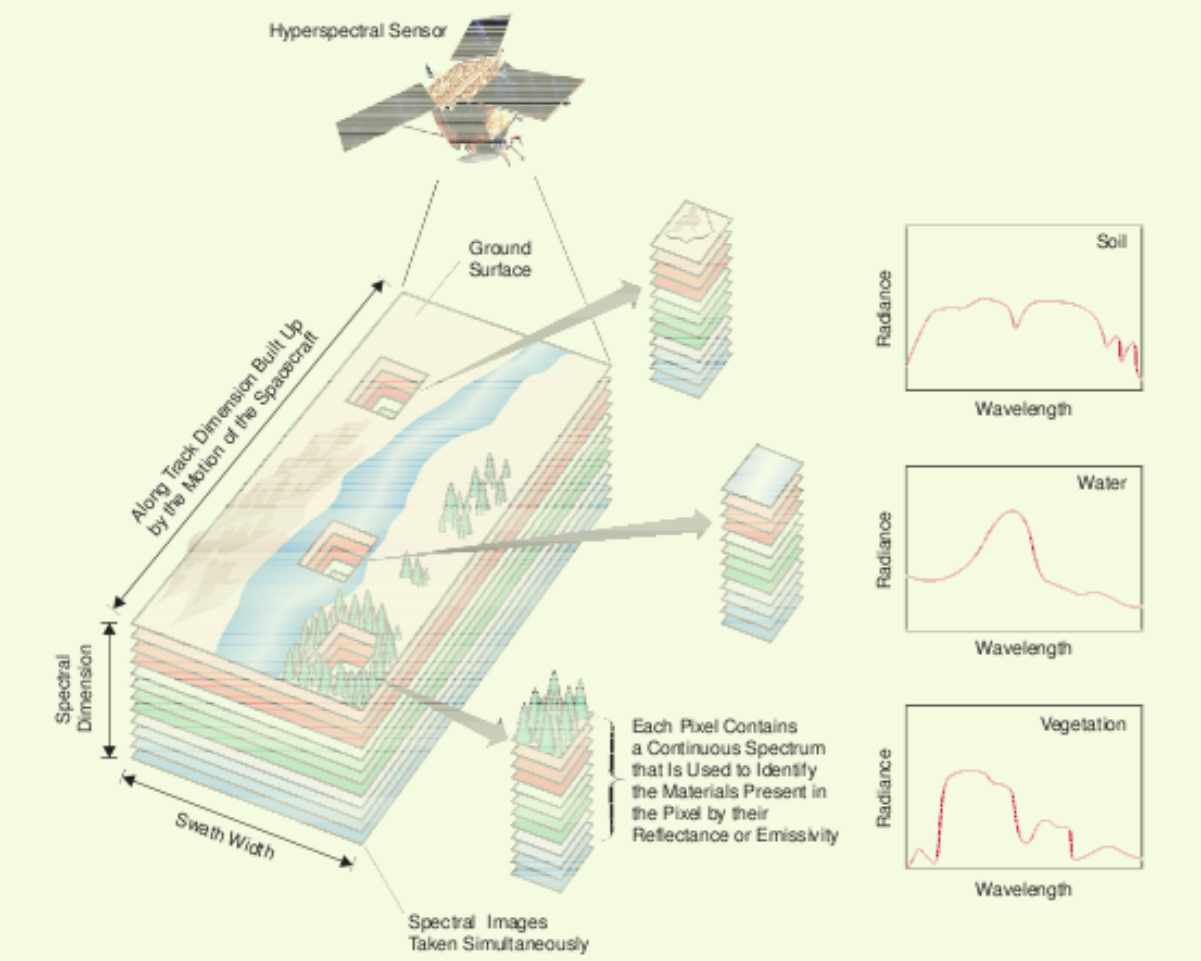

Hyperspectral Models

Linear mixing model

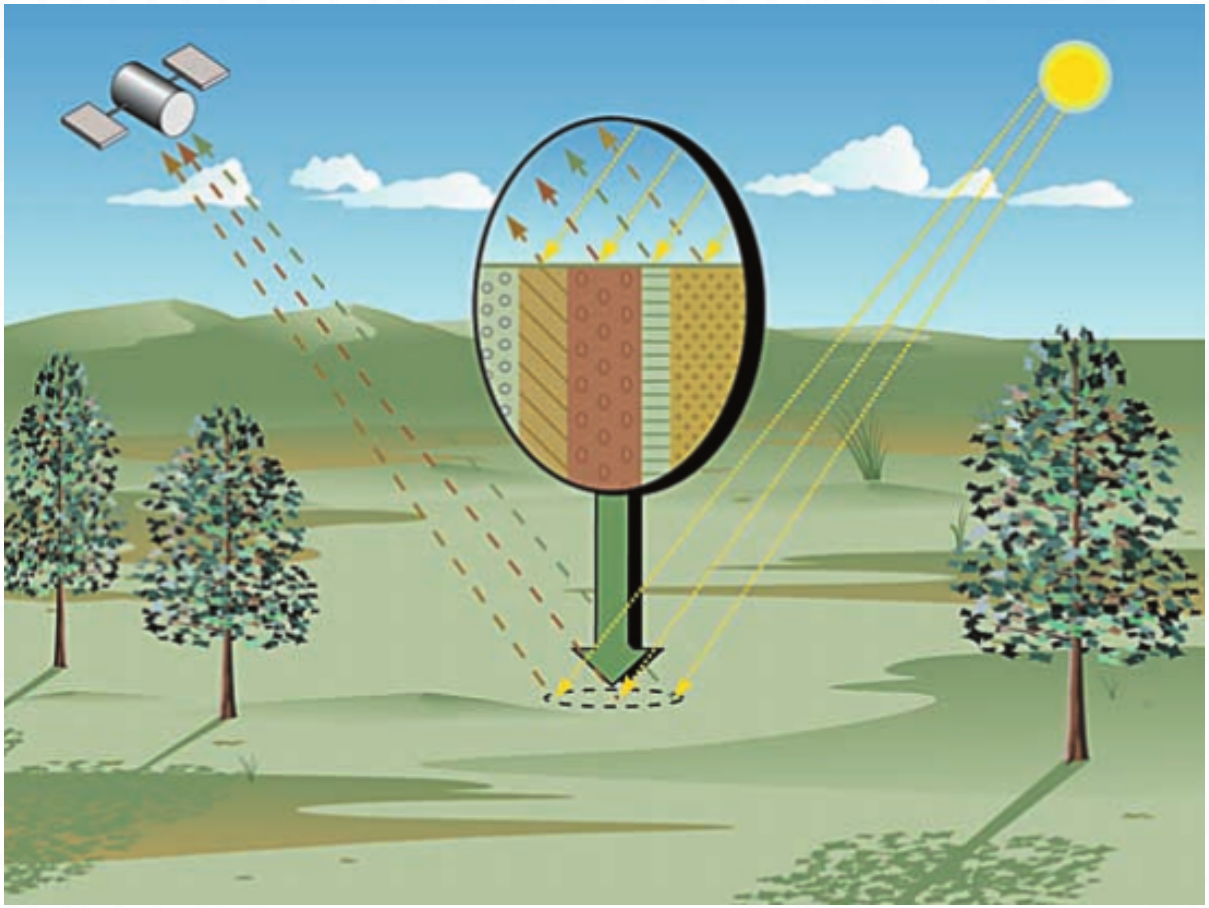

Hyperspectral Models

Non-Linear mixing model

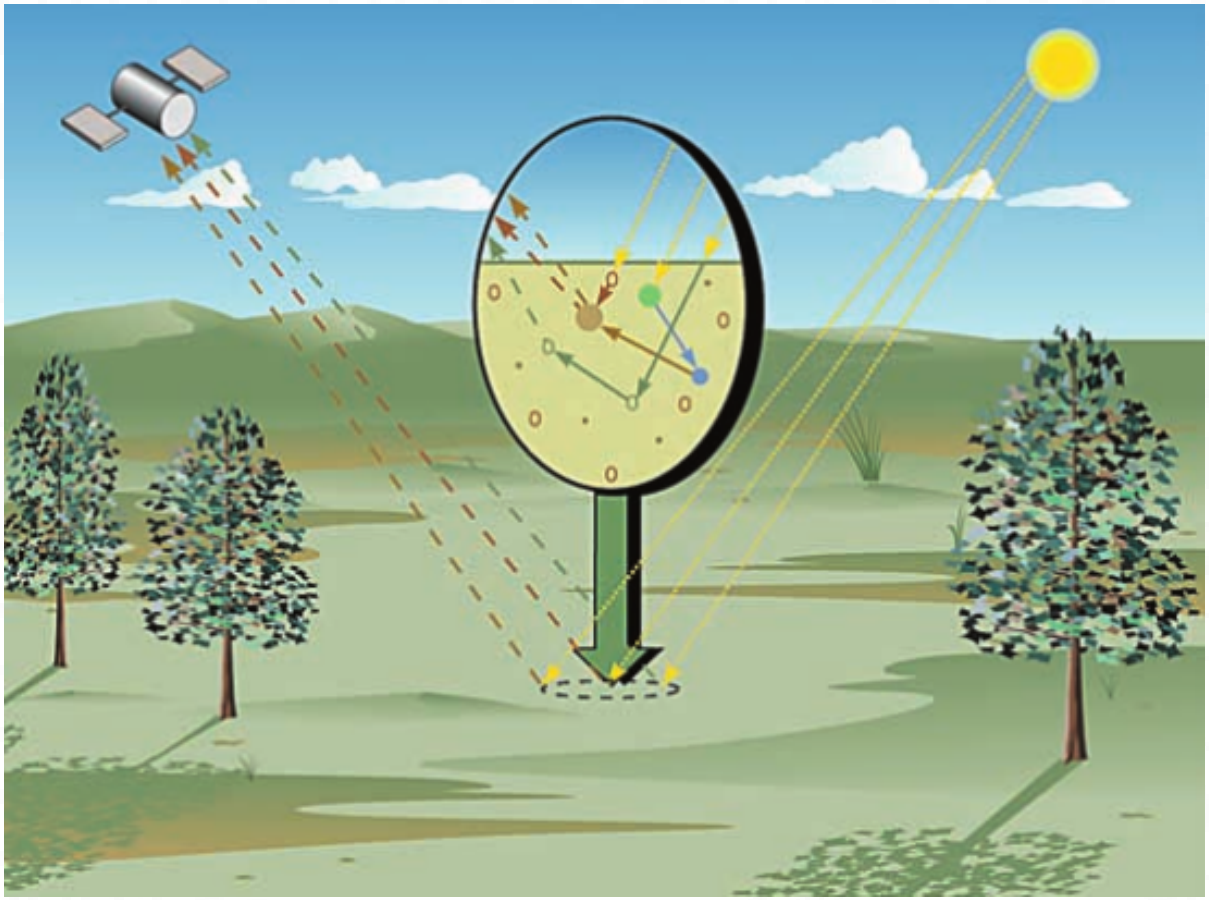

Hyperspectral Models

Non-Linear mixing model

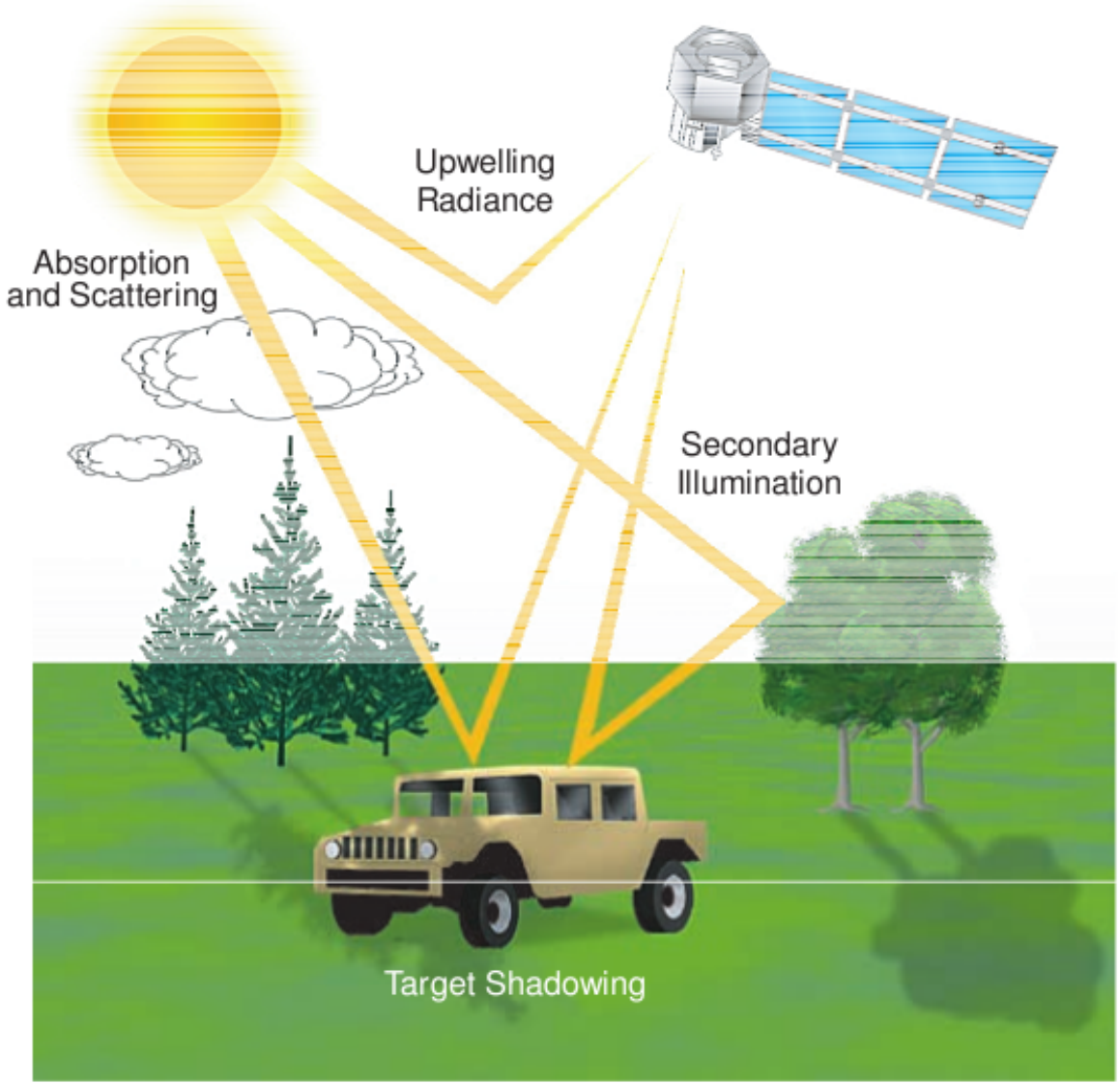

Linear Mixing Model
Definition

Linear mixing model definition

- $H = A \cdot E + \eta$
- $h(i,j) = a(i,j)_1 \cdot \mathbf{e_1} + \ldots + a(i,j)_p \cdot \mathbf{e_p} + \eta(i,j)$

Where:

- H is an hyperspectral image with mxn spatial dimensions and d spectral bands.
- E is the set of p d-dimensional spectral signatures in the image (endmembers).
- A is the image with mxn spatial dimensions of spectral fractional abundances.
- η is the additive noise.

Linear Mixing Model
Definition

Linear mixing model definition

- $H = A \cdot E + \eta$
- $h(i,j) = a(i,j)_1 \cdot \mathbf{e_1} + \ldots + a(i,j)_p \cdot \mathbf{e_p} + \eta(i,j)$

Where:

- H is an hyperspectral image with mxn spatial dimensions and d spectral bands.
- E is the set of p d-dimensional spectral signatures in the image (endmembers).
- A is the image with mxn spatial dimensions of spectral fractional abundances.
- η is the additive noise.

Linear Mixing Model
Definition

Linear mixing model definition

- $H = A \cdot E + \eta$
- $h(i,j) = a(i,j)_1 \cdot \mathbf{e_1} + \ldots + a(i,j)_p \cdot \mathbf{e_p} + \eta(i,j)$

Where:

- H is an hyperspectral image with mxn spatial dimensions and d spectral bands.
- E is the set of p d-dimensional spectral signatures in the image (endmembers).
- A is the image with mxn spatial dimensions of spectral fractional abundances.
- η is the additive noise.

Linear Mixing Model
Definition

Linear mixing model definition

- $H = A \cdot E + \eta$
- $h(i,j) = a(i,j)_1 \cdot \mathbf{e_1} + \ldots + a(i,j)_p \cdot \mathbf{e_p} + \eta(i,j)$

Where:

- H is an hyperspectral image with mxn spatial dimensions and d spectral bands.
- E is the set of p d-dimensional spectral signatures in the image (endmembers).
- A is the image with mxn spatial dimensions of spectral fractional abundances.
- η is the additive noise.

Hyperspectral Imagery Analysis

- Virtual dimensionality: estimates the number of sources forming the hyperspectral image which are relevant for the analysis.
- Endmember induction methods: induce the set of endmembers in hyperspectral images from the data.
- Unmixing methods: extract the images of spectral abundances given an hyperspectral image and the set of endmembers.

Hyperspectral Imagery Analysis

- Virtual dimensionality: estimates the number of sources forming the hyperspectral image which are relevant for the analysis.
- Endmember induction methods: induce the set of endmembers in hyperspectral images from the data.
- Unmixing methods: extract the images of spectral abundances given an hyperspectral image and the set of endmembers.

Hyperspectral Imagery Analysis

- Virtual dimensionality: estimates the number of sources forming the hyperspectral image which are relevant for the analysis.
- Endmember induction methods: induce the set of endmembers in hyperspectral images from the data.
- Unmixing methods: extract the images of spectral abundances given an hyperspectral image and the set of endmembers.

Applications

- Classification.
- Target detection.
- Synthesis.
- *CBIR Systems*.

Linear unmixing

- Linear mixing model: $H = A \cdot E + \eta$.
- Linear unmixing: find the image of abundances A for a given hypespectral image and a given set of endmembers.
- Full Constrained Least Squares Inversion:

$$A = (E^T E)^{-1} E^T I$$

subjet to the following restrictions: $a_i(x,y) \geq 0$ and $\sum_i a_i(x,y) = 1$.

- There are other aproximations subject to different restrictions or purposes.

Linear unmixing

- Linear mixing model: $H = A \cdot E + \eta$.
- Linear unmixing: find the image of abundances A for a given hypespectral image and a given set of endmembers.
- Full Constrained Least Squares Inversion:

$$A = (E^T E)^{-1} E^T I$$

subjet to the following restrictions: $a_i(x,y) \geq 0$ and $\sum_i a_i(x,y) = 1$.

- There are other aproximations subject to different restrictions or purposes.

Linear unmixing

- Linear mixing model: $H = A \cdot E + \eta$.
- Linear unmixing: find the image of abundances A for a given hypespectral image and a given set of endmembers.
- Full Constrained Least Squares Inversion:

$$A = (E^T E)^{-1} E^T I$$

subjet to the following restrictions: $a_i(x,y) \geq 0$ and $\sum_i a_i(x,y) = 1$.

- There are other aproximations subject to different restrictions or purposes.

Linear unmixing

- Linear mixing model: $H = A \cdot E + \eta$.
- Linear unmixing: find the image of abundances A for a given hypespectral image and a given set of endmembers.
- Full Constrained Least Squares Inversion:

$$A = (E^T E)^{-1} E^T I$$

subjet to the following restrictions: $a_i(x,y) \geq 0$ and $\sum_i a_i(x,y) = 1$.

- There are other aproximations subject to different restrictions or purposes.

Outline

1 Motivation

2 Linear unmixing

3 Virtual Dimensionality
- Introduction
- Neyman-Pearson Detection Theory-Based Eigen-Thresholding Analysis (HFC Method)
- Noise Whitening HFC Analysis (NWHFC Method)
- Noise Subspace Projection Analysis (NSP Method)

4 Endmember induction methods
- Geometric approaches
- Lattice computing approaches
- Heuristic approaches

Intrinsic Dimensionality (ID)

- Definition: minimum number of parameters required to account for the observed properties of the data.
- Suitable for multispectral imagery but difficult to implement with hyperspectral data.
  - High spectral resolution sensors can extract many unknown subtle material substances.
  - Determining ID of hyperspectral imagery is very problematic.
- Principal Component Analysis (PCA).

Intrinsic Dimensionality (ID)

- Definition: minimum number of parameters required to account for the observed properties of the data.
- Suitable for multispectral imagery but difficult to implement with hyperspectral data.
  - High spectral resolution sensors can extract many unknown subtle material substances.
  - Determining ID of hyperspectral imagery is very problematic.
- Principal Component Analysis (PCA).

Intrinsic Dimensionality (ID)

- Definition: minimum number of parameters required to account for the observed properties of the data.
- Suitable for multispectral imagery but difficult to implement with hyperspectral data.
  - High spectral resolution sensors can extract many unknown subtle material substances.
  - Determining ID of hyperspectral imagery is very problematic.
- Principal Component Analysis (PCA).

Virtual Dimensionality (VD)

- Definition: minimum number of spectrally distinct signal sources that characterize the hyperspectral data from a perspective view of target detection and classification.
- May include unknown interfering sources, which cannot be identified by a priori knowledge.
- Three eigen-thresholding based methods are presented to determine VD for hyperspectral imagery. They all are derived from the Neyman-Pearson detection theory.

Virtual Dimensionality (VD)

- Definition: minimum number of spectrally distinct signal sources that characterize the hyperspectral data from a perspective view of target detection and classification.
- May include unknown interfering sources, which cannot be identified by a priori knowledge.
- Three eigen-thresholding based methods are presented to determine VD for hyperspectral imagery. They all are derived from the Neyman-Pearson detection theory.

Virtual Dimensionality (VD)

- Definition: minimum number of spectrally distinct signal sources that characterize the hyperspectral data from a perspective view of target detection and classification.
- May include unknown interfering sources, which cannot be identified by a priori knowledge.
- Three eigen-thresholding based methods are presented to determine VD for hyperspectral imagery. They all are derived from the Neyman-Pearson detection theory.

Outline

1. Motivation
2. Linear unmixing
3. Virtual Dimensionality
   - Introduction
   - Neyman-Pearson Detection Theory-Based Eigen-Thresholding Analysis (HFC Method)
   - Noise Whitening HFC Analysis (NWHFC Method)
   - Noise Subspace Projection Analysis (NSP Method)
4. Endmember induction methods
   - Geometric approaches
   - Lattice computing approaches
   - Heuristic approaches

Introduction

- Use of the sample correlation-eigenvalues and covariance-eigenvalues.
- Each eigenvalue specifies a component dimension with a certain level of significance in terms of energy or variance.
- If both correlation/covariance-eigenvalues are equal, the signal represents just noise.
- *Idea: to make a test of hypothesis where the null hypothesis represents the eigenvalues being equal.*
- The number of times the test fails indicates how many signal sources are present in the image.

Introduction

- Use of the sample correlation-eigenvalues and covariance-eigenvalues.
- Each eigenvalue specifies a component dimension with a certain level of significance in terms of energy or variance.
- If both correlation/covariance-eigenvalues are equal, the signal represents just noise.
- *Idea: to make a test of hypothesis where the null hypothesis represents the eigenvalues being equal.*
- The number of times the test fails indicates how many signal sources are present in the image.

Introduction

- Use of the sample correlation-eigenvalues and covariance-eigenvalues.
- Each eigenvalue specifies a component dimension with a certain level of significance in terms of energy or variance.
- If both correlation/covariance-eigenvalues are equal, the signal represents just noise.
- *Idea: to make a test of hypothesis where the null hypothesis represents the eigenvalues being equal.*
- The number of times the test fails indicates how many signal sources are present in the image.

Introduction

- Use of the sample correlation-eigenvalues and covariance-eigenvalues.
- Each eigenvalue specifies a component dimension with a certain level of significance in terms of energy or variance.
- If both correlation/covariance-eigenvalues are equal, the signal represents just noise.
- *Idea: to make a test of hypothesis where the null hypothesis represents the eigenvalues being equal.*
- The number of times the test fails indicates how many signal sources are present in the image.

Introduction

- Use of the sample correlation-eigenvalues and covariance-eigenvalues.
- Each eigenvalue specifies a component dimension with a certain level of significance in terms of energy or variance.
- If both correlation/covariance-eigenvalues are equal, the signal represents just noise.
- *Idea: to make a test of hypothesis where the null hypothesis represents the eigenvalues being equal.*
- The number of times the test fails indicates how many signal sources are present in the image.

The Basis

1. Calculate the sample correlation matrix, R_{LxL}, and the sample covariance matrix, K_{LxL}.
2. Found their eigenvalues:
   - Let $\left\{\hat{\lambda}_1 \geq \hat{\lambda}_2 \geq \ldots \geq \hat{\lambda}_L\right\}$ be the set of eigenvalues generated by R_{LxL}.
   - Let $\{\lambda_1 \geq \lambda_2 \geq \ldots \geq \lambda_L\}$ be the set of eigenvalues generated by K_{LxL}.
3. Assume that signal sources have positive energies and noise variance in band l is given by σ_l^2.
4. Supposition: $\hat{\lambda}_l = \lambda_l + \sigma_l^2$ for $l = 1, 2, \ldots, VD$; and $\hat{\lambda}_l = \lambda_l = \sigma_l^2$ for $l = VD+1, \ldots, L$.

The Basis

1. Calculate the sample correlation matrix, R_{LxL}, and the sample covariance matrix, K_{LxL}.
2. Found their eigenvalues:
   - Let $\left\{\hat{\lambda}_1 \geq \hat{\lambda}_2 \geq \ldots \geq \hat{\lambda}_L\right\}$ be the set of eigenvalues generated by R_{LxL}.
   - Let $\{\lambda_1 \geq \lambda_2 \geq \ldots \geq \lambda_L\}$ be the set of eigenvalues generated by K_{LxL}.
3. Assume that signal sources have positive energies and noise variance in band l is given by σ_l^2.
4. Supposition: $\hat{\lambda}_l = \lambda_l + \sigma_l^2$ for $l = 1, 2, \ldots, VD$; and $\hat{\lambda}_l = \lambda_l = \sigma_l^2$ for $l = VD+1, \ldots, L$.

The Basis

1. Calculate the sample correlation matrix, R_{LxL}, and the sample covariance matrix, K_{LxL}.
2. Found their eigenvalues:
   - Let $\left\{\hat{\lambda}_1 \geq \hat{\lambda}_2 \geq \ldots \geq \hat{\lambda}_L\right\}$ be the set of eigenvalues generated by R_{LxL}.
   - Let $\{\lambda_1 \geq \lambda_2 \geq \ldots \geq \lambda_L\}$ be the set of eigenvalues generated by K_{LxL}.
3. Assume that signal sources have positive energies and noise variance in band l is given by σ_l^2.
4. Supposition: $\hat{\lambda}_l = \lambda_l + \sigma_l^2$ for $l = 1, 2, \ldots, VD$; and $\hat{\lambda}_l = \lambda_l = \sigma_l^2$ for $l = VD+1, \ldots, L$.

The Basis

1. Calculate the sample correlation matrix, R_{LxL}, and the sample covariance matrix, K_{LxL}.
2. Found their eigenvalues:
   - Let $\left\{\hat{\lambda}_1 \geq \hat{\lambda}_2 \geq \ldots \geq \hat{\lambda}_L\right\}$ be the set of eigenvalues generated by R_{LxL}.
   - Let $\{\lambda_1 \geq \lambda_2 \geq \ldots \geq \lambda_L\}$ be the set of eigenvalues generated by K_{LxL}.
3. Assume that signal sources have positive energies and noise variance in band l is given by σ_l^2.
4. Supposition: $\hat{\lambda}_l = \lambda_l + \sigma_l^2$ for $l = 1, 2, \ldots, VD$; and $\hat{\lambda}_l = \lambda_l = \sigma_l^2$ for $l = VD+1, \ldots, L$.

Test of hypothesis

Test of hypothesis

$$\begin{cases} H_0 : z_l = \hat{\lambda}_l - \lambda_l = 0 \\ H_1 : z_l = \hat{\lambda}_l - \lambda_l > 0 \end{cases} \qquad for\, l = 1, 2, \ldots, L$$

- Acording to that, $\hat{\lambda}_l$ and λ_l can be modelled as random variables with their asymptotic conditional probability densities:

$$\begin{cases} p_0(z_l) = p(z_l|H_0) \cong N(0, \sigma^2_{z_l}) \\ p_1(z_l) = p(z_l|H_1) \cong N(\mu_l, \sigma^2_{z_l}) \end{cases} \qquad for\, l = 1, 2, ..., L$$

Test of hypothesis

Test of hypothesis

$$\begin{cases} H_0 : z_l = \hat{\lambda}_l - \lambda_l = 0 \\ H_1 : z_l = \hat{\lambda}_l - \lambda_l > 0 \end{cases} \qquad for\, l = 1, 2, \ldots, L$$

- Acording to that, $\hat{\lambda}_l$ and λ_l can be modelled as random variables with their asymptotic conditional probability densities:

$$\begin{cases} p_0(z_l) = p(z_l|H_0) \cong N(0, \sigma^2_{z_l}) \\ p_1(z_l) = p(z_l|H_1) \cong N(\mu_l, \sigma^2_{z_l}) \end{cases} \qquad for\, l = 1, 2, ..., L$$

Mean and Variance I

- The mean μ is an unknown constant.
- The variance $\sigma^2_{z_l}$ is given by:

$$\sigma^2_{z_l} = Var[\hat{\lambda}_l - \lambda_l] = \sigma^2_{\hat{\lambda}_l} + \sigma^2_{\lambda_l} - 2Cov(\hat{\lambda}_l, \lambda_l) \quad for\, l = 1, 2, ..., L$$

- With $\sigma^2_{\hat{\lambda}_l}$ and $\sigma^2_{\lambda_l}$ given by:

$$\begin{cases} \sigma^2_{\hat{\lambda}_l} = Var[\hat{\lambda}_l] \cong \frac{2\hat{\lambda}_l^2}{N} \\ \sigma^2_{\lambda_l} = Var[\lambda_l] \cong \frac{2\lambda_l^2}{N} \end{cases} \quad for\, l = 1, 2, ..., L$$

Mean and Variance I

- The mean μ is an unknown constant.
- The variance $\sigma^2_{z_l}$ is given by:

$$\sigma^2_{z_l} = Var[\hat{\lambda}_l - \lambda_l] = \sigma^2_{\hat{\lambda}_l} + \sigma^2_{\lambda_l} - 2Cov(\hat{\lambda}_l, \lambda_l) \quad for\, l = 1, 2, ..., L$$

- With $\sigma^2_{\hat{\lambda}_l}$ and $\sigma^2_{\lambda_l}$ given by:

$$\begin{cases} \sigma^2_{\hat{\lambda}_l} = Var[\hat{\lambda}_l] \cong \frac{2\hat{\lambda}_l^2}{N} \\ \sigma^2_{\lambda_l} = Var[\lambda_l] \cong \frac{2\lambda_l^2}{N} \end{cases} \quad for\, l = 1, 2, ..., L$$

Mean and Variance I

- The mean μ is an unknown constant.
- The variance $\sigma^2_{z_l}$ is given by:

$$\sigma^2_{z_l} = Var[\hat{\lambda}_l - \lambda_l] = \sigma^2_{\hat{\lambda}_l} + \sigma^2_{\lambda_l} - 2Cov(\hat{\lambda}_l, \lambda_l) \quad for\, l = 1, 2, ..., L$$

- With $\sigma^2_{\hat{\lambda}_l}$ and $\sigma^2_{\lambda_l}$ given by:

$$\begin{cases} \sigma^2_{\hat{\lambda}_l} = Var[\hat{\lambda}_l] \cong \frac{2\hat{\lambda}_l^2}{N} \\ \sigma^2_{\lambda_l} = Var[\lambda_l] \cong \frac{2\lambda_l^2}{N} \end{cases} \quad for\, l = 1, 2, ..., L$$

Mean and Variance II

- The covariance $Cov(\hat{\lambda}_l, \lambda_l)$ is given by:

$$Cov(\hat{\lambda}_l, \lambda_l) \leq \sqrt{Var[\hat{\lambda}_l] Var[\lambda_l]} \cong (2/N)(\hat{\lambda}_l \cdot \lambda_l)$$

  - As $Cov(\hat{\lambda}_l, \lambda_l) \to 0$ as $N \to \infty$:

$$\sigma^2_{z_l} \cong (2/N)(\hat{\lambda}_l + \lambda_l) \quad as \quad N \to \infty$$

False Alarm and Detection Probabilities

- False alarm probability:

$$P_F = \int_{\tau}^{\infty} p_0(z)dz$$

- Detection probability (detection power):

$$P_D = \int_{\tau}^{\infty} p_1(z)dz$$

- The maximum detection probability, P_D, in determining VD for any given false alarm probability, P_F, is given by the Neyman-Pearson detector, δ_{NP}.

False Alarm and Detection Probabilities

- False alarm probability:

$$P_F = \int_{\tau}^{\infty} p_0(z)dz$$

- Detection probability (detection power):

$$P_D = \int_{\tau}^{\infty} p_1(z)dz$$

- The maximum detection probability, P_D, in determining VD for any given false alarm probability, P_F, is given by the Neyman-Pearson detector, δ_{NP}.

False Alarm and Detection Probabilities

- False alarm probability:

$$P_F = \int_{\tau}^{\infty} p_0(z)dz$$

- Detection probability (detection power):

$$P_D = \int_{\tau}^{\infty} p_1(z)dz$$

- The maximum detection probability, P_D, in determining VD for any given false alarm probability, P_F, is given by the Neyman-Pearson detector, δ_{NP}.

Outline

1. Motivation
2. Linear unmixing
3. Virtual Dimensionality
   - Introduction
   - Neyman-Pearson Detection Theory-Based Eigen-Thresholding Analysis (HFC Method)
   - Noise Whitening HFC Analysis (NWHFC Method)
   - Noise Subspace Projection Analysis (NSP Method)
4. Endmember induction methods
   - Geometric approaches
   - Lattice computing approaches
   - Heuristic approaches

Introduction

- HFC method does not decorrelate data.
- New approach: include a noise whitening process in the HFC method to remove the second order statistical correlation.
- A method to estimate the noise covariance matrix is needed:
  - Nearest Neighbor Difference (NDD): poor estimations (not explained).
  - Residual Based Estimation.
  - Linear Regression Model-based Prediction.

Introduction

- HFC method does not decorrelate data.
- New approach: include a noise whitening process in the HFC method to remove the second order statistical correlation.
- A method to estimate the noise covariance matrix is needed:
  - Nearest Neighbor Difference (NDD): poor estimations (not explained).
  - Residual Based Estimation.
  - Linear Regression Model-based Prediction.

Introduction

- HFC method does not decorrelate data.
- New approach: include a noise whitening process in the HFC method to remove the second order statistical correlation.
- A method to estimate the noise covariance matrix is needed:
  - Nearest Neighbor Difference (NDD): poor estimations (not explained).
  - Residual Based Estimation.
  - Linear Regression Model-based Prediction.

Residual Analysis I

Use of the sample covariance matrix

- Let K_{LxL} be the sample covariance matrix:

$$K_{LxL} = \frac{1}{N}\left[\sum_{i=1}^{N}(\vec{x}_i - \mu)(\vec{x}_i - \mu)^T\right]$$

- K_{LxL} can be decomposed by $K_{LxL} = D_K R_K D_K$ where:
  - D_K is a diagonal matrix given by $D_K = diag\{\sigma_1^2, \sigma_2^2, ..., \sigma_L^2\}$
  - R_K is the correlation matrix:

$$R_K = \begin{bmatrix} 1 & \rho_{12} & \rho_{13} & \cdots & \rho_{1L} \\ \rho_{21} & 1 & \rho_{23} & \cdots & \rho_{2L} \\ \rho_{31} & \rho_{32} & \ddots & \ddots & \vdots \\ \vdots & \vdots & \ddots & \ddots & \rho_{(L-1)L} \\ \rho_{L1} & \rho_{L2} & \cdots & \rho_{L(L-1)} & 1 \end{bmatrix}$$

Residual Analysis I

Use of the sample covariance matrix

- Let K_{LxL} be the sample covariance matrix:

$$K_{LxL} = \frac{1}{N}\left[\sum_{i=1}^{N}(\vec{x}_i - \mu)(\vec{x}_i - \mu)^T\right]$$

- K_{LxL} can be decomposed by $K_{LxL} = D_K R_K D_K$ where:
  - D_K is a diagonal matrix given by $D_K = diag\left\{\sigma_1^2, \sigma_2^2, ..., \sigma_L^2\right\}$
  - R_K is the correlation matrix:

$$R_K = \begin{bmatrix} 1 & \rho_{12} & \rho_{13} & \cdots & \rho_{1L} \\ \rho_{21} & 1 & \rho_{23} & \cdots & \rho_{2L} \\ \rho_{31} & \rho_{32} & \ddots & \ddots & \vdots \\ \vdots & \vdots & \ddots & \ddots & \rho_{(L-1)L} \\ \rho_{L1} & \rho_{L2} & \cdots & \rho_{L(L-1)} & 1 \end{bmatrix}$$

Residual Analysis II

Use of the inverse sample covariance matrix

- Similarly, K_{LxL}^{-1} can be decomposed by: $K_{LxL}^{-1} = D_{K^{-1}} R_{K^{-1}} D_{K^{-1}}$ where:
  - $D_{K^{-1}}$ is a diagonal matrix given by $D_{K^{-1}} = diag\left\{\varsigma_1^2, \varsigma_2^2, ..., \varsigma_L^2\right\}$ with $\left\{\varsigma_l^2\right\}_{l=1}^{L}$ being the diagonal elements of K_{LxL}^{-1}.
  - ς_l can be related to σ_l by $\varsigma_l = \sigma_l^{-1}(1 - r_{L-l}^2)^{-1/2}$ where:
    - r_{L-l}^2 is the multiple correlation coefficients of band B_l on the other $L-l$ bands $\{B_k\}_{k=1,k\neq l}^{L}$ obtained by using the multiple regression theory.
  - So, ς_l^2 is the reciprocal of a good noise variance estimate of band B_l.
  - The major advantage of using ς_l over σ_l is that ς_l removes its correlation on others ς_k's for $k \neq l$ while σ_l does not.

Residual Analysis II

Use of the inverse sample covariance matrix

- Similarly, K_{LxL}^{-1} can be decomposed by: $K_{LxL}^{-1} = D_{K^{-1}} R_{K^{-1}} D_{K^{-1}}$ where:
  - $D_{K^{-1}}$ is a diagonal matrix given by $D_{K^{-1}} = diag\left\{\varsigma_1^2, \varsigma_2^2, ..., \varsigma_L^2\right\}$ with $\left\{\varsigma_l^2\right\}_{l=1}^{L}$ being the diagonal elements of K_{LxL}^{-1}.
  - ς_l can be related to σ_l by $\varsigma_l = \sigma_l^{-1}(1 - r_{L-l}^2)^{-1/2}$ where:
    - r_{L-l}^2 is the multiple correlation coefficients of band B_l on the other $L-l$ bands $\{B_k\}_{k=1,k\neq l}^{L}$ obtained by using the multiple regression theory.
  - So, ς_l^2 is the reciprocal of a good noise variance estimate of band B_l.
  - The major advantage of using ς_l over σ_l is that ς_l removes its correlation on others ς_k's for $k \neq l$ while σ_l does not.

Residual Analysis II

Use of the inverse sample covariance matrix

- Similarly, K_{LxL}^{-1} can be decomposed by: $K_{LxL}^{-1} = D_{K^{-1}} R_{K^{-1}} D_{K^{-1}}$ where:
  - $D_{K^{-1}}$ is a diagonal matrix given by $D_{K^{-1}} = diag\left\{\varsigma_1^2, \varsigma_2^2, ..., \varsigma_L^2\right\}$ with $\left\{\varsigma_l^2\right\}_{l=1}^{L}$ being the diagonal elements of K_{LxL}^{-1}.
  - ς_l can be related to σ_l by $\varsigma_l = \sigma_l^{-1}(1 - r_{L-l}^2)^{-1/2}$ where:
    - r_{L-l}^2 is the multiple correlation coefficients of band B_l on the other $L-l$ bands $\{B_k\}_{k=1,k\neq l}^{L}$ obtained by using the multiple regression theory.
  - So, ς_l^2 is the reciprocal of a good noise variance estimate of band B_l.
  - The major advantage of using ς_l over σ_l is that ς_l removes its correlation on others ς_k's for $k \neq l$ while σ_l does not.

Residual Analysis II

Use of the inverse sample covariance matrix

- Similarly, K_{LxL}^{-1} can be decomposed by: $K_{LxL}^{-1} = D_{K^{-1}} R_{K^{-1}} D_{K^{-1}}$ where:
  - $D_{K^{-1}}$ is a diagonal matrix given by $D_{K^{-1}} = diag\left\{\varsigma_1^2, \varsigma_2^2, ..., \varsigma_L^2\right\}$ with $\left\{\varsigma_l^2\right\}_{l=1}^{L}$ being the diagonal elements of K_{LxL}^{-1}.
  - ς_l can be related to σ_l by $\varsigma_l = \sigma_l^{-1}(1 - r_{L-l}^2)^{-1/2}$ where:
    - r_{L-l}^2 is the multiple correlation coefficients of band B_l on the other $L-l$ bands $\{B_k\}_{k=1,k\neq l}^{L}$ obtained by using the multiple regression theory.
  - So, ς_l^2 is the reciprocal of a good noise variance estimate of band B_l.
  - The major advantage of using ς_l over σ_l is that ς_l removes its correlation on others ς_k's for $k \neq l$ while σ_l does not.

Inter/Intra-Band Prediction Noise Estimation

Intra/Inter band correlation

- Let $x_{l,(i,j,k)}$ be the pixel at the spatial location (i,j) in $B_{l,k}$ wich is the k-th spatial block of the l-th band B_l.
- Linear regression model to describe the intra/inter band correlation:

$$\hat{x}_{l,(i,j,k)} = a_1 x_{l-1,(i,j,k)} + a_2 x_{l+1,(i,j,k)} + a_3 x_{l,(i-1,j,k)} + a_0$$

  - where a_0, a_1, a_2, a_3 are the linear regression coefficients need to be determined.
- The residual error of $x_{l,(i,j,k)}$ is given by: $e_{l,(i,j,k)} = x_{l,(i,j,k)} - \hat{x}_{l,(i,j,k)}$.
- The residual error of $B_{l,k}$ is $e^2_{l,k} = \sum_{(i,j)} e^2_{l,(i,j,k)}$.

Inter/Intra-Band Prediction Noise Estimation

Intra/Inter band correlation

- Let $x_{l,(i,j,k)}$ be the pixel at the spatial location (i,j) in $B_{l,k}$ wich is the k-th spatial block of the l-th band B_l.
- Linear regression model to describe the intra/inter band correlation:

$$\hat{x}_{l,(i,j,k)} = a_1 x_{l-1,(i,j,k)} + a_2 x_{l+1,(i,j,k)} + a_3 x_{l,(i-1,j,k)} + a_0$$

  - where a_0, a_1, a_2, a_3 are the linear regression coefficients need to be determined.

- The residual error of $x_{l,(i,j,k)}$ is given by: $e_{l,(i,j,k)} = x_{l,(i,j,k)} - \hat{x}_{l,(i,j,k)}$.
- The residual error of $B_{l,k}$ is $e^2_{l,k} = \sum_{(i,j)} e^2_{l,(i,j,k)}$.

Inter/Intra-Band Prediction Noise Estimation

Intra/Inter band correlation

- Let $x_{l,(i,j,k)}$ be the pixel at the spatial location (i,j) in $B_{l,k}$ wich is the k-th spatial block of the l-th band B_l.
- Linear regression model to describe the intra/inter band correlation:

$$\hat{x}_{l,(i,j,k)} = a_1 x_{l-1,(i,j,k)} + a_2 x_{l+1,(i,j,k)} + a_3 x_{l,(i-1,j,k)} + a_0$$

  - where a_0, a_1, a_2, a_3 are the linear regression coefficients need to be determined.

- The residual error of $x_{l,(i,j,k)}$ is given by: $e_{l,(i,j,k)} = x_{l,(i,j,k)} - \hat{x}_{l,(i,j,k)}$.
- The residual error of $B_{l,k}$ is $e^2_{l,k} = \sum_{(i,j)} e^2_{l,(i,j,k)}$.

Inter/Intra-Band Prediction Noise Estimation

Intra/Inter band correlation

- Let $x_{l,(i,j,k)}$ be the pixel at the spatial location (i,j) in $B_{l,k}$ wich is the k-th spatial block of the l-th band B_l.
- Linear regression model to describe the intra/inter band correlation:

$$\hat{x}_{l,(i,j,k)} = a_1 x_{l-1,(i,j,k)} + a_2 x_{l+1,(i,j,k)} + a_3 x_{l,(i-1,j,k)} + a_0$$

  - where a_0, a_1, a_2, a_3 are the linear regression coefficients need to be determined.
- The residual error of $x_{l,(i,j,k)}$ is given by: $e_{l,(i,j,k)} = x_{l,(i,j,k)} - \hat{x}_{l,(i,j,k)}$.
- The residual error of $B_{l,k}$ is $e^2_{l,k} = \sum_{(i,j)} e^2_{l,(i,j,k)}$.

Inter/Intra-Band Prediction Noise Estimation

Noise variance of $B_{l,k}$

- Proposed method: subject to the constraint that the mean of the residual errors within the block must be zero: $\sum_{(i,j)} e_{l,(i,j,k)} = 0$.
- The resulted constrained solution was obtained by $\sigma^2_{l,k} = (N(B_{l,k}) - 4)^{-1} e^2_{l,(i,j,k)}$ where $N(B_{l,k})$ is the total number of pixels within $B_{l,k}$.
- So the variance of B_l can be estimated by the mean or the median of $\left\{\sigma^2_{l,k}\right\}_k$.
- The band-to-band noise correlation can be assumed to be uncorrelated or weak, so the noise covariance matrix K_n can be estimated by a diagonal matrix $K_n = diag\left\{\sigma^2_1, \sigma^2_2, ..., \sigma^2_L\right\}$.

Inter/Intra-Band Prediction Noise Estimation

Noise variance of $B_{l,k}$

- Proposed method: subject to the constraint that the mean of the residual errors within the block must be zero: $\sum_{(i,j)} e_{l,(i,j,k)} = 0$.
- The resulted constrained solution was obtained by $\sigma^2_{l,k} = (N(B_{l,k}) - 4)^{-1} e^2_{l,(i,j,k)}$ where $N(B_{l,k})$ is the total number of pixels within $B_{l,k}$.
- So the variance of B_l can be estimated by the mean or the median of $\left\{\sigma^2_{l,k}\right\}_k$.
- The band-to-band noise correlation can be assumed to be uncorrelated or weak, so the noise covariance matrix K_n can be estimated by a diagonal matrix $K_n = diag\left\{\sigma^2_1, \sigma^2_2, ..., \sigma^2_L\right\}$.

Inter/Intra-Band Prediction Noise Estimation

Noise variance of $B_{l,k}$

- Proposed method: subject to the constraint that the mean of the residual errors within the block must be zero: $\sum_{(i,j)} e_{l,(i,j,k)} = 0$.
- The resulted constrained solution was obtained by $\sigma^2_{l,k} = (N(B_{l,k}) - 4)^{-1} e^2_{l,(i,j,k)}$ where $N(B_{l,k})$ is the total number of pixels within $B_{l,k}$.
- So the variance of B_l can be estimated by the mean or the median of $\left\{\sigma^2_{l,k}\right\}_k$.
- The band-to-band noise correlation can be assumed to be uncorrelated or weak, so the noise covariance matrix K_n can be estimated by a diagonal matrix $K_n = diag\left\{\sigma_1^2, \sigma_2^2, ..., \sigma_L^2\right\}$.

Inter/Intra-Band Prediction Noise Estimation

Noise variance of $B_{l,k}$

- Proposed method: subject to the constraint that the mean of the residual errors within the block must be zero: $\sum_{(i,j)} e_{l,(i,j,k)} = 0$.
- The resulted constrained solution was obtained by $\sigma^2_{l,k} = (N(B_{l,k}) - 4)^{-1} e^2_{l,(i,j,k)}$ where $N(B_{l,k})$ is the total number of pixels within $B_{l,k}$.
- So the variance of B_l can be estimated by the mean or the median of $\left\{ \sigma^2_{l,k} \right\}_k$.
- The band-to-band noise correlation can be assumed to be uncorrelated or weak, so the noise covariance matrix K_n can be estimated by a diagonal matrix $K_n = diag\left\{ \sigma^2_1, \sigma^2_2, ..., \sigma^2_L \right\}$.

Outline

1. Motivation
2. Linear unmixing
3. Virtual Dimensionality
   - Introduction
   - Neyman-Pearson Detection Theory-Based Eigen-Thresholding Analysis (HFC Method)
   - Noise Whitening HFC Analysis (NWHFC Method)
   - Noise Subspace Projection Analysis (NSP Method)
4. Endmember induction methods
   - Geometric approaches
   - Lattice computing approaches
   - Heuristic approaches

Introduction

- Effectiveness of the HFC and NWHFC methods relies on $Cov(\hat{\lambda}_l, \lambda_l) \rightarrow 0$ as $N \rightarrow \infty$.
- For the case that the number of samples is not large enough, $Cov(\hat{\lambda}_l, \lambda_l)$ may be not zero.
- To resolve this, a Noise Subspace Projection (NSP) is developed.

Introduction

- Effectiveness of the HFC and NWHFC methods relies on $Cov(\hat{\lambda}_l, \lambda_l) \rightarrow 0$ as $N \rightarrow \infty$.
- For the case that the number of samples is not large enough, $Cov(\hat{\lambda}_l, \lambda_l)$ may be not zero.
- To resolve this, a Noise Subspace Projection (NSP) is developed.

Introduction

- Effectiveness of the HFC and NWHFC methods relies on $Cov(\hat{\lambda}_l, \lambda_l) \rightarrow 0$ as $N \rightarrow \infty$.
- For the case that the number of samples is not large enough, $Cov(\hat{\lambda}_l, \lambda_l)$ may be not zero.
- To resolve this, a Noise Subspace Projection (NSP) is developed.

Covariance Matrix of Signals

- De data sample covariance matrix, K_{LxL}, can be represented by $K_{LxL} = K_s + K_n$ where K_s is the covariance matrix of signals present in the image data.
- Using the eigendecomposition:

$$K_{LxL} = \sum_{l=1}^{VD} (\lambda_l + \sigma_l^2) u_l u_l^T + \sum_{l=VD+1}^{L} \sigma_l^2 u_l u_l^T$$

  - where $\{u_l\}_{l=1}^{VD}$ and $\{u_l\}_{l=VD+1}^{L}$ represent two sets of orthonormal vectors to span signal space and noise space respectively.
  - λ_l and σ_l^2 correspond to the energies of signals and noise in the l-th band respectively.

Covariance Matrix of Signals

- De data sample covariance matrix, K_{LxL}, can be represented by $K_{LxL} = K_s + K_n$ where K_s is the covariance matrix of signals present in the image data.
- Using the eigendecomposition:

$$K_{LxL} = \sum_{l=1}^{VD} (\lambda_l + \sigma_l^2) u_l u_l^T + \sum_{l=VD+1}^{L} \sigma_l^2 u_l u_l^T$$

  - where $\{u_l\}_{l=1}^{VD}$ and $\{u_l\}_{l=VD+1}^{L}$ represent two sets of orthonormal vectors to span signal space and noise space respectively.
  - λ_l and σ_l^2 correspond to the energies of signals and noise in the l-th band respectively.

Finding the Virtual Dimensionality

- Taking advantage of the eigen-decomposition of K_{LxL}:

$$K_n^{-1} K_{LxL} = \sum_{l=1}^{VD} (\lambda_l / \sigma_l + 1) u_l u_l^T + \sum_{l=VD+1}^{L} u_l u_l^T$$

- If it is assumed that the energies of signals are greater than noise energies, $\lambda_l > \sigma_l$ for $l = 1, 2, ..., VD$ the following hypothesis test can be used:

$$\begin{cases} H_0 : z_l = \mu_l = 1 \\ H_1 : z_l = \mu_l = \lambda_l / \sigma_l + 1 > 1 \end{cases} \quad for \; l = 1, 2, ..., L$$

- where:

$$\begin{cases} p_0(z_l) = p(z_l | H_0) \cong N(1, \sigma_{z_l}^2) \\ p_1(z_l) = p(z_l | H_1) \cong N(\mu_l, \sigma_{z_l}^2) \end{cases} \qquad \sigma_{z_l}^2 = \sigma_{\lambda_l}^2$$

Finding the Virtual Dimensionality

- Taking advantage of the eigen-decomposition of K_{LxL}:

$$K_n^{-1} K_{LxL} = \sum_{l=1}^{VD} (\lambda_l / \sigma_l + 1) u_l u_l^T + \sum_{l=VD+1}^{L} u_l u_l^T$$

- If it is assumed that the energies of signals are greater than noise energies, $\lambda_l > \sigma_l$ for $l = 1, 2, ..., VD$ the following hypothesis test can be used:

$$\begin{cases} H_0 : z_l = \mu_l = 1 \\ H_1 : z_l = \mu_l = \lambda_l / \sigma_l + 1 > 1 \end{cases} \quad for \quad l = 1, 2, ..., L$$

  - where:

$$\begin{cases} p_0(z_l) = p(z_l | H_0) \cong N(1, \sigma_{z_l}^2) \\ p_1(z_l) = p(z_l | H_1) \cong N(\mu_l, \sigma_{z_l}^2) \end{cases} \quad \sigma_{z_l}^2 = \sigma_{\lambda_l}^2$$

Outline

1. Motivation
2. Linear unmixing
3. Virtual Dimensionality
   - Introduction
   - Neyman-Pearson Detection Theory-Based Eigen-Thresholding Analysis (HFC Method)
   - Noise Whitening HFC Analysis (NWHFC Method)
   - Noise Subspace Projection Analysis (NSP Method)
4. Endmember induction methods
   - Geometric approaches
   - Lattice computing approaches
   - Heuristic approaches

Introduction

- Geometric methods follow the formal definition of the endmembers, they search for the vertices of a convex set that covers the image data.
- Because the distribution of the data in the hyperspace is usually tear-shaped they look for the minimum simplex that covers all the data.

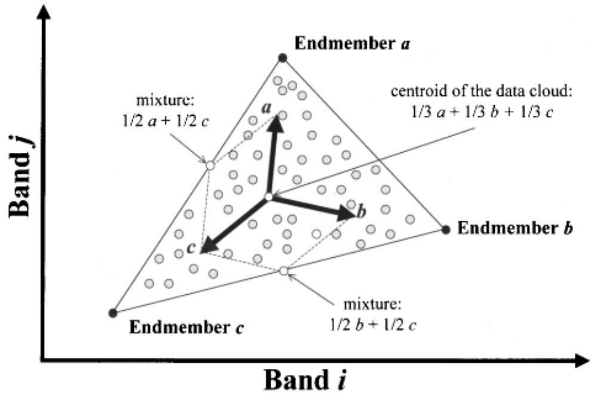

Figure: 2-dimension spectral data plot illustrating the geometrics of a mixture model based on endmembers

Introduction

- Geometric methods follow the formal definition of the endmembers, they search for the vertices of a convex set that covers the image data.
- Because the distribution of the data in the hyperspace is usually tear-shaped they look for the minimum simplex that covers all the data.

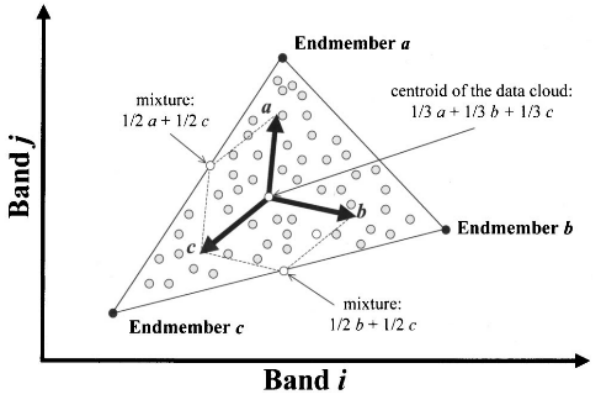

Figure: 2-dimension spectral data plot illustrating the geometrics of a mixture model based on endmembers

Minimum Volume Transform (MVT)

- Introduces two non-orthonormal transformations.
- Dark Point Fixed transformation (DPF): obtained by first normalizing the data, by projection from the origin O, to lie within the hyperplane $u^T x = 1$. New coordinates are then to be taken with respect to the vector edges, through O, of a minimum-volume circunscribing simplex having one vertex at O.
- Fixed Point Free transformation (FPF): coordinates barycentric with respect to the vertices of a circunscribing simplex in n space, provided only that the simplex be of minimum volume.
- Neither transform is uniquely determined.

Minimum Volume Transform (MVT)

- Introduces two non-orthonormal transformations.
- Dark Point Fixed transformation (DPF): obtained by first normalizing the data, by projection from the origin O, to lie within the hyperplane $u^T x = 1$. New coordinates are then to be taken with respect to the vector edges, through O, of a minimum-volume circunscribing simplex having one vertex at O.
- Fixed Point Free transformation (FPF): coordinates barycentric with respect to the vertices of a circunscribing simplex in n space, provided only that the simplex be of minimum volume.
- Neither transform is uniquely determined.

Minimum Volume Transform (MVT)

- Introduces two non-orthonormal transformations.
- Dark Point Fixed transformation (DPF): obtained by first normalizing the data, by projection from the origin O, to lie within the hyperplane $u^T x = 1$. New coordinates are then to be taken with respect to the vector edges, through O, of a minimum-volume circunscribing simplex having one vertex at O.
- Fixed Point Free transformation (FPF): coordinates barycentric with respect to the vertices of a circunscribing simplex in n space, provided only that the simplex be of minimum volume.
- Neither transform is uniquely determined.

Minimum Volume Transform (MVT)

- Introduces two non-orthonormal transformations.
- Dark Point Fixed transformation (DPF): obtained by first normalizing the data, by projection from the origin O, to lie within the hyperplane $u^T x = 1$. New coordinates are then to be taken with respect to the vector edges, through O, of a minimum-volume circunscribing simplex having one vertex at O.
- Fixed Point Free transformation (FPF): coordinates barycentric with respect to the vertices of a circunscribing simplex in n space, provided only that the simplex be of minimum volume.
- Neither transform is uniquely determined.

N-FINDER

Preprocessing

- Dimensionality reduction to $k-1$ dimensions being k the number of endmembers in image.
- Orthogonal Subspace Projection (OSP):
  - Maximun power for the single value decomposition.
  - Noise weighted variation for the Maximun Noise Fraction (MNF).

N-FINDER
Preprocessing

- Dimensionality reduction to $k-1$ dimensions being k the number of endmembers in image.
- Orthogonal Subspace Projection (OSP):
  - Maximun power for the single value decomposition.
  - Noise weighted variation for the Maximun Noise Fraction (MNF).

N-FINDER
Algorithm

- Initialize the set of endmembers.
- For each pixel:
  - Replace each endmember with the pixel.
  - Calculate simplex volume.
  - If volume decreases substitute the endmember with the pixel in the set.
- Some random initializations are required to avoid local maximums.

N-FINDER
Algorithm

- Initialize the set of endmembers.
- For each pixel:
  - Replace each endmember with the pixel.
  - Calculate simplex volume.
  - If volume decreases substitute the endmember with the pixel in the set.
- Some random initializations are required to avoid local maximums.

N-FINDER
Algorithm

- Initialize the set of endmembers.
- For each pixel:
  - Replace each endmember with the pixel.
  - Calculate simplex volume.
  - If volume decreases substitute the endmember with the pixel in the set.
- Some random initializations are required to avoid local maximums.

Convex Cones Analysis (CCA)

Algorithm

- Dimensionality reduction to $k-1$ dimensions being k the number of endmembers in image (PCA).
- Given the data S, the correlation matrix $C = S^T S$ has to be calculated.
- Use of Single Value Decomposition (SVD) to obtain the eigenvectors and eigenvalues of C.
- Select the eigenvectors p_i corresponding to the k largest eigenvalues.
- Find the convex cone limits defined by:

$$\mathbf{x} = \mathbf{p_1} + a_1\mathbf{p_2} + \ldots + a_{k-1}\mathbf{p_{k-1}}$$

Convex Cones Analysis (CCA)

Algorithm

- Dimensionality reduction to $k-1$ dimensions being k the number of endmembers in image (PCA).
- Given the data S, the correlation matrix $C = S^T S$ has to be calculated.
- Use of Single Value Decomposition (SVD) to obtain the eigenvectors and eigenvalues of C.
- Select the eigenvectors p_i corresponding to the k largest eigenvalues.
- Find the convex cone limits defined by:

$$\mathbf{x} = \mathbf{p_1} + a_1\mathbf{p_2} + \ldots + a_{k-1}\mathbf{p_{k-1}}$$

Convex Cones Analysis (CCA)

Algorithm

- Dimensionality reduction to $k-1$ dimensions being k the number of endmembers in image (PCA).
- Given the data S, the correlation matrix $C = S^T S$ has to be calculated.
- Use of Single Value Decomposition (SVD) to obtain the eigenvectors and eigenvalues of C.
- Select the eigenvectors p_i corresponding to the k largest eigenvalues.
- Find the convex cone limits defined by:

$$\mathbf{x} = \mathbf{p_1} + a_1\mathbf{p_2} + \ldots + a_{k-1}\mathbf{p_{k-1}}$$

Convex Cones Analysis (CCA)

Algorithm

- Dimensionality reduction to $k-1$ dimensions being k the number of endmembers in image (PCA).
- Given the data S, the correlation matrix $C = S^T S$ has to be calculated.
- Use of Single Value Decomposition (SVD) to obtain the eigenvectors and eigenvalues of C.
- Select the eigenvectors p_i corresponding to the k largest eigenvalues.
- Find the convex cone limits defined by:

$$\mathbf{x} = \mathbf{p_1} + a_1\mathbf{p_2} + \ldots + a_{k-1}\mathbf{p_{k-1}}$$

Convex Cones Analysis (CCA)

Algorithm

- Dimensionality reduction to $k-1$ dimensions being k the number of endmembers in image (PCA).
- Given the data S, the correlation matrix $C = S^T S$ has to be calculated.
- Use of Single Value Decomposition (SVD) to obtain the eigenvectors and eigenvalues of C.
- Select the eigenvectors p_i corresponding to the k largest eigenvalues.
- Find the convex cone limits defined by:

$$\mathbf{x} = \mathbf{p_1} + a_1 \mathbf{p_2} + \ldots + a_{k-1} \mathbf{p_{k-1}}$$

Convex Cone Analysis (CCA)

Observations

- If the number of bands b is greater than k: overdeterminated linear ecuation system. It suposses $\begin{pmatrix} b \\ c-1 \end{pmatrix}$ possible solutions.
- The number of solutions grows with order $O(b^k)$.
- Example: if $b = 100$ and $k = 5$ there are about 4 million possible solutions.
- Each ecuation defines an hyperplane in a k-dimensional space.

Convex Cone Analysis (CCA)

Observations

- If the number of bands b is greater than k: overdeterminated linear ecuation system. It suposses $\begin{pmatrix} b \\ c-1 \end{pmatrix}$ possible solutions.
- The number of solutions grows with order $O(b^k)$.
- Example: if $b = 100$ and $k = 5$ there are about 4 million possible solutions.
- Each ecuation defines an hyperplane in a k-dimensional space.

Convex Cone Analysis (CCA)

Observations

- If the number of bands b is greater than k: overdeterminated linear ecuation system. It suposses $\begin{pmatrix} b \\ c-1 \end{pmatrix}$ possible solutions.
- The number of solutions grows with order $O(b^k)$.
- Example: if $b = 100$ and $k = 5$ there are about 4 million possible solutions.
- Each ecuation defines an hyperplane in a k-dimensional space.

Convex Cone Analysis (CCA)

Observations

- If the number of bands b is greater than k: overdeterminated linear ecuation system. It suposses $\begin{pmatrix} b \\ c-1 \end{pmatrix}$ possible solutions.
- The number of solutions grows with order $O(b^k)$.
- Example: if $b = 100$ and $k = 5$ there are about 4 million possible solutions.
- Each ecuation defines an hyperplane in a k-dimensional space.

Convex Cones Analysis (CCA)

Geometric representation

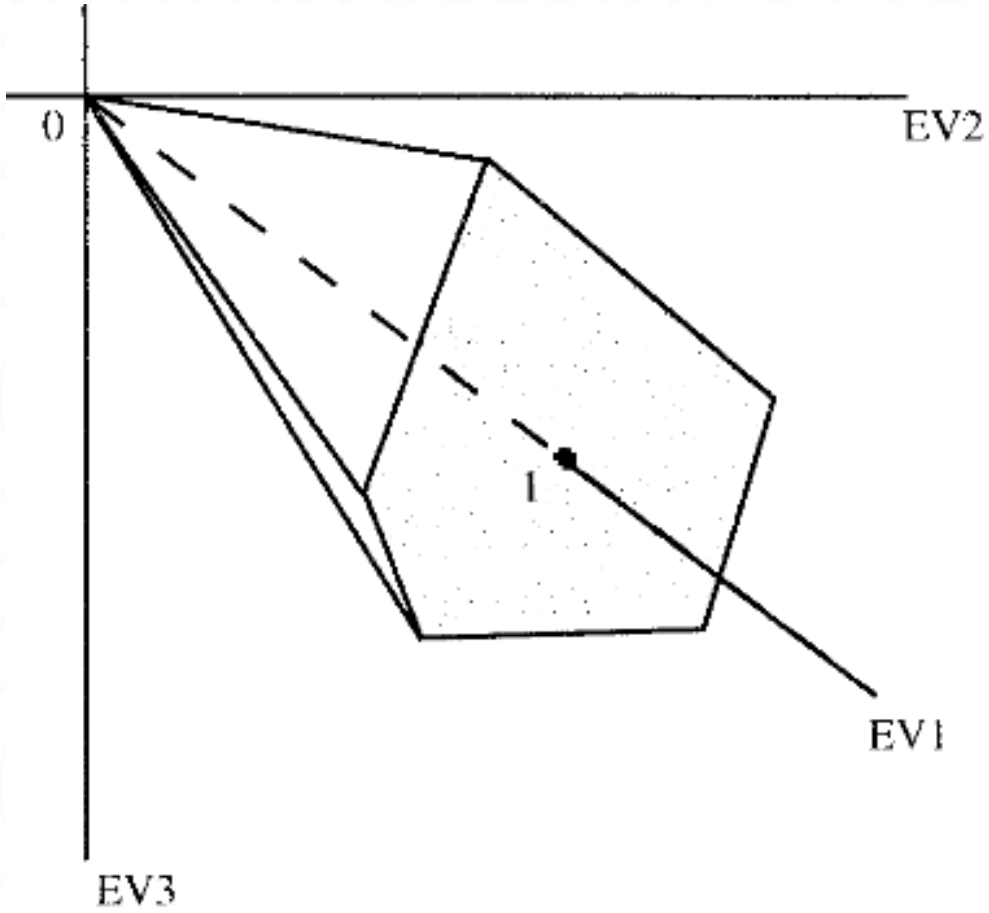

Simulated Annealing (SA)

Algorithm

- Dimensionality reduction to $k-1$ dimensions being k the number of endmembers in image (MNF).
- The partition in the configuration space defines a simplex convering the image data whose vertices are the candidate endmembers.
- The objective function minimized is the simplex volume.

Simulated Annealing (SA)

Algorithm

- Dimensionality reduction to $k-1$ dimensions being k the number of endmembers in image (MNF).
- The partition in the configuration space defines a simplex convering the image data whose vertices are the candidate endmembers.
- The objective function minimized is the simplex volume.

Simulated Annealing (SA)

Algorithm

- Dimensionality reduction to $k-1$ dimensions being k the number of endmembers in image (MNF).
- The partition in the configuration space defines a simplex convering the image data whose vertices are the candidate endmembers.
- The objective function minimized is the simplex volume.

Iterated Constrained Endmembers (ICE)

Algorithm

- Dimensionality reduction to $k-1$ dimensions being k the number of endmembers in image (MNF).
- Performs the minimization of a regularized residual sum of squares (RSS). The regularization term is the volume of the simplex.
- First the proportions are computed by quadratic programming problem solving assuming that the endmembers are known, then the endmembers are computed as the direct minimization of the RSS functional.

Iterated Constrained Endmembers (ICE)

Algorithm

- Dimensionality reduction to $k-1$ dimensions being k the number of endmembers in image (MNF).
- Performs the minimization of a regularized residual sum of squares (RSS). The regularization term is the volume of the simplex.
- First the proportions are computed by quadratic programming problem solving assuming that the endmembers are known, then the endmembers are computed as the direct minimization of the RSS functional.

Iterated Constrained Endmembers (ICE)

Algorithm

- Dimensionality reduction to $k-1$ dimensions being k the number of endmembers in image (MNF).
- Performs the minimization of a regularized residual sum of squares (RSS). The regularization term is the volume of the simplex.
- First the proportions are computed by quadratic programming problem solving assuming that the endmembers are known, then the endmembers are computed as the direct minimization of the RSS functional.

Vertex Component Analysis (VCA)

Algorithm

- The algorithm is unsupervised and exploits that the affine transformation of a simplex is also a simplex.
- It works with projected and unprojected data.
- The algorithm iteratively projects data onto a direction orthogonal to the subspace spanned by the endmembers already determined. The new endmember signature corresponds to the extreme of the projection. The algorithm iterates until all endmembers are exhausted.

Vertex Component Analysis (VCA)

Algorithm

- The algorithm is unsupervised and exploits that the affine transformation of a simplex is also a simplex.
- It works with projected and unprojected data.
- The algorithm iteratively projects data onto a direction orthogonal to the subspace spanned by the endmembers already determined. The new endmember signature corresponds to the extreme of the projection. The algorithm iterates until all endmembers are exhausted.

Vertex Component Analysis (VCA)

Algorithm

- The algorithm is unsupervised and exploits that the affine transformation of a simplex is also a simplex.
- It works with projected and unprojected data.
- The algorithm iteratively projects data onto a direction orthogonal to the subspace spanned by the endmembers already determined. The new endmember signature corresponds to the extreme of the projection. The algorithm iterates until all endmembers are exhausted.

Simplex Growing Analysis (SGA)

Algorithm

- SGA improves N-FINDR by including a process of growing simplexes one vertex at a time until the desired number of vertices is reached, which results in a high computational complexity reduction.
- Selects an appropiate initial vector to avoid the use of random vectors as initial condition, which produces different sets of final endmembers if different sets of randomly generated initial endmembers are used.
- Use of Virtual Dimensionality (VD) to select the number of endmembers in image.

Simplex Growing Analysis (SGA)

Algorithm

- SGA improves N-FINDR by including a process of growing simplexes one vertex at a time until the desired number of vertices is reached, which results in a high computational complexity reduction.
- Selects an appropiate initial vector to avoid the use of random vectors as initial condition, which produces different sets of final endmembers if different sets of randomly generated initial endmembers are used.
- Use of Virtual Dimensionality (VD) to select the number of endmembers in image.

Simplex Growing Analysis (SGA)

Algorithm

- SGA improves N-FINDR by including a process of growing simplexes one vertex at a time until the desired number of vertices is reached, which results in a high computational complexity reduction.
- Selects an appropiate initial vector to avoid the use of random vectors as initial condition, which produces different sets of final endmembers if different sets of randomly generated initial endmembers are used.
- Use of Virtual Dimensionality (VD) to select the number of endmembers in image.

Minimun Volume Constrained Non-negative Matrix Factorization (MVC-NMF)

Algorithm

- Method for endmember extraction for highly mixed data, when there are not pure pixels in the hyperspectral image.
- Takes advantage of the fast convergence of NMF schemes and at the same time eliminates the pure-pixel assumption.
- It consists in the reformulation of an NMF cost function introducing a volume regularization term, much like the ICE, substituting the RSS by the NMF criteria.

Minimun Volume Constrained Non-negative Matrix Factorization (MVC-NMF)

Algorithm

- Method for endmember extraction for highly mixed data, when there are not pure pixels in the hyperspectral image.
- Takes advantage of the fast convergence of NMF schemes and at the same time eliminates the pure-pixel assumption.
- It consists in the reformulation of an NMF cost function introducing a volume regularization term, much like the ICE, substituting the RSS by the NMF criteria.

Minimun Volume Constrained Non-negative Matrix Factorization (MVC-NMF)

Algorithm

- Method for endmember extraction for highly mixed data, when there are not pure pixels in the hyperspectral image.
- Takes advantage of the fast convergence of NMF schemes and at the same time eliminates the pure-pixel assumption.
- It consists in the reformulation of an NMF cost function introducing a volume regularization term, much like the ICE, substituting the RSS by the NMF criteria.

Outline

1. Motivation
2. Linear unmixing
3. Virtual Dimensionality
   - Introduction
   - Neyman-Pearson Detection Theory-Based Eigen-Thresholding Analysis (HFC Method)
   - Noise Whitening HFC Analysis (NWHFC Method)
   - Noise Subspace Projection Analysis (NSP Method)
4. Endmember induction methods
   - Geometric approaches
   - Lattice computing approaches
   - Heuristic approaches

Introduction

- Lattice computing can be defined as the collection of computational methods that either are defined on the algebra of lattice operators inf and sup, with the addition, or employ lattice theory to generalize previous approaches.

Automated Morphological Endmember Extraction (AMEE)

Multispectral morphological erosion/dilation

- Dilation: most spectrally singular.

$$\mathbf{d}(\mathbf{x},\mathbf{y}) = (f \circ K)(x,y) = \arg \max_{(s,t)\in K} \{D(\mathbf{f}(\mathbf{x}+\mathbf{s},\mathbf{y}+\mathbf{t}),K)\}$$

- Erosion: most spectrally mixed.

$$\mathbf{e}(\mathbf{x},\mathbf{y}) = (f \circ K)(x,y) = \arg \min_{(s,t)\in K} \{D(\mathbf{f}(\mathbf{x}-\mathbf{s},\mathbf{y}-\mathbf{t}),K)\}$$

Automated Morphological Endmember Extraction (AMEE)

Multispectral morphological erosion/dilation

- Dilation: most spectrally singular.

$$\mathbf{d}(\mathbf{x},\mathbf{y}) = (f \circ K)(x,y) = \arg \max_{(s,t)\in K} \{D(\mathbf{f}(\mathbf{x}+\mathbf{s},\mathbf{y}+\mathbf{t}),K)\}$$

- Erosion: most spectrally mixed.

$$\mathbf{e}(\mathbf{x},\mathbf{y}) = (f \circ K)(x,y) = \arg \min_{(s,t)\in K} \{D(\mathbf{f}(\mathbf{x}-\mathbf{s},\mathbf{y}-\mathbf{t}),K)\}$$

Automated Morphological Endmember Extraction (AMEE)

Cumulative distance

- Cumulative Distance for Pixel Ordering in Terms of Spectral Purity ($O(n^3)$):

$$D(\mathbf{f}(\mathbf{x},\mathbf{y}),K) = \sum_s \sum_t dist(\mathbf{f}(\mathbf{x},\mathbf{y})\mathbf{f}(\mathbf{s},\mathbf{t})) \qquad \forall (s,t) \in K$$

- Distance to the Centroid of the Data Cloud($O(n^2)$):

$$D(\mathbf{f}(\mathbf{x},\mathbf{y}),K) = dist(\mathbf{f}(\mathbf{x},\mathbf{y})\mathbf{c}(\mathbf{K})) \qquad \forall (s,t) \in K$$

$$\mathbf{c}(\mathbf{K}) = \frac{1}{M} \sum_s \sum_t \mathbf{f}(\mathbf{s},\mathbf{t}) \qquad \forall (s,t) \in K$$

Automated Morphological Endmember Extraction (AMEE)

Cumulative distance

- Cumulative Distance for Pixel Ordering in Terms of Spectral Purity ($O(n^3)$):

$$D(\mathbf{f}(\mathbf{x},\mathbf{y}),K) = \sum_s \sum_t dist(\mathbf{f}(\mathbf{x},\mathbf{y})\mathbf{f}(\mathbf{s},\mathbf{t})) \qquad \forall (s,t) \in K$$

- Distance to the Centroid of the Data Cloud($O(n^2)$):

$$D(\mathbf{f}(\mathbf{x},\mathbf{y}),K) = dist(\mathbf{f}(\mathbf{x},\mathbf{y})\mathbf{c}(\mathbf{K})) \qquad \forall (s,t) \in K$$

$$\mathbf{c}(\mathbf{K}) = \frac{1}{M} \sum_s \sum_t \mathbf{f}(\mathbf{s},\mathbf{t}) \qquad \forall (s,t) \in K$$

Automated Morphological Endmember Extraction (AMEE)

Graphic representation

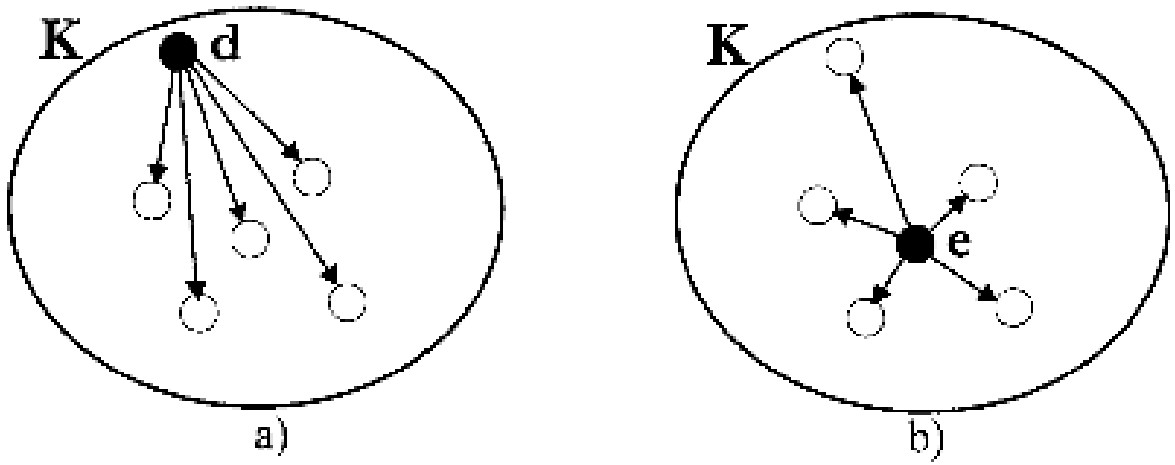

Figure: Cumulative Distance for Pixel Ordering in Terms of Spectral Purity

Automated Morphological Endmember Extraction (AMEE)

Graphic representation

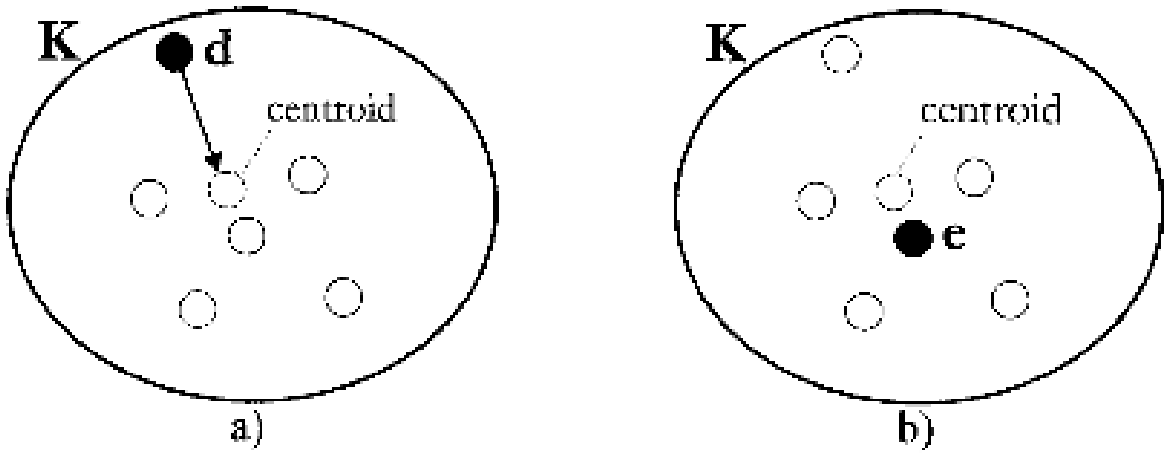

Figure: Distance to the Centroid of the Data Cloud

Automated Morphological Endmember Extraction (AMEE)

"Voting" Approach to endmember selection

- Given a pixel $p(x,y)$, the pixel $p(m,n)$ is obtained by the dilation operation over $p(x,y)$.
- The pixel counter is increased by one.
- Iterate over all the pixels in the image.
- The most voted pixels are the endmembers candidates.

Automated Morphological Endmember Extraction (AMEE)

"Voting" Approach to endmember selection

- Given a pixel $p(x,y)$, the pixel $p(m,n)$ is obtained by the dilation operation over $p(x,y)$.
- The pixel counter is increased by one.
- Iterate over all the pixels in the image.
- The most voted pixels are the endmembers candidates.

Automated Morphological Endmember Extraction (AMEE)

"Voting" Approach to endmember selection

- Given a pixel $p(x,y)$, the pixel $p(m,n)$ is obtained by the dilation operation over $p(x,y)$.
- The pixel counter is increased by one.
- Iterate over all the pixels in the image.
- The most voted pixels are the endmembers candidates.

Automated Morphological Endmember Extraction (AMEE)

"Voting" Approach to endmember selection

- Given a pixel $p(x,y)$, the pixel $p(m,n)$ is obtained by the dilation operation over $p(x,y)$.
- The pixel counter is increased by one.
- Iterate over all the pixels in the image.
- The most voted pixels are the endmembers candidates.

Automated Morphological Endmember Extraction (AMEE)

"Evaluating" Approach to endmember selection

- Given a pixel $p(x,y)$, dilation and erosion operations are evaluated over $p(x,y)$.
- The Morphological Eccentricity Index (MEI) is calculated for $p(x,y)$:

$$MEI(x,y) = dist(\mathbf{d}(\mathbf{x},\mathbf{y}),\mathbf{e}(\mathbf{x},\mathbf{y}))$$

- Iterate over all the pixels in the image.

Automated Morphological Endmember Extraction (AMEE)

"Evaluating" Approach to endmember selection

- Given a pixel $p(x,y)$, dilation and erosion operations are evaluated over $p(x,y)$.
- The Morphological Eccentricity Index (MEI) is calculated for $p(x,y)$:

$$MEI(x,y) = dist(\mathbf{d}(\mathbf{x},\mathbf{y}),\mathbf{e}(\mathbf{x},\mathbf{y}))$$

- Iterate over all the pixels in the image.

Automated Morphological Endmember Extraction (AMEE)

"Evaluating" Approach to endmember selection

- Given a pixel $p(x,y)$, dilation and erosion operations are evaluated over $p(x,y)$.
- The Morphological Eccentricity Index (MEI) is calculated for $p(x,y)$:

$$MEI(x,y) = dist(\mathbf{d}(\mathbf{x},\mathbf{y}),\mathbf{e}(\mathbf{x},\mathbf{y}))$$

- Iterate over all the pixels in the image.

Automated Morphological Endmember Extraction (AMEE)

Diferences between "Voting" and "Evaluating" approaches

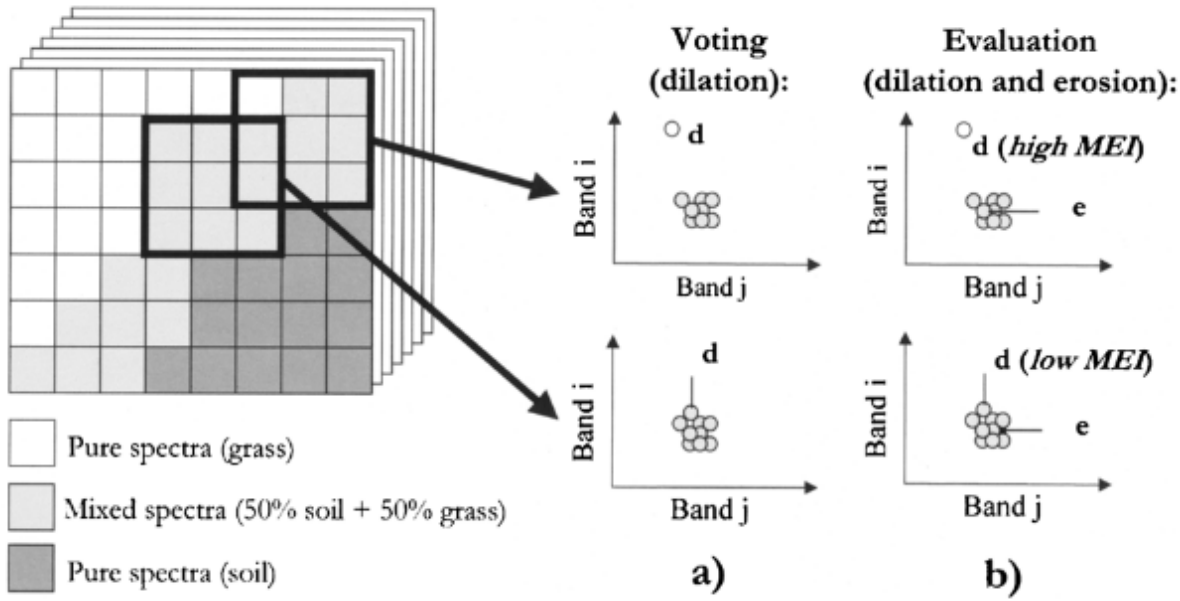

Automated Morphological Endmember Extraction (AMEE)

Algorithm

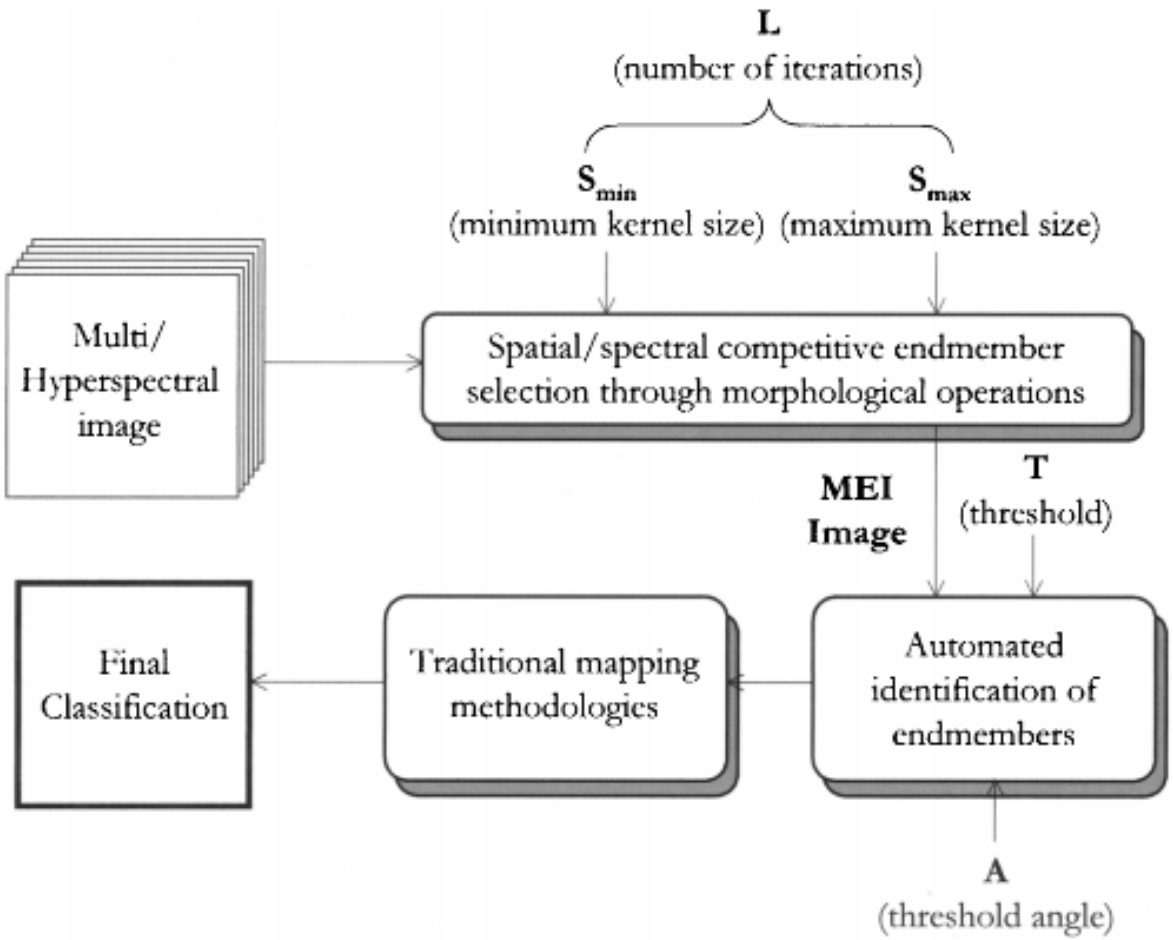

Automated Morphological Endmember Extraction (AMEE)

Observations

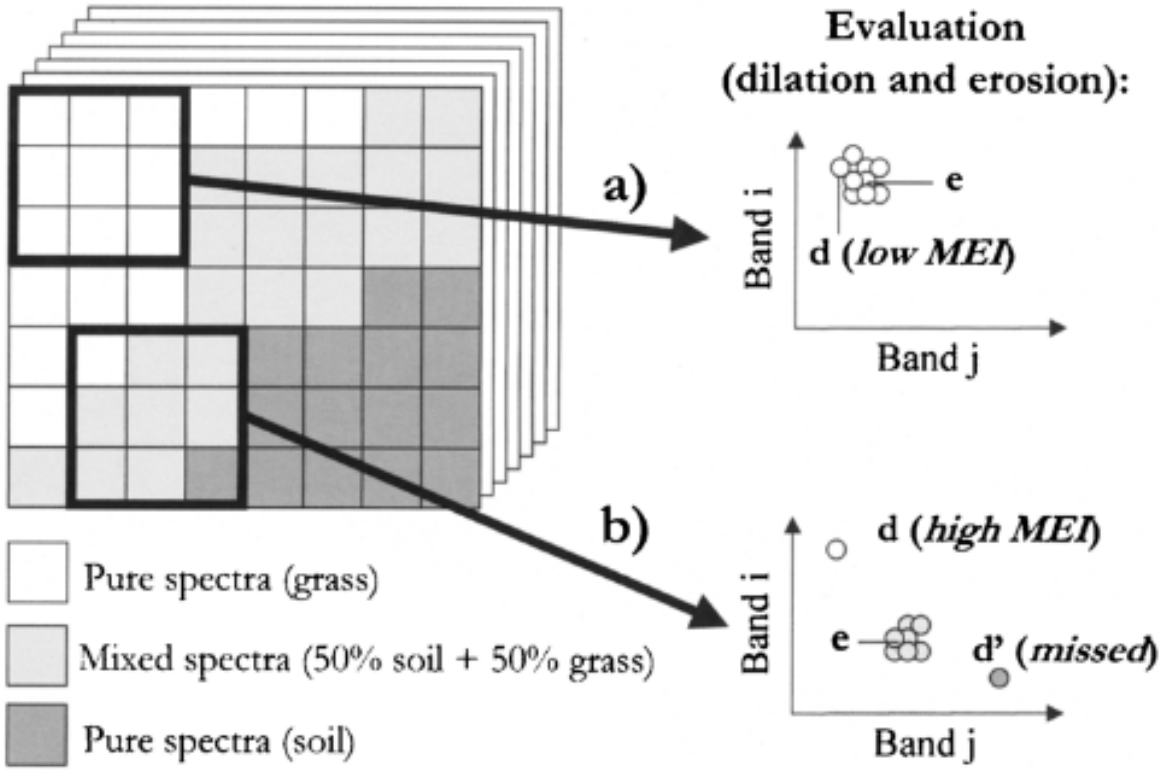

Associative Morphological Memories (AMM)

Introduction

- Based on the concept of morphological independence, later reformulated as lattice independence.
- The set of endmembers is formulated as a set of morphologically independent vectors, either in a dilative or erosive sense, or both.
- The Associative Morphological Memories, later renamed Lattice Associative Memories, are proposed as detectors of morphologically independent vectors.
- The algorithm works in a single pass over the sample data.

Associative Morphological Memories (AMM)

Introduction

- Based on the concept of morphological independence, later reformulated as lattice independence.
- The set of endmembers is formulated as a set of morphologically independent vectors, either in a dilative or erosive sense, or both.
- The Associative Morphological Memories, later renamed Lattice Associative Memories, are proposed as detectors of morphologically independent vectors.
- The algorithm works in a single pass over the sample data.

Associative Morphological Memories (AMM)

Introduction

- Based on the concept of morphological independence, later reformulated as lattice independence.
- The set of endmembers is formulated as a set of morphologically independent vectors, either in a dilative or erosive sense, or both.
- The Associative Morphological Memories, later renamed Lattice Associative Memories, are proposed as detectors of morphologically independent vectors.
- The algorithm works in a single pass over the sample data.

Associative Morphological Memories (AMM)

Introduction

- Based on the concept of morphological independence, later reformulated as lattice independence.
- The set of endmembers is formulated as a set of morphologically independent vectors, either in a dilative or erosive sense, or both.
- The Associative Morphological Memories, later renamed Lattice Associative Memories, are proposed as detectors of morphologically independent vectors.
- The algorithm works in a single pass over the sample data.

Asociative Morphological Memories (AMM)

Heteroassociative Morphological Memories

- Given a pair of in/out patterns, $(X,Y) = \{(x^\varepsilon, y^\varepsilon); \varepsilon = 1, \ldots, k\}$ an heteroassociative neural network absed in the cross correlation is building over the function $W = \sum_\varepsilon y^\varepsilon \cdot (x^\varepsilon)^T$.

$$W_{XY} = \bigwedge_{\varepsilon=1}^{k} [y^\varepsilon \times (-x^\varepsilon)']$$

$$M_{XY} = \bigvee_{\varepsilon=1}^{k} [y^\varepsilon \times (-x^\varepsilon)']$$

being $\times$ any of the $\min, \max$ operators, $\wedge, \vee$.

- If $X = Y$, then the HMM are denoted as Autoassociative Morphological Memories (AMM).

Asociative Morphological Memories (AMM)

Heteroassociative Morphological Memories

- Given a pair of in/out patterns, $(X,Y) = \{(x^\varepsilon, y^\varepsilon); \varepsilon = 1, \ldots, k\}$ an heteroassociative neural network absed in the cross correlation is building over the function $W = \sum_\varepsilon y^\varepsilon \cdot (x^\varepsilon)^T$.

$$W_{XY} = \bigwedge_{\varepsilon=1}^{k} [y^\varepsilon \times (-x^\varepsilon)']$$

$$M_{XY} = \bigvee_{\varepsilon=1}^{k} [y^\varepsilon \times (-x^\varepsilon)']$$

being $\times$ any of the $\min, \max$ operators, $\wedge, \vee$.

- If $X = Y$, then the HMM are denoted as Autoassociative Morphological Memories (AMM).

Asociative Morphological Memories (AMM)

Algorithm

- Initialize the set of endmembers with a random pixel, $E = \{e_1\}$, and the set of binary morphological independent signs, $X = \{x_1\} = \{e_k^1 > 0; k = 1, \ldots, d\}$.
- Build the AMM with the binary morphological independent signs, M_{XX}, W_{XX}.
- For each pixel in the image:
  1. Calculate the array of signs of the Gaussian noise corrections: $f^+(i) = (f^c(i) + \alpha\sigma > 0)$ and $f^-(i) = (f^c(i) - \alpha\sigma > 0)$.
  2. Calculate: $y^+ = M_{XX} \wedge f^+(i)$ and $y^- = W_{XX} \vee f^-(i)$.
  3. If $y^+ \notin X$ or $y^- \notin X$ then $f^c(i)$ is added to the set of endmembers (try next pixel).
  4. If $y^+ \notin X$ and $f^c(i) > e_{y^+}$ then substitute e_y with the pixel $f^c(i)$.
  5. If $y^- \notin X$ and $f^c(i) < e_{y^-}$ then substitute e_y with the pixel $f^c(i)$.

Asociative Morphological Memories (AMM)

Algorithm

- Initialize the set of endmembers with a random pixel, $E = \{e_1\}$, and the set of binary morphological independent signs, $X = \{x_1\} = \{e_k^1 > 0; k = 1, \ldots, d\}$.
- Build the AMM with the binary morphological independent signs, M_{XX}, W_{XX}.
- For each pixel in the image:
  1. Calculate the array of signs of the Gaussian noise corrections: $f^+(i) = (f^c(i) + \alpha\sigma > 0)$ and $f^-(i) = (f^c(i) - \alpha\sigma > 0)$.
  2. Calculate: $y^+ = M_{XX} \wedge f^+(i)$ and $y^- = W_{XX} \vee f^-(i)$.
  3. If $y^+ \notin X$ or $y^- \notin X$ then $f^c(i)$ is added to the set of endmembers (try next pixel).
  4. If $y^+ \notin X$ and $f^c(i) > e_{y^+}$ then substitute e_y with the pixel $f^c(i)$.
  5. If $y^- \notin X$ and $f^c(i) < e_{y^-}$ then substitute e_y with the pixel $f^c(i)$.

Asociative Morphological Memories (AMM)

Algorithm

- Initialize the set of endmembers with a random pixel, $E = \{e_1\}$, and the set of binary morphological independent signs, $X = \{x_1\} = \{e_k^1 > 0; k = 1, \ldots, d\}$.
- Build the AMM with the binary morphological independent signs, M_{XX}, W_{XX}.
- For each pixel in the image:
  1. Calculate the array of signs of the Gaussian noise corrections: $f^+(i) = (f^c(i) + \alpha\sigma > 0)$ and $f^-(i) = (f^c(i) - \alpha\sigma > 0)$.
  2. Calculate: $y^+ = M_{XX} \wedge f^+(i)$ and $y^- = W_{XX} \vee f^-(i)$.
  3. If $y^+ \notin X$ or $y^- \notin X$ then $f^c(i)$ is added to the set of endmembers (try next pixel).
  4. If $y^+ \notin X$ and $f^c(i) > e_{y^+}$ then substitute e_y with the pixel $f^c(i)$.
  5. If $y^- \notin X$ and $f^c(i) < e_{y^-}$ then substitute e_y with the pixel $f^c(i)$.

Lattice Auto-associative Memories (LAM)

Overview

- Improve the AMM method by proving the relationship between strong lattice independence and affine independence.
- Then it is found that most vectors in the erosive and dilative lattice memories are strong lattice independent.
- Therefore, the mere construction of the lattice memories provide a way to obtain the convex hull of the data.
- Provided an endmember selection mechanism, the algorithm can obtain in a single pass over the image a set of endmembers.

Lattice Auto-associative Memories (LAM)

Overview

- Improve the AMM method by proving the relationship between strong lattice independence and affine independence.
- Then it is found that most vectors in the erosive and dilative lattice memories are strong lattice independent.
- Therefore, the mere construction of the lattice memories provide a way to obtain the convex hull of the data.
- Provided an endmember selection mechanism, the algorithm can obtain in a single pass over the image a set of endmembers.

Lattice Auto-associative Memories (LAM)

Overview

- Improve the AMM method by proving the relationship between strong lattice independence and affine independence.
- Then it is found that most vectors in the erosive and dilative lattice memories are strong lattice independent.
- Therefore, the mere construction of the lattice memories provide a way to obtain the convex hull of the data.
- Provided an endmember selection mechanism, the algorithm can obtain in a single pass over the image a set of endmembers.

Lattice Auto-associative Memories (LAM)

Overview

- Improve the AMM method by proving the relationship between strong lattice independence and affine independence.
- Then it is found that most vectors in the erosive and dilative lattice memories are strong lattice independent.
- Therefore, the mere construction of the lattice memories provide a way to obtain the convex hull of the data.
- Provided an endmember selection mechanism, the algorithm can obtain in a single pass over the image a set of endmembers.

Outline

1. Motivation
2. Linear unmixing
3. Virtual Dimensionality
   - Introduction
   - Neyman-Pearson Detection Theory-Based Eigen-Thresholding Analysis (HFC Method)
   - Noise Whitening HFC Analysis (NWHFC Method)
   - Noise Subspace Projection Analysis (NSP Method)
4. Endmember induction methods
   - Geometric approaches
   - Lattice computing approaches
   - Heuristic approaches

Introduction

- The heuristic methods collects a set of heterogeneus endmember extraction methods that use different approaches not grouped under a strict theorical background for endmember induction.

Fast Iterative Pixel Purity Index (FIPPI)

Introduction

- Improves the Pixel Purity Index (PPI) algorithm included in the ENVI software in several ways: iterative, fast and unsupervised.
- It uses the Virtual Dimensionality concept to detect the number of endmembers in image.
- Dimensionality reduction to $k-1$ dimensions being k the number of endmembers in image (MNF).
- Use of ATGP initialization algorithm to select the p initial skewers, $\left\{ skewers_j^{(0)} \right\}_{j=1}^{p}$.

Fast Iterative Pixel Purity Index (FIPPI)

Introduction

- Improves the Pixel Purity Index (PPI) algorithm included in the ENVI software in several ways: iterative, fast and unsupervised.
- It uses the Virtual Dimensionality concept to detect the number of endmembers in image.
- Dimensionality reduction to $k-1$ dimensions being k the number of endmembers in image (MNF).
- Use of ATGP initialization algorithm to select the p initial skewers, $\left\{ skewers_j^{(0)} \right\}_{j=1}^{p}$.

Fast Iterative Pixel Purity Index (FIPPI)

Introduction

- Improves the Pixel Purity Index (PPI) algorithm included in the ENVI software in several ways: iterative, fast and unsupervised.
- It uses the Virtual Dimensionality concept to detect the number of endmembers in image.
- Dimensionality reduction to $k-1$ dimensions being k the number of endmembers in image (MNF).
- Use of ATGP initialization algorithm to select the p initial skewers, $\left\{ skewers_j^{(0)} \right\}_{j=1}^{p}$.

Fast Iterative Pixel Purity Index (FIPPI)

Introduction

- Improves the Pixel Purity Index (PPI) algorithm included in the ENVI software in several ways: iterative, fast and unsupervised.
- It uses the Virtual Dimensionality concept to detect the number of endmembers in image.
- Dimensionality reduction to $k-1$ dimensions being k the number of endmembers in image (MNF).
- Use of ATGP initialization algorithm to select the p initial skewers, $\left\{ skewers_j^{(0)} \right\}_{j=1}^{p}$.

Fast Iterative Pixel Purity Index (FIPPI)

Algorithm

- For each iterartion i:
  1. For each skewer j:
     1. Project all the data over the skewer.
     2. Subjects in extreme positions build an extrema set, $s_{extrema}(skewer_j^{(i)})$.
  2. For each data subject $\mathbf{x}$, the indicator $N_{PPI}(\mathbf{x})$ is obtained:

$$N_{PPI}(\mathbf{x}) = \sum_j I_{s_{extrema}(skewer_j^{(m)})}(\mathbf{x})$$

$$I_{s_{extrema}(skewer_j^{(m)})}(\mathbf{x}) = \begin{cases} 1 & if \quad \mathbf{x} \in S \\ 0 & if \quad \mathbf{x} \notin S \end{cases}$$

Fast Iterative Pixel Purity Index (FIPPI)

Algorithm

- For each iterartion i:
  1. For each skewer j:
     1. Project all the data over the skewer.
     2. Subjects in extreme positions build an extrema set, $s_{extrema}(skewer_j^{(i)})$.
  2. For each data subject $\mathbf{x}$, the indicator $N_{PPI}(\mathbf{x})$ is obtained:

$$N_{PPI}(\mathbf{x}) = \sum_j I_{s_{extrema}(skewer_j^{(m)})}(\mathbf{x})$$

$$I_{s_{extrema}(skewer_j^{(m)})}(\mathbf{x}) = \begin{cases} 1 & if \quad \mathbf{x} \in S \\ 0 & if \quad \mathbf{x} \notin S \end{cases}$$

Fast Iterative Pixel Purity Index (FIPPI)

Algorithm

- Stop rule:
  - In each iteration i, find the data subject $\mathbf{x}^{(\mathbf{i})}$ with the largest $N_{PPI}(\mathbf{x}^{(\mathbf{i})})$.
  - Join the sets: $\left\{skewers_j^{(i+1)}\right\} = \left\{skewers_j^{(i)}\right\} \cup \left\{\mathbf{x}_\mathbf{j}^{(\mathbf{i})}\right\}$.
  - Stop if $\left\{skewers_j^{(i+1)}\right\} = \left\{skewers_j^{(i)}\right\}$.

ICA-based Abundance Quantification Algorithm (ICA-AQA)

Overview

- Is a high-order statistics-based technique, that can accomplish endmember extraction and abundance quantification simultaneously in one-shot operation using the Independent Component Analysis (ICA) algorithm.
- The use of ICA and Independent Factor Analysis (IFA) for unmixing tasks is controversed, because the statistically independent of the sources assumed by ICA and IFA, is violated in the hyperspectral unmixing, compromising the performance of ICA/IFA algorithms for this purpose.
- It is concluded that the accuracy of this ICA/IFA-based methods tends to improve with the increase of the signature variability and the signal-to-noise ratio.

ICA-based Abundance Quantification Algorithm (ICA-AQA)

Overview

- Is a high-order statistics-based technique, that can accomplish endmember extraction and abundance quantification simultaneously in one-shot operation using the Independent Component Analysis (ICA) algorithm.
- The use of ICA and Independent Factor Analysis (IFA) for unmixing tasks is controversed, because the statistically independent of the sources assumed by ICA and IFA, is violated in the hyperspectral unmixing, compromising the performance of ICA/IFA algorithms for this purpose.
- It is concluded that the accuracy of this ICA/IFA-based methods tends to improve with the increase of the signature variability and the signal-to-noise ratio.

ICA-based Abundance Quantification Algorithm (ICA-AQA)

Overview

- Is a high-order statistics-based technique, that can accomplish endmember extraction and abundance quantification simultaneously in one-shot operation using the Independent Component Analysis (ICA) algorithm.
- The use of ICA and Independent Factor Analysis (IFA) for unmixing tasks is controversed, because the statistically independent of the sources assumed by ICA and IFA, is violated in the hyperspectral unmixing, compromising the performance of ICA/IFA algorithms for this purpose.
- It is concluded that the accuracy of this ICA/IFA-based methods tends to improve with the increase of the signature variability and the signal-to-noise ratio.

Spatial-Spectral Endmember Extraction Algorithm (SSEE)

Overview

- Another projection based method that works by analyzing a sc4ene in parts (subsets), such that it increases the spectral contrast of low contrast endmembers, thus improving the potential for these endmembers to be selected.
- The SSEE method uses a singular value decomposition (SVD) to determine a set of basis vectors that describe most of the spectral variance for subsets of the image.
- Then the full image dataset is projected onto the locally defined basis vectors to determine a set of candidate endmember pixels from where the final endmembers are selected.
- For that, it searchs for spectrally similar but spatially independent endmembers. This is realized by imposing spatial constraints for averaging spectrally similar endmembers.

Spatial-Spectral Endmember Extraction Algorithm (SSEE)

Overview

- Another projection based method that works by analyzing a sc4ene in parts (subsets), such that it increases the spectral contrast of low contrast endmembers, thus improving the potential for these endmembers to be selected.
- The SSEE method uses a singular value decomposition (SVD) to determine a set of basis vectors that describe most of the spectral variance for subsets of the image.
- Then the full image dataset is projected onto the locally defined basis vectors to determine a set of candidate endmember pixels from where the final endmembers are selected.
- For that, it searchs for spectrally similar but spatially independent endmembers. This is realized by imposing spatial constraints for averaging spectrally similar endmembers.

Spatial-Spectral Endmember Extraction Algorithm (SSEE)

Overview

- Another projection based method that works by analyzing a sc4ene in parts (subsets), such that it increases the spectral contrast of low contrast endmembers, thus improving the potential for these endmembers to be selected.
- The SSEE method uses a singular value decomposition (SVD) to determine a set of basis vectors that describe most of the spectral variance for subsets of the image.
- Then the full image dataset is projected onto the locally defined basis vectors to determine a set of candidate endmember pixels from where the final endmembers are selected.
- For that, it searchs for spectrally similar but spatially independent endmembers. This is realized by imposing spatial constraints for averaging spectrally similar endmembers.

Spatial-Spectral Endmember Extraction Algorithm (SSEE)

Overview

- Another projection based method that works by analyzing a sc4ene in parts (subsets), such that it increases the spectral contrast of low contrast endmembers, thus improving the potential for these endmembers to be selected.
- The SSEE method uses a singular value decomposition (SVD) to determine a set of basis vectors that describe most of the spectral variance for subsets of the image.
- Then the full image dataset is projected onto the locally defined basis vectors to determine a set of candidate endmember pixels from where the final endmembers are selected.
- For that, it searchs for spectrally similar but spatially independent endmembers. This is realized by imposing spatial constraints for averaging spectrally similar endmembers.

Summary

- Linear mixing model is a good aproximation for hyperspectral imagery and analitically computable.
- The endmember induction is a well investigated problem but not fully resolved and depends highly in the presence of pure pixels in image.
- Unmixing is an heuristic technique with different aproaches subject to the target objetive.
- Outlook
  - Implement and try different endmember induction methods to extract the spectral/spatial information in the hiperspectral imagery.
  - Characterize that information.
  - Provide similarity functions based in the spectral/spatial characterization for CBIR purposes.

Summary

- Linear mixing model is a good aproximation for hyperspectral imagery and analitically computable.
- The endmember induction is a well investigated problem but not fully resolved and depends highly in the presence of pure pixels in image.
- Unmixing is an heuristic technique with different aproaches subject to the target objetive.
- Outlook
  - Implement and try different endmember induction methods to extract the spectral/spatial information in the hiperspectral imagery.
  - Characterize that information.
  - Provide similarity functions based in the spectral/spatial characterization for CBIR purposes.

Summary

- Linear mixing model is a good aproximation for hyperspectral imagery and analitically computable.
- The endmember induction is a well investigated problem but not fully resolved and depends highly in the presence of pure pixels in image.
- Unmixing is an heuristic technique with different aproaches subject to the target objetive.
- Outlook
  - Implement and try different endmember induction methods to extract the spectral/spatial information in the hiperspectral imagery.
  - Characterize that information.
  - Provide similarity functions based in the spectral/spatial characterization for CBIR purposes.

Summary

- Linear mixing model is a good aproximation for hyperspectral imagery and analitically computable.
- The endmember induction is a well investigated problem but not fully resolved and depends highly in the presence of pure pixels in image.
- Unmixing is an heuristic technique with different aproaches subject to the target objetive.
- Outlook
  - Implement and try different endmember induction methods to extract the spectral/spatial information in the hiperspectral imagery.
  - Characterize that information.
  - Provide similarity functions based in the spectral/spatial characterization for CBIR purposes.

For Further Reading I

Miguel A. Veganzones, Manuel Graña.
Endmember induction techniques: a short review.
KES, 2008.

Markov Random Fields

Campos Aleatorios de Markov

C. Hernández

Grupo de Inteligencia Computacional

JIC 2008

Índice

1. Introducción
2. Campos Aleatorios de Gibbs
3. Campos Aleatorios de Markov
4. Problemas relacionados con los campos aleatorios de Markov
5. Bibliografía
6. Anexos

Introducción

- La Teoría de los Campos Aleatorios de Markov o markovianos (*Markov Random Fields*, MRF) es una rama de la teoría de la probabilidad que analiza las dependencias espaciales o contextuales de los fenónemos físicos.
- Los campos aleatorios proporcionan medidas de probabilidad sobre un dominio de definición que posee relaciones de tipo espacial o temporal.

Introducción. Ejemplo de campo aleatorio

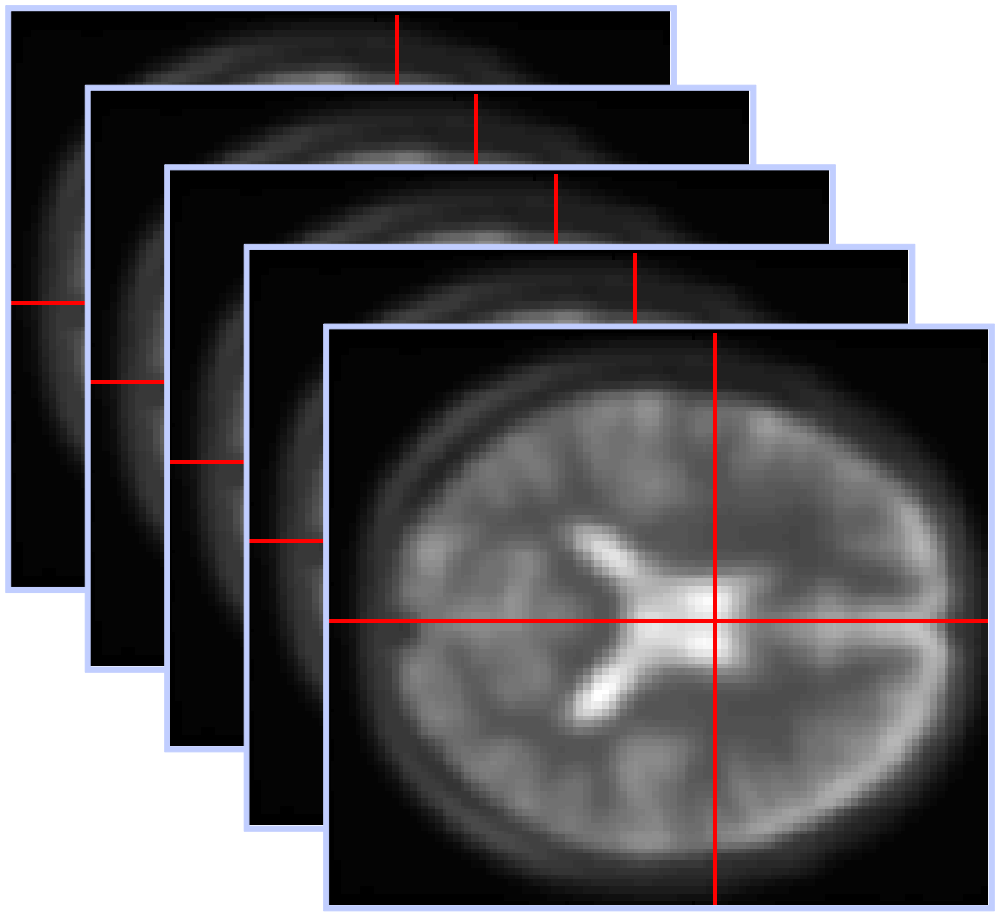

Introducción. Definición: Malla

Definición

Una **malla**, **rejilla**, **retícula** *o* **lattice** *(regular) de tamaño n, que se denota como $\mathcal{I}_n$, está formada por un conjunto finito de índices S que representa al conjunto de posiciones de la malla:*

$$S = \{s_0, s_1, \ldots, s_m\} \subseteq \mathcal{I}_n$$

donde $s_i \in S \subseteq \mathbb{R}^d$ es una posición de una malla d-dimensional[a].

[a] Por simplificación en la notación, decimos que la malla se denota por S, el conjunto de índices o posiciones de la malla.

Introducción. Ejemplos: Malla

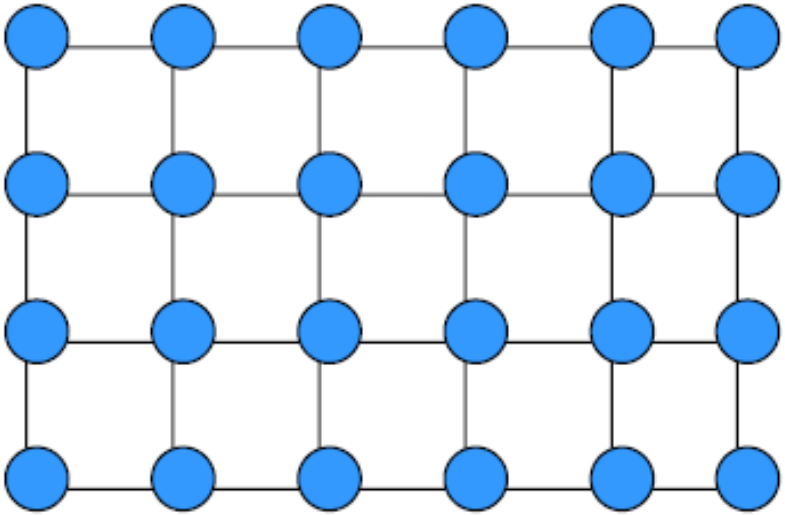

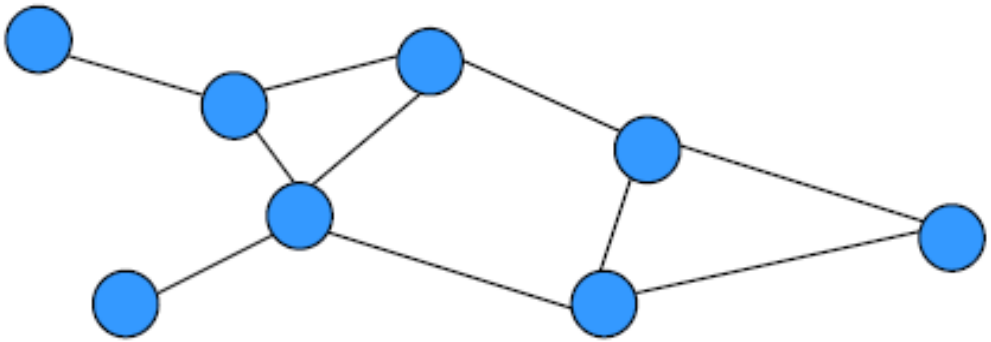

Introducción. Definición: Malla toroidal

Definición

Una **malla toroidal**, **toro** *o* **torus** *es una malla cuyos bordes cumplen una serie de condiciones cíclicas o toroidales y se denota como* $\mathcal{T}_n$.

- Esto es, para un toro 2D de dimensiones $n = (n_1, n_2)$, los índices de las posiciones de la malla son números módulo n:

$$s = (i, j) \in S \subseteq \mathcal{T}_n$$

con

$$i = 0, \ldots, n_1 - 1$$

$$j = 0, \ldots, n_2 - 1$$

Introducción. Definición: Configuración

Definición

Una **configuración** *es el vector:*

$$\mathbf{x} = (x_s)_{s \in S}$$

donde $x_s \in \Lambda_s$ *es el* **estado** *de la posición* $s \in S$ *de la malla y* Λ_s *es un espacio de estados finito.*

- Generalmente, el espacio de estados es el mismo para todas las posiciones de la malla; esto es, $\Lambda_s = \Lambda$ para todo $s \in S$.

Introducción. Definición: Espacio de configuraciones

Definición

El conjunto de todas las posibles configuraciones en la malla S se denomina **espacio de estados** *o* **espacio finito de configuraciones** *y se denota como Ω:*

$$\Omega = \prod_{s \in S} \Lambda_s$$

Introducción. Ejemplos: Imagen

Podemos modelar las imágenes a partir de mallas donde la posición $s_l \in S$ es un píxel de la imagen.

Ejemplo

Para una imagen en niveles de gris, la malla asociada es bidimensional y, por tanto, el píxel l-ésimo puede ser representado como la posición

$$s_l = s_{ij} = (i, j) \in S \subseteq \mathbb{R}^2$$

siendo i y j los índices de la posición l de la malla.

1. x_l *es el nivel de gris del píxel l-ésimo y*
2. *el espacio de estados,* Λ_s*, es el conjunto de niveles de grises*

Introducción. Ejemplos: Imagen

Ejemplo

Para una imagen RGB, la malla asociada a dicha imagen es tridimensional y, por tanto, el el píxel l-ésimo puede ser representado como la posición

$$s_l = s_{ijk} = (i, j, k) \in S \subseteq \mathbb{R}^3$$

siendo i, j y k los índices de la posición l de la malla.

1. *x_l es el valor RGB del píxel l-ésimo y*
2. *el espacio de estados, Λ_s, es la tabla de colores RGB de la imagen*

Introducción. Ejemplos: Imagen

Ejemplo

Para una imagen multiespectral, la malla asociada a dicha imagen es d-dimensional siendo d la dimensión espectral. El píxel l-ésimo es $s_l \in S \subseteq \mathbb{R}^d$.

Introducción. Ejemplos: Imagen

La siguiente imagen binaria de tamaño $n \times m$ puede ser vista como una configuración $\mathbf{x} = (x_s)_{s \in S}$ donde $x_s \in \{0, 1\}$ es el color negro o blanco del píxel $s = (i, j) \in S$.

- Malla: $S = \{1, \ldots n \times m\}$
- Conjunto de posibles valores: $\Lambda_s = \Lambda = \{0, 1\}$
- Espacio de configuraciones: $\Omega = \{0, 1\}^{|S|}$

Definición: Campo Aleatorio

Definición

Un **campo aleatorio** *(Random Field, RF) es un proceso estocástico* $X = \{X_s\}_{s=0}^{m}$ *sobre un dominio de definición en el cual se pueden establecer relaciones de tipo espacial o temporal. Cada variable aleatoria* X_s *se encuentra asociada a una posición de una malla* $s \in S$ *y toma el valor* $x_s \in \Lambda_s$ *siendo* Λ_s *un conjunto finito.*

Campo Aleatorio. Definición: Realización y configuración

Definición

El suceso conjunto $X_0 = x_0, \ldots, X_m = x_m$ *es una* **realización del campo aleatorio** $X = \{X_s\}_{s=0}^{m}$.

- Para simplificar la notación, no utilizaremos una notación diferente entre una variable aleatoria X_i y la realización específica de dicha variable, x_i.

Definición

Denominamos **configuración del suceso conjunto x** *del campo aleatorio* $X = \{X_s\}_{s=0}^{m}$ *al vector:*

$$\mathbf{x} = (x_0, \ldots, x_m) \in \Omega$$

siendo Ω *el espacio de todas las configuraciones.*

Campo Aleatorio. Configuración del suceso conjunto

- Dado un subconjunto de posiciones de la malla $A \subset S$, definimos la configuración del suceso conjunto, $\mathbf{x}_A$, en dicho subconjunto A como:

$$\mathbf{x}_A = (x_s)_{s \in A} \in \Omega_A$$

con $\Omega_A \subset \Omega$.

- La función definida como:

$$\begin{array}{rccc} X_A : & \Omega & \rightarrow & \Omega_A \\ & \mathbf{x} = (x_s)_{s \in S} & \rightarrow & \mathbf{x}_A = (x_s)_{s \in A} \end{array}$$

es la proyección del espacio de configuraciones Ω en Ω_A.

Campo Aleatorio. Definición: Probabilidad conjunta

Definición

Definimos una distribución de probabilidad P para toda configuración $\mathbf{x} \in \Omega$ del campo aleatorio $X = \{X_s\}_{s=0}^{m}$:

$$\begin{aligned} P(\mathbf{x}) &> 0 \\ \sum_{\mathbf{x} \in \Omega} P(\mathbf{x}) &= 1 \end{aligned}$$

Entonces la **probabilidad conjunta** *del campo aleatorio es:*

$$P(X = \mathbf{x}) = P(X_0 = x_0, \ldots, X_m = x_m) = P(\mathbf{x})$$

Campo Aleatorio. Definición: Características locales

Definición

Las **características locales**[a] *del campo aleatorio* $X = \{X_s\}_{s=0}^{m}$ *en los subconjuntos de la malla* $A \subset S$ *son las* **probabilidades condicionadas** *definidas como:*

$$P\left(X_A = \mathbf{x}_A \,|X_{-A} = \mathbf{x}_{-A}\right) = \frac{P\left(X = \mathbf{x}\right)}{P\left(X_{-A} = \mathbf{x}_{-A}\right)} \propto P\left(\mathbf{x}\right)$$

donde $-A$ *es el complementario*[b] *del conjunto* A *y la configuración conjunta* $\mathbf{x} \in \Omega$ *viene dada por:*

$$\mathbf{x} = \mathbf{x}_A \mathbf{x}_{-A} \in \Omega = \Omega_A \times \Omega_{-A}$$

---

[a] A esta probabilidad condicionada también se le conoce como **kernel de Markov**.

[b] También denotado como $S \backslash A$.

Campo Aleatorio. Definición: Características locales

Definición (cont.)

y las configuraciones en el conjunto A y en el complementario de A son:

$$\mathbf{x}_A \in \Omega_A \quad y \quad \mathbf{x}_{-A} \in \Omega_{-A}$$

- Por definición, ya que un campo aleatorio es estrictamente positivo, siempre se pueden definir las características locales del campo.

Campo Aleatorio Estacionario

Definición

Un campo aleatorio se denomina **estacionario** *si su distribución de probabilidad P no varía ante traslaciones del dominio.*

Campo Aleatorio Isotrópico

Definición

Un campo aleatorio se denomina **isotrópico** *si su distribución de probabilidad P no varía ante rotaciones del dominio.*

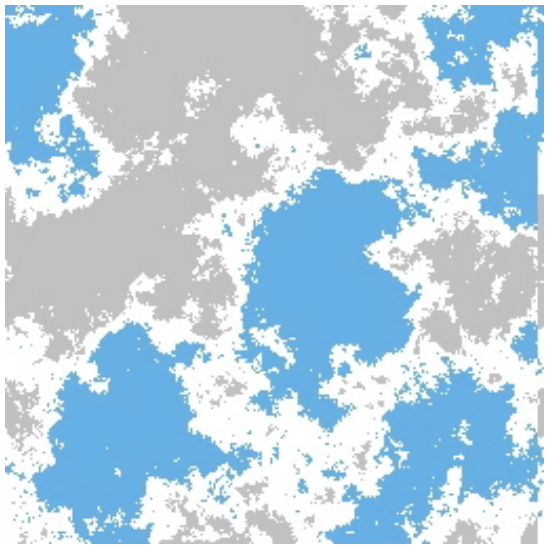

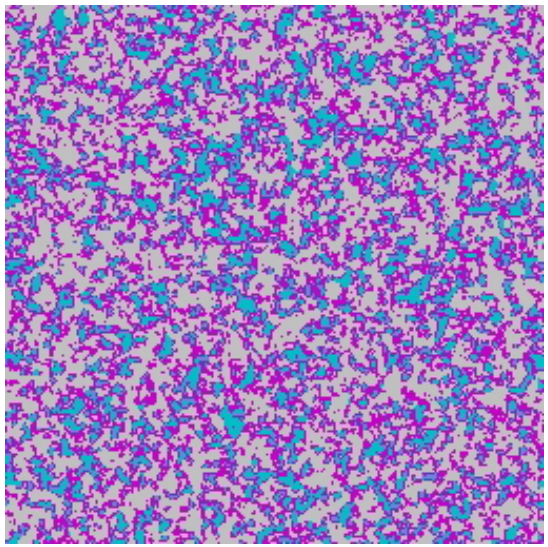

Campo Aleatorio. Representación mediante grafos

- Utilizaremos **grafos no dirigidos**, $\mathcal{G} = (\mathcal{V}, \mathcal{E})$, para representar la estructura de la **independencia condicional** en el campo aleatorio $X = \{X_s\}_{s=0}^{m}$.
- El conjunto de nodos $\mathcal{V}$ es el conjunto de posiciones de la malla

$$\mathcal{V} = \{s_0, s_1, \ldots, s_m\} = S$$

y el conjunto de aristas $\mathcal{E}$ es el conjunto de conexiones entre dichas posiciones[1].

[1] En algunos casos, y por simplificación en la notación, utilizaremos indistintamente la notación s_i o el índice i para referirnos a una posición de la malla.

Campo Aleatorio. Definición: Vecino y vecindario

Definición

Dado un grafo $\mathcal{G} = (S, \mathcal{E})$, los **vecinos** *de la posición i-ésima de la malla, $i \in S$, son todas las posiciones de la malla, $j \in S$, que comparten una arista con dicha posición. Esto es, el* **vecindario** *de la posición i-ésima es el conjunto:*

$$\partial_i = \{j \in S : \{i, j\} \in \mathcal{E}\}$$

Campo Aleatorio. Definición: Sistema de vecinos

Definición

Un **sistema de vecinos** *asociado a un grafo* $\mathcal{G} = (S, \mathcal{E})$ *se define como:*

$$\partial = \{\partial_i \,|\forall i \in S\}$$

donde ∂_i *es el vecindario de la posición i-ésima de la malla:*

$$\partial_i = \{j \in S : \{i, j\} \in \mathcal{E}\}$$

- Podemos extender esta definición cualquier subconjunto de la malla $A \subset S = \mathcal{V}$, donde los vecinos del conjunto A son:

$$\partial = \bigcup_{s \in A} \partial_s$$

Campo Aleatorio. Sistema de vecinos

Propiedades de un sistema de vecinos

Una relación de vecindad posee las siguientes propiedades:

1. Un nodo no es vecino de sí mismo: $i \notin \partial_i$
2. La relación de vecindad es recíproca: $i \in \partial_j \Longleftrightarrow j \in \partial_i$

Campo Aleatorio. Definición: Clique

Definición

Sea $X = \{X_s\}_{s=0}^{m}$ *un campo aleatorio definido en una malla* S *con un sistema de vecinos* ∂ *y representado por el grafo* $\mathcal{G} = (S, \partial)$*, una* **clique** C *es un subconjunto de posiciones de la malla* S *para el cual sus elementos (cliques de 1, 2 o más elementos) son vecinos con respecto al vecindario* ∂*.*

Campo Aleatorio. Clique

- Todos los conjuntos completos del grafo dan lugar a las cliques.
- El tipo de una clique de una malla regular viene dado por su tamaño, forma y orientación.
- En el caso de sistemas de vecinos homogéneos, las cliques de un grafo se pueden clasificar en tipos según la relación espacial entre los elementos que la forman.

Campo Aleatorio. Clique

- Los conjuntos de localizaciones únicas[2], $\{i\}$, de pares, $\{i,j\}$, y de tripletas de posiciones, $\{i,j,k\}$, se denominan cliques C_1, C_2 y C_3 respectivamente y se definen como:

$$\begin{aligned} C_1 &= \{i \,|\, i \in S\} \\ C_2 &= \{(i,j) \,|\, i,j \in S, i \sim j\} \\ C_3 &= \{(i,j,k) \,|\, i,j,k \in S : i,j,k \text{ son vecinos entre ellos}\} \end{aligned}$$

- El conjunto de todas las cliques definidas en la malla S es:

$$\mathcal{C} = C_1 \cup C_2 \cup C_3 \cup \ldots$$

[2] También denominadas **cliques simples** o **únicas**.

Campo Aleatorio. Ejemplos: Clique

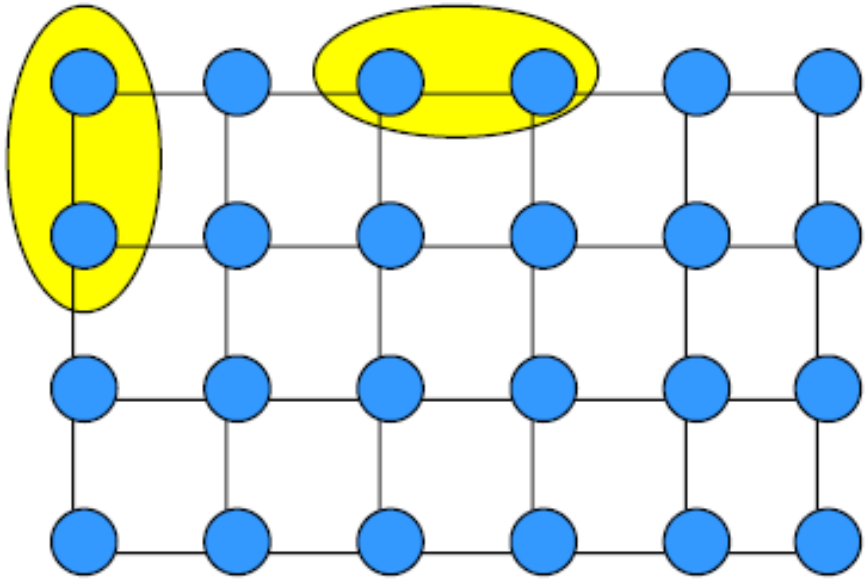

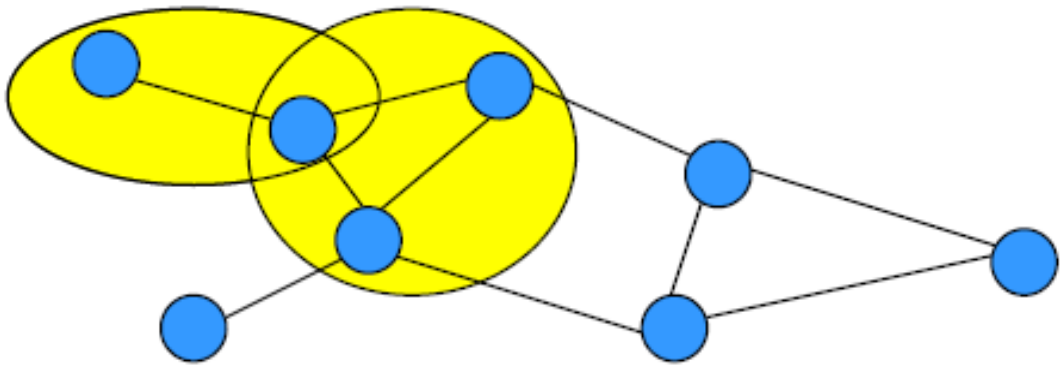

Campo Aleatorio. Ejemplos: Clique

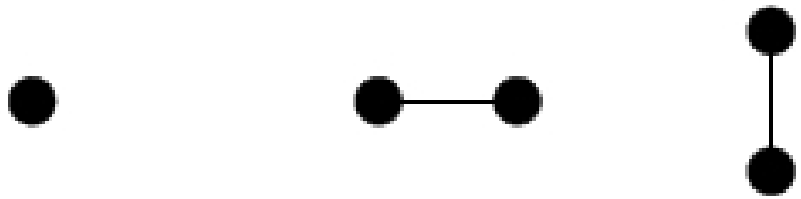

Tipos de cliques únicas o simples definidas a partir del vecindario de orden uno.

Campo Aleatorio. Ejemplos: Clique

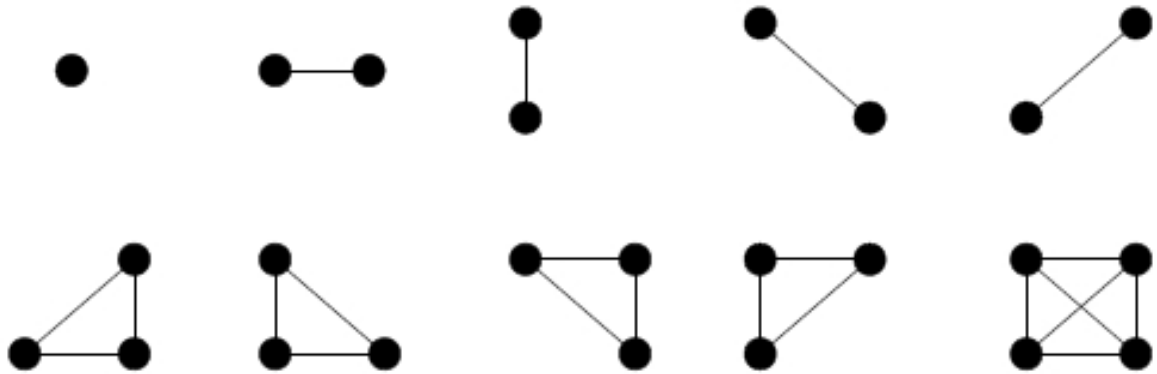

Tipos de cliques definidas a partir del vecindario de orden dos.

Campo Aleatorio. Ejemplos: Clique

5	4	3	4	5
4	2	1	2	4
3	1	○	1	3
4	2	1	2	4
5	4	3	4	5

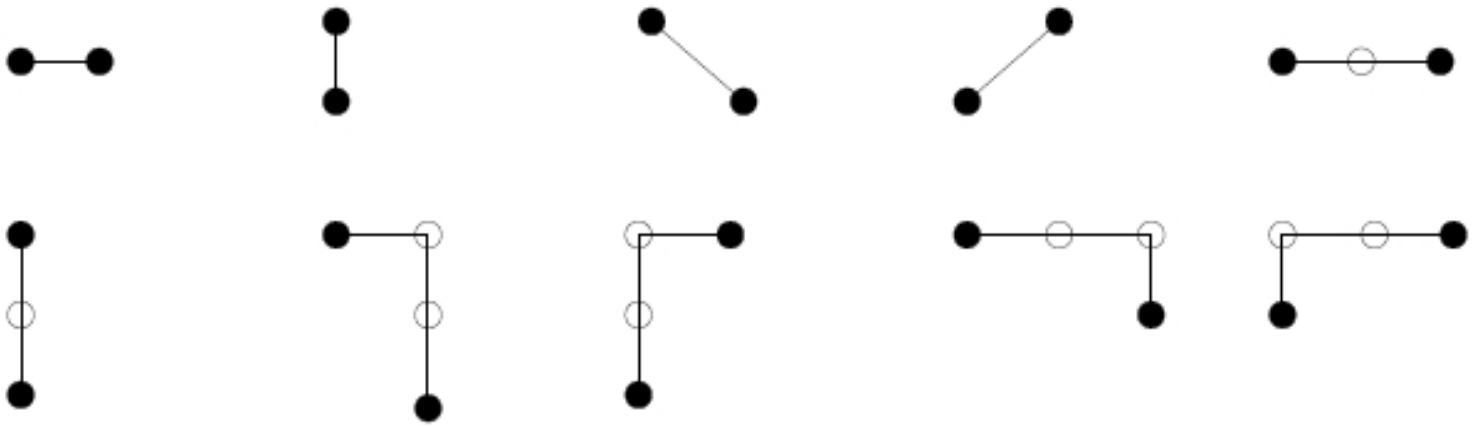

Tipos de cliques de pares para el vecindario de orden cuatro.

Campo Aleatorio. Definición: Potencial

Definición

Dado un campo aleatorio $X = \{X_s\}_{s=0}^{m}$ *definido en una malla* S, *un* **potencial** *es una familia de funciones* $\{V_A(\mathbf{x}) : \mathbf{x} \in \Omega\}$, *para todos los subconjuntos* $A \subset S$ *de la malla, tal que:*

1. *La función potencial para el conjunto vacío es la función nula:*

$$V_{\varnothing} = 0$$

2. *La función potencial sólo depende de la configuración en el subconjunto* $A \subset S$ *de la malla. Esto es,*

$$\forall \mathbf{x}, \mathbf{y} \in \Omega \qquad V_A(\mathbf{x}) = V_A(\mathbf{x}) \Longleftrightarrow \mathbf{x}_A = \mathbf{y}_A$$

siendo Ω *el espacio de configuraciones del campo aleatorio*[a].

[a] Es decir, podemos escribir: $V_A(\mathbf{x}) = V_A(\mathbf{x}_A)$.

Campo Aleatorio. Potencial

- El número de funciones potenciales es el número de subconjuntos posibles $A \subset S$ en la malla. Es decir, es $2^{|S|}$.
- La forma de esta función potencial $V_A(\mathbf{x})$ puede ser todo lo arbitraria que se desee.

Campo Aleatorio. Definición: Función de energía

Definición

La **función de energía** $U(\mathbf{x})$ *para una configuración* $\mathbf{x} \in \Omega$ *del campo aleatorio* $X = \{X_s\}_{s=0}^{m}$ *definido en una malla* S *viene dada por la suma de los potenciales* $V_A(\mathbf{x})$ *en todos los subconjuntos de la malla* $A \subset S$*:*

$$U(\mathbf{x}) = \sum_{A \subset S} V_A(\mathbf{x})$$

Campo Aleatorio. Definición: Potencial de vecindario y de pares

Definición

Dado un sistema de vecinos ∂, un potencial V_A se dice que es un **potencial de vecindario** *con respecto a ∂ si:*

$$V_A = 0$$

cuando el subconjunto A no es una clique para ese sistema de vecinos. Si $V_A = 0$ para $|A| > 2$ decimos que el potencial V_A es un **potencial de pares**.

Definición: Campo Aleatorio de Gibbs

Definición

Un campo aleatorio $X = \{X_s\}_{s=0}^{m}$ *se denomina un* **campo aleatorio de Gibbs** *(Gibbs RF) con respecto a un sistema de vecinos* ∂ *si y sólo si las configuraciones* $\mathbf{x} \in \Omega$ *siguen una distribución de Gibbs*[a]*. Esto es, la distribución de probabilidad del campo aleatorio de Gibbs viene dada por:*

$$P(\mathbf{x}) = \frac{1}{Z} e^{-U(\mathbf{x})}$$

donde Z *es una constante de normalización denominada* **función de partición**,

$$Z = \sum_{\mathbf{y} \in \Omega} e^{-U(\mathbf{y})}$$

y $U : \Omega \rightarrow \mathbb{R}$ *es la función de energía del campo aleatorio.*

[a] También conocida como **distribución canónica**.

Campo Aleatorio de Gibbs. Potencial y función de energía

- Debido al gran tamaño del espacio de configuraciones Ω, el cálculo de la función de energía es una tarea impracticable.
- No obstante, en el caso de que las dependencias sean locales y dadas por un sistema de vecinos ∂ tenemos que:
  - el número de funciones potenciales no nulas se reduce considerablemente y
  - pueden ser calculadas solamente en las cliques ya que, como hemos visto anteriormente, la función potencial $V_A(\mathbf{x})$ es nula siempre y cuando el subconjunto A no sea una clique

Campo Aleatorio de Gibbs. Potencial y función de energía

- Si las funciones potenciales son potenciales de vecindario, que toman valores no nulos para las cliques, decimos que la familia de potenciales $\{V_C(\mathbf{x}) : C \in \mathcal{C}\}$ **induce un campo aleatorio** con respecto al sistema de vecinos ∂.

Campo Aleatorio de Gibbs. Potencial y función de energía

- La función de energía $U(\mathbf{x})$ se define a partir de dichos potenciales como:

$$U(\mathbf{x}) = \sum_{C \in \mathcal{C}} V_C(\mathbf{x})$$

y la distribución de probabilidad del campo aleatorio de Gibbs $X = \{X_s\}_{s=0}^{m}$ en el espacio de configuraciones Ω con respecto al sistema de vecinos ∂ viene dada por:

$$P(\mathbf{x}) = \frac{1}{Z} \cdot \exp\left(-\sum_{C \in \mathcal{C}} V_C(\mathbf{x})\right)$$

con Z:

$$Z = \sum_{\mathbf{y} \in \Omega} \exp\left(-\sum_{C \in \mathcal{C}} V_C(\mathbf{y})\right)$$

Campo Aleatorio de Gibbs. Definición: Características locales

Definición

Las **características locales** *del campo aleatorio de Gibbs,* $X = \{X_s\}_{s=0}^{m}$, *en el conjunto de la malla* $A \subset S$ *son las probabilidades condicionadas:*

$$P\left(\mathbf{x}_A \left| \mathbf{x}_{-A} \right.\right) = \frac{1}{Z} \cdot \exp\left(- \sum_{\substack{C \in \mathcal{C}, \\ C \cap A \neq \varnothing}} V_C\left(\mathbf{x}\right) \right)$$

con Z*:*

$$Z = \sum_{\mathbf{x}_A \in \Omega_A} \exp\left(- \sum_{\substack{C \in \mathcal{C}, \\ C \cap A \neq \varnothing}} V_C\left(\mathbf{x}_A \mathbf{x}_{-A}\right) \right)$$

Campo Aleatorio de Gibbs. Definición: Características locales

Definición (cont.)

siendo la configuración conjunta:

$$\mathbf{x} = \mathbf{x}_A \mathbf{x}_{-A} \in \Omega = \Omega_A \times \Omega_{-A}$$

y las configuraciones en el conjunto A y el complementario de A:

$$\mathbf{x}_A \in \Omega_A \quad y \quad \mathbf{x}_{-A} \in \Omega_{-A}$$

Campo Aleatorio de Gibbs. Características locales

- Las características locales también pueden denotarse en función de las probabilidades condicionadas con respecto al sistema de vecinos ∂ para cada subconjunto de la malla $A \subset S$ como:

$$P\left(X_A = \mathbf{x}_A \,|X_{-A} = \mathbf{x}_{-A}\right) = P\left(X_A = \mathbf{x}_A \,|X_s = x_s, s \in \partial_A\right)$$

donde el conjunto de vecinos ∂_A es:

$$\partial_A = \bigcup_{s \in A} (\partial_s \backslash A)$$

Campo Aleatorio de Gibbs Homogéneo e Isotrópico

Definición

Un campo aleatorio de Gibbs se dice **homogéneo** *si la función potencial* $V_C(\mathbf{x})$ *es independiente de la posición relativa de la clique* C.

- Esta propiedad permite que utilicemos una única función potencial para cada tipo de clique del campo aleatorio.

Definición

Un campo aleatorio de Gibbs se dice **isotrópico** *si la función potencial* $V_C(\mathbf{x})$ *es independiente de la orientación de la clique* C.

- No obstante, debemos destacar que, aunque el sistema de vecinos sea isotrópico, generalmente las funciones potenciales no lo son.

Definición: Campo Aleatorio de Markov

Definición

Un campo aleatorio $X = \{X_s\}_{s=0}^{m}$ *sobre una malla* S *con respecto a un sistema de vecinos* ∂*, representado por el grafo* $\mathcal{G} = (S, \partial)$*, es un* **campo aleatorio de Markov** *o markoviano (Markov Random Field, MRF) si y sólo si satisface la condición de positividad y la* **propiedad markoviana** *denominada* **característica local del campo**.

- Esto es, para toda realización del campo $\mathbf{x} \in \Omega$ y para toda posición de la malla $i \in S$, se cumplen las dos condiciones:

$$\begin{aligned} P(\mathbf{x}) &> 0 \\ P(X_i = x_i \,|X_j = x_j, j \neq i) &= P(X_i = x_i \,|X_j = x_j, j \in \partial_i) \end{aligned}$$

Campo Aleatorio de Markov

- La primera condición (positividad) es necesaria para que el campo $X = \{X_s\}_{s=0}^{m}$ sea un campo aleatorio.
- La segunda condición es la **característica local**, **propiedad local de Markov** o **kernel de Markov** vista anteriormente.
- Puede demostrarse que la probabilidad conjunta $P(\mathbf{x})$ de cualquier campo aleatorio viene dada únicamente por estas probabilidades condicionales locales [Bes74].

Equivalencia entre un MRF y un Gibbs RF

- Como hemos dicho anteriormente, un campo aleatorio markoviano se caracteriza por su propiedad local de Markov:

$$P\left(X_i = x_i \left| X_j = x_j, j \neq i \right.\right) = P\left(X_i = x_i \left| X_j = x_j, j \in \partial_i \right.\right)$$

  mientras que un campo aleatorio de Gibbs se caracteriza por su distribución de Gibbs:

$$P\left(\mathbf{x}\right) = \frac{1}{\sum\limits_{\mathbf{y} \in \Omega} \exp\left(-\sum_{C \in \mathcal{C}} V_C\left(\mathbf{y}\right)\right)} \cdot \exp\left(-\sum_{C \in \mathcal{C}} V_C\left(\mathbf{x}\right)\right)$$

- El teorema de Hammersley-Clifford establece la equivalencia entre estos dos campos aleatorios.

Equivalencia entre un MRF y un Gibbs RF

Teorema (Hammersley-Clifford)

Un campo aleatorio $X = \{X_s\}_{s=0}^{m}$ *es un campo aleatorio de Markov definido en una malla* S *con respecto al sistema de vecinos* ∂ *si y sólo si* $X = \{X_s\}_{s=0}^{m}$ *es un campo aleatorio de Gibbs definido en la misma malla* S *con respecto al mismo sistema de vecinos* ∂*. Esto es:*

$$X \text{ es un MRF} \Leftrightarrow X \text{ es un Gibbs RF}$$

Equivalencia entre un MRF y un Gibbs RF

- Esta equivalencia nos permite especificar la probabilidad conjunta $P(\mathbf{x})$ de un campo aleatorio de Markov en función de las funciones potenciales de las cliques $V_C(\mathbf{x})$.
- La demostración (Markov RF $\Rightarrow$ Gibbs RF) es compleja ya que, en general, la relación entre un campo aleatorio de Gibbs o de Markov y un potencial no es unívoca puesto que dos potenciales diferentes pueden inducir el mismo campo aleatorio.

Definición: Campo Aleatorio de Markov Homogéneo

Definition

Un campo aleatorio de Markov se dice que es **homogéneo** si las características locales del campo o kernel de Markov son independientes ante traslaciones del dominio.

- Esto es, en un campo aleatorio de Markov homogéneo, la probabilidad condicional $P\left(X_i = x_i \,|X_j = x_j, j \in \partial_i\right)$ es independiente de la posición relativa de la malla $s_i \in S$.
- Es decir, dados los vecinos de una posición de la malla $s \in S$ se pueden conocer los vecinos de cualquier otra posición $t \in S$ simplemente trasladando el sistema de vecinos de la posición s a la posición t.

Definición: Campo Aleatorio de Markov Isotrópico

Definition

Un campo aleatorio de Markov se dice que es **isotrópico** si es independiente de la orientación de la posición en la malla. Es decir, el sistema de vecinos se comporta de la misma forma en todas las direcciones.

Tipos de Campos Aleatorios de Markov

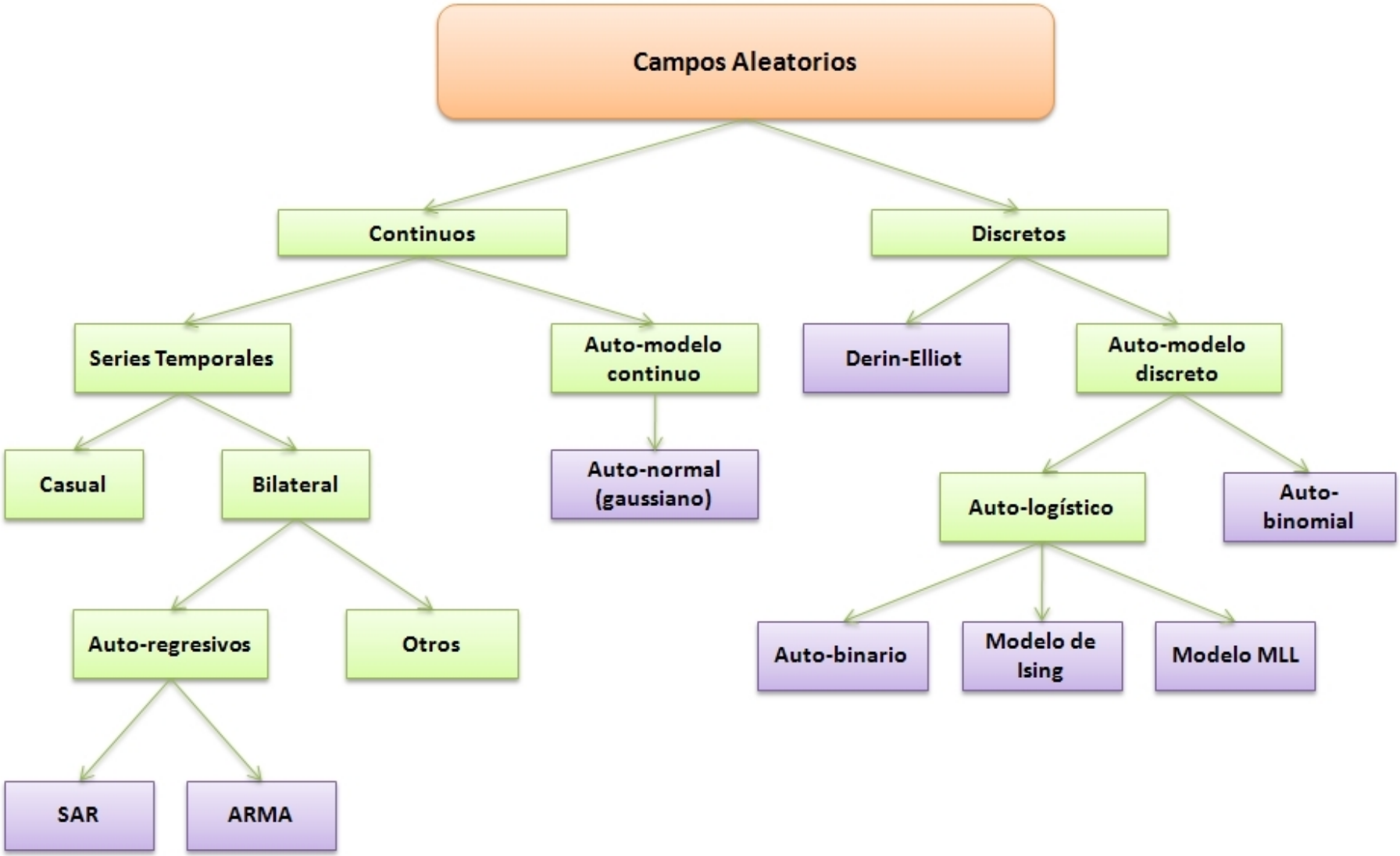

Tipos de MRF. Definición: Automodelo

Definición

Dado el campo aleatorio de Markov $X = \{X_s\}_{s=0}^{m}$ *definido en una malla* S *con un sistema de vecinos* ∂*, se dice que este campo aleatorio es un* **automodelo** *si las cliques* $\mathcal{C}$ *definidas en la malla* S *son cliques de pares:*

$$\mathcal{C} = C_1 \cup C_2$$

Tipos de MRF. Automodelo

- Los automodelos son los campos aleatorios de Markov más simples.
- Su función de energía $U(\mathbf{x})$, denominada **energía de segundo orden**, se calcula a partir de las funciones potenciales, V_1 y V_2, correspondientes a los dos tipos de cliques, C_1 y C_2 respectivamente:

$$U(\mathbf{x}) = \sum_{\{i\} \in C_1} V_1(x_i) + \sum_{\{i,j\} \in C_2} V_2(x_i, x_j)$$

Tipos de MRF. Automodelo

- Los potenciales son de la forma

$$V_1(x_i) = x_i \cdot g_i(x_i)$$

y

$$V_2(x_i, x_j) = x_i \cdot x_j \cdot h_{ij}(x_i, x_j)$$

con $g_i(.)$ y $h_{ij}(.)$ funciones arbitrarias.

- Entonces, la función de energía $U(\mathbf{x})$ del automodelo es:

$$U(\mathbf{x}) = \sum_{\{i\} \in C_1} x_i \cdot g_i(x_i) + \sum_{\{i,j\} \in C_2} x_i \cdot x_j \cdot h_{ij}(x_i, x_j)$$

Tipos de MRF. Automodelo

- Si las funciones $g_i(.)$ y $h_{ij}(.)$ son las constantes α_i e β_{ij} respectivamente, la función de energía $U(\mathbf{x})$ es:

$$U(\mathbf{x}) = \sum_{i \in S} \alpha_i \cdot x_i + \sum_{i,j \in S, i \sim j} \beta_{ij} \cdot x_i \cdot x_j$$

Tipos de MRF. Definición: Modelo auto-logístico

Definición

El automodelo $X = \{X_s\}_{s=0}^{m}$ *se dice que es un* **modelo auto-logístico** *si los valores que pueden tomar las variables* $x_i \in \Lambda$ *pertenecen al conjunto discreto* $\Lambda = \{-1, 1\}$ *ó* $\Lambda = \{0, 1\}$. *Su función de energía es:*

$$U(\mathbf{x}) = \sum_{i \in S} \alpha_i \cdot x_i + \sum_{i,j \in S, i \sim j} \beta_{ij} \cdot x_i \cdot x_j$$

- En general, el modelo auto-logístico tiene una distribución homogénea. Es decir,

$$\alpha_i = \alpha \quad \text{y} \quad \beta_{ij} = \beta \qquad \forall i, j \in S$$

Tipos de MRF. Definición: Modelo de Ising

Definición

Dado el modelo auto-logístico $X = \{X_s\}_{s=0}^{m}$, *si su sistema de vecinos* ∂ *es de primer orden; es decir, consta de 4 vecinos (norte, sur, este y oeste), y el conjunto de valores discreto es* $\Lambda = \{-1, 1\}$, *este automodelo es un* **modelo de Ising**. *Las características locales de este modelo son:*

$$P\left(x_i \,|x_j, j \in \partial_i\right) = \frac{\exp\left(\alpha_i \cdot x_i + \sum_{j\in\partial_i} \beta_{ij} \cdot x_i \cdot x_j\right)}{\exp\left(-\alpha_i - \sum_{j\in\partial_i} \beta_{ij} \cdot x_j\right) + \exp\left(\alpha_i + \sum_{j\in\partial_i} \beta_{ij} \cdot x_j\right)}$$

- Si las constantes son positivas, $\beta_{ij} > 0$, este modelo es atractivo. Por el contrario si las constantes son negativas, $\beta_{ij} < 0$, este modelo es repulsivo [KS80].

Tipos de MRF. Definición: Modelo auto-binario

Definición

Dado el modelo auto-logístico $X = \{X_s\}_{s=0}^{m}$, *si el conjunto de valores discreto es* $\Lambda = \{0, 1\}$, *este automodelo se denomina* **modelo auto-binario**. *Las características locales del modelo son:*

$$P\left(x_i \,|x_j, j \in \partial_i\right) = \frac{\exp\left[x_i \cdot \left(\alpha_i + \sum_{j\in\partial_i} \beta_{ij} \cdot x_j\right)\right]}{1 + \exp\left(\alpha_i + \sum_{j\in\partial_i} \beta_{ij} \cdot x_j\right)}$$

Tipos de MRF. Definición: Modelo auto-binomial

Definición

El automodelo $X = \{X_s\}_{s=0}^{m}$ *se dice que es un* **modelo auto-binomial** *si los valores que toman las variables* $x_i \in \Lambda = \{0, \ldots, n\}$ *vienen dados por una distribución binomial* $B(n, p_i)$. *Su función de energía es:*

$$U(\mathbf{x}) = -\sum_{i \in S} \left[\log \binom{n}{x_i} + \alpha_i \cdot x_i \right] - \sum_{i,j \in S, i \sim j} \beta_{ij} \cdot x_i x_j$$

y las características locales son:

$$P(x_i \,|x_j, j \in \partial_i) = \binom{n}{x_i} p_i^{x_i} (1 - p_i)^{n - x_i}$$

Tipos de MRF. Definición: Modelo auto-binomial

Definición (cont.)

con

$$p_i = \frac{\exp\left(\alpha_i + \sum_{j \in \partial_i} \beta_{ij} \cdot x_j\right)}{1 + \exp\left(\alpha_i + \sum_{j \in \partial_i} \beta_{ij} \cdot x_j\right)}$$

- El modelo auto-binomial se reduce al modelo auto-binario cuando $n = 1$.

Tipos de MRF. Ejemplo: Modelo auto-binomial

Modelo Binomial:1 iteraciones

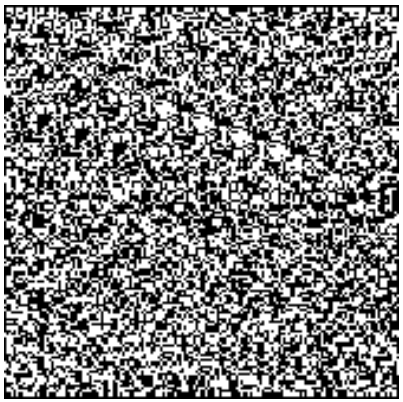

```
beta =
[3.9,3.9]
alfa = -7.8
```

Modelo Binomial:10 iteraciones

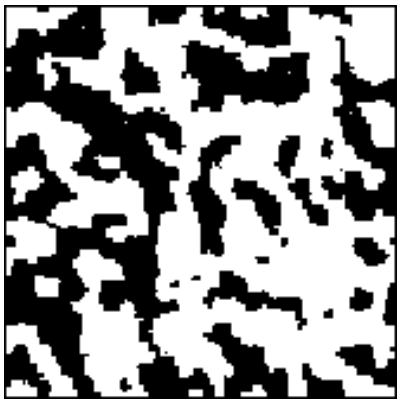

Modelo Binomial:25 iteraciones

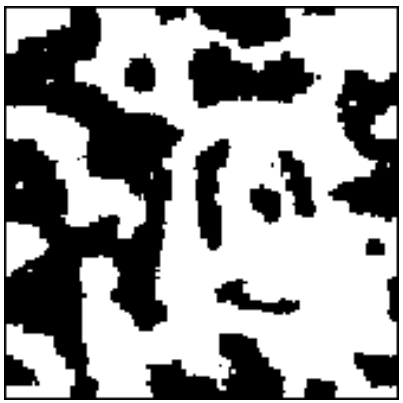

Modelo Binomial:50 iteraciones

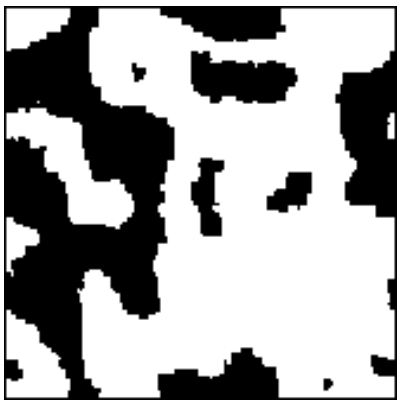

Tipos de MRF. Definición: Modelo de Derin-Elliot

Definición

El automodelo $X = \{X_s\}_{s=0}^{m}$ *se dice que es un* **modelo de Derin-Elliot** *si su función de energía viene dada por:*

$$U(\mathbf{x}) = -\sum_{i \in S} \alpha_i \cdot x_i - \sum_{i,j \in S, i \sim j} \beta_{ij} \cdot I(x_i, x_j)$$

donde la función $I(x_i, x_j)$ *se define como:*

$$I(x_i, x_j) = \begin{cases} 1 & x_i = x_j \\ -1 & x_i \neq x_j \end{cases}$$

Tipos de MRF. Definición: Modelo auto-normal

Definición

El automodelo $X = \{X_s\}_{s=0}^{m}$ *se dice que es un* **modelo auto-normal** *o un* **campo aleatorio de Markov gaussiano** *(Gaussian Markov Random Field, GRMF) si los valores que pueden tomar las variables* $x_i \in \Lambda = \mathbb{R}$ *vienen dados por la distribución de probabilidad conjunta normal multivariante:*

$$P\left(x_i \,|x_j, j \in \partial_i\right) = \frac{1}{\sqrt{2\pi\sigma^2}} \cdot$$

$$\cdot \exp\left\{-\frac{1}{2\sigma^2}\left[\left(x_i - \mu_i\right) - \sum_{j\in\partial_i} \beta_{ij}\left(x_j - \mu_j\right)\right]^2\right\}$$

Tipos de MRF. Definición: Modelo auto-normal

Definición (cont.)

con media condicional:

$$E\left[x_i \left| x_j, j \in \partial_i \right.\right] = \mu_i - \sum_{j \in \partial_i} \beta_{ij} \left(x_j - \mu_j\right)$$

y varianza condicional:

$$var\left[x_i \left| x_j, j \in \partial_i \right.\right] = \sigma^2$$

Tipos de MRF. Modelo auto-normal

- Las funciones potencial, $V_1(x_i)$ y $V_2(x_i, x_j)$, para las cliques simples y dobles de un modelo auto-normal son respectivamente:

$$V_1(x_i) = \frac{(x_i - \mu_i)^2}{2\sigma^2}$$

$$V_2(x_i, x_j) = \frac{\beta_{ij}(x_i - \mu_i)\left(x_j - \mu_j\right)}{2\sigma^2}$$

Tipos de MRF. Modelo auto-normal

- La distribución conjunta del modelo auto-normal es una distribución de Gibbs:

$$P(\mathbf{x}) = \frac{\sqrt{\det(B)}}{\sqrt{(2\pi\sigma^2)^d}} \cdot \exp\left(\frac{1}{2\sigma^2}(\mathbf{x}-\boldsymbol{\mu})^T \cdot B \cdot (\mathbf{x}-\boldsymbol{\mu})\right)$$

donde $\boldsymbol{\mu} = (\mu_i)_{d\times 1}$ es el vector de las medias condicionales y $B = (b_{ij})_{d\times d}$ es la matriz de interacción o dispersión cuyos elementos de la diagonal son 1 y el resto de elementos de dicha matriz son $b_{ij} = -\beta_{ij}$ con $\beta_{ii} = 0$.

Tipos de MRF. Modelo auto-normal

- La matriz de dispersión B es la inversa de la matriz de covarianza:

$$B = \Sigma^{-1}$$

- Debemos recordar que la condición necesaria y suficiente para que la distribución de probabilidad conjunta sea una función de probabilidad es que la matriz B sea simétrica y definida positiva.

Tipos de MRF. Ejemplo: Modelo auto-normal

Ejemplo

Un campo con ruido gaussiano independiente es un caso especial de un campo aleatorio de Markov gaussiano cuya función de energía consta únicamente de potenciales para cliques simples.

- Esto es debido a que los potenciales en las cliques de órdenes superiores son cero.
- Es decir, no existe interacción del contexto en el ruido gaussiano independiente.

Tipos de MRF. Ejemplo: Modelo auto-normal

Modelo Autonormal
beta = [0.5, 5, 0.5, 0.5]

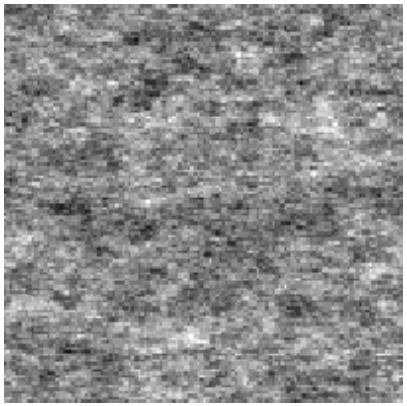

Modelo Autonormal
beta = [0.05, 0.05, 0.05, 100]

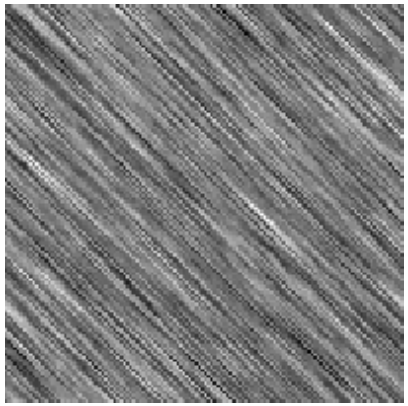

Modelo Autonormal
beta = [15, 0.05, 0.5, 2.5]

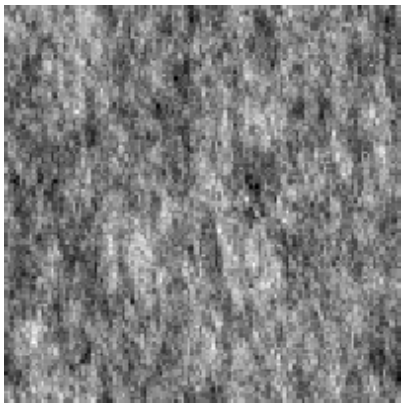

Modelo Autonormal
beta = [15 100 0.5 0.5]

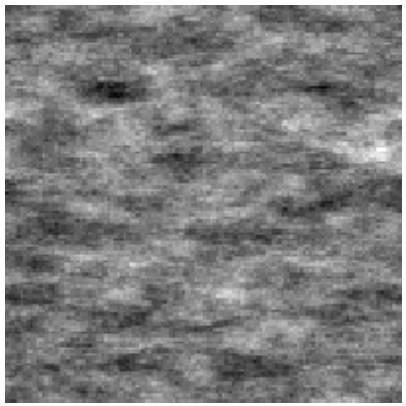

Tipos de MRF. Definición: Modelo simultáneo de auto-regresión

Definición

El campo aleatorio $X = \{X_s\}_{s=0}^{m}$ *se dice que es un* **modelo simultáneo de auto-regresión (SAR)** *si los valores que pueden tomar las variables* $x_i \in \Lambda$ *vienen dados por* d *funciones de probabilidad condicional tales como:*

$$x_i = \mu_i + \sum_{j \in \partial_i} \beta_{ij} \left(x_j - \mu_j \right) + \varepsilon_i$$

siendo $\varepsilon_i = N\left(0, \sigma^2\right)$ *funciones gaussianas independientes.*

Tipos de MRF. Modelo simultáneo de auto-regresión

- La distribución conjunta del modelo SAR es una distribución de Gibbs:

$$P(\mathbf{x}) = \frac{\sqrt{\det(B)}}{\sqrt{(2\pi\sigma^2)^d}} \exp\left(\frac{1}{2\sigma^2}(\mathbf{x}-\boldsymbol{\mu})^T \cdot B^T \cdot B \cdot (\mathbf{x}-\boldsymbol{\mu})\right)$$

donde $\boldsymbol{\mu} = (\mu_i)_{d\times 1}$ es el vector de las medias condicionales y $B = (b_{ij})_{d\times d}$ es la matriz de interacción o dispersión cuyos elementos de la diagonal son 1 y el resto de elementos son $b_{ij} = \delta_{ij} - \beta_{ij}$ con $\beta_{ii} = 0$.

Tipos de MRF. Definición: Modelo logístico multinivel

Definición

Una generalización del modelo auto-logístico $X = \{X_s\}_{s=0}^{m}$ *es el* **modelo logístico multinivel (MLL)** *también denominado* **proceso de Strauss**, **modelo de Potts** *o* **modelo generalizado de Ising** *donde los valores que pueden tomar las variables son valores discretos,* $x_i \in \Lambda = \{1, \ldots, n\}$ *con* $n > 2$, *y el potencial* V_C *depende del tipo de la clique* $C \in \mathcal{C}$ *y de la configuración local* $\mathbf{x}_C = \{x_i : i \in C\}$.

Tipos de MRF. Modelo logístico multinivel

- Los potenciales del modelo logístico multinivel vienen dados por la siguiente función:

$$V_C(\mathbf{x}) = \begin{cases} \zeta_C & \text{si } x_i = k \in \Lambda \qquad \forall i \in C \\ -\zeta_C & \text{c.c.} \end{cases}$$

- Es decir, son positivos si todas las posiciones de la clique toman el mismo valor y negativos en caso contrario.

Tipos de MRF. Modelo logístico multinivel

- Para las cliques simples, el potencial del modelo es:

$$V_C(\mathbf{x}) = V_C(x_i) = \alpha_k \qquad \text{donde} \quad x_i = k \in \Lambda$$

- El potencial para las cliques dobles es:

$$V_2(x_i, x_j) = \begin{cases} \beta_C & \text{si } x_i = x_j = k \in \Lambda \\ -\beta_C & \text{c.c.} \end{cases}$$

con $C = \{i, j\} \in C_2$.

Tipos de MRF. Modelo logístico multinivel

Teorema

El modelo logístico multinivel es un **modelo de segundo orden** *si y sólo si los valores* α_k *(para cliques simples) y* β_C *(para cliques dobles) son distintos de cero.*

Tipos de MRF. Modelo logístico multinivel

- Cuando el modelo es isotrópico, las constantes β_C son iguales para toda clique doble, $\beta_C = \beta$, y la probabilidad condicional o característica local del campo es:

$$P\left(x_i = k \,|x_j, j \in \partial_i\right) = \frac{\exp\left(-\alpha_k - \beta \cdot n_i\left(k\right)\right)}{\sum_{k=1}^{n} \exp\left(-\alpha_k - \beta \cdot n_i\left(k\right)\right)}$$

donde $n_i\left(k\right)$ es el número de vecinos de la posición i-ésima, $s_i \in S$, que toman el valor $k \in \Lambda$.

Tipos de MRF. Ejemplo: Modelo logístico multinivel

Modelo MLL:1 iteraciones

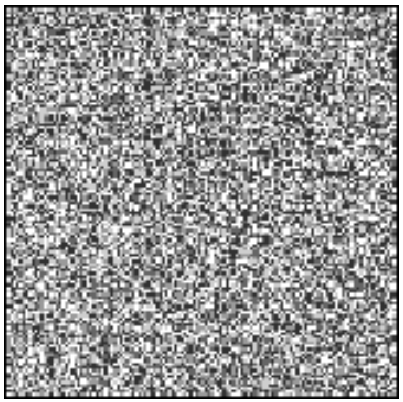

beta = 5
5 estados

Modelo MLL:5 iteraciones

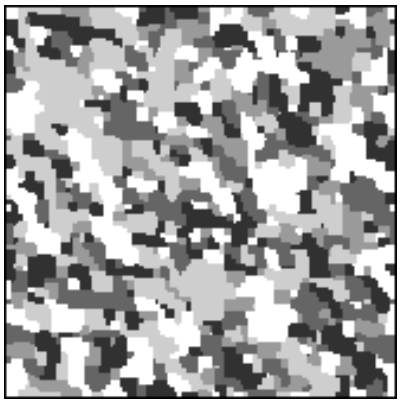

Modelo MLL:20 iteraciones

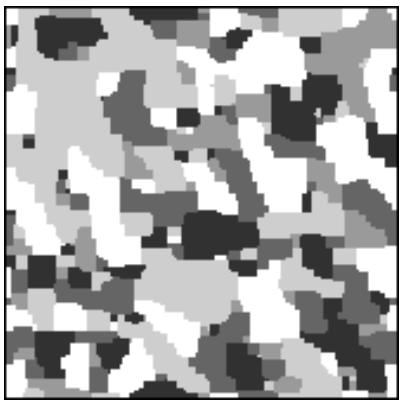

Modelo MLL:50 iteraciones

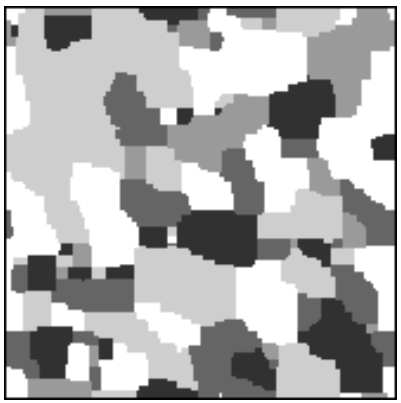

Tipos de MRF. Ejemplo: Modelo logístico multinivel

Modelo MLL
beta = 5, 3 estados

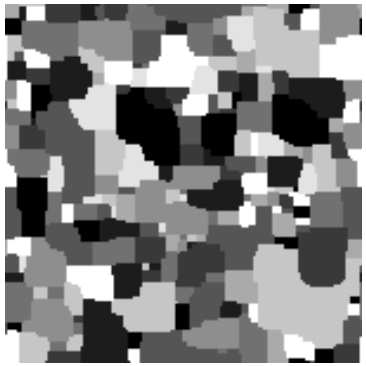

Modelo MLL
beta = 5, 5 estados

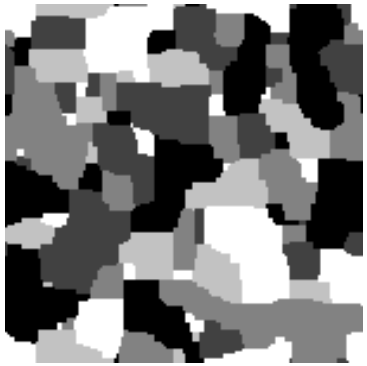

Modelo MLL
beta = 5, 10 estados

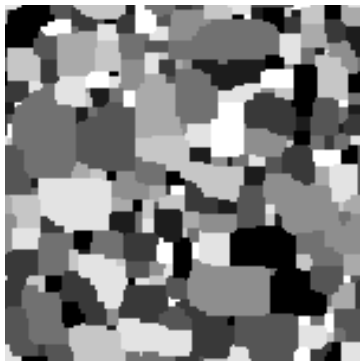

Modelo MLL
beta = 1, 3 estados

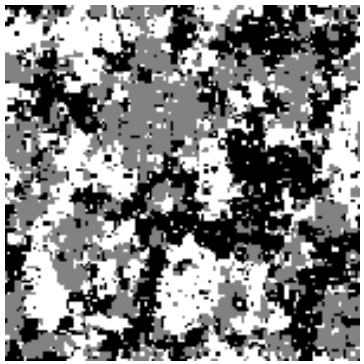

Problemas relacionados con los Campos Aleatorios de Markov

- Los principales problemas asociados a un campo aleatorio son:
  - La **estimación de los parámetros** de su sistema de vecinos.
  - La obtención de un buen algoritmo de **simulación del campo aleatorio** a fin de obtener muestras del mismo.

Estimación de los parámetros de un Campo Aleatorio de Markov

- La estimación de máxima verosimilitud (*Maximum Likelihood, ML*) de los parámetros de un campo aleatorio de Markov es computacionalmente intratable ya que el cálculo de la función de partición (Z), en la definición de la distribución de probabilidad conjunta, es imposible de calcular.
- Por ello, se utilizan ciertos métodos para la estimación de los parámetros como dos de los planteados por Besag:
  - Un método de estimación conocido como *coding estimation* [Bes74].
  - El *estimador de máxima pseudo-verosimilitud* [Bes75].

Simulación de un Campo Aleatorio de Markov

- Un problema que nos podemos plantear es el cálculo de la media de un campo aleatorio para el cual conocemos todos los parámetros de su distribución de probabilidad $P(\mathbf{x})$[1].
- Dado un campo aleatorio de Markov el cual se caracteriza por su distribución de probabilidad $P(\mathbf{x})$ definida en una malla S con un sistema de vecinos ∂, esta media se calcula como:

$$\mu_{\mathbf{x}} = \int_{\Omega} \mathbf{x} \cdot P(\mathbf{x}) \; d\mathbf{x}$$

[1] Por ejemplo, podemos incluso conocer la función de partición Z.

Simulación de un Campo Aleatorio de Markov

- Sin embargo, para la mayoría de los campos aleatorios markovianos, el cálculo de su media resulta impracticable debido a la gran dimensionalidad del espacio de configuraciones Ω.
- Por otra parte, generalmente se desconocen ciertos parámetros de la distribución de probabilidad del campo aleatorio como por ejemplo, la función de partición Z.
- Por todo ello, nos interesan métodos de generación de realizaciones del campo aleatorio a fin de obtener estadísticas del mismo o, simplemente, instancias del campo para la síntesis de texturas.

Algoritmos de simulación de Campos Aleatorios de Markov

- Los métodos de Monte-Carlo toman muestras de modo uniforme sobre el espacio de las posibles configuraciones.
  - No obstante, estas muestras se obtienen, generalmente, a partir de configuraciones con una probabilidad muy baja.
- Por ello, utilizaremos otro conjunto de algoritmos de muestreo como:
  - Algoritmo *Gibbs sampler*
  - Algoritmo de Metrópolis
  - Algoritmo *Simulated Annealing*
  - Algoritmo ICM (*Iterated Conditional Modes*)

Algoritmos de simulación de Campos Aleatorios de Markov

- Estos algoritmos obtienen una secuencia de muestras:

$$\left\{\mathbf{x}^{(0)}, \mathbf{x}^{(1)}, \ldots, \mathbf{x}^{(k)}\right\}$$

  a partir de una secuencia de distribuciones, que en el límite o equilibrio, son la distribución de Gibbs.
- Una vez alcanzada la situación de equilibrio, podemos utilizar las muestras de la secuencia para calcular estadísticas.
  - Por ejemplo, la media del campo aleatorio puede ser obtenida como:

$$\hat{\mu}_{\mathbf{x}} = \frac{1}{M} \sum_{m=1}^{M} \mathbf{x}^{(m)}$$

    donde $\mathbf{x}^{(m)}$ son realizaciones del campo aleatorio una vez alcanzado el equilibrio.

Algoritmos de simulación de Campos Aleatorios de Markov: Gibbs sampler secuencial

Modelo Ising:1 iteraciones

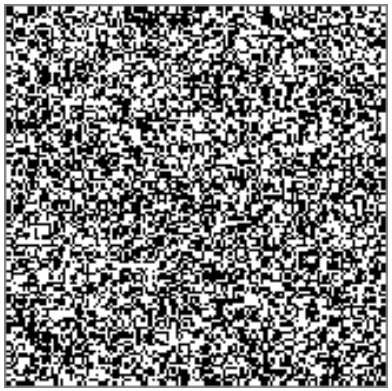

Gibbs sampler secuencial beta = 0.8

Modelo Ising:10 iteraciones

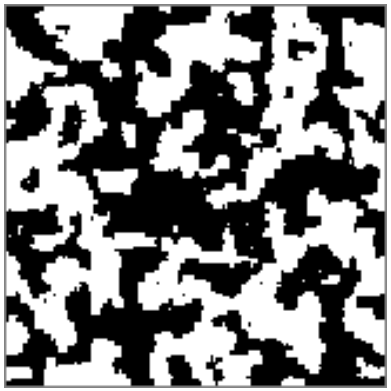

Modelo Ising:50 iteraciones

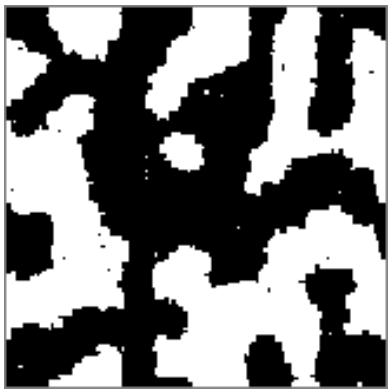

Modelo Ising:100 iteraciones

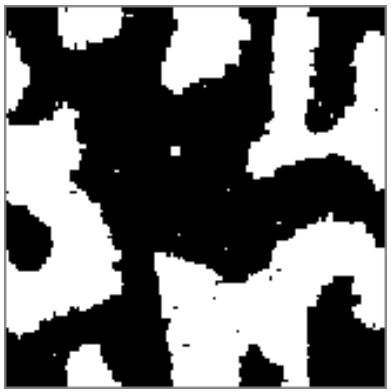

Algoritmos de simulación de Campos Aleatorios de Markov: Gibbs sampler secuencial

Modelo Ising:1 iteraciones

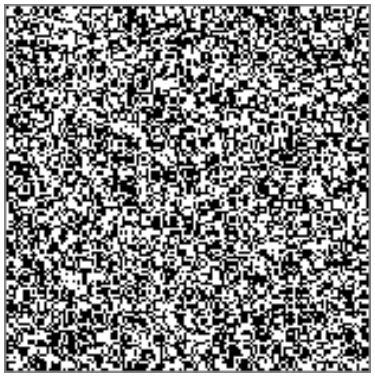

Gibbs sampler secuencial beta = 4.0

Modelo Ising:10 iteraciones

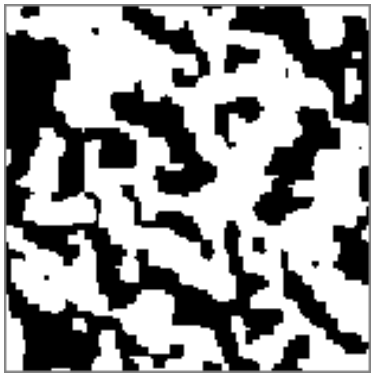

Modelo Ising:50 iteraciones

Modelo Ising:100 iteraciones

Algoritmos de simulación de Campos Aleatorios de Markov: Modelo Ising

Modelo Ising:
1 iteraciones

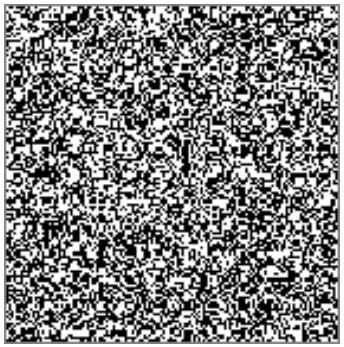

Modelo Ising:
5 iteraciones

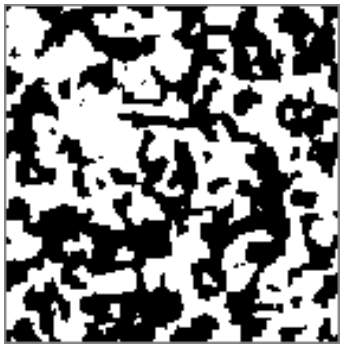

Modelo Ising:
10 iteraciones

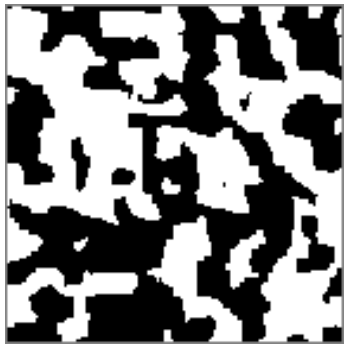

Modelo Ising:
20 iteraciones

Modelo Ising:
40 iteraciones

Modelo Ising:
50 iteraciones

Campos Aleatorios de Markov. Aplicaciones

- Los campos aleatorios de Markov se utilizan en una gran variedad de áreas de conocimiento como por ejemplo:
  - Problemas de visión de bajo y alto nivel
  - Econometría espacial, epidemiología, agronomía, ...
  - Sociología: análisis del comportamiento social, votaciones, estudio de las redes sociales,...
  - Biología celular: análisis de *clusters*, modelado de proteínas, ...
  - Etc.

Campos Aleatorios de Markov. Aplicaciones: Visión a bajo nivel

- En problemas de visión a **bajo nivel** debemos destacar las siguientes aplicaciones:
  - Eliminación de ruido en las imágenes o restauración de imágenes
  - Segmentación de imágenes o texturas
  - Filtrado de una imagen
  - Visión estereoscópica
  - Reconstrucción de superficies o recuperación de forma 3D
  - Detección de aristas
  - Análisis de texturas
  - Flujos ópticos
  - Fusión de datos, ...

Campos Aleatorios de Markov. Aplicaciones: Visión a alto nivel

- En problemas de visión a **alto nivel** debemos destacar las siguientes aplicaciones:
  - Correspondencia entre imágenes
  - Reconocimiento de objetos
  - Clasificación, ...

Bibliografía I

Howard C. Berg.
Random Walks in Biology.
Princeton University Press, rev new su edition, September 1993.

J. Besag.
Spatial interaction and the statistical analysis of lattice systems.
J. Royal Statistical Society B, 36:192–225, 1974.

J. Besag.
Statistical analysis of non-lattice data.
The Statistician, 24:179–195, September 1975.

H. Dym and H.P. Mckean.
Gaussian Processes, Function Theory, and the Inverse Spectral Problem. Probability and Mathematical Statistics, Volume 31.
Academic Press, 1976.

Bibliografía II

Barry D. Hughes.
Random Walks and Random Environments: Volume 1: Random Walks.
Oxford University Press, USA, May 1995.

Barry D. Hughes.
Random Walks and Random Environments: Volume 2: Random Environments.
Oxford University Press, USA, August 1996.

Davar Khoshnevisan.
Multiparameter Processes. An Introduction to Random Fields.
Springer Monographs in Mathematics, Nov 2002.

R. Kinderman and S.L. Snell.
Markov random fields and their applications.
American mathematical society, 1980.

Bibliografía III

S. Z. Li.
Markov random field modeling in computer vision.
Springer-Verlag, 1995.

Kurt Marti.
Stochastic Optimization Methods.
Springer, 1 edition, December 2004.

G. Parisi M. Mezard and M. A. Viraroso.
Spin Glass Theory and Beyond.
World Scientific, Singapore, 1987.

András Telcs.
The Art of Random Walks.
Springer, 1 edition, June 2006.

Bibliografía IV

E.H. van Marcke.
Random Fields: Analysis and Synthesis.
MIT Press, Cambridge MA, 1983.

Gerhard Winkler.
Image Analysis, Random Fields and Dynamic Monte Carlo Methods: A Mathematical Introduction.
Springer, 1 edition, February 1995.

Anexo A. Definición: Evento

- Consideramos ciertas distribuciones o medidas de probabilidad P en el espacio de estados o configuraciones Ω. Es decir, el conjunto $P = \{P(\mathbf{x})\}_{\mathbf{x}\in\Omega}$ tal que:

$$P(\mathbf{x}) \geq 0$$
$$\sum_{\mathbf{x}\in\Omega} P(\mathbf{x}) = 1$$

Definición

Los subconjuntos de configuraciones o estados $E \subset \Omega$ se denominan **eventos** *y su probabilidad viene dada por:*

$$P(E) = \sum_{\mathbf{x}\in E\subset\Omega} P(\mathbf{x})$$

Anexo A. Definición: Probabilidad condicionada

Definición

En el espacio de configuraciones Ω, la **probabilidad condicionada** *del evento $F \subset \Omega$ dado el evento $E \subset \Omega$ es:*

$$P(F|E) = \frac{P(F \cap E)}{P(E)}$$

▸ Características Locales

Anexo A. Definición: Independencia

Definición

Dos variables aleatorias X e Y son **independientes** *si y sólo si:*

$$P(X, Y) = P(X) \cdot P(Y)$$

y se denota como $X \perp Y$.

Anexo A. Definición: Independencia condicional

Definición

Dos variables aleatorias X e Y son **condicionalmente independientes** *dada la variable aleatoria Z si y sólo si:*

$$P(X, Y \,|Z) = P(X \,|Z) \cdot P(Y \,|Z)$$

y se denota como $X \perp Y \,|Z$.

▸ Representación Grafos

Anexo A. Teorema: Independencia condicional

Definición

Dadas tres variables aleatorias X, Y y Z, las variables X e Y son **condicionalmente independientes** *dada la variable Z para cualquier función $f(.)$ y $g(.)$ y $\forall Z$ con $P(Z) > 0$. Esto es,*

$$X \perp Y \,|Z \Leftrightarrow P(X, Y, Z) = f(X, Z) \cdot g(Y, Z)$$

Anexo B. Definición: Grafo no dirigido

Definición

Un **grafo no dirigido** *es un tupla* $\mathcal{G} = (\mathcal{V}, \mathcal{E})$ *donde* $\mathcal{V}$ *es el conjunto de nodos del grafo y* $\mathcal{E}$ *es el conjunto de aristas* $\{i, j\}$ *con* $i, j \in \mathcal{V}$ *e* $i \neq j$.

- Si $\{i, j\} \in \mathcal{E}$, existe una arista no dirigida del nodo i-ésimo al j-ésimo. En caso contrario, no existe arista.
- Un grafo se dice que está totalmente conectado si existe una arista, $\{i, j\} \in \mathcal{E}$, para todo par de nodos del grafo, $\forall i, j \in \mathcal{V}$.

Anexo B. Definición: Camino

Definición

Un **camino** *del nodo* i_0 *al nodo* i_m *(representado como* $i_0, i_1, \ldots, i_m$*) es una secuencia de nodos distintos de* $\mathcal{V}$*, para los cuales existe una arista* $\{i_j, i_{j+1}\} \in \mathcal{E}$ *con* $j = 0, \ldots, m-1$.

Anexo B. Ejemplo: Camino

Ejemplo

Un camino del nodo 1 *al nodo* 6 *es* $1, 2, 4, 5, 6$.

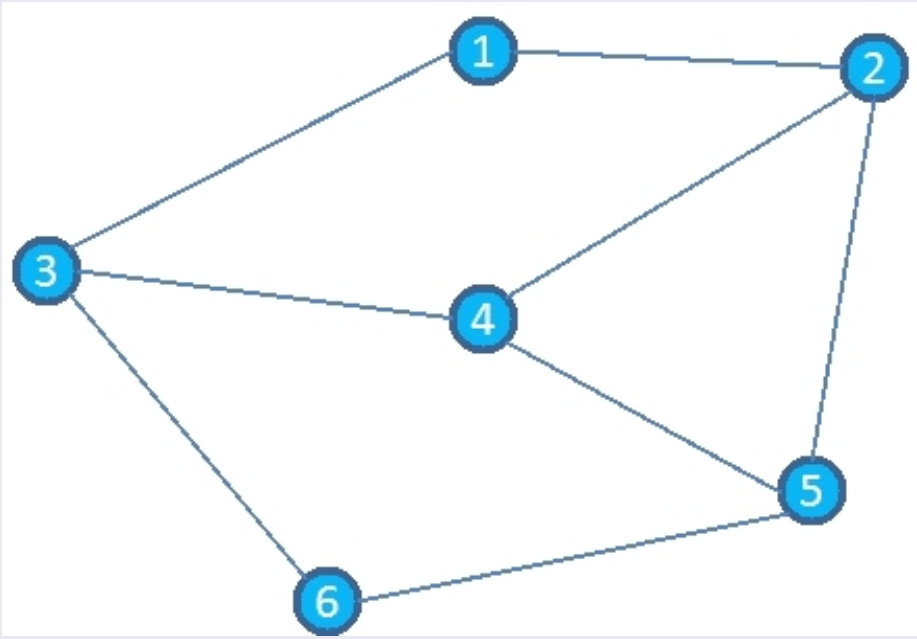

Anexo B. Definición: Conjunto Separador

Definición

Un subconjunto $C \subset \mathcal{V}$ **separa** *dos nodos $i, j \notin C$, si cada camino del nodo i al nodo j contiene al menos un nodo del subconjunto C.*

Definición

Dos conjuntos disjuntos $A \subset \mathcal{V} \backslash C$ y $B \subset \mathcal{V} \backslash C$ están separados por el subconjunto C o dicho conjunto C es el **conjunto separador** *entre los conjuntos A y B si:*

$$\forall i \in A \quad y \quad \forall j \in B \qquad \text{los nodos } i \text{ y } j \text{ están separados por } C$$

- Es decir, no podemos pasearnos por el grafo comenzando en algún lugar de A y finalizando en algún lugar de B sin pasar por algún nodo del conjunto C.

Anexo B. Ejemplo: Conjunto Separador

Ejemplo

El conjunto $C = \{1, 4, 6\}$ *separa al conjunto* $A = \{3\}$ *del conjunto* $B = \{2, 5\}$.

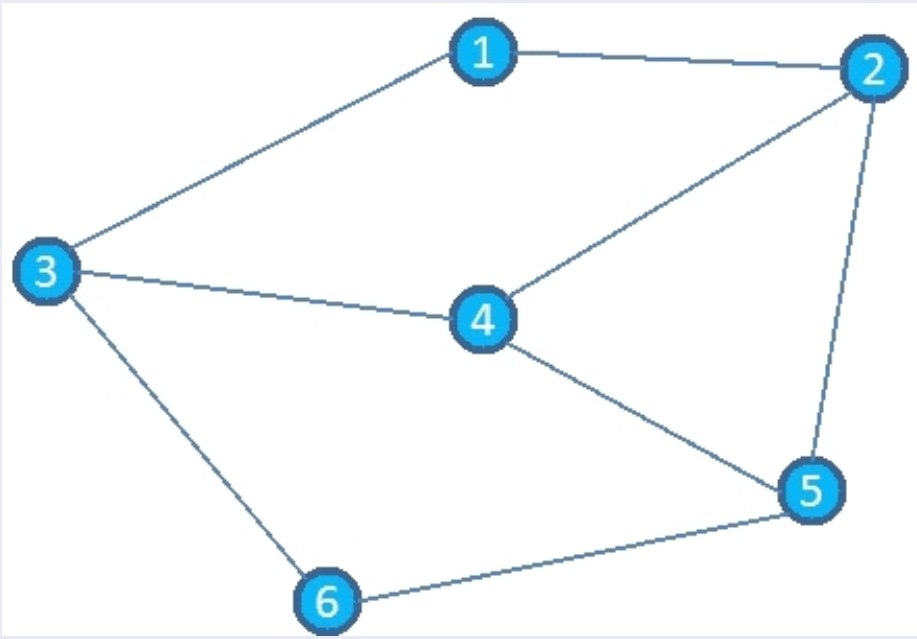

▸ Representación Grafos

Anexo B. Definición: Vecino y vecindario

Definición

Dado un grafo $\mathcal{G} = (\mathcal{V}, \mathcal{E})$, los **vecinos** *del nodo i-ésimo, $i \in \mathcal{V}$, son todos los nodos del grafo, $j \in \mathcal{V}$, que comparten una arista con dicho nodo. Esto es, el* **vecindario** *del nodo i-ésimo es el conjunto:*

$$\partial_i = \{j \in \mathcal{V} : \{i, j\} \in \mathcal{E}\}$$

Anexo B. Ejemplo: Vecino y vecindario

Ejemplo

Los vecinos del nodo 1 *son* $\partial_1 = \{2, 3\}$ *y los vecinos del nodo* 4 *son* $\partial_4 = \{2, 3, 5\}$.

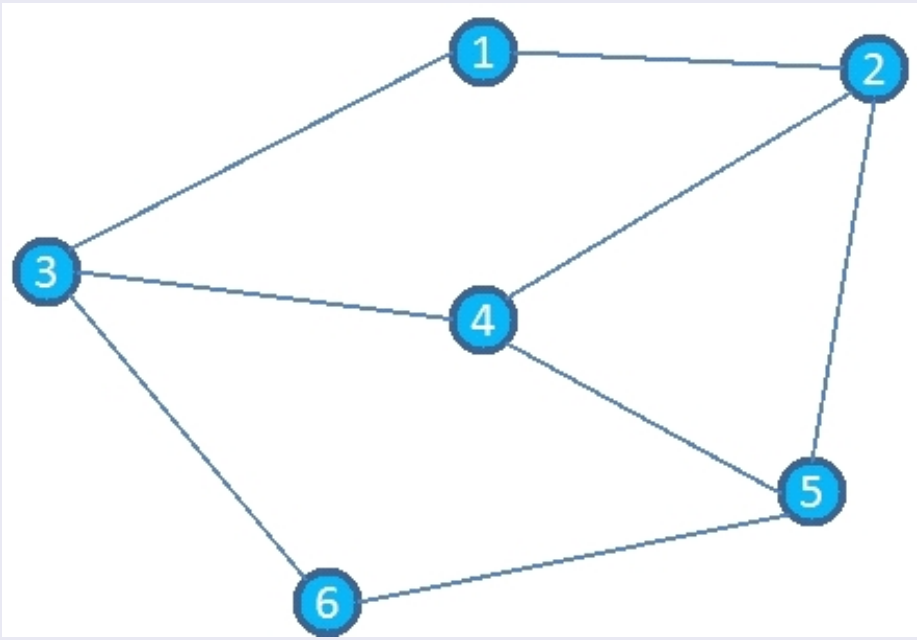

Anexo B. Vecino y vecindario

- Dados los nodos i-ésimo y j-ésimo, podemos utilizar las siguientes notaciones al referirnos a los vecinos:
  - $i \sim j$, indica que son vecinos el uno del otro respectivamente
  - $i \nsim j$, indica que no son vecinos
- En algunos casos cuando pueden establecerse orientaciones entre los nodos, por ejemplo para los píxeles de una imagen, podemos utilizar la siguiente notación:
  - $i \leftrightarrow j$, indica que son vecinos en el sentido horizontal el uno del otro respectivamente
  - $i \updownarrow j$, indica que son vecinos en el sentido vertical el uno del otro respectivamente

Anexo B. Definición: Sistema de vecinos

Definición

Un **sistema de vecinos** *asociado a un grafo* $\mathcal{G} = (\mathcal{V}, \mathcal{E})$ *se define como:*

$$\partial = \{\partial_i \,|\forall i \in \mathcal{V}\}$$

donde ∂_i *es el vecindario del nodo i-ésimo:*

$$\partial_i = \{j \in \mathcal{V} : \{i,j\} \in \mathcal{E}\}$$

Anexo B. Ejemplo: Sistema de vecinos

Ejemplo

Para una imagen bidimensional, el vecindario de orden k-ésimo del píxel del centro contiene a los píxeles con números menores o iguales a k. En este caso, mostramos el vecindario de orden 5 ($k = 5$).

5	4	3	4	5
4	2	1	2	4
3	1	○	1	3
4	2	1	2	4
5	4	3	4	5

Anexo B. Sistema de vecinos

Propiedades de un sistema de vecinos

Una relación de vecindad posee las siguientes propiedades:

1. Un nodo no es vecino de sí mismo: $i \notin \partial_i$
2. La relación de vecindad es recíproca: $i \in \partial_j \Longleftrightarrow j \in \partial_i$

Anexo B. Sistema de vecinos

- La relación de vecindario induce un grafo no dirigido $\mathcal{G} = (\mathcal{V}, \partial)$ tal que:
  - las aristas del grafo vienen dadas por el sistema de vecinos ya que existe un arista entre dos nodos s y t si y sólo si s y t son vecinos
- Por otra parte, todo grafo no dirigido induce un sistema de vecinos o vecindario.

Anexo B. Sistema de vecinos

- Generalmente, los sistemas de vecinos son *homogéneos* o *invariantes en el espacio*.
- Es decir, la estructura de vecinos (∂_i) del nodo $i \in \mathcal{V}$ se mantiene para todo el conjunto de nodos del grafo $\mathcal{V}$.

Anexo B. Ejemplo: Sistema de vecinos homogéneo

Ejemplo

Una estructura de vecinos homogénea puede definirse a partir de una matriz donde el valor 1 *indica que dicho elemento es vecino del elemento central:*

0	1	0
1	0	1
0	1	0

1	1	0
0	0	0
0	1	1

1	1	1
1	0	1
1	1	1

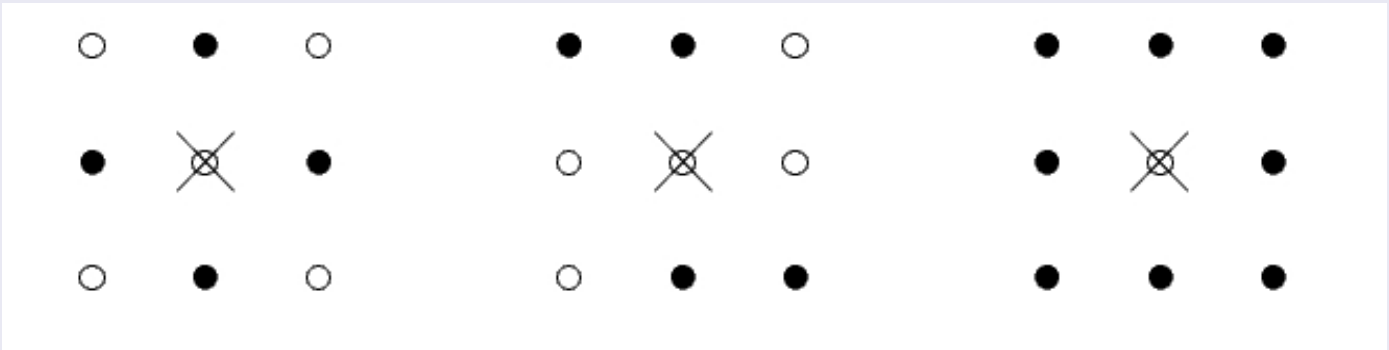

▸ Vecino y vecindario

Anexo C. Propiedades de Markov

Teorema

Sea $\mathbf{x} \in \Omega$ *una realización del campo aleatorio* $X = \{X_s\}_{s=0}^{m}$ *representado por el grafo* $\mathcal{G} = (S, \partial)$. *Entonces las siguientes propiedades son equivalentes:*

1. *La propiedad de Markov entre pares, si* $\{i, j\} \notin \partial$ *e* $i \neq j$*:*

$$x_i \perp x_j \,|\mathbf{x}_{-ij}$$

2. *La propiedad local de Markov, para todo* $i \in S$*:*

$$x_i \perp \mathbf{x}_{-\{i,\partial_i\}} \,|\mathbf{x}_{\partial_i}$$

3. *La propiedad global de Markov:*

$$\mathbf{x}_{A_1} \perp \mathbf{x}_{A_2} \,|\mathbf{x}_{A_3}$$

Teorema (cont.)

para los conjuntos disjuntos A_1, A_2 y A_3 donde A_3 separa a A_1 y a A_2 y los conjuntos A_1 y A_2 son conjuntos no vacíos.

Anexo C. Propiedad de Markov entre pares

- La propiedad de Markov entre pares (1) nos indica que si dos posiciones $i, j \in S$ no son vecinas, $\{i, j\} \notin \partial$, entonces ambas posiciones son independientes condicionalmente al resto de posiciones de la malla.

Anexo C. Ejemplo: Propiedad de Markov entre pares

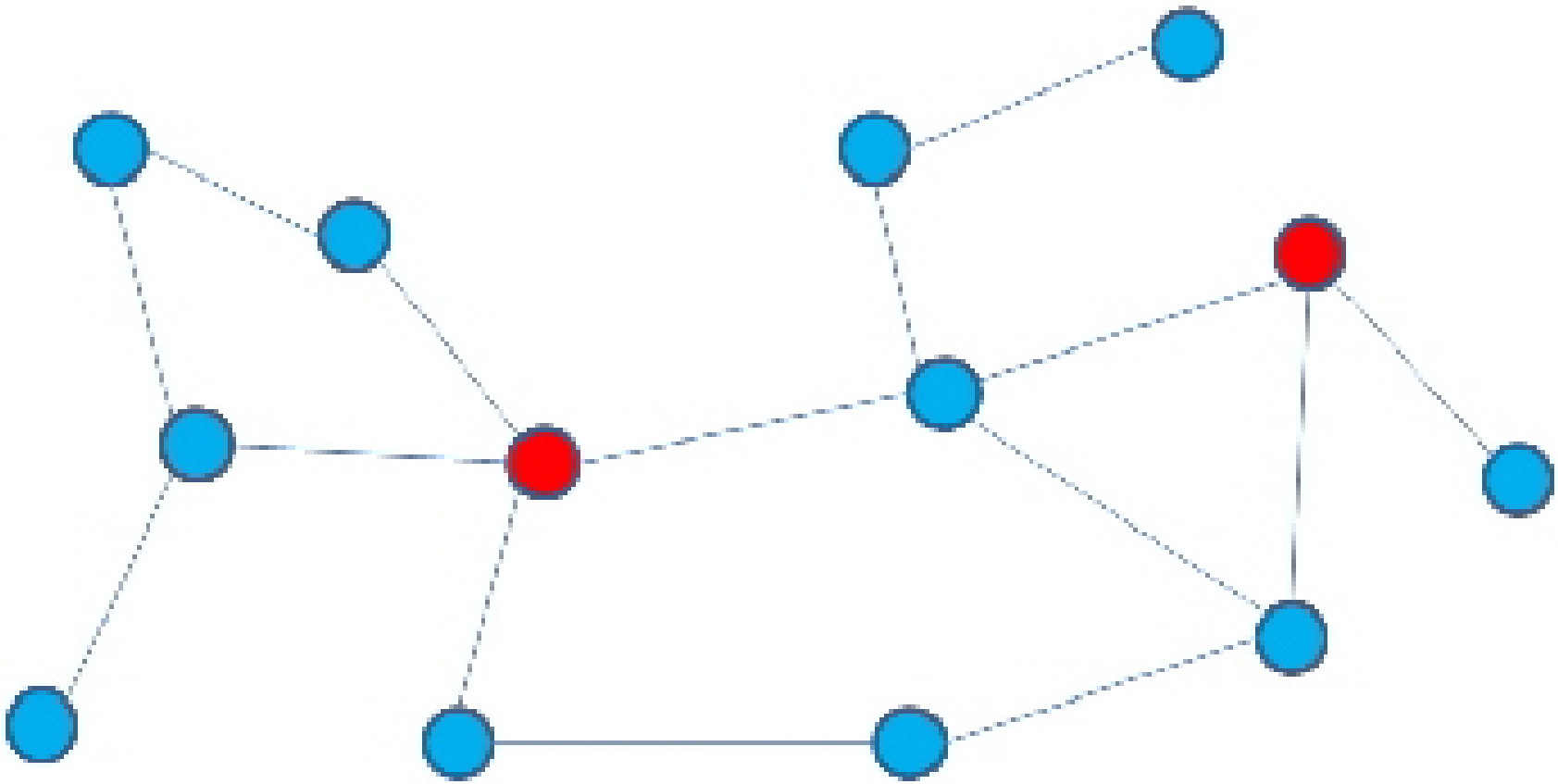

Anexo C. Propiedad local de Markov

- La propiedad local de Markov (2) nos indica que, dado su vecindario, una posición es independiente del resto de posiciones de la malla.

Anexo C. Ejemplo: Propiedad local de Markov

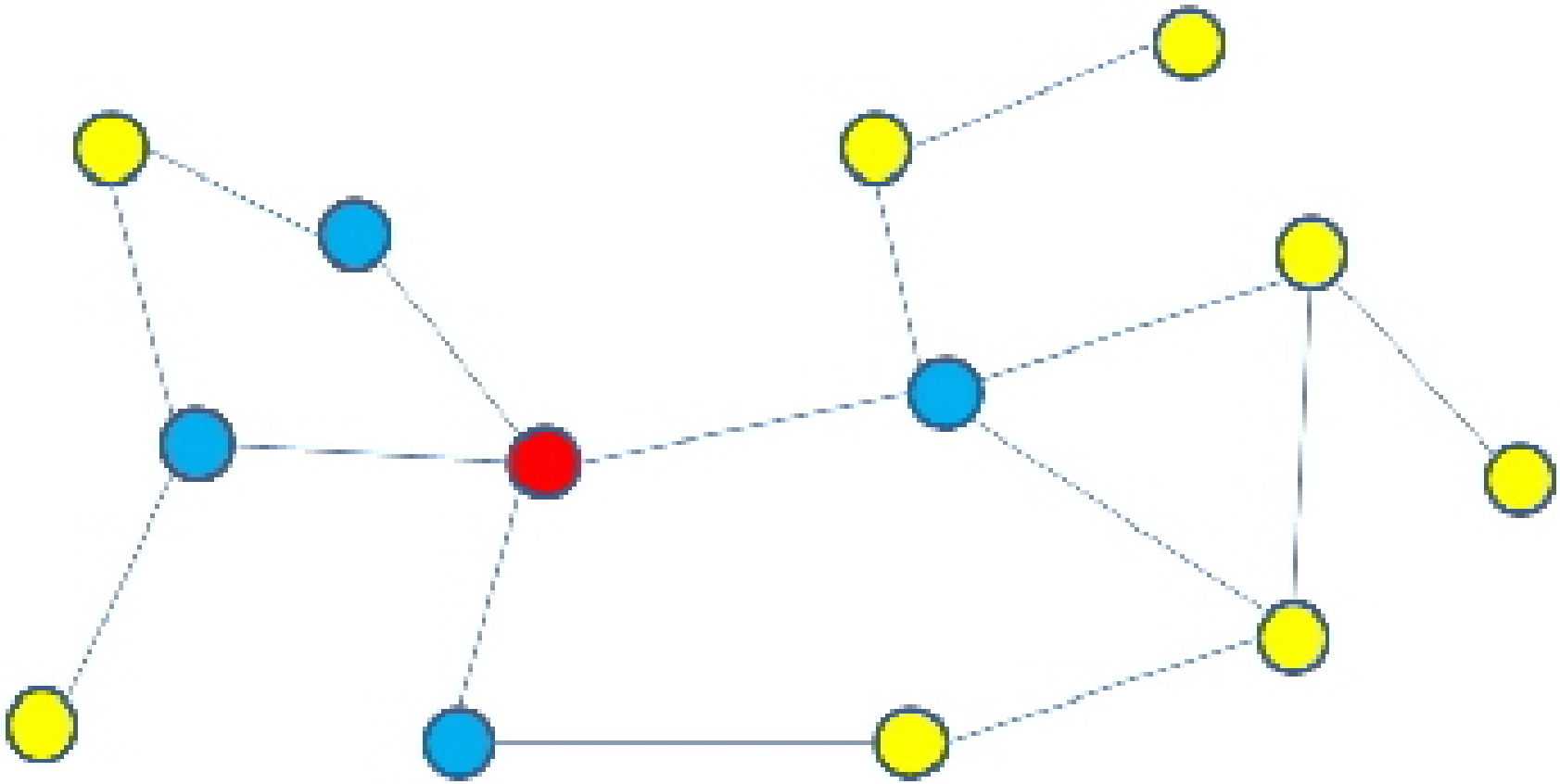

Anexo C. Ejemplo: Propiedad local de Markov

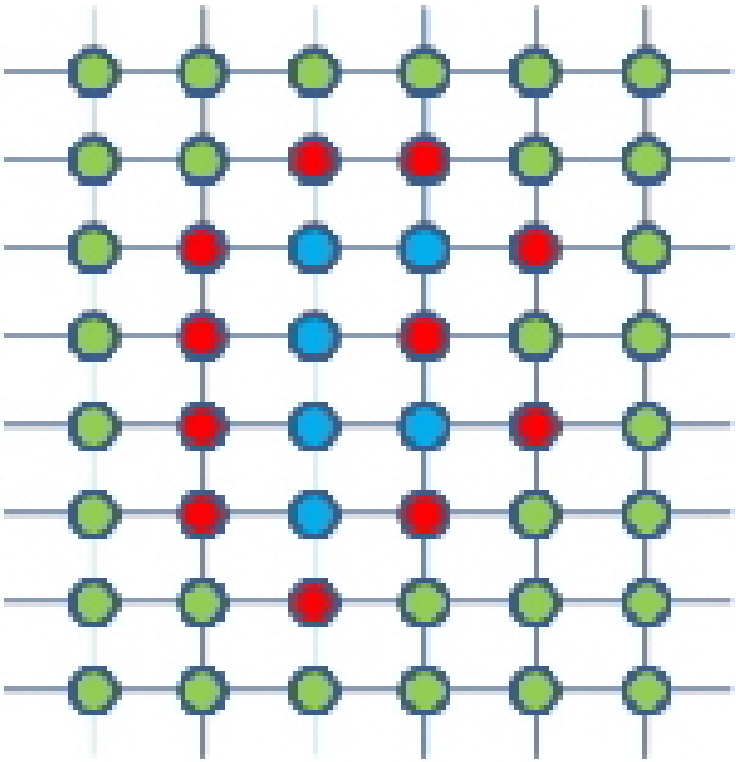

Anexo C. Propiedad global de Markov

- La propiedad global de Markov (3) implica directamente las propiedades de Markov locales (2) y entre pares (1).
- Sin embargo, la implicación en el sentido contrario es un poco sorprendente ya que la unión de los tres conjuntos A_1, A_2 y A_3 no debe ser necesariamente el conjunto de nodos del grafo o la malla S.
- La propiedades de la distribución marginal pueden ser derivadas a partir del grafo $\mathcal{G} = (S, \partial)$.
- Además, si el conjunto de cliques C es el conjunto vacío, a partir de la propiedad global de Markov (3)

$$\mathbf{x}_{A_1} \perp \mathbf{x}_{A_2} | \mathbf{x}_{A_3}$$

obtenemos que $\mathbf{x}_{A_1}$ y $\mathbf{x}_{A_2}$ son realizaciones independientes.

Anexo C. Ejemplo: Propiedad global de Markov

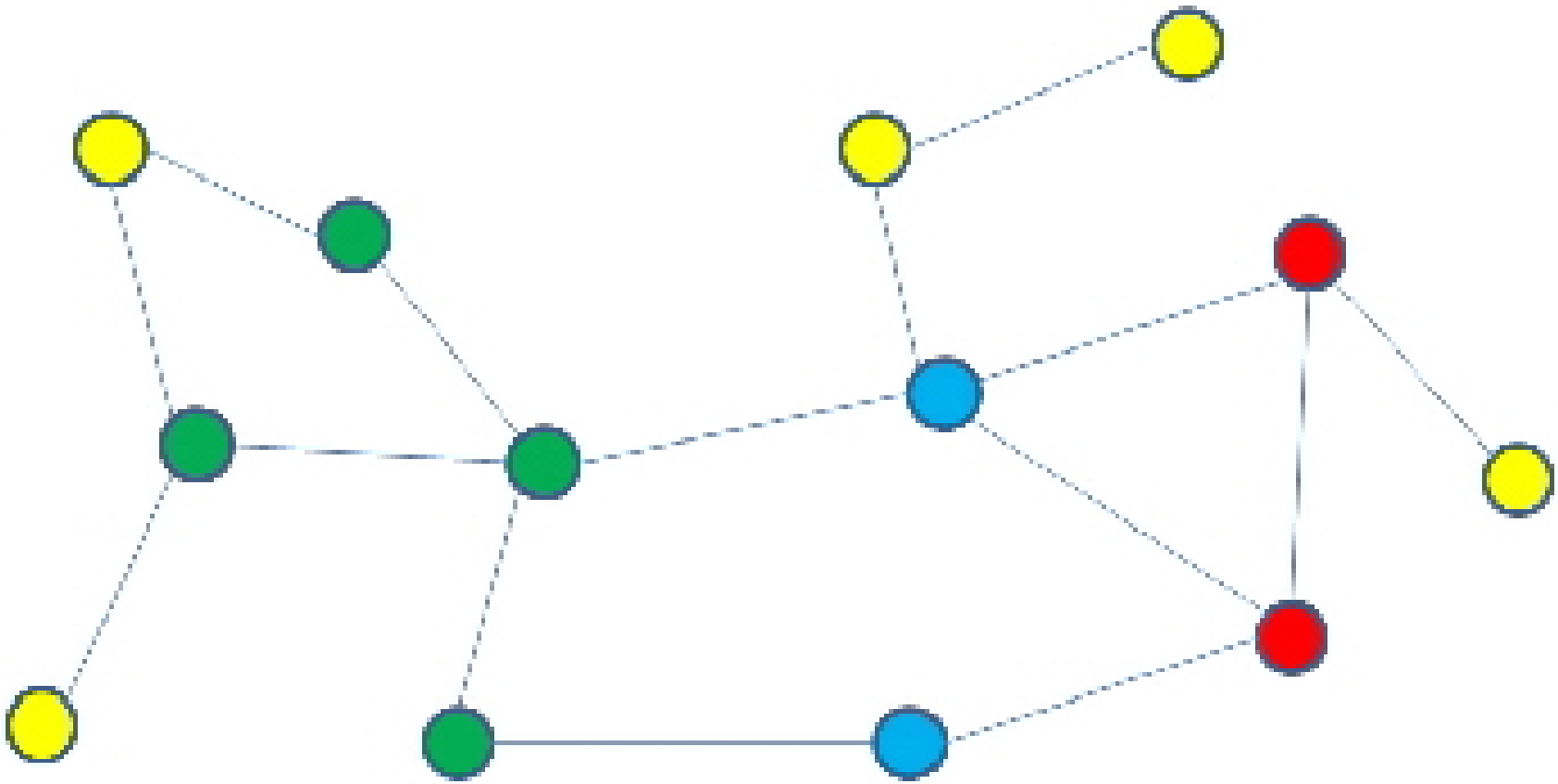

▸ Campo Aleatorio de Markov

Contraste de Hipótesis

José Luis Jiménez Josune Gallego

24 de septiembre de 2008

Índice

Introducción
- Tipos de hipótesis

Prueba de una hipótesis estadística
- Región de aceptación de H_0 y Región de rechazo de H_0
- Tipos de errores
- Decisión: hipótesis nula vs. hipótesis alternativa

Clasificación de los contrastes
- Tipos de contrastes sobre parámetros

Lema Neyman-Pearson

Test de razón de verosimilitud

Aplicaciones de los Test de Hipótesis
- Diseño del Test de Hipótesis
- Ejemplo general

Test de medias
- Test de medias con varianza conocida.
  - Influencia del tamaño muestral.
  - La potencia del contraste
- Test de diferencias entre medias
  - Estadístico de contraste.
- Significado e interpretación de los P-valores
- Los contrastes unilaterales.
- Contraste con varianza desconocida.
  - Test de medias.
  - Test de diferencias de medias.

Resumen Sección

Introducción

Tipos de hipótesis

¿Qué es una hipótesis estadística?

Definición

Una **hipótesis estadística** *es una afirmación o una conjetura acerca de la distribución de una o más variables aleatorias, o bien sobre algunas características de las mismas.*

La hipótesis que se desea contrastar se denomina **hipótesis nula** H_0, mientras que la que se acepta cuando la evidencia muestral está en contra de ésta se denomina **hipótesis alternativa** H_1.

Si se quiere contrastar la hipótesis de que un cierto parámetro θ de una población toma un valor dentro de una región Θ_0, siendo Θ el campo de variación de dicho parámetro, la hipótesis alternativa debe contemplar que el parámetro tome valores en una región Θ_1.

Tipos de hipótesis

Definición

- *Se denomina* **hipótesis simple** *a aquella que asigna valores particulares a todos los parámetros desconocidos e identifica la forma funcional de la distribución de interés. En este caso el campo de variación* Θ *toma un único valor.*
- *e* **hipótesis compuestas** *a aquellas en las que el campo de variación* Θ *puede tomar más de un valor o hay más parámetros a identificar.*

Resumen Sección

Prueba de una hipótesis estadística

- Región de aceptación de H_0 y Región de rechazo de H_0
- Tipos de errores
- Decisión: hipótesis nula vs. hipótesis alternativa

Una **prueba de una hipótesis estadística** con respecto a alguna característica desconocida de la población de interés es cualquier conjunto de reglas para decidir si se rechaza o no la hipótesis nula en base al análisis de una muestra aleatoria de la población y teniendo en cuenta la hipótesis alternativa.

A partir de una muestra generada en un experimento se calcula el valor del **estadístico de prueba** $\hat{\theta}$ que permitirá decidir que acción tomar para cada resultado del espacio muestral. Lo que hace el contraste es particionar los posibles valores del estadístico en dos subconjuntos: **región de aceptación de** H_0 y **región de rechazo de** H_0.

La aceptación de la hipótesis nula no supone ninguna garantía de que sea cierta, sino la falta de evidencia en contra. Por lo que se podría decir que el contraste es una regla de decisión. Y cuando tomamos una decisión podemos cometer errores.

		Decisión	
		H_0	H_1
Verdad	H_0	*acierto*	*error tipo I*
	H_1	*error tipo II*	*acierto*

Tipos de errores

Definición

- **Error tipo I** *Rechazar la hipótesis nula cuando esta es verdadera. La probabilidad de cometer este tipo de error se denota por* α, **nivel de significación del contraste**. *Y la probabilidad de aceptar* H_0 *cuando ésta es verdadera,* $1-\alpha$, *se denomina* **nivel de confianza**.
- **Error tipo II** *Aceptar la hipótesis nula cuando esta es falsa. La probabilidad de cometer este tipo de error se denota por* β, **riesgo del contraste**.

Se conoce como **región crítica** del test a la región de rechazo de H_0. La probabilidad de obtener un valor del estadístico dentro de esta región cuando H_0 es cierta se la denomina **tamaño** de la región crítica.

El valor $1 - \beta$ se conoce como **función potencia del contraste**. En esencia, la potencia de una prueba es la probabilidad de detectar que H_0 es falsa cuando realmente lo es.

Decisión: hipótesis nula vs. hipótesis alternativa

Un principio sencillo y razonable para obtener las reglas de decisión para la prueba de hipótesis estadísticas es seleccionar aquel procedimiento de prueba que para un error de tipo I (nivel de significación) dado tenga el menor error de tipo II (riesgo del contraste menor y mayor potencia) . Este es el test **uniformemente más potente**.

Por último, una vez seleccionado el contraste a utilizar, el aumento del tamaño muestral permitirá mejorar los valores de ambos errores puesto que añadimos más información cuantos más datos tengamos.

Resumen Sección

Clasificación de los contrastes

Tipos de contrastes sobre parámetros

Dependiendo del grado de conocimiento de la distribución de la población bajo estudio, se distingue entre contrastes **parámetricos** y **no paramétricos**. Si se conoce la distribución y se intenta obtener información sobre los parámetros desconocidos de la distribución sería el primer tipo y cuando se desconoce la distribución el segundo.

- En primer lugar, se distingue entre contrastes con hipótesis nula y alternativa simples y aquellos que tienen alguna de ellas compuesta.
- Entre estos últimos se distingue, dependiendo de la estructura de su hipótesis:
  - **Contrastes bilaterales**. En el caso de la hipótesis nula simple $H_0 : \theta = \theta_0$, se dice que H_1 es una hipótesis **alternativa bilateral** si $H_1 : \theta \neq \theta_0$. Esto es, los valores de θ bajo H_1 se encuentran a ambos lados del valor propuesto bajo H_0.
  - **Contrastes unilaterales**. Hay dos posibilidades para la la hipótesis nula compuesta $H_0 : \theta \geq \theta_0$ o bien, $H_0 : \theta \leq \theta_0$ y sus correspondientes hipótesis alternativas compuestas $H_1 : \theta < \theta_0$ y $H_1 : \theta > \theta_0$

Resumen Sección

Lema Neyman-Pearson

Las mejores pruebas. ¿Cómo construir una buena prueba?

Sea $X_1, X_2, \cdots, X_n$ una muestra aleatoria de tamaño n de una población cuya función de densidad de probabilidad es $f(x;\theta)$, y considérese la hipótesis $H_0 : \theta = \theta_0$ frente a $H_1 : \theta = \theta_1$ siendo θ_0 y θ_1 valores especificados. Entonces la mejor prueba para H_0 frente a H_1 es aquélla que tiene el valor más pequeño para el error de tipo II (mayor potencia) de entre todas las pruebas que tengan un valor del error de tipo I no mayor que α.

Lema Neyman-Pearson

Para construir la región crítica óptima en esta situación calculamos las verosimilitudes $L_0 = \prod_i f(x_i; \theta_0)$ y $L_1 = \prod_i f(x_i; \theta_1)$ cuando son ciertas las hipótesis nula y alternativa respectivamente.

Y si existe una región crítica $\mathbf{C}$ de tamaño α y una constante positiva k tal que

$$\frac{L_0(x_i;\theta_0)}{L_1(x_i;\theta_1)} \leq k \in \mathbf{C}$$

$$\frac{L_0(x_i;\theta_0)}{L_1(x_i;\theta_1)} \geq k \notin \mathbf{C}$$

entonces $\mathbf{C}$ es la mejor región crítica para probar H_0 frente a H_1 donde L_0 y L_1 son las funciones de verosímilitud relativa a H_0 y H_1, respectivamente.

Resumen Sección

Test de razón de verosimilitud

- Se trata de medir la discrepancia entre el valor asignado al parámetro en la hipótesis nula y el que se obtiene a partir de un estimador del mismo.
- La medida de la discrepancia se basa en la comparación del máximo de la función de verosimilitud evaluada en la hipótesis nula y el máximo absoluto de la misma. Este método se llama **test de razón de verosimilitud**.

Test de razón de verosimilitud

Dada una población representada por la variable X cuya distribución depende del parámetro θ, se desea contrastar

$$\begin{cases} H_0 : \theta \in \Theta_0 \\ H_1 : \theta \in \Theta_1 \end{cases}$$

con $\Theta = \Theta_0 \cup \Theta_1$.

Para realizar el contraste se toma una muestra aleatoria $x_1, x_2, \cdots, x_n$, y se calcula

$$\lambda(x_1, x_2, \cdots, x_n) = \frac{max_{\theta \in \Theta_0} L(x_1, x_2, \cdots, x_n, \theta)}{max_{\theta \in \Theta} L(x_1, x_2, \cdots, x_n, \theta)}$$

Una vez calculado $\lambda(x_1, x_2, \cdots, x_n)$ se busca un número $k \in (0, 1)$ tal que si $\lambda(x_1, x_2, \cdots, x_n) \leq k$ se rechaza H_0.

Para calcular el valor de k, fijado un nivel de significación α se procede como sigue

$$P[x_1, x_2, \cdots, x_n \in C/\theta \in \Theta_0] = P[\lambda(x_1, x_2, \cdots, x_n) \leq k/\theta \in \Theta_0] \leq \alpha$$

Sólo se tiene garantizado que el valor de k queda univocamente determinado cuando la hipótesis nula es simple.

Como consecuencias intuitivas del contraste, se tiene que:

1. Si se verifica que $\lambda(x_1, x_2, \cdots, x_n) = 1 > k$ entonces no hay evidencias para rechazar H_0.
2. El no rechazar H_0 depende de
   - lo próximo que se encuentre Θ_0 del estimador máximo-verosímil, caso de existir.
   - de la curvatura de la función de verosimilitud. De forma que cuando dicha curvatura es muy pequeña resulta más difícil rechazar H_0, haciéndose menor la capacidad de discriminación de $\lambda(x_1, x_2, \cdots, x_n)$

Resumen Sección

Aplicaciones de los Test de Hipótesis

- Diseño del Test de Hipótesis
- Ejemplo general

Diseño del Test de Hipótesis

1. Determinar la hipótesis nula y la alternativa.
2. Fijar un nivel de significación. Normalmente 0,05(5 %) y 0,01(1 %).
3. Determinar cual es el estadístico de contraste y su distribución muestral.
4. Determinar la región crítica y la región de aceptación.
5. Seleccionar una muestra y calcular el valor experimental del estadístico de contraste.
6. Tomar la decisión estadística de acuerdo con el valor experimental obtenido.
7. Sacar conclusiones acerca del problema planteado.

Ejemplo general

Supongamos que pertenecemos al consejo regulador de la denominación de origen de los vinos de Ribera de Duero. Sabemos que los vinos jóvenes de años anteriores tienen un grado alcohólico medio de 12.5 grados, tal como aparece en la etiqueta. Para el año actual, el consejo regulador, de acuerdo con todos sus miembros, ha decidido cambiar algunos de los pasos del proceso de fabricación. El primer problema que se plantea es: ¿Se ha modificado el grado alcohólico al modificar el proceso de fabricación?
Para responder a esta pregunta utilizaremos el **TEST DE MEDIAS**.

Tenemos por lo tanto definido el problema en los siguientes términos:

- Población: los vinos jóvenes de Ribera de Duero en el año actual.
- Variable que queremos medir: el grado alcohólico de los mismos.
- Hipótesis de trabajo: ¿Se ha modificado el grado alcohólico?

- El paso siguiente consiste en suponer un modelo de comportamiento teórico para la población.
- En el caso que nos ocupa, parece razonable suponer, a priori, que el grado alcohólico se concentra de forma simétrica alrededor de un valor medio. Por lo que suponemos que la varible que estamos midiendo en la población sigue una distribución normal.

Resumen Sección

Test de medias

- Test de medias con varianza conocida.
  - Influencia del tamaño muestral.
  - La potencia del contraste
- Test de diferencias entre medias
  - Estadístico de contraste.
- Significado e interpretación de los P-valores
- Los contrastes unilaterales.
- Contraste con varianza desconocida.
  - Test de medias.
  - Test de diferencias de medias.

Determinar la hipótesis nula y la alternativa.

Formularemos ahora la hipótesis de trabajo en términos de los parámetros del modelo (en el caso de la distribución normal, media y/o desviación típica). Supondremos, por el momento, que la varianza de la población es conocida, $\sigma^2 = (0{,}5)^2$. Por lo que tenemos una hipótesis nula simple.

$$H_0 : \mu = \mu_0 = 12{,}5$$

Los vinos tienen un grado alcohólico medio de 12.5 grados.

$$H_1 : \mu \neq \mu_0 = 12{,}5$$

Hipótesis alternativa bilateral. Los vinos no tienen un grado alcohólico medio de 12.5 grados.

Seleccionar una muestra

- Seleccionamos al azar $n = 14$ individuos y medimos su grado alcohólico.
- Trabajaremos con la media muestral como estimador de la media poblacional desconocida, $\overline{x} = 12{,}529$.

Determinar cual es el estadístico de contraste y su distribución muestral.

La media muestral para distintas muestras sigue una distribución normal $N(\mu, \frac{\sigma}{\sqrt{n}})$, luego, cuando la hipótesis nula es cierta

$$\overline{x} \approx N(\mu_0, \frac{\sigma}{\sqrt{n}})$$

Intuitivamente, aceptaremos la hipótesis nula cuando la media muestral sea próxima a μ_0 y la rechazaremos cuando sea muy diferente, es decir, utilizaremos la media muestral como estadístico de contraste.

Fijar un nivel de significación

- Nos queda por determinar cual es el criterio para decidir si la media muestral está próxima o no al valor teórico propuesto utilizando el concepto de error tipo I, $\alpha = 0{,}05$ o $\alpha = 0{,}01$.
- Nos plantearemos el contraste como un juicio en el que la media muestral es inocente (procede de una población con media μ_0) y no la declararemos culpable (no procede de una población con media μ_0) hasta que no se demuestre claramente lo contrario.

Determinar la región crítica y la región de aceptación

Sobre la distribución de la media seleccionamos dos puntos $\mu_0 - a$ y $\mu_0 + a$, simétricos alrededor de μ_0 de forma que si la hipótesis nula es cierta, en el $(1-\alpha)100\,\%$ de las muestras la media muestral esté entre estos dos valores.

$$P(\mu_0 - a \leq \overline{X} \leq \mu_0 + a) = 1 - \alpha$$

Aceptaremos la hipótesis nula si la media muestral está dentro del intervalo seleccionado y la rechazaremos en caso contrario. El conjunto de valores que nos llevan a aceptar la hipótesis nula forma la región de aceptación y el conjunto de valores que nos llevan a rechazarla, la región crítica.

En la práctica no se trabaja directamente con la media muestral y su distribución asociada sino con la distribución normal estándar. Por lo que reescribiremos el estadístico de la siguiente manera:

$$P(\mu_0 - a \leq \overline{X} \leq \mu_0 + a) = P(-z_{\alpha/2} \leq \frac{\overline{X} - \mu_0}{\sigma/\sqrt{n}} \leq z_{\alpha/2}) = 1 - \alpha$$

Este estadístico mide ahora la discrepancia entre el valor observado de la media y el valor teórico de la misma en la escala de la desviación típica. Y los valores $z_{\alpha/2}$ se denominan **valores críticos** ya que determinan la frontera entre la región crítica y la región de aceptación.

Contraste a partir de la media muestral estandarizada.

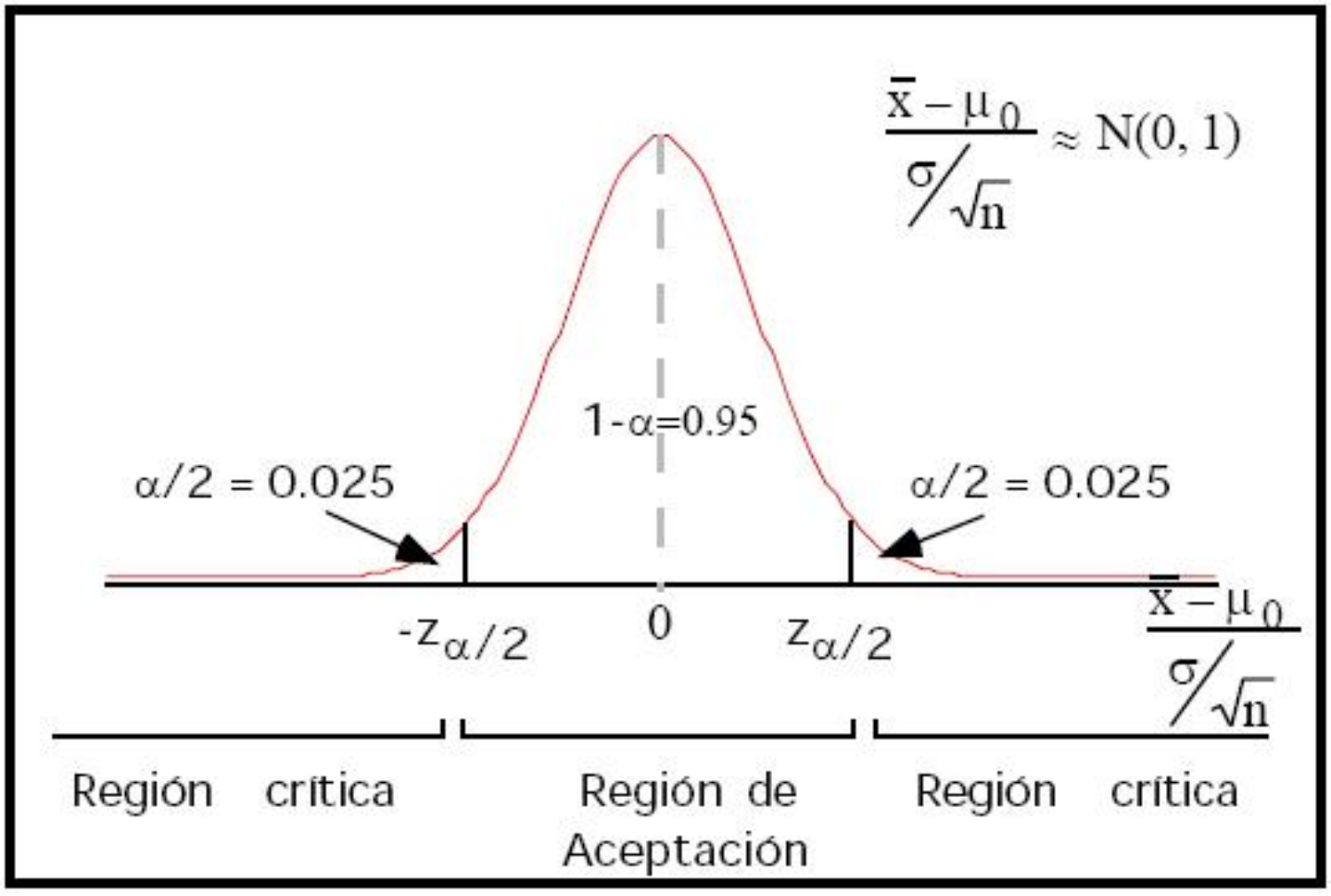

En nuestro ejemplo el valor del estadístico de contraste es:

$$Z = \frac{\overline{X} - \mu_0}{\sigma/\sqrt{n}} = \frac{12{,}529 - 12{,}5}{0{,}5/\sqrt{14}} = 0{,}217$$

Y los correspondientes valores críticos:

- Para $\alpha = 0{,}05$, $z_{0{,}025=1{,}96}$
- Para $\alpha = 0{,}01$, $z_{0{,}005=2{,}57}$

Por lo que el valor del estadístico pertenece a la región de aceptación de la hipótesis nula y podemos concluir que la modificación en el proceso de fabricación no ha modificado significativamente el grado alcohólico.

- Debemos precisar que, aunque hemos tomado la decisión de aceptar la hipótesis nula, no sabemos si ésta es correcta o no, sólo esperamos que en el 95 % de los casos sea cierta.
- Sería más correcto interpretar que, con la información de la que disponemos, no hemos encontrado evidencia suficiente de que la media sea distinta de 12.5.
- Evidentemente los valores muestrales son compatibles con otros posibles valores teóricos.

- Si aumentamos el tamaño de la muestra indefinidamente, la variabilidad de la media sería cada vez menor y conseguiríamos que la pequeña diferencia observada sea lo suficientemente grande como para considerarla significativa.
- Es por esto que se considera tan malo tener un tamaño de muestra demasiado alto como tenerlo demasiado bajo, ya que en el primer caso cualquier pequeña diferencia es considerada como significativa mientras que en el segundo no se declara significación incluso en el caso en el que la diferencia sea elevada.

La potencia del contraste

- Hemos desarrollado el contraste teniendo en cuenta sólo el riesgo de tipo I (la probabilidad de rechazar la hipótesis nula cuando ésta es cierta) pero en un contraste es necesario tener en cuenta también la probabilidad de aceptar la hipótesis nula cuando ésta es falsa (error de tipo II).
- Ambos tipos están asociados, de forma que cuando uno aumenta el otro disminuye.
- En el caso de que la hipótesis alternativa no sea simple hay que calcular el valor de la potencia del contraste para los distintos valores de la misma (función de potencia).

La potencia del contraste. Ejemplo

¿Cúal sería la potencia del contraste obtenido para detectar que la media no es 12.5 si en realidad la media fuera 13 y suponiendo un nivel de significación del 5 %?

$$\begin{cases} H_0 : \mu_0 = 12{,}5 \\ H_1 : \mu_1 = 13 \end{cases}$$

La potencia del contraste se calcularía: $1 - P(H_0 \mid H_1) = 1 - \beta$

- En términos de la media muestral el procedimiento de contraste consiste en aceptar la hipótesis nula si la media muestral está entre $\mu_0 - 0{,}262 \leq \overline{X} \leq \mu_0 + 0{,}262$ con $\mu_0 = 12{,}5$. La probabilidad de cometer un error de tipo II si la media real fuera 13 se podría calcular como la probabilidad de $P(12{,}238 \leq \overline{X} \leq 12{,}762)$ en una normal $N(13, \frac{0{,}5}{\sqrt{14}})$ de forma que la potencia del test es
$\beta = 1 - P(\frac{\overline{X} - \mu_a}{\sigma/\sqrt{n}} \leq \frac{12{,}762 - 13}{0{,}5/\sqrt{14}} = -1{,}776) = 1 - 0{,}037 = 0{,}963$

Cálculo de la potencia de un contraste para una alternativa predeterminada.

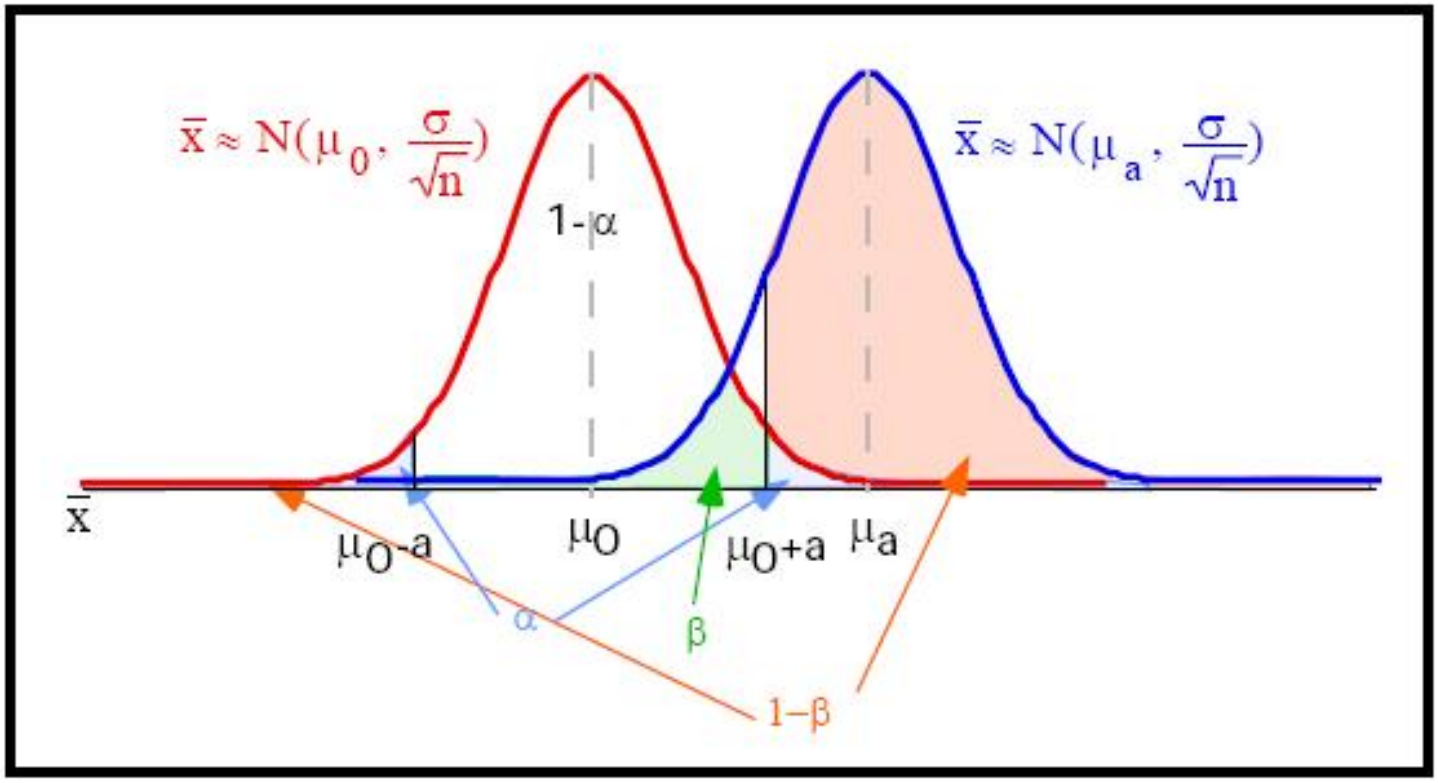

Estudio de potencia para los contrastes no significativos

En la práctica suele hacerse un estudio de potencia para los contrastes no significativos, calculando cual sería el tamaño muestral necesario para que la diferencia observada en los datos sea significativa. Si este tamaño muestral es muy grande es difícil declarar la significación por lo que consideramos que estamos haciendo lo correcto. Si el tamaño muestral necesario es pequeño conveniene revisar el experimento.

El cálculo es muy simple cuando se trabaja con distribuciones normales. La hipótesis nula se rechaza cuando $\frac{\overline{X}-\mu_0}{\sigma/\sqrt{n}} > z_{\frac{\alpha}{2}}$ de forma que, para que la diferencia sea significativa, el valor de n será:

$$\frac{\|\overline{X}-\mu_0\|}{\sigma/\sqrt{n}} > z_{\frac{\alpha}{2}} = 1{,}96$$

con lo que el tamaño de la muestra debería ser mayor que 1142:

$$\sqrt{n}\|\overline{X}-\mu_0\| > z_{\frac{\alpha}{2}}\sigma$$

$$\sqrt{n}\|12{,}529-12{,}5\| > 0{,}98 \rightarrow \sqrt{n} > 33{,}793 \rightarrow n > 1141{,}974$$

Contraste para la diferencias de medias de dos poblaciones normales con datos independientes.

En la investigación aplicada la situación más habitual es aquella en la que se quieren comparar dos poblaciones a las que se les ha aplicado, por ejemplo, dos tratamientos distintos.

Ejemplo.

Siguiendo con el ejemplo anterior vamos ahora a suponer que lo que deseamos conocer es si los vinos de nuestra denominación de origen tienen el mismo contenido alcohólico que los de otra denominación, por ejemplo la de Toro. Se trata de saber si existe una clara diferenciación en los mismos, ya que debido a la proximidad geográfica de ambas regiones, es posible que haya fraudes y se intercambien vinos de ambas dependiendo del mercado de los mismos. La hipótesis de trabajo inicial es, ¿Existen diferencias en el grado alcohólico de ambas denominaciones?.

Hipótesis de trabajo en términos de los parámetros de los modelos.

- Suponemos que en la primera población (Ribera de Duero) el grado alcohólico sigue una distribución normal $N(\mu_1, \sigma_1)$ y en la segunda población (Toro) el grado alcohólico sigue una distribución normal $N(\mu_2, \sigma_2)$.
- Las hipótesis nula y alternativa para el contraste bilateral son ahora:

$$\begin{cases} H_0 : \mu_1 = \mu_2 & (\mu_1 - \mu_2) = 0 \\ H_1 : \mu_1 \neq \mu_2 & (\mu_1 - \mu_2) \neq 0 \end{cases}$$

- Suponemos las varianzas conocidas, $\sigma_1 = 0{,}5$ y $\sigma_2 = 0{,}6$
- Se supone que las muestras se han obtenido de forma independiente en ambas denominaciones.

Estadística descriptiva básica del grado alcohólico.

Descriptiva básica

	grado, Total	grado, Ribera	grado, Toro
Media	12,805	12,529	13,450
Desv. Tip.	,557	,338	,409
Error Estd.	,124	,090	,167
n	20	14	6
MinimO	11,900	11,900	13,000
Maximo	14,000	13,000	14,000

Estadístico de contraste.

- Conocemos la distribución de la media muestral en ambas poblaciones:

$$\overline{x}_1 \approx N(\mu_1, \frac{\sigma_1}{\sqrt{n_1}}) \qquad \overline{x}_2 \approx N(\mu_2, \frac{\sigma_2}{\sqrt{n_2}})$$

- y ambas distribuciones son independientes.
- El estimador de la diferencia de medias poblacionales será la diferencia de medias muestrales y, como la diferencia de normales independientes es también una distribución normal,

$$\overline{x}_1 - \overline{x}_2 \approx N(\mu_1 - \mu_2, \sqrt{\frac{\sigma_1^2}{n_1} + \frac{\sigma_2^2}{n_2}})$$

- Estandarizando se obtiene:

$$Z = \frac{(\overline{x}_1 - \overline{x}_2) - (\mu_1 - \mu_2)}{\sqrt{\frac{\sigma_1^2}{n_1} + \frac{\sigma_2^2}{n_2}}} \approx N(0,1)$$

- Cuando la hipótesis nula es cierta $\mu_1 - \mu_2 = 0$ se tiene

$$Z = \frac{(\overline{x}_1 - \overline{x}_2)}{\sqrt{\frac{\sigma_1^2}{n_1} + \frac{\sigma_2^2}{n_2}}} \approx N(0,1)$$

- Y se realizan el contraste bilateral y los unilaterales como antes.

Valor del estadístico en el ejemplo.

$$Z = \frac{(12{,}529 - 13{,}450)}{\sqrt{\frac{0{,}25}{14} + \frac{0{,}36}{6}}} = -10{,}829$$

- Y para un nivel de significación $\alpha = 0{,}05$ el valor del contraste será $z_{0{,}025} = 1{,}96$
- Y para un nivel de significación $\alpha = 0{,}01$ el valor del contraste será $z_{0{,}005} = 2{,}57$
- **Decisión estadística:** El valor del estadístico de contraste pertenece a la región crítica, por tanto rechazamos la hipótesis nula.
- **Conclusión:** El grado alcohólico medio es significativamente diferente en las denominaciones de origen Ribera de Duero y Toro.

Contraste para la diferencias de medias de dos poblaciones normales con varianzas desconocidas pero iguales.

La distribución de la diferencia de medias muestrales es ahora:

$$Z = \frac{(\overline{x}_1 - \overline{x}_2) - (\mu_1 - \mu_2)}{\sigma\sqrt{\frac{1}{n_1} + \frac{1}{n_2}}} \approx N(0,1)$$

- Tenemos que eliminar el parámetro σ, para lo cual utilizaremos las distribuciones muestrales asociadas a las cuasi-varianzas muestrales por ser estas estimadores insesgados de la varianza poblacional.

$$\frac{(n_1 - 1)\hat{S}_1^2}{\sigma^2} \approx \chi^2_{n_1-1} \qquad \frac{(n_2 - 1)\hat{S}_2^2}{\sigma^2} \approx \chi^2_{n_2-1}$$

- La suma de dos ji-cuadrado es también una ji-cuadrado, con lo que sumando las dos anteriores:

$$\frac{(n_1-1)\hat{S}_1^2}{\sigma^2}+\frac{(n_2-1)\hat{S}_2^2}{\sigma^2}=$$

$$\frac{(n_1-1)\hat{S}_1^2+(n_2-1)\hat{S}_2^2}{\sigma^2}\approx\chi^2_{n_1+n_2-2}$$

- Suponiendo que ambas distribuciones son independientes, podemos combinarlas par obtener una distribución t de Student con $n_1 + n_2 - 2$ grados de libertad.

$$t = \frac{\frac{(\overline{x}_1 - \overline{x}_2) - (\mu_1 - \mu_2)}{\sigma\sqrt{\frac{1}{n_1} + \frac{1}{n_2}}}}{\sqrt{\frac{\frac{(n_1-1)\hat{S}_1^2 + (n_2-1)\hat{S}_2^2}{\sigma^2}}{n_1+n_2-2}}}$$

- Si la hipótesis nula es cierta utilizaremos el siguiente estadístico:

$$t = \frac{\frac{(\overline{x}_1 - \overline{x}_2)}{\sigma\sqrt{\frac{1}{n_1}+\frac{1}{n_2}}}}{\sqrt{\frac{\frac{(n_1-1)\hat{S}_1^2+(n_2-1)\hat{S}_2^2}{\sigma^2}}{n_1+n_2-2}}}$$

- Se ha estimado la varianza común de ambas poblaciones mediante una media ponderada de las varianzas estimadas en cada población.

- Es necesario que las varianzas sean iguales para poder despejarlas y eliminarlas en el cálculo del estadístico de contraste. La comprobación de la igualdad de varianzas se hace posteriormente aunque sea un paso previo a la decisión del tipo de contraste.
- Las cuestiones relacionadas con la potencia del contraste se interpretan de la misma manera que en todos los casos anteriores.

Valor del estadístico en el ejemplo.

$$Z = \frac{(12{,}529 - 13{,}450)}{0{,}359\sqrt{\frac{1}{14} + \frac{1}{6}}} = -5{,}256$$

- Y para un nivel de significación $\alpha = 0{,}05$ el valor del contraste será $t_{18,0,025} = 2{,}101$
- Y para un nivel de significación $\alpha = 0{,}01$ el valor del contraste será $z_{18,0,005} = 2{,}878$
- **Decisión estadística:** El valor del estadístico de contraste pertenece a la región crítica, por tanto rechazamos la hipótesis nula.
- **Conclusión:** El grado alcohólico es significativamente diferente en las denominaciones de origen Ribera de Duero y Toro.

Significado e interpretación de los P-valores

Definición. En el ámbito del test de hipótesis estadísticas se define el p-valor como la probabilidad de obtener un resultado al menos tan extremo como el encontrado realmente, suponiendo que la hipótesis nula es cierta. Esta suposición de que la hipótesis nula es cierta es crucial para la correcta interpretación de los p-valores.

El P-valor, que depende directamente de la muestra dada, intenta dar una medida de la veracidad de los resultados obtenidos en el test de la hipótesis nula, frente al enfoque clásico de rechazar o no la hipótesis. Si la hipótesis nula es cierta y la variación aleatoria es la única explicación de las diferencias entre las muestras, entonces el p-valor es un medida cuantitativa a tener en cuenta como evidencia en el proceso de decisión.

Interpretación.

- El p-valor mide la evidencia en contra de la hipótesis nula. Cuanto más pequeño, mayor evidencia en contra.
- En este sentido está relacionado únicamente con la hipótesis nula y no tiene nada que ver con la alternativa.

Por ejemplo, el p-valor para el contraste se puede calcular en una distribución normal como:

$$P(|Z| > \frac{\overline{X} - \mu_0}{\sigma/\sqrt{n}})$$

Y para el ejemplo anterior el p-valor es
$1 - P(-0{,}217 < Z < 0{,}217) = 2P(Z > 0{,}217) = 0{,}8285$. En este caso el p-valor puede considerarse grande por lo que se aceptaría la hipótesis nula.
En la práctica se suele adoptar el criterio de aceptar la hipótesis cuando el p-valor es mayor que el nivel de significación fijado en el procedimiento de contraste.

El p-valor de un contraste bilateral.

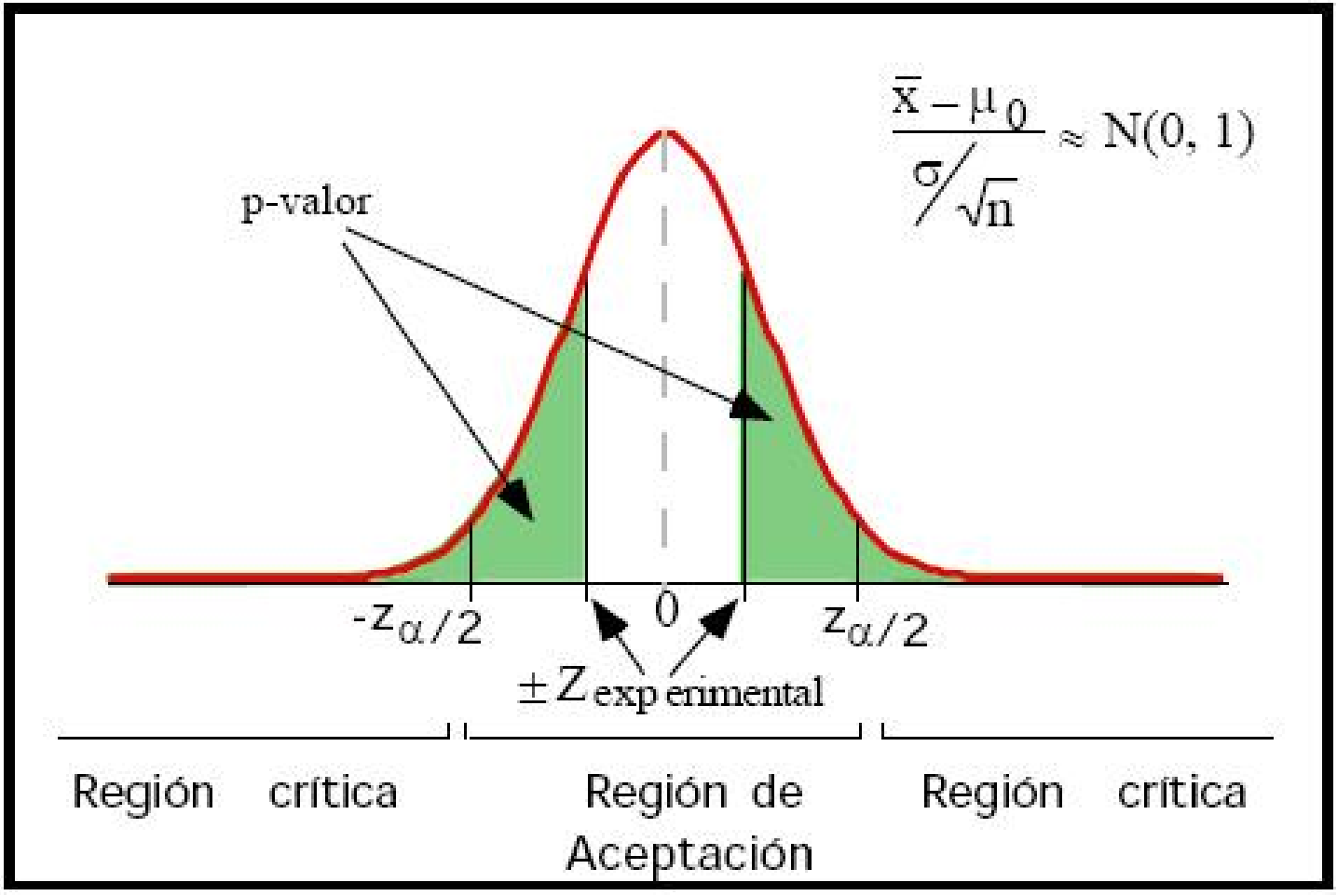

Los contrastes unilaterales.

En algunas situaciones no estamos interesados en todos los posibles valores de la hipótesis alternativa propuesta en un contraste bilateral. En este caso es conveniente modificar la hipótesis alternativa para que sea de la forma $H_a : \mu > \mu_0$ o $H_a : \mu > \mu_0$

Contraste con varianza desconocida.

En la mayor parte de las aplicaciones prácticas la varianza de la distribución es también desconocida y ha de ser estimada a partir de los datos. El problema es que ya no es posible seguir utilizando la distribución normal para el procedimiento de contraste ya que es necesario eliminar el parámetro σ del estadístico de contraste.

Test de medias. Eliminación del parámetro σ

De acuerdo con la teoría:

- Usando la media muestral tenemos el estadístico $\frac{\overline{X}-\mu_0}{\sigma/\sqrt{n}}$ que sigue una distribución normal $N(0,1)$
- Usando la varianza muestral tenemos el estadístico $\frac{(n-1)\hat{S}}{\sigma^2}$ que sigue una distribución ji-cuadrado con n-1 grados de libertad.
- Si suponemos que media y varianza son independientes, es posible combinar las correspondientes distribuciones muestrales para obtener una distribución t de Student y eliminar el parámetro σ.

Usando la definición de la t de Student con n-1 grados de libertad como el cociente entre una normal estándar y la raiz cuadrada de una ji-cuadrado con n-1 grados de libertad dividida por sus grados de libertad, y ambas independientes, obtenemos que la variable aleatoria formada por el cociente sigue una distribución t de Student con n-1 grados de libertad.

$$t = \frac{\frac{\overline{X}-\mu_0}{\sigma/\sqrt{n}}}{\sqrt{\frac{\frac{(n-1)\hat{S}}{\sigma^2}}{(n-1)}}} = \frac{\overline{X}-\mu_0}{\frac{\hat{S}}{\sqrt{n}}}$$

Contraste para la diferencias de medias de dos poblaciones normales con varianzas desconocidas pero iguales.

Supongamos ahora que las varianzas son desconocidas y distintas ($\sigma_1 \neq \sigma_2$) de forma que ya no es posible eliminar el parámetro en el cálculo de la t de Student. Se han propuesto distintas aproximaciones para el cálculo de la distribución de Welch.

El estadístico de contraste que utilizamos es:

$$t = \frac{(\overline{x}_1 - \overline{x}_2)}{\sqrt{\frac{\hat{S}_1^2}{n_1} + \frac{\hat{S}_2^2}{n_2}}}$$

La distribución del estadístico cuando la hipótesis nula es cierta es una t de Student t_f donde f es el entero más próximo a :

$$f = \frac{(\frac{\hat{S}_1^2}{n_1} + \frac{\hat{S}_2^2}{n_2})^2}{\frac{(\frac{\hat{S}_1^2}{n_1})^2}{n_1+1} + \frac{(\frac{\hat{S}_2^2}{n_2})^2}{n_2+1}} - 2$$

Métodos de segmentación y corrección de la inhomogeneidad de intensidad en imágenes de RM

Maite García-Sebastián & Manuel Graña

Grupo de Inteligencia Computacional

www.ehu.es/ccwintco

JIC II (13/05/2008)

maite.garciasebastian@gmail.com

Índice

- Introducción
- Fuentes físicas de la inhomogeneidad
- Revisión de varias aproximaciones
  - Modelo imagen
  - Función de energía
  - Modelo computacional
  - Validación: datos experimentales y resultados
- Métodos de validación
  - Bases de datos benchmark
  - Estrategias de evaluación
- Referencias

Introduction (Definitions)

- [1] (*Magnetic Resonance - Technology Information Portal)*
  - (NMR) **Nuclear Magnetic Resonance** is a physical phenomenon of the magnetic property of nuclei, which have a positive nuclear spin quantum number. The use of nuclear magnetic resonance principles produces extremely detailed pictures of the body tissue without the need for x-ray exposure and gives diagnostic information of various organs.
  - (MRI) **Magnetic resonance imaging** is a noninvasive medical imaging technique that uses the interaction between radio frequency pulses, a strong magnetic field and body tissue to obtain images of slices/planes from inside the body.

- An **image artifact** is a structure not normally present but visible as a result of
  - a limitation or malfunction in the hardware
  - or software of the MRI device
  - or in other cases a consequence of environmental influences as heat or humidity or it can be caused by the human body (blood flow, implants etc.).

  The knowledge of MRI artifacts (brit. artefacts) and noise producing factors is important for continuing maintenance of high image quality. Artifacts may be very noticeable or just a few pixels out of balance but can give confusing artifactual appearances with pathology that may be misdiagnosed.

- (IIH) **Intensity inhomogeneity** is an MRI artifact. It is also termed as
  - Intesity nonuniformity
  - Shading
  - Bias field
  - Gain field

  The sources of IIH are generally divided in two groups [2]
  - Related to properties of the MRI device such as static field inhomogeneity, RF signal energy spatial distribution and others
  - Related to the imaged object itself such as the specific magnetic permeability and dielectric properties of the imaged object

Fuentes físicas de la IIH

- Inhomogeneidad del emisor-receptor de RF: poca uniformidad de la bobina emisora-receptora de RF
- Remolinos magnéticos en el campo debido a los movimientos de los magnetos-gradiente
- Anatomía del paciente
- Geometría y propiedades eléctricas del sujeto
- Parámetros de la adquisición de la imagen
  - Secuencia de pulsos y polarización de la bobina

Articulos revisados

- Algoritmos no paramétricos
  - [3] Sled, 1998
  - [4] Rajapakse, 1998
  - [7] Ahmed, 2002
- Algoritmos paramétricos
  - [8] Styner, 2000
  - [9] Zagorodnov, 2005
  - [10] Maite G-S, Elsa F., Manuel G., 2007

Sled et al. 1998 [3]

- Algoritmo N3 (http://www.bic.mni.mcgill.ca/software/N3/)
- Método de normalización de intensidad no uniforme y no paramétrico
- Muy utilizado para la corrección del artefacto de intensidad en T1

Modelo de la imagen

$$v(\mathbf{x}) = u(\mathbf{x})f(\mathbf{x}) + n(\mathbf{x})$$

u is the true signal emitted by the tissue,

f is an unknown smoothly varying bias field

n is white Gaussian noise assumed to be independent of u.

$$\hat{u}(\mathbf{x}) = \log[u(\mathbf{x})]$$

$$\hat{v}(\mathbf{x}) = \hat{u}(\mathbf{x}) + \hat{f}(\mathbf{x}).$$

Let U, V, and F be the probability densities of $\hat{u}$, $\hat{v}$, and $\hat{f}$, respectively.

- f y u se suponen variables aleatorias e independientes.
- La ddp de V es la convolución de las ddp F y U,

$$V(\hat{v}) = F(\hat{v}) * U(\hat{v}) = \int F\left(\hat{v} - \hat{f}\right) U\left(\hat{f}\right) d\hat{f}.$$

Método computacional

- La tarea de corregir la IIH corresponde a restaurar las frecuencias de U (la ddp de la imagen original)
- Objetivo: encontrar F que maximiza el contenido frecuencial de U

- Aproximación:
  - Considera F gausiana
  - Puesto que una gausiana puede descomponerse en convolucion de gausianas mas estrechas
  - Es posible explorar el espacio de ddp U deconvolucionando progresivamente

- ddp de IIH calculados sobre diferentes scans segmentados manualmente T1, T2 y PD.

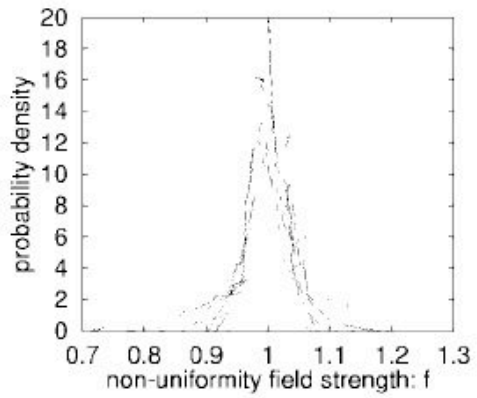

(a)

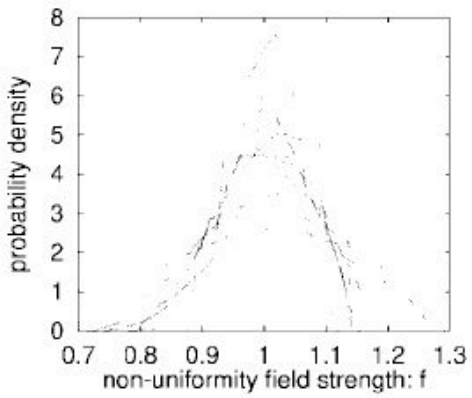

(b)

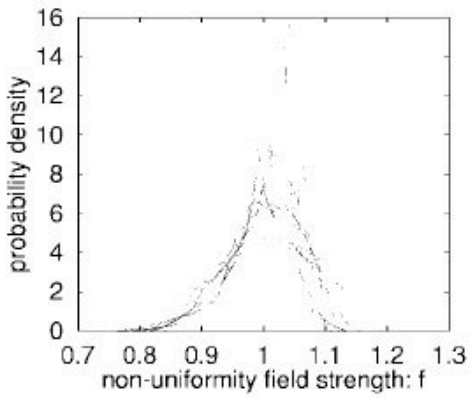

(c)

Fig. 1. Probability densities for fields estimated from white matter on MR scans of 12 individuals taken with 12 different MR scanners. Note that these are the distributions of the intensities f rather than log intensities $\hat{f}$. The T1 scan is a gradient-echo 3-D acquisition with TE = 11 ms and TR = 35 ms, while the proton density (PD) and T2 scans are two echoes TE = 30 ms and TE = 80 ms of a multislice spin echo acquisition with TR = 3 s. (a) T1-weighted, (b) T2-weighted, and (c) PD-weighted.

- Estimación de *u* en un voxel **x** a partir de la observacion *v* conocidos *F y U*

$$E[\hat{u}|\hat{v}] = \frac{\int_{-\infty}^{\infty} \hat{u}F(\hat{v}-\hat{u})U(\hat{u})\,d\hat{u}}{\int_{-\infty}^{\infty} F(\hat{v}-\hat{u})U(\hat{u})d\hat{u}}.$$

- Podemos estimar el campo de inhomogeneidad en **x** como

$$\hat{f}_e(\hat{v}) = E\left[\hat{f}|\hat{v}\right] = \hat{v} - E[\hat{u}|\hat{v}]$$

- Y suavizarlo con un operador *S*

$$\hat{f}_s(\hat{v}) = S\left\{\hat{f}_e(\hat{v})\right\} = S\{\hat{v} - E[\hat{u}|\hat{v}]\}$$

- Dadas las distribuciones F y V, la ddp U puede estimarse usando un filtro de deconvolución

$$\tilde{G} = \frac{\tilde{F}^*}{|\tilde{F}|^2 + Z^2}$$
$$\tilde{U} \approx \tilde{G}\,\tilde{V}$$

where * denotes complex conjugate, $\tilde{F}$ is the Fourier transform of F, and Z is a constant term to limit the magnitude of $\tilde{G}$.

Ilustración de la transformación que da el campo de IIH

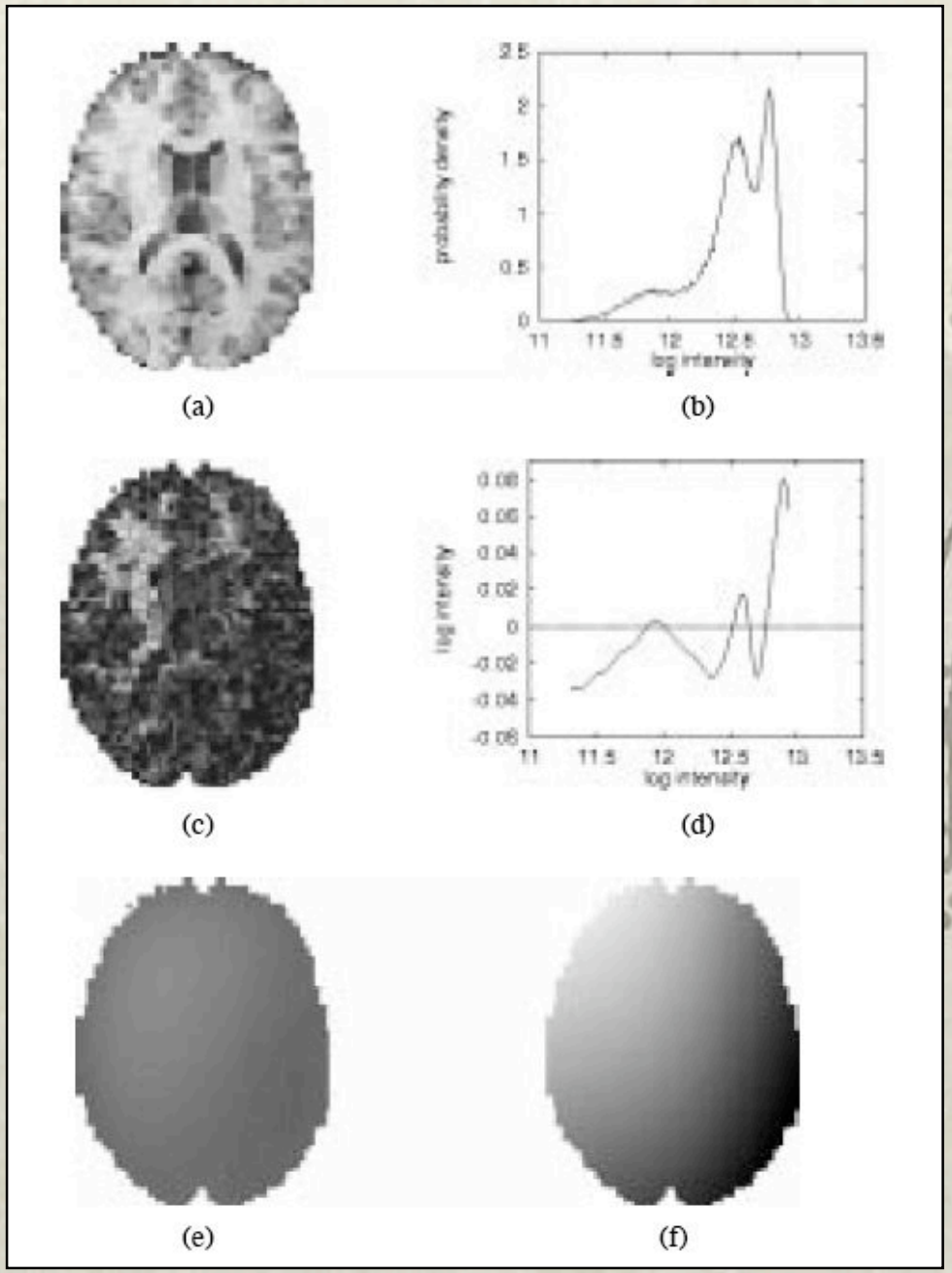

Dependencia de los parámetros

•d, el suavizado de f_e

•FWHM, anchura del kernel de deconvolución

El equilibrio entre la exactitud y la convergencia del algoritmo depende de FWHM

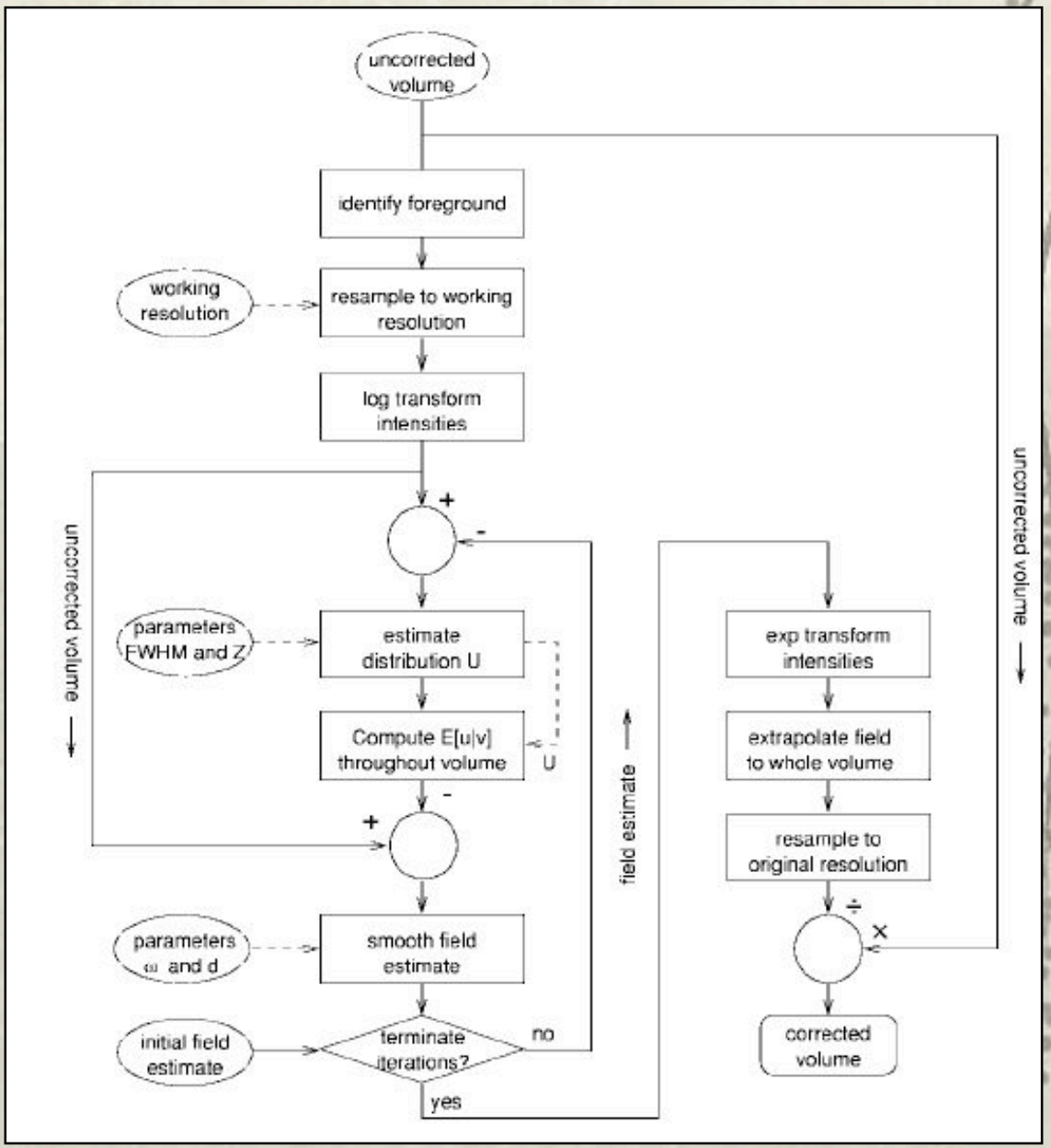

- Estimación de V (parzen windows)

$$V(\hat{v}_j) = \frac{1}{N}\sum_{i=1}^{N}\frac{1}{h}\varphi\left[\frac{\hat{v}_j - \hat{v}(\mathbf{x}_i)}{h}\right]$$

$$\varphi(s) = \begin{cases} 1-|s| & |s|<1 \\ 0, & \text{elsewhere} \end{cases}$$

Suavizado

- Una resolución menor de los datos no tiene efectos sigificativos en la estimación del bias.
- Es un paso crítico
  - Aproximación con B splines

Validación

- Imágenes reales y simuladas
- Imágenes simuladas
  - Ruido aditivo con distribución de Rician
  - Ruido multiplicativo aleatorio creado por *rejection sampling* (resolución inicial 10-mm, se va remuestreando hasta 1-mm)

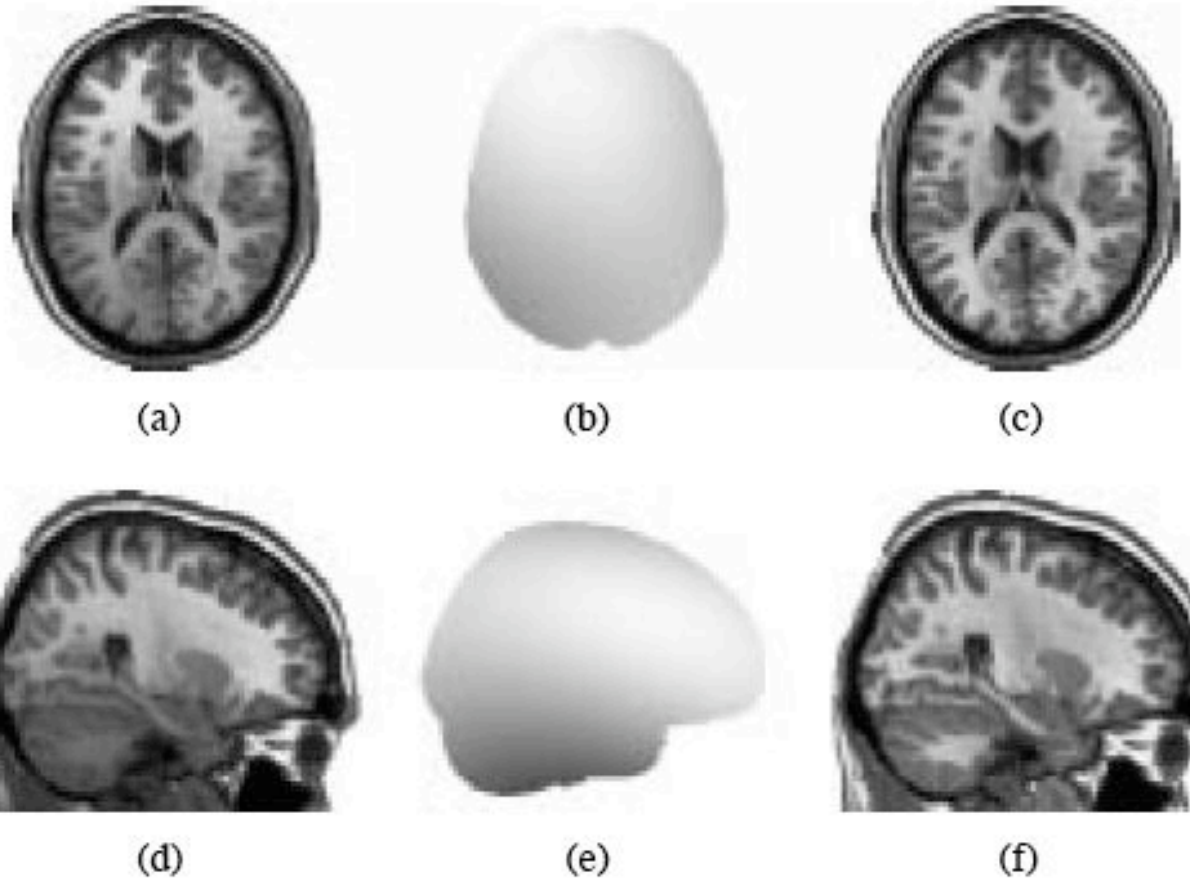

Fig. 12 Intensity nonuniformity correction of a T1 weighted 27-scan averaged gradient-echo MR scan: (a) and (d) transaxial and sagittal views of uncorrected data; (b) and (e) nonuniformity field estimated by the N3 method; (c) and (f) corrected data.

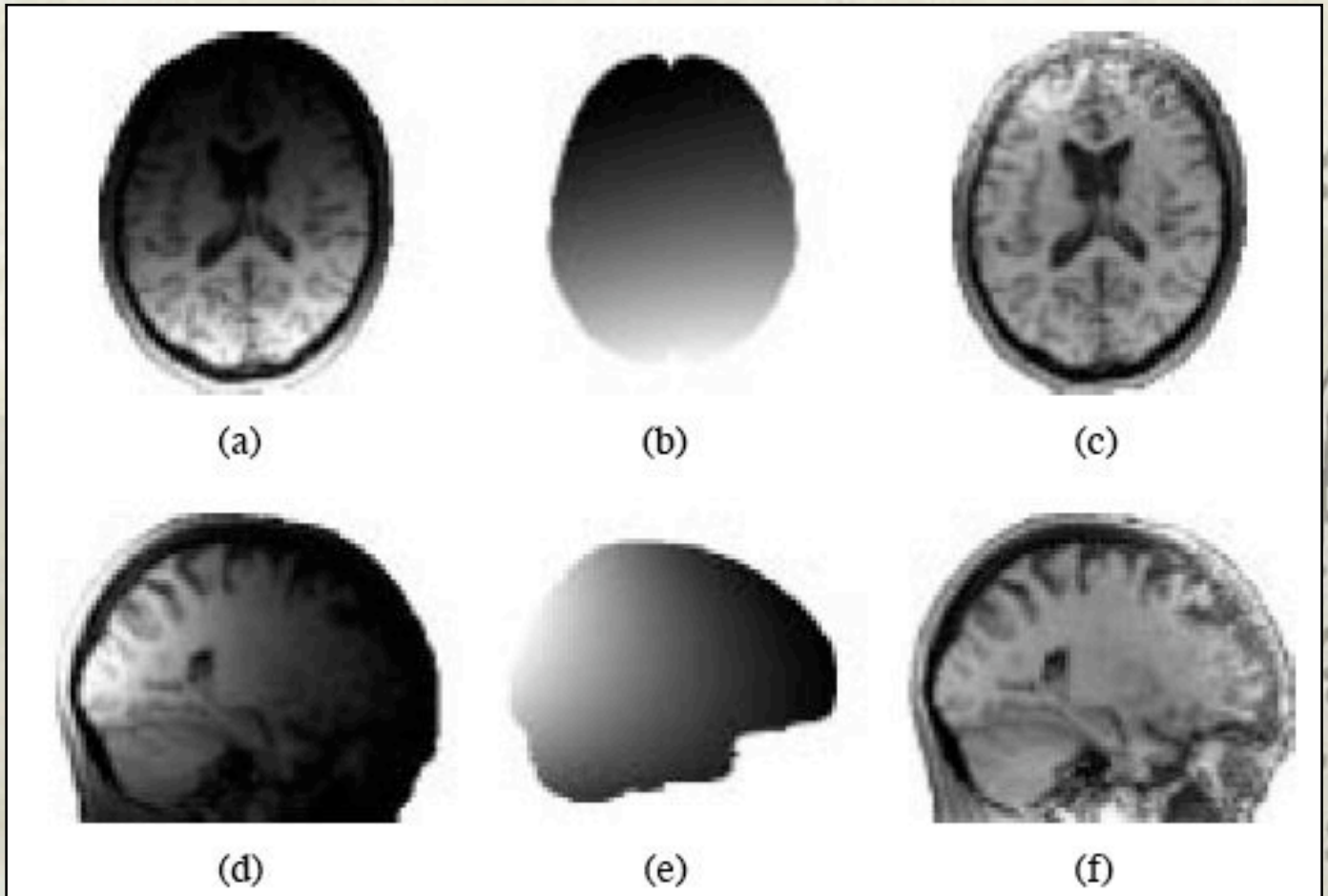

Fig. 13. Intensity nonuniformity correction of a surface coil MR scan: (a) and (d) transaxial and sagittal views of uncorrected data; (b) and (e) nonuniformity field estimated by the N3 method; (c) and (f) corrected data.

Rajapakse,1998 [4]

- Algoritmo Biased MAP (BMAP)
- Algoritmo Bayesiano basado en MRF
- Dos estimaciones interdependientes
  - estimación MAP de la clasificación dado un campo de inhomogeneidad
  - estimación ML del campo de inhomogeneidad dada una clasificación

Modelo de formación de la imagen

The image is denoted by $\mathbf{y} = (y_i: i \in I)$ where y_i is the intensity of the voxel at site i.

$i \subset I$; $I \subset \mathbf{N}^3$.

the space of the tissue classes is $\Lambda = \{1, 2, \ldots, K\}$

K different classes

segmentation of the image $\mathbf{x} = (x_i: i \in I)$.

$x_i = k$

Modelo de formación de la imagen

$$y_i = (1 + \beta_i)\mu_{x_i} + \eta_i,$$

μ_{x_i} denotes the mean intensity of the tissue class,

η_i denotes the random noise signal

β_i the varia tion of the gain of the intensity due to the intensity inhomo-geneities at the site i.

if $x_i = k$, $\eta_i \sim N(0, \sigma_k^2)$

Inhomogeneidades dependientes de la localización

Modelo computacional

Rajapakse 1998- modelo bayesiano basado en MRF

The class conditional probability at the voxel site i is written as:

$$p(y_i|x_i=k)\frac{1}{\sqrt{2\pi\sigma_k^2}}\exp\left\{-\frac{1}{2}\left(\frac{y_i-(1+\beta_i)\mu_k}{\sigma_k}\right)^2\right\},$$

$\beta = (\beta_i: i \in I)$ represents the bias field.

$\theta_k = (\mu_k, \sigma_k)$ and $\theta = (\theta_k: k \in \Lambda)$, the measurement model parameters are given by (β, θ).

$$p(\mathbf{y}|\mathbf{x}) = \prod_{i\in I} p(y_i|x_i).$$

Ruido blanco

Por el teorema de Hammersly-Clifford [5], la probabilidad a priori de un MRF viene dada por una distribución de Gibbs [6]

The *prior model*

$$p(\mathbf{x}) = \frac{1}{Z} \exp\{ - \sum_{c \in C} V_c(\mathbf{x})\},$$

The potential energy of the MRF may be written as:

$$\sum_{c \in C} V_c(\mathbf{x}) = \sum_{i \in I} \{V_1(x_i) + V_2(x_i)\},$$

singletons

$$V_1(x_i) = \sum_{k \in \Lambda} - \alpha_{0k} \delta(x_i = k),$$

doubletons,

$$V_2(x_i) = \sum_{i,j \in c_l} \{ - \alpha_l \delta(x_i = x_j) + \alpha_l \delta(x_i \neq x_j) \},$$

c_l Cliqués de orden 2 en un vecindario de radio l

$$c_l(i) = \left\{ j : j \in I, \|i - j\| < \sqrt{l}, i \neq j \right\}$$

prior model parameters

$$\alpha = (\alpha_{0k}, \alpha_1, \alpha_2 : k \in \Lambda).$$

MAP estimation

the optimal segmentation $\mathbf{x} = \mathbf{x}^*$

$$\mathbf{x}^* = \arg \max_{\mathbf{x}} \; p(\mathbf{x}|\mathbf{y}).$$

La probabilidad a priori de la imagen es independiente de la segmentación

$$p(\mathbf{x}|\mathbf{y}) \propto p(\mathbf{y}|\mathbf{x})p(\mathbf{x}).$$

$$\mathbf{x}^* = \arg \max_{x} \; p(\mathbf{y}|\mathbf{x}, \beta^*, \theta^*)p(\mathbf{x}|\alpha^*),$$

Segmentación

- El ruido es independiente en cada pixel, por lo que las probabilidades condicionadas también lo son

$$p(\mathbf{y}|\mathbf{x}) = \prod_{i \in I} p(y_i|x_i).$$

- La probabilidad a posteriori es proporcional a la exponencial de la energia global

$$p(\mathbf{x}|\mathbf{y}) \propto \exp\{-U(\mathbf{x}|\mathbf{y})\},$$

$$U(\mathbf{x}|\mathbf{y}) = \sum_{i \in I} U_i(x_i|x_j, y_i,\ j \neq i)$$

- Energias locales en cada voxel

$$U_i(x_i|x_j,\ y_i,\ j \neq i) = \frac{1}{2}\left(\frac{y_i - (1+\beta_i)\mu_{x_i}}{\sigma_{x_i}}\right)^2 + \log(\sigma_{x_i}) + V_1(x_i) + V_2(x_i).$$

Ruido gausiano

Campo markoviano que modela la distribución a priori

- Pasos de la estimación MAP rigurosa

$$\hat{\mathbf{x}} = \arg \min_{x} U(\mathbf{x}|\mathbf{y}, \hat{\beta}, \hat{\theta}, \hat{\alpha}),$$

$$(\hat{\beta}, \hat{\theta}) = \arg \max_{\beta, \theta} p(\mathbf{y}|\hat{\mathbf{x}}, \boldsymbol{\beta}, \boldsymbol{\theta}),$$

$$\hat{\alpha} = \arg \max_{\alpha} p(\boldsymbol{\alpha}|\hat{\mathbf{x}}),$$

- Algoritmo Iterated Conditioned Means (ICM) aproximación voraz (greedy): Biased MAP (BMAP)
  - Minimiza la energía local para la segmentación

$$\hat{x}_i = \arg \min_{x_i} U_i(x_i | x_j,\ y_i,\ \hat{\beta},\ \hat{\theta},\ \hat{\alpha},\ j \neq i).$$

Incialización del ICM

- Energía inicial sin bias ni prior

$$U^0(\mathbf{x}|\mathbf{y}) = \sum_{k\in\Lambda}\sum_{i\in R_k}(y_i-\mu_k)^2,$$

$$R_k = \{i : x_i = k,\ i \in I\}.$$

La segmentación inicial se puede hacer con el k-means.

- Estimación de los parámetros del modelo a priori (depende de la segmentación)

$$\hat{\alpha}_{0k} = \log \frac{|R_k|}{\sum_{j \in \Lambda} |R_j|},$$

- Estimación de los parámetros del modelo de medida (conditional prob.):
  - Minimización log-verosimilitud

$$-\log P(\mathbf{y}|\hat{\mathbf{x}}\,\boldsymbol{\beta},\,\boldsymbol{\theta}) = \frac{1}{2}\sum_{k\in\Lambda}\sum_{i\in R_k}\left(\frac{y_i-(1+\beta_i)\mu_k}{\sigma_k}\right)^2 + \sum_{k\in\Lambda}\sum_{i\in R_k}\log(\sigma_k).$$

- Diferenciando e igualando a cero

$$\hat{\mu}_k = \frac{\sum_{i \in R_k} y_i (1 + \beta_i)}{\sum_{i \in R_k} (1 + \beta_i)^2},$$

$$\hat{\sigma}_k^2 = \frac{\sum_{i \in R_k} (y_i - (1 + \beta_i)\hat{\mu}_k)^2}{|R_k|}.$$

$$\hat{\beta}_i = \frac{y_i}{\hat{\mu}_{x_i}} - 1.0.$$

El bias se filtra con un filtro pasa bajo

begin
Initialize segmentation with k-means algorithm
Find $\hat{\alpha}$ and $\hat{\theta}$ using initial segmentation
Set Flips = LARGE and $\hat{\beta} = 0$
Until (Flips > threshold)
Flips = 0
For all sites $i \in I$
  Find $\hat{x} = \arg\min_{k \in \Lambda} U_i(x_i = k|\mathbf{y}, \mathbf{x})$
  If (x_i is not the previous class at i)
  Flips = Flips + 1
  Update β_i
Repeat

Filter the bias field
Compute $\hat{\theta}$ using current segmentation

Continue
end

Validación experimental

- Rajapkse 1998
  - Cuatro conjuntos de datos reales
  - Segmentación manual de referencia en slices seleccionados
  - Datos sintéticos

Table 1
The image model parameters obtained for a two-class {Gray matter, White matter} segmentation of a shelled representative three-dimensional SPGR head scans with a T_{sk}-means initialization and the final BMAP segmentation

Model Parameters	Initial (T_{sk}-means)	Final (BMAP)
$(\mu_{\text{Gray}}, \sigma_{\text{Gray}})$	(63.34, 6.16)	(61.23, 13.40)
$(\mu_{\text{White}}, \sigma_{\text{White}})$	(84.0, 6.0)	(96.00, 7.16)
$(\alpha_{0\text{Gray}}, \alpha_{0\text{White}})$	(0.599, 0.401)	(0.522, 0.355)
(α_1, α_2)	(0.706, − 0.022)	(0.713, − 0.002)
$(\beta_{\max}, \beta_{\min})$	–	(− 0.256, 0.188)

Segmentación en dos clases (WM y GM)

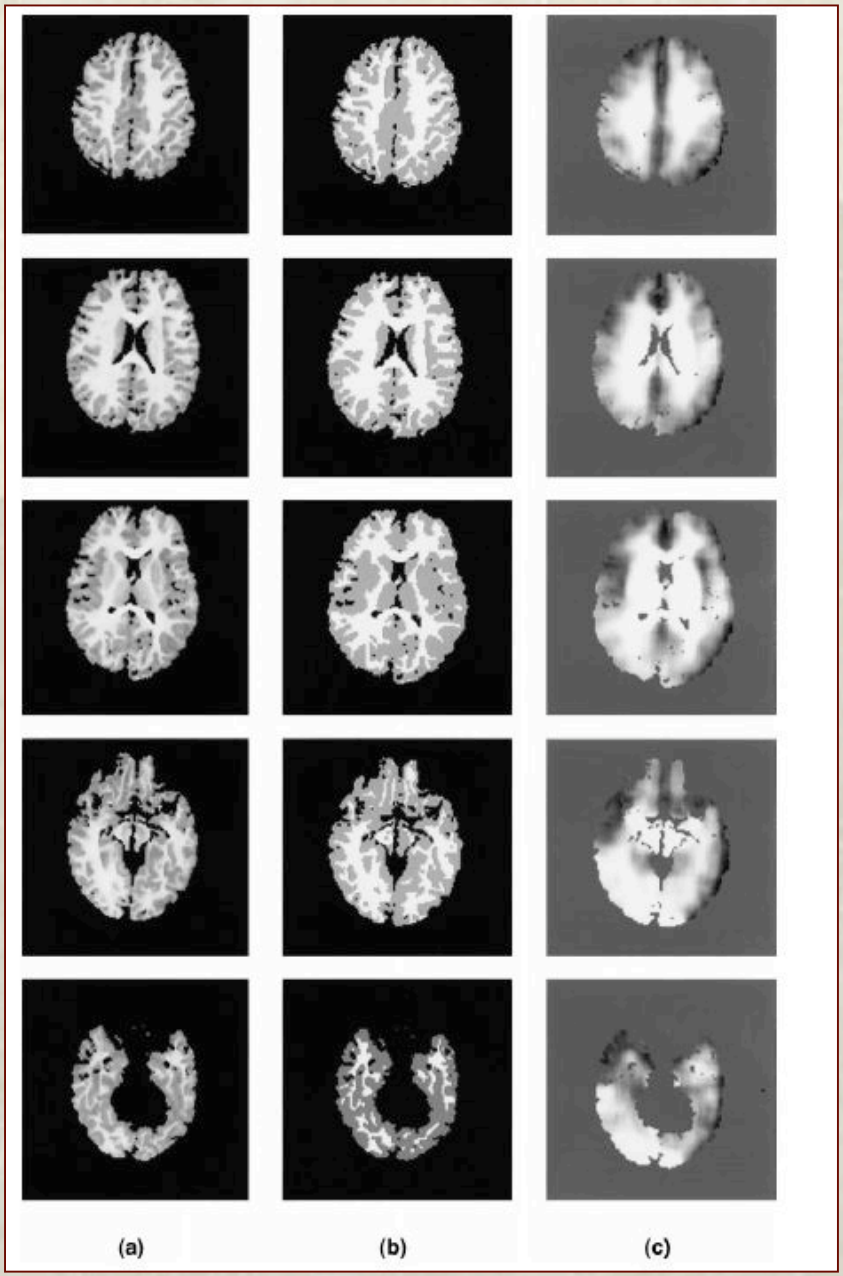

Ahmed 2002 [7]

- Algoritmo no paramétrico
- Segmentación Fuzzy de imágenes de RM
- Estimación de la IIH utilizando *fuzzy logic*

Modelo de la imagen

- Modelo de la imagen

$$Y_k = X_k G_k \qquad \forall\, k \in \{1, 2, \ldots, N\}$$

logaritmo

$$y_k = x_k + \beta_k \qquad \forall\, k \in \{1, 2, \ldots, N\}$$

Función objetivo

- Fuzzy C means objective function

$$J = \sum_{i=1}^{c} \sum_{k=1}^{N} u_{ik}^{P} \|x_k - v_i\|^2$$

$\{v_i\}_{i=1}^{c}$ are the prototypes of the clusters

$[u_{ik}] = U$ represents a partition matrix, $U \in \mathcal{U}$,

$$\mathcal{U}\left\{u_{ik} \in [0, 1] \left| \sum_{i=1}^{c} u_{ik} = 1 \ \forall k \text{ and } 0 < \sum_{k=1}^{N} u_{ik} < N \ \forall i \right.\right\}. \quad (4)$$

- Regularización de la función objetivo de FCM

$$J_m = \sum_{i=1}^{c}\sum_{k=1}^{N} u_{ik}^{p}\|x_k - v_i\|^2 + \frac{\alpha}{N_R}\sum_{i=1}^{c}\sum_{k=1}^{N} u_{ik}^{p}\left(\sum_{x_r \in \mathcal{N}_k}\|x_r - v_i\|^2\right)$$

$\mathcal{N}_k$ stands for the set of neighbors

N_R is the cardinality of $\mathcal{N}_k$

- Aplicada a las imagenes MRI

$$J_m = \sum_{i=1}^{c}\sum_{k=1}^{N} u_{ik}^{p}\|y_k - \beta_k - v_i\|^2 + \frac{\alpha}{N_R}\sum_{i=1}^{c}\sum_{k=1}^{N} u_{ik}^{p}\left(\sum_{y_r \in \mathcal{N}_k}\|y_r - \beta_r - v_i\|^2\right)$$

- Formalización del problema de estimación

$$\min_{U,\{v_i\}_{i=1}^{c},\{\beta_k\}_{k=1}^{N}} J_m, \qquad \text{subject to } U \in \mathcal{U}.$$

Usando multiplicadores de Lagrange

$$F_m = \sum_{i=1}^{c}\sum_{k=1}^{N}\left(u_{ik}^{p} D_{ik} + \frac{\alpha}{N_R} u_{ik}^{p}\gamma_i\right) + \lambda\left(1 - \sum_{i=1}^{c} u_{ik}\right)$$

$$D_{ik} = \|y_k - \beta_k - v_i\|^2$$

$$\gamma_i = \left(\sum_{y_r \in \mathcal{N}_k} \|y_r - \beta_r - v_i\|^2\right)$$

Estimación mediante optimización

- Coeficientes de pertenencia

$$\left[\frac{\delta F_m}{\delta u_{ik}} = p u_{ik}^{p-1} D_{ik} + \frac{\alpha p}{N_R} u_{ik}^{p} \gamma_i - \lambda\right]_{u_{ik}=u_{ik}^*} = 0.$$

$$u_{ik}^* = \frac{1}{\sum_{j=1}^{c} \left(\frac{D_{ik} + \frac{\alpha}{N_R}\gamma_i}{D_{jk} + \frac{\alpha}{N_R}\gamma_j} \right)^{1/(p-1)}}.$$

- Cluster centers

$$\left[\sum_{k=1}^{N} u_{ik}^{p}(y_k-\beta_k-v_i)+\sum_{k=1}^{N} u_{ik}^{p}\,\frac{\alpha}{N_R}\sum_{y_r\in\mathcal{N}_k}(y_r-\beta_r-v_i)\right]_{v_i=v_i^*} = 0. \quad (14)$$

$$v_i^* = \frac{\sum_{k=1}^{N} u_{ik}^{p}\left((y_k-\beta_k)+\frac{\alpha}{N_R}\sum_{y_r\in\mathcal{N}_k}(y_r-\beta_r)\right)}{(1+\alpha)\sum_{k=1}^{N} u_{ik}^{p}}.$$

- Campo bias

$$\left[\sum_{i=1}^{c} \frac{\partial}{\partial \beta_k} \sum_{k=1}^{N} u_{ik}^{p} (y_k - \beta_k - v_i)^2\right]_{\beta_k = \beta_k^*} = 0.$$

$$\beta_k^* = y_k - \frac{\sum_{i=1}^{c} u_{ik}^{p} v_i}{\sum_{i=1}^{c} u_{ik}^{p}}.$$

Styner et al. 2000 [8]

- Parametric Bias Field Correction (PABIC)
- Modelo paramétrico del campo bias
- Incluido en ITK

Modelo de la imagen

$$s(\underline{x}) = (o(\underline{x}) + n_{\text{bio}}(\underline{x})) * h(\underline{x}) + b(\underline{x}) + n_{\text{MR}}(\underline{x})$$

$$\tilde{s}(\underline{x}) = o(\underline{x}) + b(\underline{x}) + n(\underline{x})$$

$$\tilde{s}(\underline{x}) - b(\underline{x}) = o(\underline{x}) + n(\underline{x}).$$

$$\tilde{s}(\underline{x}) = o(\underline{x}) \cdot b(\underline{x}) + n(\underline{x})$$

$$\log \tilde{s}(\underline{x}) - \log b(\underline{x}) = \log \left(o(\underline{x}) + \frac{n(\underline{x})}{b(\underline{x})} \right).$$

¡La corrección amplifica el ruido !

Corrección

$$\begin{aligned}\hat{o}(\underline{x}) &= \tilde{s}(\underline{x}) - \hat{b}(\underline{x}, \underline{p}) \\ &= o(\underline{x}) + b(\underline{x}) - \hat{b}(\underline{x}, \underline{p}) + n(\underline{x}) \\ &\approx o(\underline{x}) + n(\underline{x}).\end{aligned}$$

Efectos de volumen parcial

- Removing partial volume voxels: styner

> In order to robustize the bias field correction to account for the large partial volume effect, we apply a preprocessing step to partially mask out these voxels. The masking method assumes that partial volume voxels mainly occur at the borders of class regions. The gradient magnitude of a slightly blurred image is calculated and voxels with large gradient magnitude are considered as partial voluming voxels and masked out.

Función de energía

- El elemento básico es la funcón valley, pensada para ignorar outliers

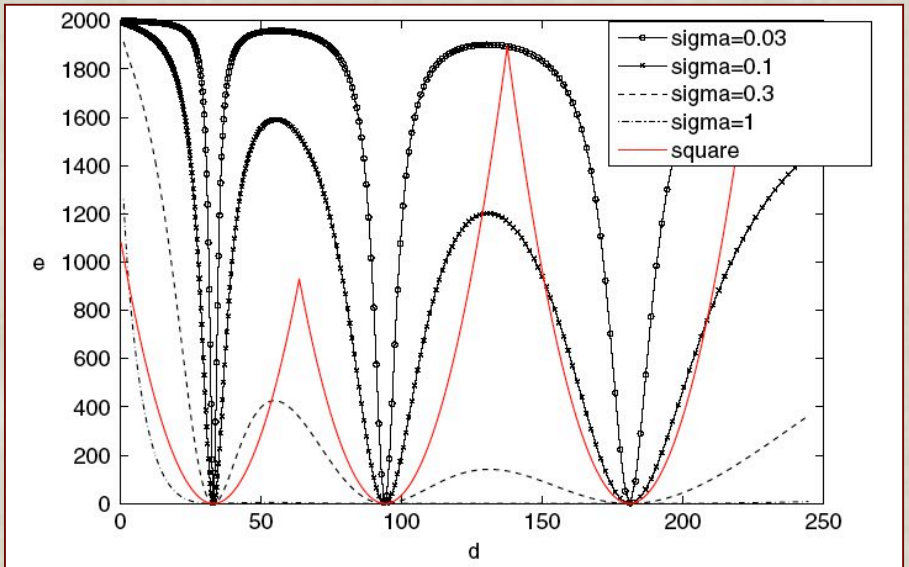

Fig. 1. Energy plot versus pixel intensity showing the basins of attraction to intensity class means.

$$\text{valley}(d) = \frac{d^2}{d^2 + 3\sigma^2}.$$

- Campos producto de polinomios de Legendre

$$\text{in 2-D:} \quad \hat{b}(\underline{x},\underline{p}) = \sum_{i=0}^{m-1} p_i f_i(\underline{x})$$

$$= \sum_{i=0}^{l} \sum_{j=0}^{l-i} p_{ij} P_i(x) P_j(y) \qquad (6)$$

$$\text{in 3-D:} \quad \hat{b}(\underline{x},\underline{p}) = \sum_{i=0}^{l} \sum_{j=0}^{(l-i)} \sum_{k=0}^{(l-i-j)} p_{ijk} P_i(x) P_j(y) P_k(z)$$

$$(7)$$

Función de energía

$$e_{tot} = \sum_i e_0(\hat{d}_i) = \sum_i \prod_k \text{valley}(\hat{d}_i - \mu_k)$$

$$e_{\text{tot_img}}(\underline{p}) = \sum_{\underline{x} \in \text{img}} \prod_k \text{valley}(\tilde{s}(\underline{x}) - \hat{b}(\underline{x}, \underline{p}) - \mu_k).$$

Los píxeles a los que se les ha corregido el campo bias realizan una mínima contribución a la energía total, ya que tienen un valor cercano a μ_k.

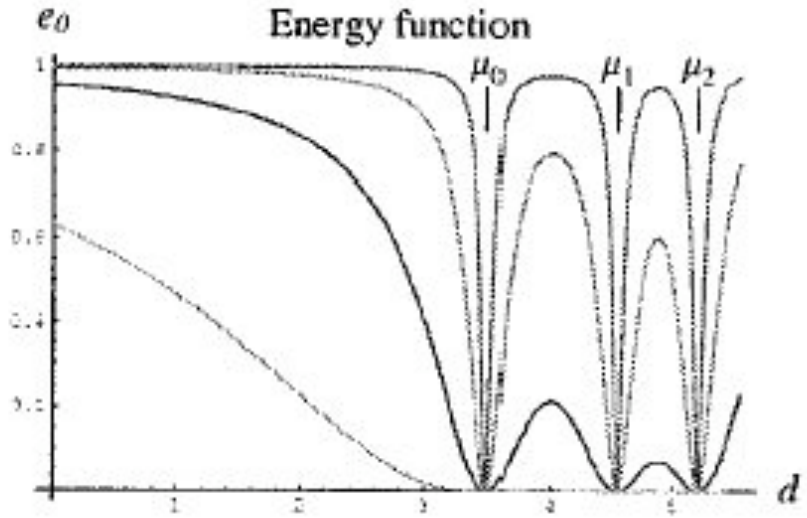

Fig. 3. Multivalued energy function. The class values are chosen as $\mu_0 = \log 33 = 3.49$, $\mu_1 = \log 94 = 4.54$, and $\mu_2 = \log 181 = 5.20$ with $\sigma_1 = \sigma_2 = \sigma_3 = 0.03, 0.1, 0.3$, and 1.0 from top to bottom, respectively.

- Algoritmo de minimización ¿(1+1)-ES?

$$
\begin{aligned}
\underline{r}_t &\sim N(\underline{0}, I) \\
\underline{x}_{t+1} &= \underline{x}_t + a_t \underline{r}_t \\
a_{t+1} &= \begin{cases} a_t \cdot c_{\text{grow}}, & \text{if } f(\underline{x}_{t+1}) < f(\underline{x}_{\text{opt}}) \\ a_t \cdot c_{\text{shrink}}, & \text{otherwise} \end{cases} \\
\underline{x}_{\text{opt}} &= \begin{cases} \underline{x}_{t+1}, & \text{if } f(\underline{x}_{t+1}) < f(\underline{x}_{\text{opt}}) \\ \underline{x}_{\text{opt}}, & \text{otherwise.} \end{cases}
\end{aligned} \tag{20}
$$

Maite G-S, Elsa F., Manuel G., 2007 [10]

- Grad Class Leg (GCL)
- Modelo paramétrico del campo IIH
- Descenso de gradiente de la función de energía para estimar
  - Campo IIH
  - Medias de intensidad de cada clase de tejido

Modelo de la imagen

$$y_i = \beta_i \cdot r_i + \eta_i,$$

logaritmo

$$Y_i = B_i + R_i,$$

- Función energía

$$e(y, \Gamma) = (y - \mu_{x_i})^2$$

En vez de la funcion valley

$$\beta_i(\boldsymbol{p}) = \sum_{j=0}^{m} \sum_{k=0}^{m-j} \sum_{l=0}^{m-k-j} p_{jkl} P_j(i_x) P_k(i_y) P_l(i_z),$$

$$e(\boldsymbol{p}, \Gamma) = \sum_{i \in I} \left(\frac{y_i}{\hat{\beta}_i(\boldsymbol{p})} - \mu_{x_i} \right)^2,$$

- Convexidad de la función de energía

$$\frac{\partial^2 e(\boldsymbol{p},\Gamma)}{\partial^2 p_{jkl}} = \sum_{i\in I} \hat{\mu}_{\hat{x}_i} \frac{y_i (P_j(i_x) P_k(i_y) P_l(i_z))^2}{\hat{\beta}_i^3(\boldsymbol{p})}, \tag{24}$$

$$\frac{\partial^2 e(\boldsymbol{p},\Gamma)}{\partial p_{jkl} \partial p_{mno}} = \sum_{i\in I} \frac{\hat{\mu}_{\hat{x}_i} y_i P_j(i_x) P_k(i_y) P_l(i_z) P_m(i_x) P_n(i_y) P_o(i_z)}{\hat{\beta}_i^3(\boldsymbol{p})}. \tag{25}$$

Minimización

- Descenso de gradiente

$$\boldsymbol{p}_{t+1} = \boldsymbol{p}_t + \boldsymbol{\alpha}_t^{\boldsymbol{p}} \nabla_{\boldsymbol{p}} e(\boldsymbol{p}, \Gamma),$$

or on the intensity class means:

$$\Gamma_{t+1} = \Gamma_t + \alpha_t^{\Gamma} \nabla_{\Gamma} e(\boldsymbol{p}, \Gamma).$$

tor in Eq. (19) is $\nabla_{\boldsymbol{p}} e(\boldsymbol{p}, \Gamma) = \left\{ \frac{\partial}{\partial p_{jkl}} e(\boldsymbol{p}, \Gamma) \right\}$, where:

$$\frac{\partial}{\partial p_{jkl}} e(\boldsymbol{p}, \Gamma) = \sum_{i \in I} \left(\frac{y_i}{\hat{\beta}_i(\boldsymbol{p})} - \hat{\mu}_{\hat{x}_i} \right) \frac{-y_i P_j(i_x) P_k(i_y) P_l(i_z)}{\hat{\beta}_i^2(\boldsymbol{p})}, \tag{21}$$

nent of the gradient vector in Eq. (20) is $\nabla_{\Gamma} e(\boldsymbol{p}, \Gamma) = \left\{ \frac{\partial}{\partial \mu_\omega} e(\boldsymbol{p}, \Gamma) \right\}$ where:

$$\frac{\partial}{\partial \mu_\omega} e(\boldsymbol{p}, I) = \sum_{i \in I | \hat{x}_i = \omega} -\frac{1}{2} \left(\frac{y_i}{\widehat{\beta}_i(\boldsymbol{p})} - \widehat{\mu}_\omega \right). \tag{22}$$

Zagorodnov 2005 [9]

- Algoritmo paramétrico
- Igual que Styner aproxima el IIH mediante una combinación lineal de productos de polinomios de Legendre

Modelo de la imagen

$$o(s) = c(s) + b(s) + e(s)$$

$$b(s) = \sum_{k=1}^{P} a_k \varphi_k(s).$$

Función de energía y estimación por mínimos cuadrados

$$o = Am + e$$

$$m = (a_1, \cdots, a_P | c_1, \cdots, c_M)^\top$$

$$A = \begin{bmatrix} \varphi_1(v_1) & \dots & \varphi_P(v_1) & 1 & 0 & \dots & 0 \\ \vdots & \ddots & \vdots & \vdots & \vdots & \dots & \vdots \\ \varphi_1(v_{N_1}) & \dots & \varphi_P(v_{N_1}) & 1 & 0 & \dots & 0 \\ \varphi_1(v_{N_1+1}) & \dots & \varphi_P(v_{N_1+1}) & 0 & 1 & \dots & 0 \\ \vdots & \ddots & \vdots & \vdots & \vdots & \dots & \vdots \\ \varphi_1(v_{N_1+N_2}) & \dots & \varphi_P(v_{N_1+N_2}) & 0 & 1 & \dots & 0 \\ \vdots & \ddots & \vdots & \vdots & \vdots & \dots & \vdots \\ \varphi_1(v_N) & \dots & \varphi_P(v_N) & 0 & 0 & \dots & 1 \end{bmatrix}$$

$$\hat{m} = (A^T A)^{-1} A^T o$$

Validation methods

- Image data sets, benchmark
- Evaluation strategies

Image data sets

- **Three types of images are typically used**:
  - **Synthetic**, containing abstract objects such as checkboards.
  - **Simulated** (e.g., the BrainWeb simulator [11, 51, 53])
  - **Real** (e.g., Internet Brain Segmentation Repository [12])

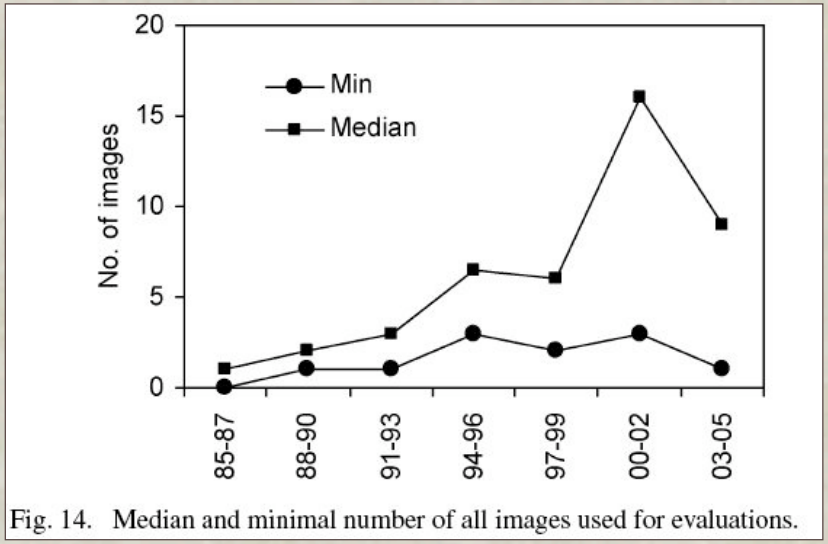

Fig. 14. Median and minimal number of all images used for evaluations.

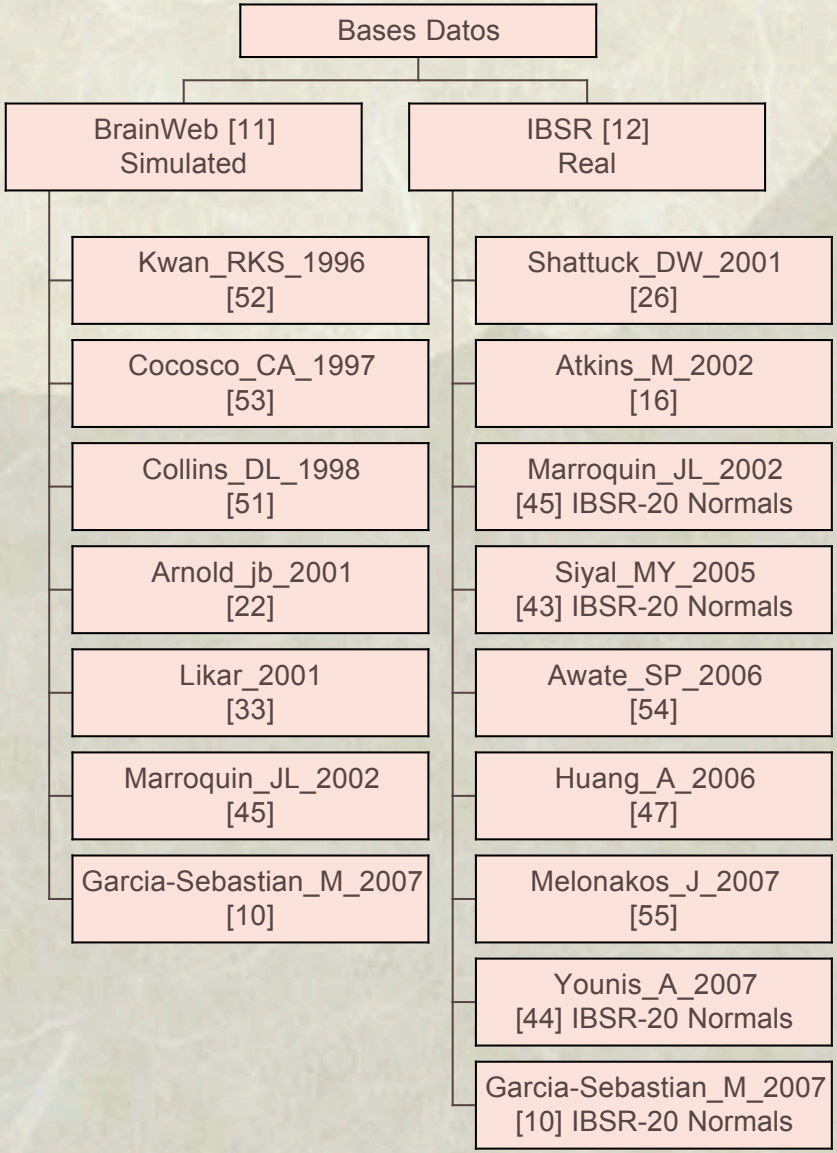
Bases Datos
BrainWeb [11]
Simulated
IBSR [12]
Real
Kwan_RKS_1996
[52]
Cocosco_CA_1997
[53]
Collins_DL_1998
[51]
Arnold_jb_2001
[22]
Likar_2001
[33]
Marroquin_JL_2002
[45]
Garcia-Sebastian_M_2007
[10]
Shattuck_DW_2001
[26]
Atkins_M_2002
[16]
Marroquin_JL_2002
[45] IBSR-20 Normals
Siyal_MY_2005
[43] IBSR-20 Normals
Awate_SP_2006
[54]
Huang_A_2006
[47]
Melonakos_J_2007
[55]
Younis_A_2007
[44] IBSR-20 Normals
Garcia-Sebastian_M_2007
[10] IBSR-20 Normals

Synthetic data sets

[13]

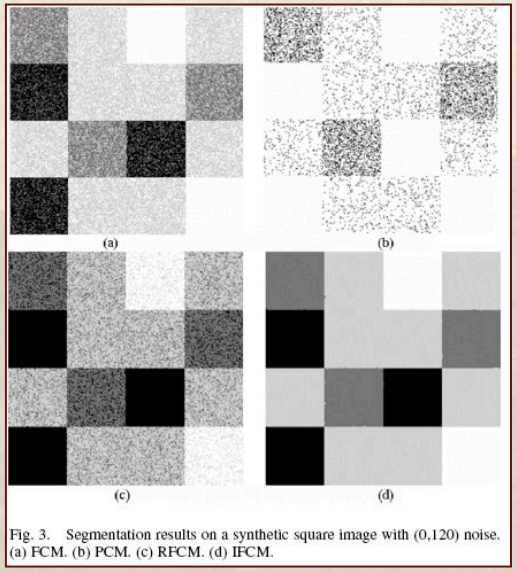

Fig. 3. Segmentation results on a synthetic square image with (0,120) noise. (a) FCM. (b) PCM. (c) RFCM. (d) IFCM.

[14]

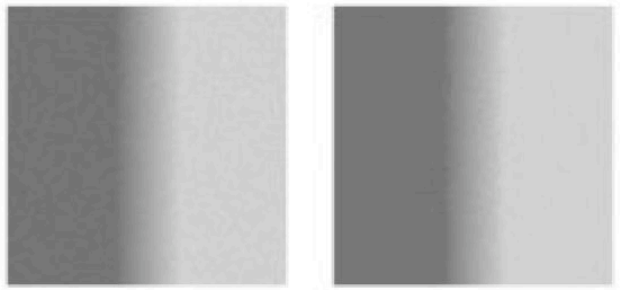

Figure 3: (*left*) Synthetic image, (*right*) corresponding recomputed image with $M = 6$

[10]

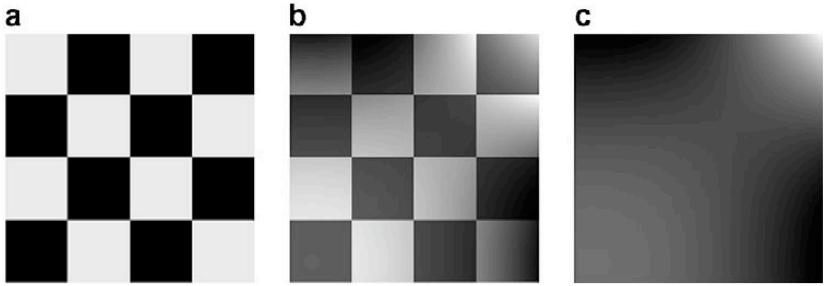

Fig. 2. Chessboard image. (a) Original. (b) The instance of IIH corrupted image. (c) The inhomogeneity field multiplying (a) to obtain (b).

[15]

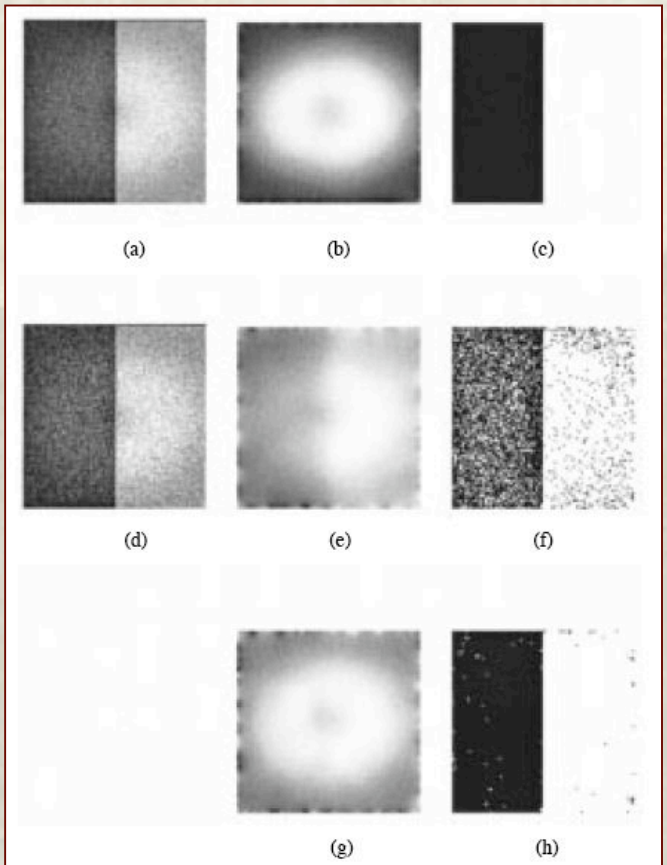

Fig. 8. Comparison of the MEM and the HMRF-EM algorithm on simulated 2-D images. (a) The original image with 3% noise. (b) Bias field estimation for (a) by both the algorithms. (c) Segmentation for (a) by both the algorithms. (d) The original image with 15% noise. (e) Bias field estimation for (d) by the MEM algorithm. (f) Segmentation for (d) by the MEM algorithm. (g) Bias field estimation for (d) by HMRF-EM algorithm. (h) Segmentation for (d) by the HMRF-EM algorithm.

[8]

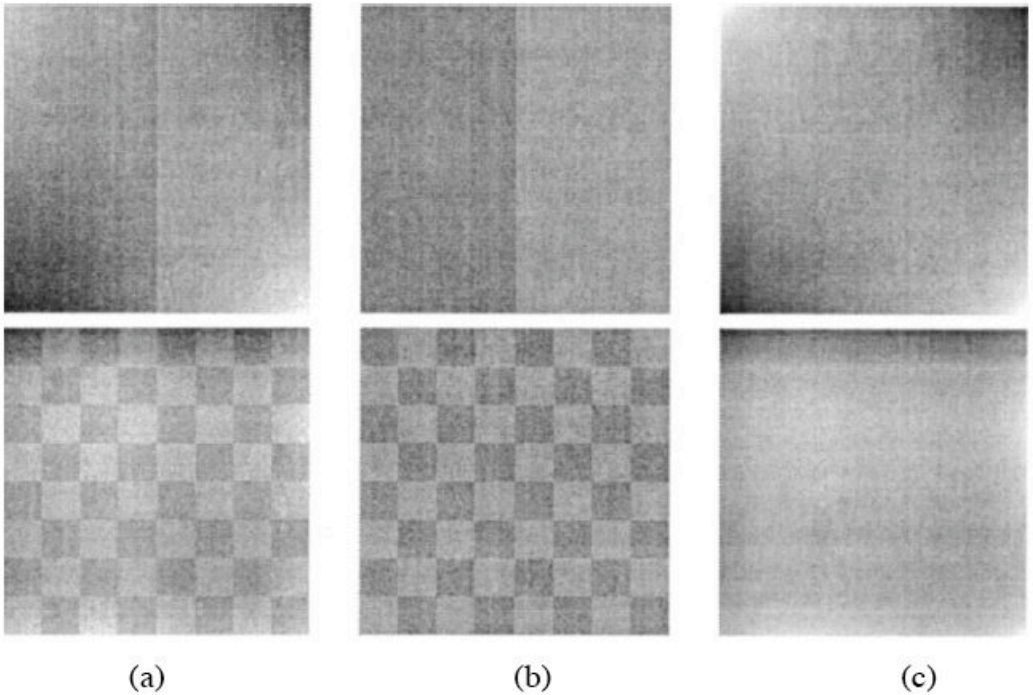

Fig. 7. Bias field correction of a step edge (top row) and a checkerboard (bottom row) (Gaussian noise $\sigma = 40\%$ contrast). (a) Noisy, distorted image. (b) Corrected image. (c) Calculated bias field.

Simulated data sets: BrainWeb [11] Normal brain database

- Pre-generated Simulated Brain Database (SBD) **parameters:**
- pulse sequence: T1, T2, PD
- noise:
  - the reference tissue for the noise computation was: White Matter for T1, and CSF for T2 and PD images.
- INU (intensity non-uniformity):
  - the field A was used for T1 images, field B for T2 images, and field C for PD images.

BrainWeb[11]
Normal brain database

- Custom simulation feature to obtain images with any other combination of parameters.
- **Intensity non-uniformity fields:** There are three fields available: field A, field B, field C. These files are the 20% INU version. For other INU levels, these fields are rescaled linearly to provide alternate inhomogeneity percentages.

Real data set: IBSR [12]

- T1-weighted MRI brain data sets for 20 Normal Subjects
  - The coronal three-dimensional T1-weighted spoiled gradient echo MRI scans were performed on two different imaging systems:

1. Ten FLASH scans on four males and six females
   - were performed on a 1.5 tesla Siemens Magnetom MR System (Iselin, NJ) with the following parameters: TR = 40 msec, TE = 8 msec, flip angle = 50 degrees, field of view = 30 cm, slice thickness = contiguous 3.1 mm, matrix = 256x256, and averages =1.

2. Ten 3D-CAPRY scans on six males and four females
   - were performed on a 1.5 tesla General Electric Signa MR System (Milwaukee, WI), with the following parameters: TR = 50 msec, TE = 9 msec, flip angle = 50 degrees, field of view = 24 cm, slice thickness = contiguous 3.0mm, matrix = 256x256, and averages = 1.

IBSR discussion

- The 20 coronal brain have various levels of difficulty.
- The worst ones have low contrast and relatively large intensity gradients.
- Better quality data should result better overlap scores for the automated methods.

IBSR, 20 Normal Subjects [16] (Atkins_M_2002)

- Intensity range of 0-216
- Slices of 256x256 pixels
- Voxel dimensions are 1.17x1.17x3.1mm^3
- Ten data sets with intensity values starting at 1024. They had a greater range of intensity values than the data sets that had minimum intensity values of 0.
- The ten data sets with intensities starting at 1024 had their intensity ranges shifted back to a minimum of 0 for this experiment, and the resulting intensity ranges are

Table 1: Intensity ranges for IBSR data sets

Set Number	1_24	100_23	11_3	111_2	112_2	12_3	13_3	101_3	202_3	205_3
Max Intensity	712	871	958	822	952	956	1107	1369	1240	1740
Slices	65	63	63	63	63	63	63	63	63	63

Evaluation Strategies

[2] A Review of Methods for Correction of Intensity Inhomogeneity in MRI, Uros Vovk et al. Transactions on Medical Imaging, vol. 26 no.3 2007

IIH correction

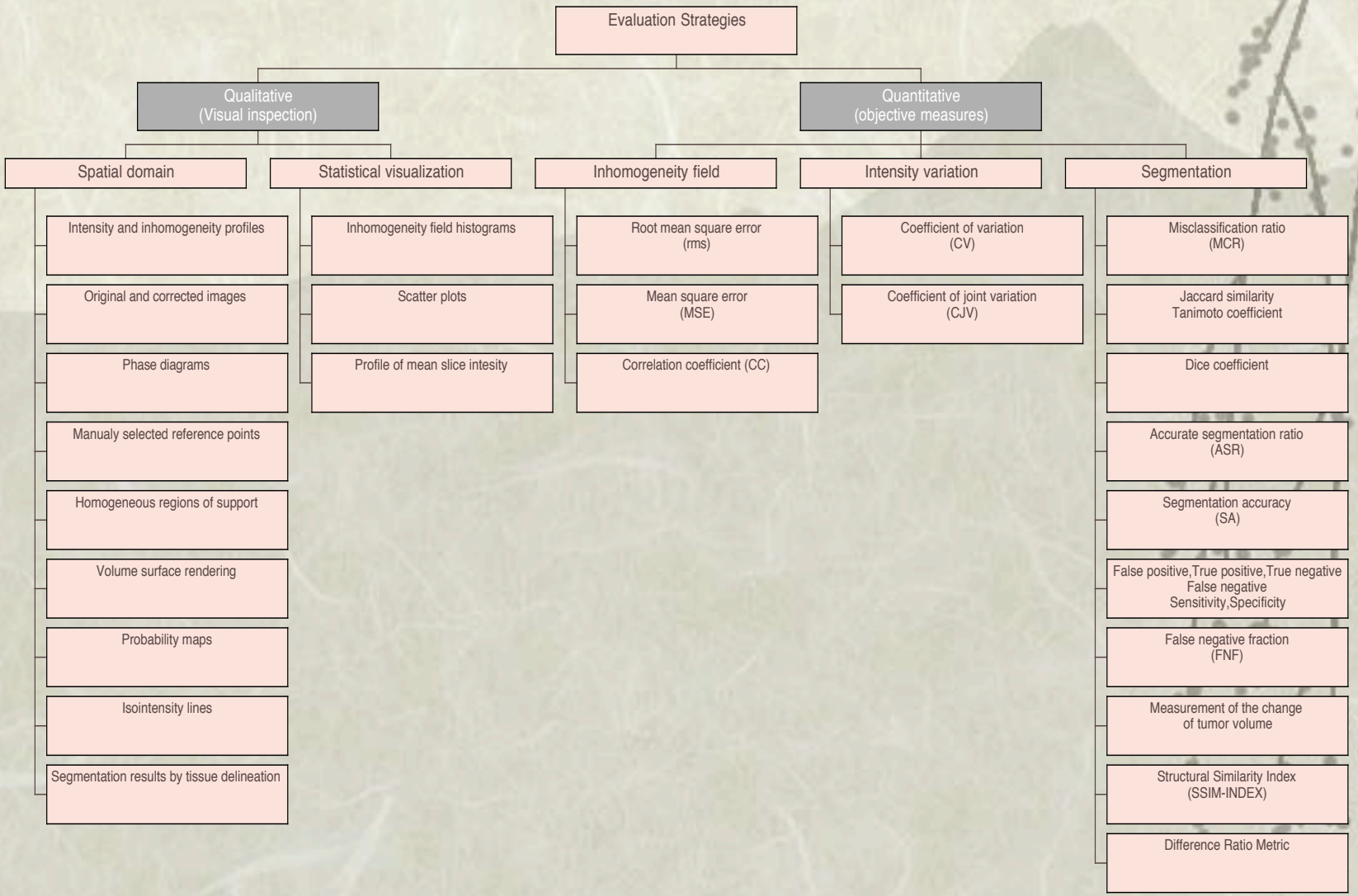

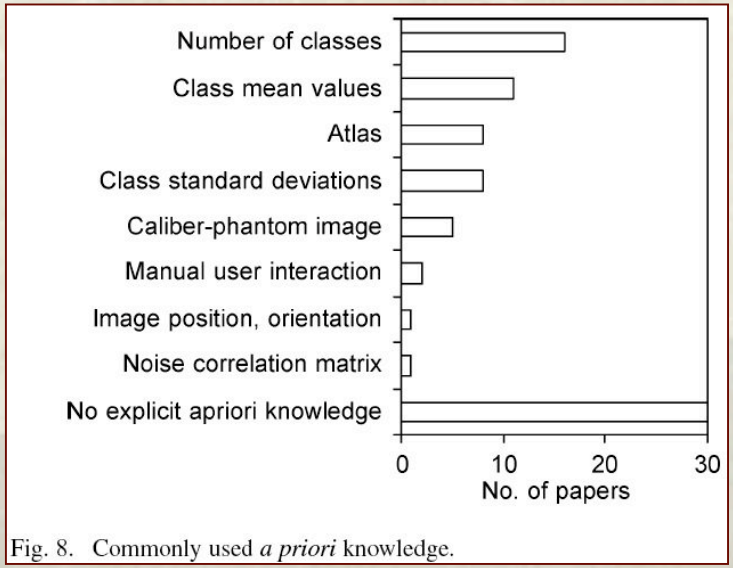

Fig. 8. Commonly used *a priori* knowledge.

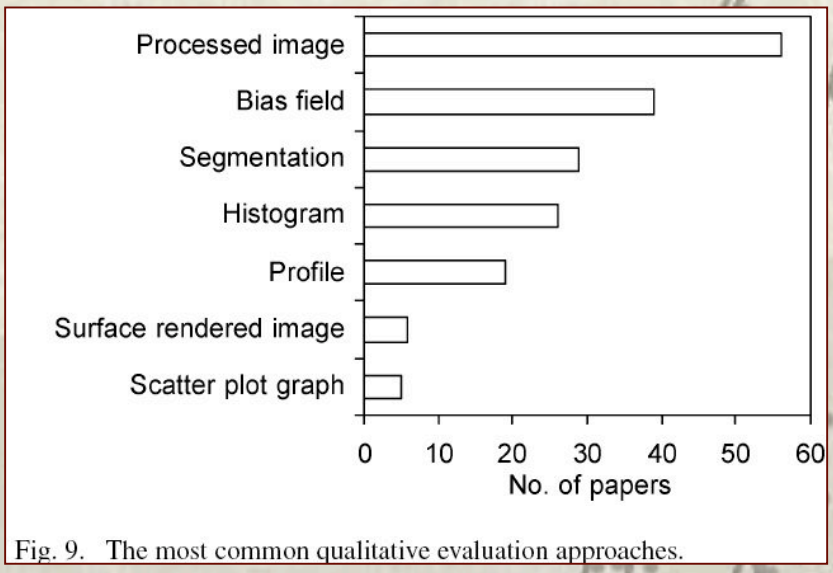

Fig. 9. The most common qualitative evaluation approaches.

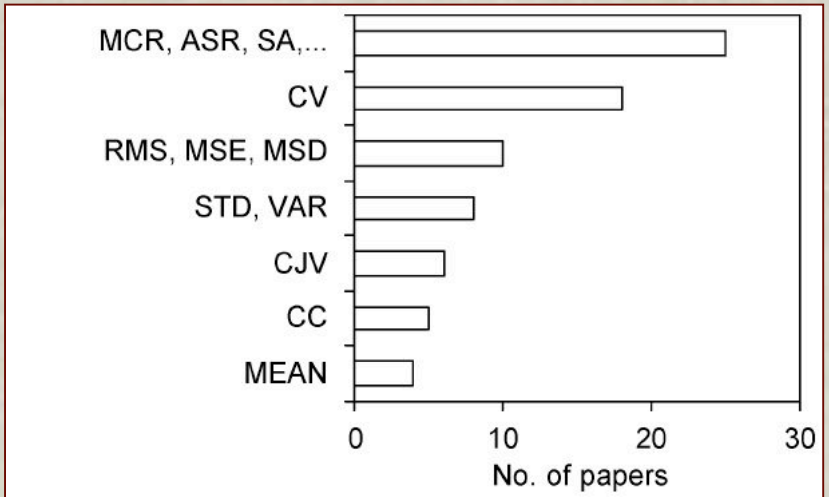

Fig. 11. The most common quantitative metrics.

Qualitative Evaluation (Spatial domain)
Intensity and inhomogeneity profiles [17, 18]

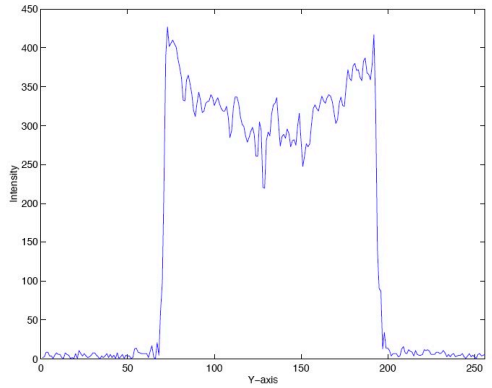

(a)

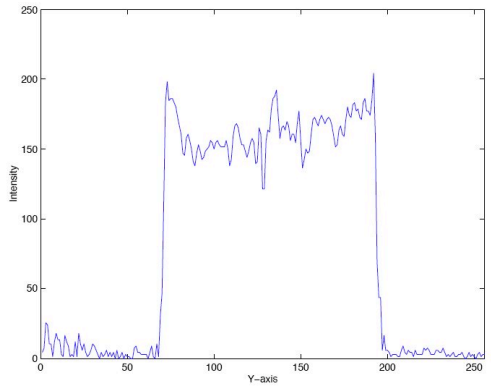

(b)

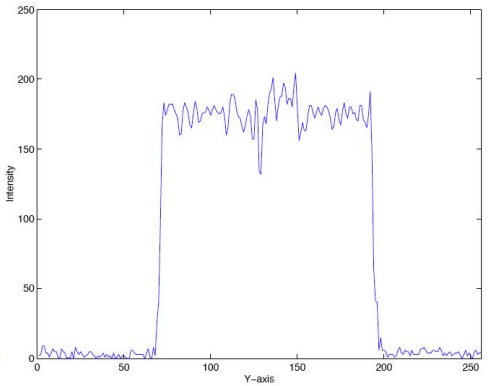

(c)

Figure 4. The intensity profiles at the 120th column in (**a**) the original bias-field corrupted mamma image and the corrected images using the proposed algorithm with (**b**) a 32 × 32 grid and (**c**) a 64 × 64 grid for the finite-element discretization of the bias field.

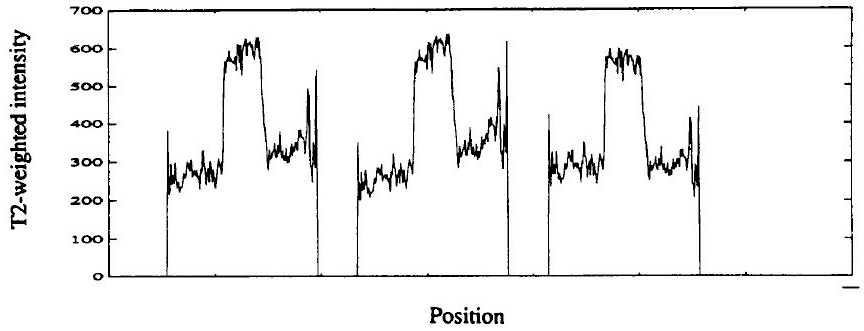

Fig. 1. Intensity profile of T2-weighted image cross section. Left: before correction. Middle: after correction with a correction surface computed on the corresponding PD-weighted image. Right: after correction with a correction surface computed on the T2-weighted image itself.

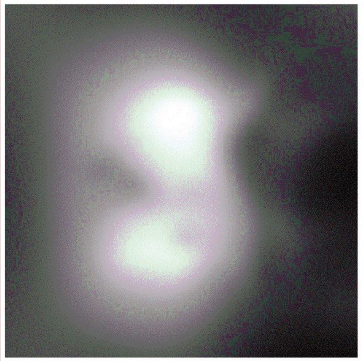

(a)

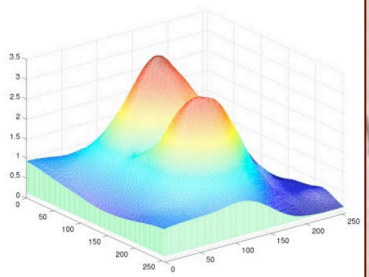

(b)

Figure 5. The recovered bias-field function is displayed (**a**) with an image and (**b**) with a surface plot.

Qualitative Evaluation (Spatial domain)
Original and corrected images [4, 19]

their differences, intensity coded inhomogeneity fields, intensity coded segmentation results

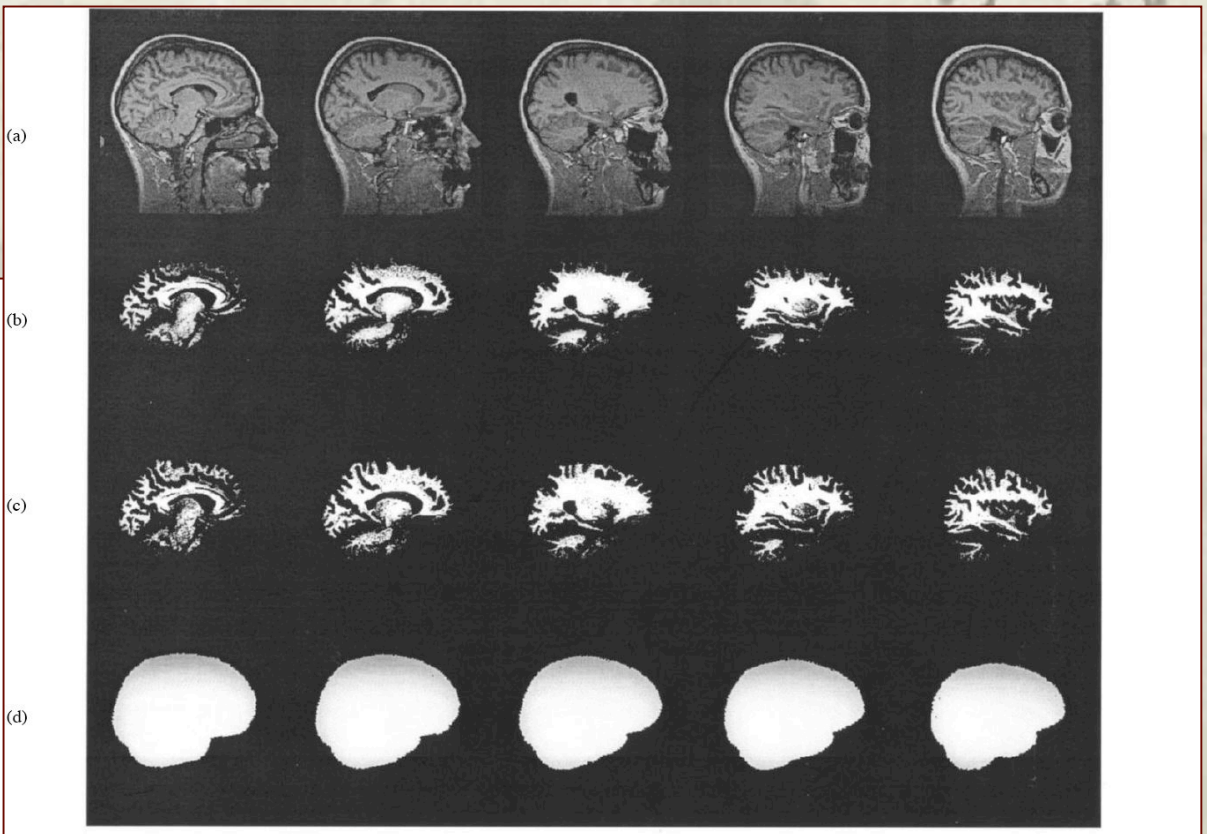

Fig. 4. Slices of a high-resolution T1-weighted MR image illustrating the performance of the method on single-channel data. (a) Original data. (b) White-matter classification with the two-step classification algorithm without bias correction. (c) White-matter classification with our three-step algorithm with bias correction. (d) Estimated bias field.

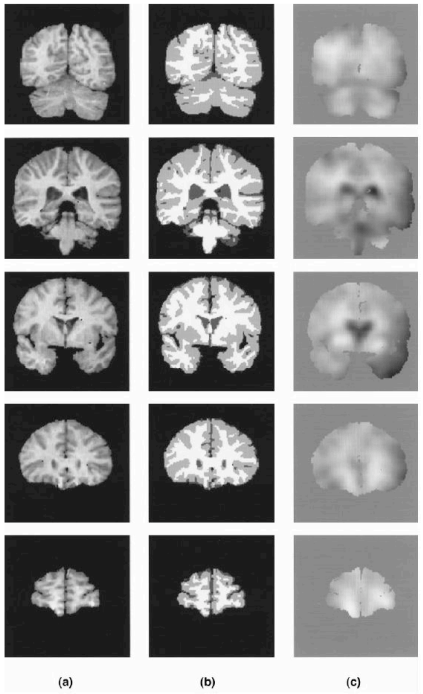

Fig. 2. Illustration of the segmentation of shelled three-dimensional CAPRY cerebral MR images into three classes representing white matter, gray matter and cerebrospinal fluid (CSF) using the BMAP algorithm: (a) original image slices; (b) segmented slices; and (c) the recovered bias fields at five different coronal levels of the brain.

Qualitative Evaluation (Spatial domain)
Manually selected reference points [18]

Fig. 2. Left: T1-weighted image with white matter reference points selected by the user overlaid in white. Middle: reference points identified after the preclassification stage with a confidence level of 0.8. Right: reference points identified after the preclassification stage with a confidence level of 0.6.

Qualitative Evaluation (Spatial domain)
Volume surface rendering [19,20]

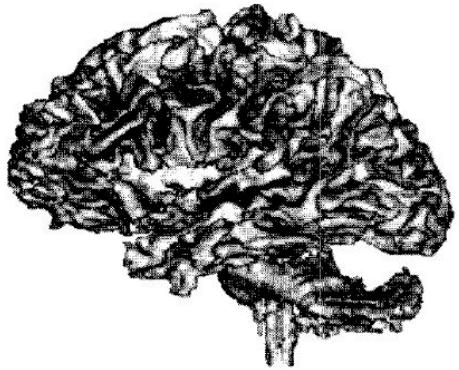

Fig. 8. White matter surface determined by adaptive segmentation.

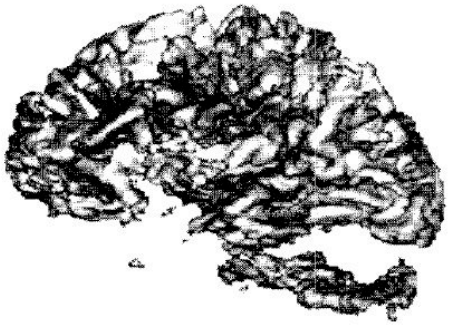

Fig. 9. White matter surface determined by conventional intensity-based segmentation.

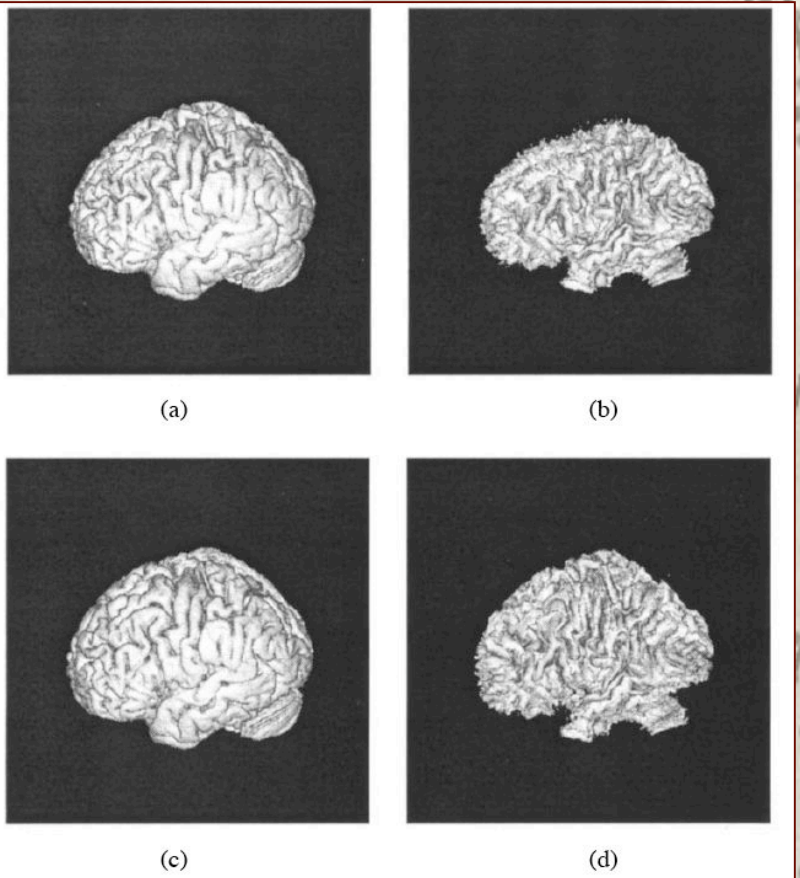

Fig. 5. 3-D rendering of the gray-matter (left) and white-matter (right) segmentation of the MR image of Fig. 4. (a) and (b) Two-step algorithm without bias correction. (c) and (d) Three-step algorithm with bias correction.

Qualitative Evaluation (Spatial domain)
Probability maps [19]

Digital brain atlas distributed with the SPM package.

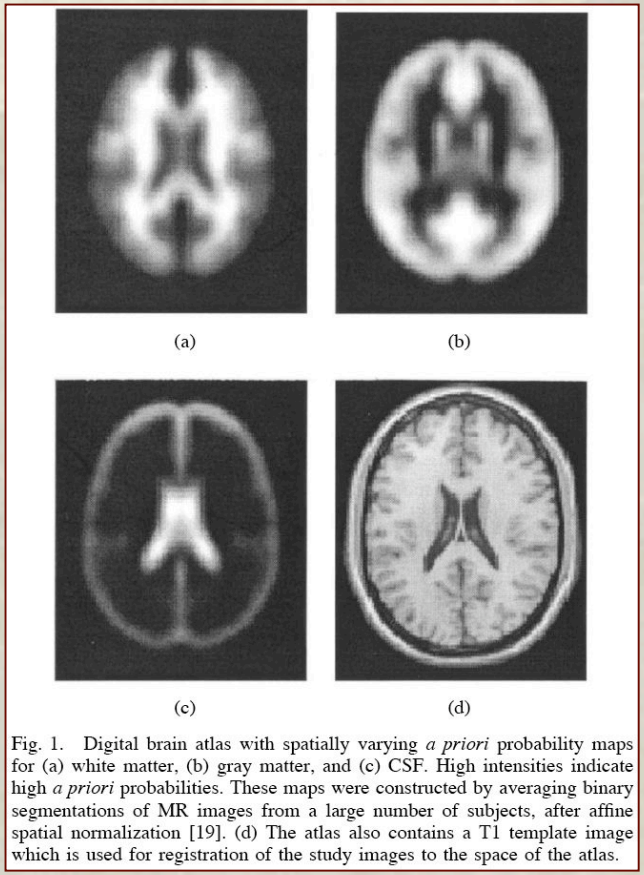

Fig. 1. Digital brain atlas with spatially varying *a priori* probability maps for (a) white matter, (b) gray matter, and (c) CSF. High intensities indicate high *a priori* probabilities. These maps were constructed by averaging binary segmentations of MR images from a large number of subjects, after affine spatial normalization [19]. (d) The atlas also contains a T1 template image which is used for registration of the study images to the space of the atlas.

Qualitative Evaluation (Spatial domain)
Isointensity lines [8]

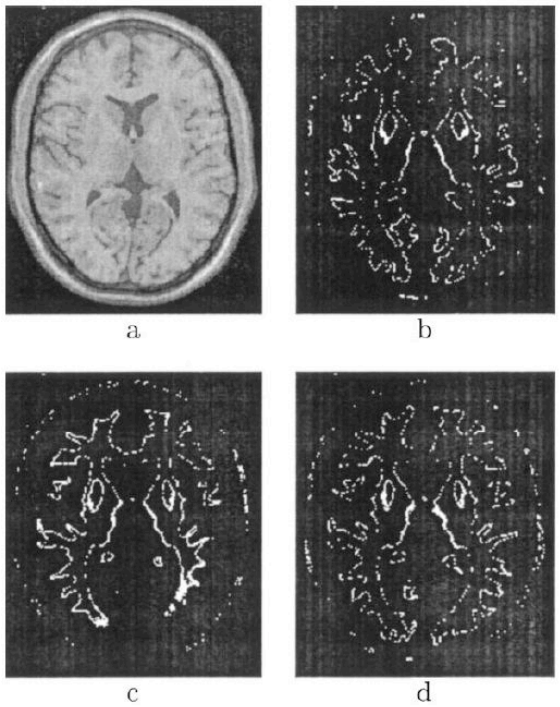

Fig. 9. Bias field correction of a simulated 3-D MRI head image of the MNI-SBD-database. Visualization of intensity isolines in a slice (a) of the undistorted base image (b), the distorted image (c) and the bias corrected image (d). The incorrect course of the GM-WM boundary in the distorted image is clearly visible.

Qualitative Evaluation (Spatial domain)
Segmentation results by tissue delineation [21]

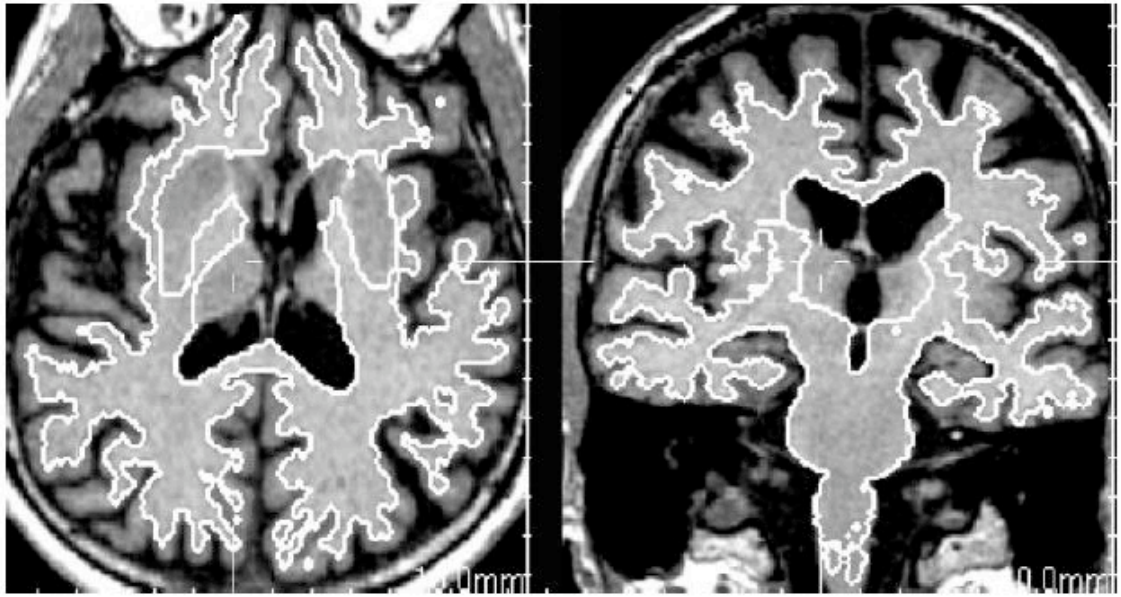

Fig. 2. Example slices (transaxial left, sagittal, coronal right) through MRI of a subject with contour showing a manually delineated volume of white matter used for manual bias field estimation. Note exclusion of caudate, lenticular nucleus and thalamus to ensure that nonwhite matter voxels do not corrupt the local bias field estimate.

Qualitative Evaluation (Spatial domain)

- Others
  - Phase diagrams (less common)
  - Homogeneous regions of support

Qualitative Evaluation (Statistical visualization of the original and corrected images features)

- Inhomogeneity field histograms [3]
- Scatter plots [22]
- Profile of mean slice intensity [23]

Intensity histograms are the most common and informative.

Quantitative Evaluation (IIH)

- The obtained IIH is compared to a reference field.
- The intensities of the corrected and reference image are compared.
- The image background is masked out.
- Ideal inhomogeneity-free images or true inhomogeneity fields must be known.

Quantitative Evaluation (IIH)

- The **root mean square error (rms)** [24,25]
  - to measure the differences between two inhomogeneity fields or image intensities, corrected image versus unbiased volume.

$$\mathrm{rms}\left(b_1(x), b_2(x)\right) = \sqrt{\frac{1}{N}\sum_{x\in\Omega}\left(b_1(x) - b_2(x)\right)^2}$$

where Ω is a region of interest of size N.

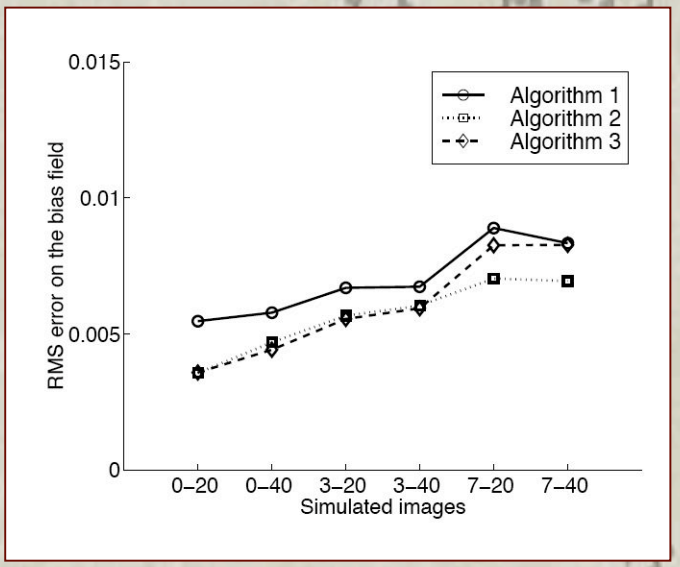

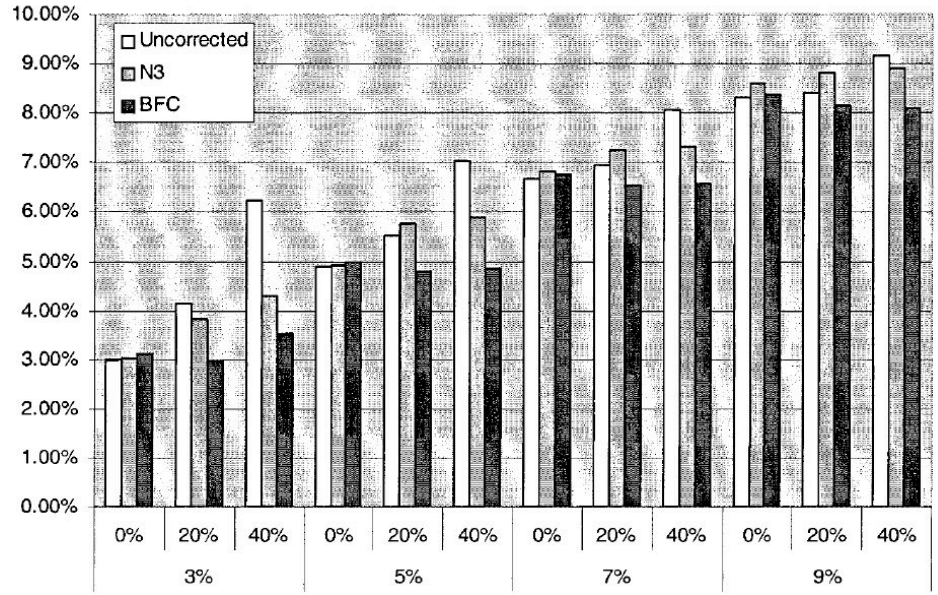

FIG. 5. Normalized RMS error metrics as a percentage of WM ground truth intensity calculated between the ground truth image and the uncorrected phantom image, the N3-corrected image, and the BFC-corrected image.

[26]

TABLE 3

MNI BrainWeb Phantom Tissue Fraction Results

	Fractional content RMS error											
	3% noise			5% noise			7% noise			9% noise		
	0% RF	20% RF	40%	0%	20%	40%	0%	20%	40%	0%	20%	40%
	Maximum a posteriori classification											
WM	0.088	0.084	0.102	0.129	0.122	0.125	0.165	0.160	0.159	0.359	0.184	0.187
GM	0.137	0.139	0.159	0.178	0.172	0.176	0.215	0.211	0.220	0.384	0.240	0.245
	Maximum likelihood classification											
WM	0.096	0.090	0.105	0.158	0.146	0.142	0.253	0.249	0.214	0.353	0.304	0.293
GM	0.144	0.145	0.163	0.206	0.196	0.194	0.299	0.297	0.277	0.420	0.366	0.362

Note. RMS error of the fractional voxel content computed by BSE/BFC/PVC for the MNI BrainWeb phantom.

Quantitative Evaluation (IIH)

- **The mean square error (MSE)** and the **mean square distance (MSD),** two similar measures [8, 27, 28].

Because scaling of the **IIH fields** or **image intensities** affect these measures, they **have to be normalized before these measures are calculated**. In this way, only the difference in shape of the IIH fields is measured and not their absolute values that contain no useful information on inhomogeneity correction.

	$\boldsymbol{y}_{\mathrm{B}}$	B-N	$\hat{\boldsymbol{f}}$, $\gamma = 0$	$\hat{\boldsymbol{f}}$, $\gamma = 0.014$
MSE (tissue)	196,542	20,820	20,428	10,901
MAE (tissue)	353.91	113.59	112.64	81.99
GM errors	64.4%	14.6%	14.3%	9.9%
WM errors	24.7%	3.6%	3.3%	2.4%

Table 1. Quantitative comparisons using the MNI brain phantom. Corrected images are generated using Brey-Narayana and the proposed method with $\gamma = 0$ and $\gamma = 0.014$. The first two lines are the mean squared error and mean absolute error (based on the true image $\boldsymbol{f}^*$) computed only in tissue regions. The last two lines are the percentage of misclassified points in GM and WM regions. Results averaged over 20 random trials.

Table 1
Mean squared difference, as a percentage of grey–white contrast, between applied differential bias field and the bias field obtained using the differential bias correction method for varying differential bias fields for simulated scan pairs, simulated scan pairs with simulated misregistration and simulated scan pairs with simulated atrophy

Scan pair	Mean squared difference
0–20%	0.0053
20–40%	0.0053
0–40%	0.0056
0–40% (atrophy)	0.040
0–20% (misregistered)	0.0099
20%–40% (misregistered)	0.0095
0%–40% (misregistered)	0.010
0%–20% (atrophy)	0.035
20%–40% (atrophy)	0.035

Quantitative Evaluation (IIH)

❖ The correlation coefficient (CC) [22]

This measure **is inherently insensitive to the absolute values of IIH fields**.

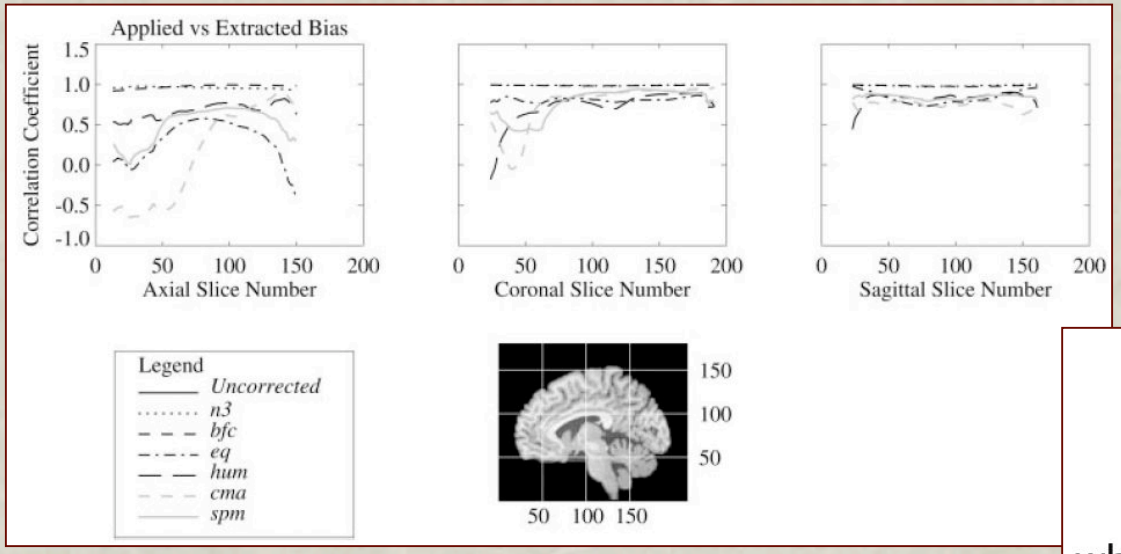

Corr2 in Matlab

$$r = \frac{\sum_m \sum_n (A_{mn} - \bar{A})(B_{mn} - \bar{B})}{\sqrt{\left(\sum_m \sum_n (A_{mn} - \bar{A})^2\right)\left(\sum_m \sum_n (B_{mn} - \bar{B})^2\right)}}$$

where $\bar{A}$ = `mean2(A)`, and $\bar{B}$ = `mean2(B)`.

Quantitative Evaluation (Intensity Variation)

- We have to estimate the mean and/or variance of intensities of a tissue of interest estimation before and after correction.
- The variance or standard deviation of the spatial intensity distribution of a tissue of interest should be reduced if IIH is removed.
- The mean intensity of a tissue can be used to estimate global intensity scaling due to IIH correction or to measure the change in contrast between two tissues of interest.

Quantitative Evaluation (Intensity Variation)

- **Means and/or variances** can be used separately [29, 30] or combined like in coefficient of variation (CV) and coefficient of joint variation (CJV).

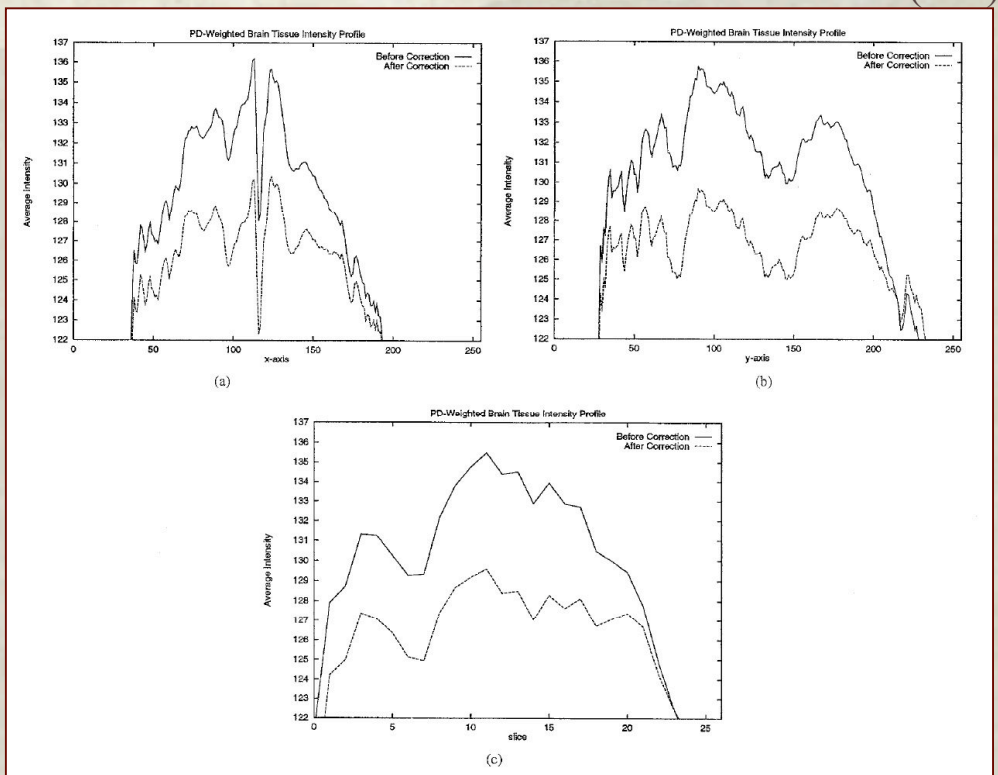

Fig. 4. Average brain tissue intensity variation in each dimension before and after RF correction. The uncorrected and corrected images from which the graphs were calculated have equivalent dynamic ranges. (a) x-axis, (b) y-axis, and (c) slice.

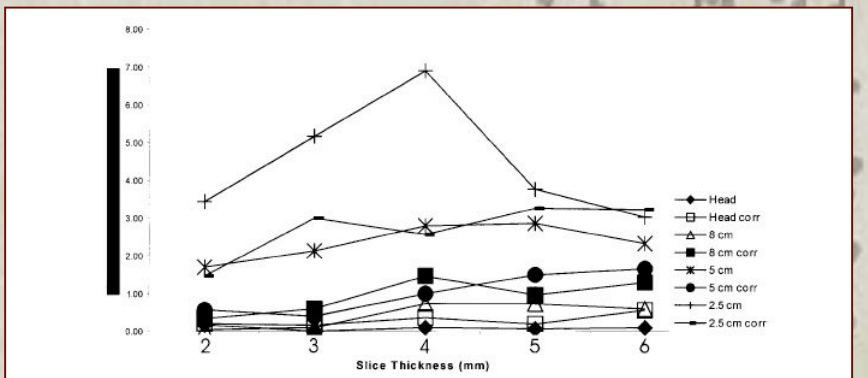

Figure 3. Plot of similarity against slice thickness. The similarity measure is calculated from the mean and variance of the signal intensities in two regions of interest in the superficial and deep parts of the vitreous humor. These were used to calculate the position at which the distributions of the regions of interest overlap. This measurement is expressed in units of SD from mean intensity of the second region of interest (deep in the globe). The distance between distributions tends to zero with increased similarity.

Quantitative Evaluation (Intensity Variation)

- **Coefficient of variation (CV) [19]:**

$$\mathrm{CV}(C) = \frac{\sigma(C)}{\mu(C)}.$$

  - It is defined as a quotient between standar deviation σ and mean value μ of selected tissue class (C).
  - This coefficient is zero if the true bias field has been totally recovered
  - It is invariant to multiplicative uniform intensity transformation (intensity scaling or contrast).
  - The quality of IIH correction has been quantitatively assessed by change/reduction of the CV of a tissue of interest [19, 3, 31, 32].

TABLE I
COEFFICIENT OF VARIATION FOR THE DATA OF FIG. 6

		T2		PD	
class	samples	original	corrected	original	corrected
white matter	1744	9.47 %	6.76 %	5.65 %	3.45 %
gray matter	925	11.18 %	8.03 %	9.64 %	5.56 %

Quantitative Evaluation (Intensity Variation)

- Disadvantajes of CV :
  - Sensitivity to uniform additive intensity tranformation (bightness), which changes the mean but not the variance of a tissue.
  - It is computed for a single tissue class, which makes the assessment of the overall IIH correction difficult when CV improves for one tissue class but not for others.
  - It doesn't provide any information on the overlap between intensity distributions of distinct tissue classes *.

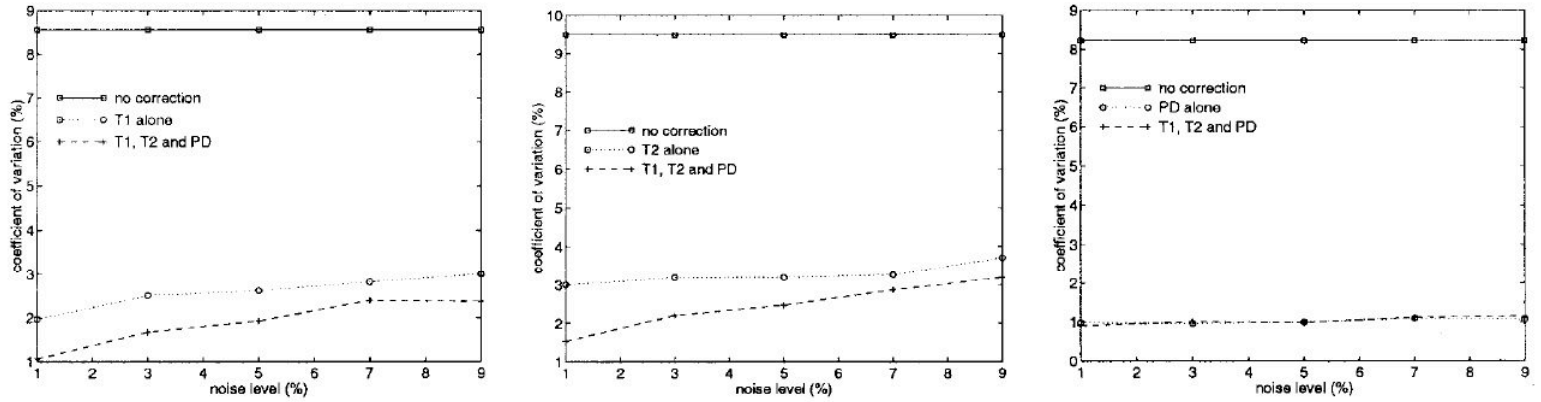

(c)

Fig. 3. Validation of the bias correction algorithm on simulated data. (a) Simulated T1-, T2-, and PD-weighted MR images obtained from the BrainWeb simulator [22]. (b) Known bias fields imposed on the T1-, T2-, and PD-weighted images. The amplitude of the bias fields is exaggerated for visualization purposes. (c) Coefficient of variation before correction, after single-channel correction and after three-channel correction for different noise levels.

Quantitative Evaluation (Intensity Variation)

- **The coefficient of joint variation (CJV) [33]:**
  - It estimates the overlap between two tissue classes (C_1 and C_2)
  - It is **invariant to the uniform linear**, i.e., multiplicative and additive, **intensity transformation**.

$$cjv(C_1, C_2) = \frac{\sigma(C_1) + \sigma(C_2)}{|\mu(C_1) - \mu(C_2)|}$$

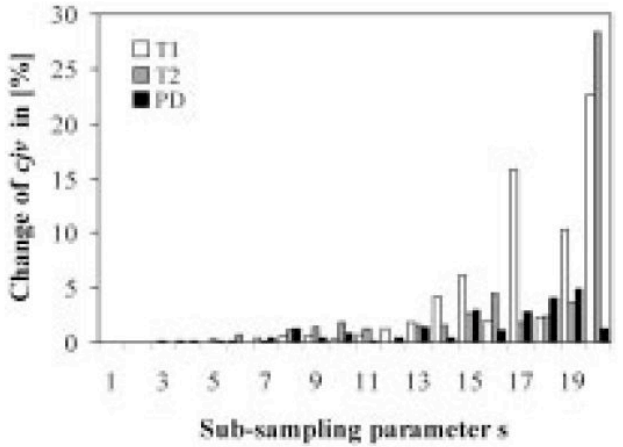

Fig. 4. Sensitivity to subsampling.

TABLE I
CORRECTION OF SIMULATED AND REAL DATA OF IMAGE SETS 1 AND 2

			cv(GM) in [%]						*cv*(WM) in [%]						*cjv*(GM,WM) in [%]					
Set	Mod	Bias	Orig.	MA2	M2	M4	N3	FMI	Orig.	MA2	M2	M4	N3	FMI	Orig.	MA2	M2	M4	N3	FMI
1 - Normal (simulated)	T1	0%	9.9	10.0	9.9	9.9	9.9	11.5	5.2	5.2	5.1	5.1	5.2	7.3	51.6	52.0	52.1	52.1	51.9	72.5
		40%	13.5	10.0	9.9	10.0	10.0	13.7	9.2	5.2	5.2	5.0	5.2	9.2	69.3	51.6	51.5	51.7	51.8	96.4
	T2	0%	17.7	18.2	17.9	17.8	17.7	22.3	12.0	12.9	12.2	12.2	12.0	17.6	83.2	82.1	82.6	82.5	83.1	125.5
		40%	20.3	18.2	17.9	17.8	20.0	20.3	13.3	12.3	11.9	11.8	13.0	14.8	106.4	82.3	82.4	82.4	103.9	116.8
	PD	0%	4.5	4.5	4.5	4.5	4.6	6.3	4.9	4.9	4.9	4.9	4.9	6.6	64.9	64.7	64.7	65.0	66.4	93.5
		40%	9.7	4.5	4.5	4.5	4.6	6.9	7.5	4.8	4.7	4.7	4.6	6.1	163.0	64.3	64.5	64.1	66.7	107.9
1 - MS lesions (simulated)	T1	0%	10.1	10.2	10.1	10.1	10.1	13.2	5.4	5.3	5.3	5.3	5.3	8.5	50.9	51.4	51.5	51.5	51.3	88.0
		40%	13.7	10.2	10.1	10.2	10.2	11.4	9.3	5.4	5.3	5.3	5.3	6.9	68.0	50.8	50.8	51.1	51.1	65.3
	T2	0%	9.7	10.1	9.9	9.9	9.9	15.0	8.3	8.9	8.5	8.5	8.4	12.4	74.9	74.1	74.2	74.3	74.9	150.3
		40%	13.7	10.3	9.9	9.9	10.1	11.3	10.6	9.1	8.4	8.4	8.2	9.6	123.8	73.7	74.1	74.2	77.8	98.3
	PD	0%	3.8	3.9	3.9	3.9	4.0	6.3	4.5	4.5	4.5	4.5	4.5	6.9	66.9	66.7	66.7	67.0	68.7	117.3
		40%	9.4	3.9	3.9	3.8	4.0	6.8	7.4	4.4	4.3	4.3	4.3	6.3	195.6	66.5	66.6	66.1	68.7	125.9
2 - Normal (real)	T1		12.3	10.3	10.4	10.4	10.6	10.6	8.2	5.8	5.8	5.8	6.0	6.2	138.0	131.4	133.0	134.0	127.0	144.3
	T2		15.9	16.2	16.0	15.8	15.9	17.5	10.0	10.4	10.0	9.9	10.0	12.1	90.7	88.4	90.4	89.8	90.7	105.0
	PD		6.9	6.3	6.4	6.3	6.4	7.4	5.3	5.3	5.2	5.1	5.2	6.7	77.8	70.7	72.1	72.1	73.2	87.1
2 - Tumor (real)	T1		8.9	8.2	8.1	8.3	8.5	8.4	6.7	5.6	5.6	5.9	6.2	5.5	175.7	167.5	168.6	170.4	168.1	173.6
	T2		14.0	12.7	12.6	13.2	12.8	13.3	10.3	9.4	9.5	9.4	9.7	9.8	169.3	164.7	166.6	175.5	161.3	163.8
	PD		6.5	5.3	5.1	5.3	5.0	5.9	5.0	4.2	4.3	4.2	4.3	4.6	133.8	118.0	115.2	118.2	114.6	121.3

Quantitative Evaluation (Intensity Variation)

- The CJV approximates the classification error [23, 33, **34**, 35, 36]

TABLE II. Mean and range of the four quality criteria

Method	CV_{WM} (%)	CV_{GM} (%)	CJV_{WG} (%)	CER (%)
0.5 T (n = 12)				
Uncorrected	5.39 (4.81, 5.96)	15.12 (13.27, 17.36)	108.75 (100.50, 138.71)	10.29 (9.40, 13.81)
SPM99-L	9.14 (5.03, 34.77)	14.59 (10.60, 20.40)	129.15 (116.17, 177.92)	11.14 (10.49, 16.15)
SPM99-S	10.13 (4.71, 33.82)	13.54 (10.17, 17.48)	132.03 (110.65, 170.94)	10.83 (9.63, 17.37)
SPM2	5.29 (4.63, 6.24)	19.19 (10.73, 25.72)	122.17 (102.62, 156.21)	10.53 (9.38, 15.34)
N3	5.15 (4.55, 5.42)	14.29 (12.90, 16.71)	113.65 (105.27, 135.79)	10.51 (9.73, 14.36)
NIC	5.02 (4.39, 5.29)	14.48 (12.73, 16.56)	105.81 (99.84, 126.69)	9.79 (8.86, 13.44)
1.5 T (n = 12)				
Uncorrected	6.52 (5.79, 7.59)	16.75 (12.74, 20.74)	83.92 (76.37, 97.10)	9.08 (8.74, 12.79)
SPM99-L	6.26 (4.70, 7.41)	17.34 (14.44, 21.49)	105.97 (86.30, 135.33)	12.90 (10.08, 18.87)
SPM99-S	5.53 (4.57, 6.22)	16.31 (13.80, 19.89)	93.40 (78.19, 107.37)	10.61 (8.99, 14.64)
SPM2	7.50 (5.39, 8.67)	15.97 (12.00, 20.52)	88.69 (76.80, 99.76)	9.77 (8.69, 12.37)
N3	5.88 (5.36, 6.45)	16.47 (14.75, 19.82)	83.95 (77.03, 91.37)	8.84 (8.15, 11.39)
NIC	5.84 (5.30, 6.57)	15.70 (12.32, 19.88)	80.77 (74.95, 88.85)	8.04 (7.18, 10.96)

Coefficient of variation of white matter (CV_{WM}), coefficient of variation of the gray matter (CV_{GM}), coefficient of joint variation of white and gray matter (CJV_{WG}), and classification error rate (CER) in the uncorrected original and corrected real images when using the SPM99, SPM2, N3, and NIC methods. Lower values denote lower bias field in the images.

TABLE I. Quality criteria measured on the Brain Web phantom with 0, 20, and 40% bias field magnitude

Brain Web	CV_{WM} (%)	CV_{GM} (%)	CJV_{WG} (%)	CER (%)
0% bias field	4.84	7.03	43.02	0.65
20% bias field	5.89	8.97	48.91	1.32
40% bias field	7.56	12.26	59.84	3.22

All quality parameters represent the amount of bias field in the images. CV_{WM}, coefficient of variation of white matter; CV_{GM}, coefficient of variation of the gray matter; CJV_{WG}, coefficient of joint variation of white and gray matter; CER, classification error rate.

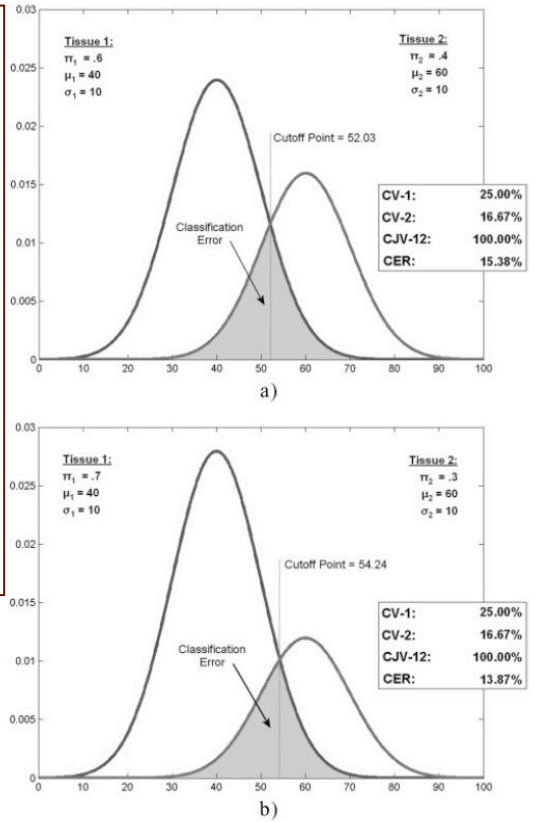

Figure 4.
Examples of probability density functions with the same mean, variance (thus presenting the same coefficient of variation CV), and coefficient of joint variation (CJV). CER, however, is higher when the relative amounts of the two tissues (π_1 and π_2) are closer.

CV and CJV don't provide information on the amount of inhomogeneity remaining after correction, unless ideal inhomogeneity-free images are avalilable.

Quantitative Evaluation (Segmentation)

- Inhomogeneity correction is evaluated via segmentation results.
- Measures
  - The misclassification ratio (MCR)
  - **The Jaccard similarity or Tanimoto coefficient**
  - **Dice coefficient**
  - The accurate segmentation ratio (ASR)
  - Segmentation accuracy (SA)
  - False positive (FPF)
  - False negative fraction (FNF)
  - False positives and true negatives
  - Measurement of the change of tumor volume

Quantitative Evaluation (Segmentation)

The misclassification ratio (MCR) [20, 37, 38, 39, 40]

- Defined as the number of pixels misclassified by the algorithm divided by the total number of pixels in the image.

TABLE III
MISCLASSIFICATION RATE FOR THE SAME DATASET REFORMATTED AT DIFFERENT SLICE PLANES

	0% INU	20% INU	40% INU
Transverse slices	3.717 %	3.676 %	3.832 %
Coronal slices	3.825 %	3.823 %	4.065 %
Sagittal slices	3.815 %	3.802 %	3.879 %

TABLE I
MISCLASSIFICATION RATE FOR DIFFERENT INU CORRECTION AND SEGMENTATION METHODS AT DIFFERENT INU LEVEL

Method	0% INU	20% INU	40% INU
FCM	3.988 %	5.450 %	9.016 %
FM-AFCM	4.171 %	4.322 %	5.065 %
TM-AFCM	4.168 %	4.322 %	4.938 %
EM1	6.344 %	7.591 %	13.768 %
EM2	4.242 %	5.638 %	9.604%
AMRF	3.876 %	4.795 %	6.874 %
MNI-FCM	4.979 %	4.970 %	5.625 %
Proposed	3.717 %	3.676 %	3.832 %

TABLE II
COMPARISON BETWEEN OUR ALGORITHM AND THE EM-MRF ALGORITHM: IN TERMS OF OVERLAP METRIC (IN %) FOR DIFFERENT TISSUE CLASS, AND THE MCR (IN %), FOR DIFFERENT INU LEVEL. "NO MRF" DENOTES THE EM-MRF ALGORITHM WITHOUT MRF REGULARIZATION, "WITH MRF" DENOTES THE EM-MRF ALGORITHM WITH MRF REGULARIZATION

	0% INU			20 % INU			40% INU		
	our algorithm	no MRF	with MRF	our algorithm	no MRF	with MRF	our algorithm	no MRF	with MRF
WM	96.44	93.70	93.31	96.62	93.52	93.53	96.59	93.49	93.13
GM	95.87	94.03	92.12	96.02	93.95	91.81	95.97	93.89	91.24
CSF	96.68	86.67	85.03	96.67	87.17	85.37	96.61	86.66	85.33
GM+WM	99.22	98.98	97.97	99.22	99.01	97.73	99.20	98.98	97.52
MCR (%)	3.717	9.294	11.810	3.676	9.224	12.002	3.832	9.459	12.557

Quantitative Evaluation (Segmentation)

The **misclassification ratio** is calculated for all image voxels of interest,

while the **Jaccard similarity** and the **Dice coefficient** estimate the segmentation of voxels of one segmented tissue.

Quantitative Evaluation (Segmentation)

The Jaccard similarity also termed the Tanimoto coefficient [26, 41]

- Measures the similarity of two sets as the ratio of the size of their intersection divided by the size of their union, and ranges from 0 for sets that have no common elements to 1 for sets that are identical.

$$J(S_1, S_2) = \frac{|S_1 \cap S_2|}{|S_1 \cup S_2|},$$

- There is a monotonic transformation between the scores of Jaccard and Dice
- The Jaccard similarity measure in terms of true positives (tp), false positives (fp) and false negatives (fn):

$$J = \frac{tp}{tp + fp + fn}$$

***

Quantitative Evaluation (Segmentation)

The Dice coefficient [29, 40, 42]

- Used for comparing set similarity
- **It is a special case of the *k* index,** appropiate for assessment of image segmentation.

$$\kappa(S_1, S_2) = \frac{2|S_1 \cap S_2|}{|S_1| + |S_2|}.$$

it can be rewritteng as

$$\kappa(S_1, S_2) = \frac{|S_1 \cap S_2|}{\frac{1}{2}(|S_1| + |S_2|)} = \frac{|S_1 \cap S_2|}{|S_1 \cup S_2| - \frac{1}{2}(|S_1 \backslash S_2| + |S_2 \backslash S_1|)},$$

- This metric is always larger than the Jaccard metric, except at 0 and 1 where they are equal.
- This case of the k index **is related to the Jaccard metric**:

$$\kappa = \frac{2J}{J+1}$$

Both metrics agree that **0 means the two sets are completely dissimilar** and that 1 **means the two sets are identical**.
The **Dice and Jaccard** measures **are fully equivalent**, i.e. there is a monotonic transformation between their scores.

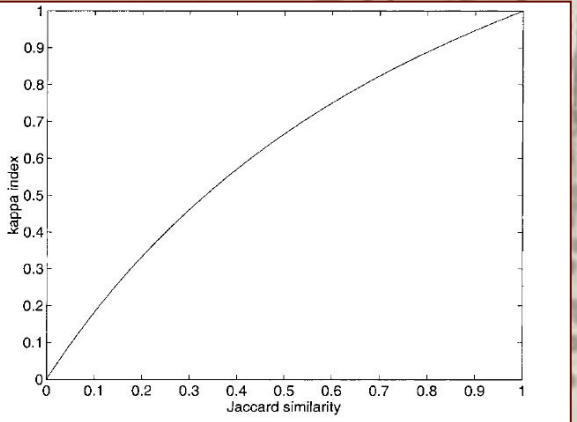

FIG. 4. Comparison of the Jaccard similarity metric and the κ index.

Quantitative Evaluation (Segmentation)

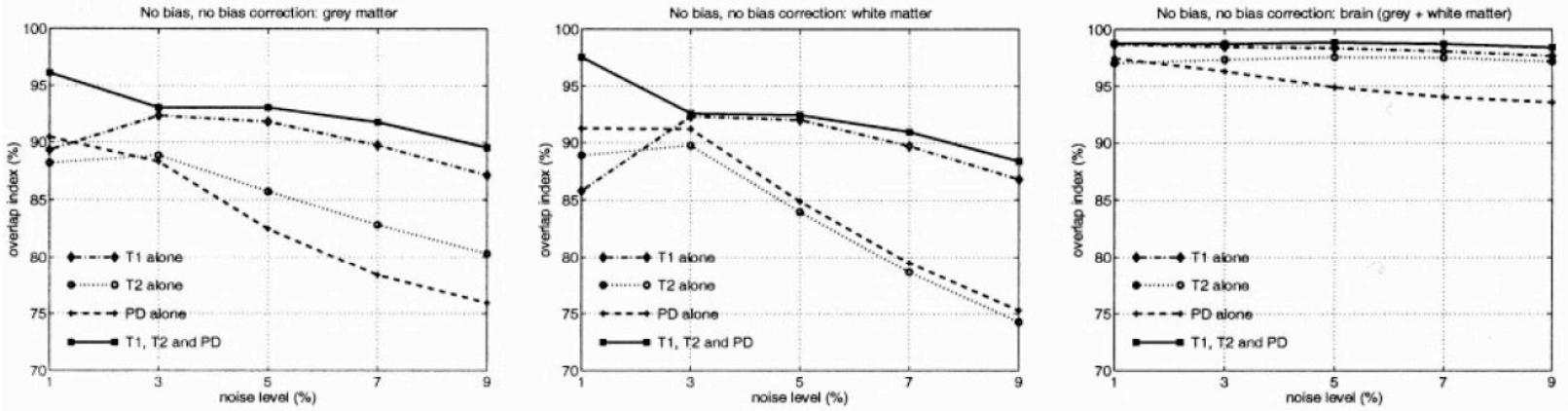

Fig. 3. Overlap metric between the automatic segmentation and the known ground truth for simulated MR images without bias field as a function of noise level for (a) gray matter, (b) white matter, and (c) total brain.

The overlap is estimated by Dice coefficient.

Table 1
Dice metrics computed from segmented BrainWeb images using the full model

Dice metric	T1			T2			PD		
	0%	40%	100%	0%	40%	100%	0%	40%	100%
Grey matter	0.932	0.934	0.918	0.883	0.881	0.880	0.872	0.880	0.872
White matter	0.961	0.961	0.939	0.916	0.916	0.915	0.923	0.928	0.923
Whole brain	0.977	0.978	0.978	0.967	0.966	0.965	0.957	0.959	0.955

Quantitative Evaluation (Segmentation)

- (IBSR [12]) The overlap metric
  - is a method for comparing two segmentations that is more critical than comparisons using the volume.
  - It is defined for a given voxel class assignment as the sum of the number of voxels that both have the class assignment in each segmentation divided by the sum of voxels where either segmentation has the class assignment.
  - This metric approaches a value of 1.0 for results that are very similar and is near 0.0 when they share no similarly classified voxels.
  - This is the same as the Tanimoto coefficient (Pattern Classification and Scene Analysis. Duda & Hart, 1973, p. 216).

Quantitative Evaluation (Segmentation)

IBSR [12], AVERAGE OVERLAP for each brain scan

amap

bkgnd	CSF	Gray	White	
1.000	0.025	0.268	0.134	5_8
1.000	0.073	0.363	0.233	4_8
1.000	0.035	0.356	0.276	2_4
1.000	0.025	0.330	0.305	6_10
1.000	0.076	0.492	0.466	15_3
1.000	0.084	0.577	0.567	16_3
1.000	0.069	0.535	0.634	17_3
1.000	0.089	0.584	0.617	8_4
1.000	0.076	0.620	0.642	7_8
1.000	0.062	0.652	0.646	110_3
1.000	0.047	0.569	0.648	111_2
0.998	0.076	0.648	0.657	112_2
1.000	0.052	0.662	0.656	100_23
1.000	0.122	0.676	0.696	202_3
1.000	0.051	0.659	0.692	191_3
0.999	0.119	0.649	0.693	12_3
1.000	0.041	0.650	0.683	13_3
1.000	0.072	0.663	0.691	1_24
1.000	0.126	0.666	0.704	205_3
1.000	0.077	0.661	0.711	11_3
0.999	0.069	0.564	0.567	Total

bmap

bkgnd	CSF	Gray	White	
1.000	0.034	0.153	0.075	5_8
1.000	0.059	0.323	0.188	4_8
1.000	0.021	0.297	0.182	2_4
1.000	0.034	0.224	0.200	6_10
1.000	0.074	0.497	0.480	15_3
1.000	0.083	0.585	0.573	16_3
1.000	0.055	0.531	0.628	17_3
1.000	0.086	0.612	0.661	8_4
1.000	0.064	0.614	0.650	7_8
1.000	0.068	0.662	0.644	110_3
1.000	0.051	0.613	0.676	111_2
0.998	0.080	0.663	0.673	112_2
1.000	0.058	0.684	0.673	100_23
1.000	0.137	0.685	0.700	202_3
1.000	0.047	0.659	0.723	191_3
0.999	0.147	0.692	0.717	12_3
1.000	0.040	0.657	0.672	13_3
1.000	0.070	0.669	0.695	1_24
1.000	0.137	0.661	0.710	205_3
1.000	0.081	0.689	0.737	11_3
0.999	0.071	0.558	0.562	Total

fuzzy

bkgnd	CSF	Gray	White	
1.000	0.033	0.196	0.075	5_8
1.000	0.059	0.327	0.283	4_8
1.000	0.020	0.305	0.289	2_4
1.000	0.034	0.279	0.205	6_10
1.000	0.061	0.408	0.479	15_3
1.000	0.048	0.456	0.548	16_3
1.000	0.046	0.413	0.558	17_3
1.000	0.064	0.492	0.623	8_4
1.000	0.051	0.530	0.650	7_8
1.000	0.037	0.538	0.653	110_3
1.000	0.035	0.482	0.637	111_2
0.998	0.048	0.554	0.677	112_2
1.000	0.029	0.547	0.674	100_23
1.000	0.083	0.588	0.712	202_3
1.000	0.032	0.568	0.723	191_3
0.999	0.073	0.560	0.721	12_3
1.000	0.024	0.516	0.714	13_3
1.000	0.045	0.534	0.692	1_24
1.000	0.089	0.588	0.716	205_3
1.000	0.054	0.579	0.718	11_3
0.999	0.048	0.473	0.567	Total

map

bkgnd	CSF	Gray	White	
1.000	0.032	0.152	0.069	5_8
1.000	0.060	0.330	0.178	4_8
1.000	0.020	0.312	0.185	2_4
1.000	0.038	0.239	0.199	6_10
1.000	0.077	0.482	0.476	15_3
1.000	0.083	0.577	0.561	16_3
1.000	0.059	0.495	0.594	17_3
1.000	0.090	0.599	0.625	8_4
1.000	0.069	0.604	0.636	7_8
1.000	0.063	0.647	0.640	110_3
1.000	0.047	0.560	0.638	111_2
0.998	0.079	0.656	0.670	112_2
1.000	0.051	0.665	0.663	100_23
1.000	0.144	0.697	0.704	202_3
1.000	0.043	0.651	0.720	191_3
0.999	0.148	0.685	0.713	12_3
1.000	0.040	0.659	0.698	13_3
1.000	0.068	0.656	0.687	1_24
1.000	0.136	0.666	0.713	205_3
1.000	0.077	0.683	0.716	11_3
0.999	0.071	0.550	0.554	Total

Quantitative Evaluation (Segmentation)

IBSR [12], AVERAGE OVERLAP for each brain scan

mlc

bkgnd	CSF	Gray	White	
1.000	0.033	0.173	0.070	5_8
1.000	0.060	0.340	0.174	4_8
1.000	0.020	0.310	0.188	2_4
1.000	0.031	0.213	0.214	6_10
1.000	0.072	0.468	0.479	15_3
1.000	0.066	0.511	0.564	16_3
1.000	0.055	0.480	0.631	17_3
1.000	0.072	0.530	0.642	8_4
1.000	0.055	0.553	0.674	7_8
1.000	0.071	0.682	0.655	110_3
1.000	0.046	0.564	0.645	111_2
0.998	0.067	0.644	0.676	112_2
1.000	0.045	0.652	0.671	100_23
1.000	0.104	0.649	0.688	202_3
1.000	0.035	0.613	0.658	191_3
0.999	0.138	0.680	0.645	12_3
1.000	0.047	0.698	0.666	13_3
1.000	0.056	0.599	0.691	1_24
1.000	0.104	0.638	0.707	205_3
1.000	0.077	0.705	0.696	11_3
0.999	0.062	0.535	0.551	Total

tskmeans

bkgnd	CSF	Gray	White	
1.000	0.032	0.181	0.074	5_8
1.000	0.058	0.317	0.267	4_8
1.000	0.020	0.305	0.289	2_4
1.000	0.034	0.270	0.207	6_10
1.000	0.064	0.429	0.479	15_3
1.000	0.054	0.480	0.563	16_3
1.000	0.050	0.448	0.606	17_3
1.000	0.064	0.487	0.632	8_4
1.000	0.050	0.520	0.660	7_8
1.000	0.039	0.543	0.655	110_3
1.000	0.038	0.498	0.654	111_2
0.998	0.049	0.557	0.676	112_2
1.000	0.029	0.547	0.674	100_23
1.000	0.086	0.587	0.708	202_3
1.000	0.032	0.565	0.720	191_3
0.999	0.078	0.574	0.727	12_3
1.000	0.025	0.531	0.722	13_3
1.000	0.047	0.545	0.692	1_24
1.000	0.091	0.583	0.711	205_3
1.000	0.056	0.587	0.716	11_3
0.999	0.049	0.477	0.571	Total

The following graphs show the overlap scores for each of the 20 brains. Scores have been multiplied by 1000.

The bran scans have been roughly ordered by their difficulty to be segmented.

The line labeled "expert" is the average overlap between two expert operators who segmented the same four brain scans for a study using different data.

This was included to give a sense of the overlap level that has been found to be acceptable for volumetric studies.

Quantitative Evaluation (Segmentation)

*IBSR [12], Overlap of **Gray Voxels** for Each Brain Scan*

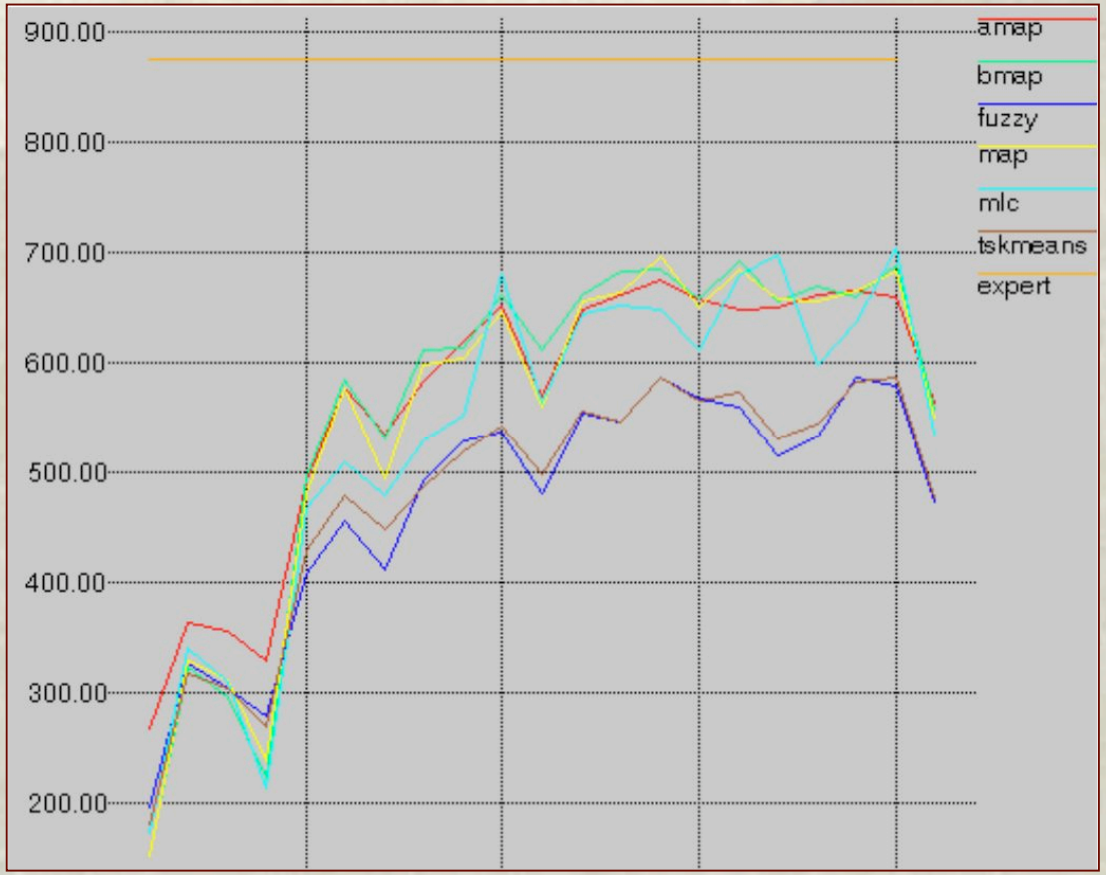

Quantitative Evaluation (Segmentation)

*IBSR [12], Overlap of **White Voxels** for Each Brain Scan*

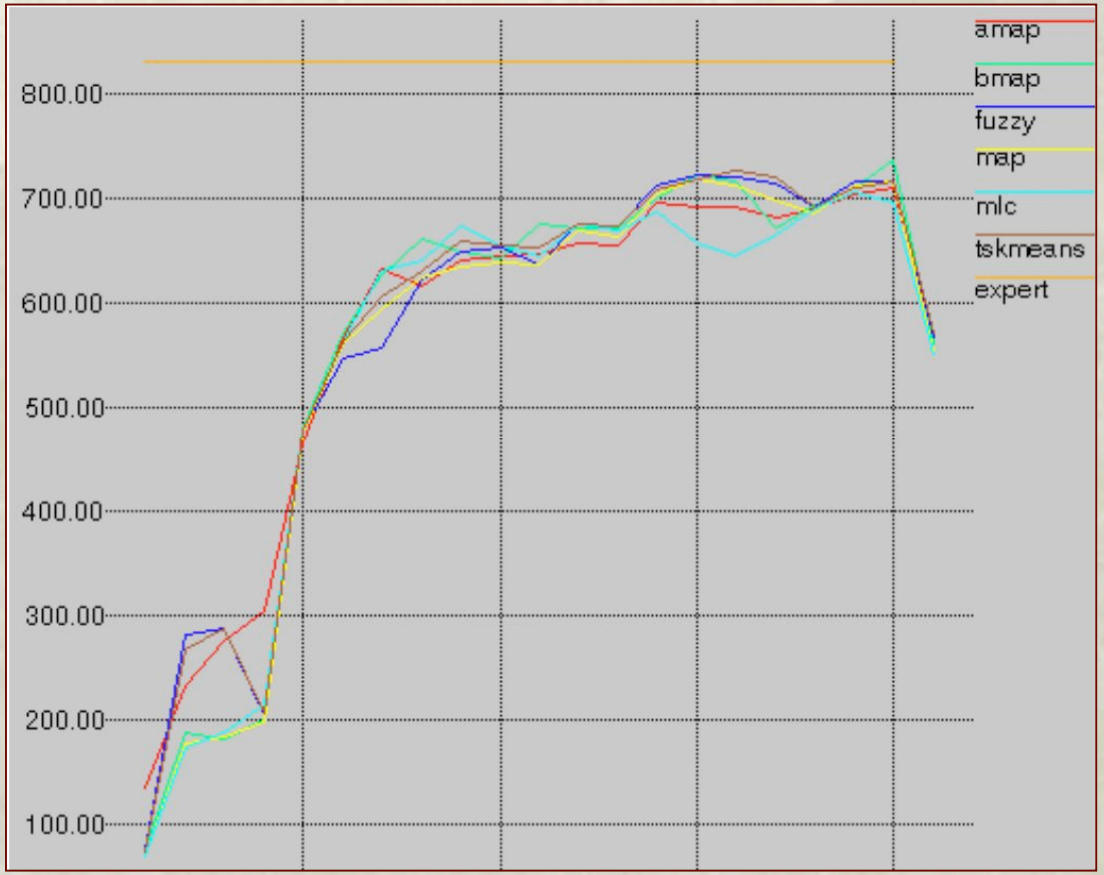

Quantitative Evaluation (Segmentation)

[43] Siyal_MY_2005

Table 2
Average overlap between manual segmentation and various methods for MGH data base

Method	GM	WM
Adaptive MAP	0.564	0.567
Biased MAP	0.558	0.562
FCM	0.473	0.567
MAP	0.550	0.554
Tree-structure *k*-means	0.477	0.571
Maximum-likelihood	0.535	0.551
MPM-MAP	0.662	0.683
M-FCM	0.647	0.658
Our proposed method	0.750	0.724
Manual (4 brain averaged over 2 experts)	0.876	0.832

[44] Younis_A_2007

Table 3. IBSR Results

White	Gray	Method
0.567	0.564	Adaptive MAP
0.562	0.558	Biased MAP
0.567	0.473	Fuzzy c-means
0.554	0.55	Maximum Aposteriori Probability (MAP)
0.551	0.535	Maximum-Likelihood
0.571	0.477	Tree-structure k-means
0.662	0.683	MPM-MAP 0
0.662	0.787	AIANN Model
0.832	0.876	Manual (4 brains averaged over 2 experts)

[10] García-Sebastián_M_2007

Table 1
Average overlap between manual segmentation and the algorithms tested in this paper

Algorithm	GM	WM
Wells	0.564	0.567
BMAP	0.558	0.562
BFCM	0.630	0.709
GradClassLeg	0.745	0.732
(Siyal, Yu, 2005)	0.750	0.724

[12] IBSR Web

Average Overlap between manually-guided segmentations
and various methods for 20 brain scans

gray	white	method
0.564	0.567	adaptive MAP
0.558	0.562	biased MAP
0.473	0.567	fuzzy c-means
0.550	0.554	Maximum Aposteriori Probability (MAP)
0.535	0.551	Maximum-Likelihood
0.477	0.571	tree-structure k-means
0.876	0.832	Manual (4 brains averaged over 2 experts)

Quantitative Evaluation (Segmentation)

MPM-MAP [45]

TABLE III
AVERAGE OVERLAP (PERFORMANCE INDEXES) BETWEEN MANUALLY-GUIDED SEGMENTATIONS AND VARIOUS METHODS FOR THE 20 BRAIN SCANS OF THE MGH DATA BASE

Method	GM	WM
adaptive MAP	0.564	0.567
biased MAP	0.558	0.562
fuzzy c-means	0.473	0.567
Maximum a Posteriori Probability (MAP)	0.550	0.554
tree-structure k-means	0.477	0.571
Maximum-Likelihood	0.535	0.551
MPM-MAP	0.662	0.683
Manual (4 brains averaged over 2 experts)	0.876	0.832

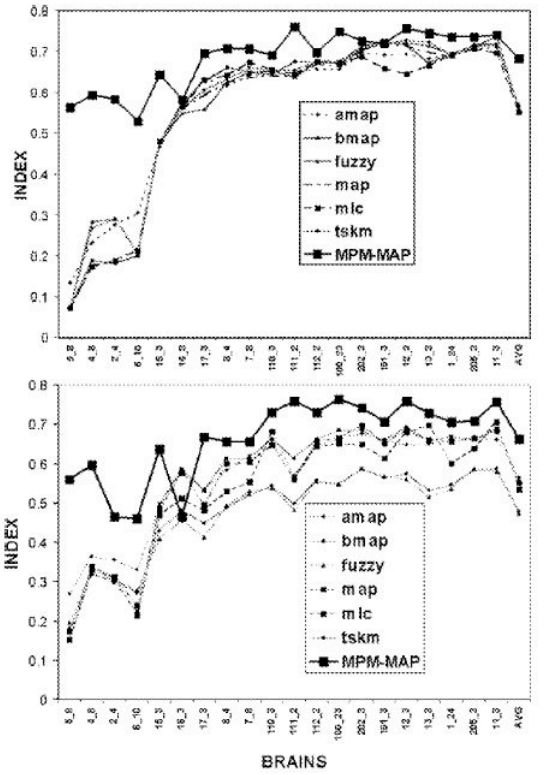

Fig. 5. Performance indexes for the individual brains of the MGH database for different segmentation methods. The bold line corresponds to our method. Above: WM; below: GM.

Quantitative Evaluation (Segmentation)

- **Accurate segmentation ratio (ASR) [42]**
- **False positive (FPF) and False negative fraction (FNF) [46]**
- **True positive fraction (TPF)**

$$TPF = \frac{Volume^{+}_{seg} \cap Volume^{+}_{true}}{Volume^{+}_{true}} \times 100\,\%\,,$$

$$FPF = \frac{Volume^{-}_{seg} \cap Volume^{-}_{true}}{Volume^{+}_{true}} \times 100\,\%\,, \qquad (23)$$

$$ASR = \frac{whole \quad volume^{+}_{seg} \cap whole \quad volume^{+}_{true}}{whole \quad volume^{+}_{true}} \times 100\,\%$$

where a + or − sign represents whether a voxel is or is not of a specific tissue type. TPF and FPF are used to measure the performance of different algorithms for a specific tissue, and ASR provides the overall evaluation based on the entire image volume. Obviously, a perfect segmentation has a TPF equal to one, FPF of zero, and ASR of one.

Quantitative Evaluation (Segmentation)

- **Segmentation accuracy (SA) [7]**

$$SA = \frac{\text{Number of correctley classifiedpixels}}{\text{Total number of pixels}} \times 100\%.$$

TABLE I
SEGMENTATION ACCURACY OF DIFFERENT METHODS WHEN APPLIED ON MR SIMULATED DATA

	SNR		
Segmentation Method	13db	10 db	8db
FCM	98.92	86.24	78.9
EM	99.12	93.53	85.11
BCFCM	99.25	97.3	93.7

Quantitative Evaluation (Segmentation)

- **False positive, False negative, True positive and True negative [26, 47]**

BSE Results on BrainWeb Phantom

Noise	RF	False positive rate	False negative rate	Similarity	κ index
0%	0%	2.28%	0.44%	0.969	0.984
3%	0%	0.98%	0.73%	0.985	0.993
	20%	1.47%	0.65%	0.976	0.988
	40%	0.98%	0.69%	1.000	1.000
5%	0%	1.09%	1.24%	0.975	0.987
	20%	1.17%	0.86%	0.978	0.989
	40%	0.99%	1.44%	0.974	0.987
7%	0%	1.02%	1.04%	0.977	0.988
	20%	1.10%	0.93%	0.977	0.989
	40%	1.56%	0.69%	0.972	0.986
9%	0%	1.07%	1.03%	0.975	0.987
	20%	0.55%	6.23%	0.917	0.957
	40%	1.13%	0.77%	0.976	0.988
Average		**1.18%**	**1.29%**	**0.973**	**0.986**

Note. False positive rates (nonbrain tissue included in mask), false negative rates (GM or WM excluded from mask), and agreement (both Jaccard and κ index) to mask found for 3% noise, 40% RF phantom. RF, or radiofrequency, refers to the level of intensity nonuniformity applied the image.

$$Sensitivity = \frac{T_+}{(T_+ + F_-)}$$

$$Specificity = \frac{T_-}{(T_- + F_+)}$$

Quantitative Evaluation (Segmentation)

- **Measure of the change of tumor volume [48]**

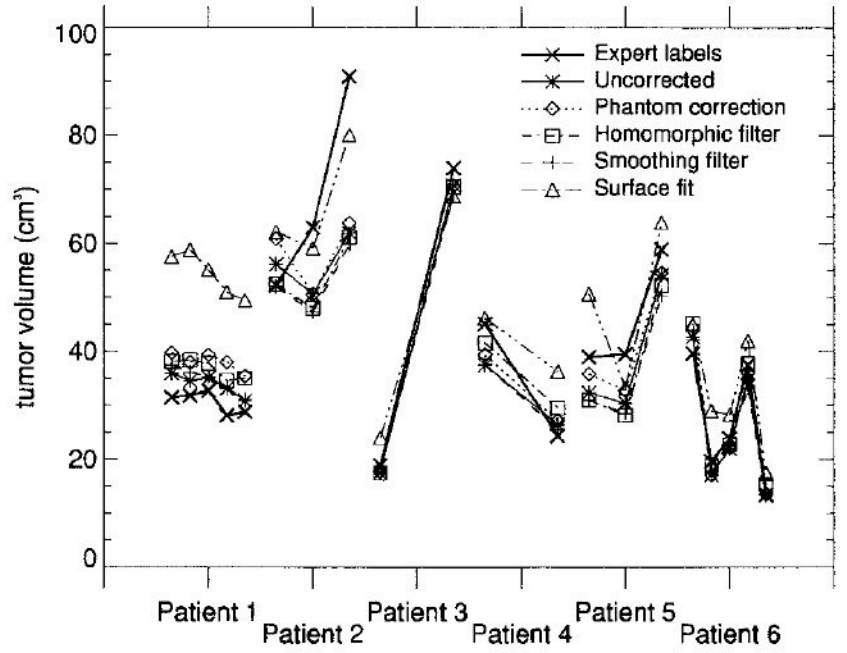

FIG. 7. Tumor volumes measured for each of the patients and each of the follow-ups. The expert labels were obtained by manual segmentation. The other volumes were obtained using k nearest neighbors segmentation, and were then averaged over the training sets (operators).

TABLE II. Pearson's correlation coefficient for segmented tumor volume against manually labeled volume.

Correction method	R_p
No correction	0.90
Phantom correction	0.88
Smoothing	0.88
Homomorphic filter	0.89
Surface fit	0.73

Quantitative Evaluation (Segmentation)

- **Structural Similarity Index measure (SSIM-INDEX) [49]**

to evaluate the degree of similarity between the original signal (groundtruth) and the distorted signal (segmented image). The SSIM-INDEX, averaged over K images, is given by:

$$\text{SSIM} - \text{INDEX} = \frac{1}{K}\sum_{k=1}^{K}\left(\frac{(2 * \mathbf{x}_k * \mathbf{y}_k + C_1)\,(2 * \sigma_{\mathbf{x}_k\mathbf{y}_k} + C_2)}{(\overline{\mathbf{x}}_k^2 + \overline{\mathbf{y}}_k^2 + C_1)\,(\sigma_{\mathbf{x}_k}^2 + \sigma_{\mathbf{y}_k}^2 + C_2)}\right)$$

where $C_1 = (K_1 * L)^2, C_2 = (K_2 * L)^2, K_1 = 0.01, K_2 = 0.03$, and $L = 255$. Such measure gives values in [0,1]; the higher the value of SSIM-INDEX, the better the segmentation result.

Quantitative Evaluation (Segmentation)

- **Difference ratio metric [50]**

Since there is a considerable loss of classified information when converting probabilistic segmentation into a non-probabilistic segmentation, to get a more reasonable comparison between the SOM-PNN classifier and the SOM classifier, we now propose a generalized difference ratio metric. For pixel n, let the probabilities of segmentation A be $P_n^A = \{P_{n1}^A, P_{n2}^A, \cdots, P_{nK}^A\}$ and that of segmentation B be $P_n^B = \{P_{n1}^B, P_{n2}^B, \cdots, P_{nK}^B\}$, the generalized difference ratio between A and B is defined as

$$r_{AB} = \frac{1}{N} \sum_{n=1}^{N} \sum_{j=1}^{K} \frac{\left(P_{nj}^A - P_{nj}^B\right)^2}{2} \times 100\% \qquad (19)$$

where N is the total number of voxels in the ROI and K is the number of materials to be segmented. Here the ROI is the brain volume without air and $K = 3$. In the non-probabilistic case, the generalized difference ratio is reduced to the percentage of difference between two segmentation used in [15].

Overview of validation methods	
Qualitative evaluation	
Profile	Ahmed et al. (1999), Cohen et al. (2000), Johnston et al. (1996), Lai and Fang (1999), Lee and Vannier (1996), Mihara et al. (1998), Sled et al. (1998), Vokurka et al. (1999), Wald et al. (1995)
Image	Ahmed et al. (1999), Axel et al. (1987), Brey and Narayana (1988), Clare et al. (2001), Collewet et al. (2002), Deichmann et al. (2002), Gilles et al. (1996), Lai and Fang (1999), Liney et al. (1998), Murakami et al. (1996), Sled et al. (1998), Thulborn et al. (1998), Wald et al. (1995), Wells III et al. (1996), Zhang et al. (2001)
Histogram	Clare et al. (2001), Collewet et al. (2002), Schroeter et al. (1998), Thulborn et al. (1998), Vokurka et al. (1999)
Quantitative evaluation	
Grayscale level	Brinkmann et al. (1998), Condon et al. (1987), Han et al. (2001), Koivula et al. (1997), Prima et al. (2001), Tincher et al. (1993), Wicks et al. (1993)
Segmented data	Dawant et al. (1993), Guillemaud and Brady (1997), Harris et al. (1994), Johnston et al. (1996), Lee and Vannier (1996), Likar et al. (2001), Meyer et al. (1995), Narayana and Borthakur (1995), Pham and Prince (1999a), Rajapakse and Kruggel (1998), Shattuck et al. (2001), Styner et al. (2000), Van Leemput et al. (1999), Vokurka et al. (1999), Wells III et al. (1996), Zhou et al. (2001), Zijdenbos et al. (1995)

Referencias

1. **Magnetic Resonance - Technology Information Portal, http://www.mr-tip.com**.
2. Uros Vovk et al. (2007). **A Review of Methods for Correction of Intensity Inhomogeneity in MRI**. Transactions on Medical Imaging, vol. 26 no.3.
3. Sled, J. G., Zijdenbos, A. P., and Evans, A. C. (1998). **A nonparametric method for automatic correction of intensity nonuniformity in MRI data**. IEEE Transactions on Medical Imaging, 17(1):87-97. PMID: 9617910.
4. Rajapakse, J. C., Kruggel, F., 1998**. Segmentation of MR images with intensity inhomogeneities.** Image and Vision Comp., 16(3):165 - 180.
5. J. Besag**, Spatial interaction and the statistical analysis of lattice systems,** Journal of the Royal Statistical Society B 36 (2) (1974) 192–225.
6. S. Geman, D. Geman**, Stochastic relaxation, Gibbs distribution, and the Bayesian restoration of images,** IEEE Transactions on Pattern Analysis and Machine Intelligence 6 (1984) 721–741.
7. Ahmed M.N., Yamany S.N., Mohamed N., Farag A. A., Moriarty T., (2002) **A Modified Fuzzy C-Means Algorithm for Bias Field Estimation and Segmentation of MRI Data**, IEEE Trans. Med. Imag., 21 (3):193-199.
8. Styner, M., Gerig, G., Brechbu¨ hler, C., Szekely, G., 2000**. Parametric estimate of intensity inhomogeneities applied to MRI.** IEEE Trans. Med. Imag. 19 (3), 153–165.

Referencias

9. Zagorodnov V.; M.F. Hansen (2005) **Performance evaluation of parametric bias field correction**, ICIP'2005, vol.3 pp.: 732-735.
10. García-Sebastián, M., Fernández, E., Graña, M., and Torrealdea, F. J. 2007. **"A parametric gradient descent MRI intensity inhomogeneity correction algorithm".** Pattern Recogn. Lett. 28, 13 (Oct. 2007), 1657-1666.
11. C. A. Cocosco, V. Kollokian, K. R. K. -S. Kwan, and A. C. Evans, "**BrainWeb: Online interface to a 3-D MRI simulated brain database**," NeuroImage, vol. 5, pp. 425–425, 1997.
12. **Internet Brain Segmentation Repository (IBSR),** http://www.cma.mgh.harvard.edu/ibsr/.
13. Shen, S., Sandham, W., Granat, M. and Sterr, A. (2005). "**MRI Fuzzy Segmentation of Brain Tissue Using Neighborhood Attraction With Neural-Network Optimization**." Information Technology in Biomedicine, IEEE Transactions on 9(3): 459-467.
14. Joshi, N. B. and Brady, M. (2005). "**A non-parametric mixture model for partial volume segmentation of MR images"**. Proceedings of British Machine Vision Conference - BMVC.
15. Zhang, Y., Brady, M. and Smith, S. (2001). **"Segmentation of brain MR images through a hidden Markov random field model and the expectation-maximization algorithm**" Medical Imaging, IEEE Transactions on 20(1): 45-57.

Referencias

16. Atkins, M. S., Siu, K., Law, B., Orchard, J. J. and Rosenbaum, W. L. (2002). "**Difficulties of T1 brain MRI segmentation techniques"**. Medical Imaging 2002: Image Processing, San Diego, CA, USA, SPIE.
17. Shang-Hong Lai and Ming Fang, **A new variational shape-from-orientation approach to correcting intensity inhomogeneities in magnetic resonance images**, Medical Image AnalysisVolume 3, Issue 4, , December 1999, Pages 409-424.
18. Dawant, B.M. and Zijdenbos, A.P. and Margolin, R.A. **Correction of intensity variations in MR images for computer-aidedtissue classification**. Medical Imaging, IEEE Transactions on, Volume: 12, Issue 4,Dec 1993, Pages 770-781.
19. Van Leemput, K.; Maes, F.; Vandermeulen, D.; Suetens, P., "**Automated model-based bias field correction of MR images of the brain**" Medical Imaging, IEEE Transactions on, vol.18, no.10, pp.885-896, Oct 1999.
20. Wells WM, Kikinis R, Grimson WEL, Jolesz F. **Adaptive segmentation of MRI data**. IEEE Transactions on Medical Imaging. 1996;15:429-442.
21. Studholme, C.; Cardenas, V.; Song, E.; Ezekiel, F.; Maudsley, A.; Weiner, M., "**Accurate template-based correction of brain MRI intensity distortion with application to dementia and aging**" Medical Imaging, IEEE Transactions on , vol.23, no.1, pp. 99-110, Jan. 2004.

Referencias

22. James B. Arnold, Jeih-San Liow, Kirt A. Schaper, Joshua J. Stern, John G. Sled, David W. Shattuck, Andrew J. Worth, Mark S. Cohen, Richard M. Leahy, John C. Mazziotta and David A. Rottenberg, **Qualitative and Quantitative Evaluation of Six Algorithms for Correcting Intensity Nonuniformity Effects**, NeuroImageVolume 13, Issue 5 , May 2001, Pages 931-943.
23. Luo, J.; Zhu, Y.; Clarysse, P.; Magnin, I., "**Correction of Bias Field in MR Images Using Singularity Function Analysis**" Medical Imaging, IEEE Transactions on , vol.24, no.8, pp. 1067-1085, Aug. 2005.
24. Sylvain Prima, Nicholas Ayache, Tom Barrick, Neil Roberts, **Maximum Likelihood Estimation of the Bias Field in MR Brain Images: Investigating Different Modelings of the Imaging Process. Medical Image Computing and Computer-Assisted Intervention** - MICCAI 2001: 4th International Conference Utrecht, The Netherlands, October 14-17, 2001, Proceedings (2001), 811.
25. Brinkmann, B.H.; Manduca, A.; Robb, R.A., "**Optimized homomorphic unsharp masking for MR grayscale inhomogeneity correction**" Medical Imaging, IEEE Transactions on , vol.17, no.2, pp.161-171, Apr 1998.
26. D. W. Shattuck, S. R. Sandor-Leahy, K. A. Schaper, D. A. Rottenberg, and R. M. Leahy, **“Magnetic resonance image tissue classification using a partial volume model,”** Neuroimage, vol. 13, pp. 856–876, 2001.

Referencias

27. A. Fan, W. M. Wells, J. W. Fisher, M. Cetin, S. Haker, R. Mulkern, C. Tempany, and A. S. Willsky, "**A unified variational approach to denoising and bias correction in MR**," Inf. Process Med Imag., vol. 18, pp. 148–159, 2003.
28. E. B. Lewis and N. C. Fox, "**Correction of differential intensity inhomogeneity in longitudinal MR images**," Neuroimage, vol. 23, pp. 75–83, 2004.
29. B. Johnston, M. S. Atkins, B. Mackiewich, and M. Anderson, "**Segmentation of multiple sclerosis lesions in intensity corrected multispectral MRI**," IEEE Trans. Med. Imag., vol. 15, no. 2, pp. 154–169, Apr. 1996.
30. E. A. Vokurka, N. A. Watson, Y. Watson, N. A. Thacker, and A. Jackson, "**Improved high resolution MR imaging for surface coils using automated intensity non-uniformity correction: Feasibility study in the orbit**," J. Magn. Reson. Imag., vol. 14, pp. 540–546, 2001.
31. Wicks DA; Barker GJ; Tofts PS, "**Correction of intensity nonuniformity in MR images of any orientation**". Magn Reson Imaging, 11(2), pp. 183-96. 1993.
32. H. Guillemaud and M. Brady, "**Estimating the bias field of MR images**," IEEE Trans. Med. Imag., vol. 16, no. 3, pp. 238-251, 1997.
33. Likar, B.; Viergever, M.A.; Pernus, F., "**Retrospective correction of MR intensity inhomogeneity by information minimization**," Medical Imaging, IEEE Transactions on , vol.20, no.12, pp.1398-1410, Dec 2001.

Referencias

34. J. D. Gispert, S. Reig, J. Pascau, J. J. Vaquero, P. Garcia-Barreno, and M. Desco, "**Method for bias field correction of brain T1-weighted magnetic resonance images minimizing segmentation error**," Hum. Brain Mapp., vol. 22, pp. 133–144, 2004.
35. E. Solanas and J.-P. Thiran, "**Exploiting voxel correlation for automated MRI bias field correction by conditional entropy minimization**," presented at the 4th Int. Medical Image Comput. Computer-Assist. Intervent. (MICCAI 2001), Utrecht, The Netherlands, 2001.
36. U. Vovk, F. Pernuˇs, and B. Likar, "**MRI intensity inhomogeneity correction by combining intensity and spatial information**," Phys. Med. Biol., vol. 49, pp. 4119–4133, 2004.
37. D. L. Pham and J. L. Prince, "**Adaptive fuzzy segmentation of magnetic resonance images**," IEEE Trans. Med. Imag., vol. 18, no. 9, pp. 737–752, Sep. 1999.
38. R. Bansal, L. H. Staib, and B. S. Peterson, "**Correcting nonuniformities in MRI intensities using entropy minimization based on an elastic model**," presented at the Medical Image Computing and Computer-Assisted Intervention (MICCAI 2004), Saint-Malo, France, 2004.
39. J. C. Rajapakse, J. N. Giedd, and J. L. Rapoport, "**Statistical approach to segmentation of single-channel cerebral MR images**," IEEE Trans. Med. Imag., vol. 16, no. 2, pp. 176–186, Apr. 1997.
40. A. W. Liew and H.Yan, "**An adaptive spatial fuzzy clustering algorithm for 3-DMRimage segmentation**," IEEE Trans. Med. Imag., vol. 22, no. 9, pp. 1063–1075, Sep. 2003.
41. K. Van Leemput, F. Maes, D. Vandermeulen, and P. Suetens, "**Automated model-based tissue classification of MR images of the brain**," IEEE Trans. Med. Imag., vol. 18, no. 10, pp. 897–908, Oct. 1999.
42. Z.-P. Liang and P. C. Lauterbur, **Principles of Magnetic Resonance Imaging: A Signal Processing Perspective**. Piscataway, NJ: IEEE Press, 1999.

Referencias

43. M.Y. Siyal and Lin Yu, **An intelligent modified fuzzy c-means based algorithm for bias estimation and segmentation of brain MRI**, Pattern Recognition LettersVolume 26, Issue 13, , 1 October 2005, Pages 2052-2062.
44. Akmal Younis, Mohamed Ibrahim, Mansur Kabuka and Nigel John. **An Artificial Immune-Activated Neural Network Applied to Brain 3D MRI Segmentation.** Journal of Digital Imaging 2007 Dec 11.
45. J.L. Marrroquin, B.C. Vemuri, S. Botello, F. Calderon and A. Fernandez-Bouzas, **"An accurate and efficient Bayesian method for automatic segmentation of brain MRI''**, IEEE Trans. On Med. Imag.21,8:934-945 2002.
46. X. Li, L. Li, H. Lu, and Z. Liang, **"Partial volume segmentation of brain magnetic resonance images based on maximum a posteriori probability,"** Med. Phys., vol. 32, pp. 2337–2345, 2005.
47. Albert Huang, Rafeef Abugharbieh, Roger Tam and Anthony Traboulsee. **"MRI Brain Extraction with Combined Expectation Maximization and Geodesic Active Contours".** Signal Processing and Information Technology, 2006 IEEE International Symposium on Volume , Issue , Aug. 2006 Page(s):107 – 111.
48. Robert P. Velthuizen and John J. Heine and Alan B. Cantor and Hongbo Lin and Lynn M. Fletcher and Laurence P. Clarke. "**Review and evaluation of MRI nonuniformity corrections for brain tumor response measurements**". Medical Physics -- September 1998 -- Volume 25, Issue 9, pp. 1655-1666.

Referencias

49. Gabriele Martino and Alfredo Petrosino. (2006). "**Fuzzy Connectivity and Its Application to Image Segmentation**". Neural Nets, Springer Berlin / Heidelberg, ISSN: 0302-9743 (Print) 1611-3349 (Online), ISBN: 978-3-540-33183-4. Volume 3931/2006.
50. Feng, M., Wenping, W., Wai Wan, T., Zesheng, T., Shaowei, X. and Xin, T. (1998). **Probabilistic segmentation of volume data for visualization using SOM-PNN classifier**. Volume Visualization, 1998. IEEE Symposium on.
51. Collins, D.L., Zijdenbos, A.P., Kollokian, V., Sled, J.G., Kabani, N.J., Holmes, C.J., Evans, A.C., 1998. **"Design and construction of a realistic digital brain phantom".** IEEE Trans. Med. Imag. 17 (3), 463–468.
52. Kwan, R.K.-S., Evans, A.C., Pike, G.B., 1996. **"An extensible MRI simulator for post-processing evaluation".** Visualization in Biomedical Computing, Proc. VBC '96, pp. 135–140.
53. Cocosco, C.A., Kollokian, V., Kwan, R.K.-S., Evans, A.C., 1997. **"Brainweb: Online interface to a 3D MRI simulated brain database".** NeuroImage 5 (4), 425.
54. Awate S.P., Tasdizen T., Foster N., Whitaker R.T., 2006. **"Adaptive Markov Modeling for Mutual-Information-Based, Unsupervised MRI Brain-Tissue Classification".** Medical Image Analysis.
55. J. Melonakos, Y. Gao, and A. Tannenbaum. **"Tissue Tracking: Applications for Brain MRI Classification".** In SPIE Medical Imaging, 2007.

Introduction to GIS

Outline

- Introduction
- Georeferenced data
- Integration of Information
- Types of data
- Functional requirements of a GIS
- GIS development
- Software for GIS

Definitions of GIS (I)

- a computer based system that provides four sets of capabilities to handle georeferenced data :
  - data input
  - data management (data storage and retrieval)
  - manipulation and analysis
  - data output.
    - **Arnoff**, S. **1989**. Geographic Information Systems: A Management Perspective. Ottawa, Canada: WDL Publications

- a system of hardware, software and procedures to facilitate the management, manipulation, analysis, modelling, representation and display of georeferenced data to solve complex problems regarding planning and management of resources
  (NCGIA, 1990)

GIS System Architecture and Components

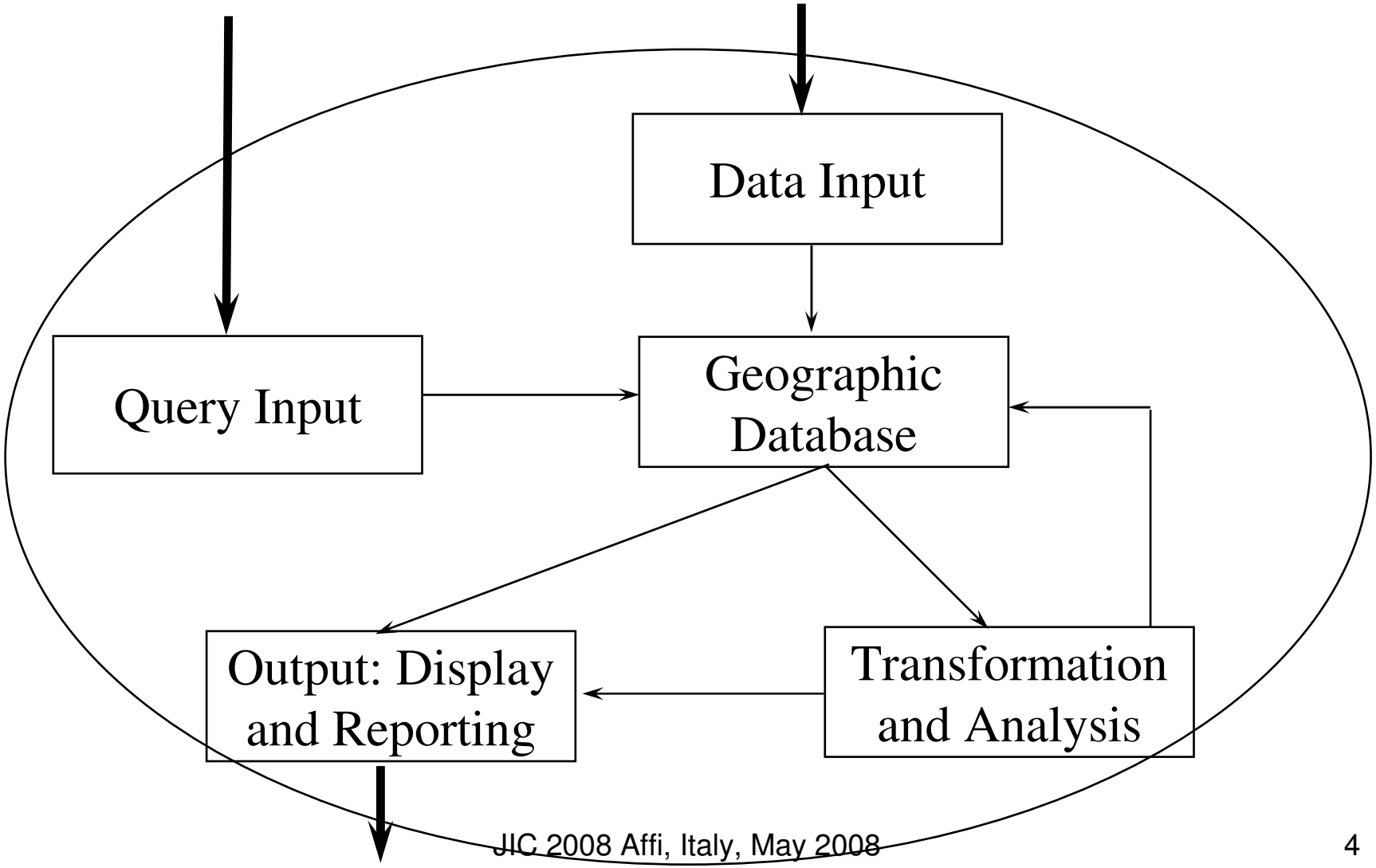

georeferenced data

- Data that contains location components as one of its dimensions, also referred to as geographically referenced data or geospacial data
  - *data are spatially referenced to the Earth*
  - Every object present on the Earth can be geo-referenced
    - » Coordinate Systems Overview

Spatial and Attribute Data

- Spatial data *(where)*
  - specifies location
  - stored in a *shape file, geodatabase* or similar geographic file
- Attribute (descriptive) data *(what, how much, when)*
  - specifies characteristics at that location, natural or human-created
  - stored in a data base *table*

GIS systems traditionally maintain spatial and attribute data separately, then “join” them for display or analysis

Geographic Integration of Information

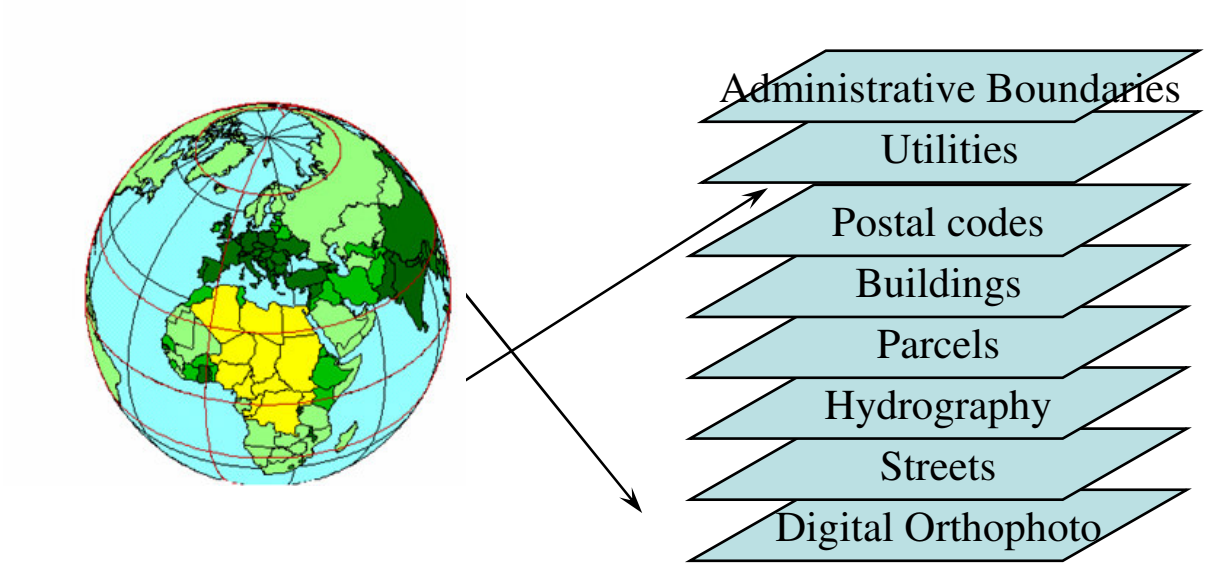

- Data is organized by layers where *each layer represents a common feature (attribute).*
- Layers are integrated using explicit location on the earth's surface

The GIS Model: example

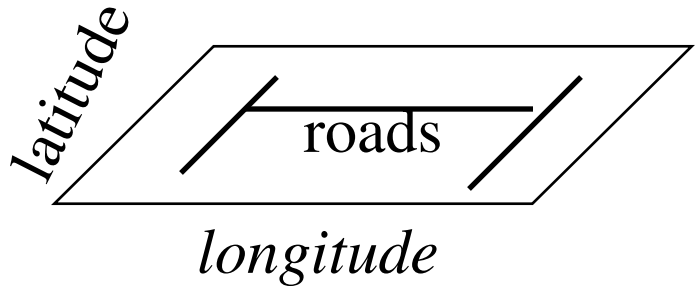

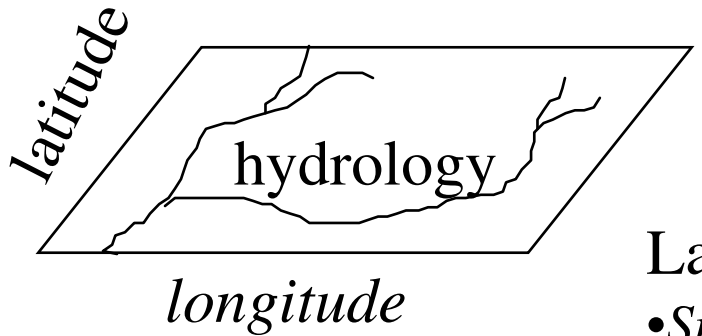

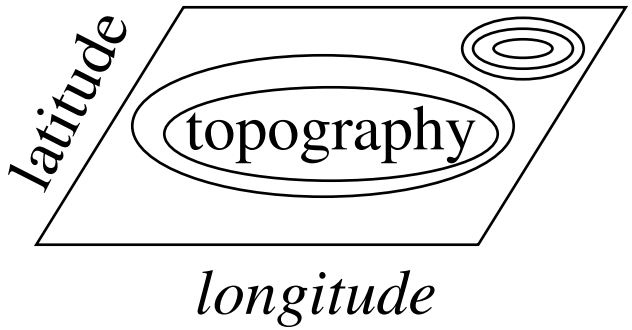

Here we have three <u>layers</u> or themes**:**

--roads,

--hydrology (water),

--topography (land elevation)

They can be related because precise geographic coordinates are recorded for each theme.

Layers are comprised of two data types

- *Spatial data* which describes location (where)
- *Attribute data* specifing what, how much,when

Layers may be represented in two ways:

- in *vector* format as points and lines
- in *raster(or image)* format as pixels

Concept of Vector and Raster

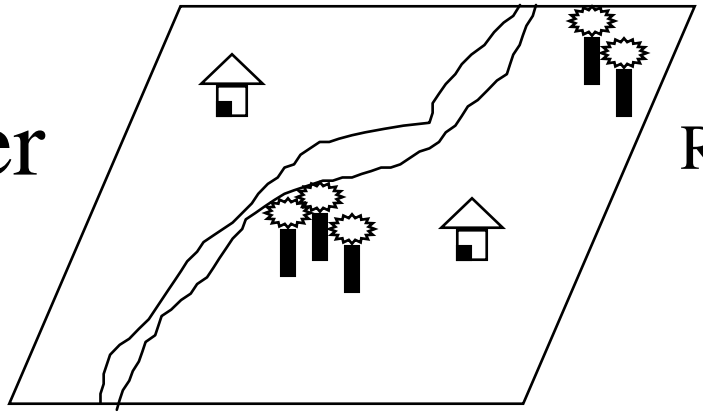

Real World

Raster Representation

	0	1	2	3	4	5	6	7	8	9
0								R	T	
1							R			T
2		H					R			
3							R			
4					R	R				
5				R						
6			R		T	T		H		
7			R		T	T				
8		R								
9		R								

Vector Representation

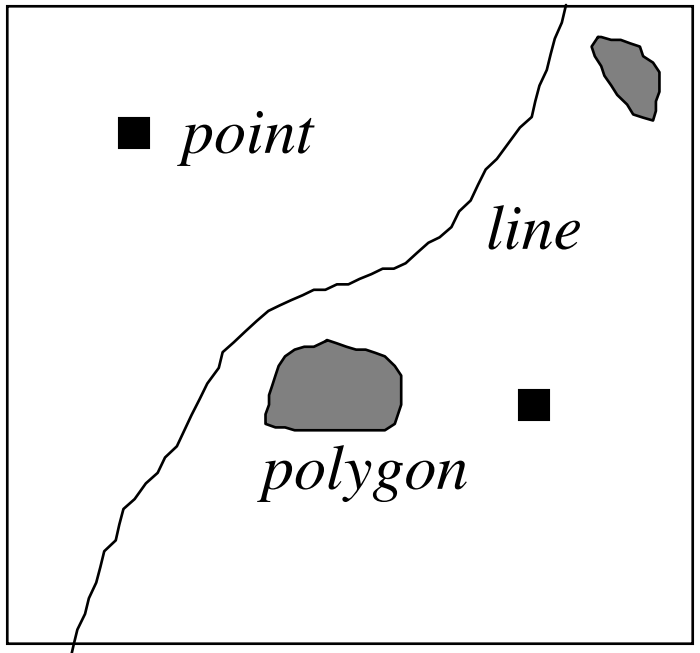

Types of data – Raster

Raster Model

- **Input**: scanner/remote sensing acquisition
- area is covered by grid with (usually) equal-sized, square cells
- *attributes* are recorded by assigning each cell a single value based on the majority feature (attribute) in the cell, such as land use type, elevation*, etc*
    - *Image* data is a special case of raster data in which the "attribute" is a reflectance value from the geomagnetic spectrum
    - cells in image data often called *pixels* (picture elements)

Raster data structures, I

- exhaustive enumeration
  - every pixel is given a single value, there is no compression

raster representation

A	A	A	A	0	0	0	0
A	A	A	A	A	0	0	0
A	A	A	A	0	B	0	0
A	A	A	A	0	0	0	0
A	A	A	0	0	0	C	C
0	0	0	0	0	C	0	0
C	C	C	C	C	0	0	0
0	0	0	0	0	0	0	0

pixel	value
1	A
2	A
3	A
4	A
5	0
6	0
7	0
8	0
9	A
10	A
11	A
12	A
13	A
14	0
15	0
16	0
.	.
.	.
.	.
62	0
63	0
64	0

Raster data structures, II

- **run-length encoding**
  - It is a raster image compression technique
    - » This technique is particularly useful for encoding monochrome images or binary images (Chrisman, 1997).

raster representation

A	A	A	A	0	0	0	0
A	A	A	A	A	0	0	0
A	A	A	A	0	B	0	0
A	A	A	A	0	0	0	0
A	A	A	0	0	0	C	C
0	0	0	0	0	C	0	0
C	C	C	C	C	0	0	0
0	0	0	0	0	0	0	0

A, 4 0, 8
A, 5 0, 8
A, 4 0, 5 B, 6 0, 8
A, 4 0, 8
A, 3 0, 6 C, 8
0, 5 C, 6 0, 8
C, 5 0, 8
0, 8

Advantages of Raster Data

- substantially easier manipulation

  - Layer overlays are really simple, since all layers are defined with the same grid over the region.
  - Topology is implicitly defined, since the location of each cell relative to all the others can be easily found.
  - no increase in complexity with son and daughter maps

Disadvantages of Raster Data

- higher data storage requirements (8-32 bytes per cell* rows* columns), but compression (run length encoding, quad trees) helps,
- decreased boundary precision
  - Increasing the *resolution* (that is, decreasing the cell size) by a factor of two, the data set sizing quadruple
- Resolution is also problematic
  - the discretization process has an effect analogous to rounding of numbers, but in a spatial sense
    - what you see in the raster image is usually larger or smaller than the real-world equivalent.
    - objects smaller than one cell may not appear at all!

Types of data - vector

- **Input** : digitizing or scanner with vectorization

  - areas usually won't "close" with digitizing errors

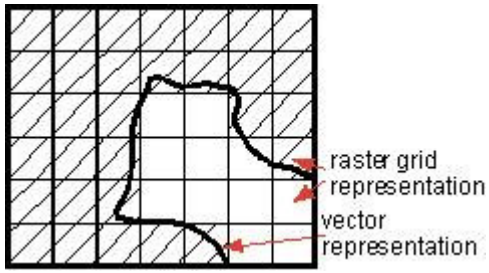

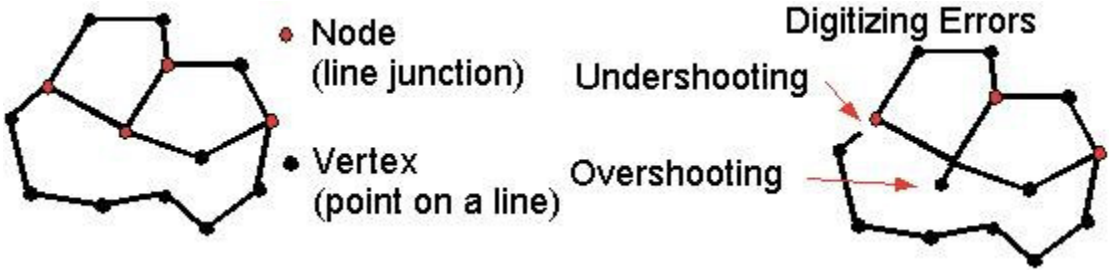

  - **points or dots (*nodes)***: trees, poles, fire plugs, airports, cities
  - **lines (*arcs)*:** streams, streets, sewers,
  - **areas (*polygons)*:** land parcels, cities, counties, forest, rock type

Topology of vector data

- Topology describes the spatial relationships of points, nodes and lines

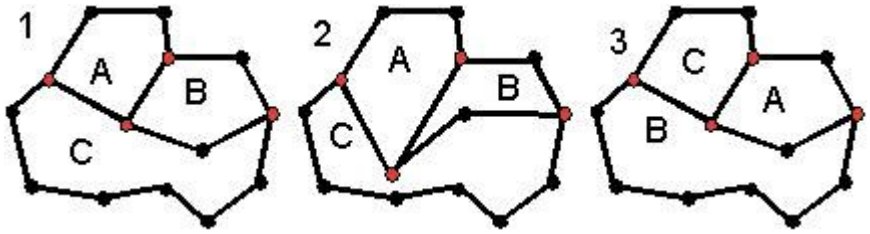

- Figures 1 and 2 have the same topology but different geometry
- Figures 1 and 3 have the same geometry but different topology

vector models I

- list of coordinates "spaghetti“
  - simple
  - easy to manage
  - no topology
  - lots of duplication, hence need for large storage space
  - very often used in CAC (computer assisted cartography)

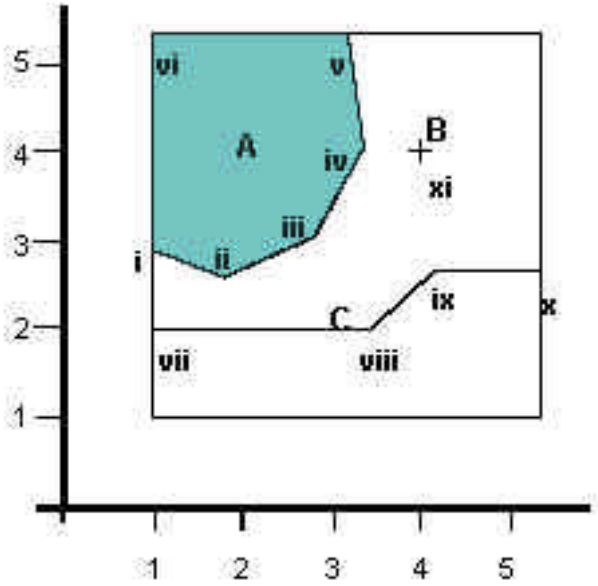

A, 6 (identifier of polygon and number of vertex)
1, 3 (coordinates of the first vertex)
1.8, 2.6
2.8, 3
3.3, 4
3.2, 5.2
1, 5.2
1, 3 (coordinates of the first vertex again)
B, 1 (identifier of the point and number of vertex)
4, 4
C, 4 (identifier of the line and number of vertex)
1, 2
3.5, 2
4.2, 2.7
5.2, 2.7

vector models II

- vertex dictionary
  - no duplication, but still this model does not use topology

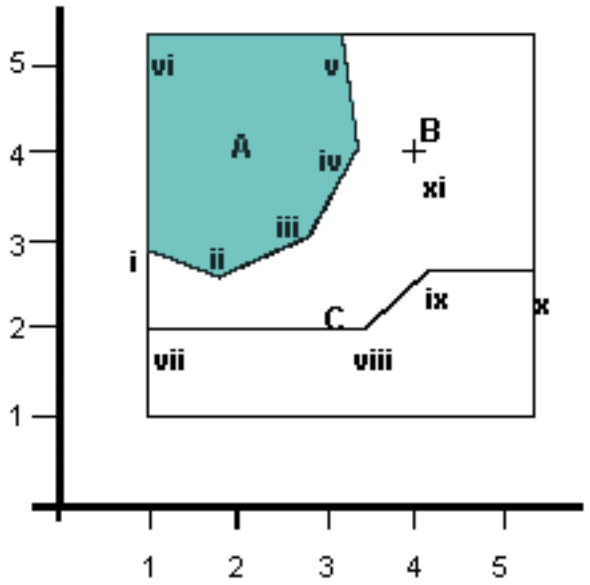

file 1

vertex	X	Y
i	1	3
ii	1.8	2.6
iii	2.8	3
iv	3.3	4
v	3.2	5.2
vi	1	5.2
vii	1	2
viii	3.5	2
ix	4.2	2.7
x	5.2	2.7
xi	4	4

file 2

polygon A: i, ii, iii, iv, v, vi
point B: xi
line C: vii, viii, ix, x

vector models III

- Dual Independent Map Encoding (DIME)
  - developed by US Bureau of the Census
  - nodes (intersections of lines) are identified with codes
  - assigns a directional code in the form of a "from node" and a "to node"
  - both street addresses and UTM coordinates are explicitly defined for each link

DIME

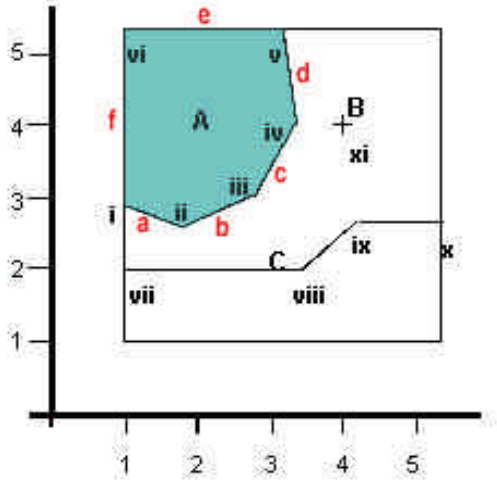

file 1

vertex	X	Y
i	1	3
ii	1.8	2.6
iii	2.8	3
iv	3.3	4
v	3.2	5.2
vi	1	5.2
vii	1	2
viii	3.5	2
ix	4.2	2.7
x	5.2	2.7
xi	4	4

segment	right polygon	left polygon	from vertex	to vertex
a	external	A	i	ii
b	external	A	ii	iii
c	external	A	iii	iv
d	external	A	iv	v
e	external	A	v	vi
f	external	A	vi	i
g	external	external	vii	viii
h	external	external	viii	ix
i	external	external	ix	x

polygon	segments
A	a, b, c, d, e, f

vector models IVa

- **POLYVRT** or arc / node structure
  - Arcs (polylines) are identified with codes

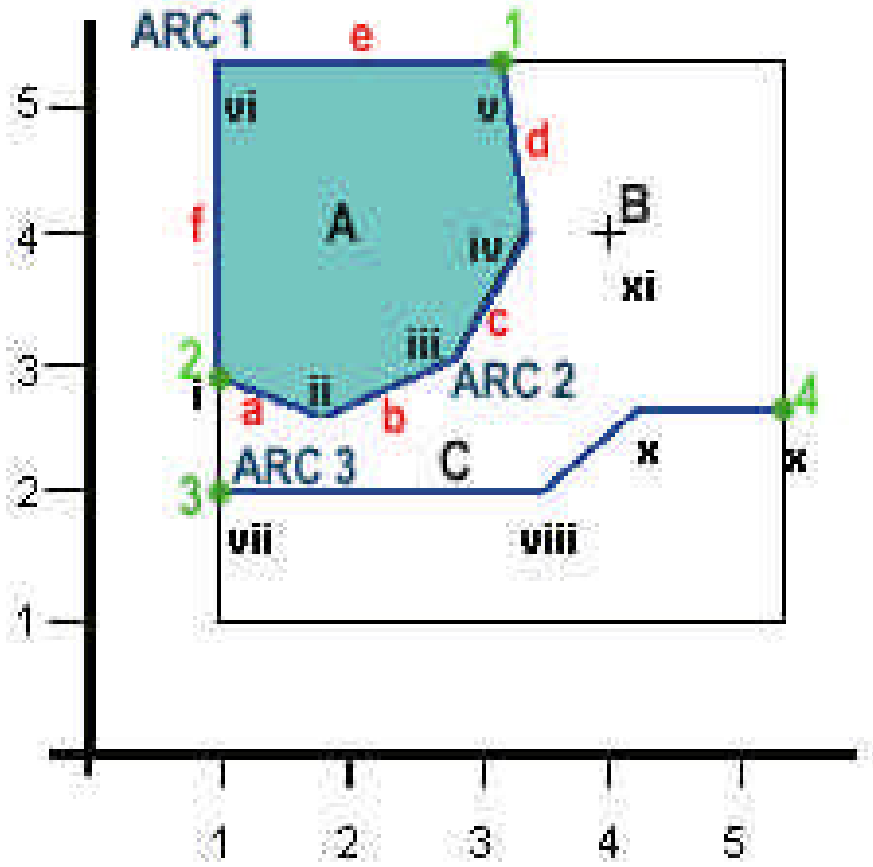

POLYVRT files

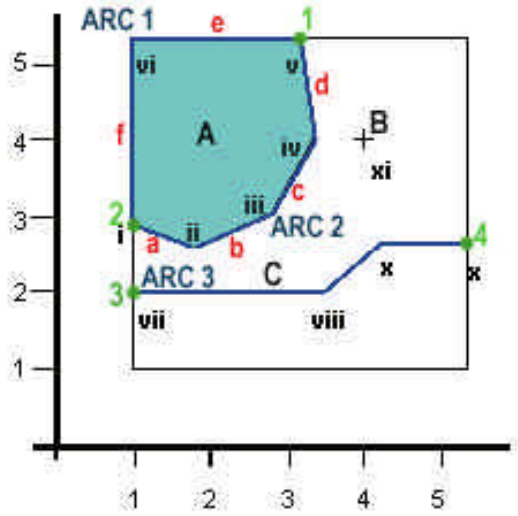

File 1. Coordinates of nodes and vertex for all the arcs			
ARC	F_node	Vertex	T_node
1	3.2, 5.2	1, 5.2	1,3
2	1,3	1.8,2.6 2.8,3 3.3,4	3.2, 5.2
3	1,2	3.5,2 4.2,2.7	5.2,2.7

File 2. Arcs topology				
ARC	F_node	T_node	R_poly	L_poly
1	1	2	External	A
2	2	1	A	External
3	3	4	External	External

File 3. Polygons topology	
Polygon	Arcs
A	1, 2

File 4. Nodes topology	
Node	Arcs
1	1,2
2	1,2
3	3
4	4
5	5

Advantages of vector data

- Much greater precision in the definition of objects is possible by defining the geometric extent of the regions in which they occur.
  - one can draw far better maps with vector data than with raster data.
  - Much less space is required to store all the information,
    - empty space on the map can be ignored.
- greater boundary precision
- complex analyses are easier

Disadvantages of vector data

- Topology between the geometric objects must be explicitly defined, though it can be done quite efficiently.
- The file structures required are more complex than the raster data files, and layer overlay operations can be very complex to perform.
  - "overlays" rapidly increase complexity and data storage needs
- Spatial variability can be represented, using a *Triangulated Irregular Network*, but it is still not as effective as the use of regularly gridded data,
- Some mathematical operations, such as derivatives, on layers or between two or more layers are impossible to perform.

raster vs. vector data models

	raster	vector
precision in graphics	✗	✓
traditional cartography	✗	✓
data volume	✗	✓
topology	✗	✓
computation	✓	✗
update	✓	✗
continuous space	✓	✗
integration	✓	✗
discontinuous	✗	✓

Properties of georeferenced data I

- **Projection:** the method by which the curved 3-D surface of the earth is represented by X,Y coordinates on a 2-D flat map/screen
  - distortion is inevitable

- **Scale:** the ratio of distance on a map to the equivalent distance on the ground
  - in theory GIS is scale independent but in practice there is an implicit range of scales for data output in any project

Properties of georeferenced data II

- **Accuracy:** how well does the database info match the real world
  - *Positional*: how close are features to their real world location?
  - *Consistency*: do feature characteristics in database match those in real world
    - is a road in the database a road in the real world?
  - *Completeness*: are all real world instances of features present in the database?
    - Are all roads included.
- **Resolution:** the size of the smallest feature able to be recognized
  - for raster data, it is the *pixel* size

The tighter the specification, the higher the cost.

Functional requirements of a GIS

- Data input
  - Existing maps, field observations, aerial photographs, sensors (airborne and satellites)
- Data storage and management
- Data processing and analysis
- Data output and presentation
  - maps, tables, figures, 3D models

Data capture/input

- Input data by digitizing, scanning, or direct coordinate entry
- Edit data in the GIS to correct errors or add features
- Label the spacial features so they can be identified (names or codes)

Management

- Link attribute data to spacial objects
- Link to external databases
- Make changes in existing databases
- Update database features
- Import/export from/to other GIS or DBMS

Manipulation

- Make maps from different sources compatible so that they can be drawn together.
- Transformation of coordinates
- Projection change

Analysis

- A GIS is distinguished from other types of information systems because of its spatial analysis functions.
- The organization of database into map layers is not simply for reasons of organizational clarity, rather it is to provide rapid access to data elements required for geographic analysis.
- The range of geographical analysis procedures can be subdivided into the following categories.
    - Database Query.
    - Overlay.
    - Proximity analysis.
    - Network analysis.
    - thematic mapping.

Database Query by attribute

- The attribute database is stored in a relational database mode, with a unique code linked to the geometric data.
  - The database can be searched with specific characteristics.
  - Complex queries can be made with the help of SQL.

Database Query by geometry

- There are five forms of primitive geometric query:
  - by point,
  - by rectangle,
  - by circle,
  - by line,
  - by polygon,
- More complex queries use both geometric and attributes search criteria together.
  - Many GIS force the separation of the two different types of query. However, some GIS, using databases to store both geometric and attribute data, allow true hybrid spatial queries.

Overlay

- Raster overlay
  - It is a relatively straightforward operation and often many data sets can be combined and displayed at once.
- Vector overlay
  - The vector overlay, however is far more difficult and complex and it involves more processing.
  - It can be performed on different types of map features:
    - » Polygon-on-polygon, line-in-polygon, point-on-polygon,….

Difference between a Topologic Overlay and a Graphic Over plot

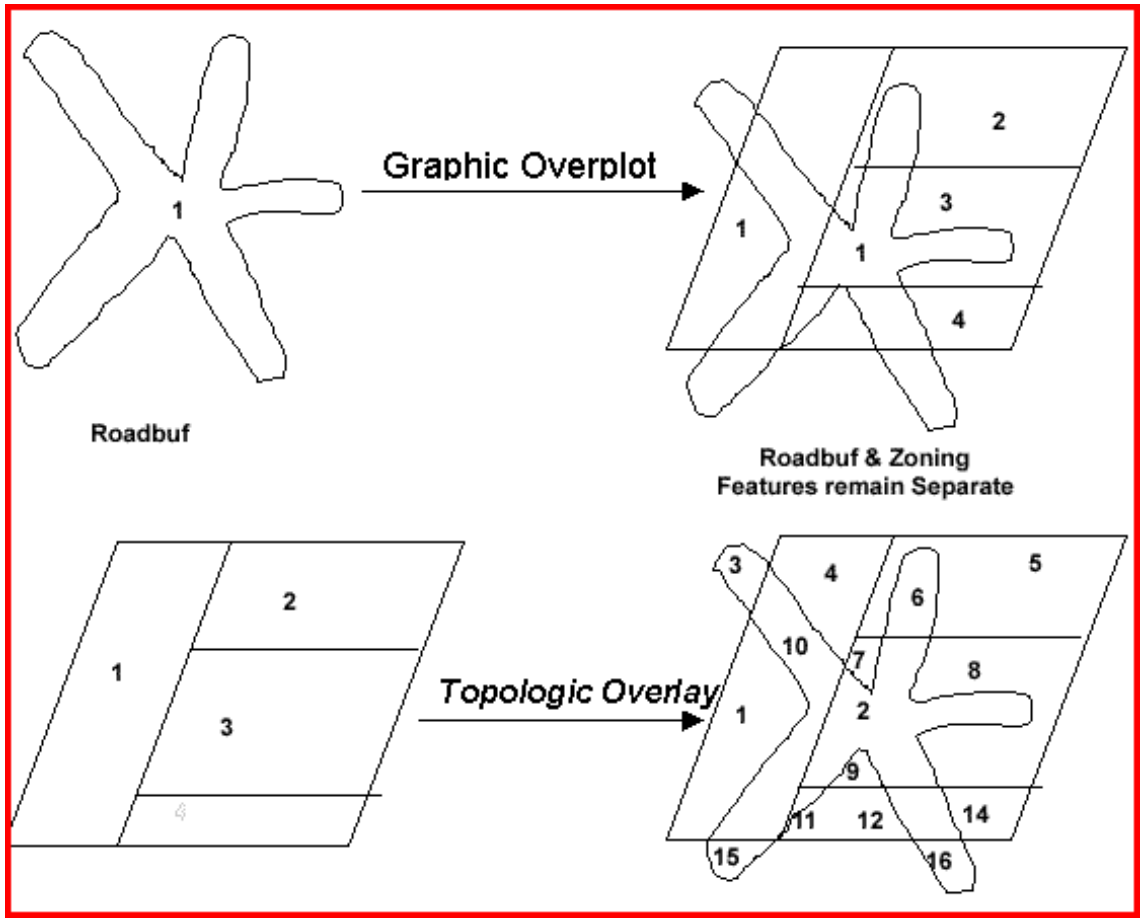

Proximity analysis

- A *buffer* is simply a region surrounding the area of interest for a given distance
- a tessellation of *Voronoi polygons (*Thiessen or proximity polygons*)*
  - All points within a Voronoi polygon are closer to a point inside the polygon than to any other point.

Network analysis

- Network models are based on interconnecting logical components, of which the most important are:
  - "Nodes" define start, end, and intersections
  - "Chains" are line features joining nodes
  - “Links" join together points making up a chain.
- *functions* include:
  - *routing and allocation*
  - *Spread and search*

- *Network load* queries involve predictions of the response of a network to an event.

Thematic mapping

- Maps used to visualize spatial relationships and patterns among information pertaining to some theme or concept (e.g. income)

- Thematic maps allow the user to present the data in a way that allows for quick and easy recognition of patterns that could not be seen by just looking at a table of numbers.
    - Superimposing two different thematic maps can allow the viewer to visually find any relationship between two variables.

- A variable, can be plotted using many different ranges, ex:
    - natural break creates ranges that, as much as possible, try to minimize the internal variation of the numbers,while maximizing the variation between the ranges.
    - Equal ranges is just that, each range is the same width.
    - equal counts, attempts to put a similar number of values in each range.

- The method of presentation of a thematic map is important.
    - colours used in a map that can emphasize or de-emphasize things you want people to notice or ignore,
    - Selection of more or fewer range divisions will add or decrease the amount of detail your map will show.

Types of Thematic Maps

- **Choropleth map**: uses zones or polygons to display information using shading, dot, density, or other techniques.
  - e.g population change, ethnicity distribution
- **Proximal (dasymetric) map**: shows zones of constant attributes, such as soil type or vegetation (similar to choropleth except that data determines boundary lines; no pre-defined polygons)
  - e.g zoning, soil map
- **Isopleth map (contour or isarithmic)** : shows a contiuous three dimensional surface such as elevation using lines connecting points of equal value (contours).
  - e.g elevation, travel time contours from a point(s), land values, income
- **Point (dot) or symbol map**: shows information relating to specific points using marker sysmbols whose size and/or frequency relates to magnitude of phenomena
  - e.g.housing sales, crimes

GIS Development

- GIS is resource-intensive and until to mid-1990 was confined to fairly large computers (mainframes, workstations).
- With de development of more powerful PCs, **Desktop GIS** became a practical proposition to a much wider (although still technically skilled) user base.
- In the late 1990s, the processing power and bandwith, resulted in **web-based GIS**, and introduced the benefits of GIS to a much wider audience.
- The third generation telecommunications will result in a explosion in **location based services**.

Web-based mapping

- It merges web and GIS technology
- It is based in the WMS(Web map Service) standard adopted by OGC (Open Geospatial consortium) that specifies the request and response protocols for open-based map client/server interaction.

Degrees of Web-based mapping complexity

- Static maps
  - Maps are downloaded as images (TIFFs or JPEGs). They may be made more interactive by embedding links
    - » If a user clicks on a particular area in a small scale map it could be linked a a larger scale image showing more detail.
- Dynamic maps
  - Maps are update on a regular basis with more up to date data (weather maps, traffic maps). However, the user does not have any input into what is displayed.
- Simple interactive maps
  - Simple maps drawn in response to a user query
    - The user types an address and the server respond by drawing a map centred on this address
- User specified themes
  - The user has control over which themes should be displayed. The themes are selected from a list provided by the server. There are also tools for zooming and panning.
- Web-based GIS

Web-based GIS

- The user is allowed to query the database using GIS tools to query either the attribute data (e.g. display only features with particular attributes) or spacial data (e.g. buffer zones).
  - They are also given more control over how the features should be rendered (e.g. colours, symbolisation, etc..)
- Web-based GIS generally tends to assume only minimal levels of expertise on behalf of the end users.

Examples of cartographic webs

- http://sitar.aragon.es/visor/
- http://sitna.cfnavarra.es/navegar/?lang=es
- http://sigpac.mapa.es/fega/visor/
- http://sigpac.mapa.es/fega/visor/

- ….

Differences between GIS and Related Systems

- **DBMS-**-typical MIS data base contains implicit but not explicit locational information
  - city, county, zip code, etc. but no geographical coordinates
- **automated mapping (AM)** --primarily two-dimensional display devices
  - thematic mapping (choropleth,etc such as SAS/GRAPH, DIDS, business mapping software) unable to relate different geographical layers (e.g zip codes and counties)
  - automated cartography--graphical design oriented; limited database ability
- **facility management (FM) systems**--
  - lack spatial analysis tools
- **CAD/CAM** (computer aided design/drafting)--primarily 3-D graphic creation (engineering design) & display systems
  - don't reference via geographic location
    - CAD sees the world as a 3-D cube, GIS as a 3-D sphere
  - limited (if any) database ability (especially for non-spatial data)
- **scientific visualization systems**--sophisticated multi-dimensional graphics, but:
    - lack database support
    - lack two-dimensional spatial analysis tools

Software for GIS: *The Main Players*

- **ESRI, Inc.,** Redlands, CA
  - clear market leader with about a third of the market
  - originated commercial GIS with their ArcInfo product in 1981
  - privately owned by Jack Dangermond, a legend in the field
  - Strong in gov., education, utilities and business logistics
- **MapInfo, Troy N.Y.**
  - Aggressive newcomer in early 1990s, but now well-established.
  - Strong presence in business, especially site selection & marketing, and telecom
- **Intergraph** (Huntsville, AL)
  - origins in proprietary CAD hardware/software
  - Older UNIX-based **MGE** (Modular GIS Environment) evolved from CAD
  - Current **GeoMedia** was the first true MS Windows-based GIS
  - strong in design, public works, and FM (facilities management), but weakening
- **Bentley Systems** (Exton, PA)
  - **MicroStation GeoGraphics,** originally developed with Intergraph, is now their exclusive and main product..
  - Strong in engineering; advertises itself as "geoengineering"
- **Autodesk** (San Rafael, CA)
  - Began as PC-based CAD, but now the dominant CAD supplier
  - First GIS product **AutoCAD *Map*** introduced in 1996
  - Primarily small business/small city customer base

The main two "pure GIS" companies.

Software for GIS: other players

Vector GIS

- **Smallworld Systems** (Englewood, CO)
  - first to use OO (early '90s), but failed to compete as established vendors did same
  - Purchased by GE in 2000
  - emphasis on FM & utilities
- **Manifold** (CDA International Corp):
  - low cost, but low market share
- **Maptitude** (Caliper Corp, Newton, MA):
  - another low cost one

Raster GIS

- **ERDAS/Imagine**
  - long established leader
  - acquired by Leica Geosystems in 2001
- **ER MAPPER**
  - aggressive newcomer originating in Australia
- **Envi,**
  - relative newcomer, radar specialization
  - acquired by Kodak in 2000
- **PCI**--Geomatica
  - long-term Canadian player
- **CARIS**
  - newer Canadian entry
- **GRASS** (Rutgers Univ.)
  - Classic old-timer originally developed by US Army Construction Engineering Research Lab(CERL) in Champaign, IL;
  - army ended dev. & support in 1996 but assumed by Baylor University.
- **IDRSI** (Clark Univ)
  - pioneering, university-developed package

ESRI Product Line-up: *ArcGIS* client products

ArcReader ("adobe acrobat" for maps) & **ArcExplorer** (spatial data viewer)

- Free viewers for geographic data.

ArcGIS 9.x Desktop: two primary modules (MS only)

1. **ArcMap:** for data display, map production, spatial analysis, data editing
2. **ArcCatalog:** for data management and preview

ArcToolbox, for specialized data conversions and analyses, available as a window in both

Available capabilities within these modules are "tiered" in three levels

- **ArcView:** viewing, map production, spatial analysis, basic editing:
- **ArcEditor:** ArcView, plus specialized editing:
- **ArcInfo:** ArcView & ArcEditor plus special analyses and conversions:

Extensions: for special apps.: *Spatial Analyst, 3D Analyst, Geostatistics, Business Analyst, etc.*

ArcObjects: to build specialized capabilities within ArcMap or ArcCatalog using VB for Applications

ArcGIS Engine (MS NT/2000/XP)

- Set of embeddable GIS components (ArcObjects software objects) for use in building custom applications
- Runs under Windows, Unix and Linux, with support for Java, C++, COM and .NET
- Replaces MapObjects which were based upon a previous generation of GIS objects

ESRI Product Line-up: *ArcGIS* server products

ArcGIS Server: three tiers of capability

Data services: ArcSDE (Spatial Database Engine)

- middleware to support spatial data storage in standard DBMS on server
- Support all major industry databases:
  - Oracle, SQL-Server, IBM DB2, Ingres

Map services: ArcIMS (Internet Map Server)

- Provide maps and simple query to a user without a desktop GIS
- Accessed via web interface

Analytic services:

- Permit the creation of server-based specialized GIS applications
- Provides full range of GIS capabilities to a user without a desktop GIS
- Accessed via web interface

(prior to version 9.2 these were sold as three separate products)

ArcGIS On-line Services

- On-line services made available on the Internet with a subscription
- Normally charged on a "per transaction" basis, but can be flat fee
- built and operated by ESRI (or other others), usually based on ArcGIS Server

ESRI ArcGIS System

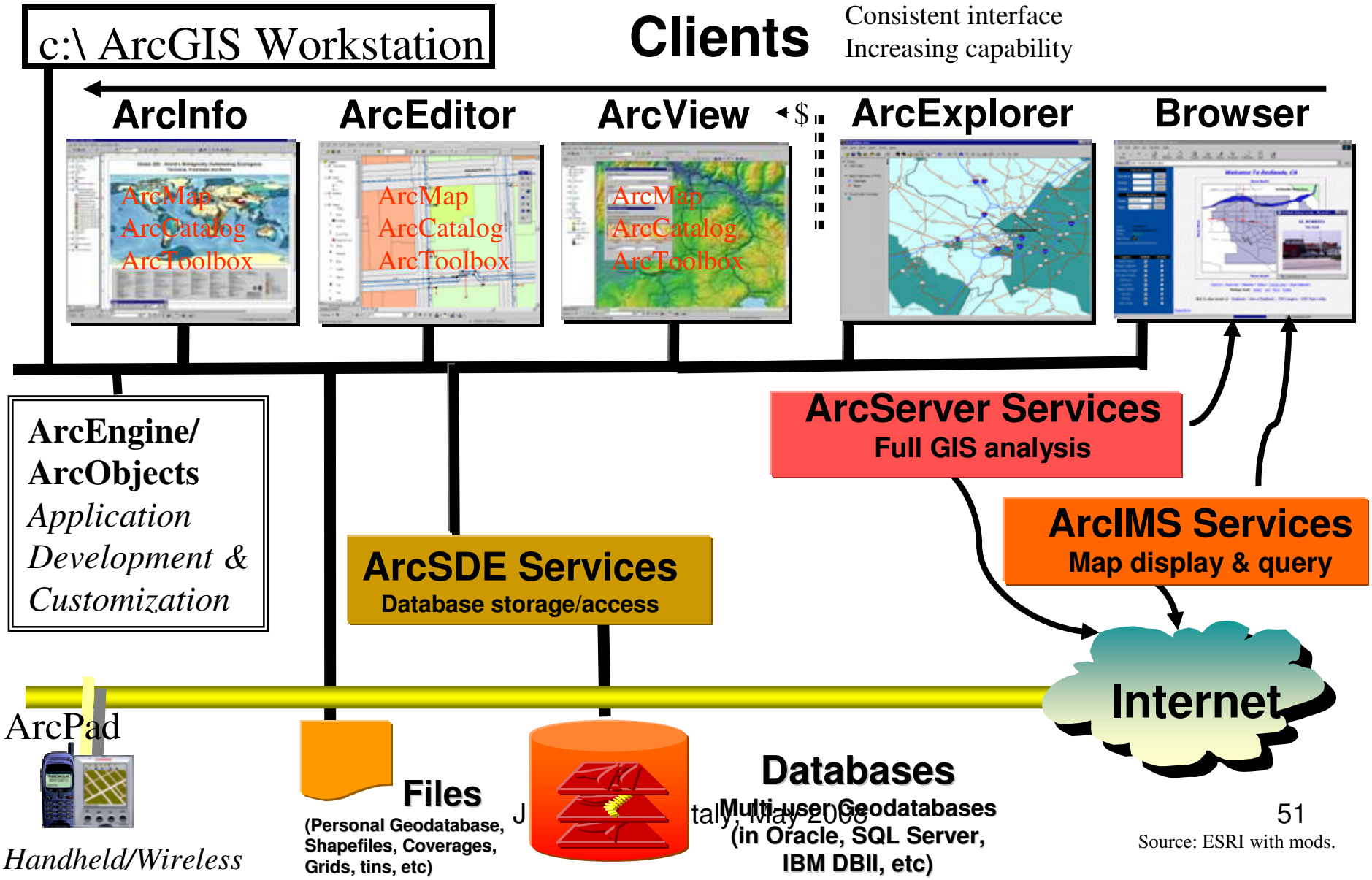

Source: ESRI with mods.

ESRI en España

- http://www.esri-es.com/esri2006/conferencia/ponencias.htm
- Ponencia ‘geoEuskadi’

Free software for GIS

http://www.mapwindow.org/

Bibliography

- http://www.gisdevelopment.net/index.html
- http://hcl.harvard.edu/libraries/maps/gis/tutorials.html
- http://www.nuim.ie/staff/dpringle/courses/hdip/main.shtml
- http://www.nr.usu.edu/Geography-Department/rsgis/GIS/Lectures/gislec.html
- http://www.ncgia.ucsb.edu/
- http://www.colorado.edu/geography/gcraft/notes/coordsys/coordsys_f.html
- Encyclopedia of GIS. S. Shekhar, H. Xiong edts, Springer, NY, 2008

Redes Sociales

Una aproximación desde la Teoría General de Sistemas

Blanca Cases, Patxi Olasagasti

Grupo de Inteligencia Computacional

JIC 2008

Parte I. La Teoría General de Sistemas como paradigma científico

Índice

1. De los filósofos griegos a la formalización de la lógica de predicados.
2. El nacimiento de las ciencias sociales y humanas: tres tipos de estructuralismo.
3. Inteligencia Artificial vs. Inteligencia Computacional.
4. La Teoría General de Sistemas.

De los filósofos griegos a la formalización de la lógica de predicados

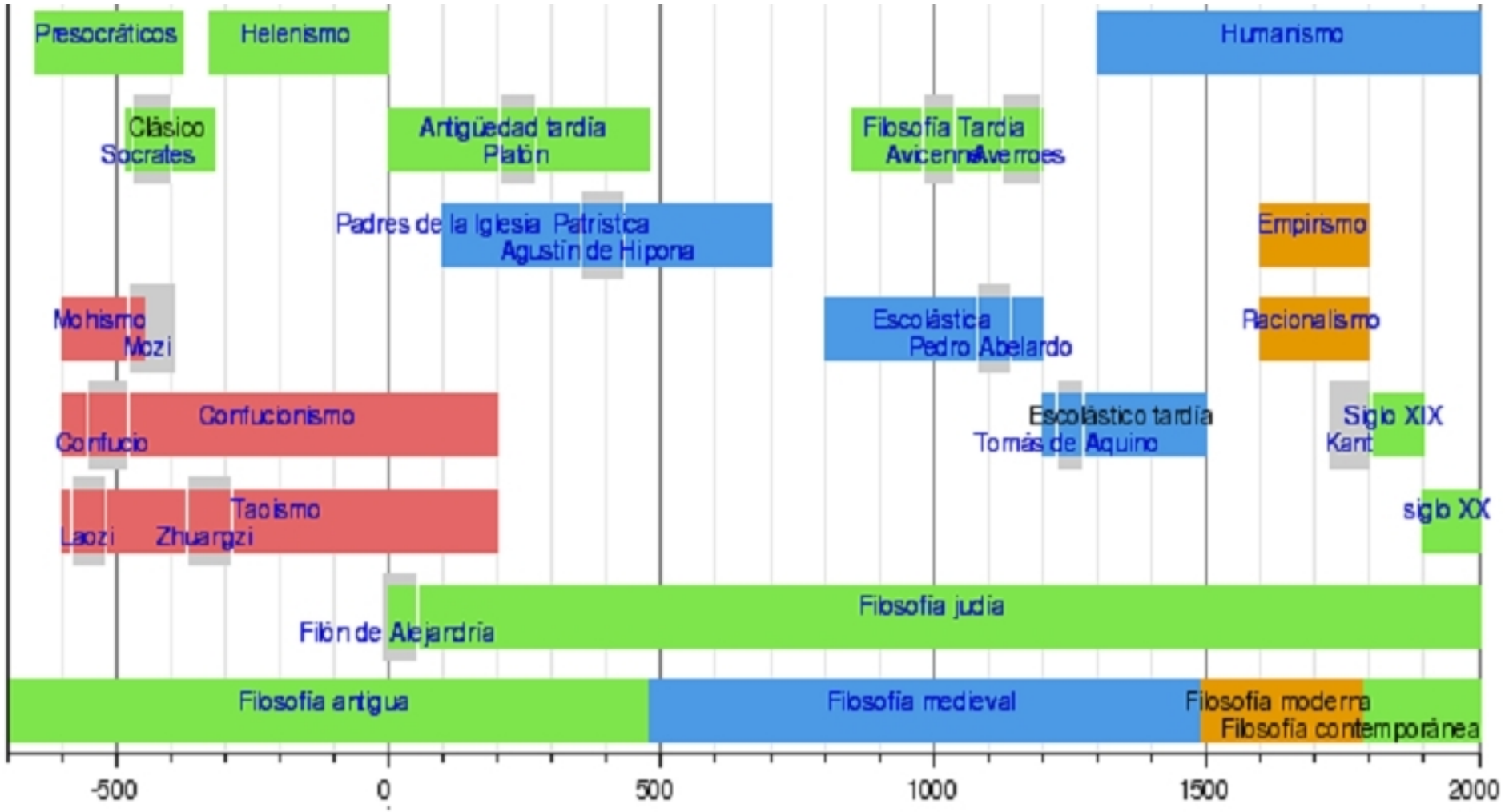

Dos áreas de la filosofía

1. Metafísica: Visión *top-down*
2. Filosofía natural o física: Visión *bottom-up*

Dos áreas de la filosofía: Metafísica

- El Universo como obra de los dioses.
- Origen divino de las capacidades humanas.
- Supremacía de la razón sobre la percepción.
  - Ejemplos: Parménides, Sócrates, Platón.
- Ejemplificación, análisis, deducción.
- Fundamentar la fe en la razón.
  - Escolástica, racionalismo.
- Desarrollo de la lógica como meta-matemática.
  - Aristóteles.

Dos áreas de la filosofía: Filosofía natural o física

- Necesidad de contrastar los objetos de la razón con los del mundo sensible.
  - Aristóteles.
- La experimentación es necesaria para la razón.
- Abstracción, síntesis, inducción.
- Empirismo, positivismo.
- Desarrollo de la aritmética y la geometría como matemáticas del mundo físico.
- La naturaleza como divinidad.
  - Ateísmo.
  - Exponentes: Heráclito, Estoicismo, Plotino, Bruno, Spinoza.

Historia de las Matemáticas: Mundo Antiguo

- **Egipto y Mesopotamia**
  - Geometría.
  - Agrimensión.
- **Grecia**
  - Inventan el razonamiento matemático deductivo: Lógica.
  - Pitágoras, Euclides, Aristóteles

Historia de las Matemáticas: Civilización Griega I

- **Pitágoras**
  - Introduce la necesidad de separar la Geometría (continua) de la Aritmética (discreta).
  - Descubrimiento de números que no son racionales.
- **Euclides**
  - Tratamiento axiomático de la Geometría.
- **Aristóteles**
  - Meta-matemática simbólica.
  - *"Silogismo es un argumento en el cual, establecidas ciertas cosas, resulta necesariamente de ellas, por ser lo que son, otra cosa diferente".*

Historia de las Matemáticas: Civilización Griega II

- Trayectoria de la lógica aristotélica[1]:
  - Imperio Islámico (s. VII):
    - Redescubrimiento de Aristóteles.
    - Desarrollo del Álgebra.
  - Escolástica (s. XI al s. XV):
    - Fundar la fe cristiana en la razón, en torno a las Universidades.

[1] Gracias a las traducciones de su obra.

Racionalismo

- Siglos XII-XVIII
  - **Rene Descartes** (s. XVII, 1596-1650)
  - **Baruch Spinoza** (s. XVII, 1632-1677)
  - **Gottfried Wilhelm von Leibniz** (s. XVII-XVIII, 1646-1716)
  - **Isaac Newton** (s. XVII-XVIII, 1653-1727)

Racionalismo

Racionalismo. René Descartes

- Francia (s. XVII, 1596-1650). Católico.
- Inicia la filosofía moderna.
- Racionalismo: Las reglas de la lógica son innatas.
- Dualismo mente-cuerpo.
- Bases del método científico en el Discurso del Método.
- Geometría analítica: coordenadas cartesianas.
- Simplificación de la notación algebraica.

Racionalismo. Baruch de Spinoza

- Amsterdam (s. XVII, 1632-1677). Origen judío-portugués. Expulsado del judaísmo.
- Identifica a Dios con la naturaleza: *"Deus sive Natura"*.
- No dualidad cuerpo-mente.
- Inspiración estoica.

Racionalismo. Gottfried Wilhelm von Leibniz I

- Alemania (s. XVII-XVIII, 1646-1716). Católico.
- Creador del Cálculo Infinitesimal.
- Filosofía:
  - Atomismo, concepto de mónada (metafísica).
  - El mejor de los mundos posibles.
  - Principio de identidad/contradicción en lógica.
  - Empirismo lógico (le siguen Kant y Hume): sólo podemos hablar del mundo si tenemos experiencia sensorial de él.

Racionalismo. Gottfried Wilhelm von Leibniz II

- Lógica formal:
  - El mayor desarrollo entre Aristóteles y Boole.
  - Principios:
    - Todas las ideas están basadas en unas pocas ideas simples que conforman el alfabeto del pensamiento humano.
    - Las ideas complejas emergen de las ideas simples a partir de combinaciones mediante un operador análogo a la multiplicación o la suma.

Racionalismo. Isaac Newton

- Inglaterra (s. XVII-XVIII, 1653-1727). Católico.
- Creador de la mecánica clásica y del cálculo diferencial independientemente de Leibniz.
- Autor de los *Philosophiae naturalis principia mathematica.*
- Importante trabajo en óptica.

Hitos s. XVII-XVIII. Jakob Bernoulli

- Suizo (1654-1705). Calvinista.
- Funda la teoría de la probabilidad en su obra *Ars Conjectandi*.

Hitos s. XVII-XVIII. Leonhard Paul Euler

- Suizo (1707-1783). Luterano.
- Análisis matemático (aplicado a la mecánica y astronomía) y Teoría de grafos.
- Notación actual de las funciones.
- Series de potencias, e^x.

Hitos s. XVII-XVIII. Georg Wilhelm Friedrich Hegel

- Alemán (1770-1831). Protestante.
- El acto mismo del conocimiento es la introducción de la contradicción.
  - Superación de la *lógica formal* y el establecimiento de la *lógica dialéctica*.
- Causa y efecto son momentos de la dependencia recíproca universal, de la conexión y concatenación recíproca de los acontecimientos, eslabones en la cadena del desarrollo de la materia y la sociedad
  - La misma cosa se presenta primero como causa y luego como efecto.

Hitos s. XVII-XVIII. Georg Wilhelm Friedrich Hegel

Hitos s. XVII-XVIII. Niels Henrik Abel

- Noruego (1802-1829). Protestante.
- Teoría de grupos abelianos y homomorfismos entre ellos.

Formalización de la Lógica de Predicados: Redes Semánticas y Teoría de Tipos

- El **retículo** es la estructura base del Álgebra de Boole de:
  - Proposiciones de la lógica.
  - Conjuntos.
  - Álgebra de probabilidades.
- La teoría de tipos en teoría de conjuntos

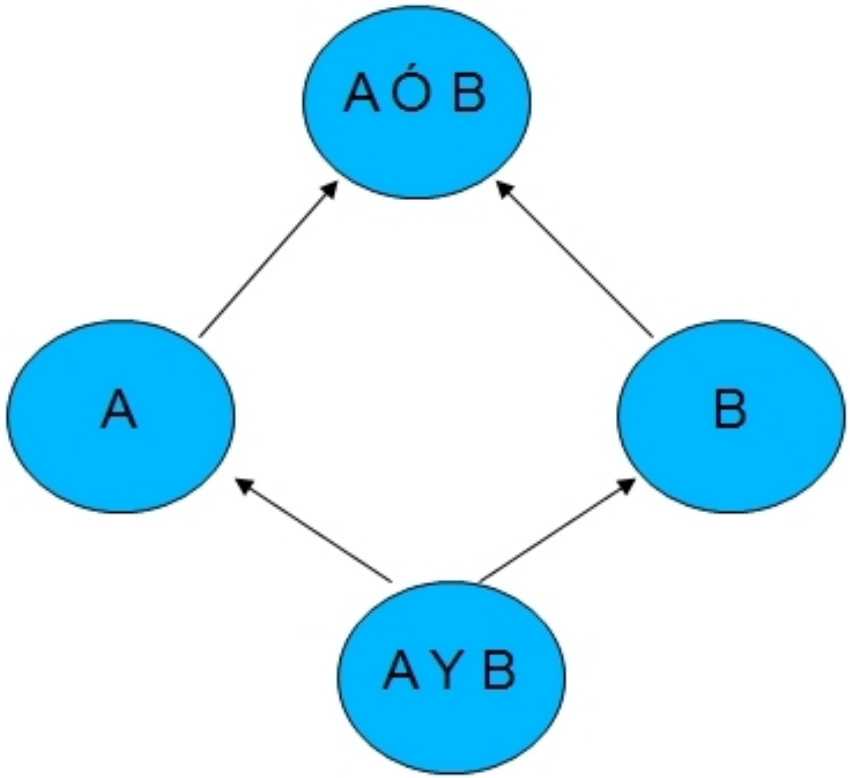

Álgebra de Boole: George Boole I

- Inglés (1815-1864).
- Álgebra de Boole: *"An Investigation of the Laws of Thought, on Which are Founded the Mathematical Theories of Logic and Probabilities"*.
- Se inspira en Aristóteles, Spinoza y Newton.

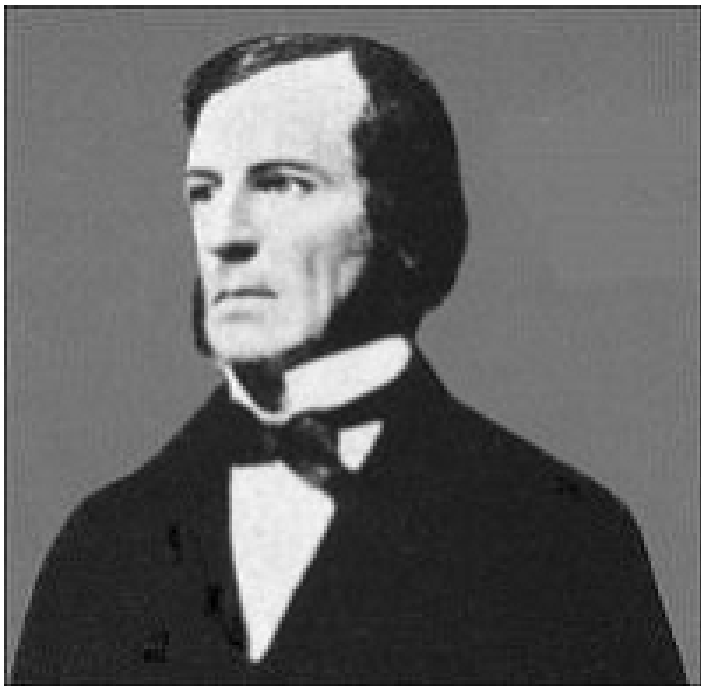

▸ Boole (wikipedia)

Álgebra de Boole: George Boole II

- Se puede definir:
  - Como retículo $(A, +, .)$: estructura algebraica en la que cada dos elementos tienen un máximo y un mínimo.
  - Como anillo: Grupo abeliano respecto a $(+)$, Grupo abeliano respecto a $(\cdot)$ Distributivo
- Operaciones : suma, producto, negación

George Boole y August De Morgan

- Leyes de **Augustus De Morgan** (1806-1871), quien inventó el término *"relación"* en matemáticas.
- Álgebra de probabilidades: $A = [0, 1]$
- Boole y De Morgan formalizan la lógica proposicional $A = \{0, 1\}$

▸ Morgan (wikipedia)

Formalización de la Lógica de Predicados: Charles Sanders Peirce I

- Cambridge MA (1839-1914). Químico de profesión.
- Contribuciones a la lógica, matemática, filosofía y semiótica.
- Fundador del pragmatismo.

▸ Peirce (wikipedia)

Formalización de la Lógica de Predicados: Charles Sanders Peirce II

- Contribuciones:
  - Demostró que la lógica proposicional se puede representar con los operadores **nand** y **nor**.
  - Primera teoría axiomática de los conjuntos y de la aritmética, antes que Dedekind y Peano.
  - Definición formal de conjunto infinito: se puede poner en correspondencia biyectiva con una de sus partes.
  - Extendió el concepto de relación de De Morgan iniciando la formalización de la lógica de predicados.
    - Distinguió entre cuantificadores de primer orden y segundo orden.

Formalización de la Lógica de Predicados: Charles Sanders Peirce III

- Creador de los grafos lógicos que son la base de los formalismos de representación del conocimiento que usa actualmente la Inteligencia Artificial (redes semánticas):
  - Los grafos conceptuales de Sowa (1984), método de representación del conocimiento en Inteligencia Artificial (IA).
  - Los frames de Minsky, base de la programación orientada a objetos.
  - La teoría de categorías.

Lógica y Teoría de Conjuntos: Georg Ferdinand Ludwig Philipp Cantor

- Alemán (1845-1918). Inventor con Dedekind y Peirce de la teoría de conjuntos.
- Concepto de cardinalidad y números transfinitos.
- Base:
  - El conjunto de partes de un conjunto A siempre tiene mayor cardinalidad que A.
- Descubre paradojas de la teoría de conjuntos y la hipótesis del continuo.
- El desarrollo de la teoría de conjuntos va paralelo al desarrollo de la lógica de predicados.

Lógica y Teoría de Conjuntos: Otros

- Frege (1848-1925), Alfred North Whitehead (1861-1847), Bertrand Russell (1872-1970) y David Hilbert avanzan en la definición de la lógica de predicados de primer orden estableciendo:
  - la Teoría de Tipos y
  - el Álgebra de Boole de los conjuntos

- Friedrich Ludwig Gottlob Frege (wikipedia)
- Alfred North Whitehead(wikipedia)
- Bertrand Russell (wikipedia)
- David Hilbert (wikipedia)

Intuicionismo

- Paradoja:
  - Producto de la existencia de fórmulas auto-contradictorias en la lógica de predicados.
- Las matemáticas son una construcción mental de los humanos.
- La existencia de un objeto es equivalente a la posibilidad de su construcción.
- Enfoque clásico: la existencia de un objeto puede ser demostrada comprobando su falsedad.
  - Para los intuicionistas esto no es válido ya que la comprobación de la falsedad de un objeto matemático no significa que es posible hallar una prueba constructiva de su existencia.
- **Brouwer** (1881-1966)
  - *"The untrustworthiness of the principles of logic"*

El problema del todo y la parte

Inteligencia artificial

Top-down:
Definición por comprensión,
Deducción,
Reducción,
Generación (gramáticas)
Lógica de predicados.

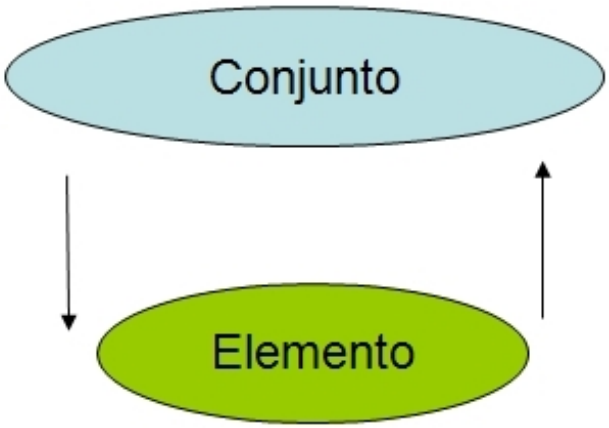

Inteligencia computacional

Bottom-up:
Definición por extensión,
Inducción,
Emergencia,
Clasificación (autómatas y estadística).

- Textos electrónicos examinados de historia de la filosofía:
  - En ninguno aparece la palabra "*network*".
  - La red, en todas sus acepciones, es un concepto del s. XX.

El nacimiento de las ciencias sociales y humanas: Tres tipos de estructuralismo

- A finales del siglo XIX.
- La física es la única ciencia positiva con leyes universales.
- Las ciencias naturales usan métodos empíricos, pero no tienen leyes universales.

El nacimiento de las ciencias sociales y humanas: Tres tipos de estructuralismo

- Las disciplinas humanistas se convierten en ciencias positivas
- Fijan:
  - un objeto de estudio
  - una metodología

El nacimiento de las ciencias sociales y humanas. Metodología

- **Teoría**:
  - ¿ Qué estructura conceptual permiten comprender y articular los datos ?
  - Análisis *top-down.*
- **Abstracción**:
  - ¿ Qué datos experimentales se van a registrar ?
  - ¿ Qué se puede decir a partir de la estructura de los datos a partir de su tratamiento masivo, sincrónico o diacrónico: abstracción ?
  - Análisis *bottom-up.*
- **Aplicación**:
  - ¿ en qué ámbitos pueden aplicarse sus resultados ?

Panorama de las Ciencias Humanas. La Psicología y la Lingüística s. XX

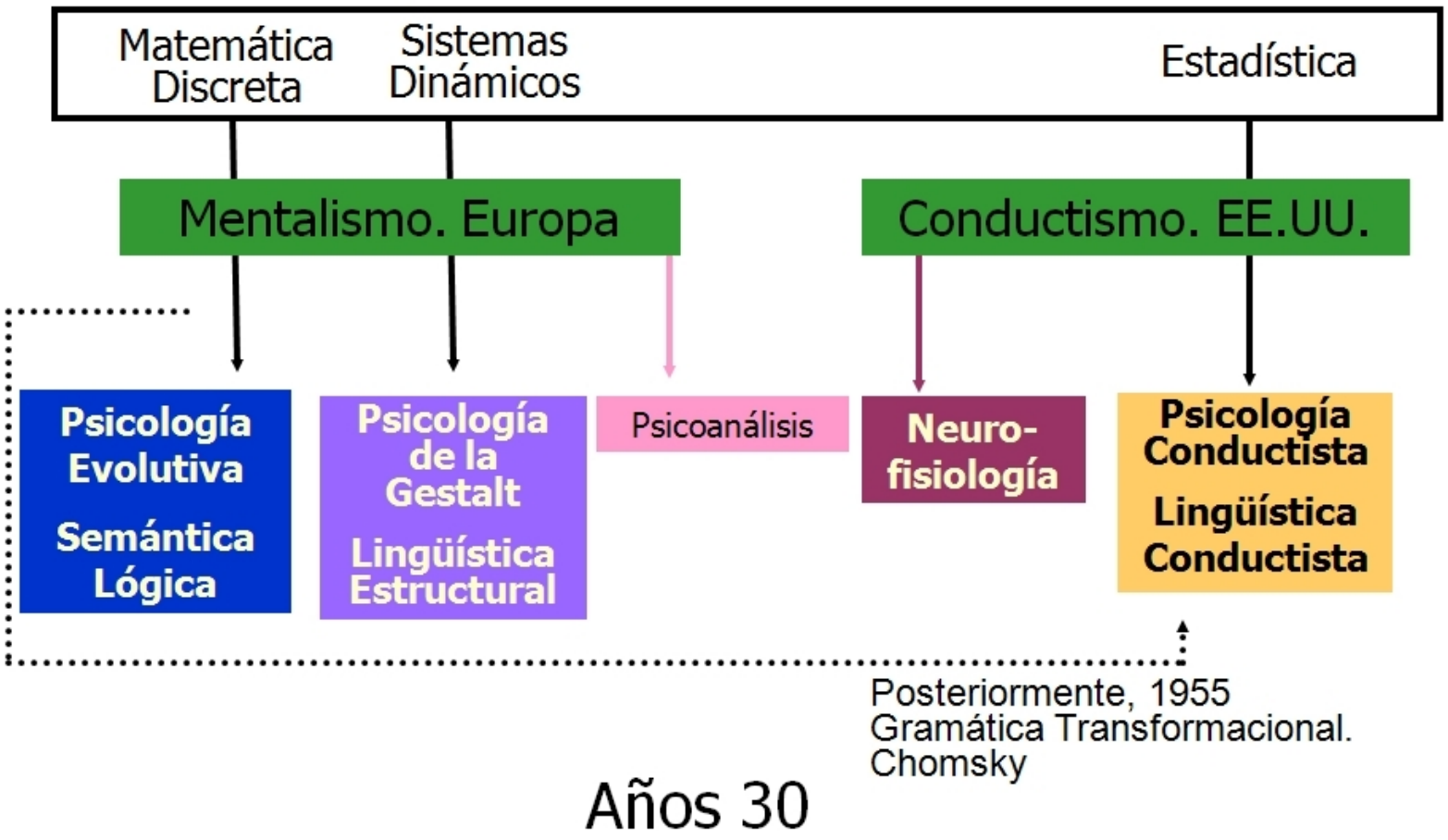

El nacimiento de la Informática

- La Informática tiene origen en la Informática Teórica y la Teoría de Circuitos.
- La Informática Teórica:
  - Teoría de la Computabilidad (años 30). Incompletitud de Gödel.
  - Teoría de Autómatas (años 50).
  - Redes neuronales (1941).
  - Autómatas finitos. Kleene.
  - Teoría de Lenguajes Formales (años 50-60).
  - Teoría de la Complejidad Computacional (años 70).
- Todas las elaboraciones de la Informática Teórica
  - Nacen en un marco interdisciplinar.
  - Son previas a la construcción de máquinas, herramientas y aplicaciones software.

El nacimiento de la Informática Teórica. Marco interdisciplinar

- Desarrollo matemático de las de ecuaciones diferenciales, de la lógica y de la estadística a finales del s. XIX.
- Las ciencias humanas se hacen ciencias positivas.
- Necesidad de determinar los datos y metodologías para su estudio.
- Integración en un corpus teórico coherente.
- Consistente también en el marco multidisciplinar.
- La Informática nace dando sustento a la formalización de las **Ciencias Humanas** y de las Ciencias Biológicas.

Antropología:
Manifestaciones
culturales
del ser humano.
Psicología
social
Sociología
Socio-
lingüística
Psicología
Fisiología
Psico-lingüística
Lingüística

Psicología conductista. Modelo externo

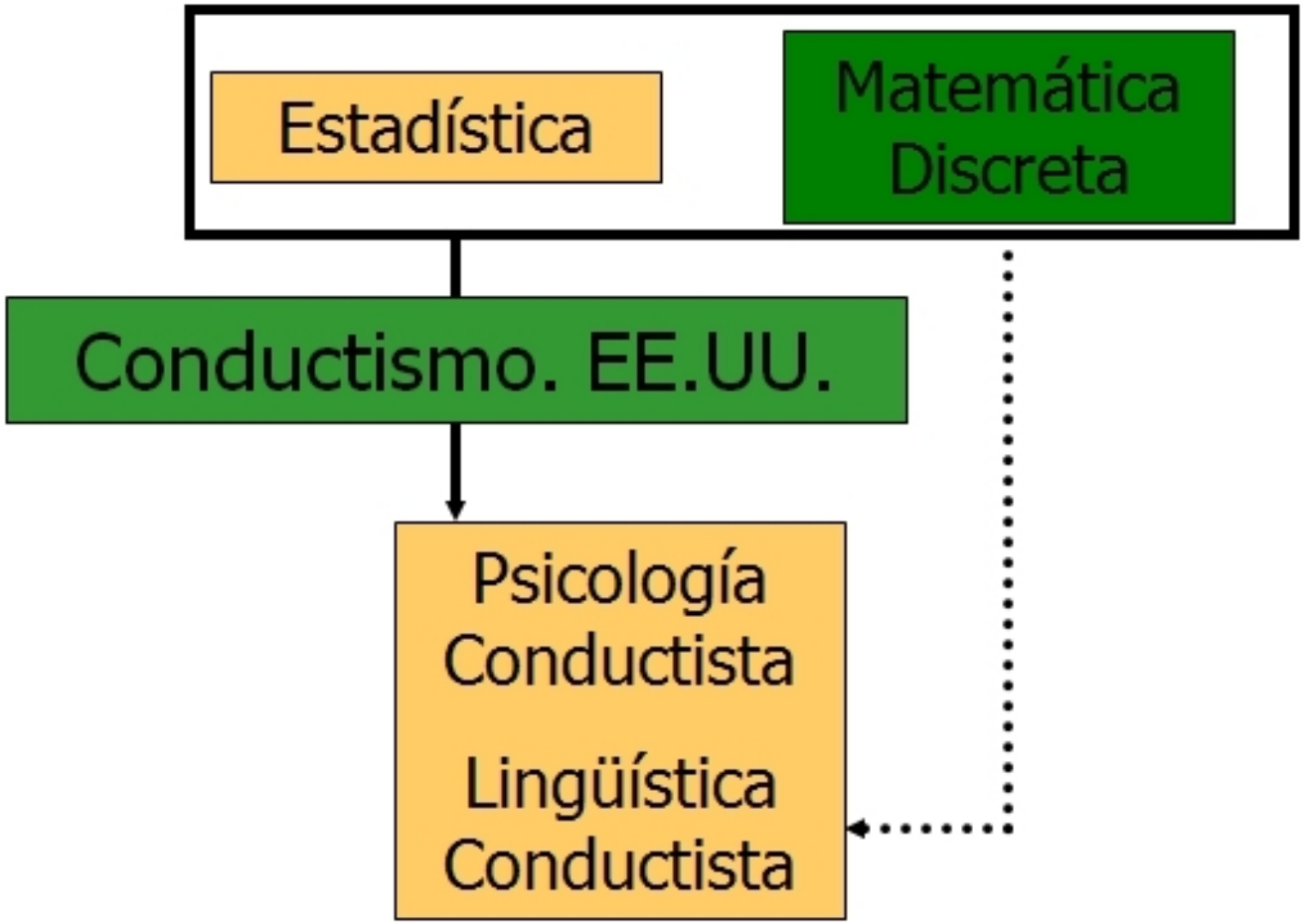

Psicología conductista. Modelo externo

Años 30:

- Descripción de la conducta y aprendizaje de los organismos.

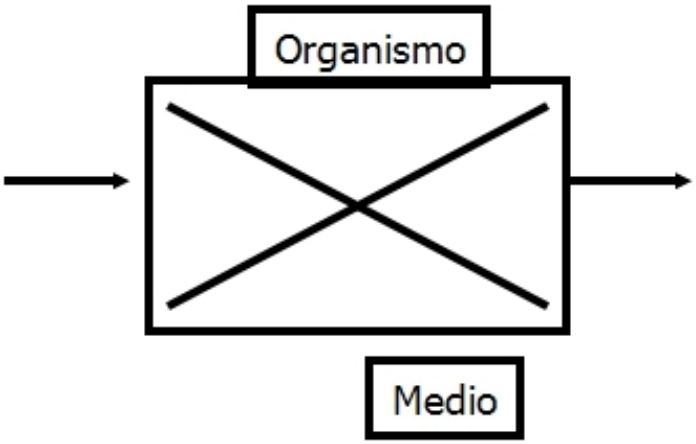

- El interior del organismo es incognoscible. La referencia al interior no es científica.
- Sólo es descriptible la conducta externa en términos de estímulo-respuesta.
- El estructuralismo americano es esencialmente "funcionalismo".

Psicología cognitiva. Modelo interno

Mentalismo Logicista

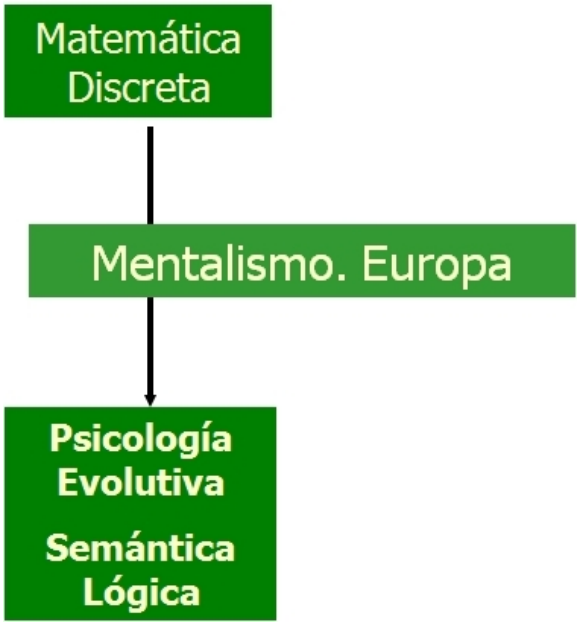

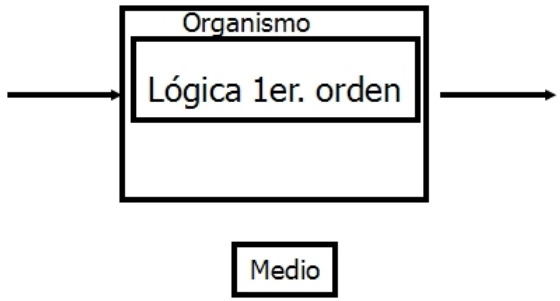

Años 30

- Explicar las capacidades humanas de razonamiento y lenguaje.
- Modelo interno de procesamiento simbólico: Lógica de Predicados de Primer Orden.

Psicología cognitiva:
Modelo interno.
Razonamiento y lenguaje.

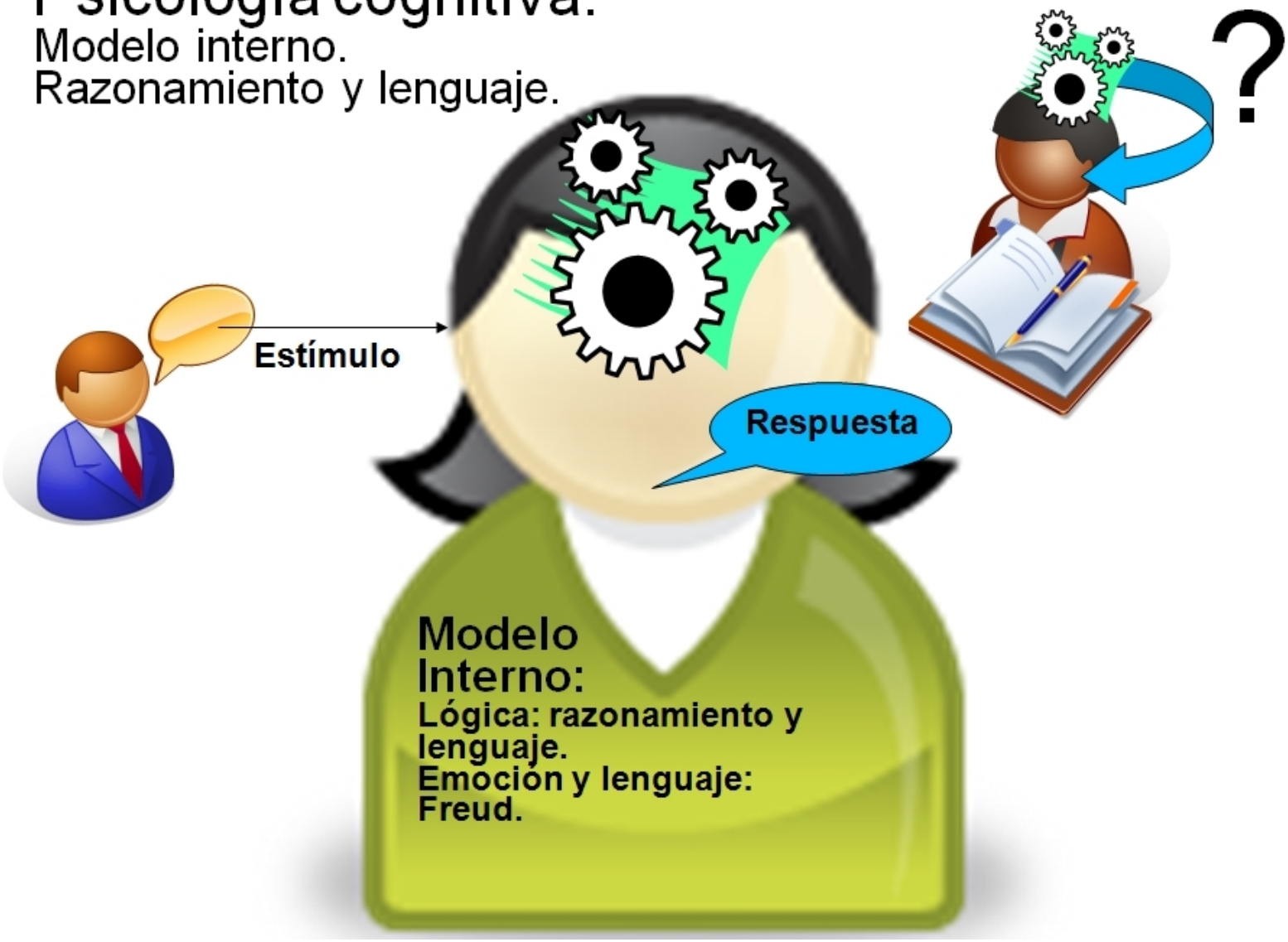

Mentalismo Sistémico

Sistemas Dinámicos

Mentalismo. Europa

Psicología de la Gestalt

Lingüística Estructural

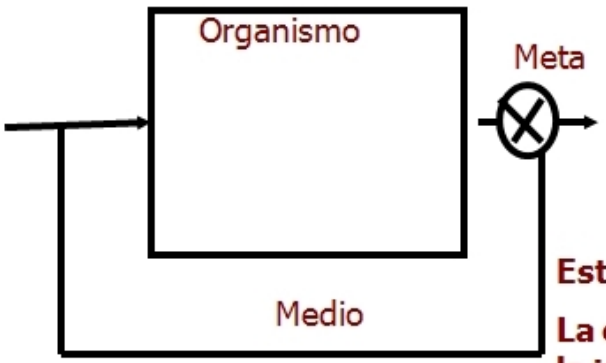

Estudia la percepción.

La conducta se explica en la interrelación del interior con el medio.

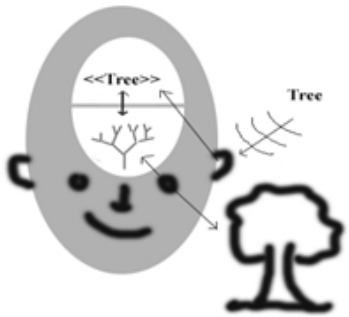

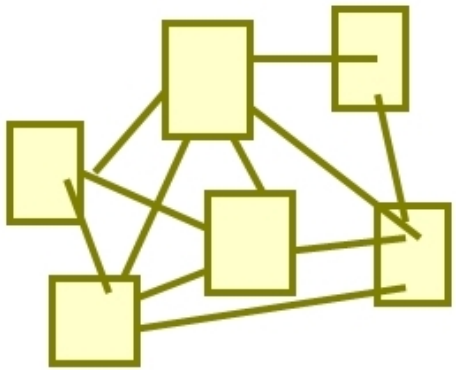

Años 30

Psicología de la Gestalt.

Motricidad. Modelo de control.

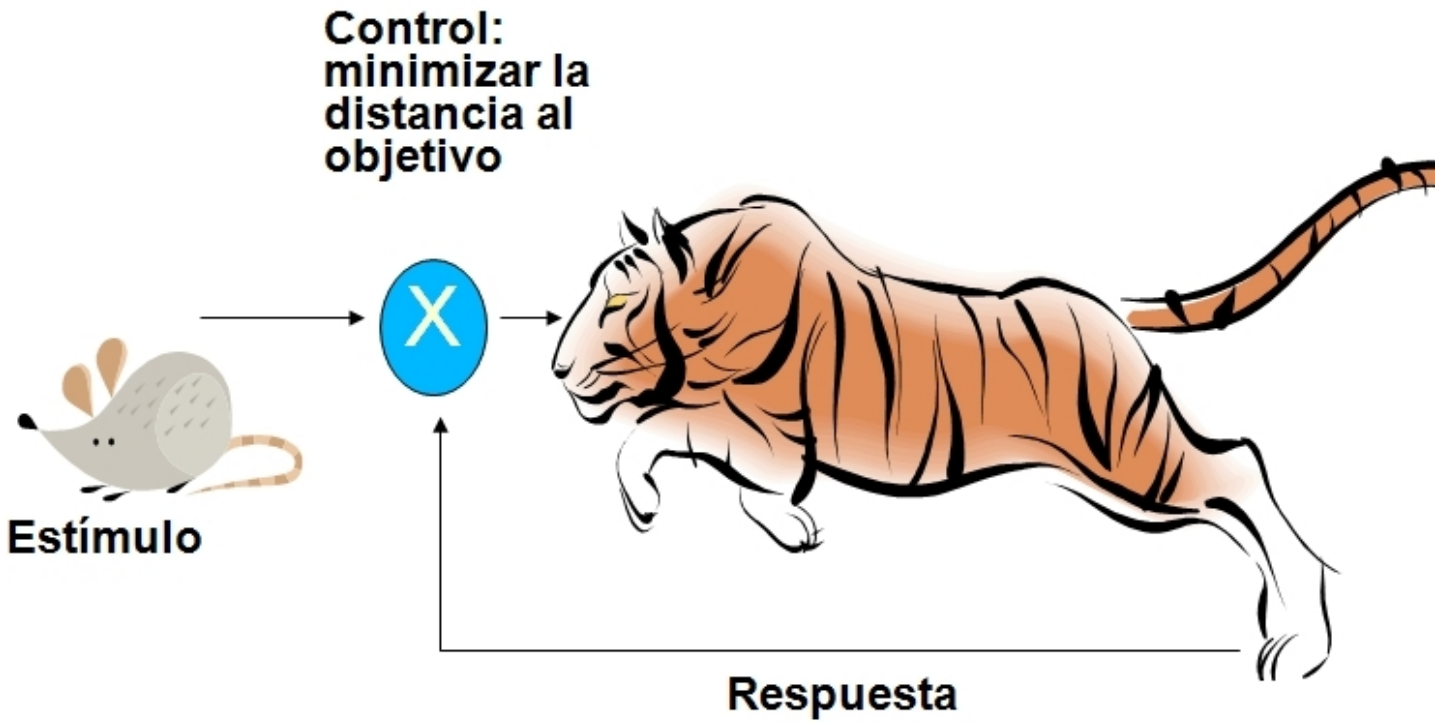

Psicología de la Gestalt.

Percepción. Holismo y antimecanicismo.

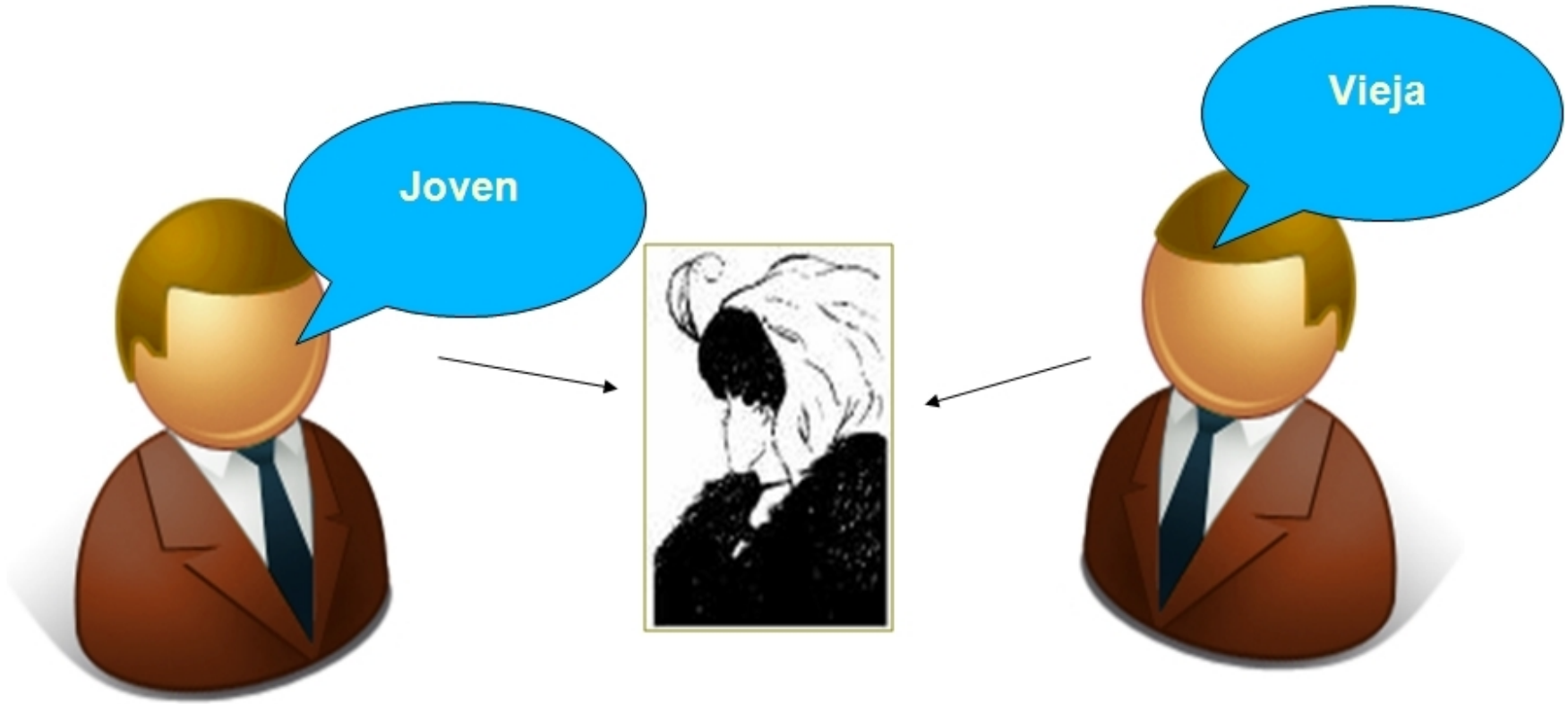

Estructuralismo en lingüística. Saussure

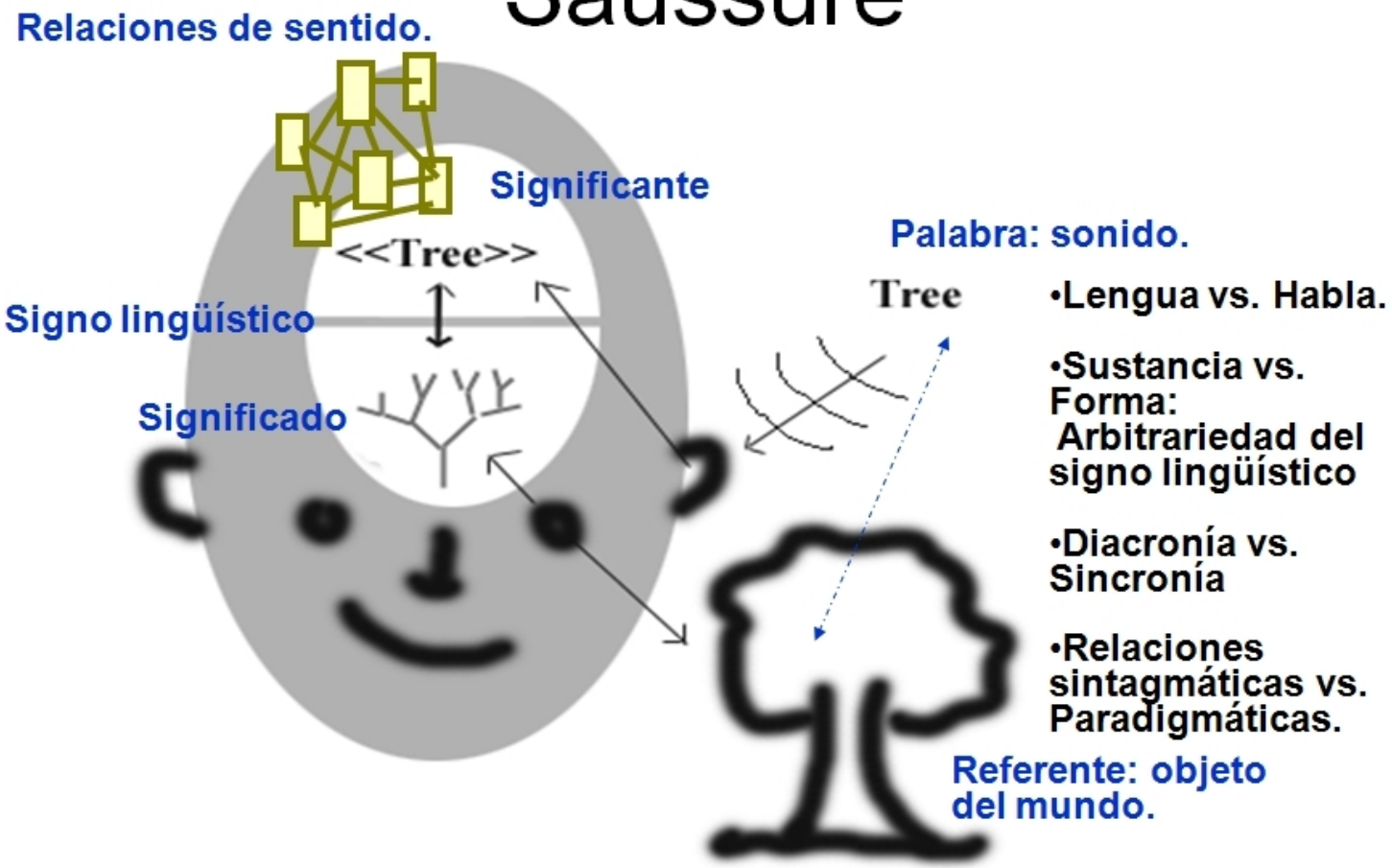

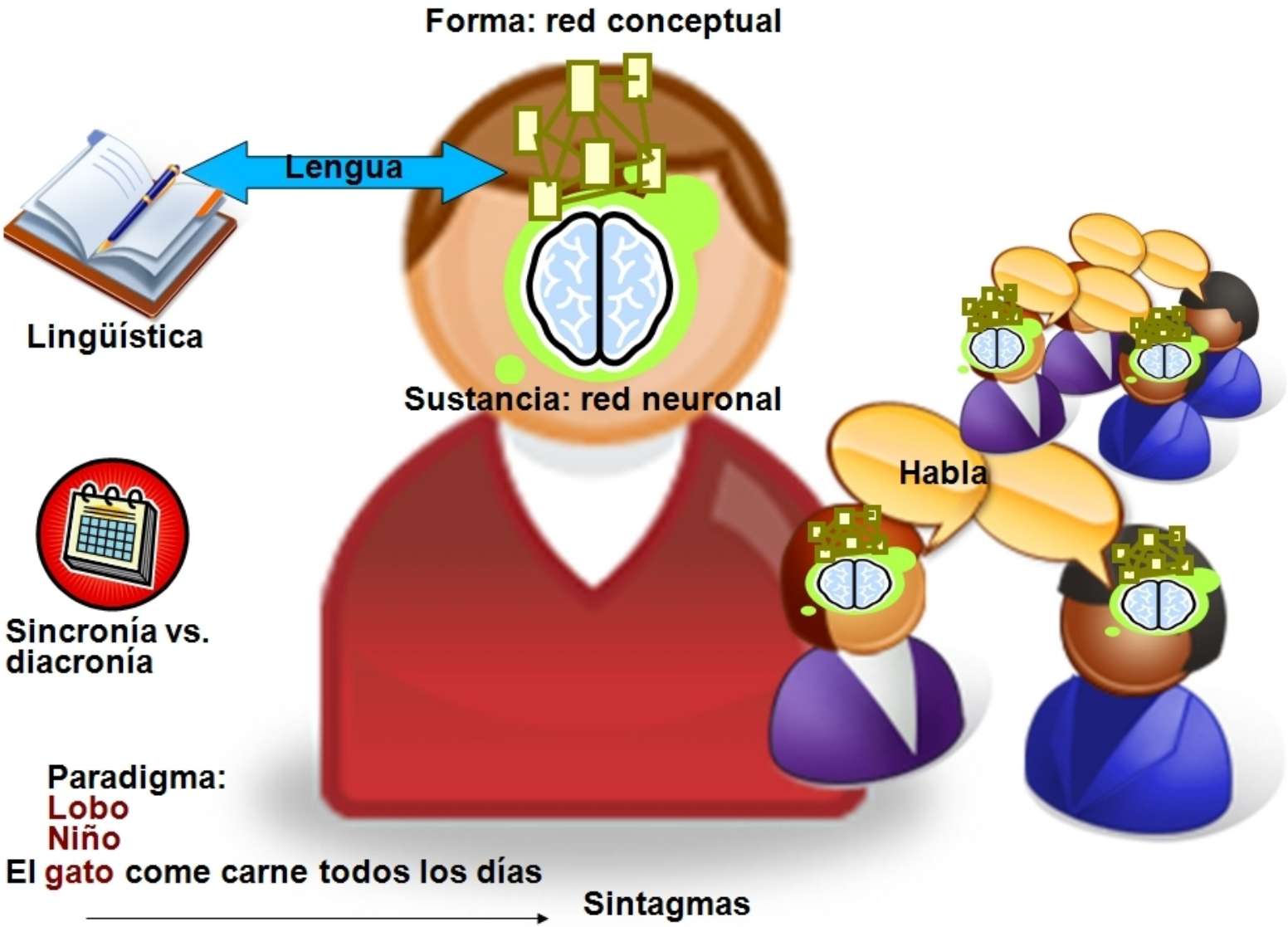
Forma: red conceptual
Lengua
Lingüística
Sustancia: red neuronal
Habla
Sincronía vs.
diacronía
Paradigma:
Lobo
Niño
El gato come carne todos los días
Sintagmas

Teoría de Sistemas

- La Teoría General de Sistemas (TGS) o Teoría de Sistemas o Enfoque de Sistemas es un esfuerzo de estudio interdisciplinario que trata de encontrar las propiedades comunes a entidades, los sistemas, que se presentan en todos los niveles de la realidad, pero que son objeto tradicionalmente de disciplinas académicas diferentes.
- Su puesta en marcha se atribuye al biólogo austríaco **Ludwig von Bertalanffy**, quien acuñó la denominación a mediados del siglo XX.

▸ Ludwig von Bertalanffy (wikipedia)

Teoría General de Sistemas

- Conjunto de entidades:
  - Interactuantes o interdependientes.
  - Reales o abstractas que forman un todo integrado. *Holismo*.
  - El todo no se reduce a las partes. *Antimecanicismo*.
- Inspiración:
  - Sistemas biológicos.
  - Sistemas humanos.

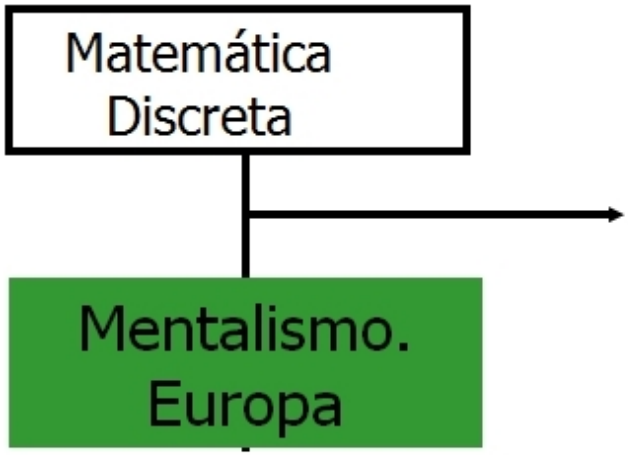

Teoría de la Computabilidad:

–Lógica de Predicados de Primer Orden. Teorema de Incompletitud de Gödel.

–Teoría de las funciones μ-Recursivas de Kleene.

–Teoría del Lambda-cálculo de Church. Tesis de Church.

–Procedimiento más general de cómputo. Máquina de Turing.

Hasta 1936

Declive del conductismo

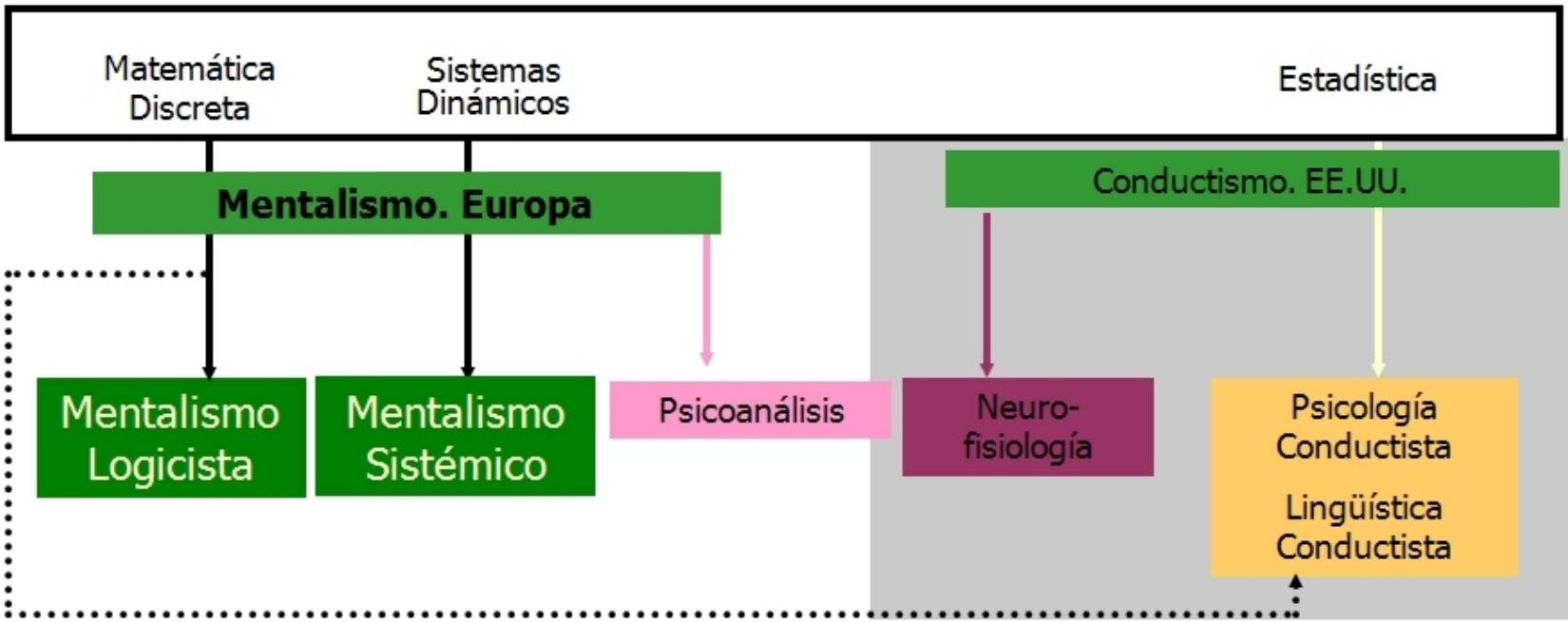

Auge del mentalismo: gracias a los ordenadores.

El conductismo deja de ser la única psicología experimental

Fin de los años 30

Construcción de los primeros ordenadores en la II G.M.

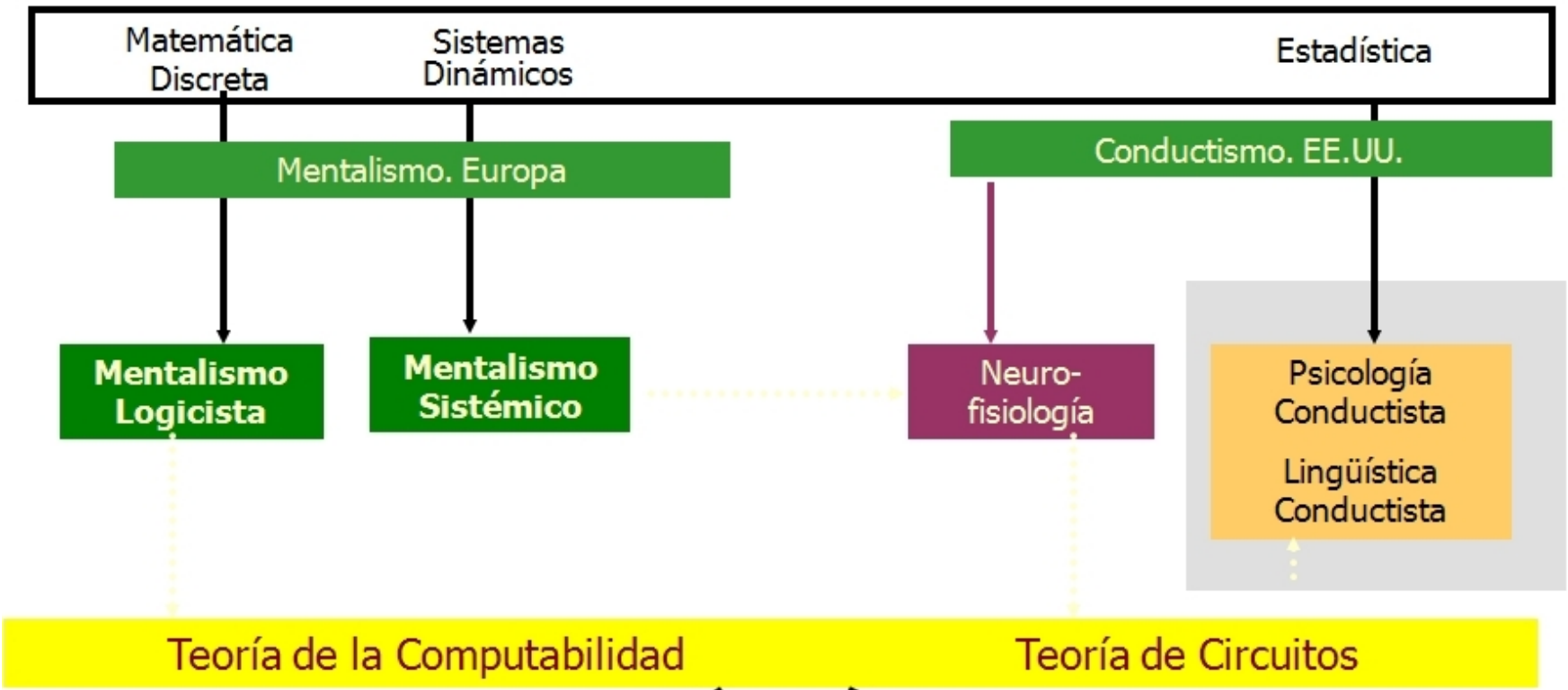

COLOSUS

- **Inglaterra**
- **Alan Turing**
- **Encriptamiento de información militar**

MARK I

- **EE.UU.**
- **Shanon, Wiener**
- **Sistemas automáticos de tiro y navegación**

1940

Movimientos interdisciplinares de la Informática, años 40.

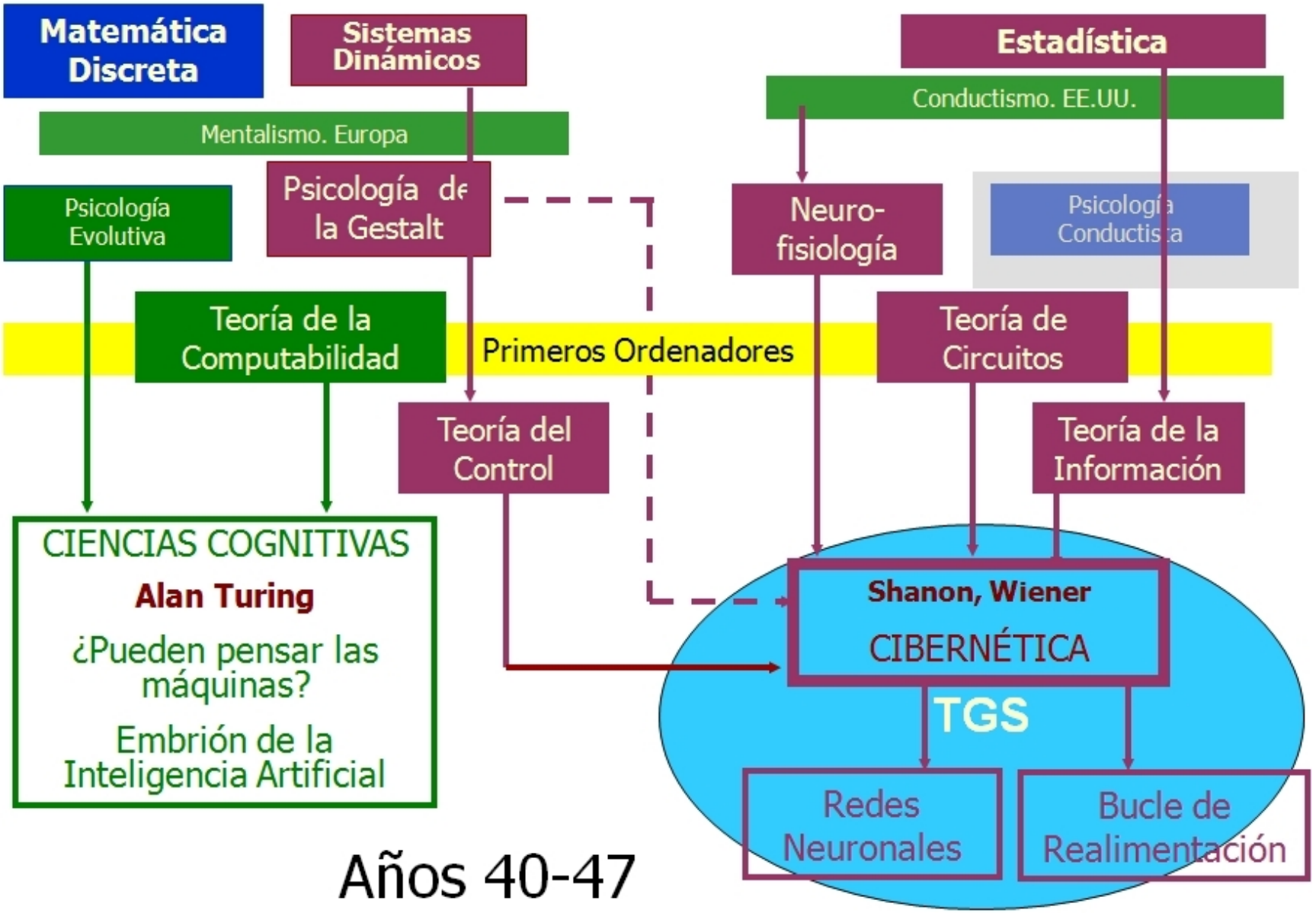

Teoría General de Sistemas de Von Bertalanffy

Definición

La **Teoría General de Sistemas** *es un área interdisciplinar de la ciencia que estudia la naturaleza de los sistemas complejos de la naturaleza, la sociedad y la ciencia. Más específicamente es un marco de trabajo mediante el cual se pueden analizar y/o describir cualquier grupo de objetos que trabajan en común para producir algún resultado. Estos grupos de objetos pueden ser tanto un simple organismo como una organización o sociedad o cualquier artefacto electro-mecánico o informativo.*

Cibernética vs. Inteligencia Artificial

"Desde sus mismos inicios, la cibernética ha estudiado los mecanismos de bajo nivel como los bucles de retroalimentación y los servomecanismos. Ha tenido una visión ascendente de cómo tales estructuras podrían interactuar en el control animal y de sistemas informáticos. La Inteligencia Artificial, sin embargo, comenzó con una visión descendente de símbolos, lenguaje y conocimiento, y se preguntaba qué clase de mecanismos y representaciones son necesarias para simular las habilidades humanas. A pesar de que tanto la I.A. como la cibernética usan redes, los elementos de éstas pertenecen a diferentes niveles del procesamiento mental. Las redes en cibernética representan neuronas individuales, pero en I.A. representan conceptos de alto nivel y relaciones, cada una de las cuales depende de millones de neuronas interactuantes."

SOWA, *Conceptual Structures*, 1984, p.339

Declive de la Cibernética. Causas

- Modelos distribuidos que requieren gran capacidad de memoria y conectividad.
- Mejor adaptada a ordenadores analógicos ya que sus modelos aplican matemática continua.
- La simulación es el método más adecuado para la investigación.
- La Teoría de Autómatas, en concreto los autómatas finitos, nacen de un intento de formalizar las redes neuronales en la matemática discreta.
- Los autómatas demuestran su superioridad como herramienta de análisis de las capacidades computacionales de las redes neuronales.

Orígenes de la Teoría de Autómatas

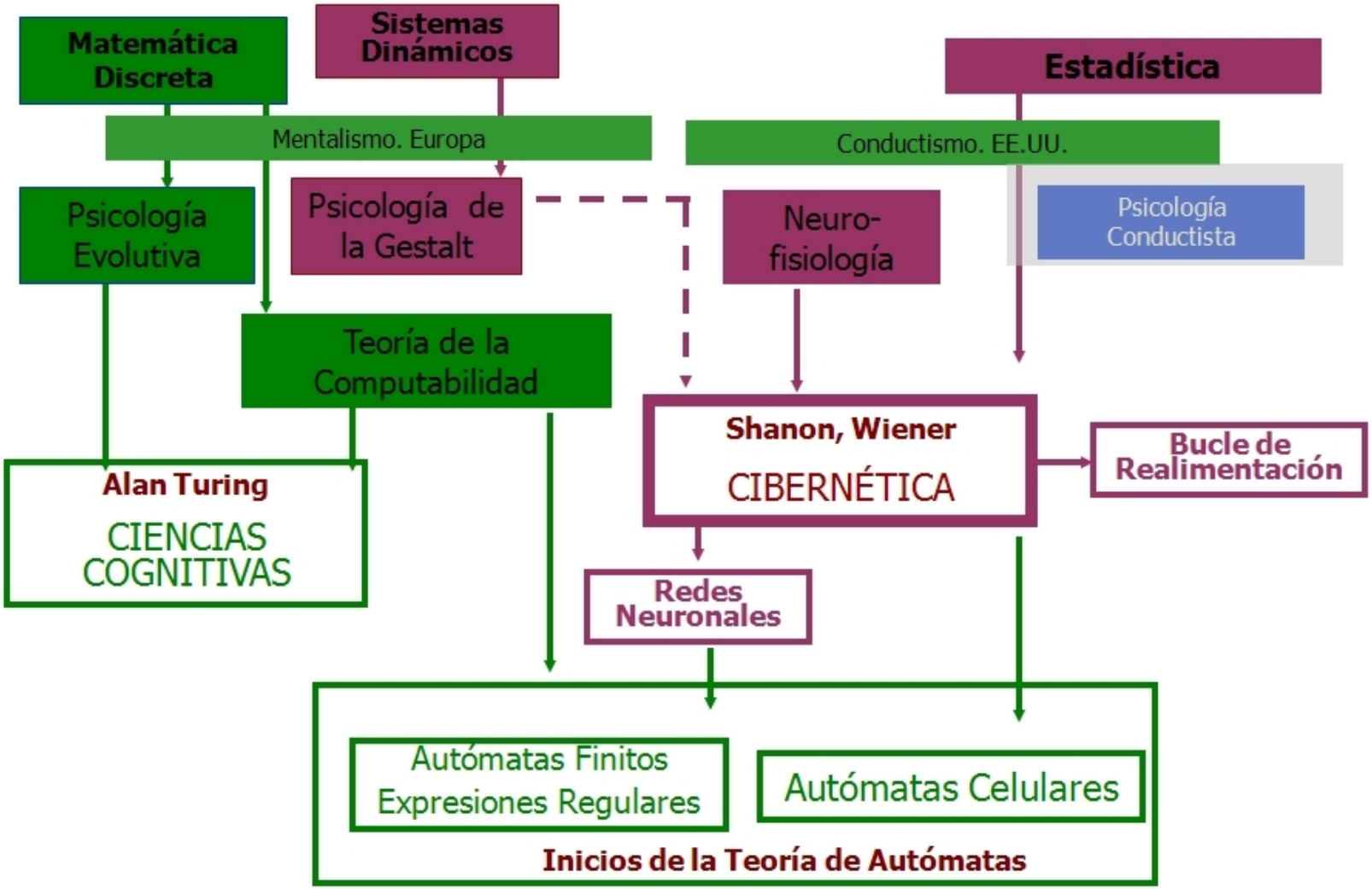

Años 48-55

Orígenes de la Teoría de Lenguajes Formales

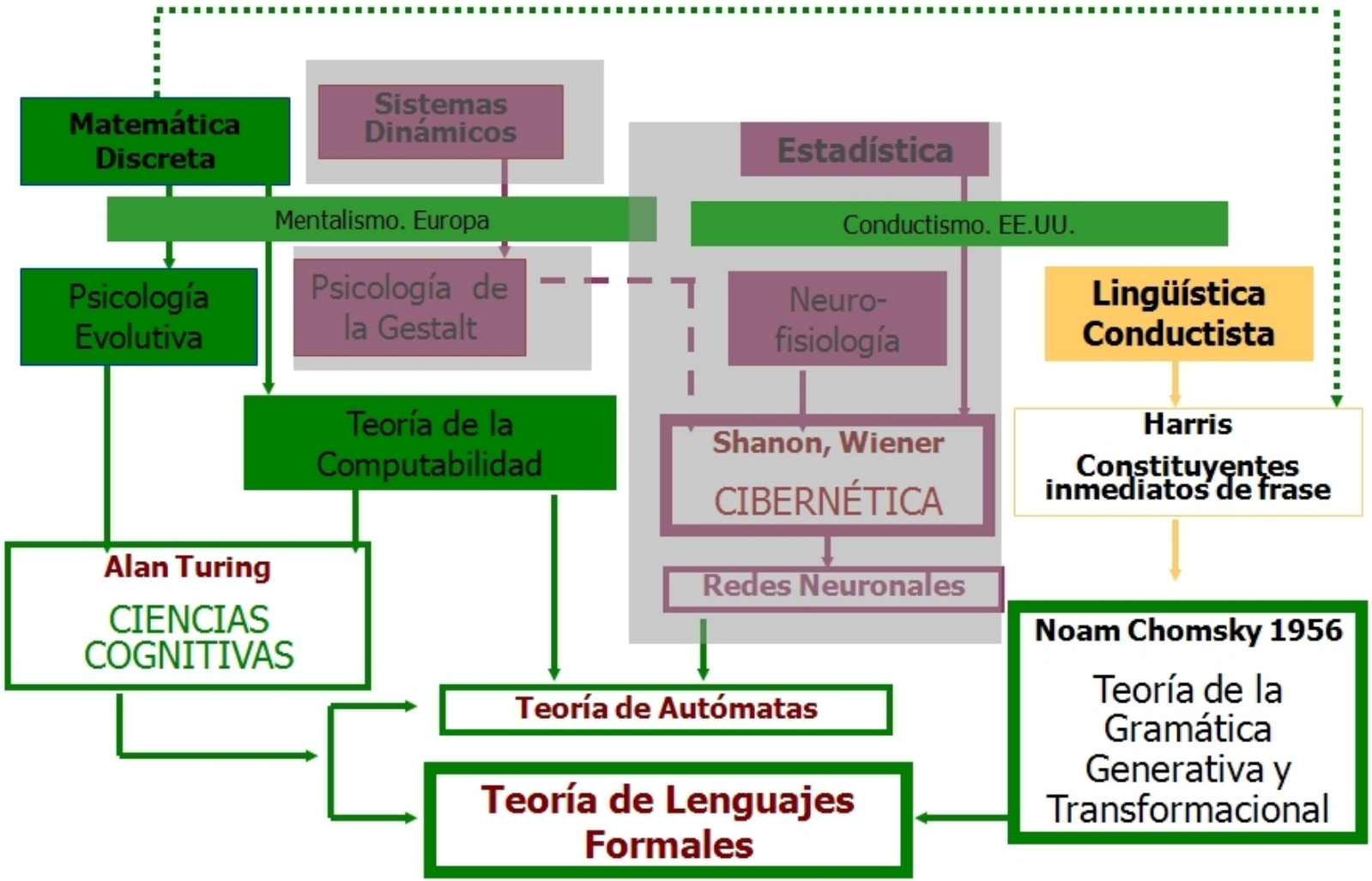

Años 55-60

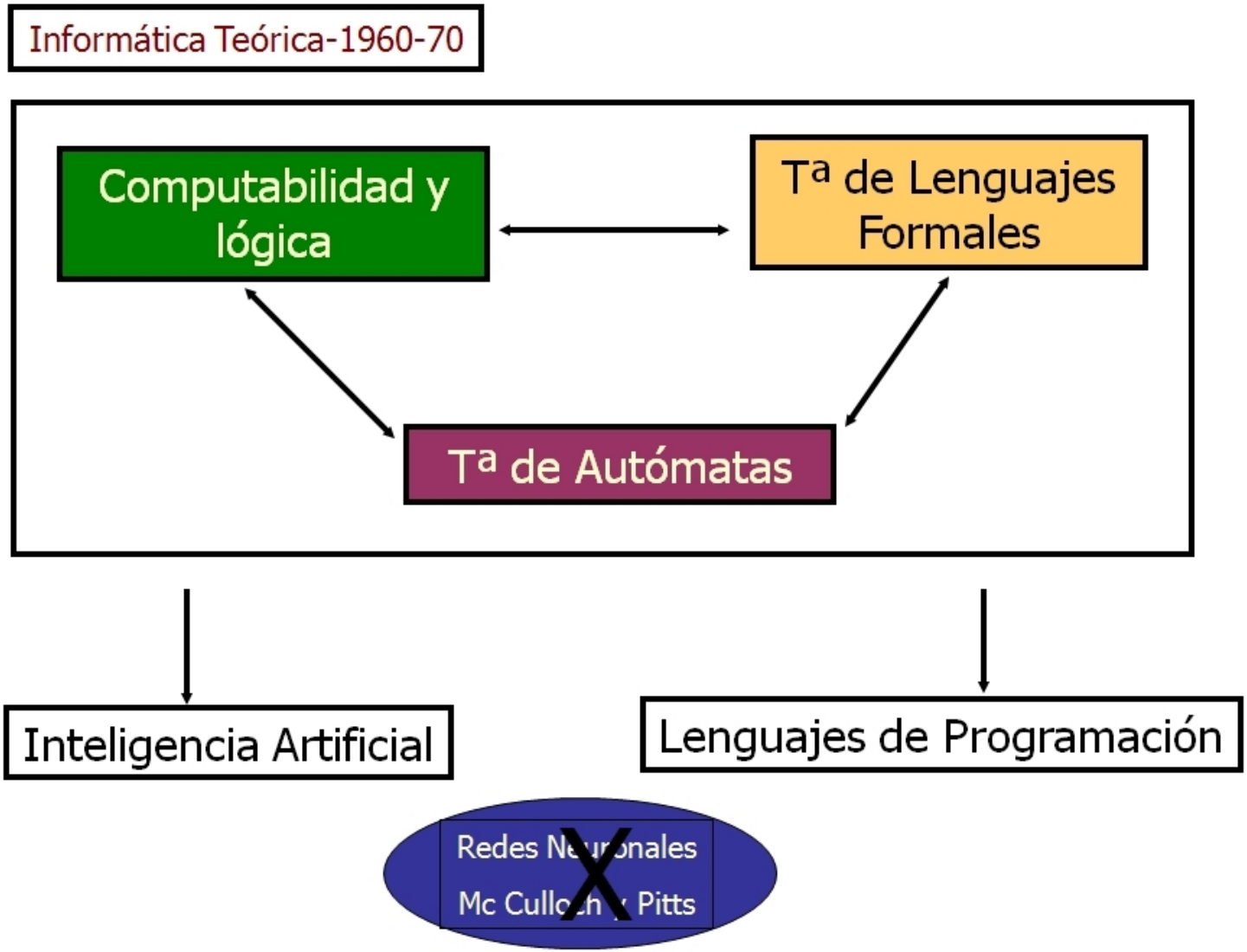
Informática Teórica-1960-70
Computabilidad y lógica
Tª de Lenguajes Formales
Tª de Autómatas
Inteligencia Artificial
Lenguajes de Programación
Redes Neuronales
Mc Culloch y Pitts

Evolución de la Cibernética y la Teoría de Sistemas

- Se cierra la investigación en Redes Neuronales hacia 1972. Minsky.
- Convergencia de la Cibernética con la Teoría de Sistemas de von Bertalanffy.
  - Idea de von Bertalanffy: Teoría de los Sistemas, que como los vivos, no son reducibles a las partes.
- Tipos de descripción sistémica que definen los gráficos.

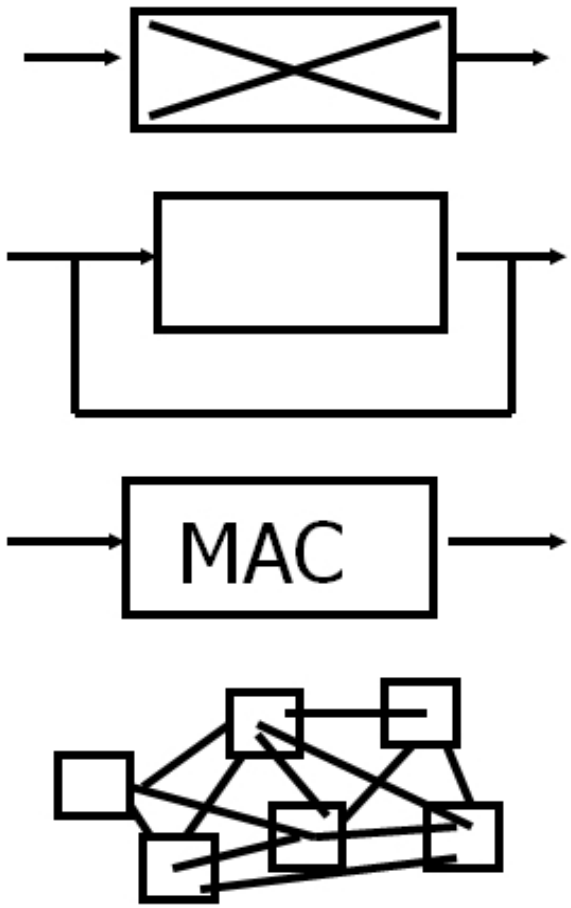

Referente biológico: Teoría de Sistemas de von Bertalanffy

- Se habla de **sistema**:
  - Conjunto de unidades interdependientes que interactúan entre sí y con el medio y llevan a cabo una tarea o comportamiento perceptible y coherente:
    - Sistema mecánico: el comportamiento global se reduce a las partes.
    - Sistema Complejo: el comportamiento percibido no se explica como suma de las partes.
- Propuesta interdisciplinar de elaborar una Teoría de Sistemas para englobar a los sistemas biológicos.

Líneas de investigación en Teoría de Sistemas en los 70-80

- Informe elaborado por Roger. E. Cavallo para la "*Society for General Systems Research*" fundada por Bertalanffy.
  - Caracterización algorítmica del aprendizaje y de los sistemas adaptativos.
  - Caracterización autopoyética de la organización de lo vivo.
  - Heurística conversacional.
  - Teoría de Sistemas *Fuzzy*.
  - Teoría General de Redes.
  - *General System Problem Solver* (GSPS).
  - Teoría Generalizada de la Información.
  - Ley de la Variedad de Requisitos.
  - Teoría de Sistemas Vivos.
  - La metodología del Q-análisis.
  - Teoría Tricotiledón del Diseño de Sistemas.

Líneas de investigación en Teoría de Sistemas en los 80

- **P. Pollack** (1989)
  - El Conexionismo introducirá a la Inteligencia Artificial en la revolución del pensamiento que actualmente se da en la Física y en las Ciencias Biológicas.

Parte II. Hacia una Teoría de las Redes Sociales

Índice

1. Origenes de la Antropología y la Sociología.
2. Interacción Social.
3. Sobre la metodología.
4. Miguel Beltrán. Las cinco vías de acceso a la Realidad Social.
5. Félix Requena. El concepto de Red Social.
6. Sistema: Red de Redes.

Orígenes de la Antropología y la Sociología

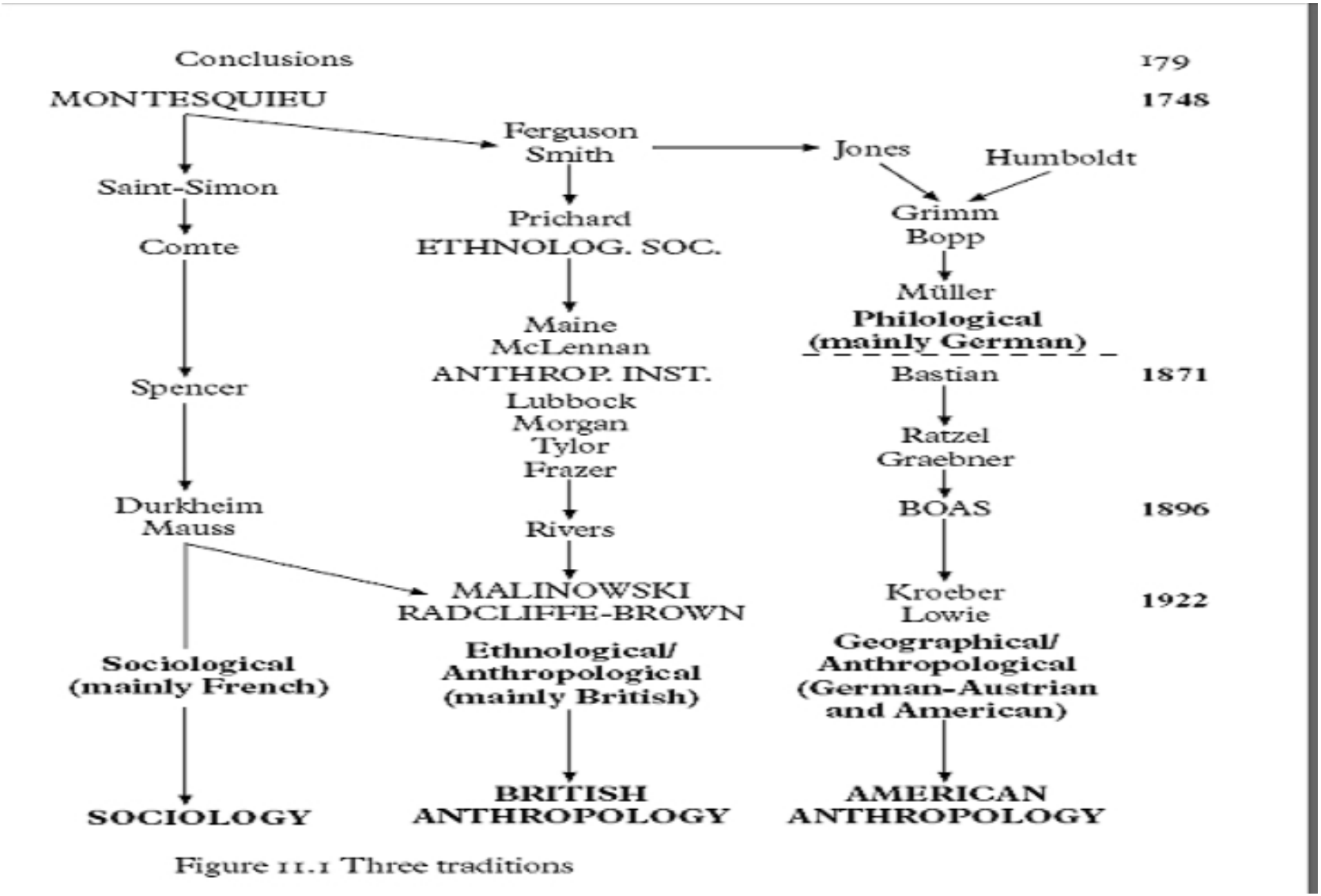

Figure 11.1 Three traditions

Orígenes de la Antropología y la Sociología. Precursores

- Comte, Saint Simon, Marx, Tokeville.
- Situación social y económica:
  - Cambios sociales profundos.
  - Triunfo de la industrialización.
  - Asentamiento del estado moderno.
  - Cambios legislativos y jurídicos.
  - Cambios de mentalidades.
    - Ya no se habla de príncipes y reinados, hablamos de la **Sociedad**.
- Período aproximado: 1800-1860.

Emile Durkheim I

- Francés (período más productivo: 1890-1910) Durkheim (wikipedia).
- Escribe en una sociedad industrial ya consolidada y un Estado "bien" formado.
- Máximo exponente de la Sociología Explicativa y del Positivismo (estadio superior).
- Temas centrales:
  - Los Hechos sociales:
    - Unos Hechos sociales explican otros y un Hecho social se explica por otros Hechos sociales. La Sociedad como **Hecho Social** se explica por otros hechos.
    - Por lo tanto trata los Hechos Sociales como "cosas". Las cosas como hechos objetivos.
  - También es muy importante el concepto de Institución social.

Emile Durkheim II

- Bibliografía fundamental:
  - *Las reglas del método sociológico*
  - *El suicidio*
  - *Las formas elementales de la vida religiosa*

Max Weber I

- Alemán (período más productivo: 1895-1920) Max Weber (wikipedia).
- Cambios profundos en la sociedad y período de mucha agitación social.
- Algún tema central: **Teoría de la acción social**.
- Máximo exponente la Sociología Comprehensiva.
- Análisis de las relaciones *microsociales*, que ayudan a comprender lo *macrosocial.*
  - Por lo tanto, trata sobre la Subjetividad.

Max Weber II

- También fundamental en él, el proceso de racionalización como elemento clave para entender la modernización o sociedad moderna y el consiguiente proceso inevitable de la burocratización.
  - Esto también tiene consecuencias fortísimas en el proceso de investigación.
- Igualmente, máximo exponente de la teoría.
  - *"Las consecuencias no queridas de la acción".*
  - Teoría básica: Teoría de la Acción Social.

Max Weber III

- En las relaciones humanas con sentido, se dan cuatro posibles tipos de relación.
- Nunca se dan en sentido puro, hay que tomarlas como Modelos teóricos o "categorías ideales" para el análisis.
  - **Acción Racional con arreglo a fines**: la acción que se realiza es "mediatizada" porque mide las consecuencias de la acción.
  - **Acción Racional con arreglo a valores**: se actúa sin medir las consecuencias de las acciones.
  - **Acción Tradicional**: se actúa por la costumbre establecida.
  - **Acción afectiva**: motivada por la emotividad, afectiva, ...

Max Weber IV

- Bibliografía fundamental:
  - *Economía y sociedad*
  - *La ética protestante y el espíritu del capitalismo*
  - *El político y el científico*

Interacción Social

- Para que haya relación social, hay que tener presente que tiene que haber interacción, **relación social**.
- La interacción puede ser como:
  - Diada (2)
  - Triada (3)
  - Grupo primario o relación cara a cara, entre 4 ó más
  - Las organizaciones formales
  - La masa

Impulso y cambios

- Años 30-40
  - Fuerte emigración intelectual a EEUU de Europa: refuerzo de la sociología americana.
  - Europa: Guerra mundial y fuertes consecuencias...
- Años 60-70:
  - Crisis social de valores y, por lo tanto, emergencia de nuevas corrientes: hipismo, valores contraculturales, feminismo, nacionalismo y todas sus variedades.
  - Nuevas y complejas identidades.
  - De la sociedad de producción a la sociedad de consumo.
  - Cambios en la estructura familiar.
  - Revolución tecnológica.

Hasta la crisis de los años 60-70. Dos paradigmas fundamentales

1. Paradigma estructural Funcionalista (Talcot Parsons):
   - Influencia en EEUU.
   - La sociedad como un Sistema y cada parte cumple su función dentro del sistema.
   - No explica los cambios sociales, aunque surgen sociólogos muy buenos de esta escuela que sí tratan la cuestión del cambio.
   - Conservadora .
   - Se va evolucionando y salen nuevos autores neo-funcionalistas. Pluralidad.

Hasta la crisis de los años 60-70. Dos paradigmas fundamentales

2. Paradigma marxista[2]:
   - Influencia en Europa.
   - El marxismo trata precisamente del cambio a lo largo de la historia:
     - Variable independiente, la **economía**.
     - Pero en el corto y medio plazo, son los valores (Weber).
   - La teoría marxista no nos explica qué cambios se están dando en la sociedad.
     - Ejemplo: el feminismo y los cambios culturales en su profundidad (mayo del 68).
   - También hay mucha pluralidad y salen buenos sociólogos "neomarxistas".

[2] También es estructuralista.

Neo-marxismo

- Pierre Bourdieu nos habla del "estructural-constructivismo", entre otras cosas.
- Probablemente nadie como él consiguió mejorar la relación entre lo subjetivo y lo objetivo y su aplicabilidad.
- Trata el estructural-constructivismo, la cuestión del habitus, la teoría del capital económico, simbólico y cultural, etc.
- La metodología bourdiana es muy buena para entender y explicar las relaciones de poder o las relaciones desiguales:
  - La distinción
  - Lo que significa hablar

Otras escuelas

- Se produce una fuerte crisis en la Sociología y esto afecta seriamente a la cuestión metodológica.
- Aparece un libro fundamental para todo el mundo *"La estructura de las revoluciones científicas"*, de Khun.
  - Plantea el tema de los Paradigmas y sus consecuencias en la investigación científica.
  - Es un historiador de la ciencia y estudia la evolución de la ciencia a lo largo del tiempo.
  - Tema central y abierto al debate.

Otras escuelas

- En los años 60 y siguientes aparecen nuevas escuelas y hay avances sustanciosos en el terreno teórico.
- Algunas de estas corrientes o escuelas son:
  - Fenomenología
  - Interaccionismo simbólico
  - Etnometodología
- Son escuelas que tienen mucho que ver con la psicología y hacen hincapié en las relaciones **micro**.
- Trabajan mucho en sociedades muy desarrolladas.
- Un libro interesante es *"La presentación de la persona en la vida cotidiana"* de E. Goffman.

Sobre la metodología

- En sociología se discute sobre este tema continuamente lo cual es bastante normal ya que la sociología se debe a la sociedad y la sociedad cambia continuamente, y en épocas de crisis fuertes todavía más; por eso nos cuestionamos continuamente las metodologías.
- Para nuevos fenómenos, nuevas herramientas de investigación.
  - Cuando las "viejas" no nos ayudan a comprender y explicar los fenómenos.
  - Por ejemplo, un tema difícil es el la sociología de la religión.
- Una cuestión que subyace a esta cuestión es:
  - ¿ existe el método científico en las ciencias sociales?
  - Pensamos que sí, aunque continuamente nos replanteamos estas cuestiones.

Sobre la metodología

- Por ejemplo, en la Ciencias naturales y físicas, al estudiar el objeto, éste no se modifica a no ser que lo modifiquemos y lo manipulemos conscientemente para ver qué reacción produce.
- En sociología es distinto, pues desde el momento que estudiamos un objeto, ya lo estamos modificando.
  - Y eso cambia mucho las reglas de cómo enfrentarnos al objeto desde la neutralidad valorativa (Weber) y lo suficientemente alejados y próximos al objeto de investigación.
  - Es decir, cual es la distancia necesaria del objeto (que, recuerdo, siempre son personas), para que se considere la investigación como científica.

Miguel Beltrán. Las cinco vías de acceso a la Realidad Social

- Miguel Beltrán, nos ofrece estas 5 vías de acceso al conocimiento de las cuestiones sociales:
  1. El método histórico
  2. El método comparativo
  3. El método crítico-racional
  4. El método cuantitativo
  5. El método cualitativo

Miguel Beltrán. El método histórico

- ¿ Cómo conocemos los procesos de largo alcance, si no tenemos en cuenta la historia ?
  - Nos tenemos que interrogar por aquello que estudia la realidad social, el curso sufrido sobre y cómo ha llegado a ser y por qué.
- A veces se confunde con la historia.
  - También es verdad que los sociólogos-as, utilizan a los historiadores como fuentes y viceversa.

Miguel Beltrán. El método comparativo

- El método comparativo es consecuencia de la conciencia de la diversidad: las variedades sociales, tanto en el espacio como en el tiempo, y esto lleva necesariamente a la curiosidad del estudioso, el examen de formas y procesos, de estructuras y comportamientos simultáneo de dos o más objetos que tienen algo en común y algo diferente.

Miguel Beltrán. El método crítico-racional

- Frente al concepto tradicional o positivista de la ciencia se opone la teoría crítica.
- Según Horkheimer:
  - *"nunca busca simplemente un incremento del conocimiento como tal: su objetivo es la emancipación del hombre de la esclavitud"*
  - *"no se pretende sustituir la racionalidad de la ciencia por la irracionalidad de la no-ciencia, sino recuperar para los fines humanos, para los valores y para el deber ser, su lugar en la ciencia"*

Miguel Beltrán. El método crítico-racional

- Para Beltrán:

"de lo que se trata es del ejercicio racional de la crítica de fines, de la negación a lo existente de su postulada condición de orden natural necesario, de mostrar el pedestal de barro en que descansan los ídolos de todo tipo"

- Por eso destaca para ello, el concepto de acción racional con arreglo a fines de Weber.

Miguel Beltrán. El método cuantitativo

- Desde el comienzo de la estadística, ésta ha tenido un desarrollo espectacular.
- Hoy día se nos hace imposible entender mínimamente el mundo, sin tener en cuenta las estadísticas.
  - La estadística está muy vinculada a la sociedad industrial y también postindustrial.
  - La estadística está muy vinculada al conocimiento y al cálculo racional, de cualquier cuestión.
- En sociología se ha empleado y se emplea mucho y básicamente en la medición de atributos: clases, rentas, opiniones, etc.

Miguel Beltrán. El método cualitativo I

- La metodología cualitativa como tal es muy amplia.
- Destacaremos algunas de las herramientas que están bajo la etiqueta de metodologías cualitativas.
- Hay que comenzar diciendo que la metodología se sustenta sobre distintas "bases" en su aplicación, pero que cobran todo su sentido, la cuestión de la ideología, es decir de los valores, la lingüística (análisis del discurso) y la propia estructura o sistema en el que se pronuncia el discurso, por ejemplo.
- Se emplea mucho en la investigación de mercado, por supuesto en la investigación académica, y se combina con la metodología cuantitativa o estadística.

Miguel Beltrán. El método cualitativo II

- En el proceso de crisis de la sociología se vivió un proceso de fuerte enfrentamiento entre los llamados cuantitativistas y los cualitativistas.
- La crítica de los segundos a los primeros iba en el sentido de que los estadísticos no dan importancia a las cuestiones discursivas, a los imaginarios sociales, a los valores que se dan detrás de los discursos y que no pueden explicar los cambios que se producen debido a la propia interacción social, etc.

Cuantitativo vs. Cualitativo

- Los cuantitativistas han acusado a los cualitivistas, de que con sus teorías, no se podía objetivar nada.
  - ¿cuánto pesa cada cuestión?
  - ¿cómo se mide, el acuerdo o desacuerdo en determinada cuestión o elemento de análisis?
- Hoy día estas barreras están superadas: hay acuerdo en que todo depende del objeto de investigación.

La herramienta de la investigación cualitativa I

- La observación participante.
  - En antropología se ha usado esta práctica investigadora.
  - Por supuesto también en sociología o psicología social.
- La entrevista en profundidad.
  - No tiene que ver con las entrevistas periodísticas.
- Los grupos de discusión.
  - Una tipología común de un grupo de ocho personas, son dirigidas o "manipuladas" por el que lleva la reunión, para analizar el discurso sobre las cuestiones que se investigan, sobre el presente, el pasado o sobre el futuro.
  - También se han utilizado grupos triangulares, que es parecida a la anterior, pero con una lógica parcialmente distinta.

La herramienta de la investigación cualitativa II

- Hay que tener presente cuestiones que por su significado mayor o menor, pero con relevancia para la investigación que se haga, puede ser de mucha validez.
- Por ejemplo, es un clásico el libro *"Metáforas de la vida cotidiana"* de Lakof.
  - Una investigación sobre el emigrante polaco a EEUU y sus vivencias y sentimientos de todo tipo.
  - Se analiza sobre todo por o a través de las cartas de correspondencia con sus familiares y amigos residentes en Polonia.

Félix Requena. El concepto de Red Social

- En la sociología desarrollada en España, apenas se ha usado el concepto de red social, entendiendo ésta como metodología para la investigación social.
- No ha sido así en otros países como EEUU e Inglaterra, en los cuales llevan ya en ello unos cuantos años.
- Sin embargo, es un concepto que se ha usado mucho, aunque en general ha sido más para hablar de manera metafórica que como metodología de investigación social.

Félix Requena. El concepto de Red Social

- Entendemos el concepto de **Red Social** como:

"una serie de vínculos entre un conjunto definido de actores sociales"
(Callon)

e igualmente

"las características de estos vínculos como un todo que tienen la propiedad de proporcionar interpretaciones de la conducta social de los actores implicados en la red"

Análisis de Redes Sociales

- El concepto de análisis de redes se puede aplicar en las más diversas especialidades como:
  - sociología política y electoral
  - sociología del trabajo
  - análisis de la estructura de organizaciones formales
  - sociología del consumo
- *"El concepto de red social, desde el punto de vista analítico, está más cerca de la idea de sociograma de J.Moreno, es decir, cual es la función o funciones de una red social".*

Análisis de Redes Sociales

- La idea de red, tal y como la usamos aquí, está tomada en gran parte de la teoría matemática de grafos.
- En esta teoría, se llama red a una serie de puntos vinculados por una serie de relaciones que cumplen determinadas propiedades, es decir, un nudo de la red está vinculado con otro mediante una línea que presenta la dirección y el sentido del vínculo.
- Una red en la teoría de grafos es un conjunto de relaciones en el cual las líneas que conectan los diferentes puntos tiene un valor concreto, sea éste numérico o no.
- Esta posibilidad de cuantificar un vínculo es una de las cualidades que mayor interés puede tener para la sociología.

Análisis de Redes Sociales

- En sociología por cuestiones pragmáticas, normalmente es necesario trabajar con un conjunto identificable de actores (personas, grupos, etc.) y las relaciones que existen entre ellos.
- En el análisis de redes no se presta tanta atención a los atributos de los actores que están en la red como los vínculos que relacionan a unos con otros, para dar una posible explicación de la conducta de los actores implicados en la red.

Sociograma (wikipedia)

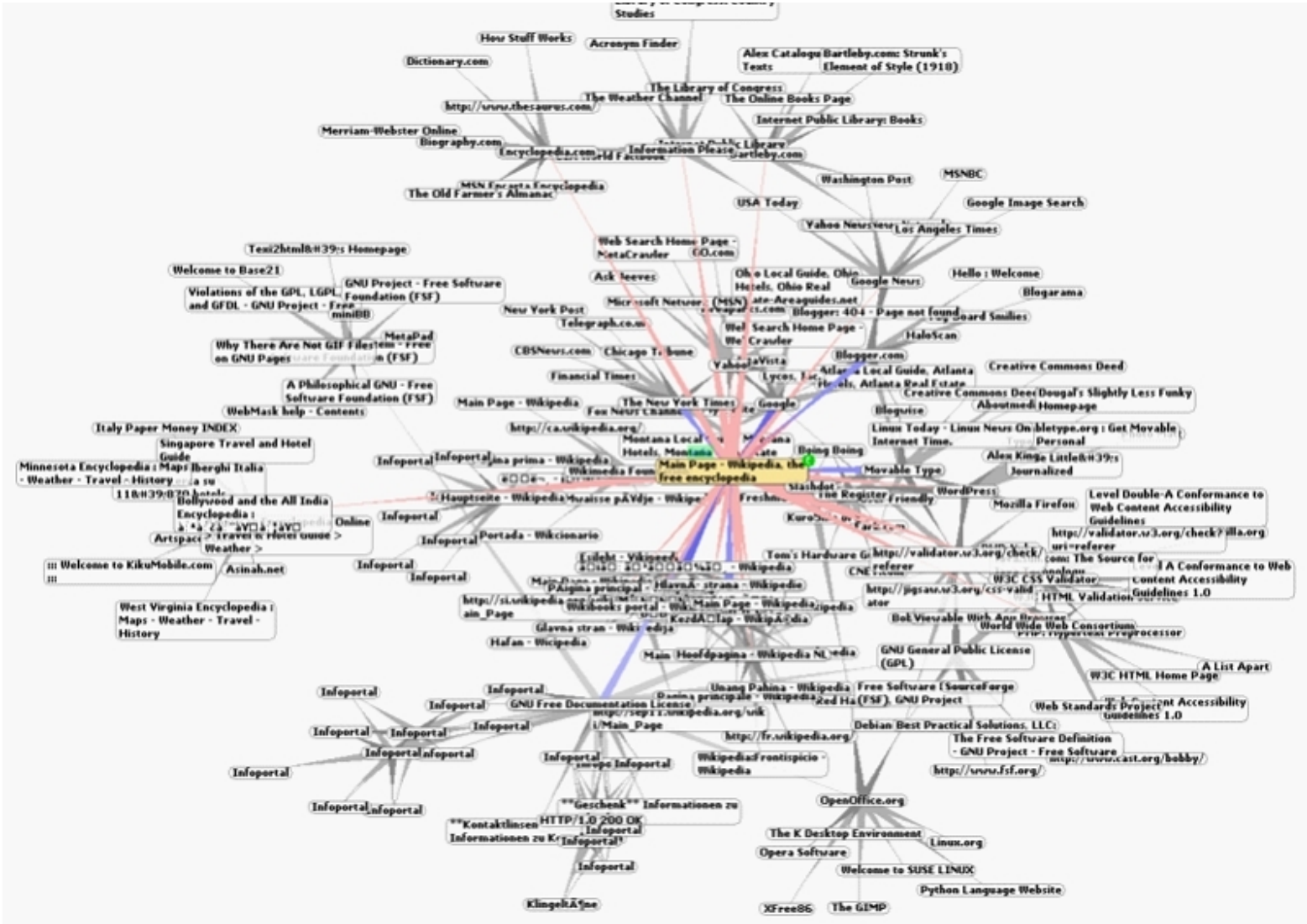

Estructura y morfología de las Redes Sociales. Posición

- La principal apreciación que hay que tener en consideración en una red social es la **posición** que ocupa un actor social dentro de la estructura de la red.
- No todas las posiciones son iguales, ni tan siquiera equivalentes.
- Se pueden distinguir a priori dos niveles de posiciones:
  - Posiciones centrales
  - Posiciones periféricas

Estructura y morfología de las Redes Sociales. Índice de centralidad

- El **índice de centralidad** de toda la red será la suma de los índices de centralidad de todas las posiciones que componen la red.
- El concepto de posición es muy importante por dos razones:
  - en primer lugar, ayuda a simplificar el análisis a medida que aumenta el nivel de complejidad de la red
  - en segundo lugar, ha demostrado ser un factor importante en la conducta de los actores de las redes de intercambio, pues en cierta forma determina el grado de autonomía o dependencia de un actor respecto a los demás
- Las posiciones de los actores en una red social determinan la "estructura de oportunidad" de un actor respecto a la facilidad de acceder a los recursos de otros actores en la red.

Estructura y morfología de las Redes Sociales

- Respecto a la morfología de las redes, Mitchel distingue cuatro elementos morfológicos en las redes sociales:
  1. Anclaje o localización de la red
  2. Accesibilidad
  3. Densidad de la red
  4. Rango de la red

Estructura y morfología de las Redes Sociales I

1. **Anclaje o localización de la red**
   - Se trata de localizar en la red en torno a determinados actores sociales, acotando en cierta forma la red, pues normalmente una red tiene que ser trazada desde algún punto o actor inicial.

2. **Accesibilidad**

- Esta se puede definir rigurosamente como la fuerza con la cual el comportamiento de un actor está influenciado por los otros.
- La accesibilidad dentro de una red se puede resumir por las distancias en una matriz, donde el número de pasos necesarios para alcanzar a otro actor aparece en la intersección de las filas con las columnas especificadas para cada actor.
- Se pueden distinguir dos magnitudes de la accesibilidad en una red:
  - la proporción de actores que pueden contactar con cada actor determinado en la red
  - el número de intermediarios que hay que usar para contactar con otros

3. **Densidad de la red**

- Esta noción está tomada directamente de la teoría de los grafos.
- La densidad de una red variará en función al número de vínculos que exista dentro de ella.
- Así, una red donde todos los actores están vinculados con todos los demás, diremos que tiene densidad máxima.
- Pero en las redes en las que unos actores están vinculados con algunos pero no con todos los actores, habrá zonas de mayor o menor densidad.

4. Rango de la red

- Un rango de primer orden es el número de actores en contacto directo con el actor sobre el que está referida o localizada la red.
  - El concepto de rango de una red es muy significativo cuando se trata de redes personales.
- En este caso particular se podría definir el rango como el número de personas que están vinculadas directamente (sin ningún intermediario) con el individuo.
  - Así, un individuo mejor relacionado que otro tendrá una red personal de rango mayor.
- Es necesario tener siempre presente, que una red se refiere a un conjunto de procesos de interacción, en los cuales hay que distinguir las siguientes cualidades o características determinantes a la hora de definir determinada relación dentro de una red.

Sistema: Red de Redes

- Estructural: **la red**.
  - Conjunto de unidades homogéneas interconectadas. punto de vista topológico.
  - Noción estática ó sincrónica: no interesan las propiedades de las unidades.
- Funcional: **Tráfico sobre una red**.
  - Noción dinámica ó diacrónica: estado y reglas o funciones que rigen el cambio de estado de las unidades.
- Semántico o Estructural-Funcional:
  - La estructura de la red canaliza el tráfico
  - El tráfico cambia la estructura de la red

Red I

- Red: Unidades conectadas por fibras o segmentos.
- Sentidos de la palabra **"red"**:
  - Natural:
    - Biológico: Tejidos, rizomas, ...
    - Físico-químico: Maya cristalina, molecular, ...
  - Antropológico:
    - Tecnológico-cultural: tejidos textiles, redes de pesca, cestos, ...
    - Psico-social: relaciones familiares, de amistad, trabajo, comercio, lingüísticas, ...

Red II

- Sentidos de la palabra **"red"** (cont.):
  - Matemático:
    - Geométrico: puntos conectados, situados en el espacio 2D ó 3D que muestran algún tipo de regularidad.
    - Grafo: conjunto de nodos conectados a través de segmentos, situados en espacios multidimensionales y que pueden o no mostrar regularidades.
  - Filosófico:
    - Parménides.
    - La ontología se ocupa de la definición del ser y de establecer las categorías fundamentales o modos generales de ser de las cosas a partir del estudio de sus propiedades.

Sistema = Red Funcional

- Natural:
  - Biológico: circulación de la sangre, incidencia de enfermedades periódicas, oscilación de poblaciones, redes neuronales naturales,...
  - Físico-químico: mecánica, reacciones químicas, electricidad, ...
- Antropológico:
  - Tecnológico-cultural: redes de transporte, música, lenguaje, ...
  - Psico-social: relaciones familiares, de amistad, trabajo, comercio, lingüísticas, ...

Sistema = Red Funcional

- Matemático:
  - Sistemas numéricos: ecuaciones en diferencia, diferenciales,. . . .
  - Sistemas axiomáticos: autómatas, gramáticas, lógica.
  - Pueden ser:
    - Deterministas o No deterministas.
    - Paralelos, distribuidos, agenciales.
    - Situados (2D, 3D) o no situados.
    - Evolutivos o no evolutivos.
- Filosófico:
  - Heráclito.
  - Filosofía natural.
  - Física.

Conclusiones

- En esta presentación hemos realizado una aproximación a las Redes Sociales desde el paradigma de la Teoría General de Sistemas.
- Para ello,
  - Hemos realizado una presentación, desde sus orígenes, de la Teoría General de Sistemas.
  - Hemos presentado la Teoría de Redes Sociales desde este paradigma científico.
  - Hemos formalizado el concepto de Red Social y de Sistema o red de redes.

Bibliografía I

Alan Barnard.
History and Theory in Anthropology.
Cambridge University Press, 1 edition, June 2000.

Pierre Bourdieu.
Social space and symbolic power.
Sociological Theory, 7(1):14–25, 1989.
Spring, 1989 / Copyright ‖ 1989 John Wiley & Sons.

Paul E. Ceruzzi.
A History of Modern Computing, 2nd Edition.
The MIT Press, 2 edition, May 2003.

Reinhard Diestel.
Graph Theory.
Springer, 3rd edition, August 2005.

Bibliografía II

Wouter de Nooy, Andrej Mrvar, and Vladimir Batagelj.
Exploratory Social Network Analysis with Pajek.
Cambridge University Press, 2005.

Holger Ebel, Jörn Davidsen, and Stefan Bornholdt.
Dynamics of social networks.
Complex., 8(2):24–27, 2002.

Victor M. Eguiluz, Martin G. Zimmermann, Camilo J. Cela-Conde, and Maxi San Miguel.
Cooperation and the emergence of role differentiation in the dynamics of social networks.
American Journal of Sociology, 110(4):977–1008, 2005.

Donald K. Freedheim and Irving B. Weiner.
Handbook of Psychology, History of Psychology.
Wiley, April 2004.

Bibliografía III

Anthony Giddens.
Politics, Sociology, and Social Theory: Encounters with Classical and Contemporary Social Thought.
Stanford University Press, 1 edition, 1995.

Michael Hechter and Christine Horne.
Theories of Social Order: A Reader.
Stanford Social Sciences, 1 edition, March 2003.

William McDougall.
Introduction to Social Psychology.
Batoche Books, fourteenth edition edition, 2001.

Bertrand Russell.
History of Western Philosophy.
Routledge, 2 edition, March 2004.

Bibliografía IV

Ludwig von Bertalanffy.
Perspectivas en la Teoría General de Sistemas.
Alianza Universidad, Madrid, 1986.

Duncan J. Watts, Peter Sheridan Dodds, and M. E. J. Newman.
Identity and search in social networks.
Science, 296(5571):1302–1305, May 2002.

L.A. Zadeh.
Fuzzy Sets and Their Applications to Cognitive and Decision Processes.
Academic Press Inc, October 1975.

Georg Wilhelm Friedrich Hegel. Contradicción I

- El acto mismo del conocimiento es la introducción de la contradicción.
  - El principio del *tercero excluido*, algo o es A o no es A, es la proposición que quiere rechazar la contradicción y al hacerlo incurre precisamente en contradicción: A debe ser $+A$ ó $-A$, con lo cual ya queda introducido el tercer término, A que no es ni $+$ ni $-$ y por lo mismo es $+A$ y $-A$.
  - Una cosa es ella misma y no es ella, porque en realidad toda cosa cambia y se transforma ella misma en otra cosa.
  - Esto significa la superación de la *lógica formal* y el establecimiento de la *lógica dialéctica*.

Georg Wilhelm Friedrich Hegel. Contradicción II

- Todas las cosas son contradictorias en sí mismas y ello es profundo y plenamente esencial.
  - La identidad es la determinación de lo simple inmediato y estático, mientras que la contradicción es la raíz de todo movimiento y vitalidad, el principio de todo automovimiento y, solamente aquello que encierra una contradicción se mueve.
  - La imaginación corriente capta la identidad, la diferencia y la contradicción, pero no la transición de lo uno a lo otro, que es lo más importante, cómo lo uno se convierte en lo otro.

▸ Georg Wilhelm Friedrich Hegel

Algunas ideas sobre redes neuronales competitivas y mixtas

Manuel Graña

contenido

- Introducción
- Algoritmo competitivo simple
- Mapas auto-organizativos de Kohonen
- Redes de contrapropagación
- Redes de base radial
- Learning Vector Quantization (LVQ)

Introducción

- Redes competitivas
  - Regla “winner takes all”
    - Corresponde con el agrupamiento duro (crisp clustering) de datos basado en representantes.
  - Aprendizaje basado en la adaptación de los representantes.
    - Búsqueda de los representantes óptimos de acuerdo a una función de energía (error).

Introducción

- Las redes competitivas tienen entrenamiento no supervisado
  - No se conoce una clasificación de los datos.
  - No se usa para el entrenamiento, aunque sea conocida.

Introducción

- Redes mixtas:
- Tienen tres capas de pesos: input, hidden y output
  - La capa hidden corresponde a una capa competitiva
  - La capa output corresponde a una capa con entrenamiento supervisado.

- Redes mixtas
- La capa competitiva realiza una partición del espacio input
- La capa supervisada se aprovecha de esta discretización para facilitar el entrenamiento
  - Equivale a un conjunto de redes definidas sobre regiones input locales

Normalización

- No es estrictamente necesaria.
  - La distancia euclídea no la necesita
- Tipos de normalización
  - Hacer que la norma del vector input sea unitaria (los datos caen en una hiperesfera)
  - Dividir por la desviación estandard y restar la media (normal N(0,1)).
  - Escalar al intervalo [0,1] o [-1,1] cada componente

Normalización

- Si los datos se normalizan, es posible que se requiera renormalización de los pesos (representantes) tras cada paso de entrenamiento si la regla de aprendizaje no garantiza la normalización

Aprendizaje competitivo simple

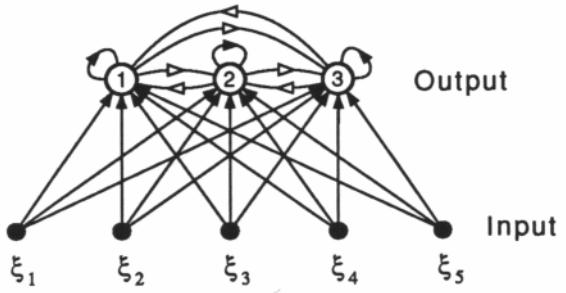

FIGURE 9.1 A simple competitive learning network. The connections shown with open arrows are inhibitory; the rest are excitatory.

Input neto

$$h_i = \sum_j w_{ij}\xi_j = \mathbf{w}_i \cdot \boldsymbol{\xi}$$

Unidad "ganadora"

$$\mathbf{w}_{i^*} \cdot \boldsymbol{\xi} \geq \mathbf{w}_i \cdot \boldsymbol{\xi}$$

$$|\mathbf{w}_{i^*} - \boldsymbol{\xi}| \leq |\mathbf{w}_i - \boldsymbol{\xi}| \qquad \text{(for all } i\text{)}.$$

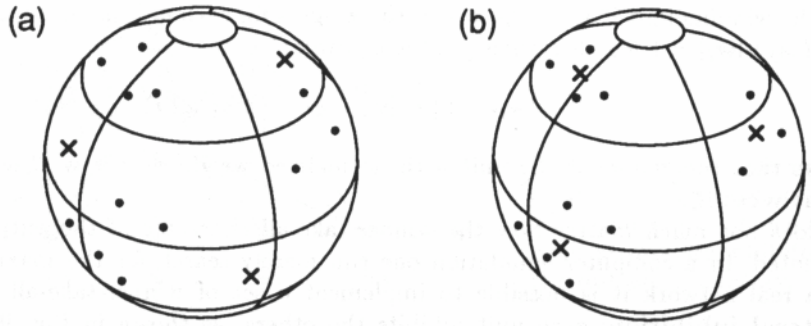

FIGURE 9.2 Competitive learning. The dots represent the input vectors, the crosses represent the weights for each of three units. (a) Before learning. (b) After learning.

Regla de aprendizaje competitivo

$$\Delta w_{i^*j} = \eta'\left(\frac{\xi_j^\mu}{\sum_j \xi_j^\mu} - w_{i^*j}\right)$$

$$\Delta w_{i^*j} = \eta(\xi_j^\mu - w_{i^*j})$$

ma

$$\Delta w_{ij} = \eta O_i(\xi_j^\mu - w_{ij}) \qquad O_{i^*} = 1 \quad O_i = 0 \text{ for } i \neq i^*$$

Aprendizaje competitivo simple

- Estructura:
  - Capa input y capa de salida
  - Unidades de salida: identificación del cluster al que se asignan los datos
- Dinámica:
  - Se calcula la distancia (Euclídea) del input a cada uno de los representantes (pesos)
    - Si el input es de norma unitaria la distancia euclídea y el producto interno son equivalentes
  - Se escoge como vencedora a la unidad de distancia mínima

Aprendizaje competitivo simple

- Entrenamiento on line:
  - La unidad ganadora “se acerca” a los datos
  - El incremento de peso es un porcentaje de la distancia al input
- Entrenamiento batch:
  - Todos los datos input asignados se usan para calcular el nuevo representante.
  - Es equivalente al algoritmo k-means.

- Problema de las unidades “muertas” (stuck units)
  - Son representantes que nunca se actualizan
  - Corresponden a clases vacias
  - Se producen por malas inicializaciones y/o por azares del entrenamiento.
  - Es un problema de convergencia básico.

- Soluciones para el problema de las unidades muertas
  - Inicialización con datos de la muestra
  - Actualizar vencedores y perdedores
  - Preservación topológica (Kohonen)
  - Ponderar el número de veces que gana una clase (conciencia)
  - Añadir ruido a los patrones

Convergencia: el algoritmo competitivo simple tiende a minimizar la distorsion de la cuantización vectorial de la muestra

Función de energía

$$E\{w_{ij}\} = \frac{1}{2}\sum_{ij\mu} M_i^\mu (\xi_j^\mu - w_{ij})^2 = \frac{1}{2}\sum_{\mu} |\boldsymbol{\xi}^\mu - \mathbf{w}_{i^*}|^2.$$

$$M_i^\mu = \begin{cases} 1 & \text{if } i = i^*(\mu); \\ 0 & \text{otherwise.} \end{cases}$$

Descenso por el gradiente

$$\langle \Delta w_{ij} \rangle = -\eta \frac{\partial E}{\partial w_{ij}} = \eta \sum_{\mu} M_i^\mu (\xi_j^\mu - w_{ij})$$

$$\eta(t) = \eta_0 t^{-\alpha} \text{ (with } \alpha \leq 1) \text{ or } \eta(t) = \eta_0(1 - \alpha t).$$

Existen muchos mínimos locales de la función de energía

La aplicación batch del descenso de gradiente es el algoritmo de k-means

SOM: mapas autoorganizativos

- Introducen la noción de preservación topológica:
  - Pesos cercanos (en el espacio input) tienen que tener unidades cercanas (en el espacio de índices de las unidades output)
  - Se actualiza la unidad ganadora y sus vecinas (en el espacio de índices)

Mapas de kohonen

winner i^* $|\mathbf{w}_{i^*} - \boldsymbol{\xi}| \leq |\mathbf{w}_i - \boldsymbol{\xi}|$ (for all i).

$$\Delta w_{ij} = \eta \Lambda(i, i^*)(\xi_j - w_{ij})$$

neighborhood function $\Lambda(i, i^*)$ 1 for $i = i^*$

$$\Lambda(i, i^*) = \exp(-|\mathbf{r}_i - \mathbf{r}_{i^*}|^2 / 2\sigma^2)$$

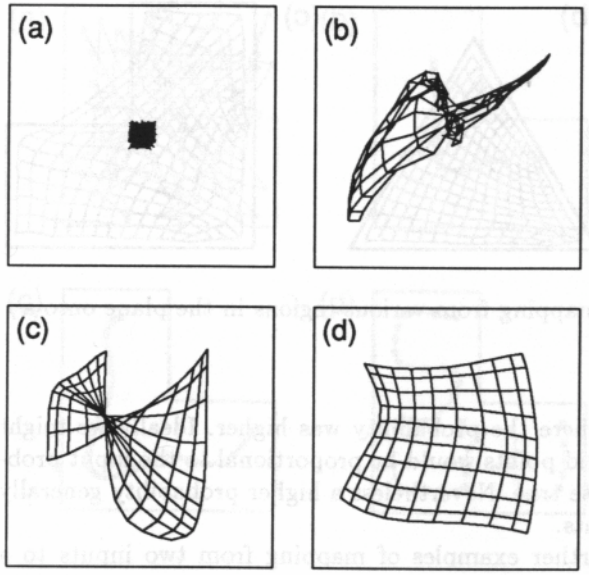

FIGURE 9.11 Kohonen feature mapping from a square region of the plane onto a 10 × 10 array of output units.

Tanto la velocidad de aprendizaje como el radio de vecindad van hacia cero muy suavemente

Convergencia

- Superponiendo el espacio input y el de índices:
  - Las unidades se disponen de forma ordenada en el espacio input
    - Si el espacio de indices es 1D tenemos una lína que no se entrecruza.
    - Si el espacio de indices es 2D tenemos una superficie (malla) que no tiene pliegues.

Convergencia

- Está demostrada la convergencia hacia el ordenamiento de la unidades en el caso de que los espacios input e índices son 1D.
- No hay resultados concluyentes para las otras situaciones.
- No hay una función de energía “bien definida”.
- Se han propuesto cosas parecidas que minimizan una función de energía bien definida

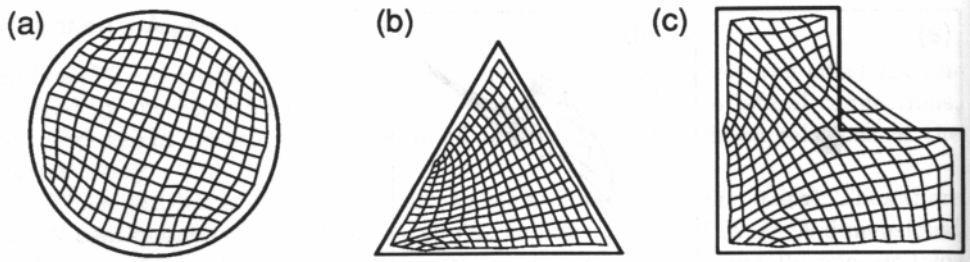

FIGURE 9.12 Kohonen feature mapping from various regions in the plane onto a 15 × 15 array of output units.

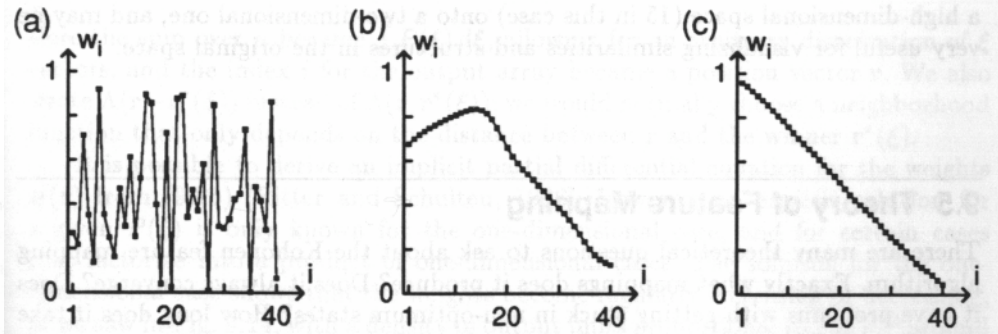

FIGURE 9.14 Kohonen feature mapping from a one-dimensional interval onto a linear array of 40 units.

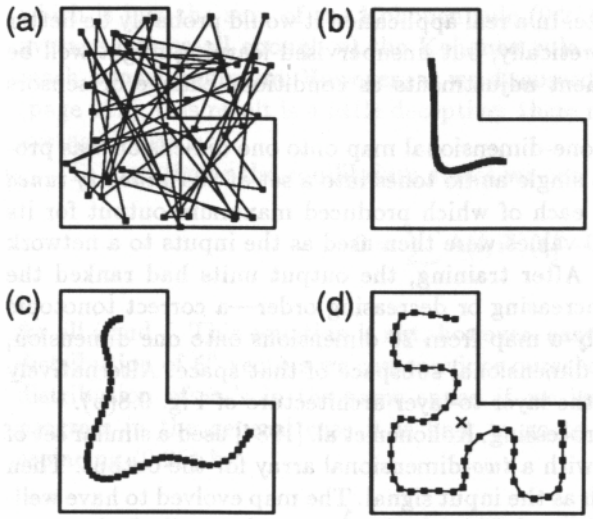

FIGURE 9.13 Kohonen feature mapping from a two-dimensional L-shaped region to a linear array of 50 units.

Redes de contrapropagación

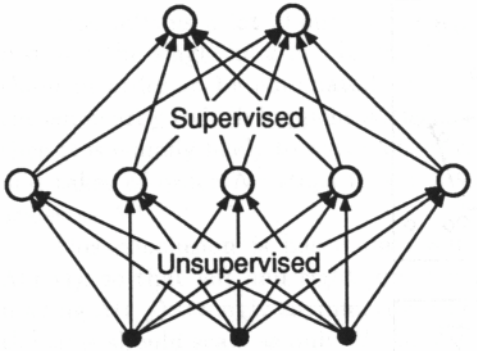

FIGURE 9.17 A hybrid learning network. Counterpropagation networks, hierarchical feature map classifiers, and radial basis function (locally tuned) networks all have this basic architecture.

La capa oculta es de unidades competitivas.

La capa de salida es de unidades lineales

Entrenamiento lineal de la capa output

$$\Delta w_{ij} = \eta(\zeta_i^\mu - O_i^\mu)V_j \,.$$

$$\Delta w_{ij} = \eta(\zeta_i^\mu - w_{ij})V_j$$

(where V_j is 1 for the winner and 0 otherwise).

$$\langle w_{ij} \rangle = \langle M_j^\mu \zeta_i^\mu \rangle$$

Redes debase radial

Las unidades ocultas tienen función de activación gausiana normalizada

Gaussian activation functions $$g_j(\boldsymbol{\xi}) = \frac{\exp[-(\boldsymbol{\xi} - \boldsymbol{\mu}_j)^2/2\sigma_j^2]}{\sum_k \exp[-(\boldsymbol{\xi} - \boldsymbol{\mu}_k)^2/2\sigma_k^2]}$$

$$\sum_j g_j(\boldsymbol{\xi}) = 1$$

Las unidades de salida son unidades lineales, con entrenamiento:

$$\Delta w_{ij} = \eta(\zeta_i^\mu - O_i^\mu)V_j \quad \text{where } O_i^\mu = w_{ij} V_j .$$

Que minimiza

$$H\{w_{ij}\} = \tfrac{1}{2} \sum_{ij\mu} [\zeta_i^\mu - w_{ij} g_j(\boldsymbol{\xi}^\mu)]^2 .$$

Métodos mixtos: LVQ

El problema es de clasificación supervisada. Los vectores input tienen una clase asociada. Los vectores peso también tienen una clase asociada.

El entrenamiento depende de la clase del vector input, es repelente o atractivo dependiendo de que sean distintos o coincidan las clases

$$\Delta w_{i^*j} = \begin{cases} +\eta(\xi_j^\mu - w_{i^*j}) & \text{if class is correct;} \\ -\eta(\xi_j^\mu - w_{i^*j}) & \text{if class is incorrect.} \end{cases}$$

LVQ2,

1. the input vector $\boldsymbol{\xi}$ is misclassified by the winning unit i^*;
2. the next-nearest neighbor i' has the correct class; and
3. the input vector $\boldsymbol{\xi}$ is sufficiently close to the decision boundary (perpendicular bisector plane) between $\mathbf{w}_{i^*}$ and $\mathbf{w}_{i'}$.

referencias

- Introduction to the Theory of Neural Computation (Santa Fe Institute Studies in the Sciences of Complexity) , John A. Hertz, Richard G. Palmer, Anders Krogh, Westview Press (January 1, 1991)

Robust Multimedia Information Retrieval in Basque Context

II Jornadas de Inteligencia Computacional

Mayo 2008, Affi, Verona

Index

- Introduction
- Information Retrieval (IR)
- Multimedia Information Retrieval
- Information Retrieval in video sources
- Information Retrieval in audio sources
- Information Retrieval in Basque Context
- Robustness
- Conclusions & Future lines

Introduction

- The **collection of written information** in some sort of repository is a practice as old as civilization itself. From ancient Mesopotamia and Alexandria to modern libraries around the globe, the need to collect information seems natural to the human kind.

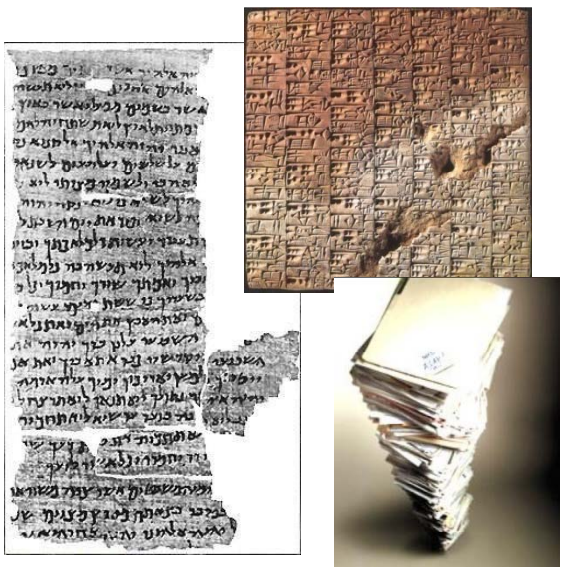

Introduction

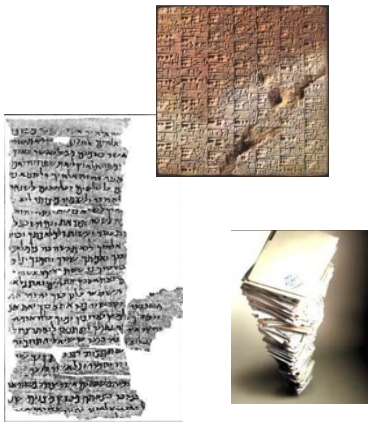

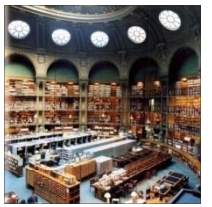

- However, as time moves forward and new information arrives, we need *new techniques* to **store** and **organize** this heritage. Main concern is how to organize this large archives in order to have fast access to desired information, for this Information Technology has developed techniques for **automatic classification, compression, storage and retrieval**.

Introduction

- The everyday more accessible use of communications, such as **radio**, **television** and **Internet**, enable us to reach information from anywhere at anytime.
- The most **natural** mean to **transmit information** among humans is by **voice**.
- Unfortunately a permanent recording of such class of information has been less common than text archiving, mainly because two reasons:
  - the large amount of storage required for acoustics
  - and its difficulties for classification or indexing.

Introduction

- Nowadays, **massive storage technologies** are more affordable than ever and **new algorithms** for **data compression** permit to record hours of video and audio in just tenths or thousands of megabytes.
- These advances outline a future where multimedia document storage will surpass text-based archiving.

- Witten I.H., et al., "*Managing gigabytes: compressing and indexing documents and images*", Van Nostrand Reinhold, New York (1994).

Introduction

- In recent years, new techniques for **text indexing** and **automatic information retrieval** has been developed and successfully used over the Internet, focusing on digital documents containing text information.
- However, the future of these search engines requires its use on **multimedia databases**.
- It is necessary to develop search engines for **multimedia digital libraries**.

- Wolf P.P.; et al., "*The MERL SpokenQuery Information Retrieval System: A System for Retrieving Pertinent Documents from a Spoken Query*", IEEE Int. Conf. on Multimedia and Expo (ICME), Vol. 2, August 2002.

Introduction

- UPV/EHU: Multidisciplinary Research Group

  The development of Automatic Index Systems

  - First stage:
    - Requires of appropriate Multimodal Resources (MR) to implement a baseline Multimodal Index System for users in the Basque Country from audio files

      Languages spoken: Basque, Spanish, and French.
    - Multilingual Continuous Speech Recognition system.
    - “Ehiztari“ project
  - New stage:
    - To continue into mass information systems (audio/visual resources).
    - Working with multimedia digital libraries
    - PROFIT project

IR - Definition

Retrieval & Access

Information

- Information Retrieval:

Basically, it is a process involved with activities which are oriented to look for and find out relevant information, for helping in the user information requirements.

- SALVADOR, J.A. "*Formación en Recuperación de Información: Análisis de los cursos y asignaturas en las escuelas de Biblioteconomía y Documentación de Norteamérica y España*", http://eprints.rclis.org, 2002.

IR - Introduction

- In 1950, Calvin N. Mooers suggested ***Information Retrieval*** as a first reference to deal with searching information in documentation.
- He defined as:

«It is information searching
into a documentation stock
focused on the specification of a field».

- *MOOERS, C.N. "The theory of digital handling of non-numerical information and its implications to machine economics". Technical Bulletin No. 48. Cambridge, MA: Zator Co., 1950*

IR - Introduction

- For 50 years, significant changes in methods and platforms, as well as formats and descriptions have been appeared.
  - Informatics Systems
  - Sources: Text, video, audio, etc.
  - WEB

… but the meaning of

«Information Retrieval»

has continued without changing

IR - Introduction

- Frederick W. Lancaster express that nowadays the "conventional" information retrieval means:

«on-line search in
electronic data bases,
in an interactive and real time way».

- LANCASTER, F.W. "*Sistemas avanzados de recuperación de información*". En: Wilfrid Lancaster y María Pinto (Coords). *Procesamiento de la información científica. Madrid: Arco/Libros, 2001.*

IR - Introduction

- Charles Meadow specifies Information Retrieval in similar terms, arguing in a basic and easy way:

«Seeking of needed information
into an information store or data base».

- MEADOW, C.T.; BOYCE, B.R.; KRAFT, D.H. "*Text Information Retrieval Systems*". *San Diego: Academic Press, 2000.*

IR - Introduction

- Jean Tague-Sutcliffe:

  In this process there exist a number of elements and variables which give it an specific denomination:

  (a) Data base and repository offices

  (b) Information representation

  (c) Users

  (d) Seeking commands –Seeking strategy

  (e) Seeking tools

  (f) Seeking process

  (g) Evaluation of the recovered files

IR - Introduction

- All these variables are located in a high level. In each variable or element several aspects can be analysed.
- The most important research lines in this field are based on those variables.
- TAGUE-SUTCLIFFE, J. "*The pragmatics of information retrieval experimentation, revisited*". *Information Processing and Management, 1992, vol. 28, nº 4.*

IR - Introduction

- There are lots of problem to solve in this field, providing an extended number of new ideas each one. Because of that, different proposals have appeared along these years. Therefrom, Information Retrieval shows different research lines . This lack of consistency is due to an emerging field, as Blair said in 1990.

- BLAIR, D.C. *Language and representation in information retrieval. Amsterdam: Elsevier Science Publishers, 1990, p. vii.*

IR - Introduction

- In fact, the weak coherency can be established by the interdisciplinarity of the Information Retrieval field.

- Information Sciences, Informatics, Data, Psychology, Computational Linguistics, Logics, Artificial Intelligence, Computational Intelligence, etc., are several of the whole items which bring benefits to the Information Retrieval research and development, with different grades of importance.

IR - Bibliography

- Baeza-Yates R. y Ribeiro-Neto B., Modern Information Retrieval. Addison Wesley. 1999.
- Chowdhury G. G., Introduction to modern information retrieval. Library Association Publishing London. 1999.
- Chu H.. «*Information Representation and Retrieval in the Digital Age». ASIST, 2003.*
- Frakes y Baeza-Yates. «*Information Retrieval: data structures and algorithms». Englewood* Cliffs: Prentice Hall, 1992.
- Rijsbergen. «*Information Retrieval». Butterworth, 1979*
- Peña, Baeza y Rodríguez. «*Gestión digital de la información». Alfaomega-Rama, 2002.*
- Chang. «*Mining the World Wide Web: an information search approach». Kluwer* Academic, 2001.
- Korfhage. «*Information Retrieval and Storage». Wiley Computer Publisher, 1997.*

IR - Bibliography

- Salton «*Automatic text processing: The transformation, analysis and retrieval of information by computer», Addison-Wesley, 1989*
- Salton y McGill*, «An introduction to modern information retrieval» McGraw-Hill, 1983.*
- ACKERMANN, E.; HARTMAN, K. Searching and researching on the Internet and the World Wide Web. 3ed. ed. Wilsonville, Oregon: Franklin, Beedle & Associates, 2003.
- Witten I. H. et al., Bell. Managing Gigabytes: Compressing and Indexing Documents and Images (2nd Edition). Morgan Kaufmann, 1999.
- Belew R. K., Finding Out About. Cambridge Press, 2001.
- Grossman D. A. and Frieder O., Information Retrieval: Algorithms and Heuristics. Kluwer Academic Publishers, 1998.

IR - Problem

- What is the IR problem?
- How to organize an IR system? (Or the main processes in IR)
- Indexing
- Retrieval
- System evaluation
- Some current research topics

IR - Problem

- **Goal** = find documents *relevant* to an information need from a large document set

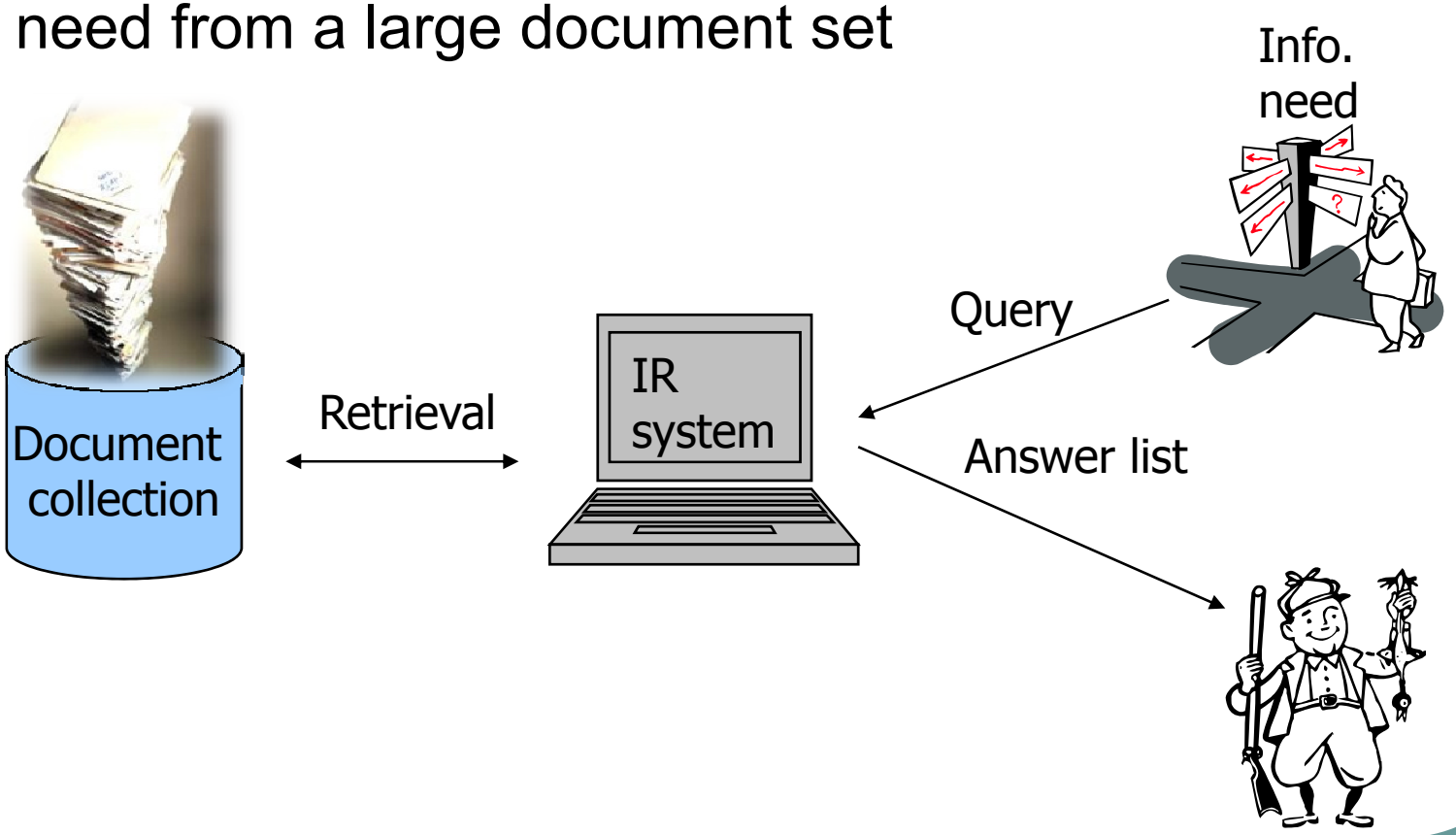

Example

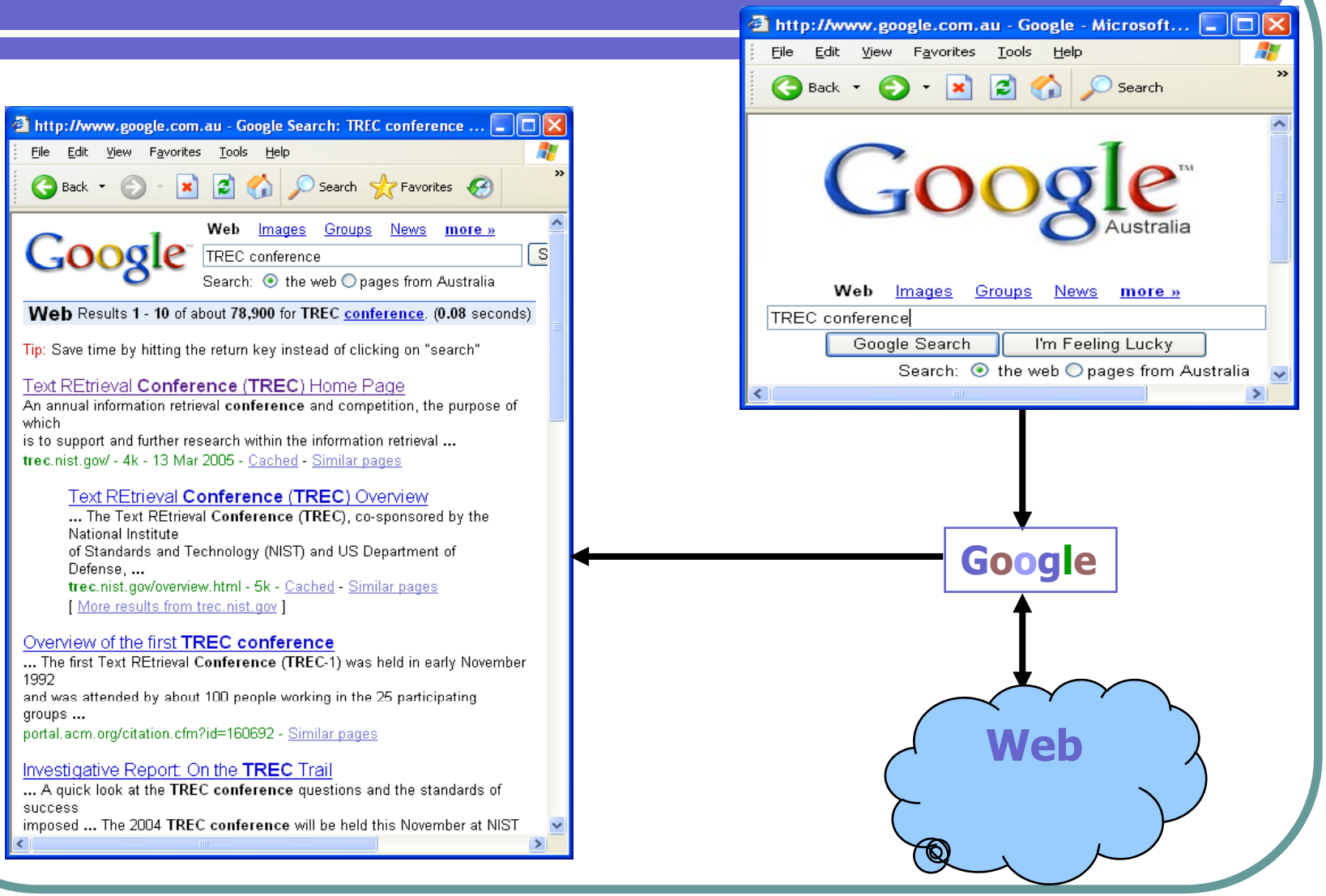
http://www.google.com.au - Google Search: TREC conference ...
File Edit View Favorites Tools Help
Back Search Favorites
Google
Web Images Groups News more »
TREC conference
Search: the web pages from Australia
Web Results 1 - 10 of about 78,900 for TREC conference. (0.08 seconds)
Tip: Save time by hitting the return key instead of clicking on "search"
Text REtrieval Conference (TREC) Home Page
An annual information retrieval conference and competition, the purpose of which
is to support and further research within the information retrieval ...
trec.nist.gov/ - 4k - 13 Mar 2005 - Cached - Similar pages
Text REtrieval Conference (TREC) Overview
... The Text REtrieval Conference (TREC), co-sponsored by the National Institute
of Standards and Technology (NIST) and US Department of Defense, ...
trec.nist.gov/overview.html - 5k - Cached - Similar pages
[More results from trec.nist.gov]
Overview of the first TREC conference
... The first Text REtrieval Conference (TREC-1) was held in early November 1992
and was attended by about 100 people working in the 25 participating groups ...
portal.acm.org/citation.cfm?id=160692 - Similar pages
Investigative Report: On the TREC Trail
... A quick look at the TREC conference questions and the standards of success
imposed ... The 2004 TREC conference will be held this November at NIST
http://www.google.com.au - Google - Microsoft...
File Edit View Favorites Tools Help
Back Search
Google Australia
Web Images Groups News more »
TREC conference
Google Search I'm Feeling Lucky
Search: the web pages from Australia
Google
Web

IR - Problem

- First applications: in libraries (1950s)

  ISBN: 0-201-12227-8

  Author: Salton, Gerard

  Title: Automatic text processing: the transformation, analysis, and retrieval of information by computer

  Editor: Addison-Wesley

  Date: 1989

  Content: <Text>

- External attributes and internal attribute (content)
- Search by external attributes = Search in DB
- IR: search by content

Comparing IR and Databases

	Databases	IR
Data	**Structured**	**Unstructured**
Fields	**Clear semantics** (SSN, age)	**No fields** (other than text)
Queries	**Defined** (relational algebra, SQL)	**Free text** ("natural language"), Boolean
Recoverability	**Critical** (concurrency control, recovery, atomic operations)	**Downplayed**, though still an issue
Matching	**Exact** (results are *always* "correct")	**Imprecise** (need to measure effectiveness)

Possible approaches

1. String matching (linear search in documents)
   - Slow
   - Difficult to improve

2. Indexing (*)
   - Fast
   - Flexible to further improvement

IR - Indexing-based

IR - Main problems

- Document and query indexing
  - How to best represent their contents?
- Query evaluation (or retrieval process)
  - To what extent does a document correspond to a query?
- System evaluation
  - How good is a system?
  - Are the retrieved documents relevant? (precision)
  - Are all the relevant documents retrieved? (recall)

IR - Document indexing

- Goal = Find the important meanings and create an internal representation
- Factors to consider:
  - Accuracy to represent meanings (semantics)
  - Exhaustiveness (cover all the contents)
  - Facility for computer to manipulate
- What is the best representation of contents?
  - Char. string (char trigrams): not precise enough
  - Word: good coverage, not precise
  - Phrase: poor coverage, more precise
  - Concept: poor coverage, precise

IR – Multimedia Databases

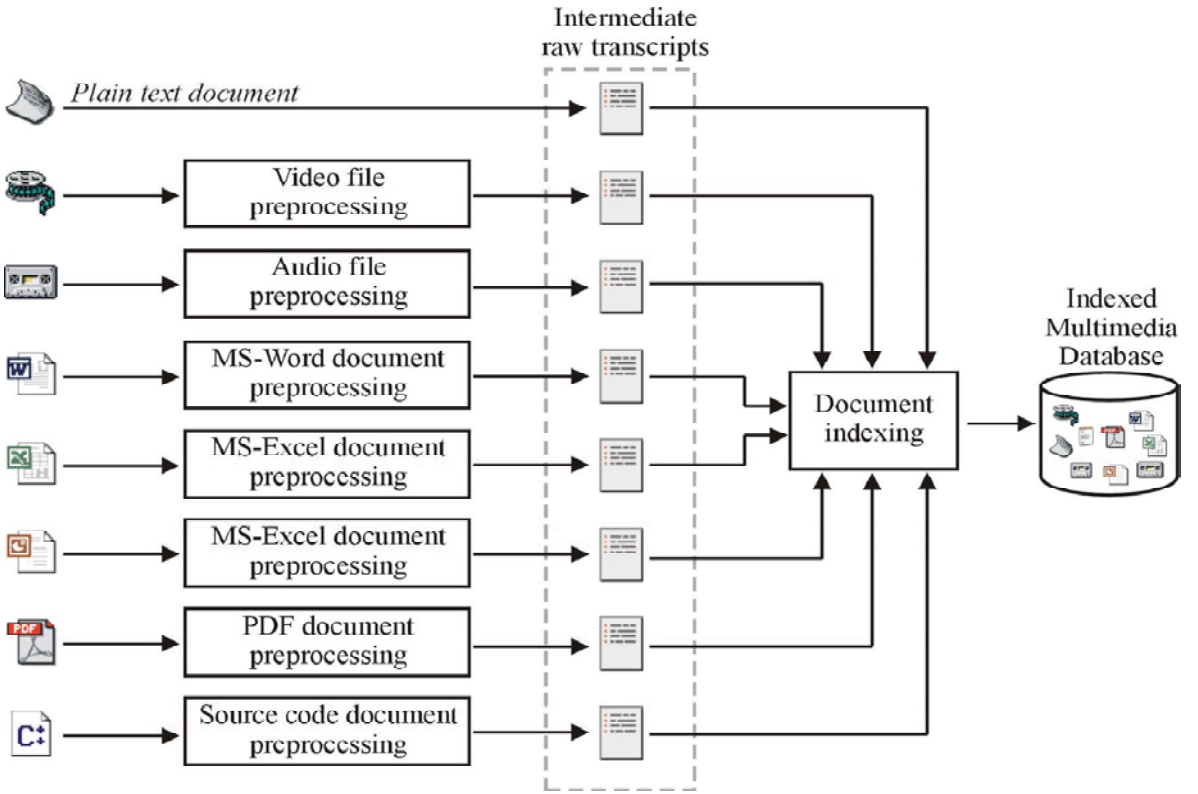

- Salgado-Garza L.R. et al., “A Proposed Architecture for a Spoken Information Retrieval with Multimedia Databases”, Taller de Tecnologías del Lenguaje Humano - INAOE, México, 2004

IR - Metadata

- Metadata:
  - Wikipedia:
    - Metadata is "data about data", of any sort in any media. An item of metadata may describe an individual *datum*, or content item, or a collection of data including multiple content items and hierarchical levels.
    - The concept of metadata is analogous to the use of indices to locate objects rather than data. For example, in a library, a set of tokens are used to specify authors, titles, etc.. Thus, the metadata helps to locate data.
    - For several fields of the information technology such as information retrieval and semantic web, metadata is an important approach to building a bridge over the interval semantic.

IR - Metadata

- Search without Metadata:

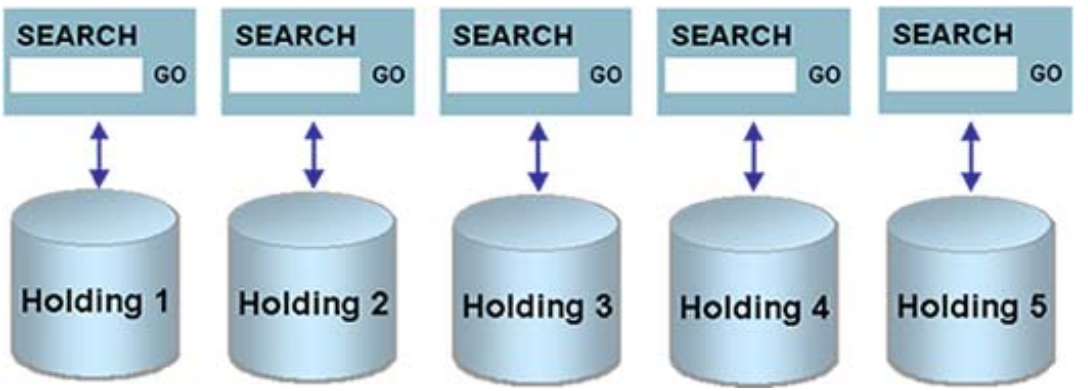

IR - Metadata

- Search based on Metadata:

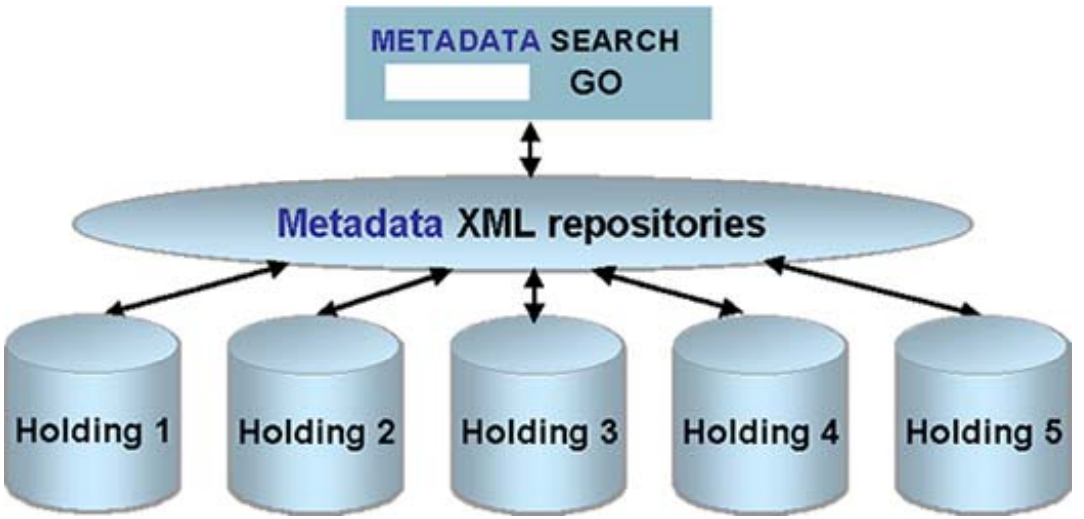

IR – Multimedia video sources

- Structure scheme:

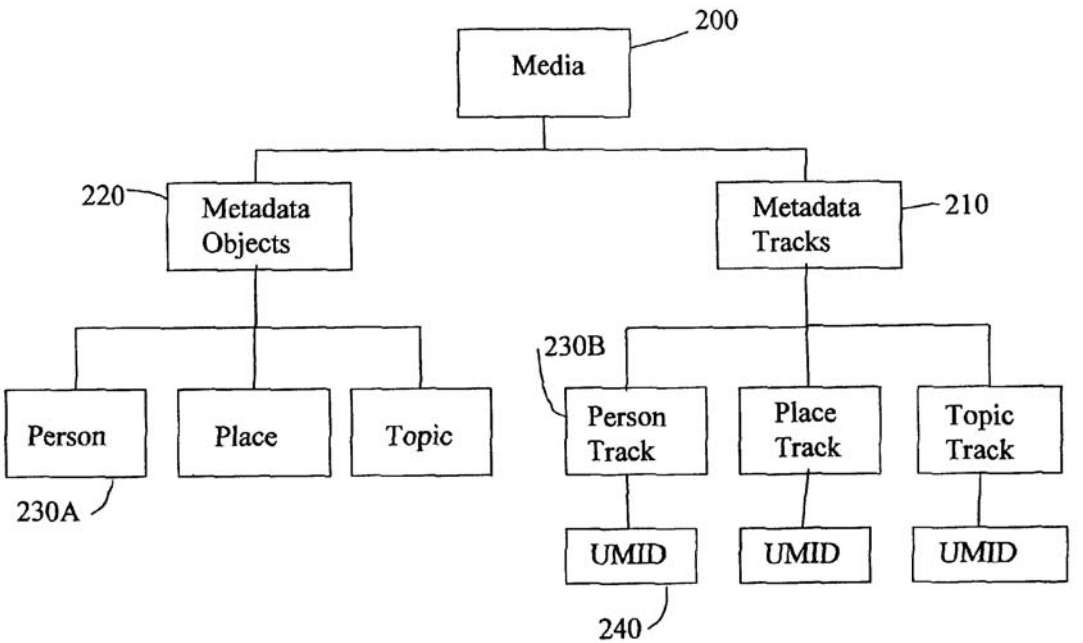

IR – Multimedia audio sources

- Structure scheme:

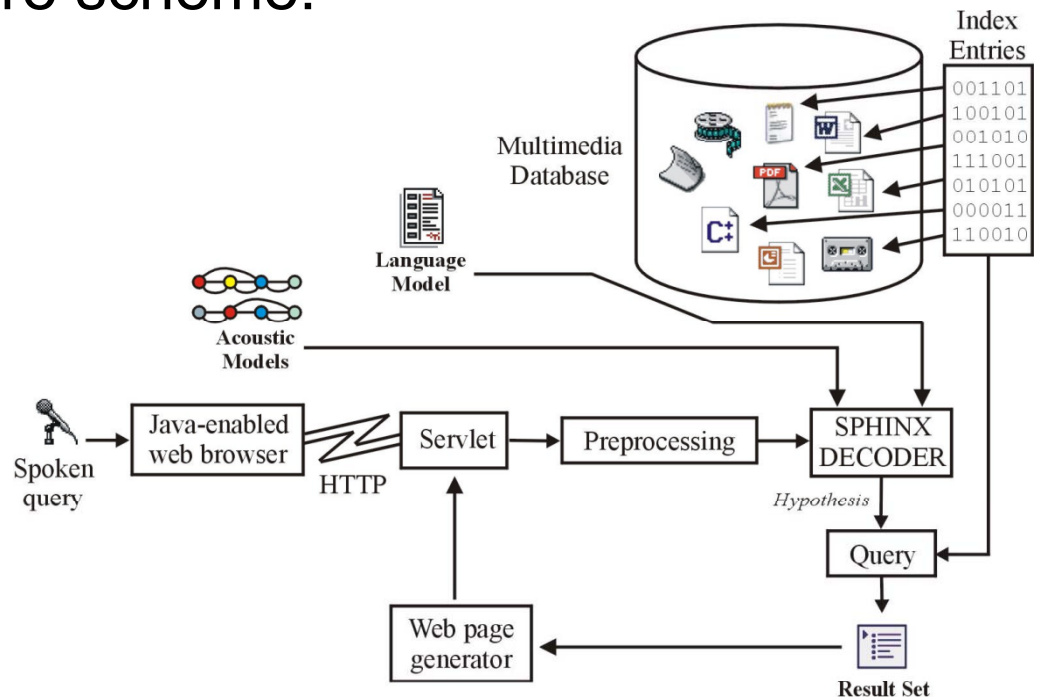

- Salgado-Garza L.R. et al., “A Proposed Architecture for a Spoken Information Retrieval with Multimedia Databases”, Taller de Tecnologías del Lenguaje Humano - INAOE, México, 2004

IR – Mult. audio/video sources

- Structure scheme:

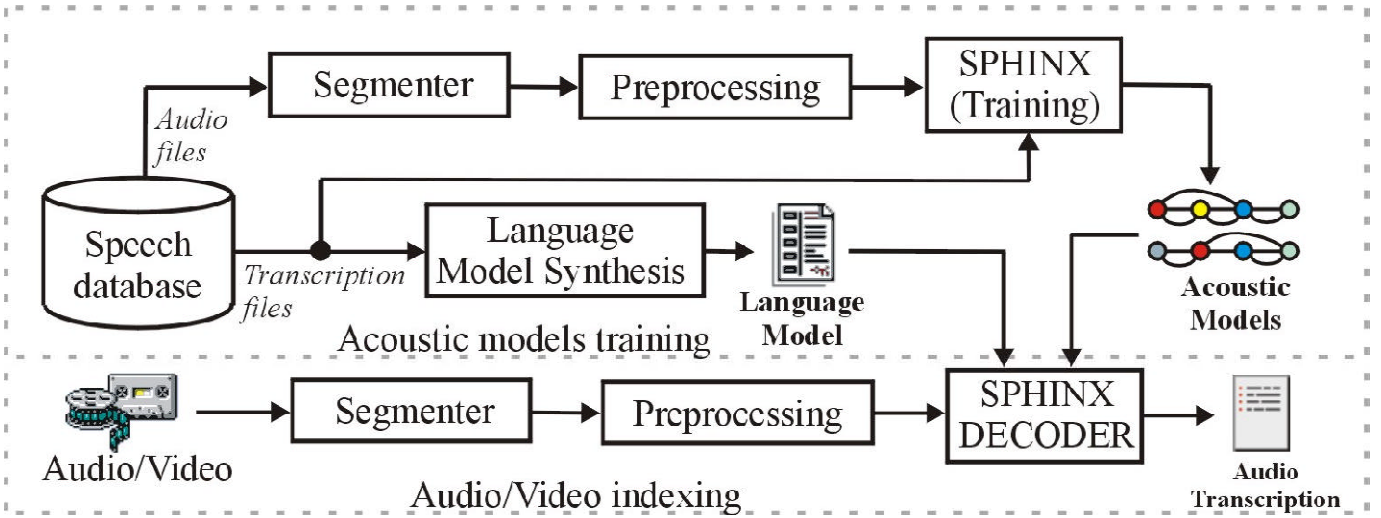

- Salgado-Garza L.R. et al., “A Proposed Architecture for a Spoken Information Retrieval with Multimedia Databases”, Taller de Tecnologías del Lenguaje Humano - INAOE, México, 2004

IR – Results in Basque Context

- Most of the mass media in Basque Country use Spanish, French, and/or Basque.
- The main goal of an Information Retrieval (IR) system is to provide effective access to on-line information, managing multimodal information such as voice, gestures or written information.
- To develop an efficient index system for IR in this context all of the tools (ASR system, NLP system, index system) and resources (digital library, Lexicon) to be developed will be oriented to create **multilingual systems**.

IR – Results in Basque Context

- In this sense, many works have been developed with several european languages (Vandecat.) and specifically French and Spanish (García-Mateo; Adda-Decker).
- But the use of Basque language introduces a new difficulty to the development of the system, since it needs specific tools and the resources available are fewer.

- Vandecatseye et al., “The COST278 pan-European Broadcast News Database”. In Proceedings of LREC 2004, Lisbon (Portugal).
- García-Mateo C. et al., “Transcrigal: A bilingual system for automatic indexing of broadcast news” LREC2004.
- Adda-Decker M. et al., “Large vocabulary speech recognition in French” Acoustics, Speech, and Signal Processing, 1999. ICASSP Proceedings., Volume 1, Issue , 15-19.

IR – Results in Basque Context

- Analysis across languages
  - *Sound inventories:*
    - Sound Inventories for Basque, French and Spanish in SAMPA (Speech Assessment Methods Phonetic Alphabet).

Sound Type	Basque	French	Spanish
Consonant			
Plosives	p b t d k g c	p b t d k g	p b t d k g
Affricates	ts ts´ tS gj		ts gj
Fricatives	jj f B T D s s´ S x G Z v h	f v s z S Z	jj f B T D s x G
Nasals	m n J	m n J N	m n J
Liquids	l L r rr	l R	l L r rr
Vowel glides	w j	w H j	w j
Vowels			
Vowels	i e a o u @	i e E a A O o u y 2 9 @ e~ a~ o~ 9~,	i e a o u
Indetermination	-	a-A e~-9~ e-E o-O 2-9	-

  - Is a crucial issue because they influence both the performance of the acoustic decoder and the vocabulary size of the general index system (text and speech).

IR – Results in Basque Context

- *Vocabulary size*:
- Basque is an agglutinative language with a special morpho-syntactic structure inside the words.
- A first approach to the problem is to use morphemes instead of words.
  - Relative Frequency of Occurrence (RFO) of the words and pseudo-morphemes in relation to their Length in Characters (LC) of the *STDBASQUE* sample

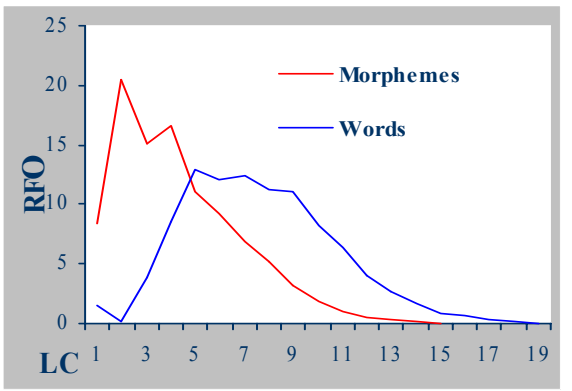

- There is a high number of units that are small (fewer than four characters) and acoustically difficult to recognize could lead to an increase of the acoustic confusion, and could also generate a high number of insertions.

IR – Results in Basque Context

- *Inventory of resources*

Language	Broadcast Video	Broadcast Audio	Transcription XML-FILE	Textual database
EU	6:37	18	12	8M
FR	-	2:58	2:58	2M
ES	9:35	12:34	12:34	4M
Total	16:12	33:12	33:12	14M

- Resources collected and developed: Broadcast (video, audio), Transcription of broadcast in XML format, text databases, and Lexical elements (Lexicons and Grammars).
- All of them were processed to include morphologic information such as each word's lemma and Part-Of-Speech tag.
- Using all this information, a Lexicon for each language was extracted taken into account the context of the word in order to eliminate ambiguity.

IR – Results in Basque Context

- *Evaluation of the audio resources:*
  - Total of Speakers (TS), Non Native Speakers (NNS), Native Speakers (NS), Size in Mb, Number Files in WAV Format (NF-WAV), Timeframe in hours (TF-H)

Media	TS	NNS	NS	SZ-Mb	NF-WAV	TF-H
Infozazpi						
EU	40	0	40	2440	134	11:23
ES	20	0	20	648	86	2:59
FR	15	0	15	657	86	2:58
EITB						
EU	187	14	173	877	7	6:37
ES	175	10	165	870	6	9:35
Total	437	24	413	5492	319	33:12

- A preliminary evaluation of digital resources oriented to robust Automatic Multilingual Information Retrieval was carried out, taken into account the future development of the system's key elements.
  - Evaluation of the audio resources: %Speech, %Non-Speech, Number of Words (NW) and Number of Distinct Words and/or Morphemes (NDW/M)

Media	%Speech	%Non-Speech	NW	NDW
Infozazpi				
EU	78	22	58855	5741-W 3445-M
ES	47	53	13625	2066
FR	42	58	20196	3494
EITB				
EU	89	11	49185	7993-W 4796-M
ES	92	18	102301	6290

IR – Results in Basque Context

- Barroso N. et al., "*Development of Multimodal Resources for Multilingual Information Retrieval in Basque context*", lecture notes in computer science, Vol. 4629, 2007, pp. 582-590.
- Ariztimuño I. et al., "*First Experiments on Acoustic-Phonetic Decoding for Multilingual Speech Recognition in the Basque context*", I Jornadas de Inteligencia Computacional JIC'07, San Sebastián-Donostia,
- Barroso N. et al., "*Development of Multimodal Resources for Multilingual Information Retrieval in the Basque Context*", INTERSPEECH, Belgium, 2007
- Bordel G. et al., "*Language Resources for a Bilingual Automatic Index System of Broadcast News in Basque and Spanish*", lecture notes in computer science, Vol. 3773, 2005, pp. 1047-1054.
- Graña M. et al., "*Selection of Lexical Units for Continuous Speech Recognition of Basque*", lecture notes in computer science, Vol. 2905, 2003, pp. 244,250.

IR – RBC: Robustness

- In the developed work, an added problem has appeared when you work with real sources of information: Noise in the samples.
- This means there are samples that are devoid of value in some of its parameters, in addition to significantly reduce the number of them.
- To give more robustness to the process, some methods are studied in order to classify small numbers of samples, and even with incomplete samples.
- Finally in a first approach Hidden Markov Models for allophonic acoustic models have been trained with noisy train sets.

IR – RBC: Robustness

- Results of the experiments clustered by sound types

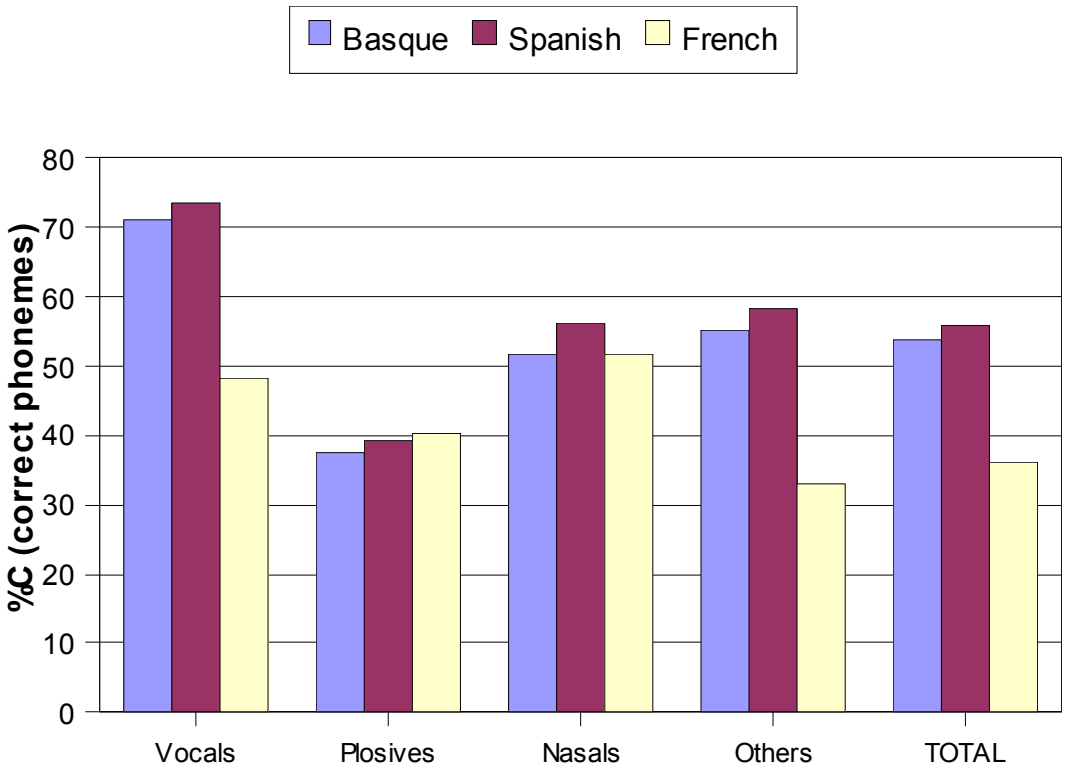

IR – RBC: Robustness

- It is obvious that the phoneme recognition rate is much better for Spanish and Basque than for French.
- This can be explained with two main reasons: on the one hand, the simple vowel structure in Basque and Spanish eases the overall recognition of phonemes.
- On the other hand, the mean noise level in French is also higher and the training data amount is smaller. Therefore, in these first experiments the results won't be comparable, but even then they encourage further work.
- Noise has more influence in plosives, affricates and fricatives.

IR – RBC: Robustness

- Results of the experiments clustered by sound types with different train sets (30%, 40%,…)

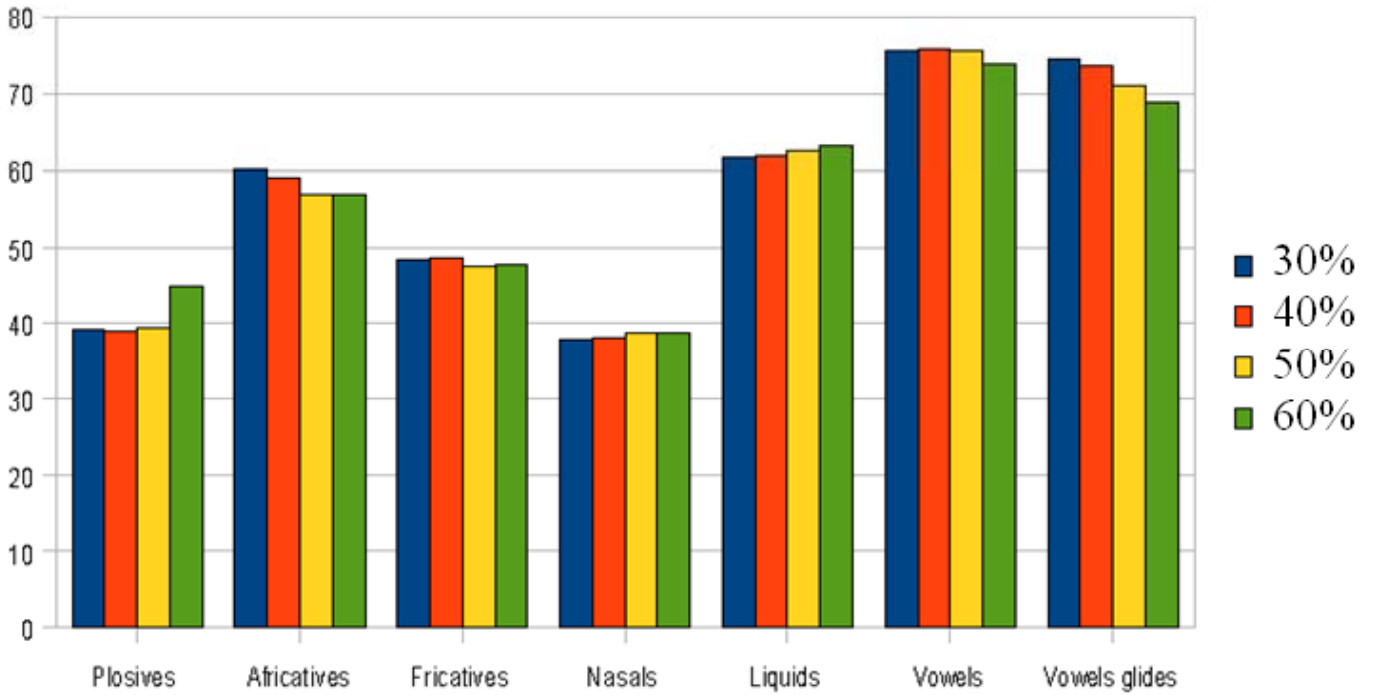

IR – RBC: Robustness Future works

- Future works

  ESTIMATION METHODS LOOC:

  - They are based on finding the best parameters to maximize a function that depends on the mean and covariance matrix of the training sample.

  - The optimal parameters are those that are better suited to the examples of the training sample so that the average likelihood of the omitted examples is maximum.

- J.P. Hoffbeck, D. Landgrebe, *"Covariance estimation and classification with limited training data"* IEEE Transactions on Pattern Analysis and Machine Intelligence, 18, no. 7, 1996, pp 763-767

IR – RBC: Robustness

ESTIMATION METHODS BLOOC:

- This method is an extension of the methods of estimating GDR and LOOC.
- Two cases are considered depending on the number of training patterns and the size of the data.
- It is supposed that the patterns are normally distributed.
- That is, the covariance matrices obtained from the training sample, Σi, are mutually independent with the distribution of Wishart.

- S. Tadjudin, D. Landgrebe, *Covariance Estimation with Limited Training Samples,* IEEE Trans. Geoscience and Remote Sensing, vol. 37, 2000

IR – RBC: Robustness

- More research works:

H.Luo, Y. Gao, Z. Liu, J.Fan, 2003

Semantic video classification with insufficient labeled samples

Proceedings of the SPIE Storage and Retrieval Methods and Applications for Multimedia, vol. 5307, pp. 340-350

K. Levi, M. Fink, Y. Weiss, 2004

Learning From a Small Number of Training Examples by Exploiting Object Categories

Proceedings of the 2004 Conference on Computer Vision and Pattern Recognition Workshop (CVPRW'04) Volume 6.

IR – RBC: Conclusions

- The development of Multimodal Resources is required for any project that involves pattern recognition on multimodal contents: Automatic Indexing tasks.
- Basque, French, and Spanish have to be taken into account because they are official in Basque mass media, as *Infozazpi Irratia* and *EITB*.
- It has been very important to lay down the foundations for Multilingual Speech Recognition Systems.
- This job tackles this issue :

  employing one less-resourced language

  like Basque in front of Spanish and French.

Future lines

- A collaboration project (PROFIT):

CATALOGADOR Y BUSCADOR MULTIMODAL PARA CONTENIDOS AUDIOVISUALES

- Enterprises involved with:

Elhuyar
VICOMTech
UPV/EHU

- Principal Objective:

A similar Google engine that looks for radio programs, TV, WEB files and any other information presented in a uniform format.

PROFIT: Purpose

- The idea of access to multimedia information based on content has been working for several years based on the success of the current search engines Google, Altavista, etc..
- Oral communication is the most natural of human beings, and therefore providing to the machines with this capacity is an important technological goal.
- This project try to develop a multimedia search engine that could be used to support television, publishing, radio or even more specialized tools such as security systems, and so on.

PROFIT: Objectives

- It is intended to give impetus to the creation of new systems and tools to develop management platforms for digital content, and for trade and copyright authorization, as well as the development of intelligent systems for the management and treatment of content.
- In this project intends to develop a search system on a multimodal database composed of heterogeneous texts, images, sounds and videos, from a multimodal input and that may also be textual, graphic or audio.

Grupo de Inteligencia Computacional
de la Universidad del País Vasco
http://www.ehu.es/ccwintco

Del 12 al 19 de Mayo de 2008
Affi,
Italia